

THE REACTIONS OF STABLE NUCLEOPHILIC CARBENES WITH MAIN GROUP COMPOUNDS

CLAIRE J. CARMALT* and ALAN H. COWLEY†

*Department of Chemistry, University College London, Christopher Ingold Laboratories, London, WC1H 0AJ, United Kingdom and †Department of Chemistry and Biochemistry, The University of Texas at Austin, Austin, Texas, 78712

- I. Introduction
- II. Group 1, 2, and 12 Complexes
 - A. Alkali Metals and Hydrogen
 - B. Alkaline Earth Metals, Zinc, and Mercury
- III. Group 13 Complexes
 - A. Group 13 Trihalides
 - B. Group 13 Trihydrides
 - C. Group 13 Trialkyls and Triaryls
- IV. Silicon, Germanium, Tin, and Lead Complexes
 - A. Silicon Halides and Organosilicon Compounds
 - B. Germanium and Tin Halides and Organotin Halides
 - C. Cyclopropenylidene Complexes of Divalent Germanium, Tin, and Lead Amides
- V. Group 15 Complexes
 - A. Phosphinidenes and Arsnidenes
 - B. Phosphoranes
- VI. Sulfur, Selenium, and Tellurium Complexes
- VII. Halogen Complexes
- VIII. Conclusions
- References

I. Introduction

Carbenes play important roles both as reactive intermediates and also as ligands; consequently, considerable effort has been devoted to understanding their molecular and electronic structures. Special interest is associated with carbenes that feature the attachment of donor groups to the carbenic carbon since they behave as nucleophiles and, in some instances, can be isolated. Pioneering work on nucleo-

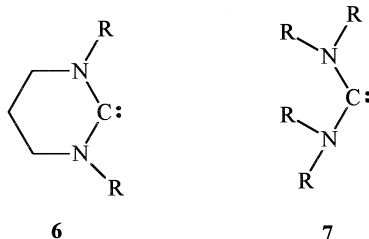
1 **2** **3**

4

5

intermediacy of this species by C-deprotonation of imidazolium salt **5** ($R' = R = \text{Ph}$; $X^- = \text{ClO}_4^-$) with KO^tBu , followed by trapping with phenylisothiocyanate (**2**) or mercuric chloride (**3**) (*vide infra*). However, several years were to elapse before Arduengo *et al.* (**4**) achieved the first isolation of a stable, crystalline nucleophilic carbene, **4** ($R' = \text{H}$; $R = \text{adamantyl}$) by C-deprotonation of the corresponding bis(1-adamantyl)imidazolium chloride with KH . This important development prompted a flurry of activity in this area of chemistry. For example, a completely new synthetic route to stable nucleophilic carbenes has been developed by Kuhn *et al.* (**5**), *viz.* the reduction of thiones with potassium in THF, and Herrmann *et al.* (**6**) demonstrated that a liquid ammonia/THF solvent system is very effective for the NaH deprotonation of imidazolium salts at relatively low temperatures. The range of stable nucleophilic carbenes has also expanded significantly, not only in terms of the elaboration of substitu-

ents on structures of type **4**, but also from the standpoint of new structural types (**7**). The isolation of saturated derivatives of types **1** ($R = \text{Mes}$) (**8**) and **6** ($R = i\text{Pr}$) (**9**) implies that the presence of a carbon-carbon double bond is not, in fact, a prerequisite for stability.



Moreover, Alder *et al.* (10) have shown that, with the appropriate substituents, it is possible to isolate acyclic nucleophilic carbenes, **7**. Polyfunctional nucleophilic carbenes have also been prepared (**6**, **11**), as have carbenes that feature additional nitrogen atoms or heteroatoms other than nitrogen (12).

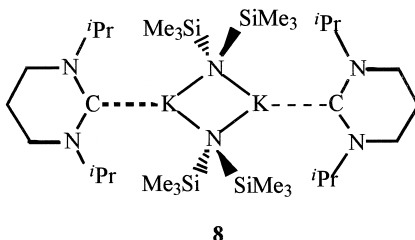
Fundamentally, the high nucleophilicity of stable carbenes, coupled with the tendency to increase the coordination number at the carbenic carbon, renders their chemical behavior very similar to that of electron-rich phosphines. As such, they have aroused considerable interest as ligands in *p*-, *d*-, and *f*-block chemistry. Earlier reviews (7*a,b*) have covered some aspects of the main group chemistry of stable nucleophilic carbenes; however, there has been considerable recent activity in this field, and thus a comprehensive, up-to-date review was considered desirable.

II. Group 1, 2, and 12 Complexes

A. ALKALI METALS AND HYDROGEN

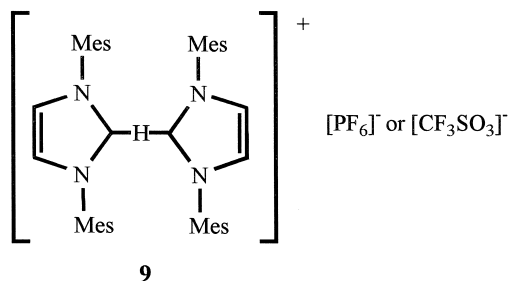
As mentioned in the Introduction, one of the synthetic approaches to stable nucleophilic carbenes involves C-deprotonation of imidazolium and related cations with alkali metal salts of strong bases such as NaH and KO^tBu. Accordingly, the interactions with alkali metal cations with stable nucleophilic carbenes could prove to be important for understanding the solution behavior of the latter. Until recently, however, there were no examples of complexes of stable carbenes with

alkali metals. The first example of such a complex (**8**) was isolated from the reaction of **6** ($R = i\text{Pr}$) with $\text{KN}(\text{SiMe}_3)_2$ (**9**). The solid-state



structure of **8** comprises dimeric molecules in which the $\text{N}(\text{SiMe}_3)_2$ groups act as bridging ligands. The $\text{K}\cdots\text{C}$ distance of 3.00 \AA suggests that the interaction is largely of an electrostatic ion-dipole nature. The interaction of carbenes **4** ($R = i\text{Pr}$, $R' = \text{Me}$), **6** ($R = i\text{Pr}$), and **7** ($R = \text{Me}$) with $\text{MN}(\text{SiMe}_3)_2$ ($M = \text{Li}, \text{Na}, \text{K}$) and LiTMP ($\text{TMP} = 2,2,6,6\text{-tetramethylpiperidide}$) in solution was also reported (9). Evidence for the complexation of these carbenes with lithium, sodium, and potassium species in solution was obtained from the ^{13}C NMR shifts for the relevant carbene center. Generally speaking, the ^{13}C chemical shift of the carbenic carbon is a very useful diagnostic and lies typically in the range $\delta 200\text{--}240$ for free imidazol-2-ylidenes, **4**.

Like I^+ (*vide infra*), H^+ can form bis(carbene) complexes, **9** (**13**). These homoleptic complexes, which feature $\text{C}\cdots\text{H}\cdots\text{C}$ interactions, were formed by treatment of **4** ($R = \text{Mes}$; $R' = \text{H}$) with the corresponding

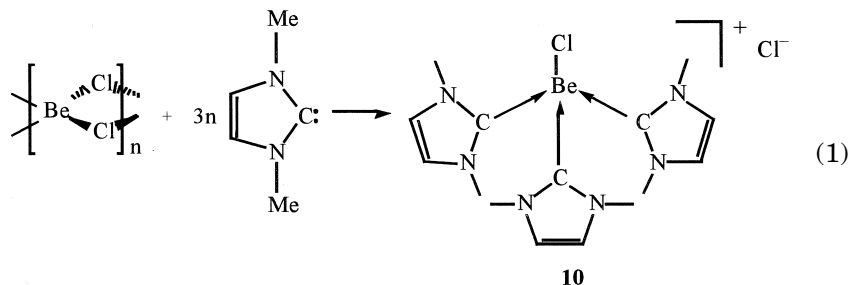


imidazolium salts, $[\mathbf{4H}]^+[\text{PF}_6]^-$ and $[\mathbf{4H}]^+[\text{CF}_3\text{SO}_3]^-$. Both salts are colorless solids that melt above 200°C . The X-ray crystal structures of both salts were determined and are very similar. The central $\text{C}\cdots\text{H}\cdots\text{C}$ unit is close to linear (172.5°); however, the two carbon-hydrogen distances in the bridge differ somewhat [$2.026(45)$ and $1.159(45) \text{ \AA}$] in

contrast to the more symmetrical I^+ analogue. The structures of both proton complexes feature secondary interactions between the anions and the 4,5 hydrogens of the imidazole rings, resulting in a one-dimensional chain motif reminiscent of the solid-state structures of the triflate salts of the bis(carbene) complexes of silver(I) and copper(I) (14).

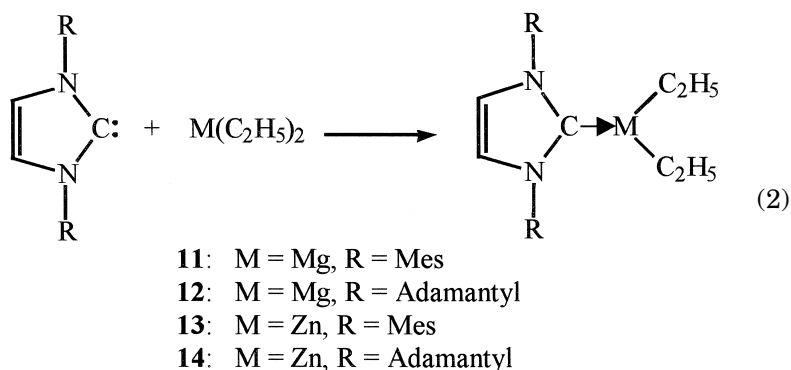
B. ALKALINE EARTH METALS, ZINC, AND MERCURY

Nucleophilic carbene **4** ($R = \text{Me}$, $R' = \text{H}$) has been shown to disrupt the polymeric structure of beryllium dichloride to form an ionic carbene complex, **10** (15). The crystal structure of **10** revealed that the cation possesses a distorted tetrahedral coordination geometry at the beryllium center. The average Be–Cl bond distance (2.083(7) Å) is

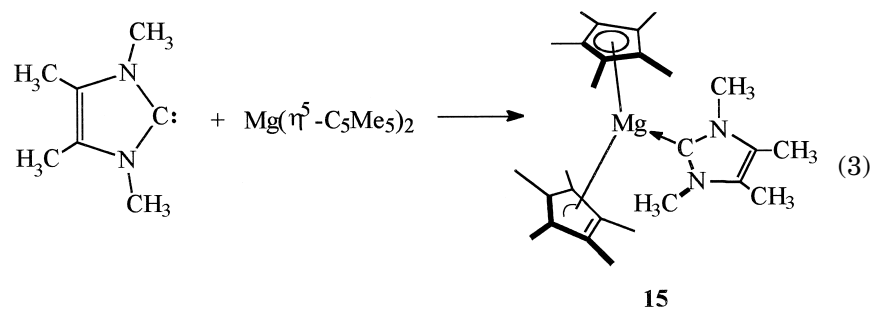


longer than those of other tetracoordinate beryllium complexes. However, the Be–C(carbene) bond distances are similar to those of conventional Be–C single bonds and the metrical parameters for the coordinated carbenes are similar to those found in the free carbene. Attempts to displace the second chloride ion by the addition of excess carbene were not successful.

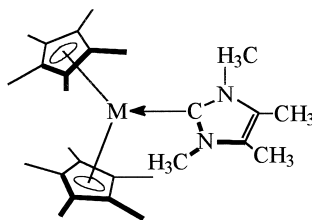
The reaction of diethyl magnesium or diethyl zinc with carbenes of type **4** ($R = \text{Mes}$ or adamantyl; $R' = \text{H}$) resulted in the isolation of complexes of composition $4 \cdot \text{MgEt}_2$ and $4 \cdot \text{ZnEt}_2$ (16). The crystal structures of $4 \cdot \text{MgEt}_2$ (**11**, $R = \text{Mes}$; **12**, $R = \text{adamantyl}$) and $4 \cdot \text{ZnEt}_2$ ($R = \text{adamantyl}$) (**14**) were reported (16). The crystalline state of **11** comprises ethyl-bridged dimers; however, the structures of **12** and **14** are monomeric and feature a trigonal planar coordination geometry at magnesium or zinc. The formation of a dimer when $R = \text{Mes}$ is not unexpected since the steric demand of a mesityl group is inferior to that of an adamantyl group (17).



Monomeric carbene complexes with 1:1 stoichiometry have also been isolated from the reaction of **4** (R = R' = Me) with bis(pentamethylcyclopentadienyl)magnesium, -calcium, -strontium, -barium, or -zinc (18). X-ray crystallographic studies showed interesting variations in the Me_5C_5 hapticities of the products. In the case of the $\text{Mg}(\eta^5\text{-C}_5\text{Me}_5)_2$ complex, one ring is pentahapto (**15**), whereas the other is intermediate between η^3 - and σ -bonded. The corresponding products isolated from the reaction of the same carbene with $\text{Ca}(\eta\text{-C}_5\text{Me}_5)_2 \cdot \text{OEt}_2$ or $\text{Ba}(\eta\text{-C}_5\text{Me}_5)_2 \cdot 2\text{thf}$ feature two pentahapto-bonded



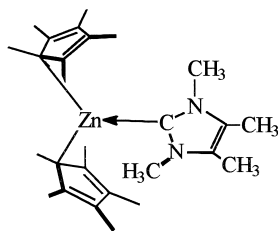
C_5Me_5 rings (**16**, **17**). (The $\text{Sr}(\eta\text{-C}_5\text{Me}_5)_2 \cdot \text{OEt}_2$ product was not suitable for complete X-ray crystallographic assay). A third coordination mode, namely bis-monohapto (**18**), was evident in the product of the $\text{Zn}(\eta^5\text{-C}_5\text{Me}_5)(\eta^1\text{-C}_5\text{Me}_5)$ reaction. For each of the complexes **15**–**18**, the shortest metal–carbon distances are those to the carbene center (2.194(2), 2.561(3), 2.951(3), and 2.022(3) Å in **15**, **16**, **17**, and **18**, respectively). If the centroids of the $\eta^5\text{-C}_5\text{Me}_5$ rings are considered to



16: M = Ca

17: M = Ba

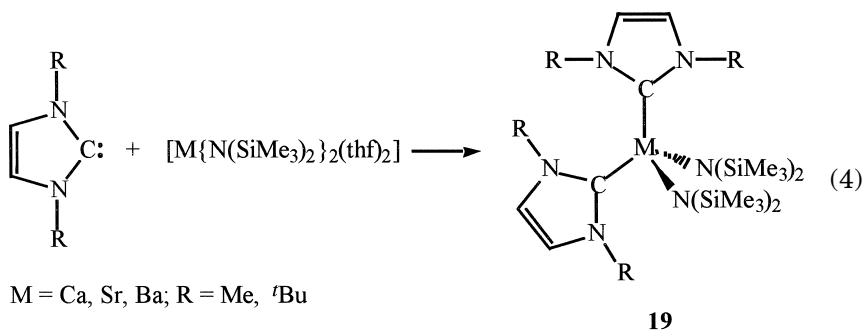
occupy single coordination sites, the metal geometries in **15** and **16** are essentially trigonal planar, whereas that of **17** is somewhat pyramidal and the carbene–barium vector does not lie in the plane of the



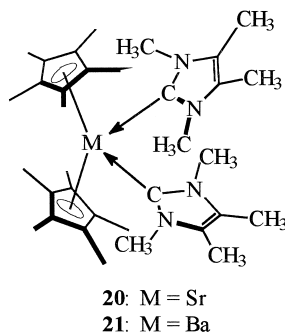
18

imidazole ring. The η^1 -bonded zinc derivative, **18**, exhibits a quasi-trigonal planar geometry. Generally, only modest structural changes accompany the coordination of the carbene. That the largest such changes take place with the zinc complex **18** is consistent with the observation that this complex possesses the shortest metal–carbene bond. As expected, complexes **15–18** possess a nonlinear $(C_5Me_5)-M-(C_5Me_5)$ arrangement (ring centroids for **15–17**; *ipso* carbons for **18**). Interestingly, the degree of bending for **16** and **17** is similar to that for the uncoordinated metallocenes.

It is also possible to isolate bis(carbene) complexes involving the heavier alkaline earth metals. Thus, the reaction of two equivalents of **4** ($R = Me$ or tBu , $R' = H$) with calcium, strontium and barium bis(trimethylsilyl)amides $[M\{N(SiMe_3)_2\}_2(thf)_2]$ ($M = Ca, Sr, Ba$) resulted in the displacement of two thf molecules to afford the corresponding biscarbene species, **19** (19). The solubilities and stabilities of these complexes were found to decrease from calcium to barium.

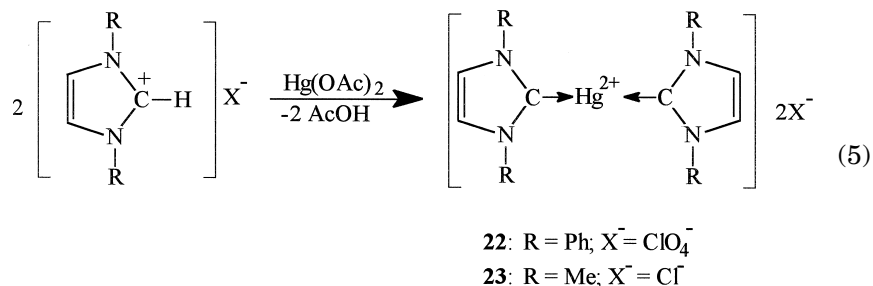


Bis(carbene) complexes of the heavier alkaline earth metals have also been prepared by treatment of $\text{Sr}(\eta\text{-C}_5\text{Me}_5)_2 \cdot \text{OEt}_2$ or $\text{Ba}(\eta\text{-C}_5\text{Me}_5)_2 \cdot 2\text{thf}$ with two equivalents of **4** ($\text{R} = \text{R}' = \text{Me}$) (**18**). The crystal structure of the strontium derivative **20** was investigated by X-ray diffraction and showed a pseudotetrahedral geometry at strontium with a carbene–Sr–carbene bond angle of $86.4(1)^\circ$ and an average Sr–carbene bond distance of $2.861(5) \text{ \AA}$.



The cationic carbene–mercury complex **22** was prepared more than 30 years ago (3) via the reaction of 1,3-diphenylimidazolium perchlorate **5** ($\text{R} = \text{Ph}$; $\text{R}' = \text{H}$) with mercuric acetate. The same synthetic approach has been used more recently for the preparation of the analogous 1,3-dimethylimidazol-2-ylidene complex, **23** (20). Thus, although **22** possesses a linear carbene–Hg–carbene skeleton (21), that of **23** is distorted toward a tetrahedral arrangement ($\text{C}(\text{carbene})\text{–Hg–C}(\text{carbene}) = 161.4(3)^\circ$) due to interactions with the chloride anions

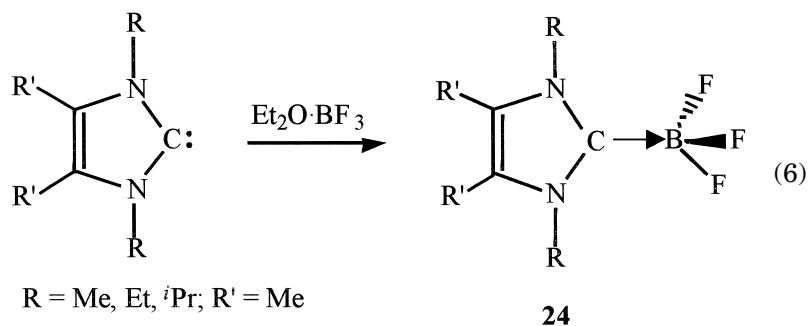
(20). Despite these secondary interactions, the Hg–carbene bond distances are very similar in **22** (2.060(1) Å) and **23** (2.092(5) Å).



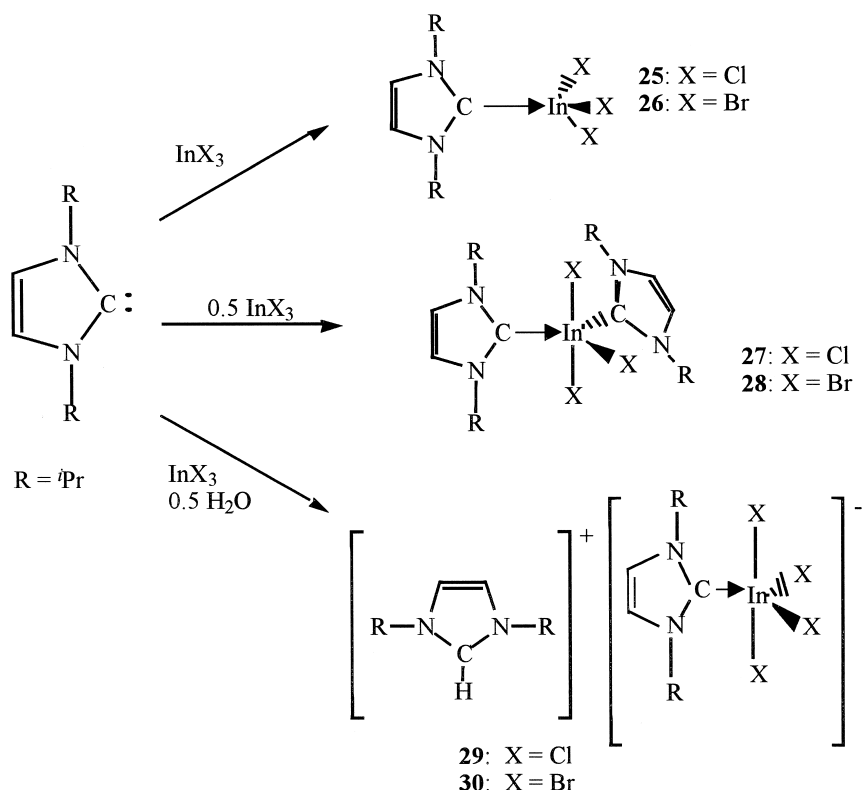
III. Group 13 Complexes

A. GROUP 13 TRIHALIDES

Treatment of carbenes **4** (R = Me, Et, *i*Pr, R' = Me) with Et₂O · BF₃ resulted in the isolation of thermally stable BF₃ complexes, **24** (22). No information regarding the structures of these complexes is available; however, a related BH₃ complex has been characterized crystallographically and is discussed later (23).



A series of complexes between stable nucleophilic carbenes and indium(III) halides has been reported (23). The reaction of **4** (R = *i*Pr, R' = Me) with 1 equiv of InX₃ (X = Cl, Br) resulted in the formation



SCHEME 1. Reactions of indium halides with 1,3-diisopropyl-4,5-dimethylimidazol-2-ylidene.

of the 1:1 complexes **25** (X = Cl) and **26** (X = Br) (Scheme 1). In contrast to other 1:1 complexes of indium(III) halides (**24**, **25**), the crystal structure of **26** showed that this complex is monomeric. The indium center in **26** adopts a distorted tetrahedral geometry and the In–Br bond distances are very similar (av. 2.500(7) Å). The In–C(carbene) bond distance of 2.199(5) Å is relatively long in comparison with conventional In–C single bond distances. The bond distances and angles within the carbene heterocycle of **26** are typical of those observed for other group 13-carbene complexes. For example, the N–C–N angle of 106.8(4)° lies between the normal value for uncoordinated nucleophilic carbenes (~102°) and that of imidazolium cations (~108°).

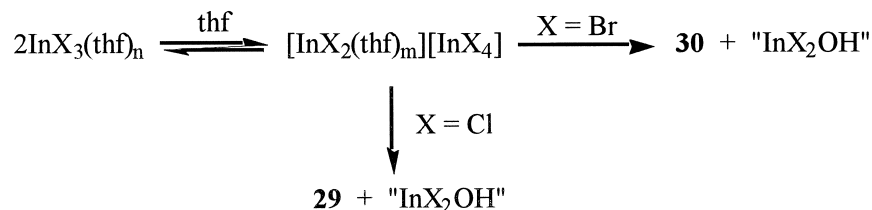
Biscarbene complexes of indium(III) halides can be isolated from the reaction of two equivalents of 1,3-diisopropyl-4,5-dimethylimida-

zol-2-ylidene with InX_3 (**27**, $\text{X} = \text{Cl}$; **28**, $\text{X} = \text{Br}$) (23). The X-ray crystal structures of **27** and **28** revealed that the pentacoordinate indium center in both compounds adopts a distorted trigonal bipyramidal geometry. In contrast to most other neutral 2:1 complexes of InX_3 in which the halide ligands occupy the equatorial sites, **27** and **28** feature two halides in the apical positions and the third halide and two carbenic atoms in the equatorial sites. It is not clear why this sterically unfavorable arrangement of the ligands is adopted. As expected, the $\text{In}-\text{C}(\text{carbene})$ distances in **27** (av. 2.228 Å) and **28** (av. 2.230 Å) are slightly longer than that in **26**. However, the geometries of the coordinated carbenes are similar.

When the reactions between **4** ($\text{R} = \text{'Pr}$, $\text{R}' = \text{H}$) and 1 equiv of the indium trihalide were carried out in the presence of water, ionic products **29** ($\text{X} = \text{Cl}$) and **30** ($\text{X} = \text{Br}$) were formed (23). The anions are, in fact, carbene complexes of the corresponding tetrahaloindates, $[\text{InX}_4]^-$, thus highlighting the strong nucleophilicity of the carbene ligand. The mechanism of the formation of **29** and **30** is unclear; however, it is believed to involve an equilibrium between $[\text{InX}_3(\text{thf})_n]$ and the corresponding ionic isomer in thf solution as suggested in Scheme 2. The other product of the reaction is thought to be an indium hydroxide, $[\text{InX}_2\text{OH}]$, although this species could not be isolated. The reaction of a 2:1 molar ratio of InBr_3 and H_2O with 1 equiv of carbene **4** ($\text{R} = \text{R}' = \text{Me}$) resulted in the corresponding imidazolium tetrabromindate (**26**).

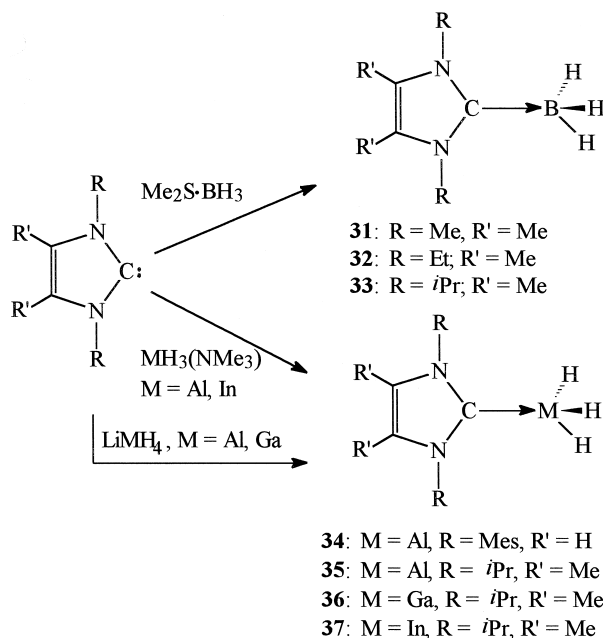
B. GROUP 13 TRIHYDRIDES

In recent years the coordination of N-, P-, or O-donor Lewis bases to aluminum and gallium trihydrides has been studied extensively (27). Interest in these complexes stems in part from their applications in a wide variety of areas, for example chemical vapor deposition technology (28) and organic synthesis (29). However, the corresponding carbene complexes of the heavier group 13 trihydrides have only been



SCHEME 2. Proposed mechanism for the formation of **29** and **30**.

reported recently (30–32). That the chemistry of carbene–borane complexes has been investigated in considerably more detail than that of the heavier congeners is partly due to the fact that borane complexes of other neutral carbon donors, such as carbon monoxide, isonitriles, and phosphine ylides, are well established. The first carbene–BH₃ complexes (**31–33**) were isolated from the reactions of Me₂S·BH₃ with 1 equiv of an *N*-heterocyclic carbene, as depicted in Scheme 3 (22). X-ray crystallographic analyses and *ab initio* calculations on **32** suggest that only weak π interactions take place between the N–C–N moiety and the C=C unit within the imidazol-2-ylidene ring; hence, as in the case of the BF₃ complex, **24**, the electronic structure is intermediate between that of the free nucleophilic carbene and that of a more delocalized imidazolium ion. In contrast to previous borane complexes of carbon bases such as H₃BCO, which rely upon some degree of back π -bonding for stability, nucleophilic carbene complexes such as **24** and **31–33** involve predominant forward donation of the carbon lone pair. The ¹¹B NMR chemical shifts for **31–33** fall in the range observed for ylide–borane adducts. Interestingly, the ¹J(¹H,¹¹B) coupling constants for these complexes are very similar to that of the borate anion [(C₆H₅)BH₃][−].

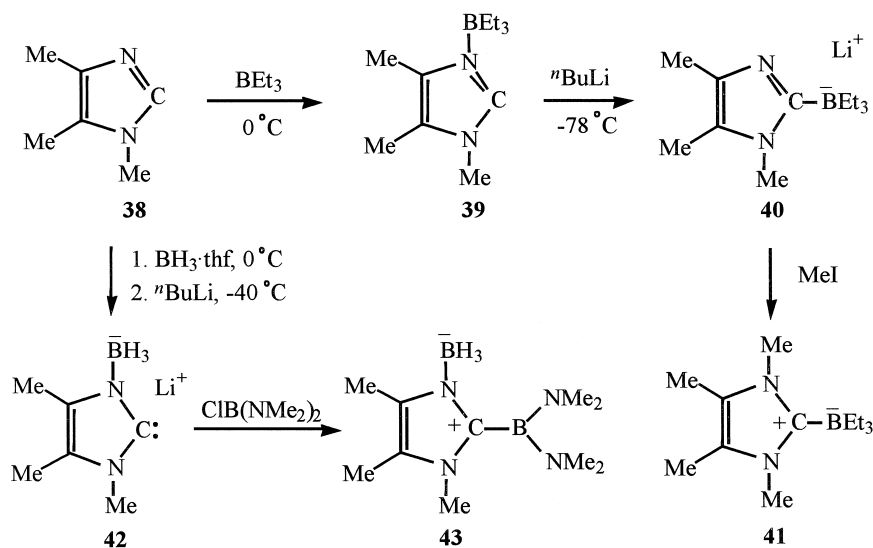


SCHEME 3. Reactions of group 13 hydrides with nucleophilic carbenes.

The reactions of $\text{MH}_3(\text{NMe}_3)$ ($\text{M} = \text{Al}, \text{In}$) or LiMH_4 ($\text{M} = \text{Al}, \text{Ga}$) with 1 equiv of **4** ($\text{R} = ^i\text{Pr}$, $\text{R}' = \text{Me}$; also when $\text{M} = \text{Al}$, $\text{R} = \text{Mes}$, $\text{R}' = \text{H}$), resulted in the formation of the analogous carbene-metal trihydride complexes **34–37**, as summarized in Scheme 3 (30–33). Interestingly, attempts to form 2:1 stoichiometry complexes via the addition of 2 equiv of carbene failed, despite the fact that such 2:1 complexes could be formed when the appropriate carbenes were allowed to react with indium halides (*vide supra*). Presumably, this observation is a consequence of the inferior Lewis acidity of an InH_3 unit in comparison with those of the indium trihalides, InX_3 ($\text{X} = \text{Cl}, \text{Br}$). The crystal structures of **34–37** are all similar in that the group 13 metal adopts a distorted tetrahedral geometry and the $\text{M}-\text{C}(\text{carbene})$ bond distances are longer than those of typical $\text{M}-\text{C}$ single bonds. The metrical parameters for the coordinated carbenes resemble those for **24** and **32**. The thermal stabilities of **34–37** decrease in the order **34** > **35** > **36** > **37** such that the indane complex, **37**, is unstable in solution above -20°C and decomposes in the solid state above -5°C , depositing indium metal and generating a gas (31, 32). Furthermore, the alane and gallane complexes, **34–36**, possess significantly greater stabilities than those normally observed for Lewis base adducts of the group 13 trihydrides, which generally decompose cleanly to the metal, hydrogen, and ligand (30–32). Again, these observations constitute evidence for the high nucleophilicities and enhanced Lewis basicities of the *N*-heterocyclic carbenes.

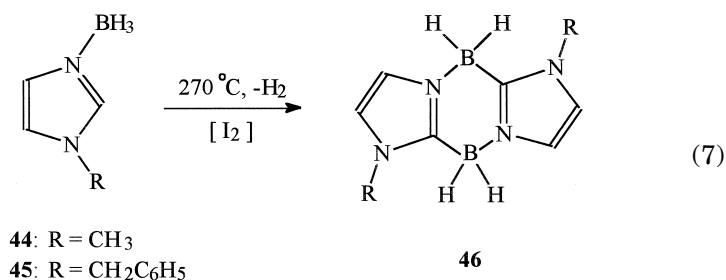
C. GROUP 13 TRIALKYLS AND TRIARYLS

A novel route for the generation of trialkylboron-carbene complexes has been reported (34). As summarized in Scheme 4, the initial step of the reaction sequence involves the N-complexation of 1,4,5-trimethylimidazole **38** with BEt_3 to form **39**, followed by deprotonation and rearrangement of resulting ionic species to **40**. The final step involves methylation with MeI to form the desired triethylboron-carbene complex, **41**. Compound **41** was characterized by mass spectroscopy and ^1H -, ^{13}C -, and ^{11}B NMR spectroscopy; the ^{11}B NMR chemical shift for **41** ($\delta -12.6$) appears in the tetracoordinate boron region. The 1,4,5-trimethylimidazole **38** is also the source of an unusual boryl-borane compound, **43** (34). Treatment with $\text{BH}_3 \cdot \text{thf}$, followed by deprotonation with $^n\text{BuLi}$, resulted in the formation of the ionic carbene/borane complex, **42**. In turn, **43** was produced via the addition of chlorobis(dimethylamino)borane to **42**. Compound **43** exhibits ^{11}B NMR chemical shifts at $\delta -21.8$ (BH_3) and $\delta 27.8$ (BNMe_2). In related work, *N*-methyl-*N*-borane complexes **44** and **45** have been de-

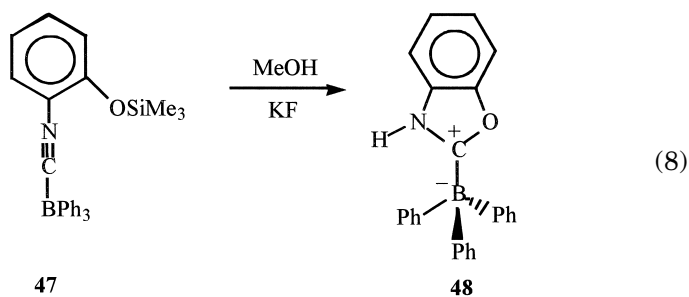


SCHEME 4. Preparation of amido- and organoboron carbene complexes.

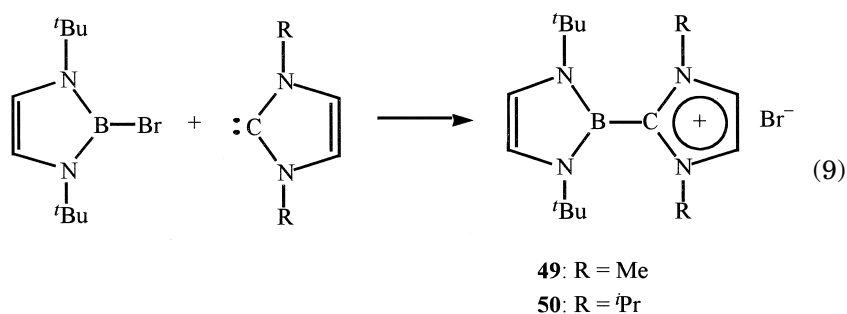
hydrogenated to tetrahydroimidazaboles **46**, which, in turn, can be regarded as dimers of carbene–borane complexes (35). Further derivatives of **46** can be prepared by exchanging B–H for B–F, B–Cl, or B–Et functionalities.



Triorganoboron complexes of *N,O*-heterocyclic carbenes are also known (36). Thus, triphenylboron–carbene complex **48** can be isolated from the reaction of methanol with an isocyanide adduct of BPh₃ (**47**) in the presence of a catalytic amount of KF. The X-ray crystal structure of **48** demonstrated that the boron atom is tetrahedrally coordinated and that all four B–C bond distances are equal within experimental error.



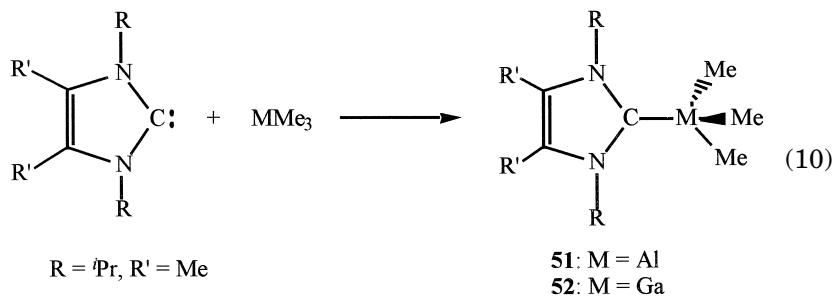
The reactivity of nucleophilic carbenes toward 2-bromo-2,3-dihydro-1*H*-1,3,2-diazaborole has also been described (37). The reaction of benzene solutions of ${}^t\text{BuNCH}=\text{CH}({}^t\text{Bu})\text{BBr}$ with carbenes **4** ($\text{R} = \text{Me}$, ${}^i\text{Pr}$; $\text{R}' = \text{H}$) resulted in high yields of ionic products **49** ($\text{R} = \text{Me}$) and



50 ($\text{R} = {}^i\text{Pr}$) via a bromide displacement process. Halide displacements have been observed previously in the reactions of carbenes with Me_3SiI (38). However, this represents the first such reaction with a haloborane. The X-ray crystal structure of **49** was determined and showed that both heterocyclic rings are planar and that the interplanar angle is 92.9° . The $\text{B}-\text{C}(\text{carbene})$ bond distance of $1.580(11) \text{ \AA}$ is comparable to that found in **32** ($1.603(3) \text{ \AA}$).

At the present time, triorgano-group 13 carbene complexes involving the heavier group 13 elements are limited to carbene complexes of AlMe_3 and GaMe_3 (39). Thus, the reaction of Me_3M with **4** ($\text{R} = {}^i\text{Pr}$, $\text{R}' = \text{Me}$) resulted in the isolation of the stable 1:1 complexes **51** ($\text{M} = \text{Al}$) and **52** ($\text{M} = \text{Ga}$). The group 13 metal centers in both **51** and **52** are tetrahedrally coordinated and the $\text{M}-\text{C}(\text{carbene})$ bond distances are relatively long (**51**: $\text{Al}-\text{C}(\text{carbene})$ $2.124(6) \text{ \AA}$, $\text{Al}-$

C(methyl) 1.940(5) Å, and 2.062(7) Å; **52**: Ga–C(carbene) 2.13(2) Å, Ga–C(methyl) 1.95(1) Å and 2.08(2) Å). The Al–C(carbene) bond distance in **51** is considerably longer than that observed in the related alane complex **35** (2.034(3) Å). This lengthening is probably a consequence of the greater steric hindrance of Me₃Al vs AlH₃ (32) and, as can be anticipated on a similar basis, the Ga–C(carbene) bond distance in **52** is much longer than that observed in the gallane complex **36** (2.071(15) Å) (32).

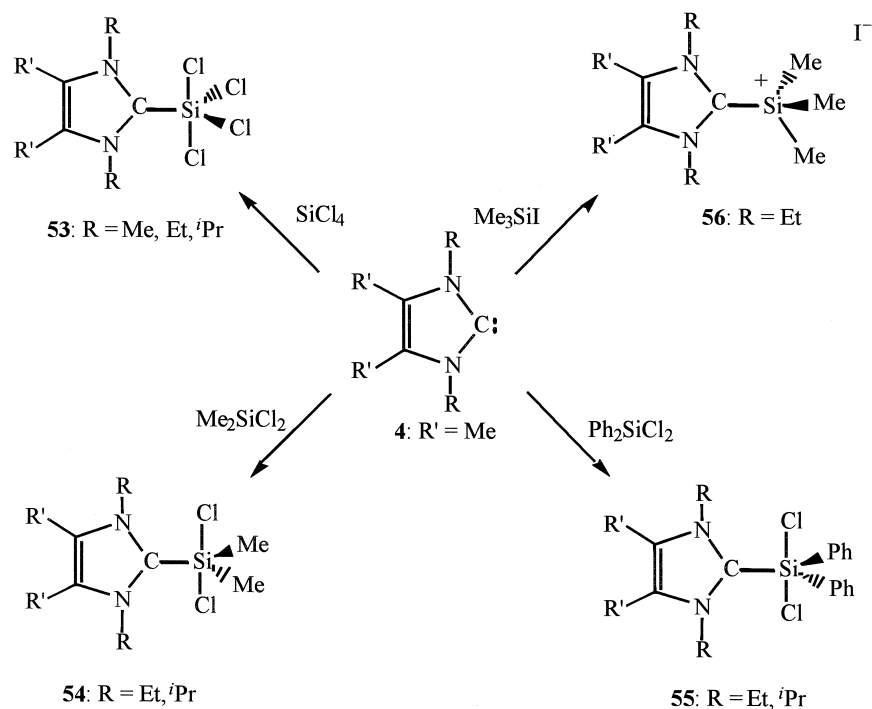


IV. Silicon, Germanium, Tin, and Lead Complexes

There is a growing interest in the organic chemistry of stable nucleophilic carbenes. However, this aspect is not covered in the present review. Attention in group 14 is therefore focused on the heavier congeners silicon, germanium, tin, and lead. Generally speaking, two pathways have been observed for the reaction of stable nucleophilic carbenes with Lewis acidic group 14 species, namely the production of simple 1:1 complexes or halide ion displacement and consequent carbene-stabilized cation formation.

A. SILICON HALIDES AND ORGANOSILICON COMPOUNDS

The reaction between carbenes **4** (R = Me, Et, ⁱPr; R' = Me) and tetrachlorosilane resulted in the 1:1 complexes, **53**, as shown in Scheme 5 (38). Characterization of the somewhat labile R = ⁱPr complex by X-ray crystallography revealed an essentially trigonal bipyramidal geometry around the pentacoordinate silicon center. The carbene ligand adopts an equatorial position and the Si–C(carbene) bond distance is 1.9711(7) Å; the bond lengths and angles within the carbene heterocycle suggest a modicum of delocalization within the ring (N–C–N angle = 107.1(6)°).

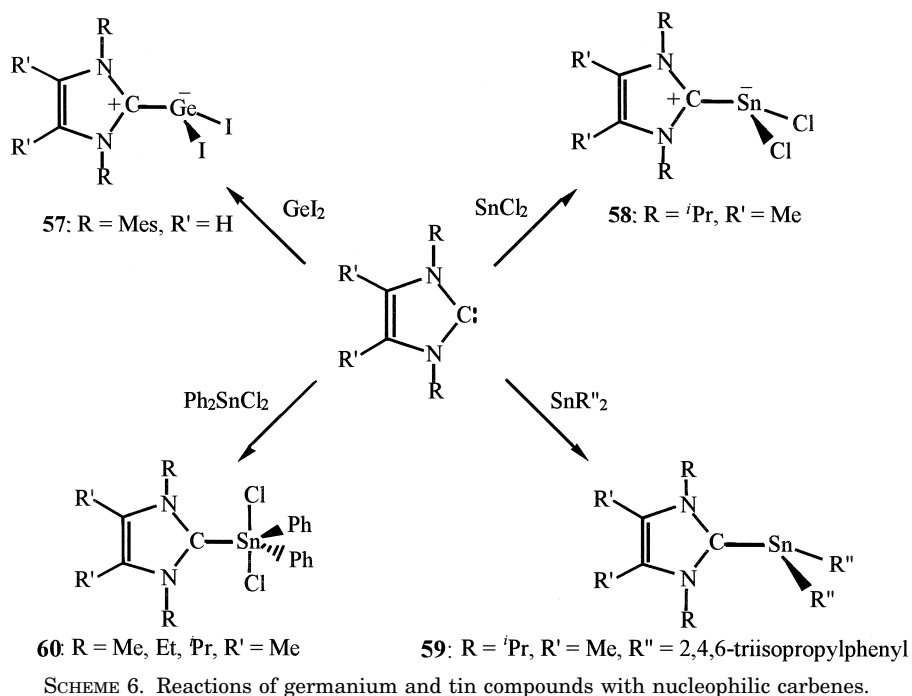


SCHEME 5. Reactions of silicon tetrachloride and organosilicon compounds with stable nucleophilic carbenes.

Pentacoordinate silicon complexes can also be prepared via the reaction of diaryldichlorosilanes with carbenes **4** ($R = \text{Et, } i\text{Pr}$; $R' = \text{Me}$). Interestingly, a 2-(trimethylsilyl)imidazolium salt (**56**) was formed when Me_3SiI was treated with **4** (39). Unfortunately, no information regarding the crystal structures of these species is available.

B. GERMANIUM AND TIN HALIDES AND ORGANOTIN HALIDES

As shown in Scheme 6, it is also possible to prepare carbene complexes of germanium and tin (**40, 41**). The reaction of 1,3-dimesitylimidazol-2-ylidene with GeI_2 was used as a model for the dimerization of singlet carbenes along a non-least-motion pathway (**40**). The ^{13}C NMR chemical shift of the carbene-germene complex **57** shows an upfield shift at δ 60.88, indicating the formation of a polarized C–Ge bond rather than a classical double bond. This view was confirmed by X-ray diffraction experiments



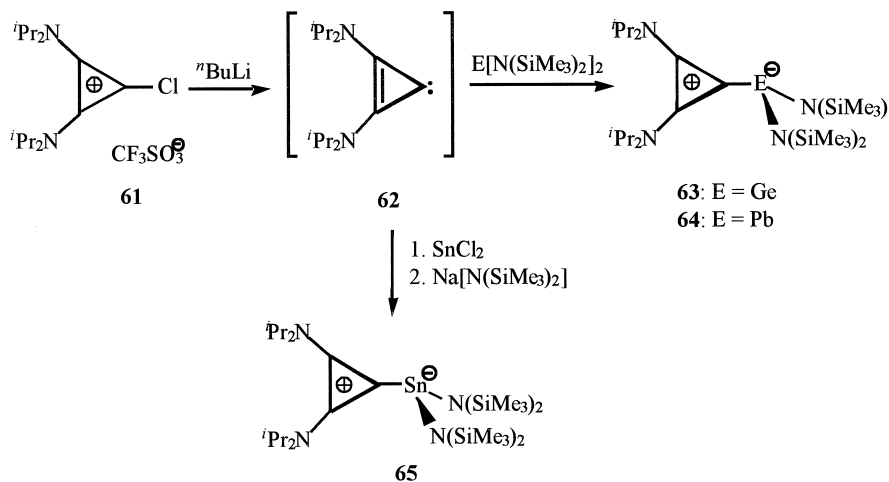
which showed that the germanium center in **57** adopts a pyramidal geometry and that the Ge–C bond distance is relatively long (2.102(12) Å). Interestingly, the two halves of the complex are twisted with respect to one another, which is probably a result of steric interactions between the iodide and mesityl substituents. Stable carbene complexes of tin(II) are also accessible from the reactions of SnCl₂ or SnR''₂ (R'' = 2,4,6-triisopropylphenyl) with 1,3-diisopropyl-4,5-dimethylimidazol-2-ylidene (**38**, **41**). The structure of the SnCl₂ complex **58** is similar to that of **57** in that the group 14 center adopts a pyramidal coordination geometry; the Sn–C(carbene) bond distance is 2.290(5) Å. As expected, the Sn–C(carbene) bond distance in the SnR''₂ complex **59** (2.379(5) Å) is longer than that observed in **58** and even exceeds the Sn–C(aryl) bond distances (2.321(2) Å and 2.308(2) Å). The long Sn–C(carbene) bond distances in **58** and **59** suggest that the complexes are best described as Lewis acid–Lewis base adducts.

Pentacoordinate tin complexes can also be isolated from the reaction of diphenyldichlorostannane with **4** (R = *i*Pr, R' = Me) (**38**). The structure of the Ph₂SnCl₂ complex **60** was shown to be very similar to that of **54** by X-ray crystallography. Thus, the geometry around

the pentacoordinate tin center is distorted trigonal bipyramidal and the three organic substituents occupy equatorial sites. The Sn–C(carbene) bond distance of 2.179(3) Å in **60** is longer than the Sn–C(phenyl) bond distances of 2.122(5) Å and 2.139(3) Å, but shorter than the Sn–C(carbene) bond distances observed in the Sn(II) complexes **58** and **59**.

C. CYCLOPROPENYLIDENE COMPLEXES OF DIVALENT GERMANIUM, TIN, AND LEAD AMIDES

Cyclopropenylidene complexes of divalent germanium, tin, and lead amides have also been reported recently (42). Bis(diisopropylamino)-cyclopropenylidene **62** can be obtained from the cyclopropenylum salt **61** by treatment with ⁿBuLi as indicated in Scheme 7. At low temperature **62** forms a stable lithium adduct that is a useful synthon. The germanium and tin cyclopropenylidene complexes **63** and **64** were formed by direct interaction of the carbene with the bis(trimethylsilylamides) E[N(SiMe₃)₂]₂ (E = Ge, Pb). However, the analogous tin compound (**65**) is only accessible via the reaction of **62** with SnCl₂ followed by amidation of the intermediate carbene complex. Compounds **63–65** are thermally stable yellow solids that are soluble in aprotic solvents. All three complexes have been characterized by means of X-ray crystallography. In each instance, the group 14 element possesses a pyramidal geometry. The E–C(carbene) distances in **63** (2.085(3) Å), **64**



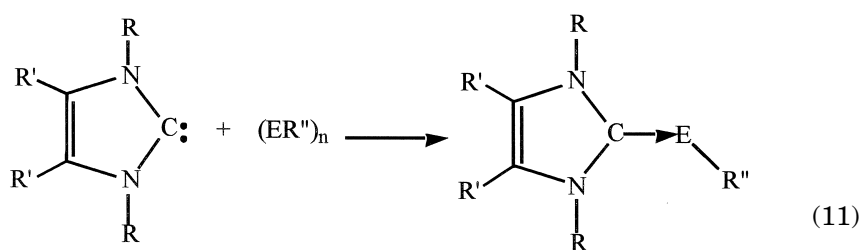
SCHEME 7. Cyclopropenylidene complexes of divalent germanium, tin, and lead.

(2.303(9) Å), and **65** (2.423(8) Å) are somewhat long and commensurate with single bond descriptions. As in the case **57–59**, the metrical parameters are indicative of ylidic resonance structures (40, 41).

V. Group 15 Complexes

A. PHOSPHINIDENES AND ARSENIDENES

More than 35 years ago, it was reported that the reaction of trimethylphosphine with the cyclotetraphosphine $(\text{CF}_3\text{P})_4$ affords the phosphine–phosphinidene complex, $\text{Me}_3\text{P} \rightarrow \text{PCF}_3$ (43). More recently, it has been demonstrated that stable carbenes are sufficiently nucleophilic to effect the depolymerization of cyclopolyphosphines and cyclopolyarsines to produce carbene–pnictinidene complexes **66–70**, the first examples of *p*-block pnictinidenes (44, 45). Two extreme canonical forms, **71** and **72**, can be written for such species. Structure **71**



66: R = R' = Me; E = P; R'' = Ph; n = 5

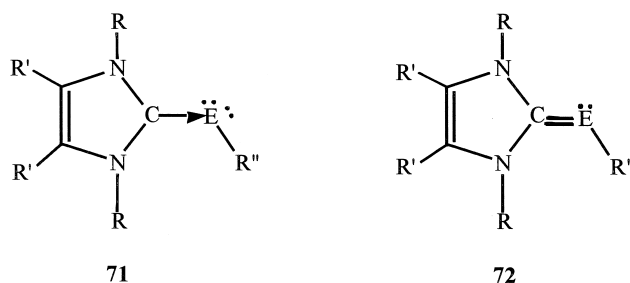
67: R = Mes; R' = H; E = P; R'' = Ph; n = 5

68: R = Mes; R' = H; E = P; R'' = C₆F₅; n = 4

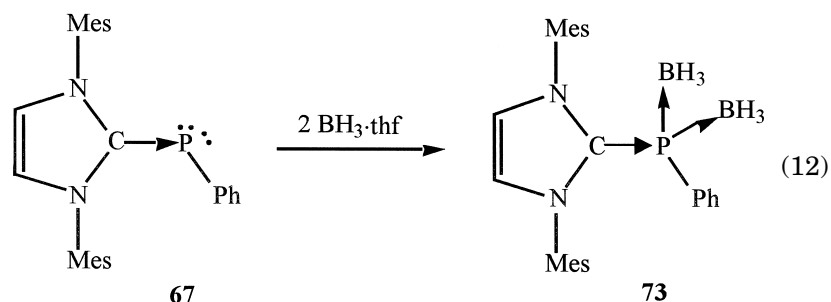
69: R = Mes; R' = H; E = P; R'' = CF₃; n = 4

70: R = Mes; R' = H; E = As; R'' = Ph; n = 6

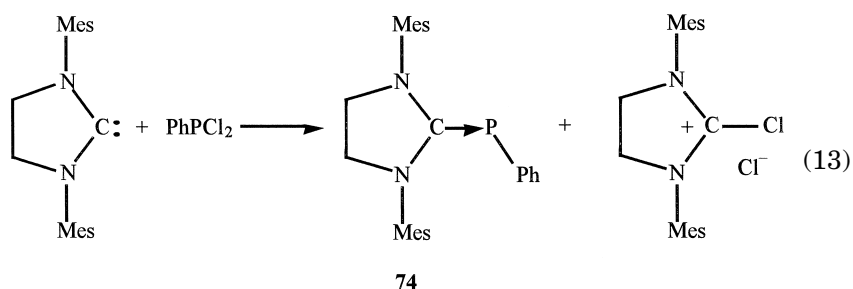
represents a phosphinidene adduct of a carbene and so involves a C–P dative bond order of 1, whereas **72** corresponds to a conventional phosphalkene and features a C=P double bond. X-ray crystallographic studies on **66–70** (44, 45) revealed that the E–C(carbene) bond is only ~4% longer than typical single bonds and that the E–C(R'') moiety is twisted out of the carbene plane by 26–46°. These data, taken in concert with the high-field ³¹P chemical shifts of **66**, **67**, and **69**, suggest the predominance of structure **71**. Further support



for structure **71** came from the reaction of **67** with $\text{BH}_3 \cdot \text{thf}$, which resulted in the exclusive formation of the bis(borane) adduct **73**, thus demonstrating the availability of two lone pairs on the phosphorus center (46).

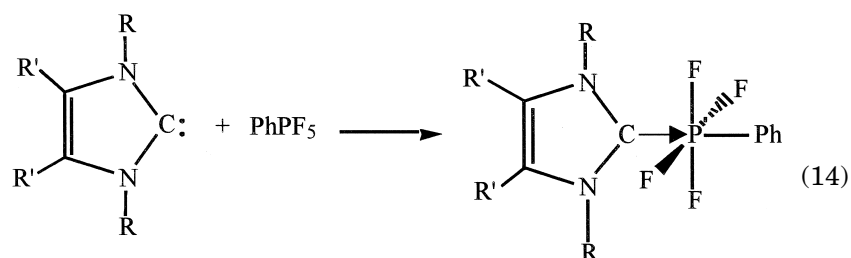


The cyclopolyphosphines that were used to prepare the carbene–phosphinidene complexes described earlier were formed by the reduction of higher oxidation state phosphorus compounds, typically dichlorophosphines, RPCl_2 (47–49). However, in some cases a separate reduction step is not necessary and it is possible to prepare the carbene–phosphinidene complex (**74**) directly by reaction of a stable nucleophilic carbene with RPCl_2 (44).



B. PHOSPHORANES

The isolation of the first carbene complex of a phosphorane has been reported recently (50). Perphosphorane (75) was formed in

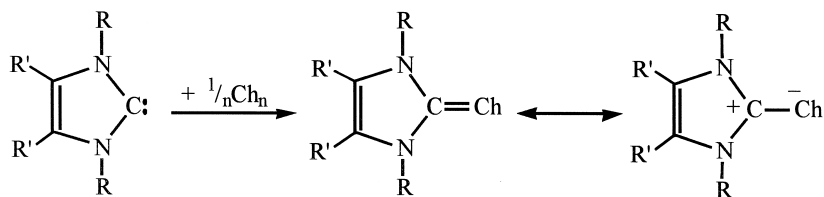


75: R = Mes, R' = H

quantitative yield by the direct reaction of **4** (R = Mes, R' = H) with phenyltetrafluorophosphorane. The X-ray crystal structure of **75** confirmed the presence of an octahedral geometry at the phosphorus center. As expected, the P–C(carbene) bond distance of 1.91 Å is somewhat longer than the P–C(phenyl) bond distance (1.84 Å). The ^{31}P resonances for **66**, **67**, and **68** appear at substantially higher fields than that for **75**, reflective of the difference between two- and six-coordinate phosphorus environments.

VI. Sulfur, Selenium, and Tellurium Complexes

N-Heterocyclic carbene complexes of sulfur or, more simply, imidazole-2-thiones, have been known for many years (51, 52) and have



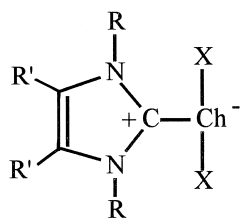
76: Ch = S, R = Me, R' = H

77: Ch = Se, R = Me, Et, i Pr, R' = Me; R = Me, R' = H

78: Ch = Te, R = Me, Et, i Pr, R' = Me

found industrial application as catalysts (53). Compounds such as **76** can be prepared by the reaction of imidazol-2-ylidenes with cyclooctasulfur (52); however, other synthetic routes are also available (51). The crystal structure of **76** was reported some time ago and revealed that the carbon–sulfur bond distance of 1.695 Å is shorter than that of a C–S single bond value (~1.81 Å) but longer than the typical carbon–sulfur double bond distance of 1.61 Å (51). Similarly, it has been demonstrated that imidazol-2-ylidenes will also react with selenium or tellurium to produce the selenones **77** and tellurones **78** (54, 55). It is of interest to note that in general tellurocarbonyl compounds, such as telluroaldehydes, can only be isolated by stabilization with metals (56), whereas **78** is relatively stable (57). The crystal structures of **77** and **78**, in concert with ^{125}Te and ^{77}Se NMR data, respectively, support an ylidic structure in both cases, rather than a formal double bond. Thus, the Ch–C(carbene) bond distances are long (**77** (R = ^iPr , R' = Me): Se–C(carbene) 1.853(4) Å, (R = Me, R' = H): Se–C(carbene) 1.884(9) Å; **78** (R = ^iPr): Te–C(carbene) 2.087(4) Å), and the signals in the ^{125}Te and ^{77}Se NMR resonances of the telluro- and selenoimidazolines, respectively, appear upfield when compared to those of other chalcocarbonyl compounds. This shielding has been attributed to the presence of π delocalization of the N–C–N moiety within the heterocyclic rings (N–C–N 106.4° for **77** (R = ^iPr , R' = Me); 106.8° for **77** (R = Me, R' = H); 106.7° for **78**).

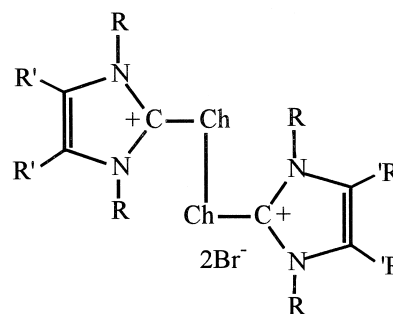
The 1:1 reaction of **76** or **77** (R = Me, R' = H) with bromine resulted in oxidation and the formation of a carbene complex of SBr_2 (**79**) or SeBr_2 (**80**), respectively (55, 58–62). The X-ray crystal structure of **79** has been reported and showed that this sulfurane possesses an almost collinear axial three-center geometry with elongated S–Br



79: Ch = S, X = Br, R = Me, R' = H

80: Ch = Se, X = Br, R = Me, R' = H

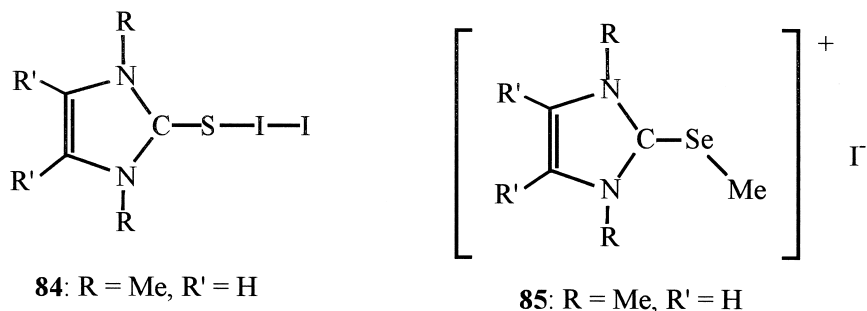
81: Ch = Se, X = I, R = ^iPr , R' = Me



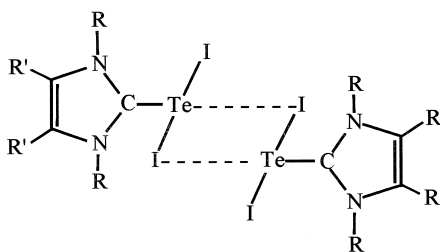
82: Ch = S, X = Br, R = Me, R' = H

83: Ch = Se, X = Br, R = Me, R' = H

bond distances of 2.520 Å and 2.477 Å (*cf.* 2.3 Å in S₂Br₂). When only half an equivalent of bromine was added to **77** or **78** (R = Me, R' = H), the disulfide (**82**) or diselenide (**83**) was isolated. Oxidation of **76** with iodine resulted in the formation of a charge-transfer complex **84**



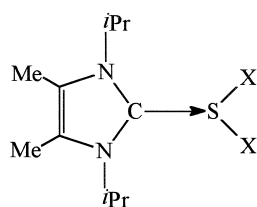
(63). In contrast, the reaction of seleno- and telluroimidazolines with iodine afforded structures in which covalent bonds are formed, i.e., complexes of SeI₂ (**81**) and TeI₂ (**86**), respectively (64–67). The X-ray crystal structure of **81** confirmed a monomeric structure in which the selenium adopts an equatorially vacant trigonal bipyramidal geometry (64). The iodide ligands occupy the axial positions and the Se–I bonds are elongated (av. Se–I 2.811(1) Å; I–Se–I 175.4°). The Se–C(carbene) bond distance for **81** (1.900(4) Å) is longer than that found for **77** (1.853(4) Å). The crystal structure of **81** showed the presence of weak iodine–iodine interactions (I...I 3.719(1) Å). Refluxing **77** (R = Me, R' = H) with iodomethane yielded the methylated cation **85**. By means of X-ray diffraction, it was shown that a dimeric structure is adopted in the case of the tellurium derivative **86** (64). The coordination geometry of each tellurium in the dimer is square planar and the Te₂I₂ unit is rhombohedral. Each tellurium atom has two



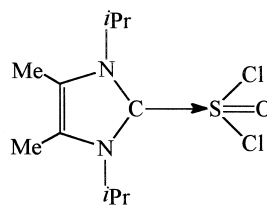
86: R = Et, R' = Me

short Te–I bonds (2.989(1) Å and 2.897(1) Å) and one long Te–I bond (3.564(1) Å). As expected, the Te–C(carbene) distance of 2.120(3) Å is longer than that observed in **78** (2.087(4) Å).

Treatment of 1,3-diisopropyl-4,5-dimethylimidazol-2-ylidene with SCl_2 and SOCl_2 resulted in **87** and **88**, respectively (67). Complex **87** can be converted into the corresponding fluoride (**89**) via reaction with AgF . Surprisingly, however, reduction of the sulfur center was ob-

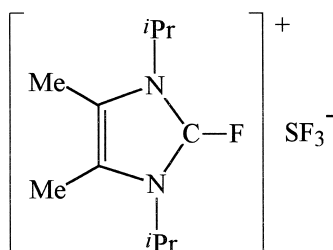


87: X = Cl
88: X = F

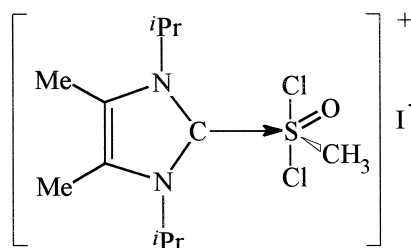


89

served when the carbene was treated with SF_4 (**90**). Alkylation of **87** with CH_3I afforded **91**.



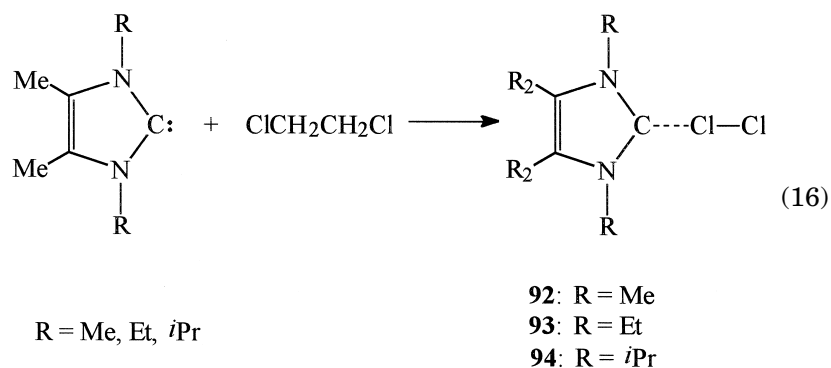
90



91

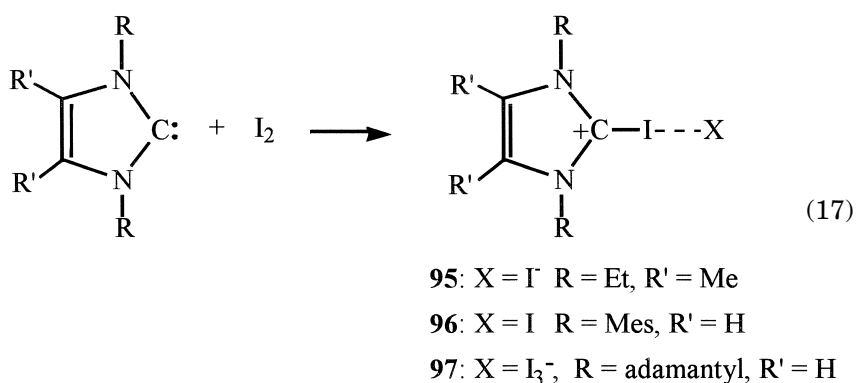
VII. Halogen Complexes

Air-sensitive carbene adducts of chlorine (**92–94**) have been isolated from the reaction of carbenes with 1,2-dichloroethane as shown below (68). The Cl–Cl bonds of these adducts are reactive. Thus, benzene is chlorinated by **92** and **93** to give chlorobenzene under mild

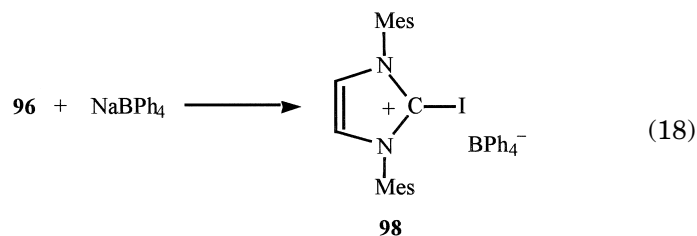


conditions and **94** reacts with AlCl_3 and SO_2 to afford chloroimidazolium salts.

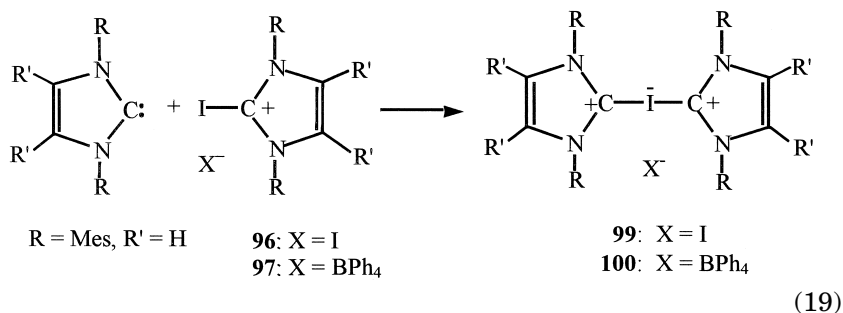
Various stable nucleophilic carbenes react with I_2 to yield 2-iodoimidazolium salts **95**–**97** (68, 69). Compounds **95** and **96** exhibit weak interactions in the solid state between the iodine in the 2-position of the imidazole ring and the iodide counterions (**95**, $\text{I} \cdots \text{I}$ 3.348 Å; **96**, $\text{I} \cdots \text{I}$ 3.249 Å). The nearly linear (176.0°) arrangement of the $\text{C}-\text{I} \cdots \text{I}$ unit suggests a hypervalent central iodine atom, and hence the $\text{C}-\text{I}$ bond distances of **95** (2.104 Å) and **96** (2.113 Å) are elongated when compared to those of iodoarenes (70). The geometries of the heterocyclic rings in both **95** and **96**, with $\text{N}-\text{C}-\text{N}$ angles of 109.3° and 107.0° , respectively, are typical of those of imidazolium cations. Imidazolium salt **97** shows a similar arrangement with weak solid-state interactions between the iodine bound to the carbene and the triiodide counterion ($\text{I} \cdots \text{I}$ 3.310 Å, $\text{C}-\text{I}$ 2.131 Å, $\text{C}-\text{I} \cdots \text{I}$ 173.1° , $\text{N}-\text{C}-\text{N}$ 109.5°). Exchange of the iodide anion in **96** by tetraphenylborate afforded **98**,



and in turn this permitted an interesting comparison of the structures of **95–97** since there is no opportunity for the $[\text{BPh}_4]^-$ anion to interact covalently with the 2-iodoimidazolium cation (**65**). As expected, the C–I bond distance in **98** (2.042 Å) is shorter than those in **95–97** and the N–C–N internal ring angle is more acute (107.7°). Interestingly, in the X-ray crystal structure of **98**, the C–I bond of the cation resides along a twofold crystallographic axis and the boron atom lies

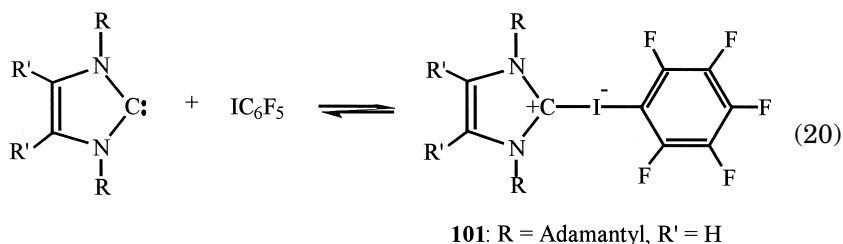


along the same axis at a distance of 4.42 Å from the iodine. Imidazolium salts **96** and **97** can react further with carbene to form the cationic bis(carbene) complexes of hypervalent iodine **99** and **100** (**69**). The ^1H and ^{13}C NMR spectra of **99** and **100** are essentially identical, suggesting that the anions do not play an important role in the bonding of the hypervalent iodine cation. The X-ray crystal structure of **100** was determined and revealed an almost linear central C–I–C unit (177.5°) with slightly longer C–I bond distances than those observed in **95–98** (**100**, C–I 2.286 Å and 2.363 Å). The structure of **100** suggests that the C–I⋯I interactions in **95** and **96** are considerably weaker than the C–I–C interaction in this case. Complexes of nucleo-



philic carbenes with iodopentafluorobenzene (**101**) have been prepared via the reaction of **4** (R = adamantyl, R' = H) with IC_6F_5 (**71**). On the basis of NMR data it was apparent that in solution **101** is in

equilibrium with free carbene and iodopentafluorobenzene, thus implying that the C–I bonds undergo facile cleavage in solution. In the crystalline state a linear C–I–C arrangement was observed ($178.9(2)^\circ$) consistent with the presence of hypervalent bonding at the iodine center. There is, however, considerable asymmetry in the two C–I bond distances (C(carbene)–I, 2.754 Å; C(arene)–I, 2.159 Å), which is probably a result of the different substituents on the carbon centers. However, it should be noted that the long C–I bond distance to the imidazole fragment is not caused by steric interactions, as can be seen by comparison with the structure of **97** (C–I 2.131 Å). The metrical parameters for the imidazole ring of **101** show some changes as a result of incorporation of the IC_6F_5 unit. In particular, the N–C–N bond angle is 2° larger than that of the free carbene and all the bonds within the ring are lengthened to some extent. This suggests that there is increased π -delocalization present as compared to free carbene. The π delocalization within the imidazole ring indicates a formal charge assignment which is the reverse of that in halonium methylides ($\text{RX}^+ - ^-\text{CR}_2$). Typically, such methylides result from reactions of electrophilic carbenes with halogen centers.



VIII. Conclusions

Stable nucleophilic carbenes are capable of forming isolable complexes with a variety of main group species in oxidation states ranging from +1 to +6. The majority of the complexes that have been reported thus far possess 1:1 stoichiometry; however, there are several instances of 2:1 complexation and one example of a 3:1 complex. Although, in principle, it is possible to write double-bonded (carbene) $\text{C}=\text{EX}_n$ canonical forms to describe the interactions between carbenes and main group entities (EX_n), in the stable nucleophilic carbene complexes considered here the bonding is predominantly of the

donor-acceptor type, *viz.* (carbene) $C \rightarrow EX_n$. As such, the chemistry of these two-electron donor carbenes bears a strong-resemblance to that of electron-rich phosphines.

Looking toward the future, significant challenges exist in terms of broadening the scope of carbene/main group complexes by employing multidentate, acyclic, and chiral carbene ligands. Further diversification can also be realized by further development of the chemistry of the heavier congeneric silylenes and germylenes. Finally, as is evident from the present review, most of the emphasis to date has been placed on synthetic and structural studies. Accordingly, exciting opportunities exist for the exploration and exploitation of the reactivity patterns of carbene/main group complexes.

Note Added in Proof:

Monomeric carbene complexes with 1:1 stoichiometry have now been isolated from the reaction of **4** ($R = 'Bu$, adamantyl or 2,4,6-trimethylphenyl; $R' = H$) with lithium 1,2,4-tris(trimethylsilyl)cyclopentadienide (**72**). The crystal structure of one such complex ($R = 'Bu$) revealed that there is a single σ -interaction between the lithium and the carbene center ($Li-C(\text{carbene})$ 1.90 Å) with the cyclopentadienyl ring coordinated in an η^5 -fashion to the lithium center. A novel hypervalent antimonide complex has also been reported (**73**). Thus, the nucleophilic addition of **4** ($R = Mes$; $R' = Cl$) to $Sb(CF_3)_3$ resulted in the isolation of the 1:1 complex with a pseudo-trigonal bipyramidal geometry at the antimony center.

ACKNOWLEDGMENTS

We are grateful to the National Science Foundation (CHE-9629088), the Science and Technology Center Program of the National Science Foundation (CHE-8920120), and the Robert A. Welch Foundation for generous financial support. CJC thanks the Royal Society for a Dorothy Hodgkin Fellowship.

REFERENCES

1. For a review, see Wanzlick, H.-W. *Angew. Chem., Int. Ed. Engl.* **1962**, *1*, 75.
2. Wanzlick, H.-W.; Schönherr, H.-J. *Leibigs Ann. Chem.* **1970**, 731, 176.
3. Wanzlick, H.; Schönherr, H. *Angew. Chem., Int. Ed. Engl.* **1968**, *7*, 141. See also, *Chem. Ber.* **1970**, *103*, 1037.

4. Arduengo, A. J., III; Harlow, R. L.; Kline, M. *J. Am. Chem. Soc.* **1991**, *113*, 361; Arduengo, A. J., III. *Acc. Chem. Res.* **1999**, *32*, 913.
5. Kuhn, N.; Kratz, T. *Synthesis* **1993**, 561.
6. Herrmann, W. A.; Elison, M.; Fischer, J.; Köcher, C.; Artus, G. R. *J. Chem. Eur. J.* **1996**, *2*.
7. For reviews, see (a) Herrmann, W. A.; Köcher, C. *Angew. Chem., Int. Ed. Engl.* **1997**, *36*, 2162; (b) Regitz, M. *Angew. Chem., Int. Ed. Engl.* **1996**, *35*, 725; (c) Arduengo, A. J., III; Krafczyk, R. *Chem. Z.* **1998**, *32*, 6.
8. Arduengo, A. J., III; Goerlich, J. R.; Marshall, W. J. *J. Am. Chem. Soc.* **1995**, *117*, 11027.
9. Alder, R. A.; Blake, M. E.; Bortolotti, C.; Bufali, S.; Butts, C. P.; Linehan, E.; Oliva, J. M.; Orpen, A. G.; Quayle, M. J. *Chem. Commun.* **1999**, 241.
10. Alder, R. A.; Allen, P. R.; Murray, M.; Orpen, A. G. *Angew. Chem., Int. Ed. Engl.* **1996**, *35*, 1121.
11. Dias, H. V. R.; Jin, W. *Tetrahedron Lett.* **1994**, *35*, 1365.
12. See, for example, (a) Enders, D.; Breurer, K.; Raabe, G.; Runsink, J.; Teles, J. H.; Melder, J.-P.; Ebel, K.; Brode, S. *Angew. Chem., Int. Ed. Engl.* **1995**, *34*, 1021; (b) Arduengo, A. J., III; Goerlich, J. R.; Marshall, W. J. *Leibigs Annl Recl.* **1997**, 365; (c) Alder, R. A.; Butts, C. P.; Orpen, A. G. *J. Am. Chem. Soc.* **1998**, *120*, 11526.
13. Arduengo, A. J., III; Gamper, S. E.; Tamm, M.; Calabrese, J. C.; Davidson, F.; Craig, H. A. *J. Am. Chem. Soc.* **1995**, *117*, 572.
14. Arduengo, A. J., III; Dias, H. V. R.; Calabrese, J. C.; Davidson, F. *Organometallics* **1993**, *12*, 3405.
15. Herrmann, W. A.; Runte, O.; Artus, G. R. *J. Organomet. Chem.* **1995**, *501*, C1.
16. Arduengo, A. J., III; Dias, H. V. R.; Davidson, F.; Harlow, R. L. *J. Organomet. Chem.* **1993**, *462*, 13.
17. For the synthesis and structures of the mesityl and adamantyl-substituted carbenes, see Arduengo, A. J., III; Dias, H. V. R.; Harlow, R. L.; Kline, M. *J. Am. Chem. Soc.* **1992**, *114*, 5530 and ref. 4, respectively.
18. Arduengo, A. J., III; Davidson, F.; Krafczyk, R.; Marshall, W. J.; Tamm, M. *Organometallics* **1998**, *17*, 3375.
19. Runte, O. Dissertation, Technische Universität München, 1977. Cited in ref. 7a.
20. Arduengo, A. J., III; Harlow, R. L.; Marshall, W. J.; Prakasha, T. K. *Heteroatom Chem.* **1996**, *7*, 421.
21. Luger, V. P.; Ruban, G. *Acta Crystallogr.* **1971**, *B27*, 2276.
22. Kuhn, N.; Henkel, G.; Kratz, T.; Kreutzberg, J.; Boese, R.; Maulitz, A. H. *Chem. Ber.* **1993**, *126*, 2041.
23. Black, S. J.; Hibbs, D. E.; Hursthouse, M. B.; Jones, C.; Malik, K. M. A.; Smithies, N. A. *J. Chem. Soc., Dalton Trans.* **1997**, 4313.
24. Alcock, N. W.; Degnan, I. A.; Howarth, O. W.; Wallbridge, M. G. H. *J. Chem. Soc., Dalton Trans.* **1992**, 2775.
25. Cowley, A. H.; Gabbai, F. P.; Isom, H. S.; Decken, A.; Culp, R. D. *Main Group Chemistry* **1995**, *1*, 9.
26. Hibbs, D. E.; Hursthouse, M. B.; Jones, C.; Smithies, N. A. *Main Group Chemistry* **1998**, *2*, 293.
27. Gardiner, M. G.; Raston, C. L. *Coord. Chem. Rev.* **1997**, *166*, 1 and references therein.
28. Simmonds, M. G.; Gladfelter, W. L. In "The Chemistry of Metal CVD"; Kodas, T.; Hampden-Smith, M., Eds.; VCH: Weinheim, **1994**.

29. Raston, C. L.; Siu, A. F. H.; Tranter, C. J.; Young, D. J. *Tetrahedron Lett.* **1994**, 35, 5915.
30. Arduengo, A. J., III; Dias, H. V. R.; Calabrese, J. C.; Davidson, F. *J. Am. Chem. Soc.* **1992**, 114, 9724.
31. Hibbs, D. E.; Hursthouse, M. B.; Jones, C.; Smithies, N. A. *Chem. Commun.* **1998**, 869.
32. Francis, M. D.; Hibbs, D. E.; Hursthouse, M. B.; Jones, C.; Smithies, N. A. *J. Chem. Soc., Dalton Trans.* **1998**, 3249.
33. Hibbs, D. E.; Hursthouse, M. B.; Jones, C.; Smithies, N. A. *Main Group Chemistry* **1998**, 2, 293.
34. Wacker, A.; Pritzkow, H.; Siebert, W. *Eur. J. Inorg. Chem.* **1998**, 843.
35. Padilla-Martínez, I. I.; Martínez-Martínez, F. J.; López-Sandoval, A.; Giron-Castillo, K. I.; Brito, M. A.; Contreras, R. *Eur. J. Inorg. Chem.* **1998**, 1547.
36. Tamm, M.; Lugger, F. E.; Hahn, F. E. *Organometallics* **1996**, 15, 1251.
37. Weber, L.; Dobbert, E.; Stämmler, H. -G.; Neumann, B.; Boese, R.; Blaser, D. *Chem. Ber.* **1997**, 130, 705.
38. Kuhn, N.; Kratz, T.; Bläser, D.; Boese, R. *Chem. Ber.* **1995**, 128, 245.
39. Li, X. W.; Su, J. R.; Robinson, G. H. *Chem. Commun.* **1996**, 2683.
40. Arduengo, A. J.; Dias, H. V. R.; Calabrese, J. C.; Davidson, F. *Inorg. Chem.* **1993**, 32, 1541.
41. Schäfer, A.; Weidenbruch, M.; Saak, W.; Pohl, S. *J. Chem. Soc., Chem. Commun.* **1995**, 1157.
42. Schumann, H.; Glanz, M.; Girgsdies, F.; Ekkehardt Hahn, F.; Tamm, M.; Grzegorzewski, A. *Angew. Chem., Int. Ed. Engl.* **1997**, 36, 2232.
43. Burg, A. B.; Mahler, W. *J. Am. Chem. Soc.* **1961**, 83, 2388. See also Cowley, A. H.; Cushner, M. C. *Inorg. Chem.* **1980**, 19, 515.
44. Arduengo, A. J., III; Calabrese, J. C.; Cowley, A. H.; Dias, H. V. R.; Goerlich, J. R.; Marshall, W. J.; Riegel, B. *Inorg. Chem.* **1997**, 36, 2151.
45. Arduengo, A. J., III; Dias, H. V. R.; Calabrese, J. C. *Chem. Lett.* **1997**, 143.
46. Arduengo, A. J., III; Carmalt, C. J.; Clyburne, J. A. C.; Cowley, A. H.; Pyati, R. *Chem. Commun.* **1997**, 981.
47. Gamon, N.; Reichardt, C.; Allman, R.; Waskowska, A. *Chem. Ber.* **1981**, 114, 3289.
48. Mahler, W.; Burg, A. B. *J. Am. Chem. Soc.* **1958**, 80, 6161.
49. Weber, L.; Meine, G.; Boese, R.; Bunghardt, D. *Z. Anorg. Allg. Chem.* **1987**, 549, 73.
50. Arduengo, A. J., III; Krafczyk, R.; Marshall, W. J.; Schmutzler, R. *J. Am. Chem. Soc.* **1997**, 119, 3381.
51. Ansell, G. B.; Forkey, D. M.; Moore, D. W. *J. Chem. Soc., Chem. Commun.* **1970**, 56.
52. Benac, B. L.; Burgess, E. M.; Arduengo, A. J., III. *Org. Synth.* **1986**, 64, 92.
53. Arduengo, A. J., III. U.S. Patent 5,104,993, 1992; Arduengo, A. J., III. U.S. Patent 5,162,482, 1992; Arduengo, A. J., III; Barsotti, R. J.; Corcoran, P. H. U.S. Patent 5,091,498, 1992; Arduengo, A. J., III; Corcoran, P. H. U.S. Patent 5,084,552, 1992.
54. Kuhn, N.; Henkel, G.; Kratz, T. *Z. Naturforsch.* **1993**, 48b, 973.
55. Williams, D. J.; Fawcett-Brown, M. R.; Raye, R. R.; VanDerveer, D.; Jones, R. L. *Heteroatom Chem.* **1993**, 4, 409.
56. Note, however, that although the telluroketone $[\text{C}_6\text{H}_4(\text{CMe}_2)_2\text{CTe}]$ is dimeric in the solid state, the monomer has been characterized spectroscopically in solution: Minoura, M.; Kawashima, T.; Okazaki, R. *J. Am. Chem. Soc.* **1993**, 115, 7019; Minoura, M.; Kawashima, T.; Okazaki, R. *Tetrahedron Lett.* **1997**, 38, 2501. For a review of terminal chalcogenido complexes, see Kuchta, M. C.; Parkin, G. *Coord. Chem. Rev.* **1998**, 176, 323.

57. Kuhn, N.; Henkel, G.; Kratz, T. *Chem. Ber.* **1993**, *126*, 2047.
58. Arduengo, A. J., III; Burgess, E. M. *J. Am. Chem. Soc.* **1976**, *98*, 5020.
59. Arduengo, A. J., III; Burgess, E. M. *J. Am. Chem. Soc.* **1977**, *99*, 2376.
60. Janulis, E. P., Jr.; Arduengo, A. J., III. *J. Am. Chem. Soc.* **1983**, *105*, 3536.
61. Arduengo, A. J., III; Burgess, E. M. *J. Am. Chem. Soc.* **1976**, *98*, 5021.
62. Koide, A.; Saito, T.; Kawasaki, M.; Motoki, S. *Synthesis* **1981**, 486.
63. Freeman, F.; Ziller, J. W.; Po, H. M.; Keindl, M. C. *J. Am. Chem. Soc.* **1988**, *110*, 2586.
64. Kuhn, N.; Kratz, T.; Henkel, G. *Chem. Ber.* **1994**, *127*, 849.
65. Kuhn, N.; Kratz, T.; Henkel, G. *Z. Naturforsch.* **1996**, *51b*, 295.
66. Kuhn, N.; Bohnen, H.; Fahl, J.; Bläser, S.; Boese, R. *Chem. Ber.* **1996**, *129*, 1579.
67. Kuhn, N.; Fahl, J.; Fawzi, R.; Maichle-Mössmer, C.; Steimann, M. *Z. Naturforsch.* **1998**, *53b*, 720.
68. Arduengo, A. J., III; Tamm, M.; Calabrese, J. C. *J. Am. Chem. Soc.* **1994**, *116*, 3625.
69. Kuhn, N.; Kratz, T.; Henkel, G. *J. Chem. Soc., Chem. Commun.* **1993**, 1778.
70. Trotter, J. In "The Chemistry of the Carbon-Halogen Bond"; Patai, S., Ed.; Wiley: Chichester, 1973, part 1, p. 49.
71. Arduengo, A. J., III; Kline, M.; Calabrese, J. C.; Davidson, F. *J. Am. Chem. Soc.* **1991**, *113*, 9704.
72. Arduengo, A. J., III; Tamm, M.; Calabrese, J. C.; Davidson, F.; Marshall, W. J. *Chem. Lett.* **1999**, 1021.
73. Arduengo, A. J., III; Krafczyk, R.; Schmutzler, R.; Mahler, W.; Marshall, W. J. *Z. Anorg. Allg. Chem.* **1999**, *625*, 1813.

GROUP I COMPLEXES OF P- AND As-DONOR LIGANDS

KEITH IZOD

Department of Chemistry, University of Newcastle, Newcastle upon Tyne, United Kingdom,
NE1 7RU

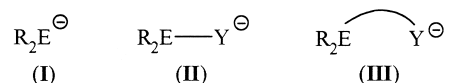
- I. Introduction
- II. Charge-Localized Ligands
 - A. Phosphides and Phosphinediides
 - B. Arsenides and Arsinediides
- III. Charge-Delocalized Ligands
 - A. Phosphinomethanides
 - B. Iminophosphides/Phosphinoamides
- IV. Tertiary Phosphine-Functionalized Ligands
- V. Miscellaneous Complexes
- VI. Conclusion
- References

I. Introduction

Complexes of the alkali metals with nitrogen donor ligands such as diorganoamides and organoimides have been studied extensively since the 1960s, and the principles that govern their chemistry are now quite well understood. This chemistry has been excellently reviewed in a number of texts (1–5). In contrast, much less attention has been paid to complexes of the alkali metals with ligands having donor atoms from the heavier elements of group 15 (P, As, Sb, Bi) (4). However, these compounds are becoming more widespread in their use, and synthetic, structural, and theoretical studies of such complexes have become increasingly common. Much of this chemistry has evolved over the past two decades, due largely to improvements in techniques for complex characterization such as X-ray crystallography and NMR spectroscopy, with some important advances only being reported in the past 3 or 4 years.

It is to be expected that interactions between alkali metal cations and P- and As-donor ligands will be weak and largely disfavored because of the mismatch between the hard alkali metal cations and soft P- and As-donors (6). Theoretical calculations certainly suggest a low affinity between the alkali metal and phosphorus-based ligands: The binding energies for the reaction $M^+ + PH_3 \rightarrow M^+PH_3$ are calculated to be -26.7 and -17.4 kcal mol $^{-1}$, for Li^+ and Na^+ respectively, compared to $Li-NH_3$ and Na^+-NH_3 binding energies of -40.2 and -28.0 kcal mol $^{-1}$ (7, 8). Overall, the relative binding strength of PH_3 is calculated to be some 68% that of NH_3 (averaged over the five cations Li^+ , Na^+ , K^+ , Mg^{2+} , Ca^{2+}).

In practice, the low affinity of the alkali metals for P- and As-donors is overcome by incorporating the P- or As-donor site into an anionic ligand. Such anionic P- and As-donor ligands fall into three broad classes: (a) ligands in which the negative charge is essentially localized on the group 15 atom E (organophosphides and arsenides) (**I**); (b) ligands in which there is a significant degree of charge delocalization toward phosphorus from an adjacent atom (e.g., phosphinomethanides and iminophosphides/phosphinoamides) (**II**); and (c) potentially chelating ligands in which the negative charge is localized on an atom distant from the phosphorus center (e.g., tertiary phosphine-functionalized alkoxides) (**III**).



The structures and aggregation states of alkali metal complexes of these ligands are highly dependent upon the nature of the metal center (charge/radius ratio, polarizability), the steric and electronic properties of the ligand substituents and the presence of coligands. The effects of these factors on complex structure parallel those observed in alkali metal organometallics (9–15), amides and imides (1, 2, 4), all of which have been well documented and will not be discussed in detail here. The formation of high-order aggregates (which are frequently insoluble in common organic solvents and thus difficult to characterize and crystallize) is often avoided by the use of coligands such as THF (tetrahydrofuran), tmeda (*N,N,N',N'*-tetramethylethylenediamine) or pmdeta (*N,N,N',N'',N''*-pentamethyldiethylenetriamine), which occupy vacant metal coordination sites, thereby preventing the formation of insoluble polymeric or lattice species. Oligomerization may similarly be hindered by the incorporation of sterically demanding substituents such as Me_3Si , Bu^t , or 2,4,6- Bu_3 -

C_6H_2 (supermesityl, mes*) into the ligand; such substituents sterically occlude vacant metal coordination sites and greatly increase the solubility of the complexes in common organic solvents. The subtle variations possible within P- and As-donor ligand complexes of the alkali metals lead to an almost bewildering array of structural types, many of which are not observed in other areas of alkali metal chemistry, and to wide variations in reactivity between complexes.

This review covers a range of phosphorus- and arsenic-containing ligands, with emphasis on those complexes in which there is an established contact between phosphorus or arsenic and an alkali metal. ^{31}P NMR spectroscopy is an invaluable tool for identifying and studying M–P interactions ($I = \frac{1}{2}$, 100%), particularly in solution, and for complexes with a Li–P contact ^{31}P and $^6\text{Li}/^7\text{Li}$ NMR studies can provide a wealth of structural and thermodynamic information (^7Li $I = \frac{3}{2}$, 92.58%; ^6Li $I = 1$, 7.42%). However, X-ray crystallography is unrivaled as a technique for elucidating the nature of species in the solid state. For this reason the present survey will focus largely on complexes in which a P–M or As–M contact has been verified by crystallography.

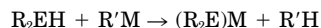
II. Charge-Localized Ligands

A. PHOSPHIDES AND PHOSPHINEDIIDES

Perhaps the simplest complexes of the alkali metals with P- or As-donor ligands are those in which there is a negative charge localized on the pnictogen atom, i.e., organophosphide and -arsenide ligands (R_2E^-). Although such complexes have been known since the early part of this century and have been used extensively for the synthesis of a wide range of transition and main group metal complexes, interest in the solution or solid state structures of these species was not expressed until the early 1980s.

1. Synthesis

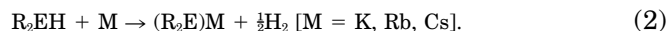
The synthesis of alkali metal organophosphides and arsenides is usually most conveniently achieved by the direct metalation of a primary or secondary phosphine/arsine with a strong deprotonating agent such as an alkyllithium or an alkali metal hydride:



$$[\text{E} = \text{P, As}; \text{R}' = \text{H, Me, Bu}^n, \text{etc.}; \text{M} = \text{Li, Na, K}]. \quad (1)$$

This is the most widely used route to alkali metal (di)organophosphide complexes. The alkali metal (di)organophosphide products are highly air and moisture sensitive and must be handled under an inert atmosphere. Alternative routes to these compounds include the following:

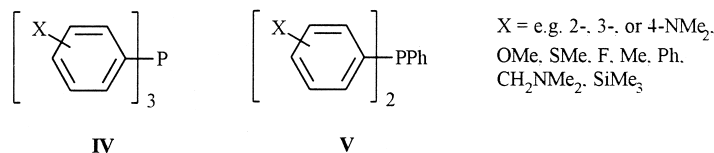
(i) Direct metalation of a primary or secondary phosphine/arsine with a heavier alkali metal (15, 16),



(ii) E–C cleavage of an aryl-substituted tertiary phosphine/arsine with an alkali metal in a donor solvent such as THF or dioxane or in liquid ammonia (17–19) (Eq. 3). Reactions in THF or dioxane may be accelerated by ultrasonication.



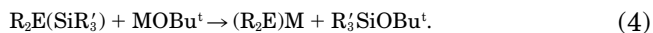
The organometallic side-product MAr is conveniently removed by selective reaction with a proton source such as Bu^tCl or NH₄Cl. This reaction is extremely effective for certain symmetrical triarylphosphines and for mixed aralkylphosphines. However, detailed investigations of P–C cleavage in functionalized and/or unsymmetrical triarylphosphines (17–19) indicate that such reactions are far from straightforward. The products obtained on treatment of triarylphosphines of type **IV** or **V** with alkali metals depend both on the nature of the substituents X and on the alkali metal.



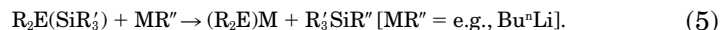
Electron-donating substituents X tend to inhibit P–C cleavage. For example, whereas PPh₃ reacts readily, (4-Me₂NC₆H₄)₃P does not react with Li/THF or Na/NH₃ (17). However, both (4-Me₂NC₆H₄)₃P and the mixed triarylphosphine (4-Me₂NC₆H₄)₂PPh undergo P–C cleavage readily on treatment with K in THF (19). Treatment of the mixed phosphine (4-Me₂NC₆H₄)₂PPh with K in THF yields [(4-Me₂NC₆H₄)PPh]K and [(4-Me₂NC₆H₄)₂P]K in a 4 : 1 ratio, whereas treatment with Li in THF yields [(4-Me₂NC₆H₄)PPh]Li and [(4-Me₂NC₆H₄)₂P]Li in a ratio approaching 1 : 4. It is also reported (17) that effective P–C cleavage in tertiary aryl phosphines requires that the LUMO (always

an aryl π^* orbital) be neither too high in energy (no reduction) or too low in energy (radical anion intermediate too stable), and that P–C cleavage is enhanced in compounds in which the coefficient of the LUMO on the carbon attached to P is large (e.g., Ph_3P). In many instances the P–C cleavage reaction is complicated by side reactions such as Birch reduction and side-group cleavage.

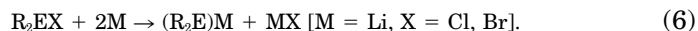
(iii) E–Si cleavage of a tertiary phosphine with an alkali metal alkoxide (20, 21) (Eq. 4) or alkali metal alkyl (22) (Eq. 5):



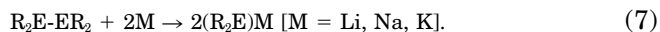
This route has proven particularly suitable for the synthesis of $(\text{Me}_3\text{Si})_2\text{PM}$ complexes (20, 21), avoiding the need for the often complex synthesis of secondary phosphines. Even in the presence of excess MOBu^t the sole product of Eq. (4) is the monometalated species $(\text{R}_2\text{E})\text{M}$.



(iv) Metalation of a halophosphine or -arsine with an alkali metal (23, 24):



(v) Reduction of a diphosphine or diarsine (25, 26):



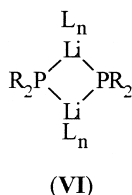
Access to heavier alkali metal complexes may also be achieved by metathesis between a lithium organophosphide and a heavier alkali metal alkoxide (27):



The alkoxide group R' is chosen so that the heavier alkali metal alkoxide MOR' is soluble in ether or hydrocarbon solvents and so the by-product LiOR' may easily be separated from the desired heavier alkali metal phosphide/arsenide (which is often insoluble in weakly or noncoordinating solvents such as ethers and hydrocarbons).

2. Homometallic Lithium (Di)organophosphides

Initial investigations of simple lithium diorganophosphides in solution using molecular weight measurements (28) and multinuclear NMR techniques (29, 30) suggested that these species existed as aggregates in solution. McFarlane and co-workers (29) reported in 1982 that the ^{31}P NMR spectrum of $\text{Li}(\text{PPh}_2)$ in Et_2O consisted of a 1:2:3:4:3:2:1 septet ($J_{\text{PLi}} = 45$ Hz) at 200 K, consistent with the presence of dimers containing a P_2Li_2 core (**VI**). The corresponding ^7Li spectrum of this complex (a well-resolved 1:2:1 triplet, $J_{\text{PLi}} = 45$ Hz) was consistent with this hypothesis. By contrast, ^{13}C NMR T_1 measurements suggest a tetrameric structure for LiPPh_2 in THF solution (31).



The first solid-state structural determination of a lithium diorganophosphide by X-ray crystallography was carried out within a year of the observations just discussed. Lithiation of Bu_2^tPH with Bu^nLi in THF, followed by crystallization from hexane, yielded the complex $[\text{Li}_2(\text{PBU}_2^t)(\text{THF})]_2$ (32, 33) (**1**). The structure consists of a four-rung ladder in which two of the phosphide groups are triply bridging and two are doubly bridging the lithium atoms (Fig. 1). The central P_4Li_4 core is essentially planar with P–Li distances ranging from 2.476(10) Å [Li(2)–P(2)] to 2.669(9) Å [Li(1)–P(1)] and internal P–Li–P angles ranging from 104.9(3)° [P(1)–Li(1)–P(2)] to 109.71(33)° [P(1)–Li(1)–P(1')]. Formation of a more extended ladder network appears to be prevented by coordination of THF to the terminal Li atoms. This ladder motif occurs in several other alkali metal phosphide complexes (*vide infra*) and is a common feature of alkali metal amide chemistry (1, 2, 4, 5).

More recently this same phosphide has been structurally characterized as the LiCl adduct, $[(\text{THF})\text{LiCl} \cdot (\text{THF})_2\text{Li}(\text{PBU}_2^t)]_2$ (34). Again the structure takes the form of a four-rung ladder; however, the central two rungs are now part of a Li_2Cl_2 cycle and the two terminal Li atoms are each coordinated by two molecules of THF. The ladder motif is broken down by the addition of the bidentate ligand DME: The recently reported complex $[\text{Li}(\text{PBU}_2^t)(\text{DME})]_2$ (DME = 1,2-dimethoxy-

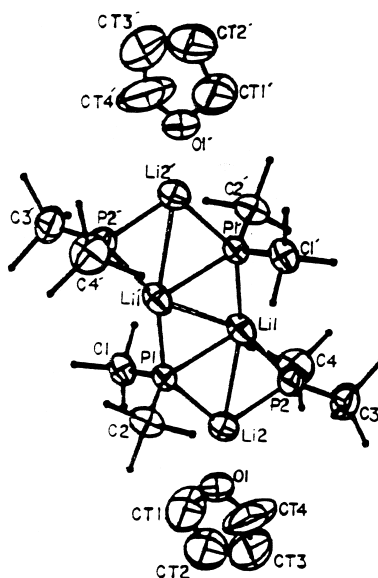


FIG. 1. Structure of $[\text{Li}_2(\text{PBu}_3)_2(\text{THF})]_2$ (1). Reproduced with permission from R. A. Jones *et al.* *J. Am. Chem. Soc.* **1983**, *105*, 7459. Copyright 1983, the American Chemical Society.

ethane), prepared by the treatment of HPBu_3 with Bu^nLi in DME/hexane, consists of a dimer with a planar Li_2P_2 core of type VI [$\text{Li}-\text{P} = 2.600(6)$; $\text{Li}-\text{P}' = 2.573(5)$ Å $\text{P}-\text{Li}-\text{P}' = 97.1(2)^\circ$] (35).

Lithium diphenylphosphide has been characterized as a number of adducts with O- or N-donor coligands, $\text{Li}(\text{PPh}_2)\text{L}$ [$\text{L} = \text{Et}_2\text{O}$ (2), $(\text{THF})_2$ (3) (36), DME (4) (35), tmeda, pmdeta (37), (12-crown-4)₂ (38)]. The Et_2O and THF adducts crystallize as infinite zigzag chains of alternating Li cations and diphenylphosphide anions, $[\text{Li}(\text{PPh}_2)(\text{OEt}_2)]_x$ and $[\text{Li}(\text{PPh}_2)(\text{THF})_2]_x$ (Fig. 2), the greater solvation in the latter complex being attributed to the larger size of Et_2O vs THF. The complex $[\text{Li}(\text{PPh}_2)(\text{DME})]_x$ adopts a similar polymeric structure in the solid state. This chain polymer motif is again common in alkali metal phosphide and arsenide chemistry (*vide infra*). As expected, as the denticity of the coligand increases (and so the coligand is consequently able to occupy more coordination sites), so the aggregation state of the complex decreases: The tmeda and pmdeta complexes are dimeric, with a planar Li_2P_2 core, and monomeric, respectively, whereas the crown ether complex exists as the solvent separated ion pair $[\text{Li}(12\text{-crown-4})_2][\text{PPh}_2]$. The C-P-C angles ($102\text{--}106^\circ$) are found to differ little within this set of compounds; the P-Li distances correlate well

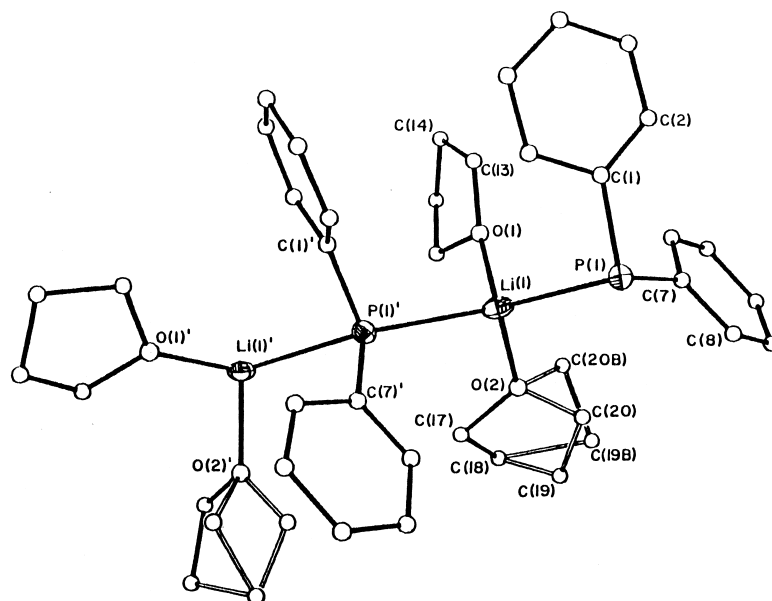
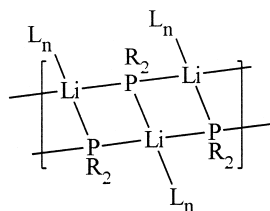


FIG. 2. Polymeric structure of $[\text{Li}(\text{PPh}_2)(\text{THF})_2]_x$ (**3**). Reproduced with permission from R. A. Bartlett *et al*, *Inorg. Chem.* **1986**, 25, 1243. Copyright 1986 the American Chemical Society.

with the coordination number of Li in each case, with lower values being found for complexes containing three-coordinate lithium [e.g., $\text{P-Li} = 2.483\text{--}2.496 \text{ \AA}$ (**2**, 3-coordinate lithium); $\text{P-Li} = 2.629$ and 2.634 \AA (**3**, 4-coordinate lithium)]. The angles along the chains of **2–4** are also noticeably dependent upon the coligands [$\text{P-Li-P} = 139.6(4)$ and $129.6(4)^\circ$ (**2**), $123.1(8)^\circ$ (**3**); $\text{Li-P-Li} = 136.9(3)$ and $126.0(3)^\circ$ (**2**), $135.0(5)^\circ$ (**3**)].

Increasing the size of the substituents on phosphorus markedly affects the structures adopted by lithium phosphide complexes: The more sterically demanding cyclohexyl groups in $[\text{Li}(\text{PCy}_2)(\text{THF})]_x$ result in a zigzag polymeric structure in which only one molecule of THF is bound to the metal center, compared to two molecules of THF in **3** (36). The lithium is three-coordinate and hence the P-Li distances [$2.455(9)$ and $2.543(9) \text{ \AA}$] are somewhat shorter than those in **3**. A more dramatic illustration of this principle is provided by $[\text{Li}\{\text{P}(\text{mes})_2\}(\text{OEt}_2)]_2$ ($\text{mes} = 2,4,6\text{-Me}_3\text{-C}_6\text{H}_2$) (**5**): Whereas $[\text{Li}(\text{PPh}_2)(\text{OEt}_2)]_x$ is a zigzag polymer (36), the more sterically hindered complex **5** is dimeric in the solid state with a planar Li_2P_2 core (39). In contrast, the less sterically demanding primary phosphide $\text{Li}\{\text{PH}(\text{mes})\}$

has been isolated in both monomeric, $[\text{Li}\{\text{PH}(\text{mes})\}(\text{THF})_3]$ (39) and $[\text{Li}\{\text{PH}(\text{mes})\}(\text{tmeda})(\text{THF})]$ (40), and helical polymeric, $[\text{Li}\{\text{PH}(\text{mes})\}(\text{THF})_2]_x$ (41), forms. The related phosphide $\text{Li}(\text{PHCy})$ adopts a one-dimensional ladder polymer arrangement (VII) in the solid state, $[\text{Li}(\text{PHCy})(\text{THF})]_x$, in which each lithium is coordinated by three P atoms and vice versa, with Li–P distances of 2.60(1) Å (ladder rung) and 2.608(8) and 2.631(8) Å (ladder edge), and an internal P–Li–P angle of 98.4° (42).



(VII)

The simplest lithium phosphide, LiPH_2 , has been isolated independently by the groups of Jones and Becker as the polymeric adduct $[\text{Li}(\text{PH}_2)(\text{DME})]_x$ (43, 44). This compound consists of infinite zigzag chains of alternating Li and P atoms with an essentially linear Li–P–Li angle of 176.9(1)°, and a P–Li–P angle of 117.0(2)°. The linearity of the Li–P–Li angle has been ascribed to the low steric demands of the H atoms on the phosphide. The Li–P distances in this prototypical complex of 2.550(8) and 2.597(8) Å are typical of those of simple lithium (di)organophosphides [see Table I for a summary of Li–P distances and NMR data for lithium (di)organophosphides]. The primary phosphide LiPHMe also crystallizes as infinite chains of alternating Li and P atoms in the adduct $[\text{Li}(\text{PHMe})(\text{diglyme})]_x$ (45); however, the Li–P–Li angle is now 132.1° [Li–P = 2.529(2) and 2.532(2) Å]. Each Li is coordinated by two P atoms and two of the O atoms of diglyme; the remaining oxygen atom of the usually tridentate diglyme ligand does not coordinate to a metal center. The chains in this complex adopt a *meso*-helical arrangement.

An unusual mixed lithium phosphide/lithium alkyl aggregate has been reported as arising from an attempted synthesis of $\text{Li}\{\text{PH}(\text{mes}^*)\}$ (46). Initial treatment of phosphorus trichloride with $\text{Li}(\text{mes}^*)$ is reported to give a mixture of the desired product, $(\text{mes}^*)\text{PCl}_2$, and the side product $(\text{mes}^*)\text{Cl}$ (via Li/Cl exchange) in an approximately 2:1 ratio. Reduction of this mixture with LiAlH_4 , followed by treatment with BuLi , then leads to rapid formation of $\text{Li}\{\text{PH}(\text{mes}^*)\}$, accompa-

TABLE I

SELECTED STRUCTURAL AND NMR DATA FOR CRYSTALLOGRAPHICALLY CHARACTERIZED
LITHIUM (DI)ORGANOPHOSPHIDE COMPLEXES

Complex ^a	Li–P (Å)	δ_P (ppm) ^b	Ref.
[Li ₂ (PBu _{1/2}) ₂ (THF)] ₂	2.669(9), 2.498(9) 2.595(10), 2.476(10)	38.51 (s, THF)	32, 33
[Li(PBu _{1/2})(THF) ₂ LiCl(THF)] ₂	2.523(4), 2.561(5)	41.8 (s, <i>d₈</i> -THF)	34
[Li(PBu _{1/2})(DME)] ₂	2.600(6), 2.573(5)	41.5 (s, DME)	35
[Li(PHCy)(THF)] _x	2.608(8), 2.60(1), 2.631(8)	–135.4 (s, C ₇ D ₈)	42
[Li(PCy ₂)(THF)] _x	2.455(9), 2.543(9)	—	36
[Li(PHMe)(diglyme)] _x	2.529(2), 2.532(2)	–197.2 (s, C ₆ D ₆)	45
[Li(PH ₂ (DME)] _x	2.550(8), 2.597(8) [2.537(5), 2.596(5)]	283 (s, DME)	43, 44
[Li(PPh ₂)(DME)] _x	2.563(3), 2.541(3)	–20.0 (s, DME)	35
[Li(PPh ₂)(OEt ₂)] _x	2.469(10), 2.486(10), 2.492(10), 2.483(10)	—	36
[Li(PPh ₂)(THF)] _x	2.629(22), 2.634(21)	—	36
[Li(PPh ₂)(tmeda)] ₂	2.574(19), 2.623(19), 2.607(18), 2.629(20) ^c	–33.3 (septet, <i>J_{PLi}</i> 45 Hz, C ₇ D ₈ , –80°C)	37
[Li(PPh ₂)(pmdeta)]	2.567(6)	–22.1 (s, C ₇ D ₈)	37
[Li{PH(mes)}(THF) ₂]	2.533(9)	–154.1 (s, C ₆ D ₆ /THF)	39
[Li{PH(mes)}(THF) ₂] _x	2.640(6), 2.656(6)	–163.2 (s, C ₇ D ₈)	41
[Li{(PH(mes)}(THF)(tmeda)]	2.560(5)	–156.3 (s, THF)	40
[Li{P(mes) ₂ }(OEt ₂)] ₂	2.483(1), 2.479(11)	–62.9 (s, THF)	39
[Li(12-c-4) ₂][PPh ₂]	—	–6.9 (s, THF)	38
[{Li(mes*)}{Li(PH(mes*))}] ₂	2.47(1), 2.47(1)	–124.8 (s, C ₇ D ₈ /THF)	46
[Li{(PPh(SiMe ₃))(tmeda)] ₂	2.62(2), 2.61(1) ^c	–145.0 (septet, <i>J_{PLi}</i> 40 Hz, C ₇ D ₈ , 258 K)	51
[Li{P(CH(SiMe ₃) ₂) ₂ }] ₂	2.481(10), 2.473(9)	–254 (septet, <i>J_{PLi}</i> 80 Hz)	23
[Li{P[CH(SiMe ₃) ₂](C ₆ H ₄ -2- CH ₂ NMe ₂)}(THF) ₂]	2.535(8) ^c	–74.3 (q, <i>J_{PLi}</i> 39.1 Hz, C ₆ D ₆ /THF)	26
[Li{P(SiMe ₃) ₂ }(DME)] ₂	2.559(4)	—	44
[Li{P(SiMe ₃) ₂ }(THF) ₂]	2.62(2), 2.62(2)	–297.6 (s, C ₇ D ₈)	22
[Li ₂ {P(SiMe ₃) ₂ }(THF)] ₂	2.55(3), 2.48(3), 2.64(2), 2.54(2), 2.44(2)	–297.7 (s, C ₇ D ₈)	22
[Li{P(SiMe ₃) ₂ }] ₆	2.52(1), 2.52(1), 2.56(1), 2.513(9), 2.63(1), 2.51(1), 2.52(1), 2.38 (1)	—	47
[Li{P(SiPh ₃) ₂ }] ₂	2.495(6), 2.449(6), 2.464(6), 2.480(6)	–308 (s, C ₇ D ₈)	49
[Li ₄ {P(SiPr ⁱ) ₂ }] ₃ {PH(SiPr ⁱ)}	2.463(14), 2.466(14), 2.494(13), 2.496(13), 2.40(2), 2.41(2), 2.40(2), 2.42(2)	–338, –351 (<i>PH</i>), –370 (singlets, C ₇ D ₈)	49
[Li(tmeda) ₂][P(SiH ₃) ₂]	—	–416.2 (s, C ₆ D ₆)	48
[Li{P(SiFBU _{1/2})Ph}(THF) ₂]	2.617(10)	–153.81 (<i>J_{PLi}</i> 49.4, –90°C)	58
[Li{P(SiFBU ^t (Is)) ₂ }(THF) ₂]	2.538(9)	–288.8 (s, C ₆ D ₆)	57
[Li{P(SiHPh ₂)(SiF(Is) ₂)} (THF) ₃]	2.527(9)	–287.4 (s, C ₆ D ₆)	52

TABLE I (Continued)

Complex ^a	Li-P (Å)	δ_P (ppm) ^b	Ref.
[Li{P(P(NPr ₂) ₂)(SiF(Is) ₂)(THF)}]	2.534(8)	−170.0 (d, J_{PP} 244.1, C_6D_6 , PLi) 90.08 (dd, J_{PP} 244.1, J_{PF} 30.5, PN_2)	52
[Li{P(SiFBU ₂)Bu ^t }(THF) ₃]	2.547(4)	−142.5 (d, J_{PF} 16.3 Hz, C_6D_6 /THF)	53
[Li{P(SiFBU ₂)(mes)}(THF) ₃]	2.503(14)	−184.7 (m, J_{PLi} 62.3, J_{PF} 17.3 Hz, Tol/ C_6D_6 , −80°C)	55
[Li{P(SiFBU ₂)(mes)}(tmeda)]	2.593(5)	−196.7 (s, Tol/ C_6D_6)	55
[Li{(P(SiFBU ₂)(mes)}(pmdeta)]	2.550(7)	−186.08 (m, J_{PLi} 70.0, J_{PF} 20.8 Hz, C_6D_6)	54
[Li{(P(SiF(Is) ₂)-Si(Is) ₂ P}(THF) ₃)]	2.568(13)	−303.3 (d, J_{PP} 46 Hz) −250.2 (dd, J_{PP} 46 Hz, J_{PF} 16 Hz, d_8 -THF)	59
[Li{P(GeBu ₂ H)(SiF(Is) ₂)(DME)}]	2.610(6)	−281.6 (s, C_6D_6)	56
[Li(12-c-4) ₂][P(SiFBU ₂)(mes)]	—	−171.5 (s, C_6D_6)	54
[Li{PH(B(NPr ₂) ₂)(DME)}] ₂	2.535(7), 2.554(7)	−213 (s)	63
[Li{P(mes)(B(mes) ₂)(OEt ₂) ₂ }]	2.451(14)	55.5 (s)	60
[Li{PCy(B(mes) ₂)(OEt ₂) ₂ }]	2.454(9)	70.1 (s)	60
[Li{P(1-Ad)(B(mes) ₂)(OEt ₂) ₂ }]	2.44(1)	90.4 (s, C_6D_6)	62
[Li{PBu ^t (B(Is) ₂)(OEt ₂) ₂ }]	2.460(4)	113.2 (s, C_6D_6 /THF)	61
[Li{P(SiMe ₃)(B(mes) ₂)(THF) ₃ }]	2.540(10)	−49.2 (s, C_6D_6 /THF)	61
[Li{P(mes)(B(PHmes)(Is))(OEt ₂) ₂ }]	2.476(6)	32.0, −117.0 (s, C_6D_6 /THF)	61
[Li(24-c-4) ₂][P(mes)(B(mes) ₂)]	—	91.3 (s)	60
[Li{P(PBu ₂) ₂ }(THF) ₂]	2.592(5), 2.599 (5)	61.9, −140.2 (s, d_8 -THF, 203 K)	64
[Li{P(PBu ₂) ₂ }(tmeda)]	2.627(6), 2640(5)	58.8, −142.5 (m, J_{PLi} 47.1 Hz, C_7D_8 , 203 K)	64
[Li{P(PPR ₂) ₂ }(THF) ₂]	2.573(4)	33.7, −188.6 (m, J_{PLi} 46.2 Hz, 203 K)	64
[{1,2-C ₆ H ₄ (PPh) ₂ P}Li(THF) ₃]	2.580(7)	31.4 (d, J_{PP} 368.5 Hz), −174.0 (d, J_{PP} 368.5 Hz, PLi , THF)	83
[1,2-C ₆ H ₄ {PPhLi(tmeda)} ₂]	2.58(3), 2.55(3), 2.59(3), 2.59(3)	−45.2 (septet, J_{PLi} 35 Hz, C_7D_8 , 203 K)	78, 79 80, 81
[1,2-C ₆ H ₄ {P(SiMe ₃)Li(tmeda)} ₂]	2.508(7), 2.544(8)	−149.6 (septet, J_{PLi} 38.3 Hz, C_7D_8 , 263 K)	81
[Li ₃ (PhPCH ₂ CH ₂ PPh)(THF) ₄] ₂	2.57(1), 2.56(2), 2.57(2), 2.53(2)	−73.0 (s, C_7D_8 , 303 K)	78
[{IsBu ^t Si(PHLi) ₂ }(LiCl)] ₂	2.20(3), 2.55–2.67(3)	—	85

(continued)

TABLE I (Continued)

Complex ^a	Li–P (Å)	δ_P (ppm) ^b	Ref.
[EtSi{PLi(SiPr ₃) ₃ }] ₂	2.464(5), 2.507(5), 2.562(5), 2.449(5), 2.511(5), 2.525(5), 2.452(5), 2.528(5), 2.554(5)	—	85
[MeC(CH ₃ PPh) ₃ {Li(THF) ₂ }- {Li(pmdeta)}]	2.52(4), 2.64(4), 2.60(4), 2.58(3), 2.62(3)	—	84
<i>Heterometallic Complexes:</i>			
[Li(THF)(PBU ₂) ₃ Sn]	2.49(3), 2.48(3)	47.2	97
[Li(THF)(PBU ₂) ₃ Pb]	2.57(6), 2.46(4)	71.5	97
[(Et ₂ O) ₂ Li{P(SiMe ₃) ₂ }GaH ₂]	2.716(8)	–277.7 (C ₇ D ₈)	94
[Cp ₂ Lu(PPh ₂) ₂ Li(tmeda)]	2.692(14), 2.691(8)	9.46 (C ₆ D ₆)	91
[MeCu(PBU ₂) ₃ Li(THF) ₃]	2.54(1)	—	99
[Sm{(PBU ₂) ₃ Li(THF) ₂ }]	2.504(9), 2.52(1), 2.52(1), 2.54(1)	—	89, 90
[Eu{(PBU ₂) ₂ Li(THF) ₂ }]	2.495(8), 2.528(9), 2.530(8), 2.530(8)	—	90
[Yb{(PBU ₂) ₂ Li(THF) ₂ }]	2.481(6), 2.504(8), 2.511(8), 2.512(7)	62.5 (q, J_{PLi} 58 Hz, J_{PYb} 873 Hz, C ₆ D ₆)	88, 90
[La(PBU ₂) ₄ Li(THF)]	2.537(5), 2.545(5)	135–180 (C ₆ D ₆ , br.)	88
[(Pr ₂ N)La{P(C ₆ H ₄ -2- OMe) ₂ }Li(THF)]	2.53(2)	–56 (q, J_{PLi} 58 Hz, C ₆ D ₆ /C ₇ D ₈ , 193 K)	92

^a Abbreviations: tmeda, *N,N,N',N'*-tetramethylethylenediamine; pmdeta, *N,N,N',N'',N''*-pentamethyldiethylenetriamine; DME, 1,2-dimethoxyethane; THF, tetrahydrofuran; 12-c-4, 12-crown-4; mes*, 2,4,6-Me₃C₆H₂; mes*, 2,4,6-Bu₃C₆H₂; Is, 2,4,6-Pr₃C₆H₂; Ad, 1-adamantyl; Tol, toluene.

^b ³¹P{¹H} chemical shifts relative to 85% H₃PO₄ at ambient temperature, unless otherwise stated (multiplicity, relevant coupling constants, solvent, temperature in parentheses).

^c Values from a representative molecule in the unit cell.

nied by slower formation of the mixed aggregate [Li(mes*)Li{PH(mes*)}]₂, which deposits in crystalline form from hexane over 3 days. An X-ray crystal structure revealed that this complex contains a central eight-membered (LiPLiC)₂ ring (Fig. 3), in which two LiPH(mes*)–Li(mes*) units, bonded via phosphorus, are joined by η^6 -interactions between a Li from one half of the dimer and the aromatic ring of the Li(mes*) subunit from the other half of the dimer.

A number of lithium phosphide complexes bearing organosilicon substituents have been synthesized and structurally characterized. Treatment of P(SiMe₃)₃ with BuⁿLi in THF yields the dimeric complex [Li{P(SiMe₃)₂}(THF)₂]₂ (**6**) (22), which contains a planar Li₂P₂ core [Li–P = Li–P' = 2.62(2); Å P–Li–P = 100.0(8)°]. Complex **6** undergoes solvent loss under vacuum (20°C, 10^{–3} torr) to give the tetramer [Li₄{ μ_2 -P(SiMe₃)₂}]₂{ μ_3 -P(SiMe₃)₂}(THF)₂] (**7**) (22), which is structurally similar to its PBU₂ analogue, **1**. In contrast, treatment of HP(SiMe₃)₂ with BuⁿLi in cyclopentane yields the solvent-free hexameric complex

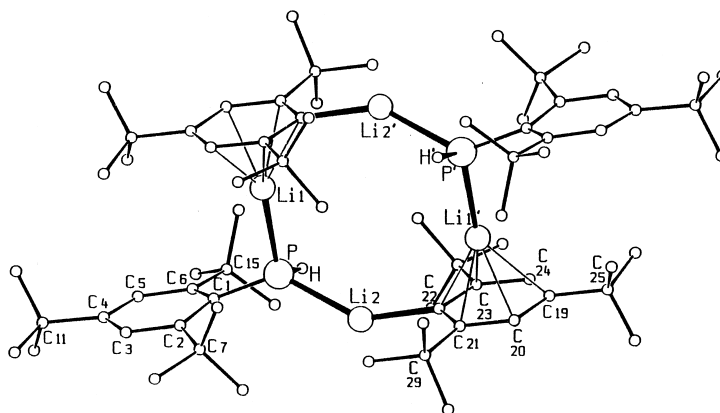


FIG. 3. Structure of $[\text{Li}(\text{mes}^*)\text{Li}\{\text{P}(\text{mes}^*)\}]_2$. Reproduced with permission from S. Kurz *et al.*, *Organometallics* **1992**, *11*, 2729. Copyright 1992, the American Chemical Society.

$[\text{Li}\{\text{P}(\text{SiMe}_3)_2\}]_6$ (**8**) (Fig. 4) (47). The hexamer adopts a six-rung ladder structure in the solid state. The formation of an extended ladder network is apparently inhibited by the steric demands of the SiMe_3 groups: The SiMe_3 groups on P(2) are displaced toward Li(3) because of unfavorable steric interactions with the SiMe_3 groups on P(1'), thus occluding the free coordination site on Li(3), which remains only two-coordinate, and preventing further oligomerisation via coordination by an additional $\text{Li}\{\text{P}(\text{SiMe}_3)_2\}$ unit. The complex $[\text{Li}\{\text{P}(\text{SiMe}_3)_2\}]$

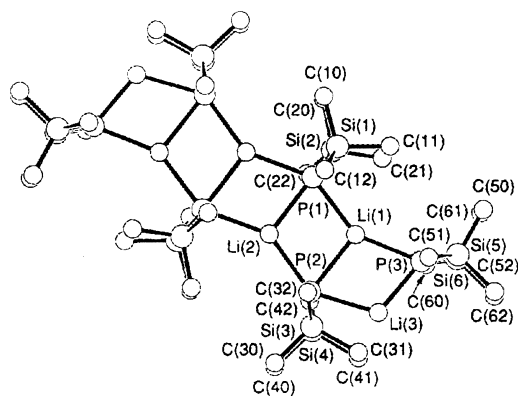


FIG. 4. Structure of hexameric $[\text{Li}\{\text{P}(\text{SiMe}_3)_2\}]_6$ (**6**). Reproduced with permission from E. Hey-Hawkins *et al.*, *Chem. Commun.* **1992**, 775. Copyright 1992, the Royal Society of Chemistry.

(DME)]₂ has also been reported and is structurally similar to **6** (44). Compounds **6** and **7** may be regarded as subunits of the solvent-free hexamer, in which coordination of lithium by two or one molecule(s) of THF prevent further oligomerization (i.e., **6** and **7** may be regarded as two- and four-rung ladder species). In **6**, **7**, and **8** the Li and P atoms are coplanar to within 0.05 Å. The solvent separated ion pair [Li(tmeda)₂][P(SiH₃)₂] has also been structurally characterized (48). The P–Si distance (2.17 Å) in this ion pair is slightly shorter than the same distances in **6** [2.196(5) and 2.194(6) Å] and **7** [2.203(6) to 2.222(6) Å].

Driess *et al.* have reported the synthesis and structures of two novel sterically hindered silicon-substituted lithium phosphides [Li{P(SiPh₃)₂}]₂ (**9**) and [Li₄{PH(SiPr₃ⁱ)}{P(SiPr₃ⁱ)₂}]₃ (**10**) (49). The large steric requirements of the Ph₃Si groups in **9** prevent oligomerization beyond a dimer and allow the isolation of a solvent-free complex. In addition to the two Li–P and contacts at each Li in the dimers [P–Li = 2.495(6), 2.449(6), 2.464(6), and 2.480(6) Å], there are contacts to the phenyl rings of the Ph₃Si groups. One ring from one P(SiPh₃)₂ ligand binds to lithium in an η²-fashion while one ring from the other P(SiPh₃)₂ ligand is bound η¹ to the metal. The unusual complex **10** arises from the lithiation of HP(SiPr₃ⁱ)₂ with *n*-butyllithium. Formation of the secondary phosphide subunit PH(SiPr₃ⁱ) is attributed to nucleophilic Si–P cleavage on treatment of the secondary phosphine with the alkylolithium. The tetrameric structure of this complex is without precedent in alkali metal phosphide chemistry and contains an essentially planar eight-membered P₄Li₄ ring in which the Li atoms are only two-coordinate [Li–PR₂ = 2.41(2) to 2.496(13) Å; Li–PHR = 2.40(2) and 2.40(2) Å], further coordination of the metal centers again being prevented by the steric requirements of the ligands. Similar planar ring systems have been observed previously in organo-alkali metal complexes such as [Na(CH₂Ph)(tmeda)]₄ (50). The short Li–P contacts in **9** and **10** reflect the low coordination number of lithium in these complexes.

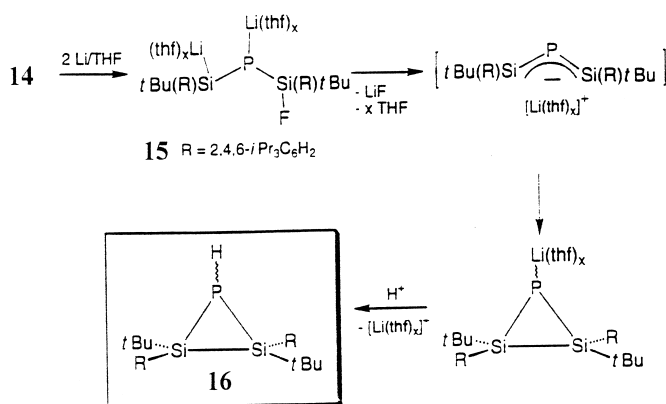
The mixed silylarylphosphide [{(Me₃Si)PhP}Li(tmeda)]₂ (51) crystallizes as dimers containing a planar Li₂P₂ core, with the phosphorus substituents in a *trans* configuration. At room temperature the ³¹P and ⁷Li NMR spectra of this compound consist of singlets, but at 0°C (³¹P) and 5°C (⁷Li) these spectra consist of a binomial septet and triplet, respectively (*J*_{P–Li} = 40 Hz), consistent with each ³¹P coupling to two ⁷Li nuclei and vice versa, indicating that the dimeric structure is preserved in solution. The lack of P–Li coupling above this temperature is attributed to rapid intermolecular Li–P exchange.

Driess *et al.* and Klingebiel *et al.* have investigated a series of fluorosilyl-substituted lithium phosphide complexes. The complexes $[\{(\text{Is})_2\text{FSi}\}(\text{Ph}_2\text{HSi})\text{P}\}\text{Li}(\text{THF})_3]$ ($\text{Is} = 2,4,6\text{-Pr}_3\text{-C}_6\text{H}_2$) (**52**), $[\{(\text{Bu}_2\text{FSi})\text{Bu}^t\text{P}\}\text{Li}(\text{THF})_3]$ (**53**), $[\{(\text{Bu}_2\text{FSi})(\text{mes})\text{P}\}\text{Li}(\text{pmdeta})]$ (**54**), and $[\{(\text{Bu}_2\text{FSi})(\text{mes})\text{P}\}\text{Li}(\text{THF})_3]$ (**11**) (**55**) are simple monomers with tetrahedral Li atoms associated with monodentate diorganophosphide ligands [$\text{Li-P} = 2.527(9)$, $2.547(4)$, $2.550(7)$, and $2.503(14)$ Å, respectively]. The crown ether complex $[(\text{Bu}_2\text{FSi})(\text{mes})\text{P}][\text{Li}(12\text{-crown-4})_2]$ (**54**) exists as solvent separated ion pairs with no Li-P contact. However, the complex $[\{(\text{Bu}_2\text{FSi})(\text{mes})\text{P}\}\text{Li}(\text{tmeda})]$ (**12**) (**55**) crystallizes as monomers in which the lithium atom is coordinated by both the phosphorus and fluorine atoms of the phosphide ligand, forming a four-membered LiPSiF chelate ring with a bite angle of $81.2(2)^\circ$. Because of the presence of such a strained chelate ring, the Li-P distance in **12** [$2.593(5)$ Å] is somewhat longer than the same distance in **11**, in which there is no $\text{Li}\cdots\text{F}$ interaction. A similar four-membered chelate ring has been observed in the complex $[\{(\text{Is})_2\text{FSi}\}(\text{Bu}^t\text{GeH})\text{P}\}\text{Li}(\text{DME})]$ (**56**), which has a chelate bite angle of $81.2(2)^\circ$ and a Li-P distance of $2.610(6)$ Å, and in $[\{(\text{IsBu}^t\text{FSi})_2\text{P}\}\text{Li}(\text{THF})_2]$ (**13**) (**57**), which has a bite angle of $81.1(3)^\circ$ and a Li-P distance of $2.538(9)$ Å.

Such fluorosilyl-substituted alkali metal phosphides are excellent precursors to a range of novel acyclic and cyclic phosphasilanes and related compounds. For example, compounds of the form $[\{(\text{Is})_2\text{FSi}\}(\text{R})\text{P}\}\text{Li}(\text{THF})_n]$ [$n = 2, 3$; $\text{R} = \text{SiMe}_3$, SiPr_3 , SiMe_2Bu^t , SiMePh_2 , SiPh_3 , $\text{Si}(\text{Naph})_3$, SiBu_2H] and $[\{(\text{Is})_2\text{FSi}\}(\text{Bu}^t\text{GeH})\text{P}\}\text{Li}(\text{DME})]$ eliminate LiF upon heating to give the corresponding silylidenephosphines, $(\text{Is})_2\text{Si}=\text{PR}$ (**56**). Thermolysis of **13** at 70°C in toluene induces LiF elimination to generate the unusual 2-phospha-1,3-disilaallyl fluoride $\text{Bu}^t(\text{Is})\text{Si}=\text{PSiF}(\text{Is})\text{Bu}^t$ (**14**), which undergoes a 1,3-sigmatropic migration of fluorine above 40°C in toluene (**57**). Treatment of **14** with elemental lithium yields the spectroscopically characterized, highly reactive intermediate **15** (Scheme 1), which readily eliminates LiF above 40°C , and, after protonation of the phosphide via a THF cleavage reaction, gives the disilaphosphacyclopropane **16**.

In contrast to **12**, the complex $[\{(\text{Bu}_2\text{FSi})\text{PhP}\}\text{Li}(\text{THF})_2]_2$ (**17**) (**58**) crystallizes as dimers in which each Li is associated with a phosphorus from one ligand and a fluorine from the other ligand, giving an eight-membered $(\text{LiPSiF})_2$ cycle [$\text{Li-P} = 2.617(10)$ Å] similar to its Na and K analogues (see Fig. 5). Above 0°C this complex eliminates LiF to give the heterocycle $\{\text{Bu}_2\text{SiP}(\text{Ph})\}_2$.

The reaction of $\{(\text{Is})_2\text{SiF}\}\text{PH-PH}\{\text{SiF}(\text{Is})_2\}$ with BuLi in THF yields the intermediate $\{(\text{Is})_2\text{SiF}\}\text{P}\{\text{Li}(\text{THF})_n\}\text{-PH}\{\text{SiF}(\text{Is})_2\}$, which on ther-

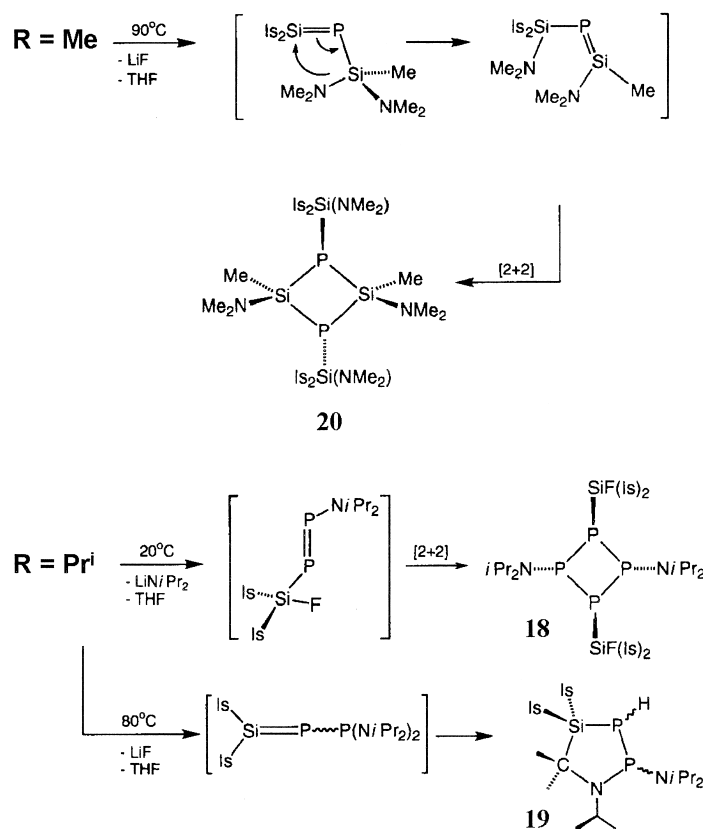


SCHEME 1. Reactions of $[\{(\text{IsBu}^t\text{FSi})_2\text{P}\}\text{Li}(\text{THF})_2]$ (**13**). Reproduced with permission from M. Driess *et al.*, *Angew. Chem. Int. Ed. Engl.* **1997**, *36*, 1326. Copyright 1997, Wiley-VCH.

molysis gives the diphosphasilacyclopropane $\{(\text{Is})_2\text{Si}\}\text{PH} - \text{P}\{\text{SiF}(\text{Is})_2\}$ (**59**). Reaction of this compound with BuLi in THF leads to the unusual lithium phosphide $[\{(\text{Is})_2\text{Si}\} - \text{P}\{\text{Li}(\text{THF})_3\} - \text{P}\{\text{SiF}(\text{Is})_2\}]$, which has been structurally characterized by X-ray crystallography. Thermolysis of this complex yields the bicyclopophosphasilane $\{(\text{Is})_2\text{Si}\}_2\text{P}_2$.

The aminophosphine-functionalized lithium phosphide complexes $[\text{Li}\{\text{P}[\text{SiF}(\text{Is})_2][\text{P}(\text{NR}_2)_2]\}(\text{THF})$ ($\text{R} = \text{Me}, \text{Pr}^i$) have also been reported to undergo novel thermally induced decomposition reactions (**52**). The complex with $\text{R} = \text{Pr}^i$ crystallizes as a monomer in which the Li is coordinated by the fluorine, the central phosphido phosphorus, and one of the NPr_2 groups, with a molecule of THF completing a distorted tetrahedral geometry about lithium [$\text{P}-\text{Li} = 2.534(8) \text{ \AA}$]; the phosphino phosphorus has no contact with the lithium atom. Thermolysis of this compound leads to the formation of two distinct heterocyclic compounds, depending on the reaction conditions. Leaving a solution of this compound in toluene to stand at room temperature for 2 days leads to the elimination of LiNPr_2 and, ultimately, to the formation of the P_4 heterocycle **18** (Scheme 2). However, heating a toluene solution to 90°C results in LiF elimination to generate the five-membered heterocycle **19**. The lithium complex with $\text{R} = \text{Me}$ undergoes a different decomposition process and yields the four-membered heterocycle **20** on heating to 90°C , via Li-F elimination.

Several boryl-substituted lithium phosphides, $[\text{Li}\{\text{PRB}(\text{Ar})_2\}\text{L}_n]$ [$\text{Ar} = \text{mes}, \text{R} = \text{Cy}, \text{Mes}, 1\text{-adamantyl}, \text{L}_n = (\text{OEt}_2)_2$; $\text{Ar} = \text{mes}, \text{R} = \text{SiMe}_3$,



SCHEME 2. Reactions of $[\text{Li}\{\text{P}[\text{SiF}(\text{Is})_2][\text{P}(\text{NR}_2)_2]\}(\text{THF})]$ ($\text{R} = \text{Pr}^i, \text{Me}$). Reproduced with permission from M. Driess *et al.*, *Chem. Ber.* **1994**, 127, 1031. Copyright 1994, Wiley-VCH.

$\text{L}_n = (\text{THF})_3$; $\text{Ar} = \text{Is}$, $\text{R} = \text{SiMe}_3$, $\text{L}_n = (\text{OEt}_2)_2$ have been structurally characterized (60–62). These monomeric complexes were found to contain planar, three-coordinate phosphorus joined to planar three-coordinate boron centers [$\text{P}-\text{Li} = 2.44(1)$ to $2.540(10)$ Å]. The planarity of the phosphorus center is attributed to some degree of B–P multiple bond character (through either $d\pi-p\pi$ interactions or hyperconjugation) and this hypothesis is supported by the coplanarity of the $\text{C}_2\text{B}-\text{PCLi}$ skeleton and by the short P–B distances of approximately 1.81–1.84 Å in these complexes (P–B bond lengths in the parent borylphosphines Ar_2BPHR typically fall in the range 1.85–1.9 Å). The monomeric complex $[\text{Li}\{\text{P}(\text{mes})[\text{B}(\text{PHmes})(\text{Is})]\}(\text{OEt}_2)_2]$ contains two different phosphorus centers attached to the same boron (61); the

(H)P–B distance is 1.927(3) Å and this P atom is highly pyramidal (sum of angles around P = 306.7°), whereas the (Li)P–B distance is 1.810(4) Å, and this P atom is essentially planar. Hence, multiple bonding by one P center appears to exclude such an interaction with the other P center. Generally, the significant B–P π -interactions in borylphosphide complexes result in an inability of the phosphide ligands to bridge two metal centers, due to the lack of an available phosphorus lone pair for bridging interactions. However, the complex [Li{PHB(NPr₂)₂}(DME)]₂ (63) crystallizes as dimers containing a planar Li₂P₂ rhombus-shaped core [P–Li = 2.535(7) and 2.554(7) Å; P–Li–P = 104.8(3)°]. The P atoms are pyramidal and the P–B distance of 1.901(5) Å is indicative of significantly reduced P–B multiple bond character due to competition between P–B and N–B π -interactions, consistent with the bridging nature of the phosphide ligands. Multi-nuclear NMR studies indicate that this dimeric structure is preserved in solution; the ⁷Li NMR spectrum consists of a well-resolved triplet ($J_{\text{PLi}} = 46.9$ Hz) below –20°C.

Several diphosphino–phosphide complexes of lithium have also been reported (64). Reaction of R₂P–P(SiMe₃)–PR'₂ with BuⁿLi yields the monomeric complexes [(L)Li{R₂P–PPR'₂}] [R = R' = Bu^t, L = (THF)₂, tmeda; R = Bu^t, R' = Prⁱ, L = (THF)₂; R = R' = Prⁱ, L = (THF)₂; R = Bu^t, R' = NEt₂, L = (THF)₂], which have all been crystallographically characterized. In each case the diphosphino–phosphide ligands bind through the two R₂P groups, there is no contact between the phosphido center and lithium; the lithium atoms achieve a distorted tetrahedral geometry by coordination to the donor atoms of the coligand(s).

Perhaps the most sterically demanding phosphide ligand used to date for the synthesis of a lithium phosphide complex is P{CH(SiMe₃)₂}₂. The complex [LiP{CH(SiMe₃)₂}]₂ (21) was synthesized by metalation of the chlorophosphine ClP{CH(SiMe₃)₂}₂ with elemental lithium (23). This unusual synthetic route helps to suppress the formation of the persistent, distillable dialkylphosphine radical ·P{CH(SiMe₃)₂}₂ (22) (65, 66). The solid state structure of the lithium phosphide consists of a dimer with a planar Li₂P₂ core [Li–P = 2.481(10) and 2.473(9) Å]. The wide P–Li–P angle of 107.8(3)° may be attributed to the steric effects of the large CH(SiMe₃)₂ substituents on phosphorus. No additional donor solvent is coordinated to the lithium centers, despite the synthesis proceeding in Et₂O; this is probably due to the large size of the CH(SiMe₃)₂ groups which prevent further coordination or oligomerization. The formation of radical species is a feature of the reactions of this lithium phosphide; reactions with either

Bu⁴Cl or SnCl₂ yield the dialkylphosphine radical **22**, whereas reactions with HCl or MeCl yield the phosphines HP{CH(SiMe₃)₂}₂ and MeP {CH(SiMe₃)₂}₂, respectively. Unusually for lithium phosphide complexes, P–Li coupling is resolved for this complex at room temperature in both the ³¹P (binomial septet, $J_{\text{PLi}} = 80$ Hz) and ⁷Li (triplet) NMR spectra, suggesting that Li–P exchange for this complex is slow on the NMR time scale, possibly as a consequence of the steric demands of the phosphide ligands.

A related lithium complex of an amino-functionalized phosphide ligand [(THF)₂Li{PCH(SiMe₃)₂(C₆H₄-2-CH₂NMe₂)₂}] **23** has been reported (27). The ligand binds to lithium through both its P and N centers to give a puckered six-membered chelate ring [P–Li = 2.535(8) Å]. The distorted tetrahedral coordination sphere of the lithium in this monomeric complex is completed by two molecules of THF.

3. Homometallic Heavier Alkali Metal (Di)organophosphides

Compared to the wealth of data concerning the solid- and solution-state structures of lithium (di)organophosphides, reports of heavier alkali metal analogues are sparse. Indeed, the first crystallographic study of a homometallic heavier alkali metal (di)organophosphide complex was reported only in 1990 (67) and the majority of such complexes have been reported in the past 3 years. Interest in these complexes stems mainly from their enhanced reactivity in comparison to equivalent lithium complexes, which is particularly useful for the synthesis of alkaline earth, lanthanide, and actinide organophosphide complexes.

The large size/charge ratio of the heavier alkali metals has the consequence that extensive aggregation is particularly common among their complexes, often leading to insoluble polymeric species that are difficult to crystallize or to characterize in solution. This is usually counteracted by the use of extremely sterically demanding substituents such as mes* and CH(SiMe₃)₂ and/or the use of polydentate coligands such as tmeda, pmdeta, and DME. The greater propensity of the heavier alkali metals to support multihapto interactions with aromatic ring systems also has significant repercussions for the aggregation states and solid state structures of (di)organophosphide complexes of these metals; multihapto M–Ar contacts are often favored over more conventional M–donor interactions.

The first heavier alkali metal phosphide species to be structurally characterized were the sodium and potassium complexes [M{P(mes)(SiFBu₂[†])}(THF)₂]₂ (M = Na, K) (67). These isostructural complexes adopt an eight-membered (MPSiF)₂ ring motif in which each alkali

metal cation is coordinated by a phosphorus from one ligand and a fluorine from the neighboring ligand (Fig. 5).

The M–P and M–F distances are 2.890(1) and 2.383(2) Å (M = Na), and 3.230(1) and 2.643(1) Å (M = K) (selected details of structurally characterized heavier alkali metal phosphide complexes are given in Table II). The related complex $[\text{Na}\{\text{P}(\text{SiF}(\text{Is})_2)\{\text{SiMe}_2(\text{CPr}^i\text{Me}_2)\}\}]_2$, prepared by treatment of the corresponding secondary phosphine with $\text{Na}\{\text{N}(\text{SiMe}_3)_2\}$ in toluene, crystallizes as rather different solvent-free dimers (16). These dimers contain a planar Na_2P_2 core in which each sodium achieves three-coordination via intramolecular Na–F contacts, giving four-membered NaPSiF chelate rings [Na–P = 2.960(4) and 2.831(4) Å]. Cryoscopic measurements indicate that the same degree of association is maintained in solution. Reaction of the related phosphine $\{\text{Is}\}_2\text{FSi}(\text{Pr}^i\text{Si})\text{PH}$ with elemental cesium in toluene containing a little THF yields the polymeric complex $[\text{Cs}\{\text{P}(\text{SiF}(\text{Is})_2)(\text{SiPr}^i_3)\}(\text{THF})_{0.5}]_x$ (16). At room temperature in the absence of THF this reaction is inhibited and above 40°C P–Si cleavage dominates. The solid-state structure of this complex consists of infinite chains of CsPRR' units linked together by intermolecular multihapto Cs–aryl contacts. There are two types of Cs atom that alternate along the chain; one Cs is in contact with one P atom, one η^6 -Is group from the same ligand, and one η^6 -Is group from an adjacent ligand in the chain,

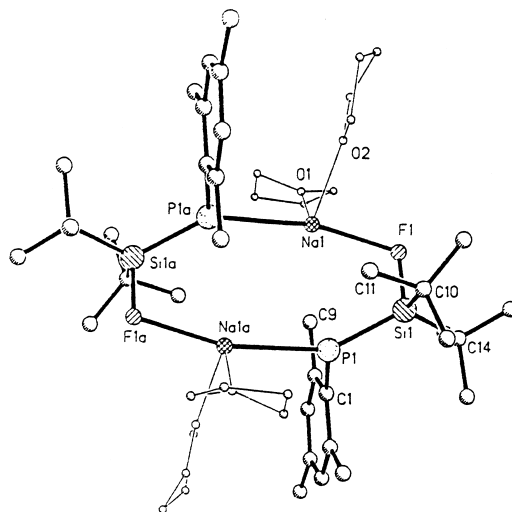


TABLE II
SELECTED STRUCTURAL AND NMR DATA FOR CRYSTALLOGRAPHICALLY CHARACTERIZED
HEAVIER ALKALI METAL (DI)ORGANOPHOSPHIDE COMPLEXES

Complex ^a	P–M (Å)	δ_P (ppm) ^b	Ref.
[Na(PHCy)(pmdeta)] ₂	2.884(8), 2.936(7)	—	68
[Na{P(C ₆ H ₄ -2-OMe) ₂ }(diglyme)] ₂	2.901(2), 2.861(2), 2.953(2), 3.047(2)	–61.4 (C ₆ D ₆ /THF)	69
[Na{P(SiFBU ₂ ^t)(mes)}(THF) ₂] ₂	2.890(1), 3.268(1)	–196.6 (C ₆ D ₆)	67
[Na{P(SiF(Is) ₂)(SiMe ₂ CMe ₂ Pr ⁱ)}] ₂	2.960(4), 2.831(4)	–269.8 (C ₆ D ₆)	16
[Na{P[CH(SiMe ₃) ₂] (C ₆ H ₄ -2-CH ₂ NMe ₂) (tmeda)]	2.8396(9)	–75.5 (<i>d</i> ₈ -THF)	26
[EtSi{PNa(SiPr ₃) ₃ }] ₃ · (toluene) ₂	2.878(2), 2.805(2), 3.012(2), 2.858(2), 2.840(2), 2.823(2), 2.778(2), 2.935(2), 3.357(2)	—	85
[K{PH(mes*)}] _x	3.271(2), 3.181(2), 3.357(2)	–89.3 (<i>d</i> ₈ -THF)	72
[K ₃ {PH(mes)} ₃ (THF) ₂] _x	3.368(1), 3.397(1), 3.364(1), 3.451(1), 3.306(2)	–141.6	71
[{K(PBu ^t Ph)} ₂ (THF)] _x	3.232(3), 3.771(4), 3.521(4), 3.318(4), 3.261(3), 3.352(4), 3.303(4), 3.321(3), 3.360(4), 3.419(4), 3.834(4), 3.296(3)	26.1 (<i>d</i> ₈ -THF)	74
[{K(PBu ^t Ph)} ₂ (<i>N</i> -MeIm)] _x	3.4422(9), 3.3037(11), 3.4224(9), 3.2322(11), 3.5069(9), 3.7934(10)	—	74
[{K(PBu ^t Ph)} ₂ (py)] _x	3.3727(14), 3.3148(14), 3.2978(14), 3.2805(14), 3.946(3), 3.2324(14)	—	74
[K{PH(Dmp)}] ₄	3.438(2), 3.162(2), 3.189(2), 3.365(2), 3.043(2)	–130.5 (C ₆ D ₆) [–123.8 (<i>d</i> ₈ -THF)]	75
[K{P[CH(SiMe ₃) ₂](C ₆ H ₄ -2- CH ₂ NMe ₂)}(pmdeta)]	3.2326(6)	–64.9 (<i>d</i> ₈ -THF)	26
[K{P(SiMe ₃) ₂ }(THF)] _x	3.3169(7), 3.4063(8), 3.4272(8)	–293.4	21
[K{P(SiFBU ₂ ^t)(mes)}(THF) ₂] ₂	3.230(1), 3.619(2)	–181.9 (C ₆ D ₆)	67

(continued)

TABLE II (Continued)

Complex ^a	P–M (Å)	δ_P (ppm) ^b	Ref.
[K{P(PH <i>tert</i> -Bu) [†] Bu [†] }(pmdeta)] ₂	3.252(2), 3.340(3), 3.658(3)	–8.90 (d, J_{PP} 321.5 Hz, PH), –57.4 (d, J_{PP} 321.5 Hz, PLi, d_8 -THF)	77
[Rb{PH(mes*)}] _x	3.381(1), 3.433(1), 3.504(1)	–82.3 (d_8 -THF)	73
[{Rb[PH(mes*)]}] ₂ (<i>N</i> -MeIm)] _x	3.518(1), 3.571(1), 3.700(1), 3.710(1), 3.898(1), 3.977(1)	—	73
[Rb{P(SiMe ₃) ₂ }(THF)] _x	3.416(1), 3.484(2), 3.486(2)	–287.1	21
[Rb{PH(Dmp)}] ₄ · Toluene	3.756(2), 3.411(2), 3.399(2), 3.520(2), 3.473(2), 3.558(2), 3.579(2), 3.425(2), 3.516(2), 3.454(2), 3.412(2), 3.480(2)	–115.7 (C ₆ D ₆), [–117.0 (d_8 -THF)]	76
[Cs{PH(mes*)}] _x	3.577(1), 3.580(2), 3.642(1)	–69.2 (d_8 -THF)	73
[{Cs[PH(mes*)]}] ₂ (THF) _{0.9}] _x	3.505(2), 3.623(3), 3.679(3), 3.802(3), 3.967(3), 4.097(3)	—	73
[{Cs[PH(mes*)]}] ₂ (<i>N</i> -MeIm)] _x	3.631(1), 3.755(1), 3.761(1), 3.782(1), 3.936(1), 3.993(1)	—	73
[{Cs[PH(mes*)]}] ₂ (py)] _x	3.626(3), 3.694(3), 3.844(3), 3.853(3), 3.865(3), 3.986(3)	—	73
[{Cs[PH(mes*)]}] ₂ (toluene) _{0.5}] _x	3.554(3), 3.567(4), 3.776(4), 3.856(3), 4.039(3), 4.442(3)	—	73
[{Cs[PH(mes*)]}] ₂ (en)] _x	3.539(2), 3.663(2), 3.724(2), 3.832(2), 4.106(2), 4.241(2)	—	73
[Cs ₃ {PH(Dmp)}] ₃ · $\frac{1}{3}$ (toluene)] _x	3.6254(14)	–99.9 (d_8 -THF)	76
[Cs{P(SiMe ₃) ₂ }(THF)] _x	3.582(1), 3.645(1), 3.667(1)	–270.0	21
[Cs{P(SiF(Is) ₂)(SiPr ₃ [†])}](THF) _{0.5}] _x	3.517(6), 3.536(7)	–296.9 (C ₆ D ₆)	16

^a Abbreviations as for Table I, except *N*-MeIm, *N*-methylimidazole; Dmp, dimesitylphenyl; py, pyridine; en, 1,2-ethylenediamine.

^b ³¹P{¹H} chemical shifts relative to 85% H₃PO₄ at ambient temperature, unless otherwise stated.

while the next Cs in the chain is in contact with one P atom, one η^3 -Is group from the same ligand, one η^6 -Is group from an adjacent ligand, and one molecule of THF [Cs–P = 3.517(6), (THF)Cs–P = 3.536(7) Å]. There is apparently no interaction between Cs and F, which has the consequence that, unlike related lithium phosphides, this complex does not eliminate CsF to give an unsaturated Si=P compound.

The first simple sodium phosphide to be structurally characterized was synthesized in 1995 by Raston and co-workers (68). The complex [Na(PHCy)(pmdeta)]₂ crystallizes as dimers with a central planar P₂Na₂ ring and a *trans* arrangement of the cyclohexyl substituents across the ring [Na–P = 2.884(8), 2.936(7) Å; Na–P–Na = 86.2(2)°].

Treatment of (*o*-MeOC₆H₄)₃P with Na in liquid ammonia/THF yields the corresponding sodium phosphide, which has been structurally characterized as its diglyme adduct [Na{μ-P(C₆H₄-2-OMe)₂}{MeO(CH₂CH₂O)₂Me}]₂ (69). Although this complex adopts a familiar P₂M₂ core arrangement, this is not planar (in contrast to other complexes containing a P₂M₂ core); the P(1)–Na(1)–P(2)–Na(2) torsion angle is –15.91(4)°. Each sodium is coordinated by the P and one O atom of the phosphide ligand to give a five-membered chelate ring; the second O atom of the ligand does not bind to the metal center. A coordination number of 6 is achieved by each sodium by coordination of the three O atoms of a diglyme molecule. In THF solution this complex decomposes to give a mixture of tetrakis(*o*-anisyl)diphosphine and (*o*-MeOC₆H₄)₂PH. The lithium analogue of this complex, which has not been structurally characterized, decomposes to give solely tetrakis(*o*-anisyl)diphosphine. The oxidant in these oxidative coupling reactions has not been identified.

The related complexes [Na{P[CH(SiMe₃)₂](C₆H₄-2-CH₂NMe₂)₂}(tmeda)] and [K{P[CH(SiMe₃)₂](C₆H₄-2-CH₂NMe₂)₂}(pmdeta)] have been isolated (27). As in the lithium analogue (**23**), the phosphide ligand binds via both its nitrogen and phosphorus centers to give puckered six-membered chelate rings in both complexes. In both the Na and K complexes, however, a significant M···C contact to the *ipso*-carbon directly attached to phosphorus increases the coordination numbers of the metals to 5 (Na) and 6 (K). The Na–P and K–P distances of 2.8396(9) and 3.2326(6) Å are short compared to other such distances reported.

The heavier alkali metal phosphides M{P(SiMe₃)₂} (M = K, Rb, Cs) have been synthesized by P–Si cleavage of the corresponding trisilylphosphine with MOBu[†] and have been structurally characterized as their THF adducts [M{P(SiMe₃)₂}(THF)]_x (21). The greater size of the

heavier alkali metal cations favors more extensive aggregation than is observed in the analogous lithium complexes **6**, **7**, and **8** (*vide supra*), and all three complexes crystallize as ladder-type polymers. The K and Rb complexes are isomorphous and adopt puckered ladder structures, such that alternate M_2P_2 squares form “steps” in a staircase-like arrangement in which the ladder-edge P–M–P angles are 140.23(2) and 139.29(5)° for the K and Rb complexes, respectively. The Cs complex adopts a more planar ladder arrangement in which the ladder-edge P–Cs–P angle is much closer to linearity (165.11(4)°).

A number of mesityl- and supermesitylphosphide complexes of the heavier alkali metals have been reported, and several of these have been the subject of a short review (70). The primary phosphide KPH(mes) crystallizes from layered THF/pentane as the unusual polymeric species $[K_3\{PH(mes)\}_3(THF)_2]_x$ (**24**) (71). The structure consists of infinite chains of edge-sharing KP_5 tetragonal pyramids in which K(1) is almost coplanar with P(1), P(2), P(1A), and P(2A), and the apical P atoms alternately point upward and downward along the chain (Fig. 6). Two further potassium atoms [K(2) and K(3)] are located over two adjacent edges of one trigonal face of the pyramid. The coordination environments of these two K atoms are completed by a molecule each of THF and multihapto interactions with the mesityl rings. This structure is in marked contrast to the corresponding helical polymer $[Li\{PH(mes)\}(THF)_2]_x$ (41).

The more sterically demanding phosphide KPH(mes*) crystallizes solvent-free, even from solutions containing THF, as the ladder polymer $[K\{PH(mes^*)\}]_x$ (**25**) (72). Coordination about each K atom is completed by multihapto interactions (approximately η^3) between the cation and the mesityl ring of an adjacent phosphide ligand. A

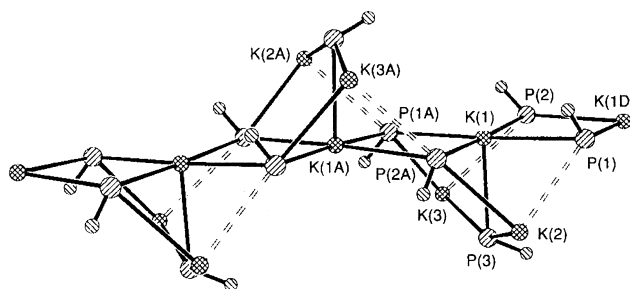


FIG. 6. Structure of $[K_3\{PH(mes)\}_3(THF)_2]_x$ (**24**). Reproduced with permission from C. Frenzel *et al.*, *Chem. Commun.* **1998**, 1363. Copyright 1998, the Royal Society of Chemistry.

systematic investigation of the heavier alkali metal complexes of supermesitylphosphide, $[M\{PH(mes^*)\}]_x$ [$M = Rb$ (**26**), Cs (**27**)], and several base adducts of these compounds, $[M\{PH(mes^*)\}_2L_n]_x$ [$M = Rb$, $L_n = N-MeIm$ (**28**); $M = Cs$, $L_n = (THF)_{0.9}$ (**29**), (py) (**30**), $(N-MeIm)$ (**31**), $(toluene)_{0.5}$ (**32**), en (**33**)] ($N-MeIm = N$ -methylimidazole; $en = 1,2$ -ethylenediamine), has revealed a number of interesting structural trends (73). The solvent-free complexes **26** and **27** crystallize from THF as ladder polymers with multihapto interactions (up to η^6 for $M = Cs$) between each metal center and an adjacent supermesityl ring system. The base adduct complexes also crystallize as ladder polymers; however, the exact form of this ladder is dependent upon the type of donor ligand(s) present (Fig. 7). Complex **29** consists of a ladder polymer in which THF ligands bridge two cesium atoms in the same square of the ladder, but only in alternate squares, with the THF molecule alternating between sites above and below the ladder. Rapid solvent loss is responsible for the <100% occupancy of the THF in the crystal, indicating the weak nature of the $Cs-THF$ interaction. The py and $N-MeIm$ adducts **28**, **30**, and **31** display a similar ladder arrangement with alternating bridged and nonbridged squares, but also exhibit a twist along the ladder by *ca.* 130° in one direction followed by an equal twist in the opposite direction. The toluene adduct **32** crystallizes from solutions containing a range of bidentate and tridentate ligands such as DME, tmeda, and pmdeta without incorporating these additional donor molecules. Interestingly, the adduct **32** is not obtained from toluene solutions in the absence of co-ligands; such recrystallization yields the solvent-free complex **27**. The structure of **32** again consists of a ladder arrangement; however, parallel ladders are linked by $\mu_2-\eta^3:\eta^3$ -toluene molecules via alternate Cs atoms along the ladder edge. There are thus two types of Cs alternating along the edges of the ladder, one coordinated by three P atoms and a multihapto interaction with an adjacent mesityl ring and one that is further coordinated to an η^3 -toluene molecule. In contrast to **32**, the adduct **33** is obtained from toluene solutions containing the bidentate en ligand. The complex again consists of an infinite ladder polymer in which alternate Cs_2P_2 squares are bridged by en ligands.

A similar investigation of the base adducts of $K(PBu^tPh)$ shows that $[K(PBu^tPh)_2(THF)]_x$ (**34**), $[K(PBu^tPh)_2(N-MeIm)]_x$ (**35**), and $[K(PBu^tPh)_2(py)]_x$ (**36**) also adopt extended polymeric ladder structures in the solid state (74). These adducts resemble the Rb and Cs complexes **28–33**; however, the base coligands in **34–36** do not bridge the potassium atoms but are bound in a terminal fashion. In each case there are two types of potassium atom in alternate positions

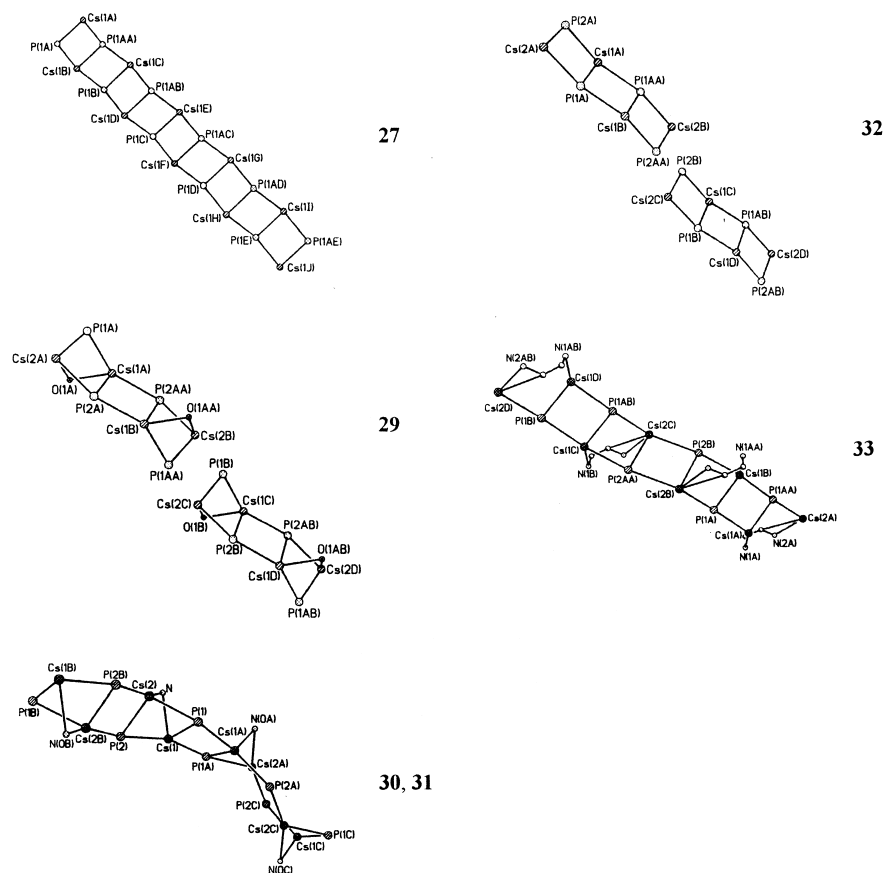


FIG. 7. Ladder motifs observed in $[\text{Cs}\{\text{PH}(\text{mes}^*)\}]$ (**27**), and $[\{\text{Cs}\{\text{PH}(\text{mes}^*)\}_2\text{L}\}]_x$ ($\text{L} = (\text{THF})_{0.9}$ (**29**); py (**30**); $N\text{-MeIm}$ (**31**); $(\text{toluene})_{0.5}$ (**32**); en (**33**)). Reproduced with permission from G. W. Rabe *et al.*, *Inorg. Chem.* **1998**, 37, 4235. Copyright 1998, the American Chemical Society.

along each edge of the chain; the coordination sphere of the first of these $[\text{K}(1)]$ principally consists of three phosphide P atoms and a molecule of the donor coligand, whereas the coordination sphere of the second $[\text{K}(2)]$ principally consists of three phosphide P atoms and a multihapto interaction with an adjacent phenyl group. In **34** the phenyl group is η^6 -bound to $\text{K}(2)$, whereas in **35** $\text{K}(2)$ has an η^4 -interaction with two adjacent phenyl groups and $\text{K}(1)$ has an η^2 -interaction with an adjacent phenyl group. In **36** $\text{K}(1)$ is coordinated by the three P atoms and the nitrogen atom of a pyridine coligand, with additional coordination by the *ipso* carbon of one adjacent phenyl ring; $\text{K}(2)$ is

coordinated by three P atoms and has an η^6 -interaction with one adjacent phenyl group and an η^2 -interaction with the phenyl group that has an η^1 contact with K(1). The structures of all three complexes are thus similar but differ subtly in the coordination environments of the potassium atoms. It is noteworthy that whereas the supermesitylphosphide complex **25** crystallizes solvent-free from solutions containing THF, complex **34** crystallizes with THF coordinated to potassium, possibly reflecting the higher steric demands of PH(mes*) over PBu^tPh.

Rabe and co-workers have also isolated the complexes $[\text{K}\{\text{PH}(\text{Dmp})\}]_4$ (**75**), $[\text{Rb}\{\text{PH}(\text{Dmp})\}]_4 \cdot (\text{toluene})$, and $[\{(\text{Dmp})\text{HP}\}_3\text{Cs}_2\text{Cs}^+] \cdot \frac{1}{3}(\text{toluene})_x$ (Dmp = 2,6-dimesitylphenyl) (**76**). Unusually, all three of these complexes adopt completely different structures in the solid state. The potassium complex crystallizes as solvent-free tetramers containing a four-rung ladder core. The coordination spheres of the two types of potassium atoms are completed by varying degrees of multihapto interaction with the mesityl rings of the Dmp ligands. The K–P distance [3.043(2) Å] for the top and bottom rungs of the tetramer is the shortest reported for any type of P–K contact, reflecting the low coordination number of the potassium atom at this site. This tetrameric four rung ladder arrangement is reminiscent of the structures of **1** and **7**, in which solvation by THF has been replaced by arene–potassium interactions. However, although the atoms in the Li_4P_4 core of **1** and **7** are essentially coplanar, only the central K_2P_2 rungs are coplanar; the top and bottom K–P rungs are significantly twisted away from the central K_2P_2 plane [the dihedral angle between the K_2P_2 core and the ladder edge P–K–P triangle is 23.6(2)°]. In contrast, the tetrameric rubidium complex adopts an unprecedented heterocubane structure with each Rb atom coordinated by three phosphide ligands, with further coordination by multihapto interactions with two mesityl rings from two different Dmp ligands (Fig. 8a). The ^1H and ^{31}P NMR spectra of this compound are essentially independent of solvent, suggesting that the tetrameric structure is retained in solution. The Cs complex crystallizes as a two-dimensional network of $\text{Cs}^+[\text{Cs}_2\{\text{PH}(\text{Dmp})\}_3]^-$ contact ion pairs (Fig. 8b). The two Cs atoms in the “anion” are bridged by three phosphide P atoms with further coordination of each Cs by two ring carbons from each of three adjacent mesityl groups. The “cation” is solvated solely by three η^3 -arene interactions, such that each Cs cation links three of the anions in a network arrangement. The network arrangement of this complex leaves large cavities in the lattice that are each filled by a molecule of toluene.

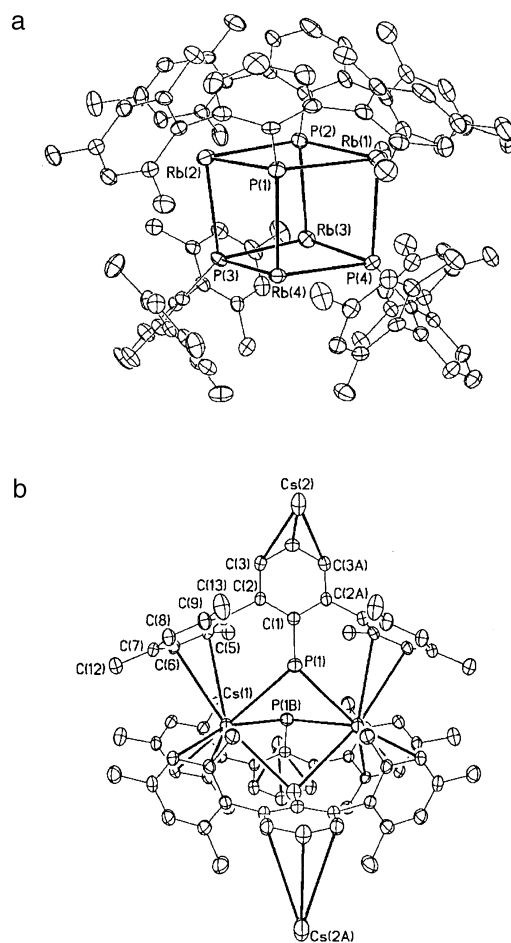


FIG. 8. (a) Structure of $[\text{Rb}\{\text{PH}(\text{Dmp})\}]_4 \cdot (\text{toluene})$; (b) structure of $[\text{Cs}^+[\text{Cs}_2\{\text{PH}(\text{Dmp})\}_3]_2] \cdot \frac{1}{2} (\text{toluene})$. Reproduced with permission from G. W. Rabe *et al.*, *Angew. Chem. Int. Ed. Engl.* **1998**, 37, 1404. Copyright 1998, Wiley-VCH.

Although the reaction of (RP)₄ with alkali metals is known to give a range of products containing anions such as (RP)₄²⁻, (RP)₂²⁻, and (R₂P₂H)⁻, it was only in 1998 that an alkali metal complex of one of these anions was structurally characterized (77). Treatment of (Bu^tP)₄ with 5 equiv of potassium in THF, followed by addition of pmdeta and stoichiometric hydrolysis, yields the complex [K{PBu^t(PHBu^t)} (pmdeta)]₂. X-ray crystallography shows that the anionic P centers of the phosphino–phosphide ligands bridge the two potassium atoms to

give a central centrosymmetric K_2P_2 core. Each K atom is further coordinated by the neutral P centers of each anion, such that the phosphino-phosphide ligands bind in an η^2 -fashion, and the three N atoms of the pmdeta coligand. The K–P distances are 3.340(3) and 3.251(2) Å (phosphide) and 3.658(3) Å (phosphine).

4. Homometallic Alkali Metal Polyphosphides and Phosphinediides.

A number of alkali metal complexes of di- or tri-anionic phosphide ligands have been reported. In 1987 the groups of Lappert (78, 79) and Craig and Gallagher (80) independently reported the crystal structure of the diphosphide $[(PhPCH_2CH_2PPh)\{Li(THF)_2\}_2]_2$, synthesized via P–C cleavage of $Ph_2PCH_2CH_2PPh_2$ (dppe) with lithium. There are two types of lithium in the complex, one of which is coordinated by two P atoms from the same ligand in a five-membered chelate ring [Li–P = 2.56(2) and 2.53(2) Å], and the other one of which bridges the P atoms of two different ligands to give a cyclic dimer with a central eight-membered P_4Li_4 ring [Li–P = 2.57(1) and 2.57(2) Å]. Each Li is further coordinated by two molecules of THF in a distorted tetrahedral geometry. This complex is a useful precursor to a range of derivatives including novel P-containing heterocycles.

Lappert and co-workers have also reported the aryl diphosphides $[C_6H_4-1,2-\{(PR)Li(tmeda)\}_2]$ [R = Ph (78, 81), SiMe₃ (81)]. These compounds crystallize as monomers in which each Li is coordinated by both P atoms and by two N atoms of the tmeda coligands, such that the two Li atoms lie in distorted tetrahedral environments on opposite sides of the planar $C_6H_4-1,2-(PR)_2$ moiety [R = Ph, Li–P = 2.55(3) to 2.59(3) Å; R = SiMe₃, Li–P = 2.508(7), 2.544(8) Å]. Low-temperature ^{31}P NMR spectroscopy confirms that this structure is preserved in solution: The $^{31}P\{^1H\}$ spectrum of $[C_6H_4-1,2-\{(PSiMe_3)Li(tmeda)\}_2]$ consists of a binomial septet ($J_{PLi} = 38.3$ Hz) at 263 K due to coupling of each of the equivalent P nuclei to two equivalent 7Li nuclei. The related bis-primary phosphide complex $[C_6H_4-1,2-\{(PH)Li(tmeda)\}_2]$ has been prepared and spectroscopically characterized, but has not been crystallographically characterized (82). Reaction of the dilithium salt $C_6H_4-1,2-(PPhLi)_2$ with white phosphorus gives Li_3P_7 and the lithium phospholide $[\{1,2-C_6H_4(PPh)_2P\}Li(THF)_3]$ (83), in which a tetrahedral Li atom is coordinated by three molecules of THF and the central phosphido phosphorus of the phospholide anion.

Two related tripodal triphosphide ligands have been isolated as their lithium or sodium derivatives. The compound $MeC(CH_2PPh_2)_3$ reacts with elemental lithium to yield the triphosphide $[(\{MeC(CH_2PPh)_3\}\{Li(THF)_2\}_2 \{Li(pmdeta)\})]$ after recrystallization

(84). This complex has two $\text{Li}(\text{THF})_2$ moieties μ_2 -bridging between the three phosphide groups with the other $\text{Li}(\text{pmdeta})$ moiety bound in a terminal fashion to one of the terminal P atoms of the triphosphide ligand. Driess and co-workers (85) have reported that treatment of the tris-secondary phosphine $\text{EtSi}\{\text{PH}(\text{SiPr}_3)\}_3$ with BuLi or BuNa yields the complexes $[\text{EtSi}\{\text{PLi}(\text{SiPr}_3)\}_3]_2$ and $[\text{EtSi}\{\text{PNa}(\text{SiPr}_3)\}_3]_2 \cdot (\text{toluene})_2$, respectively. These dimeric species contain a distorted rhombic dodecahedral $\text{Si}_2\text{P}_6\text{M}_6$ core, although in the sodium complex this core adopts a more open cage framework due to the coordination of one molecule of toluene to two of the Na atoms on opposite sides of the cage (Fig. 9).

Driess *et al.* have also reported the synthesis and crystal structure of the dilithium siladiphosphide complex $[\{\text{IsBu}^t\text{Si}(\text{PHLi})_2\}_2(\text{LiCl})_2]_2$ (85). This complex crystallizes as a “dimer of dimers” in which two $\{\text{IsBu}^t\text{Si}(\text{PHLi})_2\}$ units are linked by a central $(\text{LiCl})_2$ “deck.”

The first structural characterization of an alkali metal phosphinidide complex M_2PR was reported in 1996 by Driess *et al.* (86). A more extensive survey of phosphinidides and arsenidides is to be found in the accompanying review by Professor M. Driess. Treatment of

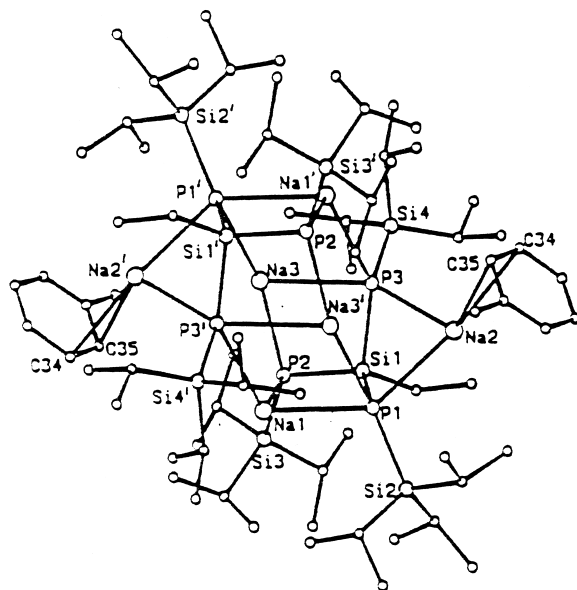


FIG. 9. Structure of $[\text{EtSi}\{\text{PNa}(\text{SiPr}_3)\}_3]_2 \cdot (\text{toluene})_2$. Reproduced with permission from M. Driess *et al.*, *Angew. Chem. Int. Ed. Engl.* **1995**, 34, 316. Copyright 1995, Wiley-VCH.

(IsPr^i_2Si) PH_2 with 2 equiv of BuLi yields (IsPr^i_2Si) PLi_2 , which cryoscopic measurements indicate is a dimer in benzene. Reaction of this compound with $\text{IsPr}^i_2\text{SiF}$ does not result in substitution of fluorine at silicon; instead, a fluorosilane adduct of the phosphinediide, [$(\text{IsPr}^i_2\text{Si})\text{PLi}_2(\text{FSiPr}^i_2\text{Is})$] $_2$, is isolated. This complex contains a central Li_2P_2 rhombus in a ladder-like $\text{P}_2\text{Li}_4\text{F}_2$ framework in which each F acts as a bridging donor between two lithium atoms (Fig. 10).

A novel oxo-centered cluster of lithium phosphinediide units, [$\{\text{Me}_2(\text{Pr}^i\text{Me}_2\text{C})\text{SiP}\}_8\text{Li}_{18}\text{O}$], has been reported as the product of double lithiation of $\{\text{Me}_2(\text{Pr}^i\text{Me}_2\text{C})\text{Si}\}\text{PH}_2$ with Bu^nLi in the presence of Li_2O (87). The origin of the Li_2O is unknown, but may be a result of hydrolysis of BuLi to LiOH. The structure is described as an ionogenic cluster formed by three closed shells and covered by a lipophilic layer of silyl groups (Fig. 11). A central Li_6O octahedral core is surrounded by a distorted cube of P atoms, and this in turn is surrounded by a Li_{12} cuboctahedral shell, where each of the 12 Li atoms lies over the edge

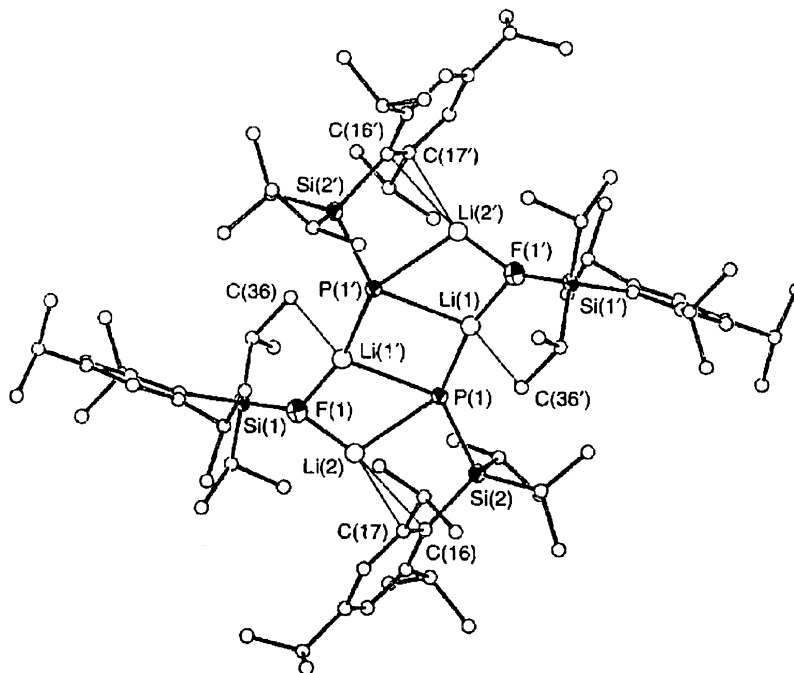


FIG. 10. Structure of [$(\text{IsPr}^i_2\text{Si})\text{PLi}_2(\text{FSiPr}^i_2\text{Is})$] $_2$. Reproduced with permission from M. Driess *et al.*, *Chem. Commun.* **1996**, 305. Copyright 1996, the Royal Society of Chemistry.

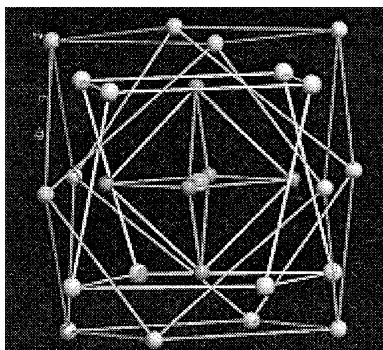
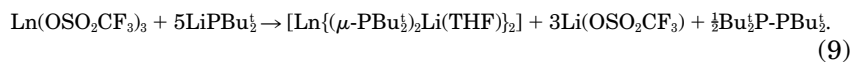


FIG. 11. Structure of the $P_8Li_{18}O$ core of $[(Me_2(Pr^iMe_2C)SiP)_8Li_{18}O]$. Reproduced with permission from M. Driess *et al.*, *Angew. Chem. Int. Ed. Engl.* **1996**, 35, 986. Copyright 1996, Wiley-VCH.

of the P_8 cube; the inner Li_6 atoms are each located over an inner face of the P_8 cube. Cryoscopic molecular weight measurements suggest that some degree of dissociation occurs in solution, and ^{31}P NMR spectroscopy indicates three P environments in benzene, two of which are attributed to the intact cluster and one to a supposed dissociate.

5. Heterometallic Alkali Metal (Di)organophosphides and Phosphinediides

Metathesis reactions between alkali metal (di)organophosphides and metal halides or related compounds occasionally yield products in which the alkali metal remains an important feature. This is particularly true of the heavier metals, such as the lanthanides, which necessarily have large radii and which, therefore, may readily incorporate an additional molecule of $LiPR_2$ in their coordination sphere. For example, treatment of $La(OSO_2CF_3)_3$ with $LiPBu_2^t$ in THF yields the “ate” complex $[(Bu_2^tP)_2La(\mu-PBu_2^t)_2Li(THF)]$ (88), in which the La atom is surrounded by four phosphide ligands, two of which bridge between the La atom and a Li atom. The Li atom is three-coordinate, its coordination sphere being completed by a molecule of THF [$Li-P = 2.537(5)$ and $2.545(5)$ Å]. Similar treatment of the trivalent lanthanide triflates $Ln(OSO_2CF_3)_3$ ($Ln = Sm, Eu, Yb$) with $LiPBu_2^t$ yields the divalent lanthanide “ate” complexes $[Ln\{(\mu-PBu_2^t)_2Li(THF)\}_2]$, according to Eq. (9) (88–90):



Lithium may also remain in the coordination sphere of a preformed "ate" complex upon reaction with a phosphine. For example, treatment of $\text{Cp}_2\text{Lu}(\mu\text{-Me})_2\text{Li(L)}$ [$\text{L} = \text{tmeda}$ or $(\text{THF})_2$] with Ph_2PH yields the diphosphide complexes $[\text{Cp}_2\text{Lu}(\mu\text{-PPh}_2)_2\text{Li(L)}]$ (91), in which Cp_2Lu and Li(L) units are doubly bridged by PPh_2 groups [$\text{Li-P} = 2.692(14)$ and $2.691(8)$ Å; $\text{L} = \text{tmeda}$]. Similar treatment of $\text{Li[La(NPr}_2)_4]$ with $(\text{C}_6\text{H}_4\text{-2-OMe})_2\text{PH}$ yields the heteroleptic complex $[(\text{Pr}_2\text{N})\text{La}\{\mu\text{-P(C}_6\text{H}_4\text{-2-OMe)}_2\}_2\text{Li(THF)}]$, in which the La atom is bound by one P and one O atom from each of the two phosphide ligands and two amide N atoms, while the Li is coordinated by the one P and the other O atom from the phosphide ligand and a molecule of THF ($\text{Li-P} = 2.53(2)$ Å) (92).

A number of complexes in which phosphide or phosphinediide ligands bridge between lithium and another main group element have been reported. Reaction of Bu_3GaCl with Bu^tPLi_2 in ether yields the heterometallic complex $[(\text{OEt}_2)_2\text{Li}\{\text{Bu}^t\text{Ga}(\mu_3\text{-PBu}^t)_2(\text{GaBu}_3^t)\}]$, which contains a $\text{Ga}_2\text{P}_2\text{Li}$ framework composed of a nonplanar Ga_2P_2 ring coordinated to a lithium atom via the two P atoms (93). Treatment of LiGaH_4 with $\text{P(SiMe}_3)_3$ yields Me_3SiH and the mixed metal phosphide species $[(\text{Et}_2\text{O})_2\text{Li}\{\mu\text{-P(SiMe}_3)_2\}_2\text{GaH}_2]$ (94), in which $\mu_2\text{-P(SiMe}_3)_2$ ligands bridge between a GaH_2 moiety and a $\text{Li(OEt}_2)_2$ moiety.

Wright *et al.* have reported two cases where LiPHCy acts as a precursor to main group phosphinidene complexes. Reaction of the primary lithium phosphide with $[\text{AlMe}\{\text{N(mes)}\}]_4$ gives the heterometallic cage complex $\{\text{Li(THF)}\}_4\{[\text{AlMe}(\mu\text{-PCy})_2(\mu\text{-PCy})]_2 \cdot \text{C}_6\text{H}_5\text{Me}\}$ (95) (Fig. 12a). Reaction of $[\text{SnNBu}^t]_4$ with 6 equiv of LiPHCy yields the complex cluster $[\{\text{Sn}_2(\text{PCy})_3\}_2\{\text{Li(THF)}\}_4] \cdot 2\text{THF}$ (96) (Fig. 12b).

Cowley, Jones, and co-workers (97) have reported that reaction of SnCl_2 or PbCl_2 with 3 equiv of LiPBu_3^t yields the "ate" complexes $[\text{Li(THF)}\{\text{M(PBu}_3^t)_3\}]$ ($\text{M} = \text{Sn, Pb}$). The two complexes are isostructural; the Sn or Pb atoms are coordinated by a terminal PBu_3^t ligand and two further phosphide ligands bridge the Li and Sn(Pb) centers. The coordination number 3 is achieved by lithium through the coordination of a molecule of THF. The Li-P distances of 2.49(3) and 2.48(3) Å ($\text{M} = \text{Sn}$) and 2.57(6) and 2.46(4) Å ($\text{M} = \text{Pb}$) are consistent with the chelate interaction of the two P atoms with a Li(THF) unit.

Heterometallic alkali metal phosphide complexes with transition metals have also been reported. The complex $[(\text{Cy}_2\text{P})_3\text{Hf}(\mu\text{-PCy}_2)_2\text{Li(DME)}]$ results from the reaction of LiPCy_2 with $\text{HfCl}_4(\text{THF})_n$ (98). This complex persists in solution. Jones *et al.* have reported the synthesis and reactivity toward a range of electrophiles of a series of lithium di-*t*-butylphosphido(alkyl)cuprates $[\text{RCu(PBu}_3^t)_2\text{Li}]$ ($\text{R} = \text{Me}$,

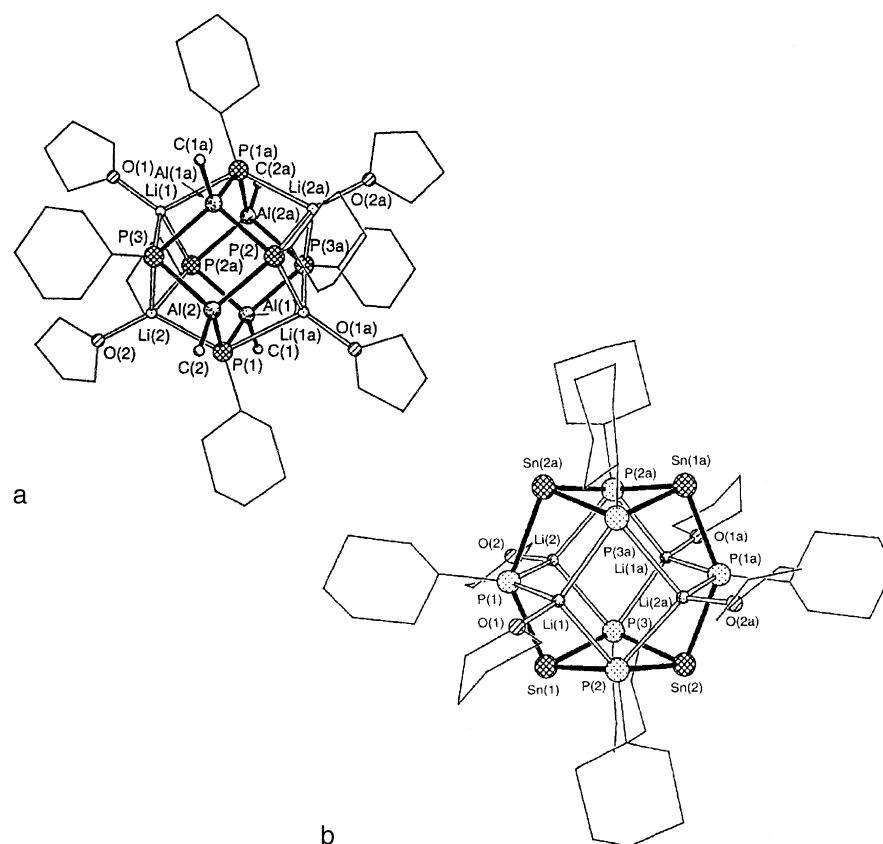


FIG. 12. (a) Structure of $\{\text{Li}(\text{THF})\}_4\{[(\text{AlMe})(\mu\text{-PCy})_2(\mu\text{-PCy})]_2\} \cdot (\text{toluene})$. Reproduced with permission from R. E. Allan *et al.*, *Chem. Commun.* **1996**, 4153. (b) Structure of $[\{\text{Sn}_2(\text{PCy})_3\}_2\{\text{Li}(\text{THF})\}_4] \cdot 2\text{THF}$. Reproduced with permission from R. E. Allan *et al.*, *Chem. Commun.* **1996**, 1501. Copyright 1996, the Royal Society of Chemistry.

Bu^n , Bu^s , Bu^t) (99). The complex with $\text{R} = \text{Me}$ crystallizes as the THF solvate $[\text{MeCu}(\text{PBU})_2\text{Li}(\text{THF})_3]$ in which the phosphido ligand bridges the two-coordinate Cu and four-coordinate Li centers. These cuprates were found to be more thermally stable than other phosphido(alkyl)-cuprates but less reactive toward electrophiles than related cyanocuprates.

Incorporation of heavier alkali metals into “ate” complexes is usually disfavored because of the large lattice energies of the simple salt elimination products MX. However, Stephan *et al.* have reported that reaction of Cp_2ZrHCl with $\text{KPH}(\text{mes}^*)$ in the presence of KH gives the

heterometallic phosphinidene complex $[\text{Cp}_2\text{ZrH}\{\text{P}(\text{mes}^*)\}\text{K}(\text{THF})_2]_2$ in low yield (100). An X-ray crystal structure of this complex shows that the phosphinidene ligands bridge the K and Zr centers, such that each P has a "terminal" Cp_2ZrH moiety, and such that the two halves of the dimer are linked via the phosphinidene ligands, forming a central P_2K_2 rhombus. These systems are highly susceptible to P–C cleavage to give P-containing transition metal products: reaction of $\{\text{Cp}^*\text{Zr}(\text{N}_2)\}_2(\mu\text{-N}_2)$ ($\text{Cp}^* = \eta^5\text{-C}_5\text{Me}_5$) with $(\text{mes}^*)\text{PH}_2$, followed by KH ultimately leads to the isolation of the crystalline polymeric complex $[\text{Cp}^*\text{Zr}(\text{P}_3)\text{K}(\text{THF})_{1.5}]_x$ via a P–C cleavage reaction (100, 101).

B. ARSENIDES AND ARSINEDIIDES

In comparison to alkali metal complexes of (di)organophosphide ligands, complexes of these metals with (di)organoarsenide ligands are relatively rare and few have been structurally characterized. This dearth of structural information is perhaps due in part to the relatively low importance of such complexes in inorganic and organic synthesis and to the lower stability (both thermal and photolytic) of arsenide complexes compared to their phosphide analogues.

Synthesis of lithium (di)organoarsenide complexes is achieved by similar methods to those outlined for organophosphide complexes (see Section I,A,1) and include (i) deprotonation of a primary or secondary arsenide with a strong base such as BuLi or LiAsH₂, (ii) As–Si cleavage using BuLi, or (iii) reaction of a chloroarsine with lithium.

Becker *et al.* reported the first structurally authenticated alkali metal arsenide complex in 1982 (102). The complex $[\text{Li}\{\text{As}(\text{SiMe}_3)_2\}(\text{DME})]_2$, synthesized by the reaction of $\text{As}(\text{SiMe}_3)_3$ with BuLi or MeLi in DME, crystallizes as centrosymmetric dimers containing a planar Li_2As_2 rhombus-shaped core [$\text{Li}–\text{As} = 2.59(2)$ Å; $\text{As}–\text{Si} = 2.307(7)$ Å; $\text{As}–\text{Li}–\text{As} = 99(1)^\circ$]. Tetrahedral coordination of the lithium atoms is achieved by coordination to the two O atoms of the chelating DME ligands. Cryoscopic measurements indicate that the dimeric structure of this complex is preserved in solution. (Selected bond lengths and angles of alkali metal arsenides are listed in Table III.)

The two related complexes $[\text{Li}_4\{\mu_2\text{-As}(\text{SiMe}_3)_2\}_2\{\mu_3\text{-As}(\text{SiMe}_3)_2\}_2(\text{THF})_2]$ (**37**) and $[\text{Li}\{\text{As}(\text{SiMe}_3)_2\}(\text{THF})_2]_2$ have been isolated and structurally characterized (103). The former complex was isolated in very low yield from the reaction of $\text{LiAs}(\text{SiMe}_3)_2$ with InCl_3 after recrystallization from pentane, whereas the latter complex was isolated by recrystallization of $\text{LiAs}(\text{SiMe}_3)_2$ from a pentane/THF mix. Complex **37** is isostructural with its phosphorus analogue **7** (*vide supra*) and con-

sists of a four-rung ladder arrangement in which the Li_4As_4 core is essentially planar [$\text{Li}-\text{As} = 2.51(2)$ to $2.69(2)$ Å; internal $\text{As}-\text{Li}-\text{As}$ angles = $105.8(7)$, $103.2(5)$, and $108.9(6)^\circ$]. The dimer $[\text{Li}\{\text{As}(\text{SiMe}_3)_2\}(\text{THF})_2]_2$ is both isostructural and isomorphous with its phosphorus analogue and contains a central planar Li_2As_2 rhombus [$\text{Li}-\text{As} = 2.67(1)$, $2.70(1)$ Å; $\text{As}-\text{Li}-\text{As} = 98.2(4)^\circ$]. This complex is also essentially isostructural with the DME adduct $[\text{Li}\{\text{As}(\text{SiMe}_3)_2\}(\text{DME})]_2$. The fluorosilyl-substituted lithium arsenide $[\text{Li}\{\text{As}(\text{SiPr}_3)(\text{SiF}(\text{Is})_2)\}(\text{THF})_2]$ is monomeric with a trigonal planar lithium atom coordinated by the arsenide ligand [$\text{Li}-\text{As} = 2.46(3)$ Å] and two molecules of THF (104). Thermolysis of this complex yielded the first example of an arsasilene $(\text{Is})_2\text{Si}=\text{As}(\text{SiPr}_3)$.

Unlike the corresponding phosphide analogues $[\text{Li}(\text{PPh}_2)(\text{THF})_2]_x$ and $[\text{Li}(\text{PPh}_2)(\text{OEt}_2)_2]_x$ (36), which are polymeric in the solid state (*vide supra*), the complex $[\text{Li}(\text{AsPh}_2)(\text{OEt}_2)_2]_2$ crystallizes as dimers containing a planar Li_2As_2 core [$\text{Li}-\text{As} = 2.708(9)$, $2.757(9)$ Å; $\text{As}-\text{Li}-\text{As} = 90.3(4)^\circ$] (105). However, the dioxane adduct $[\text{Li}(\text{AsPh}_2)(1,4\text{-dioxane})_3]$ is monomeric with a distorted tetrahedral Li atom ($\text{Li}-\text{As} = 2.660(10)$ Å) (105). The solvent-separated ion pair $[\text{Li}(12\text{-crown-4})_2][\text{AsPh}_2]$ has also been structurally characterized (105).

In contrast, the sodium complex $[\text{Na}(\text{AsPh}_2)(\text{dioxane})]_x$ is polymeric in the solid state [$\text{Na}-\text{As} = 2.962(4)$, $2.937(4)$ Å] (25). This complex was synthesized by the rather unusual method of sodium reduction of a diarsine;



The complex consists of infinite zigzag chains of $\text{Na}-\text{As}-\text{Na}-\text{As}$ units in which the $\text{Na}-\text{As}-\text{Na}$ angle is essentially linear [$173.6(1)^\circ$] and the $\text{As}-\text{Na}-\text{As}$ angle is $121.5(1)^\circ$. The sodium atoms achieve a tetrahedral geometry by coordination by two molecules of dioxane that bridge between adjacent chains to give a two-dimensional sheet arrangement.

Perhaps the most sterically hindered lithium arsenide, $[\text{LiAs}\{\text{CH}(\text{SiMe}_3)_2\}_2]_3$, was prepared from the reaction of $\text{ClAs}\{\text{CH}(\text{SiMe}_3)_2\}_2$ with lithium in ether (24). The complex crystallizes as a solvent-free cyclic trimer containing a Li_3As_3 core with a boat conformation [$\text{Li}-\text{As} = 2.60(4)$ Å (average)]. The Li_3As_3 core is asymmetric in that the $\text{Li}-\text{As}(3)-\text{Li}$ angle [$98(1)^\circ$] is significantly smaller than the other two $\text{Li}-\text{As}-\text{Li}$ angles [$103(1)$ and $105(1)^\circ$]. Like its phosphorus-containing analogue (**21**, *vide supra*), this complex may act as either a one-electron reducing agent or a pnictogen-centered nucleophile. For example, reaction of $[\text{LiAs}\{\text{CH}(\text{SiMe}_3)_2\}_2]_3$ with SnCl_2 yields the persistent radi-

cal species $\cdot\text{As}\{\text{CH}(\text{SiMe}_3)_2\}_2$, whereas reaction with MeCl yields $\text{MeAs}\{\text{CH}(\text{SiMe}_3)_2\}_2$.

An interesting reaction is observed between LiAsBu_2 and MgBr_2 , leading to the isolation of the complex $[\text{Li}\{\text{AsBu}^i(\text{AsBu}_2^i)\}(\text{THF})]_2$ in 65% yield (106). The complex process by which this compound is produced is unclear, and the authors report that the side products of this reaction were not identified. However, such a process clearly involves both As–As bond formation and As–C bond cleavage. The complex consists of a typical planar Li_2As_2 arrangement [$\text{As}–\text{Li}–\text{As} = 100.6(3)^\circ$], with the two Li–As(arsenide) distances identical to within experimental error [$2.58(2) \text{ \AA}$]. The arsino-As atoms have no short contacts with lithium.

To date only one polyanionic arsenide complex of an alkali metal has been reported. The complex $[\text{Bu}^i\text{Ge}\{\text{As}(\text{SiPr}_3^i)\text{Li}\}_3]_2$ is obtained from the reaction of Bu^iGeF_3 with 3 equiv of $\text{Li}\{\text{AsH}(\text{SiPr}_3^i)\}$ and BuLi in ether in 24% yield (107). The complex contains a $\text{Ge}_2\text{As}_6\text{Li}_6$ framework with a center of symmetry in a distorted rhombododecahedral arrangement (Fig. 13). Each As atom is thus bound to three Li atoms in addition to one Ge atom and one exocyclic SiPr_3^i group; the Li atoms are in contact with three As atoms and also with two H atoms from different SiPr_3^i groups [$\text{Li}–\text{As} = 2.52(2)$ to $2.62(2) \text{ \AA}$]. Additional solvation of the Li atoms is not observed, even though the complex is syn-

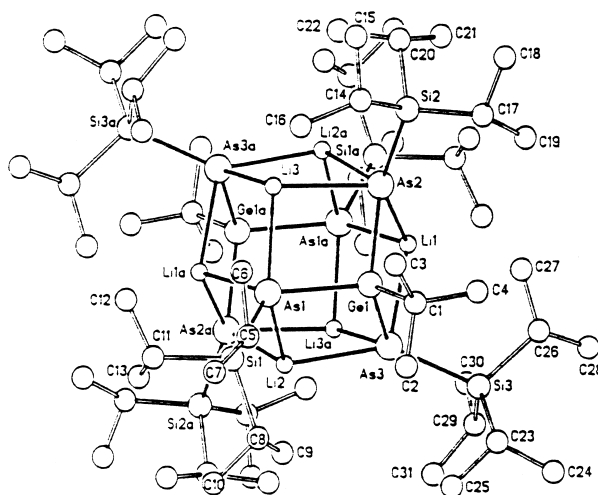


FIG. 13. Structure of $[\text{Bu}^i\text{Ge}\{\text{As}(\text{SiPr}_3^i)\text{Li}\}_3]_2$. Reproduced with permission from L. Zsolnai *et al.*, *Angew. Chem. Int. Ed. Engl.* **1993**, *32*, 1439. Copyright 1993, Wiley-VCH.

TABLE III

SELECTED STRUCTURAL DATA FOR CRYSTALLOGRAPHICALLY CHARACTERIZED ALKALI METAL
(DI)ORGANOARSENIDE COMPLEXES

Complex ^a	M–As (Å)	Ref.
[Li(AsPh ₂)(Et ₂ O) ₂] ₂	2.708(9), 2.757(9)	105
[Li(AsPh ₂)(1,4-dioxane) ₃]	2.660(10)	105
[Li{As[CH(SiMe ₃) ₂] ₂ }] ₃	2.58(4), 2.58(4), 2.63(4), 2.57(4), 2.66(4), 2.58(4)	24
[Li{As(AsBu ^t)Bu ⁱ }(THF)] ₂	2.58(2), 2.58(2)	106
[Li{As(SiMe ₃) ₂ }(DME)] ₂	2.59(2)	102
[Li{As(SiMe ₃) ₂ }(THF)] ₂	2.70(1), 2.67(1)	103
[Li ₂ {As(SiMe ₃) ₂ }(THF)] ₂	2.63(2), 2.69(2), 2.57(2), 2.51(2), 2.54(2)	103
[Li{As(SiPr ₃)(SiF(Is) ₂)}(THF)] ₂	2.46(3)	104
[Bu ^t Ge{As(SiPr ₃)Li] ₃]	2.59(2), 2.56(1), 2.62(2), 2.54(2), 2.62(1), 2.59(1), 2.52(2), 2.62(1)	107
[Na(AsPh ₂)(THF)] _x	2.962(4), 2.937(4)	25
<i>Heterometallic complexes:</i>		
[Cp ₂ Lu(AsPh ₂)Li(tmeda)]	2.65(4), 2.73(3)	108
[(Et ₂ O) ₂ Li{As(SiMe ₃) ₂ }GaH ₂]	2.736(6)	94

^a Abbreviations as in Table I.

thesized in diethyl ether, possibly due to steric shielding associated with the large SiPr₃ groups (Table III).

The first dilithium arsinediide complex was reported by Driess *et al.* (87). Treatment of {Me₂(PrⁱMe₂C)Si}AsH₂ with 2 equiv of BuLi, in the presence of a small amount of Li₂O, yields the cage complex [{Me₂(PrⁱMe₂C)Si]As}]₁₂Li₂₆O]. This is closely related to the phosphinediide complex [{Me₂(PrⁱMe₂C)SiP}]₈Li₁₈O] (87) (*vide supra*), and again the origin of the Li₂O unit is similarly unclear. An approximately icosahedral arrangement of As centers is capped on each face by one of 20 of the Li atoms to give an approximately spherical [As₁₂Li₂₀]⁴⁺ framework that binds the remaining Li atoms as an octahedral Li₆O core. Once again, cryoscopic and ⁷Li NMR measurements indicate that this structure is essentially maintained in solution.

Two heterometallic lithium arsenide complexes have been reported. The “ate” complex [Cp₂Lu(μ-AsPh₂)₂Li(tmeda)] is obtained from the reaction of [Cp₂Lu(μ-Me)₂Li(tmeda)] with Ph₂AsH in benzene (108). The complex contains a puckered LuAs₂Li core [Li–As = 2.65(4) and 2.73(3) Å] with an angle between the As₂Li and As₂Lu planes of 150.8(4)°. Reaction of LiGaH₄ with As(SiMe₃)₃ yields the complex [(Et₂O)₂Li{μ-As(SiMe₃)₂}GaH₂] via the elimination of HSiMe₃ (94).

This complex is isostructural with its phosphorus analogue (94, *vide supra*) and contains a planar LiAs_2Ga core [$\text{Li-As} = 2.736(6) \text{ \AA}$]. In solution, both ^1H and $^{13}\text{C}\{^1\text{H}\}$ NMR spectra indicate three SiMe_3 environments, consistent with either the formation of a mixture of oligomers or decomposition. The observation of signals due to free $\text{As}(\text{SiMe}_3)_3$, even for freshly prepared solutions of the complex, which grew in intensity with time, indicate the thermal sensitivity of this compound.

III. Charge-Delocalized Ligands

The ability of phosphorus to stabilize a negative charge α to the heteroatom center has been known for many years and has been used widely in organic synthesis (109). This stabilization has been variously attributed to delocalization of charge into empty phosphorus d -orbitals or P-C (or other P-X) σ^* -orbitals (hyperconjugation) and/or to the polarizability of phosphorus, although the participation of phosphorus d -orbitals in charge stabilization is now thought to be of little importance (7). One report (110) has suggested that hyperconjugation is the dominant factor in stabilizing phosphorus-substituted carbanions. The propensity of phosphorus to effect charge delocalization in this way has led to the development of two classes of anionic, potential P-donor ligands, the phosphinomethanides $[(\text{R}_2\text{P})_n\text{CR}'_{(3-n)}]$ ($n = 1-3$) and the phosphinoamides/iminophosphides $[(\text{R}_2\text{P})_n\text{NR}'_{(2-n)}]$ ($n = 1, 2$), in which charge is delocalized toward phosphorus from a formally anionic C- or N-center, respectively. A wide range of complexes of these ligands has been synthesized with main group, transition, and lanthanide metals, showing a great variation in binding modes, reactivities, and structures. Of these two classes of ligands, the phosphinomethanides have been most investigated. The following discussion will be limited to P(III)-stabilized anions. Although P(V)-stabilized carbanions [such as α -metalated phosphine oxides, $\text{MCH}_2\text{P}(\text{O})\text{R}_2$] are of great importance in organic synthesis (111) and several alkali metal complexes of such anions have been structurally characterized (112-119), there is typically no direct M-P or M-C contact, the metal preferring to bind to the more electronegative substituent at phosphorus (e.g., O, S). For example, in the complex $[\{(\text{CH}_2)_5\text{P}(\text{O})(\text{CHPh})\}\text{Li}(\text{THF})_2]_2$ the lithium is bound only to the oxygen atoms of the phosphine oxide and THF molecules and forms no short contacts with the benzylic carbon (120).

A. PHOSPHINOMETHANIDES

Creation of a carbanion center α - to phosphorus(III) results in the generation of a phosphinomethanide ligand in which the directly bonded phosphorus and carbon centers are (valence) isoelectronic and have relatively similar electronegativities [carbon and phosphorus have Pauling electronegativities of 2.55 and 2.19, respectively (121)]. This enables the P and C centers to compete as nucleophiles for metal centers and, in consequence, these ligands may adopt a range of bonding modes. The bonding mode adopted depends upon the electronic and steric properties of the substituents at P and C, the nature of the metal center (hardness, polarizability, etc.), and the presence or absence of coligands. For the alkali metals reported bonding modes of monophosphinomethanide ligands ($R_2P-CR'_2$) include η^1 -C-donation (**VIII**), η^1 -P-donation (**IX**), η^2 -PC-donation (**X**), and bridging modes (**XI**) (Scheme 3). For di- and triphosphinomethanides [$(R_2P)_2CR'$ and $(R_2P)_3C$, respectively] reported bonding modes include bidentate PP-donation (**XII**), heteroallyl coordination (**XIII**), and combined bridging/PP-donation (**XIV**).

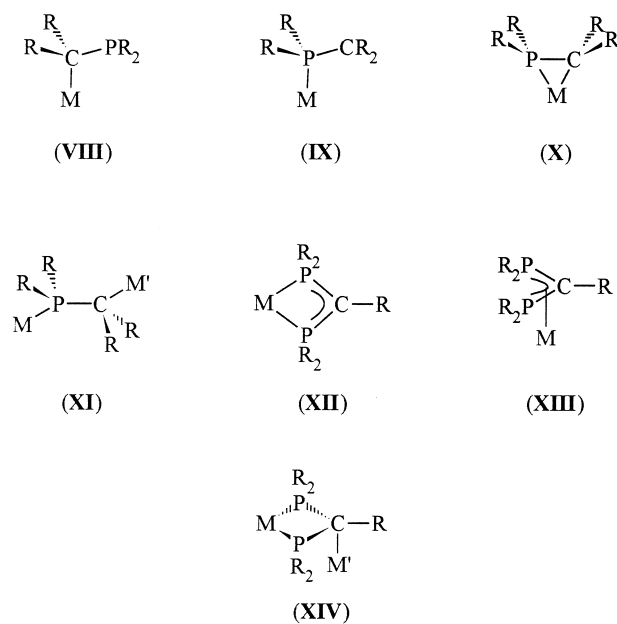
1. Synthesis

With very few exceptions, alkali metal complexes of phosphinomethanide ligands are synthesized by the deprotonation of a tertiary phosphine bearing an α -CHR₂ group with an alkali metal alkyl such as BuⁿLi:



2. Lithium Phosphinomethanides

The first alkali metal complex of a phosphinomethanide ligand to be structurally characterized was reported by H. H. Karsch and co-workers in 1984. Crystallization of $Li\{C(PMe_2)_3\}$ from pentane containing 2 equiv of THF yields the complex $[Li\{C(PMe_2)_3\}(THF)]_2$ (**38**) (122, 123) (Fig. 14). The complex consists of dimers in which each lithium is bound in an η^2 -PP fashion by a phosphinomethanide ligand via two of the phosphorus atoms, P(1) and P(2) [Li–P = 2.588(3), 2.684(3) Å]; the remaining P atom P(3) forms no contact with lithium. The two halves of the dimer are linked by Li*–C(1) interactions to give an overall bonding situation resembling **XIV** (Scheme 3); however, the close approach of Li* to P(1) and P(2) suggests that the bonding situation might best be described as resembling a π -heteroallyl complex [Li*–P = 2.945(3), 2.998(3) Å]. The Li*–C(1) interaction



SCHEME 3. Binding modes of mono-, di-, and triphosphinomethanide ligands with the alkali metals.

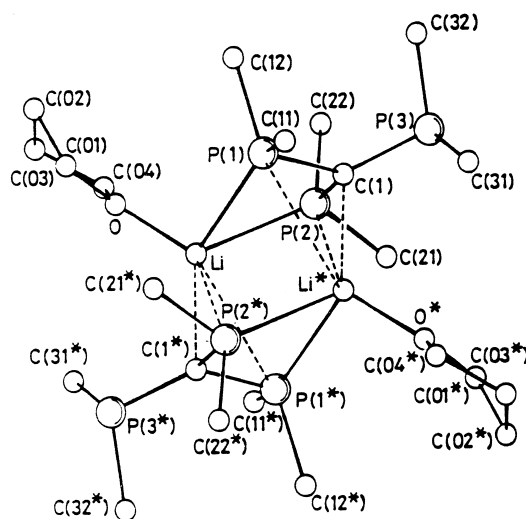


FIG. 14. Structure of $[\text{Li}\{\text{C}(\text{PMe}_2)_3\}(\text{THF})_2]$. Reproduced with permission from H. H. Karsch *et al.*, *Chem. Commun.* **1984**, 569. Copyright 1984, the Royal Society of Chemistry.

is reflected in the deviation from planarity of the CP_3 core of the phosphinomethanide ligand [sum of angles at $\text{C}(1) = 350.8^\circ$]. In common with other phosphinomethanide ligands, the $\text{P}-\text{C}(1)$ distances of 1.795(2), 1.796(2), and 1.812(2) Å are significantly shorter than the corresponding distances in the neutral triphosphine $\text{HC}(\text{PMe}_2)_3$ (average 1.856(7) Å), reflecting the partial double bond character of the $\text{P}-\text{C}$ bond caused by charge delocalization from the carbanion center to phosphorus in the anion (selected structural and NMR data for alkali metal phosphinomethanide complexes are given in Table IV).

As has been observed for (di)organophosphide complexes of the alkali metals, the structures and aggregation states of alkali metal phosphinomethanides are dramatically affected by the size and nature of the ligand substituents and the presence of additional coligands such as THF, tmeda, or pmdeta. The subtle interplay of these factors, and in particular the steric and electronic properties of substituents at both phosphorus and the α -carbon, defines the structures adopted by such complexes.

Several complexes of lithium with monophosphinomethanide ligands, $\text{R}_2\text{C}-\text{PR}'_2$, have been isolated and structurally characterized, with H. H. Karsch and co-workers making a particularly significant contribution to this work. Metalation of Ph_2PMe with Bu^nLi in the presence of tmeda yields the compound $\text{Li}(\text{CH}_2\text{PPh}_2)(\text{tmeda})$. Multinuclear NMR experiments suggested that this complex is monomeric in d_8 -THF solution, and an initial crystallographic investigation appeared to confirm that a monomeric structure was maintained in the solid state (124). However, reinvestigation of the crystal structure has indicated that the complex is dimeric in the solid state, $[\text{Li}(\text{CH}_2\text{PPh}_2)(\text{tmeda})]_2$ (**39**) (125). Each phosphinomethanide ligand bridges the two Li atoms via its C and P centers in a head-to-tail fashion to give a centrosymmetric dimer containing a six-membered $(\text{CPLi})_2$ ring in a chair conformation (Fig. 15). The $\text{P}-\text{Li}$ and $\text{C}-\text{Li}$ distances are 2.686(5) and 2.174(6) Å, respectively. This head-to-tail dimeric arrangement is a common feature of alkali metal phosphinomethanide chemistry.

The related tertiary phosphines PMe_3 and PMe_2Ph may also be metalated by $\text{Bu}^n\text{Li}(\text{tmeda})$, giving phosphinomethanide complexes that are shown by cryoscopy to be monomeric in benzene solution, but that crystallography confirms are dimeric in the solid state (126). Both complexes crystallize as dimers, $[\text{Li}(\text{CH}_2\text{PMeR})(\text{tmeda})]_2$ [$\text{R} = \text{Me}$ (**40**), Ph (**41**)], with a similar structure to that of **39**, containing a $(\text{CPLi})_2$ core. However, whereas **40** adopts a chair conformation, **41** is closer to a boat conformation with the phenyl groups in equatorial

TABLE IV

SELECTED STRUCTURAL AND NMR DATA FOR CRYSTALLOGRAPHICALLY CHARACTERIZED ALKALI METAL PHOSPHINOMETHANIDE COMPLEXES

Complex ^a	M–P (Å)	M–C (Å) ^b	δ_p (ppm) ^c	Ref.
[Li(CH ₂ PPh ₂)(tmeda)] ₂	2.593(7) ^d	2.150(8)	–1.9 (s, <i>d</i> ₈ -THF, 200 K)	124, 125
[Li(CH ₂ PPh ₂)(THF)] ₄	2.70(1)	2.21(1), 2.39(1)	8.31 (s, <i>d</i> ₈ -THF)	127
[Li{CH(SiMe ₃)(PMe ₂)}(tmeda)] ₂	2.680(7), 2.661(8), 3.042(8), 3.034(8)	2.249(9), 2.26(1)	–44.23 (s, C ₆ D ₆)	132, 133
[Li{CH(SiMe ₃)(PMe ₂)}(pmdeta)]	—	2.207(5)	—	136
[Li{C(SiMe ₃) ₂ (PMe ₂) ₂ Li(tmeda)]	2.716(9), 2.72(1), 2.88(1), 2.93(1)	2.18(1), 2.17(1)	–33.51 (s, C ₆ D ₆)	133, 134
[Li{C(SiMe ₃) ₂ (PMe ₂) ₂ }] ₄	2.519(4)	2.172(4)	—	136
[Li{C(SiMe ₃) ₂ (PMe ₂) ₂ }(THF)] ₂	2.584(6)	2.202(6)	—	137
[Li{C(SiMe ₃) ₂ P(C ₆ H ₄ -2-CH ₃ NMe ₂) ₂ }]	2.427(6)	—	–18.2 (q, <i>J</i> _{PLi} 88.9 Hz, C ₆ D ₆)	141
[Li{CH(PMe ₂) ₂ }(THF)] ₂	2.697(4), 2.685(4), 3.068(5), 3.108(5)	2.219(6)	—	131
[Li{CH(PPh ₂) ₂ }(THF)] ₂	2.607(6), 3.056(6), 2.949(6), 3.181(6)	2.242(8)	—	130
[Li{CH(PPh ₂) ₂ }(tmeda)]	2.582(4), 2.582(6)	—	—	129
[Li{C(SiMe ₃)(PPh ₂) ₂ }(tmeda)]	2.530(7), 2.532(6)	—	22.61 (q, <i>J</i> _{PLi} 48.6 Hz, C ₇ D ₈)	131
[Li{C(SiMe ₃)(PMe ₂) ₂ }(tmeda)]	2.507(6), 2.516(6)	—	—	130
[Li{C(SiMe ₃)(PMe ₂) ₂ }(THF)] ₂	2.641(8), 2.655(8), 2.959(8), 2.999(8)	2.298(9)	—	130
[Li{C(SiMe ₂ Ph)(PMe ₂) ₂ }] ₃	2.589(7), 2.606(7), 2.564(8), 2.573(7), 2.619(8), 2.641(7)	2.260(8), 2.208(9), 2.298(8)	–24.25 (q, <i>J</i> _{PLi} 51.8 Hz, C ₇ D ₈ , –100°C)	138, 139
[Li{C(SiMe ₂ Ph)(PMe ₂) ₂ }(tmeda)]	2.51(1), 2.54(1)	—	–26.30 (q, <i>J</i> _{PLi} 55.6 Hz, C ₆ D ₆)	139
[(THF) ₂ Li{(Ph ₂ P) ₂ CCH ₃ }] ₂	2.542(6), 2.559(6)	—	17.0 (s, <i>d</i> ₈ -THF)	145
[Li{C(PMe ₂) ₃ }(THF)] ₂	2.588(3), 2.684(3), 2.945(3), 2.998(3)	2.290(4)	—	122, 123
[Na{C(SiMe ₃) ₂ P(C ₆ H ₄ -2-CH ₃ NMe ₂) ₂ }(Et ₂ O) _{0.5} (DME) _{0.5} }]	2.8004(10)	—	–11.9 (C ₇ D ₈)	142
[K{C(SiMe ₃) ₂ P(C ₆ H ₄ -2-CH ₃ NMe ₂) ₂ }] ₄	3.2227(5)	—	–7.9 (<i>d</i> ₈ -THF)	144
<i>Heterometallic complexes:</i>				
[(tmeda)Li(PMe ₂ CH ₂) ₂ AlMe ₂]	2.606(5)	—	–50.76 (C ₇ D ₈)	148, 149
[(THF)(tmeda)Li(PMe ₂ CH ₂) ₂ AlMe ₂]	2.593(7)	—	–49.17 (C ₇ D ₈)	149
[(tmeda)LiClAlMe ₂]	2.669(7)	—	–32.66 (q, <i>J</i> _{PLi} 69.5 Hz, C ₇ D ₈ , –60°C)	150, 151
[{Li(THF)} ₂ Cr ₂ (CH ₂ PMe ₂) ₆]	2.549(4)	2.266(8)	–6.3 (s), –46.0 (q, <i>J</i> _{PLi} 62 Hz, <i>d</i> ₁₀ -diethyl ether)	152

^a Abbreviations as in Table I.^b M–C contact to the carbanion center.^c ³¹P{¹H} chemical shifts relative to 85% H₃PO₄ at ambient temperature unless otherwise stated (multiplicity, relevant coupling constants, solvent, and temperature in parentheses).^d Value(s) from a representative molecule in the unit cell.

positions. This is most likely a consequence of steric interactions between the large phenyl groups. Treatment of Me₂PhP with BuⁿLi in the presence of (–)-sparteine yields the complex [Li(CHPMePh)(sparteine)]₂ (**42**), which crystallizes with a structure similar to **41**,

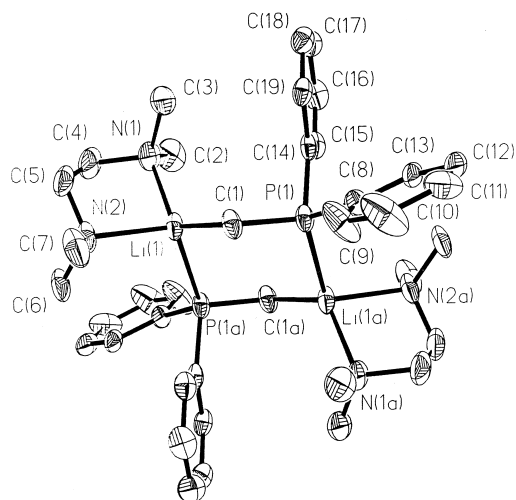
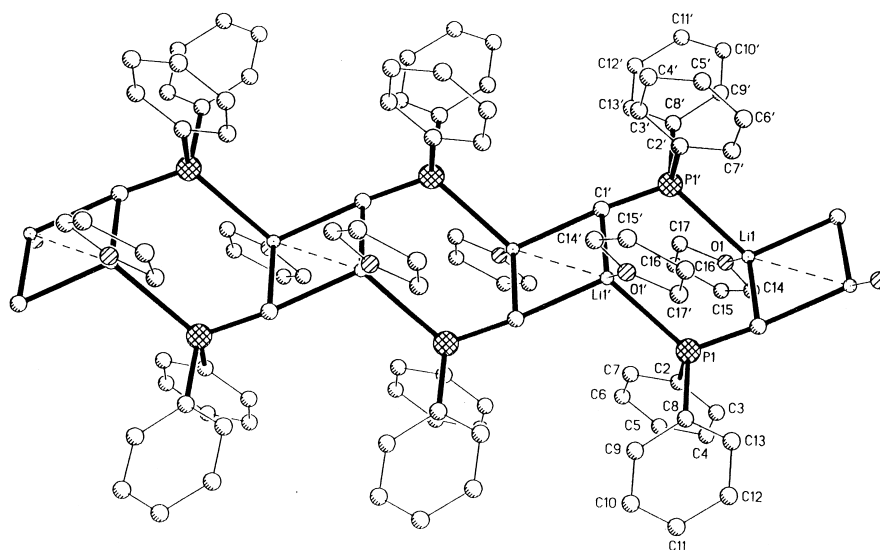


FIG. 15. Structure of $[\text{Li}(\text{CH}_2\text{PPh}_2)(\text{tmeda})]_2$ (**39**). Reproduced with permission from S. Blaurock *et al.*, *Organometallics* **1997**, *16*, 807. Copyright 1997, the American Chemical Society.

i.e., in a chair conformation. Both **41** and **42** are chiral at phosphorus and crystallize as *meso* diastereomers.

The preparation of $\text{LiCH}_2\text{PPh}_2$ in the absence of metal alkyl-activating polydentate amine donors was found to be more problematic. However, one report details the successful synthesis of $[\text{Li}(\text{CH}_2\text{PPh}_2)(\text{THF})]_x$ via a transmetalation reaction between $\text{Bu}_3\text{SnCH}_2\text{PPh}_2$ and Bu^nLi (**127**). Crystallography shows this complex to be an unusual infinite ladder polymer in the solid state. The ladders are made up from six-membered $(\text{PCLi})_2$ rings with a distorted chair conformation linked together by planar four-membered C_2Li_2 rings (Fig. 16). A distorted tetrahedral geometry is obtained by Li through the coordination of one molecule of THF per Li center. The Li–P distance [2.70(1) Å] is similar to those in **40–42**, whereas the Li–C distance [2.21(1) Å] within the $(\text{PCLi})_2$ rings is slightly longer [cf. 2.12(1)–2.174(4) Å for **40** and **42**]. The Li–C distance in the four-membered Li_2C_2 rings [2.39(1) Å] is somewhat longer than that within the six-membered $(\text{PCLi})_2$ rings. This structure is essentially similar to that of the sulfur-stabilized carbanion complex $[\text{Li}(\text{CH}_2\text{SMe})(\text{THF})]_x$ (**128**).

The structures of several simple lithium diphosphinomethanides $\text{Li}\{(\text{R}_2\text{P})_2\text{CR}\}$ have been investigated. The complex $[\text{Li}\{\text{CH}(\text{PPh}_2)_2\}(\text{tmeda})]$ (**43**) is monomeric in the solid state (**129**), the lithium being



bound by the two P atoms of the phosphinomethanide ligand (bonding mode **XII**) and a chelating tmeda coligand in a distorted tetrahedral arrangement. The CP₂Li four-membered ring is slightly puckered along the P...P vector (the angle between the normals of the P(1)–C(1)–P(2) and P(1)–Li–P(2) planes is 9.4°, but the Li...C(1) distance of 3.054(6) Å and the essentially planar carbanion center C(1) indicate that there is no significant C(1)...Li interaction.

The analogous THF complex $[\text{Li}\{\text{CH}(\text{PPh}_2)_2\}(\text{THF})]_2$ (**44**) crystallizes as centrosymmetric dimers with a core that is essentially identical to that of **38** in which each Li is in contact with two P atoms from one ligand and the carbanion center of another ligand (130). The lithium complex of the less sterically demanding ligand $\text{CH}(\text{PMe}_2)_2$ crystallizes from THF as the dimer $[\text{Li}\{\text{CH}(\text{PMe}_2)_2\}(\text{THF})]_2$ with a structure that is the same in all major features to that of **44** (131).

The nucleophilicity of the carbanion center in phosphinomethanide ligands is dramatically affected by the presence in an α -position of additional charge-stabilizing groups such as SiR_3 or PR_2 . As the number of such groups at the carbanion center increases, so the charge on the carbanion becomes increasingly delocalized toward the heteroatoms, reducing the nucleophilicity of the carbanion center and favoring coordination of metal centers by phosphorus. For example, like the

“unsubstituted” complex **38** (126), the silyl-substituted analogue $[\text{Li}\{\text{CH}(\text{SiMe}_3)(\text{PMe}_2)\}(\text{tmeda})]_2$ (**45**) crystallizes as a head-to-tail dimer with a $(\text{PCLi})_2$ core (132, 133). However, whereas **38** adopts a chair conformation in which the bond lengths and angles deviate little from those expected, complex **45** adopts a twist conformation. In **45** each Li is primarily in contact with a P atom from one ligand and a central C atom from the other ligand, supplemented by a further weak “cross-dimer” $\text{P} \cdots \text{Li}$ contact (Fig. 17a). The Li–P distances of 2.680(7) and 2.661(8) Å are significantly shorter than the “cross-dimer” $\text{Li} \cdots \text{P}$ contacts [3.042(8) and 3.034(8) Å]. The effect of the SiMe_3 group appears to be both steric and electronic in nature, tending to favor coordination by the P atom and causing an unusual twist conformation to be adopted.

Substitution of the carbanion center by a further SiMe_3 group has an even greater effect on the binding mode of the phosphinomethanide. Deprotonation of $\text{HC}(\text{SiMe}_3)_2(\text{PMe}_2)$ with $\text{Bu}^t\text{Li}/\text{tmeda}$ yields the novel complex $[\{\text{Li}(\text{tmeda})\}\{(\text{Me}_2\text{P})(\text{SiMe}_3)_2\text{C}\}_2\text{Li}]$ (133, 134). The complex may be described as a “head-to-head” dimer in which one lithium is primarily associated with the two P atoms and the two N atoms of the tmeda, while the other Li atom is coordinated by both of the central carbons of the phosphinomethanide ligands with supplementary weak coordination by the P atoms, such that the P atoms act as a bridge between the two lithiums (Fig. 17b). The Li(1)–P(2) and Li(1)–P(1) distances of 2.716(9) and 2.71(1) Å, respectively, are only slightly shorter than the Li(2)–P(1) and Li(2)–P(2) distances [2.88(1) and 2.92(1) Å]. This structure bears a striking resemblance to that of the complex $[\text{Li}(\text{THF})_4][\{(\text{Me}_3\text{Si})_3\text{C}\}_2\text{Li}]$, which crystallizes as solvent-separated ion pairs containing an anion in which lithium is coordinated solely by the two carbanion centers (135).

In the absence of coligands the complex $[\text{Li}\{\text{C}(\text{SiMe}_3)_2(\text{PMe}_2)\}]_x$ (**46**) may be isolated by the reaction of $\text{HC}(\text{SiMe}_3)_2(\text{PMe}_2)$ with Bu^nLi in refluxing hexane for 3 weeks (136). In spite of the presence of two sterically demanding, charge-stabilizing SiMe_3 groups, the complex consists of head-to-tail dimers in which the central $(\text{PCLi})_2$ core adopts a chair conformation. The dimers are linked into infinite chains via intermolecular $\text{Si}-\text{Me} \cdots \text{Li}$ contacts [$\text{Li} \cdots \text{C}(\text{Me}) = 2.514(4)$ Å], making the lithium atoms almost exactly trigonal planar (sum of angles at Li = 358.2°). The short Li–P distance [2.519(4) Å] reflects the low coordination number of lithium and compares with Li–P distances of 2.680(7) and 2.661(8) Å for the essentially four-coordinate Li atoms in **45**. Treatment of the solvent-free complex with THF yields the complex $[\text{Li}\{\text{C}(\text{SiMe}_3)_2(\text{PMe}_2)\}(\text{THF})]_2$, which crystal-

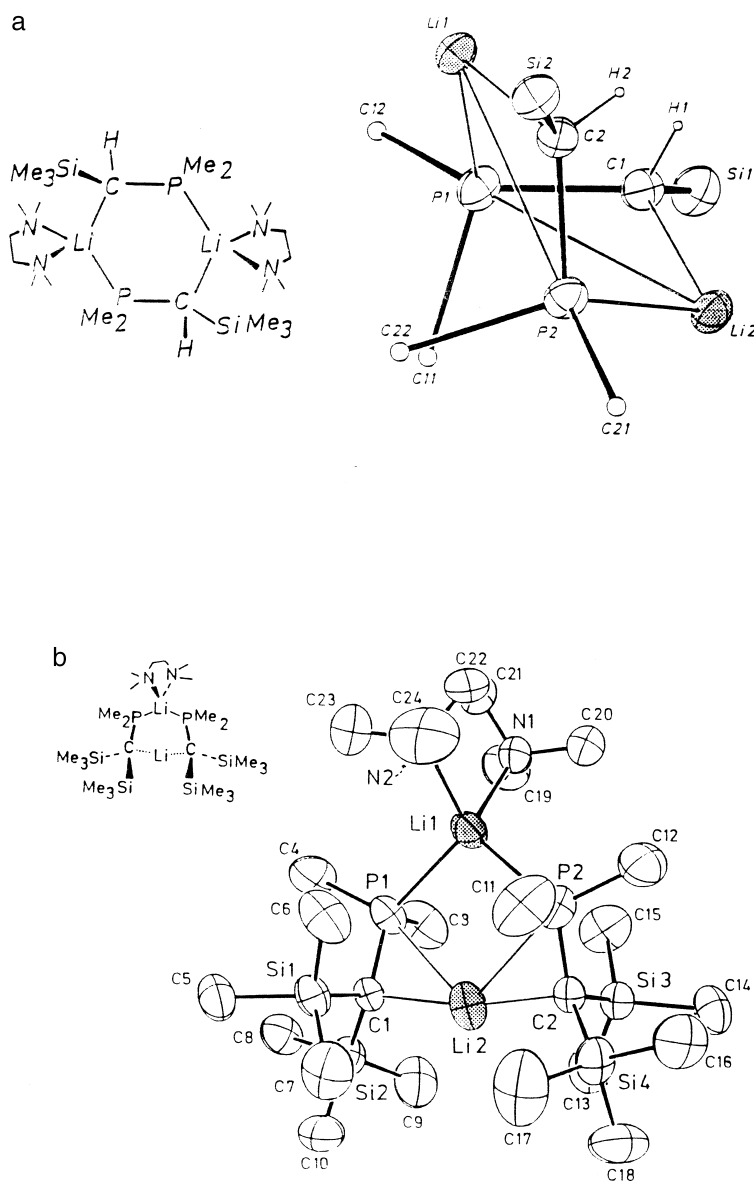


FIG. 17. Ligand bonding modes in and structures of (a) $[\text{Li}\{\text{CH}(\text{SiMe}_3)(\text{PMe}_2)\}(\text{tmeda})]_2$ and (b) $[\text{Li}(\text{tmeda})\text{Li}\{\text{C}(\text{SiMe}_3)_3(\text{PMe}_2)\}]_2$. (Reproduced with permission from (a) H. H. Karsch *et al.*, *J. Organomet. Chem.* **1988**, 342, C29, copyright 1988, Elsevier Science Ltd.; (b) H. H. Karsch *et al.*, *Chem. Commun.* **1987**, 1033, copyright 1988, the Royal Society of Chemistry.)

lizes as typical centrosymmetric dimers with a chair-type $(\text{PCLi})_2$ core ($\text{Li}-\text{P} = 2.584(6)$, $\text{Li}-\text{C} = 2.202(6)$ Å) (137). The structures adopted by the three complexes $[\{\text{Li}(\text{tmeda})\}\{\text{Me}_2\text{P}(\text{SiMe}_3)_2\text{C}\}_2\text{Li}]$, $[\text{Li}\{\text{C}(\text{SiMe}_3)_2(\text{PMe}_2)\}(\text{THF})]_2$, and $[\text{Li}\{\text{C}(\text{SiMe}_3)_2(\text{PMe}_2)\}]_x$ amply illustrate the effect of co-ligands on phosphinomethanide binding modes and aggregation states.

These effects are similarly demonstrated by the adducts of several related phosphinomethanide complexes. For example, whereas compound **45** is dimeric with a $(\text{PCLi})_2$ core, the complex $[\text{Li}\{\text{CH}(\text{SiMe}_3)(\text{PMe}_2)\}(\text{pmdeta})]$ (136) exists as a monomer in the solid state in which there are no inter- or intramolecular contacts between lithium and phosphorus; the lithium is coordinated solely by the three nitrogen atoms of the *pmdeta* and the central carbanion of the phosphinomethanide ligand. Similarly, whereas $[\text{Li}\{\text{C}(\text{SiMe}_3)(\text{PMe}_2)_2\}(\text{THF})]_2$ is a dimer in which each lithium is bound in an η^2 -PP fashion by one ligand and by the central carbon of the other ligand (binding mode **XIV**; $\text{Li}-\text{P} = 2.641(8)$, $2.655(8)$ Å, $\text{Li}-\text{C} = 2.298(9)$ Å), the adduct $[\text{Li}\{\text{C}(\text{SiMe}_3)(\text{PMe}_2)_2\}(\text{tmeda})]$ (**47**) is monomeric in the solid state, the lithium being coordinated by the two P atoms and two N atoms of the phosphinomethanide and *tmeda* ligands in a tetrahedral geometry, with no $\text{Li}\cdots\text{C}$ contacts (binding mode **XII**) (130). The complex $[\text{Li}\{\text{C}(\text{SiMe}_3)(\text{PPh}_2)_2\}(\text{tmeda})]$ (**48**) adopts a similar monomeric structure in the solid state (131), although steric buttressing by the phenyl groups increases the P–Li distances from 2.507(6) and 2.516(6) Å in **47** to 2.697(4) and 2.685(4) Å in **48**.

Incorporation of additional donor functionality into the periphery of phosphinomethanide ligands also has dramatic consequences for the structures of their alkali metal complexes. The complex $[\text{Li}\{\text{C}(\text{SiMe}_2\text{Ph})(\text{PMe}_2)_2\}]_3$ (**49**) crystallizes as solvent-free cyclic trimers (Fig. 18), in which each lithium is primarily coordinated by two P atoms from one ligand and the carbanion center of an adjacent ligand (138, 139). This is supplemented by an essentially η^2 -interaction with the *ipso* and an *ortho*-carbon of the phenyl ring associated with the carbanion bonded to lithium. Each Li is thus bound by two P atoms, two aryl carbons, and a central carbon of the phosphinomethanide ligands.

This Li–phenyl interaction is similar to the η^1 -Ph contact observed in the silicon-stabilized carbanion complex $[\text{Li}\{\text{C}(\text{SiMe}_2\text{Ph})_3\}(\text{THF})]$ (140). Addition of *tmeda* to **49** yields the monomeric compound $[\text{Li}\{\text{C}(\text{SiMe}_2\text{Ph})(\text{PMe}_2)_2\}(\text{tmeda})]$ in which the lithium is bound by the two P atoms of the phosphinomethanide ligand and the two N atoms of the *tmeda* in a distorted tetrahedral geometry (139). There

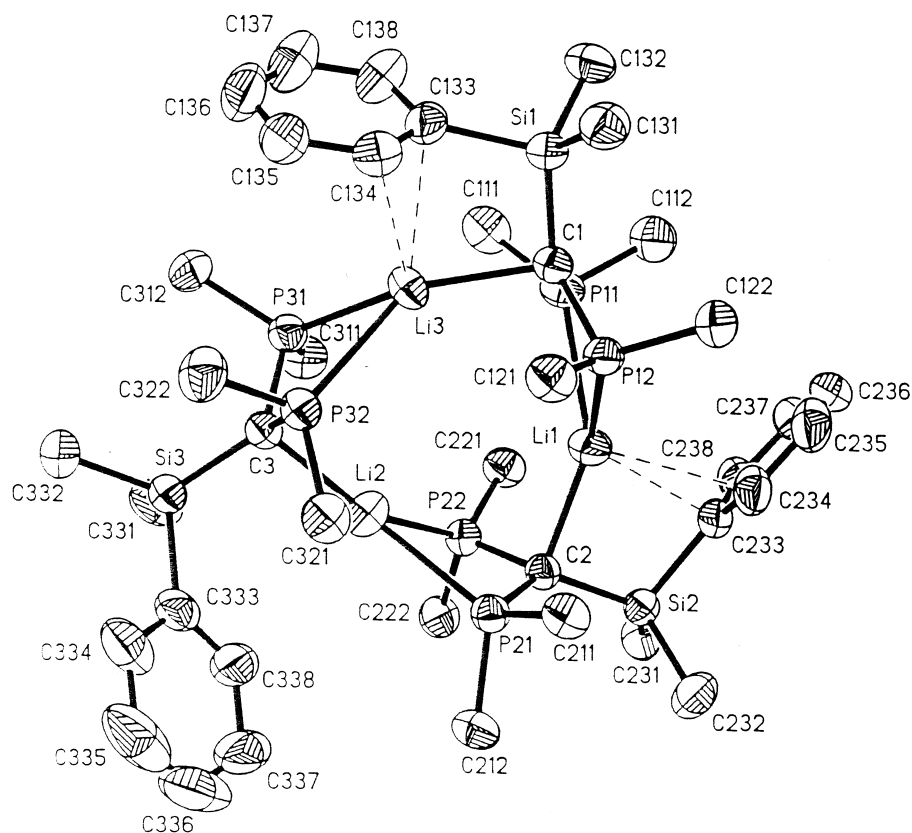


FIG. 18. Structure of $[\text{Li}\{\text{C}(\text{SiMe}_2\text{Ph})(\text{PMe}_2)_2\}]_3$. Reproduced with permission from H. H. Karsch *et al.*, *J. Organomet. Chem.* **1994**, 474, C1. Copyright 1994, Elsevier Science Ltd.

are no contacts between the lithium and carbons in the aromatic ring.

Functionalization by amino groups leads to a unique binding mode for a phosphinomethanide ligand. Metalation of $\{(\text{Me}_3\text{Si})_2\text{CH}\}\text{P}(\text{C}_6\text{H}_4\text{-2-CH}_2\text{NMe}_2)_2$ (**50**) with Bu^nLi gives the monomeric complex $[\text{Li}\{(\text{SiMe}_3)_2\text{C}\}\text{P}(\text{C}_6\text{H}_4\text{-2-CH}_2\text{NMe}_2)_2]$ (**51**) (141). In contrast to the metalation of $\text{HC}(\text{PMe}_2)(\text{SiMe}_3)_2$, which requires heating under reflux for 3 weeks in hexane, this reaction is complete within 1 hour at room temperature. The enhanced reactivity of **50** is attributed to the participation of the amino groups in the deprotonation step (chelation assistance). Unusually for a monophosphinomethanide, the ligand binds to lithium through its P and N atoms only (bonding mode **IX**),

generating two six-membered chelate rings; there is no contact between the lithium atom and the planar sp^2 -hybridized carbanion center C(1) (Fig. 19).

The P–Li distance in **51** of 2.427(6) Å is extremely short and compares with distances of 2.584(6), 2.519(4), and 2.680(7) and 2.661(8) Å in $[\text{Li}\{\text{C}(\text{SiMe}_3)_2(\text{PMe}_2)\}(\text{THF})]_2$ (**137**), $[\text{Li}\{\text{C}(\text{SiMe}_3)_2(\text{PMe}_2)\}]_x$ (**136**) and $[\text{Li}\{\text{CH}(\text{SiMe}_3)(\text{PMe}_2)\}(\text{tmeda})]_2$ (**132**), respectively. The related methoxy-substituted tertiary phosphine $\{(\text{Me}_3\text{Si})_2\text{CH}\}\text{P}(\text{C}_6\text{H}_4\text{-2-OMe})_2$ also undergoes facile deprotonation with Bu^nLi to give the complex $[(\text{Et}_2\text{O})\text{Li}\{(\text{SiMe}_3)_2\text{C}\}\text{P}(\text{C}_6\text{H}_4\text{-2-OMe})_2]$ (**52**) (**142**). However, the geometric constraints of the less flexible *o*-anisyl substituents prevent the formation of more than one chelate ring, leading to a PCO bonding mode; the ligand binds through both its P and C centers in an η^2 -fashion with supplementary coordination by the anisyl O atom in a five-membered chelate ring. This η^2 -PC binding mode (mode **X** Scheme 3) is unique in alkali metal phosphinomethanide chemistry.

3. Heavier Alkali Metal Phosphinomethanides

Although potassium complexes of phosphinomethanide ligands have been used in the synthesis of lanthanide phosphinomethanides (**143**), it is only very recently that a heavier alkali metal phosphinomethanide complex has been isolated and structurally characterized.

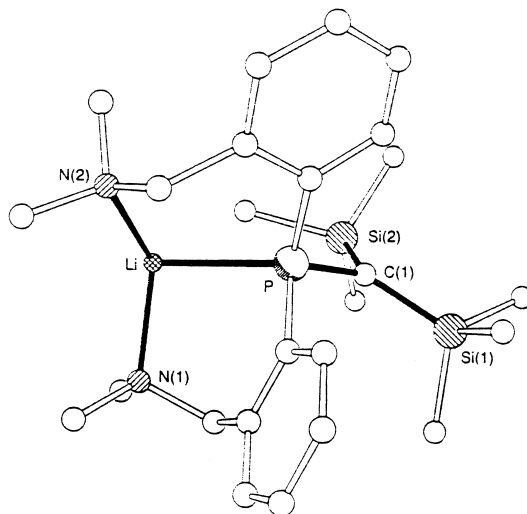


FIG. 19. Structure of $[\text{Li}\{\text{C}(\text{SiMe}_3)_2(\text{C}_6\text{H}_4\text{-2-CH}_2\text{NMe}_2)_2\}]$. Reproduced with permission from W. Clegg *et al.*, *Chem. Commun.* **1998**, 1129. Copyright 1998, the Royal Society of Chemistry.

Metathesis between the lithium complex **51** and KOBu^t (**144**) or NaOBu^t (**142**) yields $[\text{K}\{(\text{SiMe}_3)_2\text{C}\}\text{P}(\text{C}_6\text{H}_4\text{-2-CH}_2\text{NMe}_2)_2]_x$ (**53**) and $[\text{Na}\{(\text{SiMe}_3)_2\text{C}\}\text{P}(\text{C}_6\text{H}_4\text{-2-CH}_2\text{NMe}_2)_2(\text{Et}_2\text{O})_{0.5}(\text{DME})_{0.5}]$ (**54**), respectively, the first examples of such complexes to be structurally characterized. The sodium complex is essentially similar to **51** except that, in addition to coordination by the phosphorus and two nitrogen atoms of the ligand, the sodium is bound by a disordered 50/50 mix of ether and DME. The potassium complex **53** is also coordinated by the ligand in a PN_2 mode with no contact between the cation and the carbanion center (Fig. 20a). However, the greater coordination requirements of the large potassium cation result in further coordination of the metal

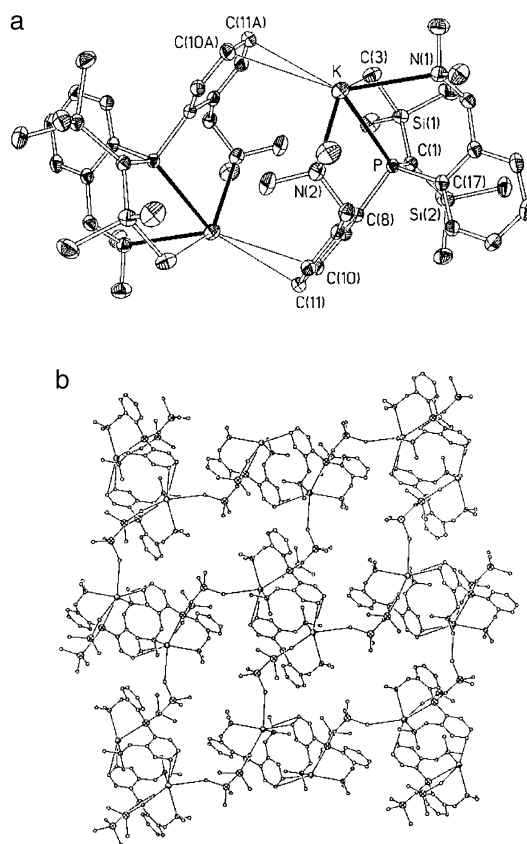


FIG. 20. (a) Structure of the dimeric subunits in $[\text{K}\{\text{C}(\text{SiMe}_3)_2(\text{C}_6\text{H}_4\text{-2-CH}_2\text{NMe}_2)_2\}]_x$ (**53**); (b) sheet arrangement of the subunits in **53**. Reproduced with permission from W. Clegg et al., *Organometallics* **1999**, *18*, 2939. Copyright 1999, the American Chemical Society.

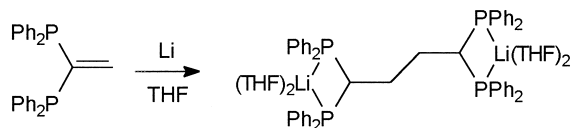
center via an intramolecular Si–Me \cdots K contact. In addition to this the complex forms dimers via η^2 -interactions between potassium and an aromatic ring from an adjacent ligand.

These dimeric units are then further linked into a two-dimensional sheet arrangement via intermolecular Si–Me \cdots K contacts (Fig. 20b). The intramolecular Me \cdots K distance, C(3) \cdots K [3.4646(17) Å], is significantly longer than the intermolecular distance, C(5B) \cdots K (3.3981(16) Å), but both are within the typical range of distances for K \cdots Me contacts (15). Once again the Na–P and K–P distances [2.8004(10) and 3.2227(5) Å, respectively] are extremely short. Complex **53** represents the first example of a crystallographically authenticated P–K contact where a negative charge is not localized on the phosphorus atom [i.e., where the phosphorus is not bound as a (di)organophosphide ligand].

4. Di- and Poly-anionic Phosphinomethanides

A handful of complexes have been reported in which a di- or poly-anionic bis(phosphinomethanide) ligand is bound to an alkali metal. For example, the novel synthesis of a bis(phosphinomethanide) complex of lithium has been reported: Reaction of the vinylidene phosphine (Ph₂P)₂C=CH₂ with elemental lithium in THF under argon gives the butane-1,4-diide salt {(THF)₂Li(Ph₂P)₂CCH₂}₂ (**55**) in high yield (145). The reaction proceeds according to Scheme 4 via the coupling of a phosphorus-stabilized radical anion, Li⁺[(Ph₂P)CCH₂][−].

The complex consists of a bis(diphosphinomethanide) ligand binding a lithium atom at each end in an η^2 -PP coordination mode [Li–P = 2.542(6) and 2.559(6) Å]. The lithium atoms achieve four-coordination through the coordination of two molecules of THF each. Hydrolysis of this complex is an excellent route to the otherwise inaccessible tetraphosphine {(Ph₂P)₂CHCH₂}₂, a potentially useful polyphosphine ligand analogous to two linked bis(diphenylphosphino)methane (dppm) moieties.



SCHEME 4. Li-mediated radical coupling of a vinylidene phosphine to give a bis(diphosphinomethanide) complex. Reproduced with permission from W. Clegg *et al.*, *Organometallics* **1998**, 17, 5231. Copyright 1998, the American Chemical Society.

An example of a bis(phosphinomethanide) tetraanion has also been reported (146). Treatment of $\text{MeP}(\text{CH}_2\text{C}_6\text{H}_4\text{-2-Br})_2$ with 2 equiv of Bu^nLi in pentane in the presence of 2 equiv of tmeda at -20°C yields the dilithium salt $\text{MeP}(\text{CH}_2\text{C}_6\text{H}_4\text{-2-Li})_2$ via Li–Br exchange. Further treatment of this dianion with 2 equiv of $\text{Bu}^n\text{Li}(\text{tmeda})$ leads to deprotonation at the benzylic site α - to phosphorus to give the pentane soluble complex $[(\text{tmeda})_2\text{Li}_2\{\text{MeP}(\text{CHC}_6\text{H}_4\text{-2-Li})_2\}]_2$ containing a quadruply charged carbanion. This compound adopts a complex dimeric structure containing a rhombus-shaped Li_4 core (Fig. 21).

In contrast, the simpler lithiobenzylphosphine $[\text{Li}(\text{CHPhPPh}_2)(\text{OEt}_2)_2]$ exhibits no short $\text{Li} \cdots \text{P}$ contacts in the solid state (147).

5. Heterometallic Phosphinomethanides

The ability of phosphinomethanide ligands to bridge between two metal centers has enabled the synthesis of a number of heterometallic complexes in which a P–Li contact is maintained. For example, reaction of $[\text{Me}_2\text{Al}(\text{CH}_2\text{PMe}_2)]_2$ with $(\text{tmeda})\text{LiCH}_2\text{PMe}_2$ in ether yields the “ate” complex $[(\text{tmeda})\text{Li}(\text{PMe}_2\text{CH}_2)_2\text{AlMe}_2]$ (56) (148, 149). The phosphinomethanide ligands bridge the Al and Li centers in a head-to-

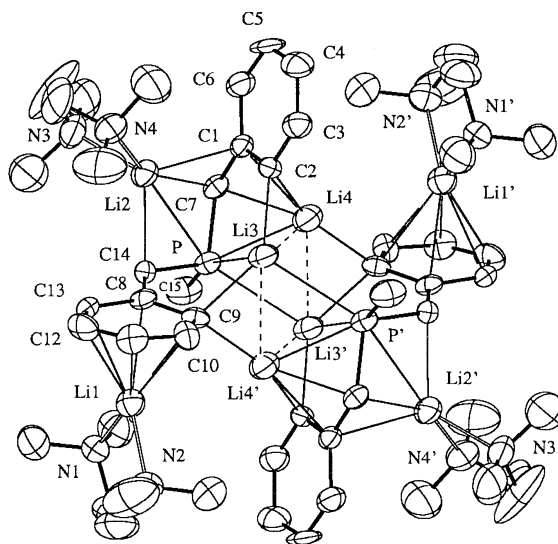


FIG. 21. Structure of $[(\text{tmeda})_2\text{Li}_2\{\text{MeP}(\text{CHC}_6\text{H}_4\text{-2-Li})_2\}]_2$. Reproduced with permission from M. Winkler *et al.*, *Angew. Chem. Int. Ed. Engl.* **1994**, 33, 2279. Copyright 1994, Wiley-VCH.

head fashion with both P atoms coordinated to lithium [Li–P = 2.606(5) Å] and both carbanion centers bound to aluminum. The six-membered $\text{AlC}_2\text{P}_2\text{Li}$ ring adopts an envelope-type conformation with the Li atom deviating from the C_2P_2 plane by only 0.14 Å to give an angle of 5° between the P_2C_2 and LiP_2 planes; the angle between the AlC_2 and P_2C_2 planes is 66.7° . This complex may also be obtained from the reaction of $[\text{Al}(\text{CH}_2\text{PMe}_2)_3]$ with MeLi/tmeda in ether, which gives a mixture of **56** and $[\text{Li}(\text{PMe}_2\text{CH}_2)_4\text{Al}]_n$ due to rapid ligand exchange. The reaction of $[\text{Me}_2\text{Al}(\text{CH}_2\text{PMe}_2)_2]$ with MeLi/tmeda in THF/ether yields the complex $[(\text{THF})(\text{tmeda})\text{Li}(\text{PMe}_2\text{CH}_2)\text{AlMe}_3]$ in which the phosphinomethanide ligand bridges the Al and Li centers, with the lithium again bound by the phosphorus end of the ligand [P–Li = 2.593(7) Å] (148, 149). This complex is unstable in solution, decomposing to **56** and $[\text{Li}(\text{tmeda})_2][\text{AlMe}_4]$ over several days. Reaction of $[(\text{tmeda})\text{Li}\{\text{PMe}_2\text{C}(\text{SiMe}_3)_2\}_2\text{Li}]$ with Me_2AlCl in pentane yields the novel heterocyclic complex $[(\text{tmeda})\text{LiClAl}(\text{Me})_2\text{C}(\text{SiMe}_3)_2\text{PMe}_2]$ (150, 151). The core of this complex consists of a five-membered Li–Cl–Al–C–P heterocycle; the phosphinomethanide and Cl ligands bridge the Al and Li centers. The coordination sphere of the lithium thus consists of the two nitrogen atoms of the tmeda, the chloride bridge and the phosphorus of the bridging phosphinomethanide ligand [Li–P = 2.669(7) Å].

Three related complexes have been reported in which a phosphinomethanide bridges between lithium and a transition metal center (152). Reaction of 2 equiv of $\text{CrCl}_2(\text{THF})_2$ with 6 equiv of $\text{LiCH}_2\text{PMe}_2$ in ether yields a deep red solution from which crystals of $[\{\text{Li}(\text{THF})\}_2\text{Cr}_2(\text{CH}_2\text{PMe}_2)_6]$ crystallize in 80% yield. The complex consists of a pair of quadruply bonded chromium atoms bridged in a *trans*- μ - η^2 head-to-tail fashion by two phosphinomethanide ligands. The remaining phosphinomethanide ligands are bound in an η^1 -fashion via their carbanion centers to the two Cr atoms, two at each end. The lithium atoms are then coordinated by the phosphorus atoms of the ligands such that a six-membered $\text{LiP}_2\text{C}_2\text{Cr}$ heterocycle is formed at each end of the complex. Each Li atom is additionally bound to one molecule of THF and has a weak contact to the carbanion center of one of the phosphinomethanide ligands bridging the Cr_2 unit. This complex is the first example of a homoleptic transition metal phosphinomethanide to be reported. In the presence of tmeda this compound crystallizes as either the molecular species $[\{\text{Li}(\text{tmeda})\}_2\text{Cr}_2(\text{CH}_2\text{PMe}_2)_6]$ or the chain polymer $[\text{Li}_2\text{Cr}_2(\text{CH}_2\text{PMe}_2)_6(\text{tmeda})]_x$, both of which contain a similar core to the THF complex. However, in the latter complex these units are linked into an infinite

chain by tmeda ligands that bridge between the lithium atoms in adjacent $\text{Cr}_2(\text{CH}_2\text{PMe}_2)_6\text{Li}_2$ units (152).

Two heterometallic lithium–lanthanide complexes have been reported; however, in neither case is a strong P–Li contact preserved (153). The complex $[\text{Li}\{\text{C}(\text{SiMe}_3)_2(\text{PMe}_2)\}_4\text{La}]$ is obtained, regardless of stoichiometry, from the reaction of $\text{La}(\text{O}_3\text{SCF}_3)_3$ and $\text{Li}\{\text{C}(\text{SiMe}_3)_2(\text{PMe}_2)\}$. The four ligands form PP-chelates with the La center in a distorted dodecahedral geometry. The lithium atom is then coordinated by the central carbons of two of the ligands, along with weak interactions with one phosphorus on each of the two ligands [$\text{Li}\cdots\text{P} = 2.879(8)$ and $2.814(7)$ Å] and two methyl groups, one from the PMe_2 group and one from the SiMe_3 group of the same ligand. The complex $[\{(\text{THF})\text{Li}\}_2\text{YbI}_2\{\text{C}(\text{SiMe}_3)_2(\text{PMe}_2)\}_2]$, prepared from YbI_2 and $\text{Li}\{\text{C}(\text{SiMe}_3)_2(\text{PMe}_2)\}$, exhibits contacts between each lithium and THF, the iodine atom and a central carbanion of one phosphinomethanide ligand, but not between lithium and phosphorus (153).

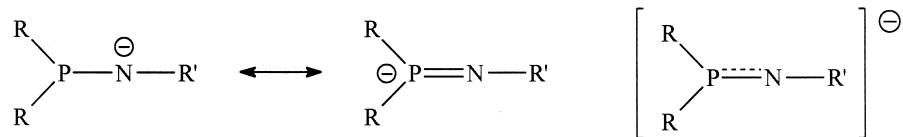
6. Arsinomethanides

Whereas alkali metal phosphinomethanides have been well studied and a large number of complexes have been structurally characterized, there are apparently no reports of alkali metal complexes with arsenic-stabilized carbanions.

B. IMINOPHOSPHIDES/PHOSPHINOAMIDES

Although alkali metal complexes of ligands in which phosphorus is α to a carbanion center are well established, similar complexes where phosphorus is α to an anionic center other than carbon are relatively rare, and few such complexes exhibit a genuine $\text{P}\cdots\text{M}$ contact. However, within the past few years the groups of Ashby and Ellermann have reported the synthesis and structural characterization of a number of iminophosphide/phosphinoamide complexes of the group 1 metals (for the purposes of this review these ligands will be termed phosphinoamides). These ligands may be regarded as deriving from deprotonation either of a phosphorus(III)-substituted secondary amine ($\text{R}_2\text{P}-\text{NHR}$) or of a phosphorus(V) imine ($\text{R}_2\text{HP}=\text{NR}$), although in practice the former route is typically used in their synthesis and is perhaps the more accurate description (*vide infra*). In the former case the formal charge on the anion would be localized on nitrogen (a phosphinoamide), whereas in the latter case the formal charge would be localized on phosphorus (an iminophosphide). The true nature of

these ligands lies somewhere between these extremes; the charge is somewhat delocalized (via hyperconjugation or $d\pi$ - $p\pi$ interactions) from the nitrogen center to phosphorus in a similar manner to the situation described for the analogous phosphinomethanide ligands.



The first such complex to be structurally characterized, $[\text{Li}(\text{PhNPPh}_2)(\text{OEt}_2)_2]$ (**57**), was synthesized by the reaction of PhNHPPh_2 with Bu^nLi in ether (*154*). The complex consists of centrosymmetric dimers with a planar Li_2N_2 core typical of lithium amides (*1, 2*). Each lithium is bound in an η^2 -fashion to both the nitrogen and phosphorus centers of a phosphinoamide ligand with $\text{Li}-\text{N}$ distances of 2.023(4) and 2.024(4) Å and a $\text{Li}-\text{P}$ distance of 2.684(3) Å; the cross-dimer $\text{Li} \cdots \text{P}$ distance of 3.004(4) Å is at the higher end of the range of known $\text{Li}-\text{P}$ contacts. Each lithium is further coordinated to a molecule of diethyl ether. Of particular interest in these complexes is the $\text{P}-\text{N}$ distance, which for **57** is 1.672(2) Å, suggesting partial $\text{P}-\text{N}$ double bond character.

The related complexes $[\text{Li}\{\text{mes}^*\text{NPPh}_2\}(\text{OEt}_2)_2]$ (**58**), $[\text{Li}\{\text{Bu}^t\text{CH}_2\text{NPPh}_2\}(\text{OEt}_2)_2]$ (**59**), and $[\text{Li}(\text{Pr}^i\text{NPPh}_2)(\text{OEt}_2)_2]$ (**60**) have all been crystallographically characterized (*155*). Complexes **59** and **60** adopt similar structures to **57** containing a central N_2Li_2 core with weak $\text{P} \cdots \text{Li}$ contacts ($\text{P} \cdots \text{Li} = 2.633(6)$ and $2.693(7)$ Å for **59** and **60**, respectively). However, the monomeric complex **58** exhibits no short contacts between Li and P; the *trans* configuration about the $\text{P}-\text{N}$ bond, caused by the steric bulk of the mes^* substituent at nitrogen, results in orientation of the phosphorus lone pair away from the lithium center. Calculations suggest that the relative energies of the *cis* and *trans* forms of simple phosphinoamides of the form $[\text{F}_n\text{H}_{(1-n)}\text{N}-\text{PF}_m\text{H}_{(2-m)}]^-$ ($n = 0, 1$; $m = 0-2$) range from ~ 0 kcal mol $^{-1}$ for $\text{HN}-\text{PH}_2^-$ to 6 kcal mol $^{-1}$ for $\text{FN}-\text{PH}_2^-$ (*156*), although a significant energy barrier of up to 22 kcal mol $^{-1}$ exists between the two forms. These calculations also indicate that the stabilizing effect of phosphorus and consequent shortening of the $\text{P}-\text{N}$ bond in these systems is best attributed to $\text{N}-\text{P}$ negative hyperconjugation (i.e., delocalization of charge from the N_p lone pair into the $\text{P}-\text{X}$ σ^* orbitals) and that the best description of these ligands is as phosphinoamides with the negative charge localized largely on nitrogen. Calculations on the model complex

[Li(HNPH₂)] do not indicate that short P···Li contacts are favored (156).

The bis(diphenylphosphino)amide complex [Li{N(PPh₂)₂}(THF)₃] has been structurally characterized (157). The complex is monomeric in the solid state with the lithium coordinated in an η^2 -fashion by the N and P atoms of the phosphinoamide ligand and three molecules of THF. The Li···P distance is 2.964(9) Å. Multinuclear NMR studies on this complex show that at low temperature restricted rotation about the P–N bond becomes evident. The activation barrier for this process at –80°C (the coalescence temperature) is 8.1 kcal mol^{–1}. The sodium and potassium analogues of this complex have also been structurally characterized. The sodium complex [Na{N(PPh₂)₂}(pmdeta)] is monomeric in the solid state with the sodium atom coordinated by the N and one of the P atoms of the phosphinoamide ligand [Na···P = 2.9619(11) Å] and the three nitrogen atoms of the pmdeta (158). Additional weak contacts to one of the *ortho* carbons of a phenyl group and one of the methylene carbons of the pmdeta are also present in the structure. The potassium complex [K{N(PPh₂)₂}(pmdeta)] is also monomeric in the solid state but exhibits no significant K···P contacts (159).

IV. Tertiary Phosphine-Functionalized Ligands

The low affinity of the alkali metals for neutral P-donor ligands has hampered efforts to synthesize complexes in which there is a genuine R₃P–M interaction (see Section I). However, this poor affinity may be overcome by incorporating a remote phosphine functionality into a potentially chelating anionic ligand, such as a phosphine-substituted alkoxide, amide, or aryl, and several alkali metal complexes of such ligands have been isolated.

1. Phosphine-Functionalized C-Donor Ligands

The synthesis of the phosphine-substituted benzyl compound Li(tmeda)(CH₂C₆H₄-2-PPh₂) by the reaction of 2-CH₃C₆H₄PPh₂ with BuⁿLi(tmeda) was reported in 1971, but the complex was not well characterized (160). However, treatment of this complex with Me₃SiCl yields the tertiary phosphine (Me₃Si)CH₂C₆H₄-2-PPh₂, which itself undergoes facile deprotonation with BuⁿLi(tmeda) to give the complex [Li(tmeda){CH(Me₃Si)C₆H₄-2-PPh₂}], which has been structurally characterized (126). The ligand binds to the metal center through both its carbanion and phosphine centers to give a five-membered

chelate ring. A distorted tetrahedral geometry about the lithium atom is achieved by the coordination of the two nitrogen atoms of the tmeda coligand. The Li–P and Li–C distances of 2.65(1) and 2.25(1) Å, respectively, are within the ranges normally found for such contacts (selected structural and NMR data for alkali metal complexes of phosphine-functionalized anionic ligands are summarized in Table V).

Another example of a tertiary phosphine-functionalized aryl ligand is obtained by treatment of 2-BrC₆H₄PPh₂ with BuⁿLi in ether, which yields the complex [Li(C₆H₄-2-PPh₂)(OEt₂)₂] (61) via a lithium–halogen exchange reaction (161). The solid-state structure of 61 consists of centrosymmetric aryl-bridged dimers with a central C₂Li₂ core, with each lithium coordinated by the C and P atoms of a chelating phosphinoaryl ligand. Interestingly, the 2-(diphenylphosphino)phenyl ligands are essentially isostructural with triphenylphosphine, having the three phenyl rings nearly perpendicular. The Li–P distances in the four crystallographically independent dimers in the unit cell range from 2.694(6) to 2.752(6) Å. This Li–P contact has the consequence that the bridging aryl rings are twisted away from the perpendicular orientation (with respect to the Li₂C₂ plane) usually found in aryl-bridged dimers. In toluene solution the ³¹P and ⁶Li NMR spectra of a ⁶Li-enriched sample consist of singlets from –50 to +20°C, suggesting rapid exchange of the P–Li bonds in the dimer and consequent loss of P–Li coupling. However, the signal due to the metalated carbon in the ¹³C{¹H} NMR spectrum consists of a doublet of quintets (*J*_{PC} = 99.9 Hz, *J*_{LiC} = 8.3 Hz), consistent with the preservation of a dimeric structure in solution. In THF solution the signal for the same carbon consists of a doublet of triplets (*J*_{PC} = 106.8 Hz, *J*_{LiC} = 14 Hz), whereas the ³¹P and ⁶Li spectra again consist of singlets across a wide temperature range, consistent with a monomeric structure in this solvent.

An interesting diphosphine-substituted aryllithium complex has been reported (162). Reaction of 2,6-(Me₂PCH₂)₂C₆H₃Br with BuⁿLi in pentane in the presence of a small amount of tmeda yields the solvent-free complex [Li{2,6-(Me₂PCH₂)₂C₆H₃}]₂ (62), in which the aryl-bridged dimers contain a central planar C₂Li₂ core. In addition to the two Li–C interactions, each lithium binds to the two P atoms of the ligand, such that each ligand acts as a PCP tridentate bis-chelate and the lithium atoms obtain a highly distorted tetrahedral geometry [P–Li = 2.668(3)/2.544(4), 2.667(3)/2.513(4), 2.668(4)/2.550(4), and 2.627(4)/2.586(4) Å for the two crystallographically independent molecules in the unit cell]. In contrast to 61, the two phenyl rings are almost perpendicular to the C₂Li₂ plane, the greater flexibility of the

TABLE V

SELECTED STRUCTURAL AND NMR DATA FOR CRYSTALLOGRAPHICALLY CHARACTERIZED
ALKALI METAL COMPLEXES OF TERTIARY PHOSPHINE-FUNCTIONALIZED LIGANDS

Complex ^a	M–P (Å)	δ_P (ppm) ^b	Ref.
[Li{2,6-(Me ₂ PCH ₂) ₂ C ₆ H ₃ }] ₂	2.668(3), 2.667(3), 2.668(4), 2.627(4) ^c	–41.8 (septet, J_{PLi} 21 Hz, C ₇ D ₈ , 298 K) [–40.5 (q, J_{PLi} 44 Hz, C ₇ D ₈ , 193 K)]	162
[Li{C ₆ H ₄ -2-PPh ₂ }(OEt ₂)] ₂	2.694(6) ^c	—	161
[Li{CH(SiMe ₃)C ₆ H ₄ -2-PPh ₂ }(tmeda)]	2.65(1)	–14.7 (C ₆ D ₆)	126
[Li{MeP(C ₆ H ₄ -2-CH ₂ NMe ₂)(C ₆ H ₄ -2-CHNMe ₂)}] ₂	2.482(4), 2.553(4)	–47.6 (septet, J_{PLi} 31.6 Hz, C ₇ D ₈ , 297 K) [–47.6 (q, J_{PLi} 63.2 Hz, C ₇ D ₈ , 208 K)]	163
[Li ₄ {PhP(C ₆ H ₃ -2-S-3-SiMe ₃) ₂ }] ₂ [–] (DME) ₂]	2.400(12) ^c	–12.9 (s, C ₇ D ₈)	171
[Li{OC(Bu ^t) ₂ CH ₂ PMe ₂ }] ₂	2.50(1)	–55.9 (septet, J_{PLi} 30 Hz, C ₇ D ₈)	169
[Li{OC(Bu ^t) ₂ CH ₂ PPh ₂ }] ₂	2.651(6)	–14.3 (septet, J_{PLi} 27 Hz, C ₇ D ₈)	169
[Li{OC(Bu ^t) ₂ CH ₂ PPh ₂ }(OCBu ^t)]	2.59(1), 2.63(1)	–14.3 (septet, J_{PLi} 27 Hz, C ₇ D ₈)	169
[Li ₂ {N(SiMe ₂ CH ₂ PPr ⁱ) ₂ }] ₂ LiCl]	2.59(1), 2.63(1), 2.61(1), 2.58(1)	–6.2 (q, J_{PLi} 48.5 Hz, C ₇ D ₈ , –27°C)	167
[Li{N(SiMe ₂ CH ₂ PPr ⁱ) ₂ }] LiAlMe ₄]	2.675(7), 2.556(7), 2.538(7), 2.656(7)	–8.6 (s, C ₇ D ₈ , –88°C)	167
[Li{N(SiMe ₂ CH ₂ PPr ⁱ) ₂ }] NaBEt ₄]	2.57(1), 2.59(1), 2.60(1), 2.60(1)	–4.2 (s, C ₆ D ₆)	167
<i>syn</i> -[Li ₂ {PhP(CH ₂ SiMe ₂ N-SiMe ₂ CH ₂)PPh}(THF)]	2.53(2), 2.53(2)	—	168
<i>anti</i> -[Li ₂ {PhP(CH ₂ SiMe ₂ N-SiMe ₂ CH ₂)PPh}(THF)] ₂]	2.722(7)	—	168
[Na{Ph ₂ P(C ₅ H ₄)}(DME)] ₂	3.056(2)	–18.1 (THF)	165
[Na{Pr ⁱ PPC(H)=C(O)Ph}] ₄	2.852(2)	–17.98 (s, C ₆ D ₆)	170
[Na{(PhCH)Ph ₂ PCHPhPh ₂ }(OEt ₂)(THF)].	2.946(6)	–16.04, 14.12 (d, J_{PP} 137.3 Hz, C ₆ D ₆)	166

^a Abbreviations as for Table I.

^b ³¹P{¹H} chemical shifts relative to 85% H₃PO₄ at ambient temperature, unless otherwise stated (multiplicity, relevant coupling constants, solvent, temperature in parentheses)

^c Values from a representative molecule in the unit cell.

CH_2PMe_2 substituents allowing Li–P contacts without disruption of the bond angles of the core. Multinuclear NMR studies indicate that the dimeric structure is preserved in solution. At 193 K the structure is static; the ^7Li and ^{31}P spectra consist of a triplet and a quartet ($J_{\text{PLi}} = 44$ Hz), respectively, indicating coordination of each lithium by two phosphorus atoms. However, at room temperature the ^7Li and ^{31}P spectra consist of a quintet and a septet, respectively ($J_{\text{PLi}} = 21$ Hz), indicating that the dimer is fluxional, with each Li coupling to all four phosphorus nuclei and vice versa. A ΔG^\ddagger of 50 kJ mol^{-1} was estimated for this process from the coalescence temperature.

A rather unusual phosphine-substituted benzyllithium complex has been prepared in our own laboratory (163). Whereas reaction of the amine-functionalized tertiary phosphine $\text{MeP}(\text{C}_6\text{H}_4\text{-2-CH}_2\text{NMe}_2)_2$ with Bu^nLi yields the phosphinomethanide complex $[\text{Li}\{\text{CH}_2\text{P}(\text{C}_6\text{H}_4\text{-2-CH}_2\text{NMe}_2)_2\}]_4$ (142), treatment of the same phosphine with Bu^iLi in light petroleum yields the benzyllithium complex $[\text{Li}\{\text{MeP}(\text{C}_6\text{H}_4\text{-2-CH}_2\text{NMe}_2)(\text{C}_6\text{H}_4\text{-2-CHNMe}_2)\}]_2$ (**63**) (Fig. 22). The solid-state structure consists of highly asymmetric, internally solvated dimers in which the two lithium atoms are primarily associated with a benzylic carbon from one ligand with supplementary coordination by a phosphorus and a nitrogen atom from the other ligand.

The ligand is chiral at both phosphorus and methine carbon centers and the compound crystallizes as pairs of *RRSS* (with reference to the

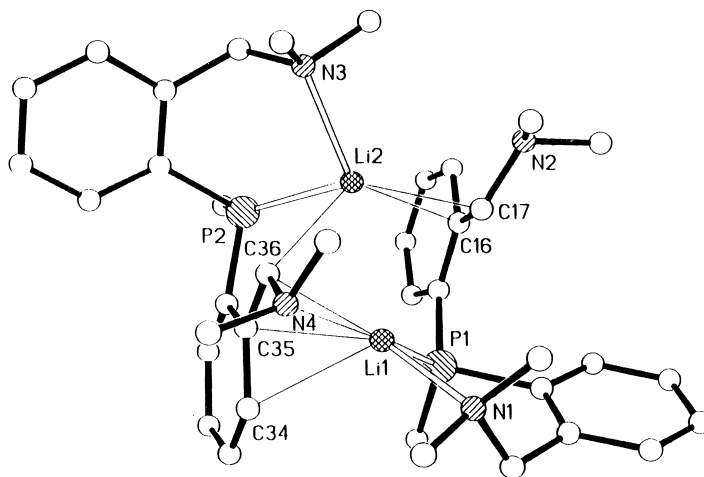


FIG. 22. Structure of $[\text{Li}\{\text{MeP}(\text{C}_6\text{H}_4\text{-2-CH}_2\text{NMe}_2)(\text{C}_6\text{H}_4\text{-2-CHNMe}_2)\}]_2$ (**63**). Reproduced with permission from W. Clegg et al., *Organometallics* **1999**, *18*, 3950. Copyright 1999, the American Chemical Society.

two P and two C centers, respectively) and *SSRR* stereoisomers. The two Li atoms in the dimer are in distinct coordination environments with Li(1) in close contact with the α -carbon C(36), adjacent *ipso*- and *ortho*-carbons C(35) and C(34), and N(4) of one ligand and P(1) and N(1) of the other ligand. The α -carbon C(36) effectively bridges the two lithium centers. Li(2) has close contacts with the α - and *ipso*-carbons C(16) and C(17) of one ligand and P(2) and N(3) of the other ligand, supplemented by weak contact with the bridging α -carbon C(36). The Li(1)–P(1) and Li(2)–P(2) distances are 2.482(4) and 2.553(4) Å, respectively, the “cross-dimer” Li(1)··P(2) and Li(2)··P(1) distances (4.432 and 3.809 Å, respectively) are greater than the sum of their van der Waals radii (3.65 Å) (164). The main features of the dimeric structure observed in the solid state are preserved in toluene solution, although ^1H , ^{13}C , ^{31}P , and ^7Li NMR spectra indicate that a much more symmetrical structure prevails in solution. Multinuclear NMR spectroscopy shows that at room temperature the complex undergoes an intramolecular dynamic process by which the two lithium atoms may be associated with either of the P atoms (but not both simultaneously) and vice versa. The room-temperature ^{31}P and ^7Li spectra thus consist of a binomial septet and a 1:2:1 triplet ($J_{\text{PLi}} = 31.6$ Hz), respectively. At 208 K this process is frozen out and the ^{31}P (1:1:1:1 quartet, $J_{\text{PLi}} = 63.2$ Hz) and ^7Li (doublet) spectra are consistent with a more symmetrical form of the solid state structure in which each lithium interacts with only one phosphorus.

Reaction of $(\text{C}_5\text{H}_5)\text{PPh}_2$ with sodium in refluxing THF, followed by recrystallization from DME/toluene, yields the cyclopentadienide complex $[\text{Na}\{\text{Ph}_2\text{P}(\text{C}_5\text{H}_4)\}(\text{DME})]_2$ (165). This is a rare example of a complex in which there is a direct contact between a heavier alkali metal and a neutral phosphine (three further such Na–P contacts have been reported (*vide infra*) but there have been no reports to date of complexes containing a similar M–PR₃ interaction [M = K, Rb, Cs]). The phosphine-substituted cyclopentadienyl ligands bridge the two sodium atoms, binding via their phosphine and η^5 -cyclopentadienyl centers to give a dimeric structure. Each sodium is further coordinated to a chelating DME ligand, giving the sodium atoms a distorted pseudotetrahedral geometry, with a Na–P distance of 3.056(2) Å.

The ylide $(\text{PhCH}_2)\text{Ph}_2\text{P}=\text{CHPh}_2$ may be deprotonated by NaNH_2 to give the complex $[\text{Na}\{(\text{PhCH})\text{Ph}_2\text{PCHPh}_2\}(\text{OEt}_2)(\text{THF})]$ (166), in which the sodium atom is coordinated by the benzylic and *ipso* carbons in an essentially η^2 -fashion, the terminal P atom of the ligand and one molecule each of ether and THF [Na–P = 2.946(6) Å].

2. Phosphine-Functionalized *N*-Donor Ligands

Fryzuk and co-workers have described the synthesis and structural characterization of several adducts of a tridentate amido diphosphine complex of lithium (167). Reaction of $\text{HN}(\text{SiMe}_2\text{CH}_2\text{Cl})_2$ with 3 equiv of LiPPr_2 leads directly to the lithium amide complex $\text{Li}\{\text{N}(\text{SiMe}_2\text{PPr}_2)_2\}$ (**64**), the first 2 equiv of the lithium phosphide displacing the chlorides and the third equivalent deprotonating the amine. Although this complex could not be crystallographically characterized, multinuclear NMR experiments support this formulation but do not provide any evidence of a P–Li interaction. However, in the presence of LiCl , the adduct $[\{\text{LiN}(\text{SiMe}_2\text{CH}_2\text{PPr}_2)_2\}_2\text{LiCl}]$ may be crystallized and structurally characterized (Fig. 23). The structure can best be described as a three-rung $\text{Li}_3\text{N}_2\text{Cl}$ ladder in which a LiCl unit is sandwiched between two $\text{Li}\{\text{N}(\text{SiMe}_2\text{PPr}_2)_2\}$ units. The two P atoms of each ligand chelate each of the terminal lithium atoms, making these lithium atoms four-coordinate. Variable-temperature ^{31}P and ^7Li NMR spectra indicate that the ladder structure is maintained in solution.

Addition of LiAlMe_4 to **64** yields the adduct $[\{\text{LiN}(\text{SiMe}_2\text{CH}_2\text{PPr}_2)_2\}_2\text{LiAlMe}_4]_2$, which is dimeric in the solid state. Two of the lithium atoms are bound by the ligand in a P_2N bis-chelate mode, the other

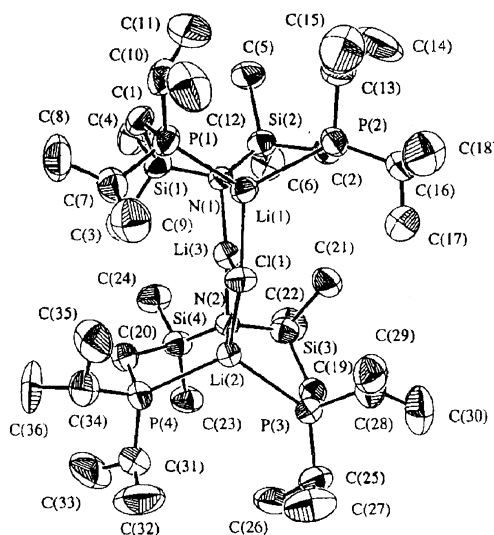
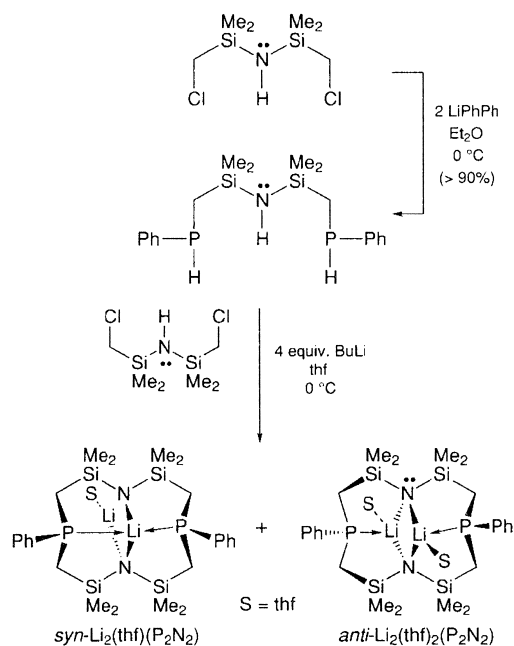


FIG. 23. Structure of $[\{\text{LiN}(\text{SiMe}_2\text{CH}_2\text{PPr}_2)_2\}_2\text{LiCl}]$. Reproduced with permission from M. D. Fryzuk *et al.*, *Organometallics* **1997**, 16, 725. Copyright 1997, the American Chemical Society.

lithium atoms are bound by the amide N and the methyl groups of the AlMe_4 moiety. Multinuclear NMR spectroscopy of a ^6Li , ^{15}N -labeled complex indicate that lithium exchange is more rapid than phosphorus exchange and that interaggregate exchange dominates at room temperature, whereas at low temperature intra-aggregate exchange predominates. Addition of LiAlEt_4 to **64** gave a complex that could not be crystallized, but addition of NaBEt_4 gave the adduct $[\{\text{LiN}(\text{SiMe}_2\text{CH}_2\text{PPr}_2)_2\}\text{NaBEt}_4]$, which adopts a one-dimensional polymer structure in the solid state. The ligand again binds lithium in a bis-chelate P_2N mode with these units being bridged by NaBEt_4 moieties. The sodium atoms are associated with the amido nitrogen and two of the ethylene carbons of the BEt_4 unit. This motif is then repeated along the chain $-\text{Li}(\text{P}_2\text{N})-\text{Na}(1)-\text{BEt}_4-\text{Na}(2)-\text{Li}(\text{P}_2\text{N})-$ with BEt_4 groups linking adjacent chains via $\text{Na}(2)-\text{BEt}_4-\text{Na}(2)$ “cross-links.”

Fryzuk *et al.* have also reported a macrocyclic diphosphine diamide ligand complexed to lithium (168). Reaction of $\text{HN}\{\text{SiMe}_2\text{CH}_2(\text{PPh})_2\}_2$ with $\text{HN}(\text{SiMe}_2\text{CH}_2\text{Cl})_2$ and 4 equiv of Bu^nLi or LDA in THF at 0°C yields two products, *syn*- $[\text{Li}_2(\text{P}_2\text{N}_2)(\text{THF})]$ (**65**) and *anti*- $[\text{Li}_2(\text{P}_2\text{N}_2)(\text{THF})_2]$ (**66**) [$\text{P}_2\text{N}_2 = \text{cyclo-PhP}(\text{CH}_2\text{SiMe}_2\text{NSiMe}_2\text{CH}_2)_2\text{PPh}$], in a ratio of 3:1 (Scheme 5). Both products have been structurally characterized by X-ray crystallography.

The two complexes both have two lithium atoms bridging the two amide nitrogen atoms in a Li_2N_2 rhombus arrangement. However, the complexes differ in the coordination of the phosphorus atoms and their stereochemistries and in their degree of solvation by THF. Complex **65** has both phosphorus atoms bound to the same lithium, making this lithium tetrahedral; the remaining lithium is three-coordinate, bound solely by the amido nitrogen atoms and a molecule of THF. The two phenyl groups are then *syn* across the macrocycle. Complex **66** has a more symmetrical arrangement: In addition to its two Li-N contacts, each Li is bound to one phosphorus and one molecule of THF, with the two Ph substituents in an *anti* relationship. The ^7Li NMR spectra of these complexes confirm their different natures: The ^7Li NMR spectrum of **65** consists of a binomial triplet and a singlet, whereas the spectrum of **66** consists of one doublet. The two complexes may be separated by fractional crystallization from hexane, the less soluble product being **66**. Interestingly, the *syn* complex **65** is the sole product if the synthesis is conducted in ether prior to workup in THF (80% yield), whereas the *anti* complex **66** predominates when the reaction is conducted at -60°C in THF (ratio **65**:**66** = 1:2.4).



SCHEME 5. Synthesis of *syn*-[Li₂(P₂N₂)(THF)] (**65**) and *anti*-[Li₂(P₂N₂)(THF)₂] (**66**) [P₂N₂ = *cyclo*-PhP(CH₂SiMe₂NSiMe₂CH₂)₂PPH]. Reproduced with permission from M. D. Fryzuk *et al.*, *Chem. Commun.* **1996**, 2783. Copyright 1996, the Royal Society of Chemistry.

3. Phosphine-Functionalized *O*- and *S*-Donor Ligands

Two phosphine-functionalized alkoxide ligands have been reported as complexes of the alkali metals. Treatment of the lithium phosphinomethanide [Li(CH₂PR₂)(tmeda)] (R = Me, Ph) with Bu₃C=O yields the complexes [Li{OC(Bu^t)₂CH₂PR₂}]₂ (R = Me, **67**, R = Ph, **68**) (169). The complexes crystallize as centrosymmetric dimers with a central Li₂O₂ core. Each ligand forms a five-membered chelate ring with one lithium, with Li–P distances of 2.50(1) and 2.651(6) Å for **67** and **68**, respectively. The shorter Li–P distance in **67** is attributed to the lower steric requirements of the Me groups on phosphorus. In solution the ⁷Li and ³¹P NMR spectra of both compounds suggest that each P is in contact with two Li nuclei, and each Li is in contact with two P nuclei. This was attributed to a rearrangement of the complex to a chair-type O(LiP)₂O arrangement; however, in light of the behavior of **62** and **63** described earlier, it is possible that these spectra may be consistent with a dynamic process involving rapid intramolecular

P–Li exchange. In the presence of a slight excess of ketone the unusual complex $[\text{Li}\{\text{OC}(\text{Bu}^t)_2\text{CPR}_2\}_2\text{Li}(\text{OCBu}_2^t)]$ may be isolated. This complex again adopts a structure with a central Li_2O_2 core. However, both phosphorus atoms chelate only one lithium atom; the remaining lithium is coordinated by the two bridging oxygens and one molecule of the ketone.

A related enolate complex $[\text{Na}\{\text{Pr}_2\text{PC}(\text{H})=\text{C}(\text{O})\text{Ph}\}]_4$ has been prepared by deprotonation of the ketone $\text{Pr}_2\text{PCH}_2\text{C}(\text{O})\text{Ph}$ with $\text{NaN}(\text{SiMe}_3)_2$ (170). In the solid state this complex adopts a cubane-type structure with a Na_4O_4 core. Each ligand bridges opposite edges of the cube, forming a five-membered chelate ring at each sodium. The Na–P distance in this complex of 2.852(2) Å is short in comparison to other similar contacts.

One phosphine-functionalized thiolate complex of lithium has been reported (171). The dithiol $\text{PhP}(\text{C}_6\text{H}_3-2\text{-SH-3-SiMe}_3)_2$ may be doubly deprotonated by Bu^nLi in hexane to give the dilithium complex $[\text{Li}_2\{\text{PhP}(\text{C}_6\text{H}_3-2\text{-S-3-SiMe}_3)_2\}(\text{DME})]_2$ after recrystallization from toluene/DME. The complex adopts a four-rung S_4Li_4 ladder motif with a chair conformation of the three edge-sharing four-membered S_2Li_2 rings. The terminal lithium atoms are coordinated by two thiolate sulfur atoms and two oxygen atoms of DME, whereas the internal Li atoms are coordinated by three thiolate sulfur atoms and one phosphorus. Thus, the dithiolate–phosphine ligand acts as a bis-chelate, forming two five-membered chelate rings with one sulfur triply bridging and one doubly bridging. Low-temperature ^7Li NMR spectroscopy indicates that this structure is maintained in solution: two Li environments are apparent, one of which exhibits coupling to phosphorus ($J_{\text{PLi}} = 53.9$ Hz).

V. Miscellaneous Complexes

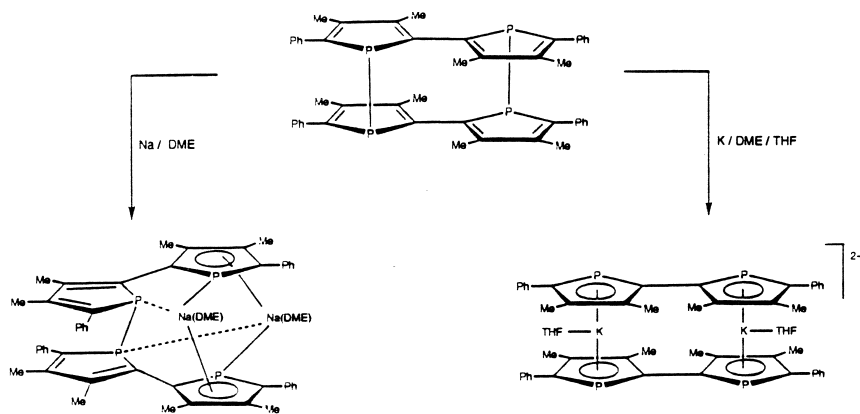
Several complexes have been isolated and structurally characterized in which an alkali metal is bound to a π -phospholide or -arsolide anion. For example, reduction of the chlorophosphole *cyclo*- $\text{C}_4\text{Me}_4\text{PCl}$ with lithium in THF in the presence of tmeda yields the lithium phospholide $[(\text{tmeda})\text{Li}(\text{PC}_4\text{Me}_4)]$ (69) (172). This complex is monomeric, with the phospholide ligand η^5 -bound to the lithium atom, the coordination sphere of lithium being completed by the two nitrogen atoms of the tmeda coligand. The Li–P distance in this complex is 2.531(7) Å and the C–C distances of 1.396–1.424 Å are indicative of a highly aromatic anion. The corresponding arsolide complex

[(tmeda)Li(AsC₄Me₄)] (**70**) has been isolated by a similar procedure from the reduction of the chloroarsole *cyclo*-C₄Me₄AsCl with lithium/tmeda in THF (173). This complex may also be prepared by reduction of the 1,1'-bis(arsole) Me₄C₄As-AsC₄Me₄ or, more effectively, by As-C cleavage of the phenylarsole 1-PhAsC₄Me₄ with lithium. The structure of **70** is essentially the same as that of its phospholide analogue (**69**) with the arsolide anion bound in an η^5 -fashion to lithium [Li-As = 2.596(12) Å].

The structure of the unusual diphospholide complex [(Me₃Si)₃Si] Li(μ - η^5 : η^5 -2,4,5-Bu₃-C₃P₂)(η^6 -toluene)] has been reported, although synthetic details were not described (174). The two lithium atoms sit either side of the diphospholide anion, each bound in an η^5 -fashion. The coordination sphere of one lithium is completed by a σ -bonded Si(SiMe₃)₃ ligand, while the other lithium is bound in an η^6 -fashion to a molecule of toluene.

The reaction of the phosphole tetramer (PC₄-2-Ph-3,4-Me₂)₄ (**71**) with either sodium or potassium yields the complexes **72** and **73**, respectively (Scheme 6) (26).

The sodium atoms are both bound η^5 to one phospholide ring and η^1 to the phosphorus atom of the other phospholide ring of the dianion. Each Na atom is further coordinated by one of the phosphole phosphorus atoms and two oxygen atoms of the DME coligand. The potassium complex is quite different; reduction of the phosphole tetramer with 4 equiv of potassium yields a tetraanion, which, after crystallization from DME containing 18-crown-6, gives the solvent separated



SCHEME 6. Reactions of (PC₄-2-Ph-3,4-Me₂)₄ (**71**) with Na and K. Reproduced with permission from F. Paul *et al.*, *Angew. Chem. Int. Ed. Engl.* **1996**, 35, 1125. Copyright 1996, Wiley-VCH.

rated ion pair **73**. Each potassium atom in the anion is sandwiched in a kalocene-type arrangement between two η^5 -bound phospholide rings and is further coordinated by a molecule of THF. The mean planes of the two directly bonded phospholide units form an angle of 47° and the THF molecules lie on the open side of the tilted sandwich (ring centroid–K–ring centroid = 137.9°).

Reaction of the tetraphosphafulvalene $((\text{Ph})\overline{\text{PC(Ph)C(Ph)P(Ph)C}}=)_2$ with excess lithium or potassium yields the corresponding 1,1'-diphospholide dianion as its Li_2 or K_2 salt, respectively, via a P-C cleavage reaction (175). The potassium complex $[\{\text{K(DME)}_2\}_2\{(\overline{\text{PC(Ph)C(Ph)PC}})_2\}]$ has been crystallographically characterized and consists of infinite chains containing planar diphospholide dianions. Each potassium is coordinated by two of the P atoms, one from each half of the phospholide dianion and the two central carbon atoms of the ligand in an η^4 -PCCP fashion. The two potassium atoms lie on opposite sides of the dianion and are further coordinated by two molecules of DME each. One of the DME ligands on each potassium bridges these K_2 (diphospholide) units via one of its oxygen atoms, forming K_2O_2 links in an infinite chain structure, and making each potassium heptacoordinate. This η^4 -coordination of the phospholide units of the dianion to potassium is in marked contrast to the η^5 -phospholide bonding observed in **73** and **69**.

A heterometallic phospholide complex has also been reported. Reaction of $\text{K(C}_4\text{Me}_4\text{P)}$ with SmCl_3 in refluxing toluene for 24 hours yields an orange solution that deposits crystals of composition $[(\text{C}_4\text{Me}_4\text{P})_6\text{Sm}_2(\text{KCl})_2(\text{toluene})_3]_x$ on cooling (176). Crystallography reveals that this compound adopts a complex structure in the solid state. The Sm atoms are coordinated by two η^5 -phospholide ligands (one of which is also η^1 -bound to K via phosphorus) and one η^1 -phospholide (via phosphorus), in addition to a chlorine atom. The chlorine atoms bridge the Sm and K centers, and the phospholide that is η^1 -bound to Sm is η^5 -bound to K, creating dimeric subunits with an eight-membered $(\text{SmClKP})_2$ ring. Each potassium is further coordinated in an η^6 -fashion to a molecule of toluene and an η^1 -phospholide, giving the potassium atoms a pseudotetrahedral geometry and linking the dimeric subunits into a three-dimensional network.

Treatment of the trichlorosilanes RSiCl_3 [$\text{R} = \text{Bu}^t$, mes, Cp^* , Is, O(mes*), Ph] with 4 equiv of $\text{LiPH(mes}^*)$ leads directly to the diphosphasilaallyl complexes $[(\text{L})\text{Li}\{(\text{mes}^*)\text{PSi(R)P(mes}^*)\}]$ in a one-pot synthesis (177, 178). Four such complexes have been crystallographically characterized: $[(\text{Et}_2\text{O})_2\text{Li}\{(\text{mes}^*)\text{PSi(Bu}^t\text{)P(mes}^*)\}]$ (**74**), $[(\text{DME})\text{Li}$

$\{(\text{mes}^*)\text{PSi}(\text{mes})\text{P}(\text{mes}^*)\}$] (**75**), $[(\text{Et}_2\text{O})_2\text{Li}\{(\text{mes}^*)\text{PSi}(\text{Bu}^t)\text{P}(\text{mes}^*)\}]$ (**76**), and the ion pair $[\text{Li}(\text{15-crown-5})][(\text{mes}^*)\text{PSi}(\text{Bu}^t)\text{P}(\text{mes}^*)]$ (**77**). Complexes **74–76** contain four-coordinate lithium, the lithium being bound by the two phosphorus atoms of the chelating diphosphasilaallyl ligand and two oxygen atoms of the ether coligand(s), with no short contacts between the lithium and central silicon atoms. The diphosphasilaallyl ligands are σ -bonded to lithium and the lithium lies approximately in the SiP_2 plane in each case. In all three complexes the substituents at phosphorus are arranged such that the complexes have approximate overall C_2 symmetry. Multinuclear NMR spectroscopy shows that **77** is obtained as a mixture of E/Z and Z/Z isomers, although only the former isomer has been isolated and crystallographically characterized. The P–Si distances differ little between the E and Z portions of the anion, however, the P–Si–P angle of $125.7(1)^\circ$ is markedly larger than that in the corresponding complex **74** [P–Si–P = $104.9(1)^\circ$]. The synthesis of the related lithium diphosphasilaallyl complex $[(\text{Et}_2\text{O})_2\text{Li}\{(\text{mes}^*)\text{PC}(\text{Me})\text{P}(\text{mes}^*)\}]$ has also been reported (179). Multinuclear NMR spectroscopy suggested that a similar structure to that of the diphosphasilaallyl complex **74** is adopted in solution. A crystallographic study confirms this hypothesis (180): The lithium is bound by the two P atoms and two ether oxygens in a distorted tetrahedral arrangement, with Li–P distances of 2.80 Å.

Three molecular complexes of the Zintl ions P_7^{3-} and As_7^{3-} have been structurally characterized. Treatment of white phosphorus with $\text{LiCH}_2\text{PPh}_2/\text{tmeda}$ yields the complex $[\{(\text{tmeda})\text{Li}\}_3\text{P}_7]$ (181). The lithium atoms bridge the three twofold bonded P atoms of the anion and are further coordinated in a distorted tetrahedral geometry by the two nitrogen atoms of the tmeda coligands. The corresponding arsenic complex $[\{(\text{tmeda})\text{Li}\}_3\text{As}_7]$ (**78**) has been synthesized in excellent yield by the reaction of $[\text{LiAl}(\text{AsHR})_4]$ ($\text{R} = \text{H}, \text{SiPr}_3^i$) with tmeda (182). This reaction proceeds with the elimination of H_2 and unidentified alanate products $[\text{Li}_x\text{Al}_y\text{H}_z]$. The structure is similar to that of its phosphorus analogue with three $\text{Li}(\text{tmeda})$ units bridging the three twofold bonded As atoms of the Zintl ion. The complex $[\{(\text{DME})\text{Li}\}_3\text{As}_7]$ has also been isolated and shown to adopt a similar structure to **78** (183).

Reaction of P_4 with NaSiBu_3 in THF or DME yields the complex $[\text{Na}(\text{Bu}_3^t\text{Si})\text{P}=\text{P}=\text{P}=\text{P}(\text{SiBu}_3^t)\text{Na}]$ (**79**) as the corresponding THF or DME adducts (184). Spectroscopic investigations indicate that this complex adopts a *cis* configuration, although a solid-state structure was not obtained. However, in the presence of Bu^tOMe , a 2+2 cycloaddition reaction occurs, yielding the complex $[\text{Na}_4\{(\text{Bu}_3^t\text{SiP})\text{P}\}_4] \cdot 4(\text{Bu}^t\text{OMe})$. The alternative adduct $[\text{Na}_4\{(\text{Bu}_3^t\text{SiP})\text{P}\}_4] \cdot 4(\text{DME})$ has

been shown by crystallography to consist of a central P_4 distorted square with the four $PSiBu_3$ groups arranged mutually *trans* around the ring. Each sodium atom is then coordinated by one of the P atoms of the central ring and two of the P atoms joined to opposite corners of the ring, along with the O atoms of a DME ligand. The two P atoms on either side of the P_4 ring thus bridge two Na atoms in a Na_2P_2 ring, such that the complex may be described as a triple-decker stack of Na_2P_2 - P_4 - Na_2P_2 rings.

VI. Conclusion

This review has sought to illustrate the wide structural diversity among group 1 complexes of P- and As-donor ligands. The structures of such compounds are highly sensitive to the nature of the metal center, the ligand substituents, the presence and nature of coligands, and the presence of functional groups at the ligand periphery.

Although much progress has been made in the past 25 years in the synthesis of complexes of the alkali metals with P- and As-donor ligands, there are still large gaps in our knowledge. The rich variety of structural types found for the alkali metal phosphides suggests that many more surprises may lie in store and that a similarly wide range of complexes may be obtained for analogous arsenide ligands, particularly in view of the fact that several of the arsenide complexes that have been structurally characterized exhibit highly unusual structural motifs. Similarly, although the chemistry of lithium phosphinomethanides is well established, reports of heavier alkali metal complexes of these ligands are sparse. There is also, as yet, no report of a structurally characterized arsinomethanide complex of the alkali metals or of contacts between uncharged tertiary phosphine and arsine groups and the heavier alkali metals.

It is to be expected that the next few years will again see major developments in this challenging and fascinating field.

REFERENCES

1. Gregory, K.; Schleyer, P. von R.; Snaith, R. *Adv. Inorg. Chem.* **1990**, *37*, 47.
2. Mulvey, R. E. *Chem. Soc. Rev.* **1991**, *20*, 167.
3. Beswick, M. A.; Wright, D. S. In "Comprehensive Organometallic Chemistry II"; Abel, E. W., Stone, F. G. A., and Wilkinson, G., Eds.; Pergamon: Oxford, 1995, Vol. 1; pp 1-34.

4. Sapse, A. M.; Schleyer, P. von R., Eds.; "Lithium Chemistry. A Theoretical and Experimental Overview"; Wiley-Interscience: New York, 1995.
5. Lappert, M. F.; Power, P. P.; Sanger, A. R.; Srivastava, R. C. "Metal and Metalloid Amides"; Wiley: New York, 1980.
6. Pearson, R. G. "Chemical Hardness"; Wiley-VCH: Weinheim, 1997.
7. Schleyer, P. von R.; Clark, T.; Kos, A. J.; Spitznagel, G. W.; Rohde, C.; Arad, D.; Houk, K. N.; Rondan, N. G. *J. Am. Chem. Soc.* **1984**, *106*, 6467.
8. Magnusson, E. *J. Phys. Chem.* **1994**, *98*, 12558.
9. Setzer, W. N.; Schleyer, P. von R. *Adv. Organomet. Chem.* **1985**, *24*, 353.
10. Schade, C.; Schleyer, P. von R. *Adv. Organomet. Chem.* **1987**, *27*, 169.
11. Williard, P. G. In "Comprehensive Organic Synthesis"; Trost, B. M, and Fleming, I., Eds.; Pergamon, Oxford, 1991; Vol. 1, pp. 1–47.
12. Lambert, C.; Schleyer, P. von R. *Angew. Chem. Int. Ed. Engl.* **1994**, *33*, 1129.
13. Weiss, E. *Angew. Chem. Int. Ed. Engl.* **1993**, *32*, 1501.
14. Wardell, J. L. In "Comprehensive Organometallic Chemistry"; Wilkinson, G, Stone, F. G. A, and Abel, E., Eds.; Pergamon, Oxford, 1982; Vol. 1; pp. 43–119.
15. Smith, J. D. *Adv. Organomet. Chem.* **1998**, *43*, 267.
16. Driess, M.; Pritzkow, H.; Skipinski, M.; Winkler, U. *Organometallics* **1997**, *16*, 5108.
17. Budzelaar, P. H. M.; van Doorn, J. A.; Meijboom, N. *Recl. Trav. Chim. Pays-Bas* **1991**, *110*, 420.
18. van Doorn, J. A.; Frijns, J. H. G.; Meijboom, N. *Recl. Trav. Chim. Pays-Bas* **1991**, *110*, 441.
19. Toth, I.; Hanson, B. E.; Davis, M. E. *Organometallics* **1990**, *9*, 675.
20. Uhlig, F.; Hummeltenberg, R. *J. Organomet. Chem.* **1993**, *452*, C9.
21. Englich, U.; Hassler, K.; Ruhlandt-Senge, K.; Uhlig, F. *Inorg. Chem.* **1998**, *37*, 3532.
22. Hey, E.; Hitchcock, P. B.; Lappert, M. F.; Rai, A. K. *J. Organomet. Chem.* **1987**, *325*, 1.
23. Hitchcock, P. B.; Lappert, M. F.; Power, P. P.; Smith, S. J. *Chem. Commun.* **1984**, 1669.
24. Hitchcock, P. B.; Lappert, M. F.; Smith, S. J. *J. Organomet. Chem.* **1987**, *320*, C27.
25. Belforte, A.; Calderazzo, F.; Morvillo, A.; Pelizzi, G.; Vitali, D. *Inorg. Chem.* **1984**, *23*, 1504.
26. Paul, F.; Carmichael, D.; Ricard, L.; Mathey, F. *Angew. Chem. Int. Ed. Engl.* **1996**, *35*, 1125.
27. Clegg, W.; Doherty, S.; Izod, K.; Kagerer, H.; O'Shaughnessy, P.; Sheffield, J. M. *J. Chem. Soc. Dalton Trans.*, **1999**, 1825.
28. Issleib, K.; Tzschach, A. *Chem. Ber.* **1959**, *92*, 1118.
29. Colquhoun, I. J.; McFarlane, H. C. E.; McFarlane, W. *Chem. Commun.* **1982**, 220.
30. Zschunke, A.; Riemer, M.; Schmidt, H.; Issleib, K. *Phosphorus, Sulphur* **1983**, *17*, 237.
31. Zschunke, von A.; Bauer, E.; Schmidt, H.; Issleib, K. *Z. Anorg. Allg. Chem.* **1982**, *495*, 115.
32. Jones, R. A.; Stuart, A. L.; Wright, T. C. *J. Am. Chem. Soc.* **1983**, *105*, 7459.
33. Rabe, G. W.; Riede, J.; Schier, A. *Acta Cryst. Sect. C* **1996**, *C52*, 1350.
34. Westerhausen, M.; Hartmann, M.; Schwarz, W. *Inorg. Chim. Acta* **1998**, *269*, 91.
35. Stieglitz, G.; Neumüller, B.; Dehnicke, K. *Z. Naturforsch. B.* **1993**, *48b*, 156.
36. Bartlett, R. A.; Olmstead, M.; Power, P. P. *Inorg. Chem.* **1986**, *25*, 1243.

37. Mulvey, R. E.; Wade, K.; Armstrong, D. R.; Walker, G. T.; Snaith, R.; Clegg, W.; Reed, D. *Polyhedron* **1987**, *6*, 987.
38. Hope, H.; Olmstead, M. M.; Power, P. P.; Xu, X. *J. Am. Chem. Soc.* **1984**, *106*, 819.
39. Bartlett, R. A.; Olmstead, M. M.; Power, P. P.; Sigel, G. A. *Inorg. Chem.* **1987**, *26*, 1941.
40. Niediek, K.; Neumüller, B. *Z. Anorg. Allg. Chem.* **1993**, *619*, 885.
41. Hey, E.; Weller, F. *Chem. Commun.* **1988**, 782.
42. Hey-Hawkins, E.; Kurz, S. *Phosphorus, Sulfur, Silicon* **1994**, *90*, 281.
43. Jones, R. A.; Koschmieder, S. U.; Nunn, C. M. *Inorg. Chem.* **1987**, *26*, 3610.
44. Becker, G.; Hartmann, H.-M.; Schwarz, W. *Z. Anorg. Allg. Chem.* **1989**, *577*, 9.
45. Becker, G.; Eschbach, B.; Mundt, O.; Seidler, N. *Z. Anorg. Allg. Chem.* **1994**, *620*, 1381.
46. Kurz, S.; Hey-Hawkins, E. *Organometallics* **1992**, *11*, 2729.
47. Hey-Hawkins, E.; Sattler, E. *Chem. Commun.* **1992**, 775.
48. Becker, G.; Eschbach, B.; Käshammer, D.; Mundt, O. *Z. Anorg. Allg. Chem.* **1994**, *620*, 29.
49. Driess, M.; Pritzkow, H. *Z. Anorg. Allg. Chem.* **1996**, *622*, 1524.
50. Schade, C.; Schleyer, P. von R.; Dietrich, H.; Mahdi, W. *J. Am. Chem. Soc.* **1986**, *108*, 2485.
51. Hey, E.; Raston, C. L.; Skelton, B. W.; White, A. H. *J. Organomet. Chem.* **1989**, *362*, 1.
52. Driess, M.; Winkler, U.; Imhof, W.; Zsolnai, L.; Huttner, G. *Chem. Ber.* **1994**, *127*, 1031.
53. Boese, R.; Bläser, D.; Andrianarison, M.; Klingebiel, U. *Z. Naturforsch. B.* **1989**, *44b*, 265.
54. Andrianarison, M.; Stalke, D.; Klingebiel, U. *J. Organomet. Chem.* **1990**, *381*, C38.
55. Andrianarison, M.; Klingebiel, U.; Stalke, D.; Sheldrick, G. M. *Phosphorus, Sulfur, Silicon* **1989**, *46*, 183.
56. Driess, M.; Pritzkow, H.; Rell, S.; Winkler, U. *Organometallics* **1996**, *15*, 1854.
57. Driess, M.; Rell, S.; Pritzkow, H.; Janoschek, R. *Angew. Chem. Int. Ed. Engl.* **1997**, *36*, 1326.
58. Stalke, D.; Meyer, M.; Andrianarison, M.; Klingebiel, U.; Sheldrick, G. M. *J. Organomet. Chem.* **1989**, *366*, C15.
59. Driess, M.; Pritzkow, H.; Rell, S.; Janoschek, R. *Inorg. Chem.* **1997**, *36*, 5212.
60. Bartlett, R. A.; Feng, X.; Power, P. P. *J. Am. Chem. Soc.* **1986**, *108*, 6817.
61. Bartlett, R. A.; Dias, H. V. R.; Feng, X.; Power, P. P. *J. Am. Chem. Soc.* **1989**, *111*, 1306.
62. Pestana, D. C.; Power, P. P. *J. Am. Chem. Soc.* **1991**, *113*, 8426.
63. Dou, D.; Wood, G. L.; Duesler, E. N.; Paine, R. T.; Nöth, H. *Inorg. Chem.* **1992**, *31*, 1695.
64. Kovacs, I.; Krautscheid, H.; Matern, E.; Sattler, E.; Fritz, G.; Hönle, W.; Borrmann, H.; von Schnering, H. G. *Z. Anorg. Allg. Chem.* **1996**, *622*, 1564.
65. Gynane, M. J. S.; Hudson, A.; Lappert, M. F.; Power, P. P.; Goldwhite, H. *J. Chem. Soc. Dalton Trans.* **1980**, 2428.
66. Gynane, M. J. S.; Hudson, A.; Lappert, M. F.; Power, P. P.; Goldwhite, H. *Chem. Commun.* **1976**, 623.
67. Andrianarison, M.; Stalke, D.; Klingebiel, U. *Chem. Ber.* **1990**, *123*, 71.
68. Koutsantonis, G. A.; Andrews, P. C.; Raston, C. L. *Chem. Commun.* **1995**, 47.
69. Aspinall, H. C.; Tillotson, M. R. *Inorg. Chem.* **1996**, *35*, 5.
70. Smith, J. D. *Angew. Chem. Int. Ed. Engl.* **1998**, *37*, 2071.

71. Frenzel, C.; Jörcchel, P.; Hey-Hawkins, E. *Chem. Commun.* **1998**, 1363.
72. Rabe, G. W.; Yap, G. P. A.; Rheingold, A. L. *Inorg. Chem.* **1997**, *36*, 1990.
73. Rabe, G. W.; Heise, H.; Yap, G. P. A.; Liable-Sands, L. M.; Guzei, I. A.; Rheingold, A. L. *Inorg. Chem.* **1998**, *37*, 4235.
74. Rabe, G. W.; Kheradmandan, S.; Heise, H.; Guzei, I. A.; Liable-Sands, L. M.; Rheingold, A. L. *Main Group Chem.* **1998**, *2*, 221.
75. Rabe, G. W.; Kheradmandan, S.; Yap, G. P. A. *Inorg. Chem.* **1998**, *25*, 6541.
76. Rabe, G. W.; Kheradmandan, S.; Liable-Sands, L. M.; Guzei, I. A.; Rheingold, A. L. *Angew. Chem. Int. Ed. Engl.* **1998**, *37*, 1404.
77. Beswick, M. A.; Hopkins, A. D.; Kerr, L. C.; Mosquera, M. E. G.; Palmer, J. S.; Raithby, P. R.; Rothenberger, A.; Stalke, D.; Steiner, A.; Wheatley, A. E. H.; Wright, D. S. *Chem. Commun.* **1998**, 1527.
78. Anderson, D. M.; Hitchcock, P. B.; Lappert, M. F.; Leung, W.-P.; Zora, J. A. *J. Organomet. Chem.* **1987**, *333*, C13.
79. Anderson, D. M.; Hitchcock, P. B.; Lappert, M. F.; Moss, I. *Inorg. Chim. Acta* **1988**, *141*, 157.
80. Brooks, P.; Craig, D. C.; Gallagher, M. J.; Rae, A. D.; Sarroff, A. *J. Organomet. Chem.* **1987**, *323*, C1.
81. Hitchcock, P. B.; Lappert, M. F.; Leung, W.-P.; Yin, P. *J. Chem. Soc. Dalton Trans.* **1995**, 3925.
82. Hey, E. *J. Organomet. Chem.* **1989**, *378*, 375.
83. Schmidpeter, A.; Burget, G.; Sheldrick, W. S. *Chem. Ber.* **1985**, *118*, 3849.
84. Walter, O.; Klein, T.; Huttner, G.; Zsolnai, L. *J. Organomet. Chem.* **1993**, *458*, 63.
85. Driess, M.; Huttner, G.; Knopf, N.; Pritzkow, H.; Zsolnai, L. *Angew. Chem. Int. Ed. Engl.* **1995**, *34*, 316.
86. Driess, M.; Rell, S.; Pritzkow, H.; Janoschek, R. *Chem. Commun.* **1996**, 305.
87. Driess, M.; Pritzkow, H.; Martin, S.; Rell, S.; Fenske, D.; Baum, G. *Angew. Chem. Int. Ed. Engl.* **1996**, *35*, 986.
88. Rabe, G. W.; Riede, J.; Schier, A. *Inorg. Chem.* **1996**, *35*, 40.
89. Rabe, G. W.; Riede, J.; Schier, A. *Inorg. Chem.* **1996**, *35*, 2680.
90. Rabe, G. W.; Yap, G. P. A.; Rheingold, A. L. *Inorg. Chem.* **1997**, *36*, 3213.
91. Schumann, H.; Palamidis, E.; Schmid, G.; Boese, R. *Angew. Chem. Int. Ed. Engl.* **1986**, *25*, 718.
92. Aspinall, H. C.; Moore, S. R.; Smith, A. K. *J. Chem. Soc. Dalton Trans.* **1993**, 993.
93. Petrie, M. A.; Power, P. P. *Organometallics* **1993**, *12*, 1592.
94. Janik, J. F.; Wells, R. L.; Young, V. G., Jr.; Halfen, J. A. *Organometallics* **1997**, *16*, 3022.
95. Allan, R. E.; Beswick, M. A.; Raithby, P. R.; Steiner, A.; Wright, D. S. *J. Chem. Soc. Dalton Trans.* **1996**, 4153.
96. Allan, R. E.; Beswick, M. A.; Cromhout, N. L.; Paver, M. A.; Raithby, P. R.; Steiner, A.; Trevithick, M.; Wright, D. S. *Chem. Commun.* **1996**, 1501.
97. Arif, A. M.; Cowley, A. H.; Jones, R. A.; Power, J. M. *Chem. Commun.* **1986**, 1446.
98. Baker, R. T.; Krusic, P. J.; Tulip, T. H.; Calabrese, J. C.; Wreford, S. S. *J. Am. Chem. Soc.* **1983**, *105*, 6763.
99. Martin, S. F.; Fishpauagh, J. R.; Power, J. M.; Giolando, D. M.; Jones, R. A.; Nunn, C. M.; Cowley, A. H. *J. Am. Chem. Soc.* **1988**, *110*, 7226.
100. Fermin, M. C.; Ho, J.; Stephan, D. W. *Organometallics* **1995**, *14*, 4247.
101. Fermin, M. C.; Ho, J.; Stephan, D. W. *J. Am. Chem. Soc.* **1994**, *116*, 6033.
102. Becker, von G.; Witthauer, C. Z. *Anorg. Allg. Chem.* **1982**, *492*, 28.
103. Jones, L. J., III; McPhail, A. T.; Wells, R. L. *J. Coord. Chem.* **1995**, *34*, 119.

104. Driess, M.; Pritzkow, H. *Angew. Chem. Int. Ed. Engl.* **1992**, *31*, 316.
105. Bartlett, R. A.; Dias, H. V. R.; Hope, H.; Murray, B. D.; Olmstead, M. M.; Power, P. P. *J. Am. Chem. Soc.* **1986**, *108*, 6921.
106. Arif, A. M.; Jones, R. A.; Kidd, K. B. *Chem. Commun.* **1986**, 1440.
107. Zsolnai, L.; Huttner, G.; Driess, M. *Angew. Chem. Int. Ed. Engl.* **1993**, *32*, 1439.
108. Schumann, H.; Palamidis, E.; Loebel, J.; Pickardt, J. *Organometallics* **1988**, *7*, 1008.
109. Edwards, G. L. In "Comprehensive Organic Functional Group Transformations"; Katritzky, A. R., Meth-Cohn, O., and Rees, C. W., Eds.; Elsevier: Oxford, 1995; pp. 579–627.
110. Römer, B.; Gatev, G. G.; Zhong, M.; Brauman, J. I. *J. Am. Chem. Soc.* **1998**, *120*, 2919.
111. Maryanoff, B. E.; Reitz, A. B. *Chem. Rev.* **1989**, *89*, 863.
112. Denmark, S. E.; Dorow, R. L. *J. Am. Chem. Soc.*, **1990**, *112*, 864.
113. Denmark, S. E.; Miller, P. C. *J. Am. Chem. Soc.*, **1991**, *113*, 1468.
114. Denmark, S. E.; Swiss, K. A.; Wilson, S. R. *J. Am. Chem. Soc.* **1993**, *115*, 3826.
115. Denmark, S. E.; Swiss, K. A. *J. Am. Chem. Soc.* **1993**, *115*, 12195.
116. Zarges, W.; Marsch, M.; Harns, K.; Haller, F.; Frenking, G.; Boche, G. *Chem. Ber.* **1991**, *124*, 861.
117. Denmark, S. E.; Cramer, C. J. *J. Org. Chem.* **1990**, *55*, 1806.
118. Denmark, S. E.; Cramer, C. J.; Miller, P. M.; Dorow, R. L.; Swiss, K. A.; Wilson, S. R. *J. Am. Chem. Soc.* **1994**, *116*, 2437.
119. Müller, J. F. K.; Neuburger, M.; Spingler, B. *Angew. Chem. Int. Ed. Engl.* **1999**, *38*, 92.
120. Denmark, S. E.; Swiss, K. A.; Wilson, S. R. *Angew. Chem. Int. Ed. Engl.* **1996**, *35*, 2515.
121. Allred, A. L. *J. Inorg. Nucl. Chem.* **1961**, *17*, 215.
122. Karsch, H. H.; Müller, G. *Chem. Commun.* **1984**, 569.
123. Karsch, H. H.; Weber, L.; Wewers, D.; Boese, R.; Müller, G. *Z. Naturforsch. B.* **1984**, *39b*, 1518.
124. Fraenkel, G.; Winchester, W. R.; Williard, P. G. *Organometallics* **1989**, *8*, 2308.
125. Blaurock, S.; Köhl, O.; Hey-Hawkins, E. *Organometallics* **1997**, *16*, 807.
126. Byrne, L. T.; Engelhardt, L. M.; Jacobsen, G. E.; Leung, W.-P.; Papasergio, R. I.; Raston, C. L.; Skelton, B. W.; Twiss, P.; White, A. H. *J. Chem. Soc. Dalton Trans.* **1989**, 105.
127. Steinborn, D.; Neumann, O.; Weichmann, H.; Heinemann, F. W.; Wagner, J.-P. *Polyhedron* **1998**, *17*, 351.
128. Becker, F.; Heinemann, F. W.; Steinborn, D. *Organometallics* **1997**, *16*, 2736.
129. Brauer, D. J.; Hietkamp, S.; Stelzer, O. *J. Organomet. Chem.* **1986**, *299*, 137.
130. Karsch, H. H.; Deubelly, B.; Müller, G. *J. Organomet. Chem.* **1988**, *352*, 47.
131. Karsch, H. H.; Grauvogl, G.; Mikulcik, P.; Bissinger, P.; Müller, G. *J. Organomet. Chem.* **1994**, *465*, 65.
132. Karsch, H. H.; Deubelly, B.; Riede, J.; Müller, G. *J. Organomet. Chem.* **1988**, *342*, C29.
133. Karsch, H. H.; Appelt, A.; Deubelly, B.; Zellner, K.; Riede, J.; Müller, G. *Z. Naturforsch. B.* **1988**, *43b*, 1416.
134. Karsch, H. H.; Appelt, A.; Deubelly, B.; Müller, G. *Chem. Commun.* **1987**, 1033.
135. Eaborn, C.; Hitchcock, P. B.; Smith, J. D.; Sullivan, A. C. *J. Chem. Soc. Chem. Commun.* **1983**, 827.

136. Karsch, H. H.; Zellner, K.; Mikulcik, P.; Lachmann, J.; Müller, G. *Organometallics* **1990**, *9*, 190.
137. Karsch, H. H.; Zellner, K.; Gamper, S.; Müller, G. *J. Organomet. Chem.* **1991**, *414*, C39.
138. Karsch, H. H.; Richter, R.; Paul, M.; Riede, J. *J. Organomet. Chem.* **1994**, *474*, C1.
139. Karsch, H. H.; Richter, R.; Deubelly, B.; Schier, A.; Paul, M.; Heckel, M.; Angermeier, K.; Hiller, W. *Z. Naturforsch. B.* **1994**, *49b*, 1798.
140. Eaborn, C.; Hitchcock, P. B.; Smith, J. D.; Sullivan, A. C. *J. Chem. Soc. Chem. Commun.* **1983**, 1390.
141. Clegg, W.; Doherty, S.; Izod, K.; O'Shaughnessy, P. *Chem. Commun.* **1998**, 1129.
142. Clegg, W.; Izod, K.; O'Shaughnessy, P., unpublished results.
143. Karsch, H. H.; Appelt, A.; Müller, G. *Angew. Chem. Int. Ed. Engl.* **1986**, *25*, 823.
144. Clegg, W.; Izod, K.; O'Shaughnessy, P. *Organometallics* **1999**, *18*, 2939.
145. Clegg, W.; Izod, K.; McFarlane, W.; O'Shaughnessy, P. *Organometallics* **1998**, *17*, 5231.
146. Winkler, M.; Lutz, M.; Müller, G. *Angew. Chem. Int. Ed. Engl.* **1994**, *33*, 2279.
147. Decken, A.; Cowley, A. H. *J. Organomet. Chem.* **1996**, *509*, 135.
148. Karsch, H. H.; Appelt, A.; Müller, G. *Chem. Commun.* **1984**, 1415.
149. Karsch, H. H.; Appelt, A.; Müller, G. *Organometallics* **1985**, *4*, 1624.
150. Karsch, H. H.; Zellner, K.; Müller, G. *Chem. Commun.* **1991**, 466.
151. Karsch, H. H.; Zellner, K.; Müller, G. *Organometallics* **1991**, *10*, 2884.
152. Steinborn, D.; Neumann, O.; Bruhn, C.; Rüffer, T.; Boese, R.; Heineman, F. W. *Chem. Eur. J.* **1998**, *4*, 11.
153. Karsch, H. H.; Ferazin, G.; Steigelmann, O.; Kooijman, H.; Hiller, W. *Angew. Chem. Int. Ed. Engl.* **1993**, *32*, 1739.
154. Ashby, M. T.; Li, Z. *Inorg. Chem.* **1992**, *31*, 1321.
155. Poetschke, N.; Nieger, M.; Khan, M. A.; Niecke, E.; Ashby, M. T. *Inorg. Chem.* **1997**, *36*, 4087.
156. Trinquier, G.; Ashby, M. T. *Inorg. Chem.* **1994**, *33*, 1306.
157. Kremer, T.; Hampel, F.; Knoch, F. A.; Bauer, W.; Schmidt, A.; Gabold, P.; Schütz, M.; Ellermann, J.; Schleyer, P. von R. *Organometallics* **1996**, *15*, 4776.
158. Ellermann, J.; Schütz, M.; Heinemann, F. W.; Moll, M. *Z. Anorg. Allg. Chem.* **1998**, *624*, 257.
159. Ellermann, J.; Schütz, M.; Heinemann, F. W.; Moll, M.; Bauer, W. *Chem. Ber. / Rec.* **1997**, *130*, 141.
160. Longoni, G.; Chini, P.; Canziani, F.; Fantucci, P. *Chem. Commun.* **1971**, 470.
161. Harder, S.; Brandsma, L.; Kanters, J. A.; Duisenberg, A.; van Lenthe, J. H. *J. Organomet. Chem.* **1991**, *420*, 143.
162. Pape, A.; Lutz, M.; Müller, G. *Angew. Chem. Int. Ed. Engl.* **1994**, *33*, 2281.
163. Clegg, W.; Izod, K.; O'Shaughnessy, P. *Organometallics* **1999**, *18*, 3950.
164. Bondi, A. *J. Phys. Chem.* **1964**, *68*, 441.
165. Lin, G.; Wong, W.-T. *Polyhedron* **1994**, *13*, 3027.
166. Schmidbaur, H.; Deschler, U.; Zimmer-Gasse, B.; Neugebauer, D.; Schubert, U. *Chem. Ber.* **1980**, *113*, 902.
167. Fryzuk, M. D.; Giesbrecht, G. R.; Rettig, S. J. *Organometallics* **1997**, *16*, 725.
168. Fryzuk, M. D.; Love, J. B.; Rettig, S. J. *Chem. Commun.* **1996**, 2783.
169. Engelhardt, L. M.; Harrowfield, J. M.; Lappert, M. F.; Mackinnon, I. A.; Newton, B. H.; Raston, C. L.; Skelton, B. W.; White, A. H. *Chem. Commun.* **1986**, 846.
170. Fryzuk, M. D.; Gao, X.; Rettig, S. J. *Can. J. Chem.* **1995**, *73*, 1175.

171. Froelich, N.; Hitchcock, P. B.; Hu, J.; Lappert, M. F.; Dilworth, J. R. *J. Chem. Soc. Dalton Trans.* **1996**, 1941.
172. Douglas, T.; Theopold, K. H. *Angew. Chem. Int. Ed. Engl.* **1989**, 28, 1367.
173. Sendlinger, S. C.; Haggerty, B. S.; Rheingold, A. L.; Theopold, K. H. *Chem. Ber.* **1991**, 124, 2453.
174. Ficker, R.; Hiller, W.; Böhringer, M.; Becker, G. Z. *Kristallogr.* **1996**, 211, 341.
175. Maigrot, N.; Ricard, L.; Charrier, C.; Mathey, F. *Angew. Chem. Int. Ed. Engl.* **1992**, 31, 1031.
176. Gosink, H.-J.; Nief, F.; Ricard, L.; Mathey, F. *Inorg. Chem.* **1995**, 34, 1306.
177. Lange, D.; Klein, E.; Bender, H.; Niecke, E.; Nieger, M.; Pietschnig, R.; Schoeller, W. W.; Ranaivonjatovo, H. *Organometallics* **1998**, 17, 2425.
178. Niecke, E.; Klein, E.; Nieger, M. *Angew. Chem. Int. Ed. Engl.* **1989**, 28, 751.
179. Gouygou, M.; Veith, M.; Couret, C.; Escudié, J.; Huch, V.; Koenig, M. *J. Organomet. Chem.* **1996**, 514, 37.
180. Gouygou, M.; Koenig, M.; Couret, C.; Escudié, J.; Huch, V.; Veith, M. *Phosphorus, Sulfur Relat. Elem.* **1993**, 77, 230.
181. Hönle, W.; von Schnering, H. G.; Schmidpeter, A.; Burget, G. *Angew. Chem. Int. Ed. Engl.* **1984**, 23, 817.
182. Driess, M.; Merz, K.; Pritzkow, H.; Janoschek, R. *Angew. Chem. Int. Ed. Engl.* **1996**, 35, 2507.
183. Hübler, K.; Becker, G. Z. *Anorg. Allg. Chem.* **1998**, 624, 483.
184. Wiberg, N.; Wörner, A.; Karaghiosoff, K.; Fenske, D. *Chem. Ber. / Rec.* **1997**, 130, 135.

AQUEOUS SOLUTION CHEMISTRY OF BERYLLIUM

LUCIA ALDERIGHI,* PETER GANS,[†] STEFANO MIDOLLINI,[‡]
and ALBERTO VACCA*

*Dipartimento di Chimica, Università di Firenze, I-50144 Firenze, Italy;

[†]School of Chemistry, The University of Leeds, Leeds LS2 9JT, England;

[‡]Istituto per lo Studio della Stereochimica ed Energetica dei Composti di Coordinazione,
CNR, I-50132 Firenze, Italy

- I. Introduction
 - A. Purpose of This Review
 - B. Scope and Organization
 - C. Notation
- II. Properties of Beryllium
- III. The Beryllium Ion
- IV. Beryllium Hydrolysis
 - A. Soluble Hydrolysis Products
 - B. Structures
 - C. Enthalpy and Entropy of Hydrolysis
 - D. Precipitation Equilibria
- V. Interaction with Inorganic Ligands
 - A. Fluorides
 - B. Other Inorganic Anions
- VI. Interaction with Organic Ligands
 - A. Monocarboxylate Ligands
 - B. Biscarboxylate Ligands
 - C. Hydroxycarboxylate Ligands
 - D. Aminocarboxylate Ligands
 - E. Aminopolycarboxylate Ligands (Complexones)
 - F. Dihydroxy Ligands
 - G. Phosphonate Ligands
 - H. Other Organic Ligands
- VII. Conclusions
 - Health and Safety Aspects
 - References

I. Introduction

Beryllium ore extraction has been on the increase recently. Data for the past 5 years are shown in Fig. 1 (1). This increase is connected

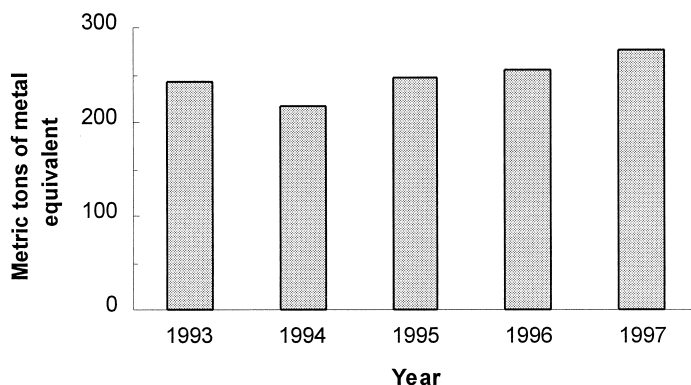


FIG. 1. Annual world production of beryllium 1993–1997 (1).

with the unique characteristics of the metal, its alloys, and its compounds, which find specialist applications in the electronic, aerospace, and other high-tech industries.

The metal is slightly more dense than magnesium metal but has a much higher melting point, rigidity, and corrosion resistance, which would make it the most useful low-density metal were it not for the very high cost (1997: 720 \$ kg⁻¹, 98.5% pure) (1). The high cost is related to the relatively low terrestrial abundance (*ca.* 2 ppm in the earth's crust). The principal ores are bertrandite, Be₄(OH)₂Si₂O₇, in the Unites States and beryl, Al₂Be₃Si₆O₁₈, elsewhere. The minerals crysoberyl, Al₂BeO₄; euclase, AlBe(OH)SiO₄; and phenacite, Be₂SiO₄, also contain beryllium but are not important commercially.

Beryllium metal is used as a window material for X-ray tubes (it has 17 times the transmittance of aluminum). Notwithstanding the high cost of the metal, it has been tested for use in high-performance sports equipment such as golf clubs, bicycles, and motorcycles.

Alloys of beryllium and of other metals with beryllium are also important. Beryllium–aluminum alloy (62%Be, 38%Al) and beryllium–copper master alloy are both available commercially: The incorporation of 2% Be into copper greatly increases the hardness and strength of the metal without reducing its electrical and thermal conductance. This is the single largest use of beryllium.

Beryllium oxide, BeO, is used in place of SiO₂ or Al₂O₃ in performance-sensitive ceramic applications. It is distinguished by having the highest melting point (2507°C) combined with excellent thermal conductivity and poor electrical conductivity.

A serious drawback to the use of beryllium is the very high toxic

hazard associated with the element and its compounds. It now appears that the primary hazard is with the inhalation of dust particles containing the element (2). Chronic beryllium disease (CBD, previously known as beryllosis) is a localized response of the immune system in the lungs to the presence of an insoluble and persistent irritant. CBD being an immune response, there is a latency period of 5–10 years between exposure and the onset of clinical symptoms. The disease was first identified in the 1940s among workers involved in the manufacture of fluorescent light tubes, when a zinc beryllium silicate was employed as a phosphor. Fortunately the incidence of CBD among workers in beryllium-related industries is now minimal thanks to the efficacy of preventative measures, chief of which is the reduction of the concentration of airborne beryllium to less than $2 \mu\text{g m}^{-3}$ in the air. This very low TLV may be compared to the value of 10 mg m^{-3} for gaseous hydrogen cyanide. Oral ingestion of beryllium compounds does not appear to pose a major threat to health. This may in part be due to the fact that in the region of the intestine where substances are absorbed into the blood stream the pH is 7–8, when most of the beryllium will be precipitated as the hydroxide. Nevertheless caution is essential, as it is well known that beryllium can interfere with the action of a wide variety of enzymes (3).

The combination of toxic hazard and high price (itself in part due to the extra measures needed in production processes to ensure the workers' safety) has been an effective brake on commercial development of beryllium chemistry. Where possible substitute, albeit less effective, materials are often used: titanium as an alternate lightweight metal or carbon fiber composites, phosphor-bronzes in place of beryllium alloys, aluminum nitride in place of BeO (1).

A. PURPOSE OF THIS REVIEW

This review is timely because of the likely increase in the use of beryllium compounds in the coming years. There is therefore a need for improved knowledge of beryllium chemistry, especially in relation to aqueous solutions. There is little doubt that fear has played a part in the relative underdevelopment of beryllium chemistry; now that the hazards are better understood it should be possible to make good progress.

What makes beryllium so special is the fact that in aqueous solution its cation, Be^{2+} , is the only cation that is both habitually 4-coordinate and forms a range of complexes with simple ligands. This means that an understanding of the chemistry of this cation should

be of great value in the development of a sound theory of solution chemistry.

Greater use of beryllium will require the consideration of its role in the environment, and a knowledge of speciation in naturally occurring waters will be needed. Further studies are needed to identify the toxicity hazards other than from the inhalation of beryllium-containing dust.

B. SCOPE AND ORGANIZATION

The literature relating to the aqueous solution chemistry of beryllium has been covered to the end of 1998. Previous reviews and relevant compilations of data are listed in Table I. The scope of this review will be to consider all the published data, with a particular emphasis on quantitative aspects, with the aim of facilitating a general discussion. A brief section relating to health and safety issues will be found at the end.

C. NOTATION

1. *Equilibrium Constants*

In this section charges on cations or anions are omitted for sake of generality. L and H_xL are used to symbolize a ligand and the corresponding uncharged Brønsted acid. The conventional symbols used for equilibrium constants are similar to those described in Ref. (8).

K_i Equilibrium constant for stepwise addition of a ligand in mononuclear complexes

$$\text{BeL}_{i-1} + \rightleftharpoons \text{BeL}_i \quad K_i = \frac{[\text{BeL}_i]}{[\text{BeL}_{i-1}][\text{L}]}$$

$*K_i$ Stepwise equilibrium constant for addition of a ligand from the acid

$$\text{BeL}_{i-1} + \text{H}_x\text{L} \rightleftharpoons \text{BeL}_i + x\text{H} \quad *K_i = \frac{[\text{BeL}_i][\text{H}]^x}{[\text{BeL}_{i-1}][\text{H}_x\text{L}]}$$

β_i Equilibrium constant for cumulative addition of ligand in mononuclear complexes

$$\text{Be} + i\text{L} \rightleftharpoons \text{BeL}_i \quad \beta_i = \frac{[\text{BeL}_i]}{[\text{Be}][\text{L}]^i}$$

TABLE I

REVIEWS AND DATA COMPILATIONS RELATING TO BERYLLIUM CHEMISTRY

Year	Author(s)	Title	Ref.
1958	Silber, P.	Glucinium	4
1960	Darwin, G. E.; Buddery, J. H.	Beryllium	5
1964	Everest, D. A.	The Chemistry of Beryllium	6
1971	Bertin, F.; Thomas, G.	Sur la Chimie de Coordination du Bérillium	7
1971	Sillén, L. G.; Martell, A. E.	Stability Constants of Metal–Ion Complexes	8
1972	Bell, N. A.	Beryllium Halides and Pseudohalides	9
1976	Baes Jr, C. F.; Mesmer, R. E.	The Hydrolysis of Cations	10
1977	Smith, R. M.; Martell, A. E.	Critical Stability Constants	11
1982	Högfeldt, E.	Stability Constants of Metal–Ion Complexes	12
1986	Seidel, A.	Beryllium	13
1987	Hertz, R. K.	General analytical Chemistry of Beryllium	14
1987	Akitt, J. W.	The Alkali and Alkaline Earth Metals	15
1987	Schmidbaur, H.	Beryllium, Organoberyllium Compounds	16
1990	Skilleter, D. N.	To Be or Not to Be—The Story of Beryllium Toxicity	2
1991	Rossmann, M. D.; Preuss, O. P.; Powers, M. B.	Beryllium: Biomedical and environ- mental aspects	17
1993	Kumberger, O.; Schmidbaur, H.	Warum ist Beryllium so toxisch?	18
1994	Rees Jr, W. S.	Alkaline Earth Metals: Inorganic Chemistry	19
1994	Wong, C. Y.; Woolins, J. D.	Beryllium Coordination Chemistry	20
1995	Bell, N. A.	Beryllium	21
1997	Mederos, A. <i>et al.</i>	Recent aspects of the coordination chemistry of the very toxic cation beryllium(II): The search for sequestering agents	22
1997	Smith R. M.; Martell, A. E.	NIST Critically Selected Stability Constants of Metal Complexes Database	23
1997	Pettit, L. D.; Powell, H. K. J.	IUPAC Stability Constants Database	24

β_{pqr} Cumulative equilibrium constant for any complex (when a subscript is zero, it is omitted)

$$p\text{Be} + q\text{L} + r\text{H} \rightleftharpoons \text{Be}_p\text{L}_q\text{H}_r \quad \beta_{pqr} = \frac{[\text{Be}_p\text{L}_q\text{H}_r]}{[\text{Be}]^p[\text{L}]^q[\text{H}]^r}$$

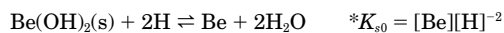
$^*\beta_{pq}$ Equilibrium constant for hydrolysis

$$p\text{Be} + q\text{H}_2\text{O} \rightleftharpoons \text{Be}_p(\text{OH})_q + q\text{H} \quad \beta_{pqr} = \frac{[\text{Be}_p(\text{OH})_q][\text{H}]^q}{[\text{Be}]^p}$$

K_{s0} Solubility product



$^*K_{s0}$ Solubility product with hydrolysis



K [equation]: In this case the equation defines the reaction to which the equilibrium constant refers.

ΔH , ΔS denote standard enthalpy (kJ mol^{-1}) and entropy ($\text{J mol}^{-1} \text{K}^{-1}$) of reaction: The notation corresponds to that used for the equilibrium constants.

2. Methods of Measurement

The method used to determine the equilibrium constant or other thermodynamic function is shown in the tables with the following abbreviations.

cal	calorimetry
col	colorimetry
con	conductivity
dis	distribution between two phases
gl	glass electrode
H, F, etc.	emf with specified selective electrode
iE	voltammetry
ix	ion exchange
kin	rate of reaction
lit	from critical survey of literature data
nmr	nuclear magnetic resonance
oth	other method (specified in the "results" column)
pol	polarography
qh	quinhydrone electrode
ram	Raman spectroscopy
red	emf with redox electrode
sol	solubility
sp	spectrophotometry

For further details see reference (8).

II. Properties of Beryllium

Some physical and chemical properties of the alkaline earth metals are shown in Table II. It can be seen that beryllium is significantly different from the elements below it in the periodic table in most respects. The fact that the density of beryllium is greater than that of magnesium is perhaps surprising, but can be understood by noting that magnesium is both a more massive and a larger atom. The density of beryllium is to be compared to that of iron (7.9 g cm^{-3}), titanium (4.5 g cm^{-3}), and aluminum (2.7 g cm^{-3}).

The standard reduction potential for Be^{2+} is the least negative of the elements in the group and by the same token beryllium is the least electropositive and has the greatest tendency to form covalent bonds. The bulk metal is relatively inert at room temperature and is not attacked by air or water at high temperatures. Beryllium powder is somewhat more reactive. The metal is passivated by cold concentrated nitric acid but dissolves in both dilute acid and alkaline solutions with the evolution of dihydrogen. The metal reacts with halogens at 600°C to form the corresponding dihalides.

III. The Beryllium Ion

In aqueous solution below pH 3 there is little doubt that beryllium is surrounded by four water molecules and exists as $[\text{Be}(\text{H}_2\text{O})_4]^{2+}$. The coordination number has been confirmed by solution ^1H NMR (25–28) and ^{17}O NMR spectroscopy (29) and X-ray diffraction (30). Vibrational spectra of aqueous beryllium solutions have been reported by Kuli-

TABLE II
SOME PHYSICAL AND CHEMICAL PROPERTIES OF THE ALKALINE EARTH METALS^a

Property	Be	Mg	Ca	Sr	Ba	Ra
Melting point/ $^\circ\text{C}$	1278	649	839	769	725	(700)
Density (20°C)/ g cm^{-3}	1.85	1.74	1.54	2.54	3.59	5.50
Atomic radius/pm	111	160	197	215	217	223
Ionic radius/pm	(27)	72	100	118	135	148
Ionization energy/ kJ mol^{-1}	900	738	590	549	503	509
E°/V , for: $\text{M}^{2+}(\text{aq}) + 2\text{e} \rightarrow \text{M}(\text{s})$	-1.85	-2.37	-2.87	-2.89	-2.91	-2.92
ΔH_{fus} (kJ mol^{-1})	15	8.9	8.6	8.2	7.8	(8.5)
ΔH_{vap} (kJ mol^{-1})	309	128	151	154	151	137

^a Taken from Ref. (19).

kova *et al.* (31). A variety of thermodynamic, kinetic, and transport properties of aqueous beryllium ions have been measured (32), but the data are rather sparse in comparison with what is available for aqueous magnesium solutions. The substitution reactions of the beryllium ion in water and nonaqueous solvents have been comprehensively reviewed (33). The diffusion behavior of aqueous solutions of beryllium sulfate have been investigated (34).

Molecular dynamics calculations have been performed (35–38). One *ab initio* calculation (39) is particularly interesting because it avoids the use of pairwise potential energy functions and effectively includes many-body interactions. It was concluded that the structure of the first hydration shell is nearly tetrahedral but is very much influenced by its own solvation.

In the solid state X-ray and neutron diffraction structure determinations have confirmed the 4-coordination in $\text{BeSO}_4 \cdot 4\text{H}_2\text{O}$ (40, 41), $\text{Be}[\text{C}_2(\text{COO})_2] \cdot 4\text{H}_2\text{O}$ (42), and $\text{Be}(\text{IO}_3)_2 \cdot 4\text{H}_2\text{O}$ (43). The Be–O distance was found to be close to 161 pm in all cases. The arrangement of oxygen atoms is tetrahedral, but the tetrahedron is usually distorted because of the fairly strong hydrogen bonds that exist between the water molecules coordinated to the beryllium atom and the anions. O–Be–O angles range between 87° and 122° .

IV. Beryllium Hydrolysis

The many attempts to quantify beryllium hydrolysis are summarized in Table III.

A. SOLUBLE HYDROLYSIS PRODUCTS

1. Acid Solutions

It has long been recognized that in solution the aqua-ion $[\text{Be}(\text{H}_2\text{O})_4]^{2+}$ exists only in strongly acidic conditions. This is due to the very high charge density at the surface of the beryllium atom occasioned by its small size. Above a pH of *ca.* 3 there is appreciable hydrolysis, which reduces the average charge per beryllium atom. In the absence of complexing ligands the insoluble hydroxide $\text{Be}(\text{OH})_2$ forms from solutions in the pH range *ca.* 5–12. The hydroxide is amphoteric and dissolves in strong alkali (pH > 12). Early attempts to understand the hydrolysis have been exhaustively reviewed by Mattock (50).

TABLE III
EQUILIBRIUM CONSTANTS RELATING TO BERYLLIUM HYDROLYSIS

Method	T (°C)	Medium	Log of equilibrium constants, remarks	Ref.
kin	99.7	BeCl ₂ var	* K_1 -4.46	44
H	25	BeCl ₂ var	* K_1 -3.63, K_1 10.28	45
sol	rt	var	$K[2\text{Be}(\text{OH})_2(\text{s}) + 2\text{OH}^- \rightarrow \text{Be}_2(\text{OH})_4^{2-}]$ -0.77, $K[\text{Be}(\text{OH})_2(\text{s}) + 2\text{OH}^- \rightarrow \text{Be}(\text{OH})_4^{2-}]$ -1.19 or -1.48 [three forms of $\text{Be}(\text{OH})_2(\text{s})$]	46
H	25	BeSO ₄ var	* β_{22} -6.85, * $K[2\text{Be}(\text{OH})_2(\text{s}) + 2\text{H}^+ \rightarrow \text{Be}_2(\text{OH})_2^{2+}]$ 8.90, $K[2\text{Be}(\text{OH})_2(\text{s}) \rightarrow \text{Be}_2(\text{OH})_2^{2+} + 2\text{OH}^-]$ -18.80	47
H	25	BeCl ₂ var	* β_{22} -6.77, * $K[2\text{Be}(\text{OH})_2(\text{s}) + 2\text{H}^+ \rightarrow \text{Be}_2(\text{OH})_2^{2+}]$ 9.32, $K[2\text{Be}(\text{OH})_2(\text{s}) \rightarrow \text{Be}_2(\text{OH})_2^{2+} + 2\text{OH}^-]$ -18.39	47
H	25	BeBr ₂ var	* β_{22} -6.23, * $K[2\text{Be}(\text{OH})_2(\text{s}) + 2\text{H}^+ \rightarrow \text{Be}_2(\text{OH})_2^{2+}]$ 9.15, $K[2\text{Be}(\text{OH})_2(\text{s}) \rightarrow \text{Be}_2(\text{OH})_2^{2+} + 2\text{OH}^-]$ -18.57	48
H	25	BeI ₂ var	* β_{22} -6.36, * $K[2\text{Be}(\text{OH})_2(\text{s}) \rightarrow \text{Be}_2(\text{OH})_2^{2+} + 2\text{H}^+]$ 9.23, $K[2\text{Be}(\text{OH})_2(\text{s}) + 2\text{OH}^- \rightarrow \text{Be}_2(\text{OH})_2^{2-}]$ -18.48	48
gl	22.5	2 M NH ₄ NO ₃	* K_1 -6.70, ev $\text{Be}_2\text{OH}^{3+}$	49
gl	25	1 M (na)ClO ₄	* K_1 -6.52, * β_{21} -3.51	50
gl, sol	rt	0 corr	K_{s0} -17.7, $K[\text{Be}(\text{OH})_2(\text{s}) \rightarrow \text{Be}(\text{OH})_2]$ -3.66, β_2 14.04	51
sol	25	0 corr	$K[\text{Be}(\text{OH})_2(\text{s}) + \text{OH}^- \rightarrow \text{Be}(\text{OH})_3^-]$ -2.49, $K[\text{Be}(\text{OH})_2(\text{s}) + 2\text{OH}^- \rightarrow \text{Be}(\text{OH})_4^{2-}]$ -2.70, * $K_{s0} \geq 6.86$, $K_{s0} \geq -21.14$ [metastable $\text{Be}(\text{OH})_2$], * β_{22} -6.80	52
sol	25	0 corr	* K_{s0} -6.86 (α - $\text{Be}(\text{OH})_2$), $K[\text{Be}(\text{OH})_2(\alpha) + \text{OH}^- \rightarrow$ $\text{Be}(\text{OH})_3^-]$ -2.49, $K[\text{Be}(\text{OH})_2(\alpha) + 2\text{OH}^- \rightarrow$ $\text{Be}(\text{OH})_4^{2-}]$ -2.70, $K[3\text{Be}(\text{OH})_2(\alpha) + 3\text{H}^+ \rightarrow$ $\text{Be}_3(\text{OH})_3^{3+}]$ -11.67, * β_{33} -8.9	52, 53
qh, H	25	3 M (Na)ClO ₄	* β_{33} -8.66, * β_{21} -3.24, * β_2 -10.9, no ev $\text{Be}_2(\text{OH})_2^{2+}$ or $\text{Be}_4(\text{OH})_4^{4+}$	54
gl	25	0 corr ?	β_{22} 21.31 or β_{33} 33.03	55
gl, sol	25	0 corr ?	$K[\text{Be}(\text{OH})_2(\text{s}) \rightarrow \text{Be}(\text{OH})^+ + \text{OH}^-]$ -10.82 or $K[2\text{Be}(\text{OH})_2(\text{s}) \rightarrow \text{Be}_2(\text{OH})_2^{2+} + 2\text{OH}^-]$ -19.95	55
pol, gl	19	→0	K_{s0} -25.7	56
gl, qh	25	3 M (Na)ClO ₄	* β_{33} -8.66, * β_{21} -3.2 [low Be(II) concn], -3.15 [1 M Be(II)]	57
cal	25	3 M (Na)ClO ₄	$\Delta^*H_{21} = 18.5$, $\Delta^*S_{21} = 0.8$, $\Delta^*H_{33} = 63.5$, $\Delta^*S_{33} = 47.3$	58
gl	20	0.1 M (NaClO ₄)	* K_1 -5.7, * $K_2 \approx -7$ (rapid flow apparatus)	59

(continued)

TABLE III (Continued)

Method	T (°C)	Medium	Log of equilibrium constants, remarks	Ref.
lit	25	0 corr	$K_{s0} - 20.8$ (amorphous), $K_{s0} - 21.1$ (α -Be(OH) ₂), $K_{s0} - 21.5$ (β -Be(OH) ₂), $K[3\text{Be}(\text{OH})_2(\text{s}) \rightarrow$ $\text{Be}_3(\text{OH})_6^{3+} + 3\text{OH}^-] - 31.4$ (β -Be(OH) ₂) $K[\text{Be}(\text{OH})_2(\text{s}) + \text{OH}^- \rightarrow \text{Be}(\text{OH})_3^-] - 2.9$, $K[\text{Be}(\text{OH})_2(\text{s}) + 2\text{OH}^- \rightarrow \text{Be}(\text{OH})_4^{2-}] - 3.1$	60
H, gl, qh	25	3 M (Na)ClO ₄	$^*\beta_{21} - 3.22$, $^*\beta_{33} - 8.664$, $^*\beta_2 - 10.87$	54, 57 61
oth	20	0.1 M (KCl)	$^*K_1 - 5.68$, $^*K_2 \leq -6.7$ (gl, rapid flow)	62
oth	20	0.1 M (NaClO ₄)	$^*K_1 - 5.71$, $^*K_2 \leq -6.7$ (gl, rapid flow)	63
gl	?	0.5 M (NaClO ₄)	$^*\beta_{21} - 3.24$, $^*\beta_{33} - 8.81$, $^*\beta_2 - 11.0$	63
dis, gl	25	dil	$^*\beta_2 - 13.65$, $^*\beta_3 - 24.11$, no ev BeOH ⁺	64
gl	25	0.5 M (NaClO ₄)	$^*\beta_{21} - 3.20$, $^*\beta_{33} - 8.81$, $^*\beta_2 - 11.0$	65
H, qh	0–60	1 M NaCl	$^*\beta_{21} - 3.64(0^\circ)$, $-3.43(25^\circ)$, $-2.93(60^\circ)$, $\Delta^*H_{21} = 21$, $\Delta^*S_{21} = 5.9$ $^*\beta_{33} - 10.08(0^\circ)$, $-8.91(25^\circ)$, $-7.67(60^\circ)$, $\Delta^*H_{33} = 66.9$, $\Delta^*S_{33} = 64.0$ $^*\beta_{57} - 28.66(0^\circ)$, $-25.33(25^\circ)$, $-22.11(60^\circ)$, $\Delta^*H_{57} = 190$, $\Delta S_{57} = 147$	66
gl	25	dioxan–H ₂ O	$^*\beta_{21} - 3.66$, $^*\beta_2 - 10.84$, $^*\beta_{22} - 7.15$, $^*\beta_{33} - 8.75$ [in 0.2 dioxan + 0.8 H ₂ O], 3 M (Li)ClO ₄]	67
gl	25	35% dioxan	$^*\beta_{21} - 3.29$, $^*\beta_{33} - 8.65$, $^*\beta_2 - 11.5$, in 35% dioxan (10 mol%), $I = 3$ M (LiClO ₄)	68
gl	25	3 M (LiClO ₄)	$^*K_1 \leq -5.4$, $^*\beta_{21} - 3.27$, $^*\beta_{33} - 8.74$, $^*\beta_2 - 11.5$	69
gl	25	2 M (K)NO ₃	$^*\beta_{21} - 3.28$, $^*\beta_{33} - 8.90$, $^*\beta_{34} - 16$, $^*\beta_{68} - 27.5$, $^*\beta_{69} - 34.5$	69
gl	25	3 M KCl	$^*\beta_{21} - 3.18$, $^*\beta_{33} - 8.91$	70
dis	19		$K_1 10.8$, $K_2 7.50$, $\beta_2 18.3$	71
gl	25	0.1 M K ₂ SO ₄	$^*\beta_{21} - 2.67$, $^*\beta_{33} - 7.45$, $^*\beta_{34} - 14.02$, $^*\beta_{68} - 23.4$, $^*\beta_{69} - 29.2$	72
gl	25	2 M KCl	$^*\beta_{21} - 3.66$, $^*\beta_{23} - 5.99$, $^*\beta_{33} - 8.03$, $^*\beta_{34} - 15.6$, $^*\beta_{68} - 28.1$	72
kin	20	0.1 M KCl	$^*K_1 - 5.7$, $^*K_2 - 5.5$	73
gl	25	3 M (Na)ClO ₄	$^*\beta_{21} - 3.16$, $^*\beta_{33} - 8.66$, $^*\beta_2 - 11.16$	74
gl	60	3 M (Na)ClO ₄	$^*\beta_{21} - 2.9$, $^*\beta_{22} - 6.25$, $^*\beta_{33} - 7.7$, $^*\beta_{34} - 13.22$	75
gl	25	1 M KNO ₃	$^*\beta_{21} - 3.22$, $^*\beta_{33} - 8.87$, $^*\beta_2 - 11.26$	76
gl	25	3 M LiClO ₄	$^*\beta_{21} - 3.50$, $^*\beta_{22} - 7.35$, $^*\beta_{33} - 8.541$, $^*\beta_2 - 11.38$	77
		31% methanol		
gl	25	0.1 M LiClO ₄	$^*K_1 \geq -6.3$, $^*\beta_{21} - 3.32$, $^*\beta_{33} - 8.807$, $^*\beta_2 - 11.35$	77
gl	25	3 M LiClO ₄	$^*\beta_{21} - 3.04$, $^*\beta_{33} - 8.671$, $^*\beta_{68} - 27.337$	77
lit	0–60	1 M NaCl	$^*\beta_{21} - 3.64(0^\circ)$, $-3.42(25^\circ)$, $-2.91(60^\circ)$ $^*\beta_{33} - 10.081(0^\circ)$, $-8.907(25^\circ)$, $-7.664(60^\circ)$ $^*\beta_{68} - 31.15(0^\circ)$, $-27.46(25^\circ)$, $-23.73(60^\circ)$	10
sol	25	0.01 M NaClO ₄ or LiClO ₄	$^*K_1 - 4.6$, $^*K_2 - 2.7$	78

TABLE III (Continued)

Method	T (°C)	Medium	Log of equilibrium constants, remarks	Ref.
gl	25	0.1 M KNO ₃	$^*\beta_{21} - 2.96, ^*\beta_{33} - 8.81, ^*\beta_2 - 11.32$	79
gl	25	3 M (Na)ClO ₄	$^*\beta_{21} - 3.23, ^*\beta_2 - 11.07, ^*\beta_{33} - 8.66, ^*\beta_{56} - 18.84,$ $^*\beta_{68} - 26.69$	80
gl	25	→ 0	$^*\beta_{21} - 3.47, ^*\beta_{33} - 8.86, ^*\beta_{56} - 19.5, ^*\beta_{68} - 26.3,$ $^*K_{s0} 6.87 (\alpha\text{-Be(OH)}_2)$	80
sol	25	3 M NaClO ₄	$K_1 - 6.02, ^*K_{s0} 6.18$	81
gl	25	0.5 M NaClO ₄ or LiClO ₄	$^*\beta_{21} - 3.20, ^*\beta_{33} - 8.92$	82
gl	25	1 M NaClO ₄ or LiClO ₄	$^*\beta_{21} - 3.52, ^*\beta_{33} - 8.70, ^*\beta_{68} - 26.82$	83
lit	20	0.1 M	$K_1 8.3, \beta_2 16.7$	23
lit	25	0.1 M	$^*\beta_{21} 10.82, \beta_2 16.2, \beta_{33} 32.54$	23
lit	25	0.5 M	$^*\beta_{21} 10.54, \beta_2 16.5, \beta_{33} 32.35$	23
lit	25	1 M	$^*\beta_{21} 10.56, \beta_2 16.3, \beta_{33} 32.64, \beta_{68} 83.42$	23
lit	25	2 M KNO ₃	$^*\beta_{21} 10.68, \beta_{33} 32.98$	23
lit	25	3 M NaClO ₄	$K_1 8.16, \beta_{21} 10.98, \beta_2 17.3, \beta_{33} 33.88, \beta_{56} 66.24,$ $\beta_{68} 86.74, K_{s0} - 21.12 (\beta\text{-Be(OH)}_2)$ $\Delta H_{21} = -36, \Delta S_{21} = 79.4$ $\Delta H_{33} = -100, \Delta S_{33} = 268$	23
lit	25	3 M LiClO ₄	$\beta_{21} 10.83, \beta_{33} 32.94, \beta_{68} 80.82$ $\Delta H_{21} = -38, \Delta S_{21} = 88.2$ $\Delta H_{33} = -107, \Delta S_{33} = 310$	23
lit	25	→ 0	$K_1 8.6, \beta_2 14.4, \beta_3 18.8, \beta_4 18.6$ $K_{s0} - 20.8 (\text{amorphous}), K_{s0} - 21.1 (\alpha\text{-Be(OH)}_2),$ $K_{s0} - 21.5 (\beta\text{-Be(OH)}_2)$	23
gl	25	0.5 M (Na)ClO ₄	$^*\beta_{21} - 3.20, ^*\beta_2 - 11.68, ^*\beta_{33} - 8.68, ^*\beta_{56} - 18.31,$ $^*\beta_{68} - 25.77$	84
gl	25	0.5 M (Na)ClO ₄ 80% dmso	$^*K_1 - 5.25, ^*\beta_{21} - 2.98, ^*\beta_2 - 9.59, ^*\beta_{33} - 9.28,$ $^*\beta_{56} - 18.03, ^*\beta_{68} - 25.16$	84
cal	25	0.5 M (Na)ClO ₄	$\Delta H_{21} = -27, \Delta S_{21} = 111, \Delta H_{33} = -100.8,$ $\Delta S_{33} = 282$ $\Delta H_{56} = -208, \Delta S_{56} = 523, \Delta H_{68} = -239,$ $\Delta S_{68} = 802$	85

The first modern study was performed by Kakihana and Sillén (54). These authors studied an extensive range of solutions in the pH range from the onset of hydrolysis to the onset of precipitation. They made a convincing case for the formation of the trimer, $\text{Be}_3(\text{OH})_3^{3+}$, as the principal product of hydrolysis, with the species $\text{Be}_2(\text{OH})^{3+}$ being formed to a minor extent under the experimental conditions used. They also found that some Be(OH)_2 was present in solution before precipitation had occurred. This model was subsequently confirmed by various authors (57–65, 74, 79, 86). The same model was found to

be valid in water/dioxan mixtures when the mole fraction of dioxan was less than 0.1, but when the mole fraction was greater than 0.2 the additional species $\text{Be}_2(\text{OH})_2^{2+}$ was proposed (68). The model was also found to apply to solutions in heavy water, with the expected reduction in the equilibrium constants (74) and confirmed again by Brown *et al.* (79).

Subsequent studies showed that other species are formed to a small extent just before precipitation begins; these species have a hydroxide to beryllium ratio greater than 1, but because their concentrations are always relatively low their identification has been dogged by controversy. Mesmer and Baes obtained data at a range of temperatures and from this data proposed the minor species $\text{Be}_5(\text{OH})_7^{3+}$ (66). Later they also suggested that the species $\text{Be}_6(\text{OH})_8^{4+}$ was formed (10), in agreement with earlier work by Lanza and Carpeni (69, 72). These last had also proposed the additional species $\text{Be}_3(\text{OH})_4^{2+}$ and $\text{Be}_6(\text{OH})_9^{3+}$.

The controversy seems to have been settled by Bruno (80) by the use of a three-pronged approach: careful and wide-ranging experimental work, a computer program (LETAGROP) (87) capable of examining all possible models and a requirement that reasonable chemical structures can be assigned to all the species proposed. The model put forward by Bruno is as follows: $\text{Be}_2(\text{OH})_3^{3+}$, $\text{Be}_3(\text{OH})_3^{3+}$, $\text{Be}_5(\text{OH})_6^{4+}$, $\text{Be}_6(\text{OH})_8^{4+}$, and $\text{Be}(\text{OH})_2(\text{aq})$ with the structures shown in Fig. 2. In each of these structures all the beryllium atoms are surrounded by a tetrahedron of oxygen atoms belonging to water molecules, hydroxide ions, or oxide ions. The hydroxide ions form bridges between two beryllium atoms, with Be–O–Be angles close to tetrahedral, and the oxide ion bridges between three beryllium atoms also with Be–O–Be angles close to tetrahedral.¹

From a structural point of view Bruno's hypothesis is sound. In chemical terms the hydrolysis proceeds with the formation of hydroxide bridges up to the formation of the trimer. Then at high concentrations trimeric units are fused together to form the higher aggregates, that can be seen as precursors to the structure adopted by $\text{Be}(\text{OH})_2$ in the solid state. (See Section IV, C, precipitation equilibria). Speciation diagrams for Bruno's model are shown in Fig. 3. Two points are noteworthy in these diagrams. In the first place the concentrations of the

¹ Hydrogen-ion concentration measurements cannot distinguish between a bis-hydroxy species and a mono-oxy species because the equilibrium $2 \text{OH}^- \rightleftharpoons \text{O}^{2-} + \text{H}_2\text{O}$ neither releases nor consumes protons. Thus the species written as $\text{Be}_5(\text{OH})_6^{4+}$ and $\text{Be}_6(\text{OH})_8^{4+}$ are "equivalent" to $\text{Be}_5\text{O}(\text{OH})_4^{4+}$ and $\text{Be}_6\text{O}(\text{OH})_6^{4+}$, as shown in Fig. 2.

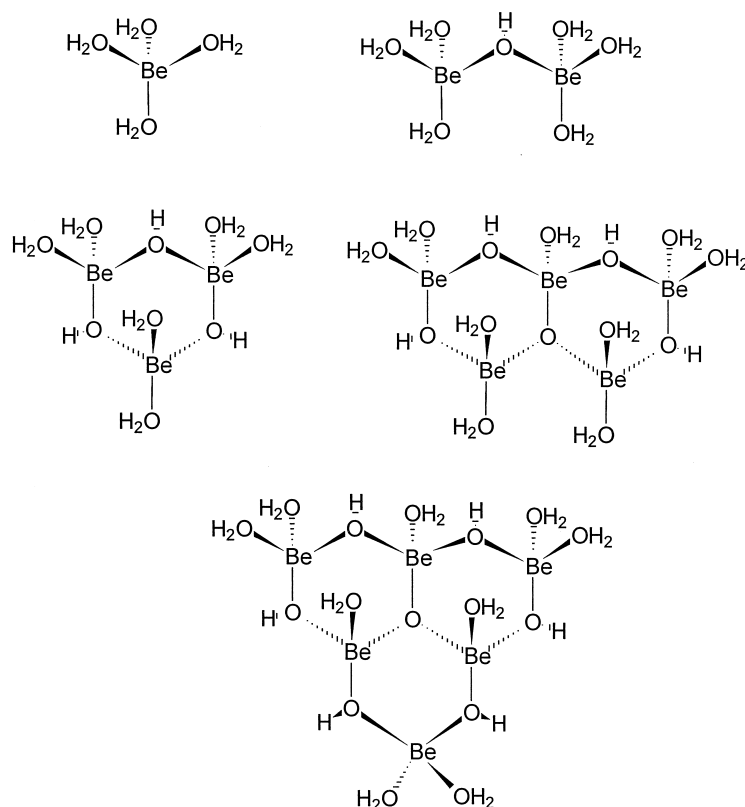


FIG. 2. Structures proposed for beryllium hydrolysis products (80).

species are strongly dependent on analytical concentration of beryllium, with the polynuclear species being formed mainly in the relatively concentrated solutions. The second point is that the pH at which $\text{Be}(\text{OH})_2$ begins to separate out from the solution is also dependent on the total beryllium concentration. The same model was successfully applied to water/dmsol solvent mixtures up to 80% dmsol (84).

^1H NMR spectroscopy has been a useful tool for confirming the model deduced by potentiometry. Akitt *et al.* (27, 28) have characterized the species $[\text{Be}_2(\text{OH})(\text{H}_2\text{O})_6]^{3+}$ and $[\text{Be}_3(\text{OH})_3(\text{H}_2\text{O})_6]^{3+}$. Very concentrated solutions were prepared by dissolving a known weight of Na_2CO_3 in a certain volume of concentrated BeCl_2 solution, and spectra were recorded at temperatures between -45 and -55°C . The ratio $[\text{H}_2\text{O}]/[\text{Be}^{2+}]$ varied between 18.47 and 22.7, which corresponds

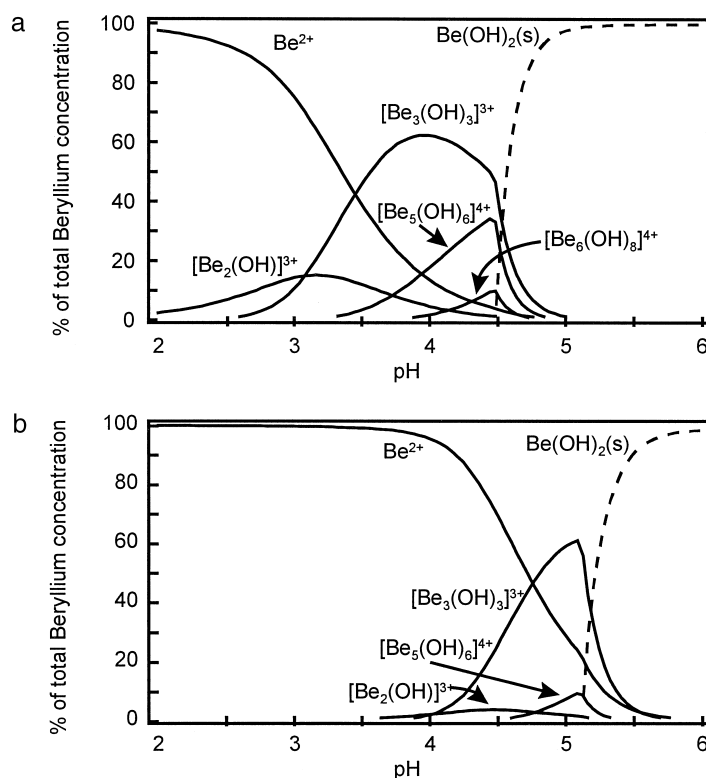


FIG. 3. Calculated distribution of beryllium hydroxo species in acid conditions. (a) $C_{\text{Be}} = 0.2 \text{ M}$, (b) $C_{\text{Be}} = 0.002 \text{ M}$.

to a beryllium concentration of ca. 3 M. The ratio $m = C_{\text{Na}}/C_{\text{Be}}$, which was termed “degree of hydrolysis,” was varied between 0 and 1.16 according to the amounts of carbonate and beryllium present. Spectra obtained at six different m values are shown in Fig. 4. The three distinct lines were assigned to the (aquated) species $[\text{Be}(\text{H}_2\text{O})_4]^{2+}$, $[\text{Be}_2(\text{OH})(\text{H}_2\text{O})_6]^{3+}$, and $[\text{Be}_3(\text{OH})_3(\text{H}_2\text{O})_6]^{3+}$ on the basis that $[\text{Be}(\text{H}_2\text{O})_4]^{2+}$ is the predominant species when $m = 0$ and the trimer is the dominant species when $m = 1$. These results were confirmed by the same author from a study of hydrogen–deuterium isotope effects (28).

^9Be NMR spectra are often referenced to “aqueous beryllium sulfate” as an external standard. Unfortunately, many workers using the standard appear to be unaware that the frequency of the observed line shifts to higher field with increasing concentration of sol-

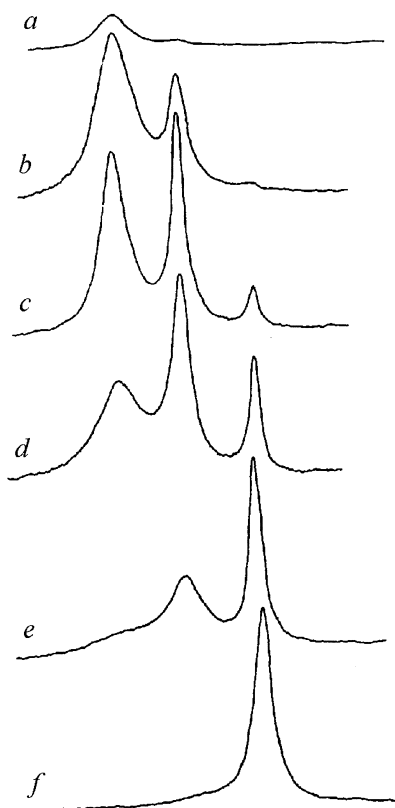


FIG. 4. ^1H NMR spectra of hydrolyzed BeCl_2 solutions showing only the low field hydration water region: $m = (a) 0.0, (b) 0.12, (c) 0.25, (d) 0.40, (e) 0.65, \text{ and } (f) 0.92$. Reproduced with permission from Ref. (27). Copyright 1980. The Royal Society of Chemistry.

ute, as illustrated in Fig. 5. Although the ^9Be nucleus is quadrupolar ($S = 3/2$), the line due to $[\text{Be}(\text{H}_2\text{O})_4]^{2+}$ is relatively narrow because the ion has near tetrahedral symmetry and quadrupolar broadening would be insignificant in an ion of T_d symmetry.

The hydrolysis products all give a single, broad, ^9Be NMR line at ca. 0.74 ppm. The intensity of this line increases with increasing pH up to the point where $\text{Be}(\text{OH})_2$ precipitates (84). The line was assigned to the trimer that is the predominant hydrolysis product. A spectrum of the trimer is shown in Fig. 6 together with the spectrum of the aqua ion for comparison purposes (88). The broadness of the

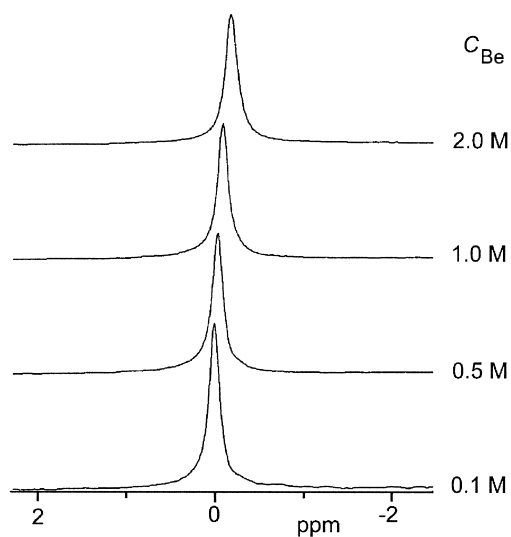


FIG. 5. ^9Be NMR spectra at 28.12 MHz of aqueous beryllium sulfate (293 K) at various concentrations: Chemical shifts are relative to $0.1 \text{ mol dm}^{-3} \text{ BeSO}_4$.

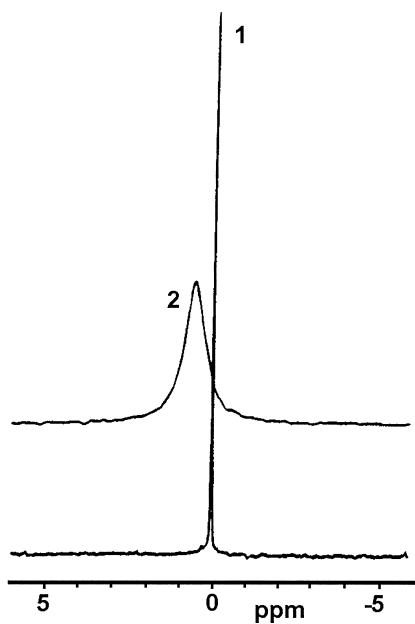


FIG. 6. ^9Be NMR spectra (H_2O , 293 K) of two picrates: **1**, $[\text{Be}(\text{H}_2\text{O})_4](\text{picrate})_2 \cdot \text{H}_2\text{O}$, $C_{\text{Be}} = 0.1 \text{ mol dm}^{-3}$; **2**, $[\text{Be}_3(\text{OH})_5(\text{H}_2\text{O})_6](\text{picrate})_3 \cdot 6\text{H}_2\text{O}$, $C_{\text{Be}} = 0.033 \text{ mol dm}^{-3}$. Reproduced with permission from Ref. (89). Copyright 1998, American Chemical Society.

line due to the trimer is obviously due to the effects of the quadrupolar ^9Be nucleus.

2. Alkaline Solutions

Between pH values of ca. 6 and 12 aqueous solutions hold very little dissolved beryllium because of the low solubility of $\text{Be}(\text{OH})_2$. When the pH is raised above 12, the hydroxide begins to dissolve with the formation of, first, $\text{Be}(\text{OH})_3^-$ and then, at even higher pH values, $\text{Be}(\text{OH})_4^{2-}$ (52). The presence of these species in strongly alkaline solutions was confirmed by means of solvent extraction experiments (90) and infrared spectroscopy (31). A speciation diagram is shown in Fig. 7, which was constructed using the values of $\log \beta_3 = 18.8$ and $\log \beta_4 = 18.6$ critically selected from Table III. The diagram illustrates clearly the precipitation and dissolution of $\text{Be}(\text{OH})_2$.

When $\text{Be}(\text{OH})_2$ is dissolved in strong alkali ($\text{pH} > 12$) a narrow ^9Be NMR signal is observed at ca. 2 ppm (91). This is probably due to the ion $[\text{Be}(\text{OH})_4]^{2-}$ which, with near tetrahedral symmetry, would be subject to little quadrupolar broadening.

B. STRUCTURES

Investigations of the equilibria obtaining in solution have provided information concerning the stoichiometry and stability of the species formed when the beryllium ion is hydrolyzed. Although the identification of the minor species can never be regarded as definitive, there is little doubt that the principal species are $\text{Be}_2(\text{OH})_3^{3+}$ and $\text{Be}_3(\text{OH})_3^{3+}$ in acid solutions and $\text{Be}(\text{OH})_3^-$ and $\text{Be}(\text{OH})_4^{2-}$ in strongly basic solutions. Further support for these conclusions is provided by some crystal structures. The structure of $[\text{Be}_3(\text{OH})_3(\text{H}_2\text{O})_6]$

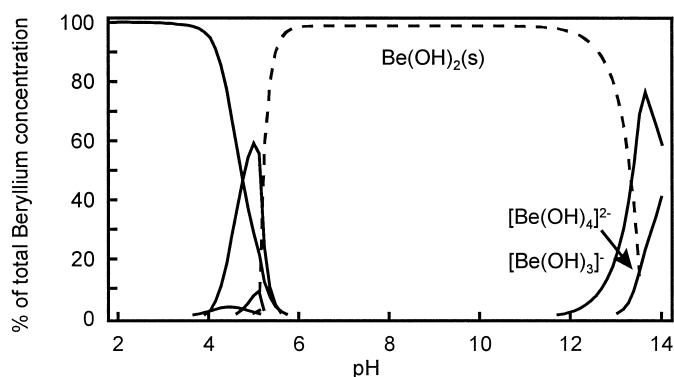


FIG. 7. Calculated distribution diagram of beryllium hydroxo species, $C_{\text{Be}} = 0.002 \text{ M}$.

(picrate)₃·6H₂O (88) confirmed the cyclic nature of the trimeric species. Each beryllium atom is bonded to two water molecules and two bridging hydroxide groups, as shown in Fig. 8. The arrangement of oxygen atoms around the beryllium atom is approximately tetrahedral with O–Be–O angles in the range 103–116° and average distances for Be–OH₂ of 165.9 pm and for Be–OH of 158.9 pm. These values are in good agreement with values for analogous beryllium complexes, where the water molecules of the hydrolysis product are replaced by other ligands: [Be₃(OH)₃(picolate)₃] (92), [Be₃(OH)₃(pyrazolylborate)₃] (93), [Be₃(OH)₃(3,5-dimethylpyrazolylborate)₃] (94) and K₃[Be₃(OH)₃(malonate)₃] (95).

There are as yet no structural data on the mononuclear hydroxo complexes formed at high pH. Schmidbaur *et al.* (91) have obtained the structure of a compound that had been crystallized from a solution at pH 13.2. The compound contains the anion [Be₄(OH)₁₀]²⁻, which has a structure resembling that of adamantane or P₄O₁₀, as shown in Fig. 9.

The solid Ca[Be(OH)₄] is known in the form of various hydrates (96, 97). Schmidbaur and his group have isolated a compound which analyzed as Ca[Be(OH)₄]·3/2H₂O (98). The crystal structure of this compound revealed the surprising fact that this compound contains the anion [(HO)₃Be(OH)Be(OH)₃]³⁻. The structure of this anion, shown in Fig. 10, is remarkably similar to the structure of the cation [(H₂O)₃Be(OH)Be(OH₂)₃]³⁺, which is a principal hydrolysis product in

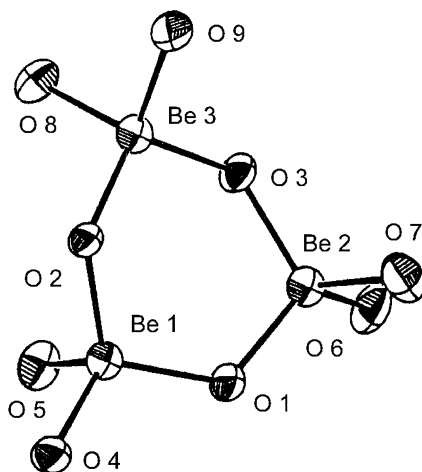


FIG. 8. Perspective view of the trimeric species [Be₃(OH)₃(H₂O)₆]³⁺. Reproduced with permission from Ref. (89). Copyright 1998, American Chemical Society.

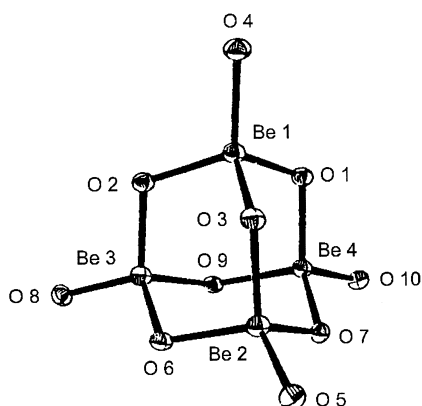


FIG. 9. Molecular structure of the hydroxoberyllate anion $[\text{Be}_4(\text{OH})_{10}]^{2-}$. Reproduced with permission from Ref. (91). Copyright 1998, American Chemical Society.

acid solutions. In fact, the two structures are related by the addition or removal of six protons. The second surprising fact about this compound was the characterization of the anion H_3O_2^- , in which a proton forms a symmetrical bridge between two hydroxide groups, as in HF_2^- . The observation of this species for the first time should serve as a reminder that the hydroxide ion, whether terminal, bridging, or "free," forms strong hydrogen bonds in solution.

The structures of the solids isolated from strongly alkaline solutions cast a shadow of doubt over the simple model in which the only species formed are $\text{Be}(\text{OH})_3^-$ and $\text{Be}(\text{OH})_4^{2-}$. Of course what crystallizes from a solution may well be a species with low equilibrium concentration as the process of crystallization is driven by the insolubility of the product. Nevertheless it is clear that relatively little effort has

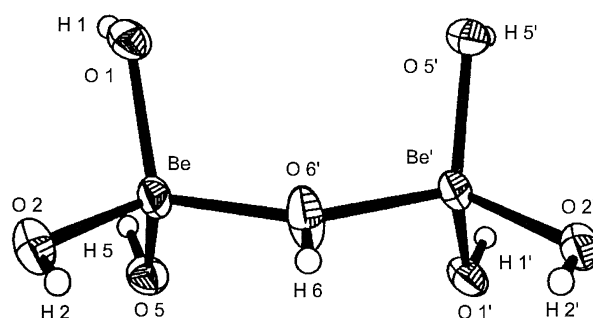


FIG. 10. Molecular structure of the hydroxoberyllate anion $[\text{Be}_2(\text{OH})_7]^{3-}$. Reproduced with permission from Ref. (98). Copyright 1998, American Chemical Society.

been directed at understanding the equilibria obtaining in very basic solutions. This is undoubtedly due in part to difficulties associated with making quantitative measurements (e.g., alkaline error problems with a glass electrode). Another difficulty is that contamination by atmospheric CO_2 can cause severe problems in analyzing the data.

The polynuclear hydroxo-anions isolated as solids will also be present in solution. Their existence points to a chemistry that is formally comparable to polynuclear oxy-anion chemistry—compare $[\text{Be}_2(\text{OH})_7]^{3-}$ to $\text{Cr}_2\text{O}_7^{2-}$. In both cases the protonation of a divalent mononuclear anion results in the formation of a binuclear bridged structure.

C. ENTHALPY AND ENTROPY OF HYDROLYSIS

Carell and Olin (58) were the first to derive thermodynamic functions relating to beryllium hydrolysis. They determined the enthalpy and entropy of formation of the species $\text{Be}_2(\text{OH})^{3+}$ and $\text{Be}_3(\text{OH})_3^{3+}$. Subsequently, Mesmer and Baes determined the enthalpies for these two species from the temperature variation of the respective equilibrium constants. They also determined a value for the species $\text{Be}_5(\text{OH})_7^{3+}$ (66). Ishiguro and Ohtaki measured the enthalpies of formation of $\text{Be}_2(\text{OH})^{3+}$ and $\text{Be}_3(\text{OH})_3^{3+}$ calorimetrically in solution in water and water/dioxan mixtures (99). The agreement between the values is satisfactory considering the fact that they were obtained with different chemical models and ionic media.

The most recent determination (85), by means of microcalorimetry, furnished thermodynamic quantities for both major and minor species in the currently accepted “best” model (84), with the exception of the enthalpy of formation of $\text{Be}(\text{OH})_2$ in solution, which proved to be impossible to determine; the results are shown in Table IV. It is interesting to note that the formation of all the hydrolyzed species is favored by both enthalpy and entropy contributions to the free energy change. The $[\text{Be}(\text{H}_2\text{O})_4]^{2+}$ ion, by virtue of its high charge density, will provoke ordering of the solvent molecules in its vicinity on purely electrostatic grounds (see also Section III). This ordering tendency will be reduced with the reduction of charge density that occurs with hydrolysis. It is therefore to be expected, on electrostatic grounds alone, that the entropy term will be favorable to hydrolysis.

However as well as electrostatics the making and breaking of bonds must be considered. The Be–O bond has considerable covalent character so that it is not obvious, *a priori*, that replacement of water molecules by bridging hydroxide should be favored by a negative enthalpy

TABLE IV
THERMODYNAMIC FUNCTIONS FOR THE FORMATION OF HYDROLYZED
BERYLLIUM(II) SPECIES^a

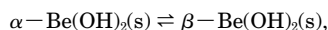
Reaction	log <i>K</i>	−Δ <i>G</i> ° (kJ mol ^{−1})	−Δ <i>H</i> ° (kJ mol ^{−1})	Δ <i>S</i> ° (J K ^{−1} mol ^{−1})
2Be ²⁺ + OH [−] → Be ₂ (OH) ³⁺	10.49(1)	59.87(8)	27(2)	111(7)
3Be ²⁺ + 3H [−] → Be ₃ (OH) ₃ ³⁺	32.39(3)	184.9(2)	100.8(4)	282(1)
5Be ²⁺ + 6H [−] → Be ₅ (OH) ₆ ³⁺	63.83(5)	364.3(3)	208(3)	523(10)
6Be ²⁺ + 8H [−] → Be ₆ (OH) ₈ ³⁺	83.75(5)	478.0(3)	239(2)	802(7)

^a 298 K, 0.5 M NaClO₄; values in parentheses are standard deviations on the last significant figure.

change. The data shown in Fig. 11 indicate that the enthalpy change increases linearly with the number of hydroxide groups present in the hydrolyzed ion. This shows that the replacement of two water molecules by a bridging hydroxide group is indeed an exothermic process and that the enthalpy change is the same for each hydroxide introduced. It is also the case that the entropy term increases with the number of hydroxide groups. Because both $-\Delta H^\circ$ and ΔS° increase linearly with the number of hydroxide groups it follows that the same is true for $-\Delta G^\circ$ and the logarithm of the corresponding equilibrium constant.

D. PRECIPITATION EQUILIBRIA

Three different forms of beryllium hydroxide in the solid state have been described (10, 52, 53, 100). The amorphous form of Be(OH)₂ is obtained as a gelatinous precipitate when alkali is added to a beryllium-containing solution at ambient temperatures. The gelatinous precipitate is slowly transformed into the metastable α form when the mixture is allowed to stand. The stable β form is obtained after the mixture has aged for some months or by precipitation at 70°C. The value of log *K* for the equilibrium between α and β forms,



was estimated from solubility measurements to be 0.37 (10). When determining the solubility product of the hydroxide, account should be taken of the hydrolysis equilibria that precede precipitation. For this reason the original results (52, 53) have been reinterpreted by successive authors as each of them proposed a new hydrolysis scheme.

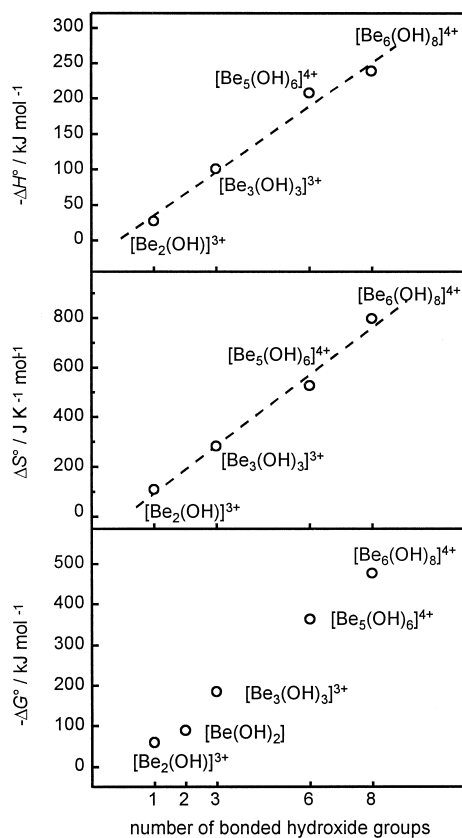


FIG. 11. Thermodynamic functions for the formation of hydroxospecies as a function of the number of contained hydroxide groups; (—) least-squares regression. Reproduced with permission from Ref. (85). Copyright 1998, Wiley-VCH Verlag GmbH.

For example, Bruno (80) found a value of $\log {}^*K_{s0} = 6.87 \pm 0.05$ (extrapolated to infinite dilution) for the equilibrium



This value is very close to the value of 6.85 ± 0.05 originally derived by Schindler and Garrett (53) and is slightly higher than the value of 6.65 ± 0.05 computed by Baes and Mesmer (10).

The crystal structure of $\beta\text{-Be}(\text{OH})_2$ has been determined using both X-ray and neutron diffraction (101). It is very similar to the structure of β -crystallite in that $\text{Be}(\text{OH})_4$ tetrahedra are linked by corner shar-

ing. The hydroxide ions form almost symmetrical bridges between the two adjacent beryllium atoms with an average Be–O distance of 164 pm. Both the structural data and detailed examination of vibrational spectra (102) show that there is hydrogen bonding in the solid state, which is weaker than in the isostructural compound ϵ -Zn(OH)₂. This result may be significant in relation to beryllium hydrolysis in solution, as the explanation proposed was that although the high polarizing power of the beryllium atom increases the hydrogen-bond donor capacity of a bound hydroxide ion, at the same time it decreases capacity of the bound hydroxide ion to accept a hydrogen bond.

V. Interaction with Inorganic Ligands

Few inorganic ligands form stable complexes with the beryllium ion in aqueous solution. This is a reflection of the fact that on the one hand Be²⁺ shows a strong preference for oxygen donor ligands such as water and the hydroxide ion, and on the other hand reacts with the more basic ligands such as ammonia to give the insoluble hydroxide. Reported equilibrium constants are in Table V.

A. FLUORIDES

The fluoride ion is the only inorganic ligand to form a complete substitution series, $[\text{Be}(\text{H}_2\text{O})_{4-n}\text{F}_n]^{(2-n)+}$ ($n = 1-4$), though there is considerable variation in the equilibrium constants that have been reported. The most reliable values are probably those of Anttila *et al.* (117) who used both glass and fluoride-ion selective electrodes and also took account of the competing hydrolysis reactions. They did not, however, make measurements in the conditions where BeF_4^{2-} would have been formed. A speciation diagram based on reported equilibrium constants is shown in Fig. 12. It can be seen that the fluoride ion competed effectively with hydroxide at pH values up to 8, when $\text{Be}(\text{OH})_2$ precipitates.

The formation of the mixed complexes $\text{Be}_3(\text{OH})_3\text{F}^{2+}$ and $\text{Be}_3(\text{OH})_3\text{F}_2^+$ is particularly interesting in that it highlights the stability of the hydroxo-bridged trimer $\text{Be}_3(\text{OH})_3^{3+}$. The ¹⁹F NMR signals in all the fluoro complexes are 1:1:1:1 quartets due to splitting by the $S = 3/2$ ⁹Be nucleus, separate signals being observed for each complex, indicating that there is slow exchange on the NMR time scale. The observation of quartets shows that the fluorides are attached to a single beryllium atom and do not form bridges between two beryllium atoms. Thus,

TABLE V

STABILITY CONSTANTS FOR BERYLLIUM COMPLEXES WITH INORGANIC LIGANDS

Ligand	Method	<i>T</i> (°C)	Medium	Log of equilibrium constants, remarks	Ref.
Fluoride	sol	25	Be(NO ₃) ₂ var	<i>K</i> ₁ 4.29, <i>β</i> ₂ 2.0	103
	col	?	var	<i>K</i> ₁ 5.89, <i>K</i> ₂ 4.94, <i>K</i> ₃ 3.56, <i>K</i> ₄ 1.99	104
	red	0–50	0.5 M NaClO ₄	* <i>K</i> ₁ 2.23, * <i>K</i> ₂ 0.85, * <i>K</i> ₃ –0.78 (at 0°C) * <i>K</i> ₁ 2.12, * <i>K</i> ₂ 0.84, * <i>K</i> ₃ 0.03 (at 25°C) * <i>K</i> ₁ 1.86, * <i>K</i> ₂ 0.67, * <i>K</i> ₃ –0.73 (at 50°C)	105
		25	0 corr	Δ* <i>H</i> ₁ = –14.2, Δ* <i>H</i> ₂ = –7.26, Δ* <i>S</i> ₁ = 6.20, Δ* <i>S</i> ₂ = –8.24	105
	sp		var	<i>K</i> ₁ 5.4	106
	sol	25	var	<i>K</i> ₁ 5.64, <i>K</i> ₂ 2.4	107
	dis	20	2 M HClO ₄	* <i>K</i> ₁ 1.99, * <i>K</i> ₂ 1.12, * <i>K</i> ₃ 0.38	108
	sol	25	Be(NO ₃) ₂ var	<i>K</i> ₁ 4.29	109
	req, qh	25	0.5 M NH ₄ ClO ₄	<i>K</i> ₁ 4.71, <i>K</i> ₂ 3.61, <i>K</i> ₃ 4.71, <i>K</i> ₄ 3.61	110
	ix	?	0.16 NaNO ₃	<i>K</i> ₁ 3.64, <i>β</i> ₂ 5.90 (cation exchange) <i>β</i> ₂ 5.93, <i>β</i> ₃ 7.76, <i>β</i> ₄ 9.12 (anion exchange)	111
	red	25	0.5 M NaClO ₄	Δ <i>H</i> ₁ = –1.7, Δ <i>S</i> ₁ = 92, <i>I</i> = 0.5 M NaClO ₄ Δ <i>H</i> ₁ = –0.8, Δ <i>S</i> ₁ = 113, <i>I</i> = 0 (corr)	112
	nmr	2–50	var	<i>K</i> ₄ 1.1, Δ <i>H</i> ₄ ≈ 0, Δ <i>S</i> ₄ = 21	113
	nmr	25	var	<i>K</i> ₁ 3.0, <i>K</i> ₂ 2.7, <i>K</i> ₃ 2.0, <i>K</i> ₄ 1.1	114
	<i>i</i> E	25	1 M NaClO ₄	<i>K</i> ₁ 5.28	115
	H, F	25	1 m NaClO ₄	<i>K</i> ₁ 4.99, <i>β</i> ₂ 8.80, <i>β</i> ₃ 11.61, <i>β</i> ₄ 13.05	116
	H, F	0–60	1 m NaCl	<i>K</i> ₁ 4.94, <i>β</i> ₂ 8.80, <i>β</i> ₃ 11.53, <i>β</i> ₄ 13.00 (at 0°C) <i>K</i> ₁ 4.90, <i>β</i> ₂ 8.66, <i>β</i> ₃ 11.45, <i>β</i> ₄ 12.88 (at 25°C) <i>K</i> ₁ 4.90, <i>β</i> ₂ 8.59, <i>β</i> ₃ 11.25, <i>β</i> ₄ 12.66 (at 60°C) Δ <i>H</i> ₁ = –1.5, Δ <i>H</i> ₂ = –4.8, Δ <i>H</i> ₃ = –1.2, Δ <i>H</i> ₄ = –1.9 Δ <i>S</i> ₁ = 89, Δ <i>S</i> ₂ = 56, Δ <i>S</i> ₃ = 49, Δ <i>S</i> ₄ = 20.9	116
	H, F	25	3 M NaClO ₄	<i>K</i> ₁ 5.21, <i>β</i> ₂ 9.57, <i>β</i> ₃₁₋₃ –4.18, <i>β</i> ₃₂₋₃ –0.67	117
Chloride	dis	20	HCl var	<i>K</i> ₁ –0.66	108
	ix	18	0.5 M NaClO ₄	<i>K</i> ₁ 1.11, <i>β</i> ₂ 0.30, <i>β</i> ₃ 1.40	118
	dis	20	0.7 M HClO ₄	<i>K</i> ₁ –0.36	119
	dis	25	4 M NaClO ₄	<i>K</i> ₁ –0.85, <i>β</i> ₂ –0.70	120
	dis	20	0.7 M NaClO ₄	<i>K</i> ₁ –0.42	119
	dis	25	4 M NaClO ₄	<i>K</i> ₁ –0.7, <i>β</i> ₂ –0.8	120
Thiocyanate	ix	18	1 M NaClO ₄	<i>K</i> ₁ 0.13, <i>β</i> ₂ 0.13	121
	dis	25	4 M NaClO ₄	<i>K</i> ₁ –0.16, <i>β</i> ₂ –0.60	120

TABLE V (Continued)

Ligand	Method	<i>T</i> (°C)	Medium	Log of equilibrium constants, remarks	Ref.
Sulfate	ix	18	0.5 NaClO ₄	<i>K</i> ₁ 0.72	122
	kin	25	0	<i>K</i> ₁ 1.95	123
	dis	25	1 M NaClO ₄	β_2 1.78, β_3 2.08	124
	Hg	35	0	<i>K</i> ₁ 2.17	125
	var	25	0	<i>K</i> ₁ 2.22 (kin), <i>K</i> ₁ 2.16 (sp)	126
Selenite	con	18	dil	<i>K</i> _s [BeL (s) → Be ²⁺ + L ²⁻] −8.0	127
Nitrate	ix	18	0.5 NaClO ₄	<i>K</i> ₁ −0.60, β_2 1.62	118
	dis	25	4 M NaClO ₄	<i>K</i> ₁ −0.63	120
Phosphate	gl, sol	19–20	dil	<i>K</i> _s [Be ₃ L ₂ (s) → 3Be ²⁺ + 2L ³⁻] −3.77, <i>K</i> _s [Be(NH ₄)L(s) → Be ²⁺ + NH ₄ ⁺ + 2L ³⁻] −19.7	128
	gl	25	3 M NaClO ₄	<i>K</i> [Be ²⁺ + H ₃ L → BeH ₂ L ⁺ + H ⁺] 0.00, <i>K</i> [Be ²⁺ + 2H ₃ L → Be(H ₂ L) ₂ + 2H ⁺] 0.59, <i>K</i> [2Be ²⁺ + H ₃ L → Be ₂ (OH)(H ₂ L) ²⁺ + 6H ⁺] −0.43, <i>K</i> [3Be ²⁺ + 3H ₃ L → Be ₃ (OH) ₃ (H ₂ L) ₃ + 6H ⁺] −2.06, <i>K</i> [3Be ²⁺ + 6H ₃ L → Be ₃ O(H ₂ L) ₆ ²⁺ + 8H ⁺] 1.57, <i>K</i> [3Be ²⁺ + H ₃ L → Be ₃ (OH) ₃ (HL) ⁺ + 5H ⁺] −8.37 or <i>K</i> [3Be ²⁺ + H ₃ L → Be ₃ (OH) ₃ L + 6H ⁺] −12.12	129
Diphosphate	gl	25	0.1 M KCl	<i>K</i> ₁ 10.08, β_2 15.45, <i>K</i> [Be ²⁺ + HL ³⁻ → BeHL ²⁻] 5.98	130
Tripolyphosphate	gl, cal	20	0.1 M (CH ₃) ₄ NNO ₃	<i>K</i> [BeL ³⁻ + H ⁺ → BeHL ²⁻] 5.35, $\Delta H_1 = 19.7$	131
Carbonate	gl	25	3 M NaClO ₄	<i>K</i> [Be ²⁺ + H ₂ L → BeL + 2H ⁺] −10.4, <i>K</i> [3Be ²⁺ + 2H ₂ O + H ₃ L → Be ₃ (OH) ₂ (HL) ³⁺ + 3H ⁺] −8.90, <i>K</i> [5Be ²⁺ + 4H ₂ O + H ₂ L → Be ₅ (OH) ₄ L ⁴⁺ + 6H ⁺] −17.24, <i>K</i> [6Be ²⁺ + 7H ₂ O + 2H ₂ L → Be ₆ (OH) ₇ (HL) ₂ ³⁺ + 9H ⁺] −29.46	132
	gl, sol	25	3 M NaClO ₄	<i>K</i> [Be ²⁺ + H ₂ L → BeL + 2H ⁺] −10.12, <i>K</i> [Be ²⁺ + H ₂ O + H ₂ L → Be(OH)L [−] + 3H ⁺] −16.82, <i>K</i> [Be ²⁺ + 2H ₂ O + H ₂ L → Be(OH) ₂ L ²⁻ + 4H ⁺] −24.22, <i>K</i> [3Be ²⁺ + 3H ₂ O + 3H ₃ L → Be ₃ (OH) ₃ L ₃ ³⁻ + 9H ⁺] −45.5 <i>K</i> [3Be ²⁺ + 3H ₂ O + 3H ₂ L → Be ₃ (OH) ₄ L ₃ ⁴⁻ + 10H ⁺] −52.0 * <i>K</i> [Be(OH) ₂ (s) + H ₂ L → BeL + 2H ⁺] 6.18	81

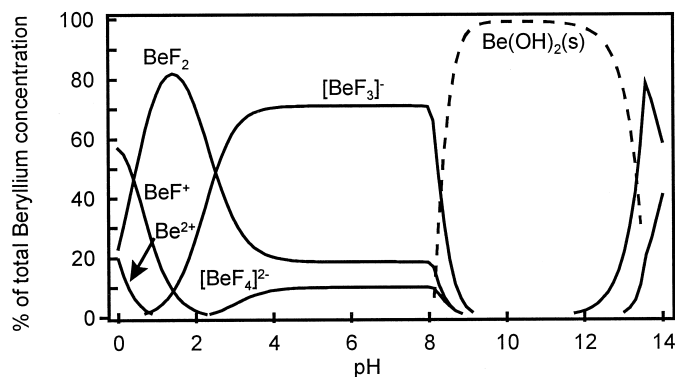
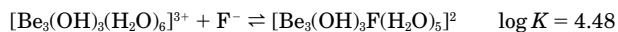


FIG. 12. Calculated species distribution for fluoro and hydroxo complexes in solution. $C_{\text{Be}} = 0.002 \text{ mol dm}^{-3}$, $C_{\text{F}} = 0.02 \text{ mol dm}^{-3}$.

the fluoride ions replace water molecules in both the monomer and the trimer (117). The stepwise equilibrium constants for the reactions



are remarkably similar. Chemical shifts and coupling constants for the species observed are given in Table VI. Values for $\text{Be}_3(\text{OH})_3\text{F}^{2+}$ and $\text{Be}_3(\text{OH})_3\text{F}_2$ are approximate as they seem to show some concentration dependence. Measurements of the area of each peak were used to estimate the concentrations of the corresponding complex in the various mixtures. This was of considerable assistance in defining the

TABLE VI

^{19}F NMR DATA FOR FLUORO COMPLEXES OF BERYLLIUM(II) IN AQUEOUS SOLUTION^a

Species	^{19}F chemical shift (ppm) ^b	$^1J(^9\text{Be}-^{19}\text{F})$ (Hz)
BeF^+	-98.0	42.2
BeF_2	-95.8	29.7
BeF_3^-	-94.6	37.3
$\text{Be}_3(\text{OH})_3\text{F}^+$	≈ -88.6	≈ 35
$\text{Be}_3(\text{OH})_3\text{F}_2^+$	≈ -89.2	≈ 34

^a Taken from Ref. (117); 298 K, 3 M NaClO_4 .

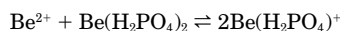
^b Relative to pure trifluoroacetic acid as external standard.

chemical model, although the authors also report the presence of some unassigned NMR peaks of very low intensity.

The kinetics of fluoride substitution reactions have been studied (133). The relatively low activation enthalpy for the reaction provoked Strehlow to suggest an unusual mechanism (see Ref. (32) for details).

B. OTHER INORGANIC ANIONS

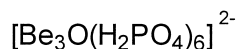
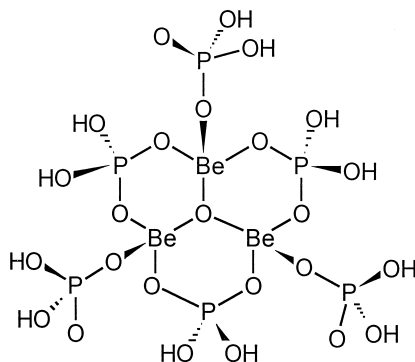
The only other inorganic ligands to form fairly stable complexes are phosphate and carbonate, and there is some similarity between the complexes formed by these ligands. Beryllium forms two mononuclear complexes with the dihydrogen phosphate ion, BeL^+ and BeL_2 ($\text{L} = \text{H}_2\text{PO}_4^-$) (129). The equilibrium constant derived for the formation of BeL^+ , $\log K_1 = 1.87$, is less than for fluoro- and carbonato-complexes, but larger than for other inorganic ligands. Curiously, the value of the equilibrium constant for the disproportionation reaction



$K = 0.3 \pm 0.1$, is much lower than the value of 4 that would be expected on purely statistical grounds. This was explained in terms of the formation of intramolecular hydrogen bonds. The H_2PO_4^- ion also replaces water molecules in the principal hydrolysis products: the complexes with stoichiometry $\text{Be}_2(\text{OH})(\text{H}_2\text{PO}_4)^{2+}$ and $\text{Be}_3(\text{OH})_3(\text{H}_2\text{PO}_4)_3$ were clearly established, while the complex $\text{Be}_3(\text{OH})_3(\text{HPO}_4)^+$ seems likely. In addition, a complex with the stoichiometry $\text{Be}_3\text{H}_8(\text{H}_3\text{PO}_4)_6$ was indicated. This complex, it was suggested, does not contain the $\text{Be}_3(\text{OH})_3$ core but should probably be formulated as $[(\text{H}_2\text{PO}_4)_6\text{Be}_3\text{O}]^{2-}$ with a structure closely related to the well-known "basic beryllium acetate" (see below): a central oxygen atom is surrounded by three beryllium atoms; three phosphate units form bridges between two beryllium atoms and the other three phosphate units are attached as monodentate ligands.

Carbonate also forms a mononuclear complex (132). Using an (ionic strength and temperature adjusted) value of $\log \beta_2$ for the formation of carbonic acid, $\text{CO}_3^{2-} + 2\text{H}^+ \rightleftharpoons \text{CO}_2(\text{aq}) + \text{H}_2\text{O}$, of 15.92 (11), $\log K$ for the equilibrium $\text{Be}^{2+} + \text{CO}_3^{2-} \rightleftharpoons \text{BeCO}_3(\text{aq})$ was derived as 5.4. The other carbonato species formed were assigned the formulas $\text{Be}_3(\text{OH})_2(\text{HCO}_3)^{3+}$ and $\text{Be}_5(\text{OH})_4(\text{CO}_3)^{4+}$, since the Raman spectra of the coordinated carbonate appeared to be different in the two complexes, but the structures proposed for these species are not imme-

diately convincing. No structure was proposed for the complex " $\text{Be}_6(\text{OH})_9(\text{CO}_2)^{3+}$."



In alkaline solutions two more monomeric complexes and a polymeric complex were found (81). The predominant monomeric complex was assigned the formula $\text{Be}(\text{OH})_2(\text{CO}_3)^{2-}$; $\text{BeCO}_3(\text{aq})$ and $\text{Be}(\text{OH})(\text{CO}_3)^-$ were found as minor species. The stoichiometry of the polymeric complex could not be established with certainty.

Halides other than fluoride form very weak complexes in aqueous solution; there are no reliable equilibrium constants to be found in the literature. The solution chemistry of aqueous solutions of beryllium chloride, bromide, and iodide have been reviewed previously (9). Some evidence for the formation of thiocyanate complexes was obtained in solvent extraction studies (134).

VI. Interaction with Organic Ligands

A. MONOCARBOXYLATE LIGANDS

Published equilibrium constants for monocarboxylato complexes are summarized in Table VII. All that can be deduced with certainty from these data is that the anions derived from monocarboxylic acids form rather weak complexes with beryllium. In all probability they act as monodentate ligands. The possibility of bidentate chelation using both carboxylate oxygen atoms can be ruled out on the grounds

TABLE VII

STABILITY CONSTANTS FOR MONOCARBOXYLATO COMPLEXES OF BERYLLIUM(II)

Ligand	Method	$T/^{\circ}\text{C}$	Medium	Log of equilibrium constants, remarks	Ref.
Formate	kin	25	dil	K_1 0.15	135
Acetate	dis	25	0.1 M	K_1 1.62, β_2 2.36	136
Propionate	gl	25–45	1 M NaClO ₄	K_1 0.30, β_2 4.2 (at 25°), K_1 0.55, β_2 4.4 (at 35°), K_1 1.00, β_2 4.4 (at 45°)	137
Cyclohexene-carboxylate	sp	?	?	K_1 3.32	138
Nitroacetate	kin	18	0.2 M Ba(NO ₃) ₂	K_1 0.26	139

of both the large bite of the CO₂ group and the formation of a four-membered ring.

A different situation obtains in compounds such as the basic beryllium monocarboxylates (140–142). In particular the acetate derivative, Be₄O(O₂CCH₃)₆, has been known in the solid state for nearly 100 years (143). A partial structure of this compound is in Fig. 13 (144). The central oxide ion is surrounded by a tetrahedron of beryllium atoms. The acetate ions form bridges across the six edges of the Be₄ tetrahedron, with each acetate bonding with two Be atoms. Each beryllium atom is surrounded by an approximate tetrahedron of

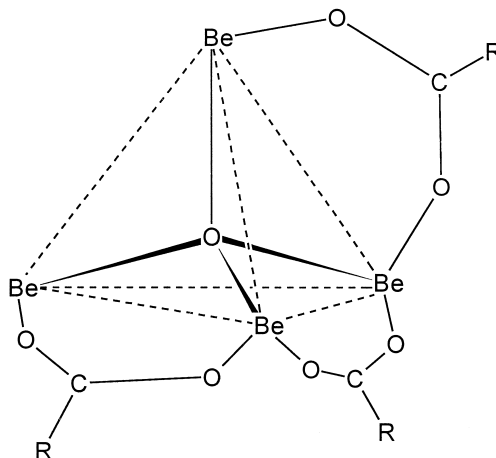
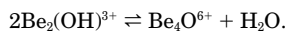


FIG. 13. Partial schematic view of the structure of Be₄O(O₂CCH₃)₆, showing three acetate groups only.

oxygen atoms. As yet there is no evidence for the existence of this species in solution, even though the central core is formally a dimer of the first hydrolysis product:



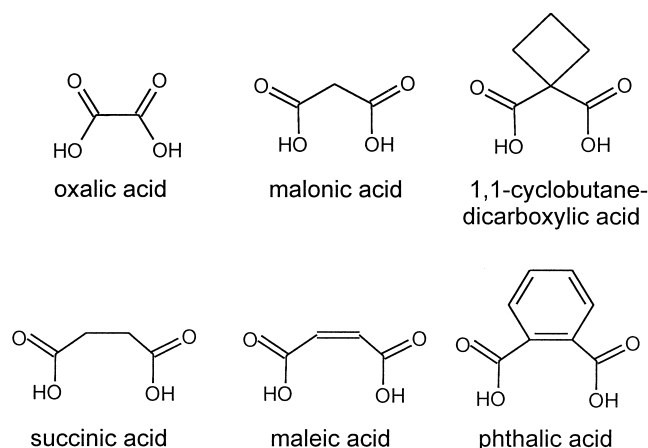
An analogous nitrato complex, $\text{Be}_4\text{O}(\text{NO}_3)_6$, is known in the solid state (145). The presence of a central 4-coordinate oxide ion and bridging nitrato ions has been confirmed by X-ray methods (146). The structures of these solid-state μ_4 -oxo complexes lend support to the μ_3 -oxo structures suggested for phosphato and carbonato complexes in solution (see Section IV).

B. BISCARBOXYLATE LIGANDS

Ligands containing more than one carboxylate group can form stable complexes with beryllium that contain one or more chelate rings. Complexes of the types $[\text{Be}(\text{L})(\text{H}_2\text{O})_2]$, $[\text{Be}(\text{L})_2]^{2-}$, $[\text{Be}_3(\text{OH})_3(\text{L})(\text{H}_2\text{O})_4]^+$, and $[\text{Be}_3(\text{OH})_3(\text{L})_3]^{3-}$ have been characterized for a number of ligands containing two carboxylate groups. Equilibrium constants for these and related complexes are given in Table VIII. It is clear that the formation of complexes with these ligands goes hand in hand with the process of beryllium hydrolysis. This is due to the fact that the acids, H_2L , are not fully dissociated in the pH range where beryllium hydrolysis is important, resulting in a relatively low concentration of the ligand L^{2-} . The wide range of equilibrium constant values in the literature is due, above all, to the effects of neglecting the hydrolysis reactions.

Vacca *et al.* have examined a series of ligands in order to determine the influence of ring size and inductive effects on the complexes formed (85, 95, 167). The size of the chelate ring formed depends on the number of carbon atoms between the carboxylate groups. Five-membered rings are formed by the oxalate ion; six-membered rings by malonate and C-substituted malonate ions; seven-membered rings by succinate, phthalate, and maleate. The results are summarized in Table IX. The ligands that give seven-membered rings form much weaker complexes than those that give six-membered rings. Further insight into thermodynamics of formation of these complexes is provided by the results of calorimetric measurements (85), summarized in Table X.

In all cases studied the standard enthalpy change accompanying the replacement of two water molecules by the chelating ligand is



positive, that is, unfavorable. The entropy change is the determining factor that makes these complexes stable. In other words, the chelate effect provides the driving force for the formation of these complexes. These results help to explain why monocarboxylate complexes are so weak.

A comparison of oxalato, malonato, and succinato complexes (Fig. 14) shows that the malonato complexes are the most stable because of the least unfavorable enthalpy term. The entropy term is virtually the same for the formation of all three ML complexes. These thermodynamic results indicate that with beryllium the formation of a six-membered ring is more favorable than the formation of five- or seven-membered rings. It is probably significant that there is little stereochemical strain with a six-membered ring, as this configuration is most compatible with both the tetrahedral geometry of the beryllium ion and the trigonal geometry at the sp^2 carbon atoms. With the oxalato complex strain is evident in the small O–Be–O angle found in the solid state (*vide infra*, Table XII).

Ligands with more than two carboxyl groups do not seem to form more stable complexes than the biscarboxylate ligands. An example is the ligand propane-1,2,3-tricarboxylate (tricarballilate) for which the equilibrium constant for the formation of the complex BeL^- is little greater than with succinate (76).

The interaction between beryllium and dicarboxylates has also been followed by ^9Be NMR spectroscopy (85, 95, 167–169). Representative spectra are shown in Figs. 15 and 16 (95).

Assignment of the spectra in Fig. 16 is straightforward, as the species distribution diagrams show the four Be-containing species have

TABLE VIII

STABILITY CONSTANTS FOR POLYCARBOXYLATO COMPLEXES OF BERYLLIUM(II)

Ligand	Method	T (°C)	Medium	Log of equilibrium constants, remarks	Ref.
Oxalate	sp	?	?	K_1 4.87	138
	gl	25	0.15 M NaClO ₄	K_1 4.08, β_2 5.91	147
	dis	20	0.1 M KClO ₄	K_1 4.12	148
	gl	30	0.2 M NaClO ₄	K_1 4.08, K_2 1.83	149
	dis	25	1 M NaClO ₄	K_1 3.55, β_2 5.40	124
	gl		2 M NaNO ₃	K_1 3.2, β_2 5.7, β_{22-2} -0.85	150
	gl	20	0.1 M KNO ₃	K_1 4.08, K_2 1.30	151
	gl	25	0.5 M NaClO ₄	K_1 3.52, β_2 5.57, β_{31-3} -3.85, β_{33-3} -0.59	152
	ram	20	var	K_1 3.26, β_2 5.32, $K[3\text{Be}^{2+} + 3\text{L}^{2-} + 3\text{OH}^- \rightarrow \text{Be}_3(\text{OH})_3\text{L}_3^{3-}]$ 39.94	153
	kin	25	0	$K[\text{Be}^{2+} + \text{HL}^- \rightarrow \text{Be}(\text{HL})^+]$ 1.23, $K[\text{BeL} + \text{H}^+ \rightarrow \text{Be}(\text{HL})^+]$ 3.0	154
	lit	20	0.1 M (K ⁺)	K_1 4.10, β_2 5.38	23
	lit	25	0.1 M (Na ⁺)	K_1 4.08	23
	lit	25	0.5 M (Na ⁺)	K_1 3.52, β_2 5.57, β_{31-3} -3.85, β_{33-3} -0.59	23
	lit	25	1 M (Na ⁺)	K_1 3.55, β_2 5.40	23
	gl	25	0.5 M NaClO ₄	K_1 3.47, β_2 5.24, $K[\text{Be}_3(\text{OH})_3^{3+} + \text{L}^{2-} \rightarrow \text{Be}_3(\text{OH})_3\text{L}^+]$ 3.78, $K[\text{Be}_3(\text{OH})_3^{3+} + 3\text{L}^{2-} \rightarrow \text{Be}_3(\text{OH})_3\text{L}_3^{3-}]$ 8.3	95
	cal	25	0.5 M NaClO ₄	ΔH_1 19.5, ΔS_1 132, ΔH_2 31, ΔS_1 138, $\Delta H[\text{Be}_3(\text{OH})_3^{3+} + \text{L}^{2-} \rightarrow \text{Be}_3(\text{OH})_3\text{L}^+]$ 10.9, $\Delta S[\text{Be}_3(\text{OH})_3^{3+} + \text{L}^{2-} \rightarrow \text{Be}_3(\text{OH})_3\text{L}^+]$ 109, $\Delta H[\text{Be}_3(\text{OH})_3^{3+} + 3\text{L}^{2-} \rightarrow \text{Be}_3(\text{OH})_3\text{L}_3^{3-}]$ 28, $\Delta S[\text{Be}_3(\text{OH})_3^{3+} + 3\text{L}^{2-} \rightarrow \text{Be}_3(\text{OH})_3\text{L}_3^{3-}]$ 254	85
Malonate	gl	?	?	K_1 4.98	138
	gl	25	0.15 M NaClO ₄	K_1 5.73, β_2 9.28	147
	gl	30	0.2 M NaClO ₄	K_1 5.15, β_2 8.48	149
	gl	25-35	1 M NaClO ₄	$K[\text{Be}^{2+} + \text{HL}^- \rightarrow \text{Be}(\text{HL})^+]$ 2.65 (at 25°C) $K[\text{Be}^{2+} + 2\text{HL}^- \rightarrow \text{Be}(\text{HL})_2]$ 5.32 (at 25°C) $K[\text{Be}^{2+} + \text{HL}^- \rightarrow \text{Be}(\text{HL})^+]$ 2.77 (at 35°C) $K[\text{Be}^{2+} + 2\text{HL}^- \rightarrow \text{Be}(\text{HL})_2]$ 5.43 (at 35°C)	155
	gl	20	0.1 M KNO ₃	K_1 5.30, K_2 3.26	151
	gl	25	0.5 M NaClO ₄	K_1 5.34, β_2 8.85, β_{33-3} 0.81	156
	kin	25	0	$K[\text{Be}^{2+} + \text{HL}^- \rightarrow \text{Be}(\text{HL})^+]$ 1.26, $K[\text{BeL} + \text{H}^+ \rightarrow \text{Be}(\text{HL})^+]$ 1.66	154

TABLE VIII (Continued)

Ligand	Method	T (°C)	Medium	Log of equilibrium constants, remarks	Ref.
Diethyl- malonate Succinate	ram	20		K_1 5.51, β_2 8.88, $K[\text{Be}_3(\text{OH})_3^{3+} + 3\text{L}^{2-} \rightarrow \text{Be}_3(\text{OH})_3\text{L}_3^{3-}]$ 2.88	157
	lit	20	0.1 M	K_1 5.30, β_2 8.56	23
	lit	25	0.5 M	K_1 5.10, β_2 8.85, $K[\text{Be}_3(\text{OH})_3^{3+} + 3\text{L}^{2-} \rightarrow \text{Be}_3(\text{OH})_3\text{L}_3^{3-}]$ 0.89	23
	gl	25	0.5 M NaClO ₄	K_1 5.36, β_2 9.21, $K[\text{Be}_3(\text{OH})_3^{3+} + \text{L}^{2-} \rightarrow \text{Be}_3(\text{OH})_3\text{L}^+]$ 5.26, $K[\text{Be}_3(\text{OH})_3^{3+} + 3\text{L}^{2-} \rightarrow \text{Be}_3(\text{OH})_3\text{L}_3^{3-}]$ 12.84	95
	cal	25	0.5 M NaClO ₄	ΔH_1 10.53, ΔS_1 138.0, ΔH_2 5.19, ΔS_1 91.2, $\Delta H[\text{Be}_3(\text{OH})_3^{3+} + \text{L}^{2-} \rightarrow \text{Be}_3(\text{OH})_3\text{L}^+]$ 8.4, $\Delta S[\text{Be}_3(\text{OH})_3^{3+} + \text{L}^{2-} \rightarrow \text{Be}_3(\text{OH})_3\text{L}^+]$ 129, $\Delta H[\text{Be}_3(\text{OH})_3^{3+} + 3\text{L}^{2-} \rightarrow \text{Be}_3(\text{OH})_3\text{L}_3^{3-}]$ 18.8, $\Delta S[\text{Be}_3(\text{OH})_3^{3+} + 3\text{L}^{2-} \rightarrow \text{Be}_3(\text{OH})_3\text{L}_3^{3-}]$ 309	85
	sp	?	?	K_1 4.99	138
	sp	?	?	K_1 3.08	138
	gl	25	0.15 M NaClO ₄	K_1 4.69, β_2 6.43	147
	gl	25–35	1 M NaClO ₄	$K[\text{Be}^{2+} + \text{HL}^- \rightarrow \text{Be}(\text{HL})^+]$ 2.48 (25°), 2.56 (35°), $K[\text{Be}^{2+} + 2\text{HL}^- \rightarrow \text{Be}(\text{HL})_2]$ 4.90 (25°), 5.23 (35°)	155
	gl	25	1 M KNO ₃	K_1 3.13, $K[\text{Be}^{2+} + \text{L}^{2-} + \text{H}^+ \rightarrow \text{BeHL}^+]$ 6.54, $K[\text{Be}^{2+} + \text{L}^{2-} \rightarrow \text{Be}(\text{OH})\text{L}^- + \text{H}^+]$ -2.64	76
	gl	25	0.5 M NaClO ₄	K_1 2.74, β_2 4.36, $K[\text{Be}^{2+} + 2\text{HL}^- \rightarrow \text{Be}(\text{HL})_2]$ 3.05, $K[\text{Be}_3(\text{OH})_3^{3+} + \text{HL}^- \rightarrow \text{Be}_3(\text{OH})_3(\text{HL})^{2+}]$ 2.0, $K[\text{Be}_3(\text{OH})_3^{3+} + 3\text{L}^{2-} \rightarrow \text{Be}_3(\text{OH})_3\text{L}_3^{3-}]$ 5.07	156
	kin	25	0	$K[\text{Be}^{2+} + \text{HL}^- \rightarrow \text{Be}(\text{HL})^+]$ 1.48, $K[\text{BeL} + \text{H}^+ \rightarrow \text{Be}(\text{HL})^+]$ 2.69	154
	lit	25	0.5 M	K_1 2.74, β_2 4.36	23
	lit	25	1 M	K_1 3.13, $K[\text{BeL} \rightarrow \text{Be}(\text{OH})\text{L}^- + \text{H}^+]$ 5.59	23
	gl	25	0.5 M NaClO ₄	K_1 3.04, β_2 4.1, $K[\text{Be}_3(\text{OH})_3^{3+} + \text{L}^{2-} \rightarrow \text{Be}_3(\text{OH})_3\text{L}^+]$ 2.03	85
	cal	25	0.5 M NaClO ₄	ΔH_1 21.1, ΔS_1 129, ΔH_2 15, ΔS_1 69, $\Delta H[\text{Be}_3(\text{OH})_3^{3+} + \text{L}^{2-} \rightarrow \text{Be}_3(\text{OH})_3\text{L}^+]$ 42, $\Delta S[\text{Be}_3(\text{OH})_3^{3+} + \text{L}^{2-} \rightarrow \text{Be}_3(\text{OH})_3\text{L}^+]$ 181	85
Maleate	sp	?	?	K_1 3.24	138
	gl	25	0.15 M NaClO ₄	K_1 4.33, β_2 6.46	147
	kin	25	0	$K[\text{Be}^{2+} + \text{HL}^- \rightarrow \text{Be}(\text{HL})^+]$ 1.48, $K[\text{BeL} + \text{H}^+ \rightarrow \text{Be}(\text{HL})^+]$ 3.5	154
Fumarate	sp	?	?	K_1 3.23	138

(continued)

TABLE VIII (Continued)

Ligand	Method	<i>T</i> (°C)	Medium	Log of equilibrium constants, remarks	Ref.
Adipate	sp	?	?	K_1 3.24	138
Phthalate	gl	25	0.15 M NaClO ₄	K_1 3.97, β_2 5.69	147
2-Oxosuccinate	sp	25	0.2 M NaClO ₄	$K[\text{Be}^{2+} + \text{HL}^- \rightarrow \text{Be}(\text{HL})^+]$ 3.1	158
	kin	25	0.2 M NaClO ₄	$K[\text{Be}^{2+} + \text{HL}^- \rightarrow \text{Be}(\text{HL})^+]$ 3.3	158
Diglycolate	gl	25	0.1 M NaClO ₄	K_1 2.62	159
Aurintricarboxylate	oth	25	0.16 M	K_1 5.38	160
	sp	25	?	K_1 4.54	161
Tricarballilate	gl	25	1 M KNO ₃	K_1 3.75, β_{111} 8.00	162
Anthranilate	gl	25	0.5 M NaClO ₄	K_1 1.95, β_{22-1} 1.50, β_{33-3} -7.34, β_{32-3} -5.62	163
Folate	gl	30	var (KNO ₃)	K_1 4.65, β_2 8.35 ($I = 0.1$ M); K_1 4.80, β_2 8.50 ($I = 0.05$ M); K_1 5.15, β_2 9.05 ($I = 0.01$ M); K_1 5.30, β_2 9.45 ($I \rightarrow 0$)	164
Mercaptoacetate	gl	25–45	0.065 M	K_1 7.17, β_2 12.58 (at 25°), K_1 6.95, β_2 11.84 (at 35°), K_1 6.82, β_2 11.68 (at 45°), $\Delta H = -102$	165
Thiophene-2-carboxylate	Gl	30	0.2 M NaClO ₄	K_1 2.15, β_2 4.21	166

maximum concentrations in distinct pH zones. Using these assignments the more complicated spectra shown in Fig. 15 could also be assigned. The ^9Be NMR spectra of the weaker succinato complexes did not show separate lines for all the complexes known to be present (85). For example, the spectrum of a mixture of beryllium sulfate and succinic acid in a molar ratio 1:2, at pH 5.9, just prior to the precipitation of the hydroxide, has a broad line at ca. 0.7 ppm due to the species $[\text{Be}_3(\text{OH})_3(\text{H}_2\text{O})_6]^{3+}$, with a shoulder on the downfield side. The two species $[\text{Be}(\text{succ})\text{H}_2\text{O}]_2$ and $[\text{Be}(\text{succ})_2]^{2-}$ (169), whose chemical shifts were determined separately to be 1.02 and 1.42 ppm, respectively, did not give rise to separate lines even though speciation calculations showed them to be present at low concentration.

The chemical shifts of the species $[\text{BeL}_2]^{2-}$ have been found in the range 4.95–1.42 ppm, $[\text{Be}_3(\text{OH})_3\text{L}_3]^{3-}$ in the range 3.19–1.55 ppm, and $[\text{BeL}(\text{H}_2\text{O})_2]$ in the range 2.90–1.02 ppm (Table XI). In general, successive substitution of water molecules by the anionic ligand L^{2-} results in a shift to lower field.

The size of the chelate ring influences the ^9Be resonance frequencies, as has been noted previously: The smaller the ring, the more

TABLE IX
STABILITY CONSTANTS OF SOME SUBSTITUTED MALONATO AND
RELATED BERYLLIUM(II) COMPLEXES^a

Ligand	log K_1	log K_2	log K_x	log K_y
Malonate	5.36(2)	3.85(1)	5.26(7)	12.84(6)
Methylmalonate	5.394(7)	3.683(7)	5.47(6)	12.64(3)
Dimethylmalonate	5.544(5)	3.737(8)	5.22(5)	12.57(3)
Phenylmalonate	5.130(7)	3.48(1)	4.92(4)	11.05(4)
CBDC ^c	5.51(7)	3.38(1)		10.68(9)
Phthalate	3.170(8)	2.15(4)	2.44(8)	
Succinate	3.04(1)	1.0(2)	2.03(6)	

^a 25°C, 3 M NaClO₄; values in parentheses are standard deviations on the last significant figure.

^b $K_x = K[\text{Be}_3(\text{OH})_3^{3+} + \text{L}^{2-} \rightarrow \text{Be}_3(\text{OH})_3\text{L}^+]$.

^c $K_y = K[\text{Be}_3(\text{OH})_3^{3+} + 3\text{L}^{2-} \rightarrow \text{Be}_3(\text{OH})_3\text{L}_3^{3-}]$.

^c Cyclobutane-1,1-dicarboxylate.

TABLE X
THERMODYNAMIC FUNCTIONS FOR THE FORMATION OF OXALATO, MALONATO, AND
SUCCINATO BERYLLIUM(II) COMPLEXES^a

Reaction	ΔG° (kJ mol ⁻¹)	ΔH° (kJ mol ⁻¹)	ΔS° (J K ⁻¹ mol ⁻¹)
L = oxalate			
$\text{Be}^{2+} + \text{L}^{2-} \rightarrow \text{BeL}$	-19.8(1)	19.5(3)	132(1)
$\text{BeL} + \text{L}^{2-} \rightarrow \text{BeL}_2^{2-}$	-10.1(4)	31(1)	138(3)
$\text{Be}^{2+} + 2\text{L}^{2-} \rightarrow \text{BeL}_2^{2-}$	-29.9(4)	49(2)	263(6)
$\text{Be}_3(\text{OH})_3^{3+} + \text{L}^{2-} \rightarrow \text{Be}_3(\text{OH})_3\text{L}^+$	-21.7(4)	10.9(8)	109(3)
$\text{Be}_3(\text{OH})_3^{3+} + 3\text{L}^{2-} \rightarrow \text{Be}_3(\text{OH})_3\text{L}_3^{3-}$	-47.7(8)	28(1)	254(6)
L = malonate			
$\text{Be}^{2+} + \text{L}^{2-} \rightarrow \text{BeL}$	-30.6(1)	10.53(6)	138.0(5)
$\text{BeL} + \text{L}^{2-} \rightarrow \text{BeL}_2^{2-}$	-21.91(5)	5.19(8)	91.2(4)
$\text{Be}^{2+} + 2\text{L}^{2-} \rightarrow \text{BeL}_2^{2-}$	-52.50(8)	15.82(8)	229.2(5)
$\text{Be}_3(\text{OH})_3^{3+} + \text{L}^{2-} \rightarrow \text{Be}_3(\text{OH})_3\text{L}^+$	-30.1(4)	8.4(8)	129(3)
$\text{Be}_3(\text{OH})_3^{3+} + 3\text{L}^{2-} \rightarrow \text{Be}_3(\text{OH})_3\text{L}_3^{3-}$	-73.3(3)	18.8(8)	309(3)
L = succinate			
$\text{Be}^{2+} + \text{L}^{2-} \rightarrow \text{BeL}$	-17.34(4)	21.1(1)	129(5)
$\text{BeL} + \text{L}^{2-} \rightarrow \text{BeL}_2^{2-}$	-6(1)	15(1)	69(5)
$\text{Be}^{2+} + 2\text{L}^{2-} \rightarrow \text{BeL}_2^{2-}$	-23.1(1)	36(1)	198(5)
$\text{Be}_3(\text{OH})_3^{3+} + \text{L}^{2-} \rightarrow \text{Be}_3(\text{OH})_3\text{L}^+$	-11.6(3)	42(1)	181(3)

^a 298 K, 3 M NaClO₄; values in parentheses are standard deviations on the last significant figure.

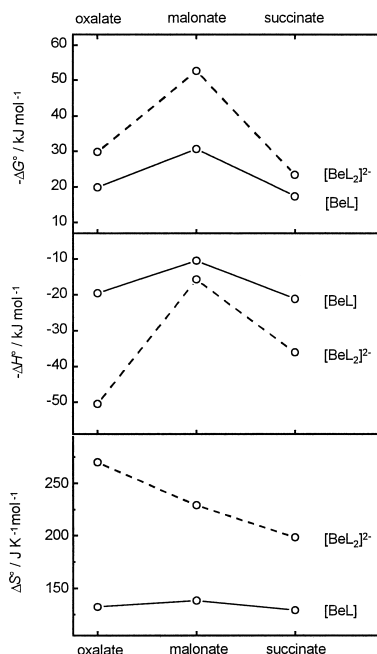


FIG. 14. Thermodynamic functions ΔG° (top), ΔH° (center), and ΔS° (bottom) for the cumulative formation of BeL and BeL_2^{2-} , where L = oxalate, malonate, and succinate. Reproduced with permission from Ref. (85). Copyright 1998, Wiley-VCH Verlag GmbH.

resonances occur at low field. The difference between malonato complexes (six-membered rings) and oxalato complexes (five-membered rings) is greater than between malonato complexes and succinato complexes (seven-membered rings). Evans attributed this effect to the rigidity of the chelate rings (170), but perhaps ring strain is also important.

Substituent effects have been observed in a series of substituted malonato complexes (167). The ^9Be resonance frequencies move to higher field as the basicity of the ligand increases, as can be seen in Table XI. Quadrupolar broadening is considerable in complexes of the hydrolyzed trimer, so much so that unless a species of this sort is present in high concentration relative to the others, its signal may be buried in the baseline noise. The tetrahedron is significantly distorted from T_d symmetry in these compounds.

Alkaline metal salts of the complexes $[\text{BeL}_2]^{2-}$ are relatively easy to obtain as crystals; some structural data are given in Table XII. Deviations from the regular tetrahedral structure are most marked with

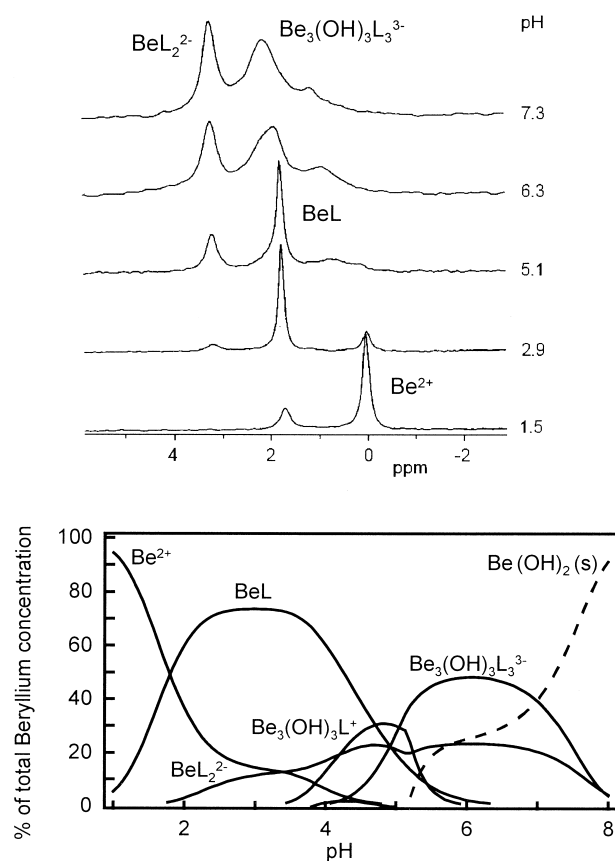


FIG. 15. ^9Be NMR spectra and calculated distribution diagram for the system BeSO_4 -malonate 1:1 ($C_{\text{Be}} = C_{\text{L}} = 0.1 \text{ M}$) (95).

the oxalato complex with O-Be-O angles of ca. 100° inside the five-membered ring. The O-Be-O angles inside the six- and 7-membered rings are much closer to the ideal tetrahedral angle. The structure of the bis(maleato) beryllate ion (169) is shown in Fig. 17. There is no obvious correlation between the structures (Table XII) and the stabilities of the complexes in solution (Table X).

The structure of the anion $[\text{Be}_3(\text{OH})_3(\text{malonate})_3]^{3-}$ (95) is illustrated in Fig. 18. The $\text{Be}_3(\text{OH})_3$ ring has a flattened chair conformation with no crystallographic symmetry. Nevertheless, the arrangement of oxygen atoms around each beryllium is near tetrahedral.

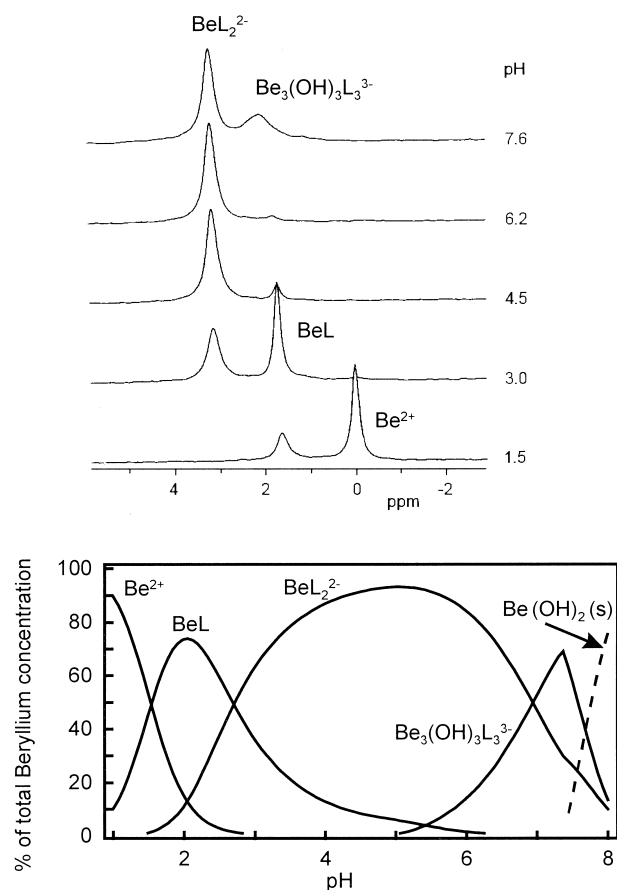


FIG. 16. ^9Be NMR spectra and calculated distribution diagram for the system BeSO_4 -malonate 1:2 ($C_{\text{Be}} = 0.1 \text{ M}$, $C_{\text{L}} = 0.2 \text{ M}$) (95).

C. HYDROXYCARBOXYLATE LIGANDS

1. Aliphatic

The tendency of aliphatic hydroxycarboxylic acids to form complexes is comparable to the tendency of the corresponding carboxylic acids to form complexes. This arises for two reasons. In the first place the hydroxide group is very resistant to deprotonation so that it is unrealistic to expect its oxygen atom to enter into the formation of a chelate ring. Also, as the hydroxide group is electron-withdrawing, the basicity of the carboxylate ligand is reduced, which should lead to weaker complexes being formed. Thus hydroxy monocarboxylic

TABLE XI

⁹Be NMR CHEMICAL SHIFTS OF DICARBOXYLATO BERYLLIUM(II) COMPLEXES^a

Ligand	Ligand basicity ^b	[BeL ₂] ²⁻	[Be ₃ (OH) ₃ L ₃] ³⁻	[BeL(H ₂ O) ₂]	Ref.
Oxalate	7.64	4.95	3.19	2.90	95
Phenylmalonate	7.11	3.29		1.76	167
Malonate	7.56	3.19	2.10	1.76	95
Methylmalonate	7.94	2.90	1.94	1.57	167
Dimethylmalonate	8.30	2.44	1.72	1.35	167
Phthalate	7.38 ^d	2.41		1.20	171
CBDC ^c	8.11	2.39	1.70	1.35	167
Maleate	7.25 ^e	2.02	1.55	1.21	169
Succinate	8.95 ^d	1.42		1.02	169

^a Values in ppm toward higher frequency from an external 0.1 M BeSO₄ aqueous solution, with the exception of phthalate, maleate, and succinate, which were referenced to “aqueous [Be(H₂O)₄]²⁺.”

^b log β₂^H, decimal logarithm of the overall basicity constant of the ligand (298 K, 0.5 M NaClO₄).

^c Cyclobutane-1,1-dicarboxylate.

^d From Alderighi *et al.* (167).

^e From Smith and Martell (23).

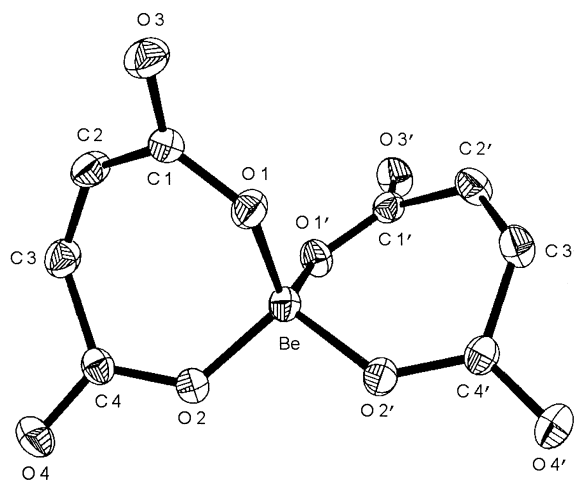


FIG. 17. Molecular structure of the anion [Be(maleate)]²⁻. Reproduced with permission from Ref. (169). Copyright 1998, Verlag der Zeitschrift für Naturforschung.

TABLE XII

SELECTED STRUCTURAL PARAMETERS OF
BIS-DICARBOXYLATO BERYLLIUM(II) COMPLEXES $[\text{BeL}_2]^{2-}$

Ligand	Be–O, average distance (pm)	Average endocyclic O–Be–O angle (°)	Ref.
Oxalate	162.2(3)	99.6(1)	95
Malonate	161.6(7)	108.8(5)	95
CBDC ^b	160.6(8)	107.0(3)	167
Phthalate	160.3(8)	109.4(3)	171
Maleate	161.2(2)	110.7(5)	169

^a Values in parentheses are standard deviations on the last significant figure.

^b Cyclobutane-1,1-dicarboxylate.

acids form very weak complexes just like the simple acids, whereas hydroxydicarboxylic acids and hydroxytricarboxylic acids form fairly stable complexes. Equilibrium constants have been reported for beryllium complexes with anions derived from the following acids: glycolic acid (172–174), lactic acid (137, 172–174), malic acid (76, 138, 173, 175), tartaric acid (76, 148, 174–177), 2-hydroxy-2-methylpropanoic acid (174, 178), 3-hydroxybutanoic acid (178), and citric acid (162, 174, 176, 179, 180).

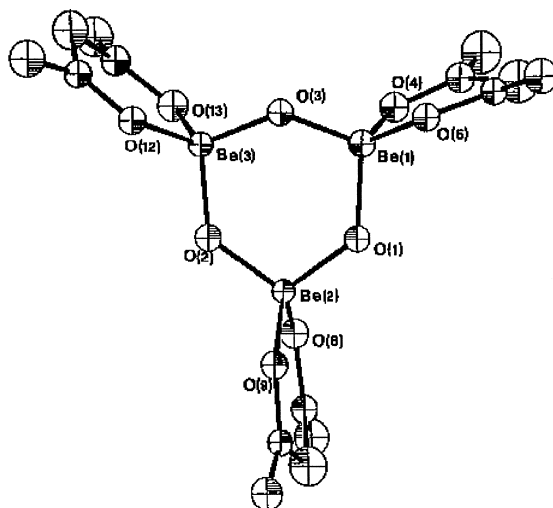


FIG. 18. Molecular structure of the anion $[\text{Be}_3(\text{OH})_3(\text{malonate})_3]^{3-}$. Reproduced with permission from Ref. (95). Copyright 1997, Elsevier Science.

The glycolate ion, $\text{HOCH}_2\text{COO}^-$, forms very weak complexes in solution. Figure 19 shows the speciation calculated on the basis of recently determined data (174) in which it is clear that the concentrations of the complexes BeL^+ and BeL_2 are very low. Nevertheless, it is a curious fact that the glycolate complex, $\text{Na}_4[\text{Be}_6(\text{OCH}_2\text{COO})_8]$, was prepared in the solid state long ago (181). The crystal structure of this compound has been determined more recently (182). The structure (Fig. 20) shows that the OH groups have indeed been deprotonated and that the alcoxy groups form bridges between pairs of beryllium atoms. The glycolate ligands bridge across edges of the Be_6 cluster.

2. Aromatic

The interaction of ligands derived from salicylic acid and its derivatives has been extensively investigated (83, 147, 149, 160, 170, 176, 183–205). A similar situation obtains with regard to 1-hydroxy-2-naphthoic acid (185, 194, 196, 198, 206–215). Salicylic acid derivatives may be useful in chelation therapy for beryllium poisoning (2).

The principal species formed by a salicylate, according to the most recent study (83), are BeL and $[\text{BeL}_2]^{2-}$, in which both the carboxyl group and the hydroxy group have lost the proton that is present in the parent acid. In addition, a “protonated” complex, $[\text{BeHL}_2]$, was found to be present. The complex $\text{Be}_3(\text{OH})_3\text{L}_3^{3-}$ was found as a minor species; a structure similar to that of the corresponding dicarboxylato complex was proposed for it. Equilibrium constants for these salicylato complexes are in Table XIII, together with some values for substituted salicylato complexes. The stability of the complexes follows

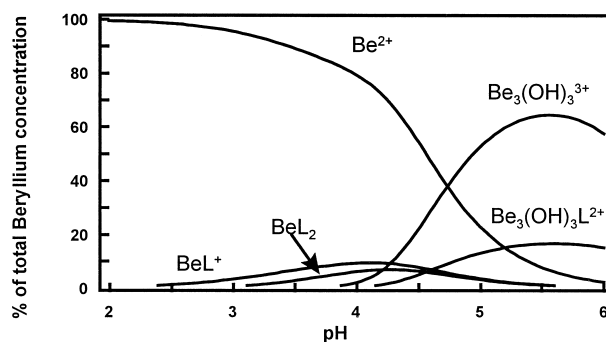
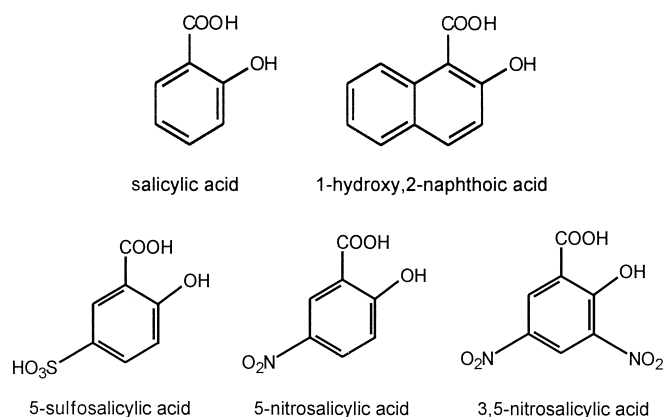


FIG. 19. Calculated species distribution for a beryllium(II)-glycolate solution. $C_{\text{Be}} = 0.003 \text{ M}$, $C_{\text{L}} = 0.015 \text{ M}$ (174).



the base strength of the ligands as determined by aromatic substitution effects.

The structure of the monosalicylato complex $\text{BeL}(\text{H}_2\text{O})_2$ is shown in Fig. 21 (216). This is one of the few examples of a known structure in

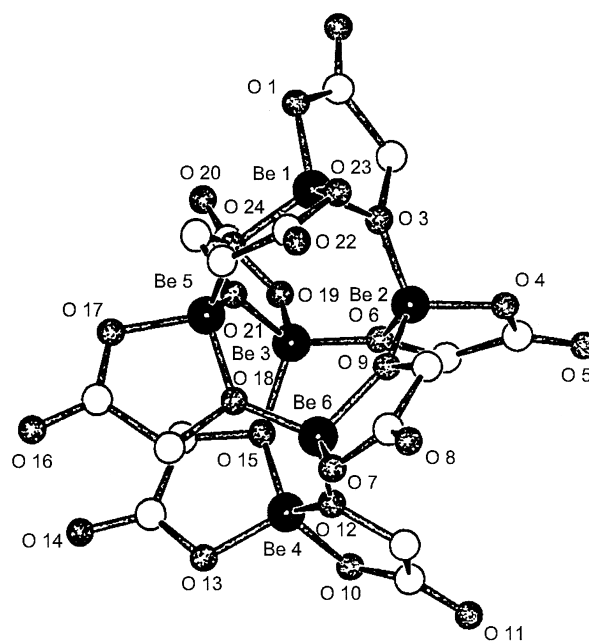


FIG. 20. Molecular structure of the glycolate complex anion $[\text{Be}_6(\text{OCH}_2\text{CO}_2)_8]^{4-}$. Reproduced with permission from Ref. (182). Copyright 1992, Verlag der Zeitschrift für Naturforschung.

TABLE XIII

STABILITY CONSTANTS FOR SALICYLATO COMPLEXES OF BERYLLIUM(II)

Reaction	log <i>K</i>			
	Salicylate (83) ^a	5-Sulfosalicylate (208) ^b	5-Nitrosalicylate (204) ^b	3,5-Dinitrosalicylate (204) ^b
$\text{Be}^{2+} + \text{L}^{2-} \rightarrow \text{BeL}$	12.4	11.74	9.64	8.5
$\text{BeL} + \text{L}^{2-} \rightarrow \text{BeL}_2^{2-}$	10.2	8.92	7.53	6.9
$\text{BeHL}^+ + \text{L}^{2-} \rightarrow \text{BeHL}_2^{2-}$	12.5			
$\text{Be}_3(\text{OH})_3^{3+} + 3 \text{L}^{2-} \rightarrow \text{Be}_3(\text{OH})_3\text{L}_3^{3-}$	32.1			
$\text{Be}^{2+} + \text{HL}^- \rightarrow \text{BeHL}^+$	1.6			
$\text{BeL}^{2+} + \text{HL}^- \rightarrow \text{BeHL}_2^{2-}$	1.7			
$\text{BeHL}^+ + \text{HL}^- \rightarrow \text{Be}(\text{HL})_2$	2.2			
$\text{BeL} + \text{H}_2\text{O} \rightarrow \text{Be}(\text{OH})\text{L}^- + \text{H}^+$	6.6			

^a 298 K, 1 M NaClO₄.^b 298 K, 0.1 M NaClO₄.

which there are water ligands attached to the beryllium atom. The structure of the bis-complex, (NH₄)₂[BeL₂], has also been determined (217).

During the investigations leading to the determination of these structures, another compound, containing a carbonate-bridged dinuclear anion, was obtained (217), whose structure is shown in Fig.

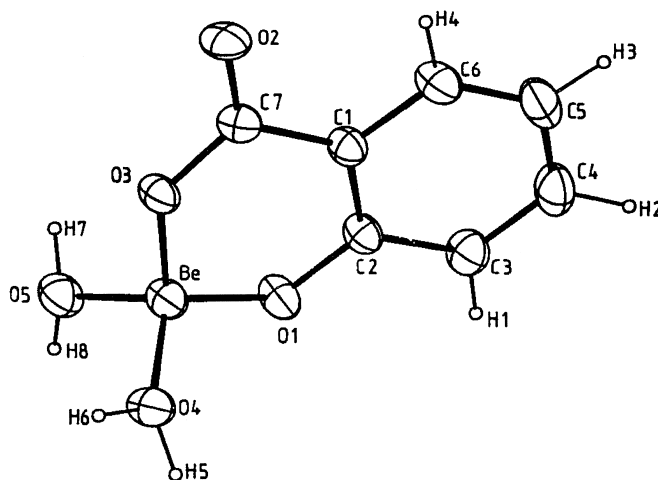


FIG. 21. Molecular structure of [Be(salicylate)(H₂O)₂]. Reproduced with permission from Ref. (216). Copyright 1991, American Chemical Society.

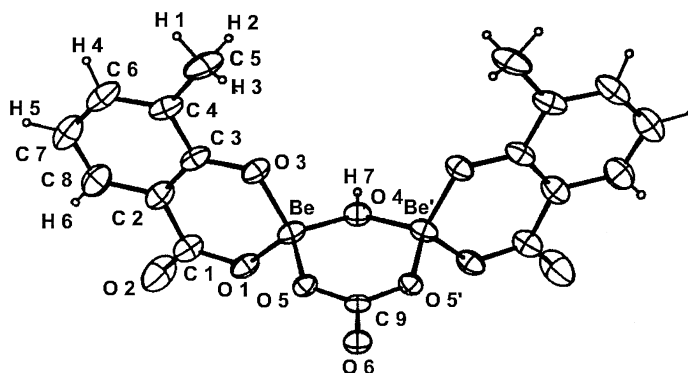
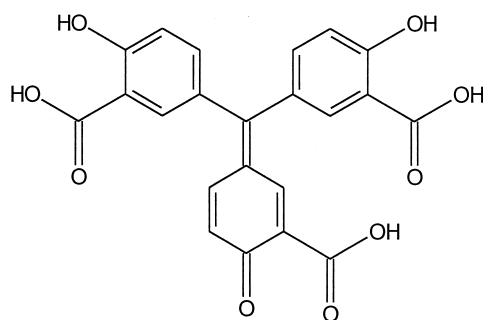


FIG. 22. Molecular structure of the carbonate-bridged 3-methylsalicylate complex anion $[\text{Be}_2(\text{OH})(\text{CO}_3)(\text{C}_7\text{H}_6\text{OCO}_2)_2]^{3-}$. Reproduced with permission from Ref. (217). Copyright 1993, Wiley-VCH Verlag GmbH.

22. This compound can be considered as a derivative of the hydrolysis product, $[(\text{H}_2\text{O})_3\text{Be}(\text{OH})\text{Be}(\text{H}_2\text{O})_3]^{3+}$, in which the bidentate 3-methylsalicylate ligands each replace two water molecules, the other two water molecules being replaced by a carbonate ion bridging between two beryllium atoms. Similar carbonate bridges have been proposed previously (132).

Aurin tricarboxylate (also known as aluminon) forms fairly stable complexes with beryllium: $\text{Log } K_1$ values of 5.38 (160) and 4.54 (161) have been reported. In the 1950s this ligand was examined as a possible antidote to beryllium poisoning in rats, but although it reduced the toxicity, serious side effects were noted; for further details see the review by Wong and Woollins (20).



aurin tricarboxylic acid

The formation of beryllium complexes of *o*-, *m*-, and *p*-hydroxyphenylacetate in aqueous solution has been also reported (218).

D. AMINOCARBOXYLATE LIGANDS

1. Amino Acids

The interaction with both synthetic and naturally occurring amino acids has been studied extensively: glycine (138, 173, 219–221), α - (173, 219) and β -alanine (138, 220), sarcosine (219), serine (222), aspartic acid (138, 173, 222–226), asparagine (222), threonine (222), proline (219), hydroxyproline (219), glutamic acid (138, 222–225), glutamine (222), valine (219, 227), norvaline (219), methionine (222, 226), histidine (228, 229), isoleucine (219), leucine (219, 230), norleucine (219), lysine (222), arginine (222), histidine methyl ester (228), phenylalanine (138, 222), tyrosine (222), 2-amino-3-(3,4-dihydroxyphenyl)propanoic acid (DOPA) (222), tryptophan (222), aminoisobutyric acid (219), 2-aminobutyric acid (219, 231), citrulline (222), and ornithine (222).

Many of the results reported are of a dubious nature. For example, Perkins (219, 222) assumed that complexes of the type ML_2 were formed and quoted $\log \beta_2$ values between 9.8 and 14.2. Not only was the possible formation of a simple complex of the type ML excluded (not to mention any other complexes), but the effects of hydrolysis (which, to be fair, were poorly understood at the time) were completely ignored. The high stability of amino acid complexes was put in doubt in successive publications (220, 229, 232, 233). It has even been suggested, on the basis of Raman spectra, that the amino group does not coordinate to the beryllium atom (232). Unfortunately the opposite conclusion was reached on the basis of IR measurements, namely that only the amino group was coordinated (234).

A potentiometric study has led to the suggestion that complexes of the type ML are formed by glycinate, α - and β -alaninate, phenylalaninate, and glutamate with $\log K$ values of 6.25, 6.39, 7.36, 6.26, and 6.89, respectively (22). The other species suggested is of the type $[Be_3(OH)_3L]$. Notwithstanding the apparently high formation constants of these complexes, the speciation diagrams show that hydrolysis reactions are predominant and the amino acid complexes are present as minor components of the equilibrium mixtures. This conclusion has been confirmed in on-going potentiometric and 9Be NMR studies in our own laboratory (235).

The formation of beryllium complexes with other ligands contain-

ing nitrogen and carboxylato oxygen as potential donor atoms, such as glycylglycinate (219), picolinate (pyridine-2-carboxylate) (236), histamine derivatives (228, 237), and 2-amino-3-mercapto-3-methylbutanoic acid (D-penicillamine) (238) has been also reported.

E. AMINOPOLYCARBOXYLATE LIGANDS (COMPLEXONES)

Much interest has been directed at this group of compounds both from the environmental and medicinal points of view. The following list gives references to the complexones that have been investigated:

Iminodiacetate (82, 239) and derivatives obtained by replacing the imino hydrogen atom by alkyl groups (82), or more complicated groups (206, 240–243)

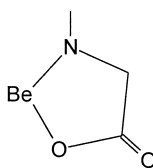
Nitrilotriacetate (148, 151, 227, 230, 239, 240, 244) and nitrilotripropionate (151, 244)

1,2-Diaminoethane-*N,N,N',N'*-tetraacetate (148, 151, 240, 245–249) and the corresponding tetrapropionate (249)

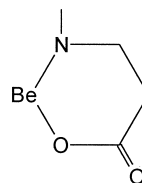
1,2-Diaminobenzene-*N,N,N',N'*-tetraacetate (248, 250) and chloro- and methyl-ring-substituted derivatives (248)

trans-1,2-Diaminocyclohexane-*N,N,N',N'*-tetraacetate (148, 249).

The expected mononuclear complexes of formula BeL are formed along with BeHL, BeH₂L, and Be₃(OH)₃(HL). It was found that when an acetate group is replaced by a propionate group the stability constant increases (249) as shown in Table XIV. This can be explained by assuming that the nitrogen atom is coordinated to the beryllium. The -NCH₂CO₂ moiety forms a five-membered ring but the -NCH₂CH₂CO₂ moiety forms the more stable six-membered ring.



imino-acetate



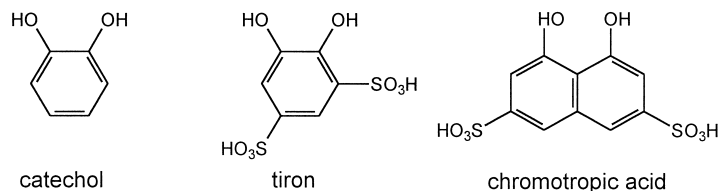
imino-propionate

The interaction of beryllium with nitrilotripropionic acid (H₃ntp) has been investigated in some detail (244). This acid forms a strong complex ($\log K_1 = 9.24$) that can be isolated as a solid. The crystal structure of the anion [Be(ntp)] is shown in Fig. 23. The structure confirms the coordination of the nitrogen atom along with an oxygen atom from each carboxyl group.

F. DIHYDROXY LIGANDS

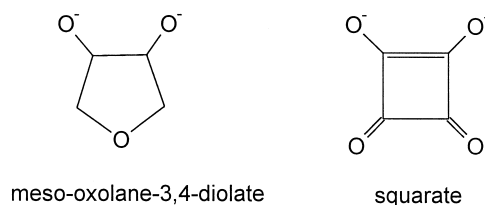
Complexes of beryllium with 1,2-dihydroxybenzene (catechol) and its more soluble sulfonate derivatives (188, 198, 251–256) have been investigated with particular reference to their possible use as antidotes for beryllium poisoning.

Equilibrium constants for some related complexes are given in Table XV (170). Chromotropic acid forms the most stable complexes, presumably with the formation of a strain-free 6-membered ring.



The structure of a salt of the bis(catecholato) complex, BeL_2^{2-} , has been determined (257). The average O–Be–O angle in the five-membered ring was found to be 99.6° , which is comparable to the angle found in the five-membered ring of the oxalato complex, shown in Table XII. The ^9Be NMR signal of this compound falls at very low field (7.5 ppm), in line with the tendency for rigid chelate rings to provoke high frequencies.

Polyalcohols do not generally interact noticeably with beryllium, probably on account of the low acidity of the alkyl-OH group. Two exceptions are known where solid compounds have been isolated. The complex anion $[\text{bis}(\text{meso-oxolane-3,4-diolato})\text{Be}]^{2-}$ has been shown to contain two anionic diolato ligands (258).



The squarato ligand, which is a resonance-stabilized pseudoaromatic, forms an unusual complex in the solid state, $[\text{Be}(\text{C}_4\text{O}_4)(\text{H}_2\text{O})_3]$, whose structure is shown in Fig. 24 (42). Here the ligand is mono-

TABLE XIV
STABILITY CONSTANTS FOR SOME AMINOPOLYCARBOXYLATO
COMPLEXES OF BERYLLIUM(II)^a

Ligand	log K_1	log β_x ^b
$\begin{array}{c} \text{OOCCH}_2 \quad \text{CH}_2\text{COO}^- \\ \diagdown \quad \diagup \\ \text{NCH}_2\text{CH}_2\text{N} \\ \diagup \quad \diagdown \\ \text{OOCCH}_2 \quad \text{CH}_2\text{COO}^- \end{array}$	7.90	36.70
$\begin{array}{c} \text{OOCCH}_2\text{CH}_2 \quad \text{CH}_2\text{CH}_2\text{COO}^- \\ \diagdown \quad \diagup \\ \text{NCH}_2\text{CH}_2\text{N} \\ \diagup \quad \diagdown \\ \text{OOCCH}_2 \quad \text{CH}_2\text{COO}^- \end{array}$	8.50	36.86
$\begin{array}{c} \text{OOCCH}_2\text{CH}_2 \quad \text{CH}_2\text{CH}_2\text{COO}^- \\ \diagdown \quad \diagup \\ \text{NCH}_2\text{CH}_2\text{N} \\ \diagup \quad \diagdown \\ \text{OOCCH}_2\text{CH}_2 \quad \text{CH}_2\text{CH}_2\text{COO}^- \end{array}$	8.45	36.71
$\begin{array}{c} \text{OOCCH}_2 \quad \text{CH}_2\text{COO}^- \\ \diagdown \quad \diagup \\ \text{NCH}_2\text{CH}_2\text{CH}_2\text{N} \\ \diagup \quad \diagdown \\ \text{OOCCH}_2 \quad \text{CH}_2\text{COO}^- \end{array}$	7.83	36.60
$\begin{array}{c} \text{OOCCH}_2\text{CH}_2 \quad \text{CH}_2\text{CH}_2\text{COO}^- \\ \diagdown \quad \diagup \\ \text{NCH}_2\text{CH}_2\text{CH}_2\text{N} \\ \diagup \quad \diagdown \\ \text{OOCCH}_2 \quad \text{CH}_2\text{COO}^- \end{array}$	7.84	36.07
$\begin{array}{c} \text{OOCCH}_2 \quad \text{CH}_2\text{COO}^- \\ \diagdown \quad \diagup \\ \text{N} \\ \diagup \quad \diagdown \\ \text{OOCCH}_2 \quad \text{CH}_2\text{COO}^- \end{array}$	6.68	34.92
$\begin{array}{c} \text{OOCCH}_2 \quad \text{CH}_2\text{CH}_2\text{COO}^- \\ \diagdown \quad \diagup \\ \text{N} \\ \diagup \quad \diagdown \\ \text{OOCCH}_2 \quad \text{CH}_2\text{COO}^- \end{array}$	8.12	35.80
$\begin{array}{c} \text{OOCCH}_2 \quad \text{CH}_2\text{CH}_2\text{COO}^- \\ \diagdown \quad \diagup \\ \text{N} \\ \diagup \quad \diagdown \\ \text{OOCCH}_2 \quad \text{CH}_2\text{CH}_2\text{COO}^- \end{array}$	9.25	—
$\begin{array}{c} \text{OOCCH}_2\text{CH}_2 \quad \text{CH}_2\text{CH}_2\text{COO}^- \\ \diagdown \quad \diagup \\ \text{N} \\ \diagup \quad \diagdown \\ \text{OOCCH}_2\text{CH}_2 \quad \text{CH}_2\text{CH}_2\text{COO}^- \end{array}$	9.24	—

^a 298 K, 1 M NaClO₄; data from (248) and references therein.

^b $\beta_x = K[3\text{Be} + 3\text{OH} + \text{HL} \rightleftharpoons \text{Be}_3(\text{OH})_3(\text{HL})]$ (generic formula, charges omitted).

dentate as far as beryllium is concerned, but the structure appears to be stabilized by the formation of a hydrogen bond between a coordinated water molecule and another oxygen atom of the squarate resulting in a sort of seven-membered chelate ring.

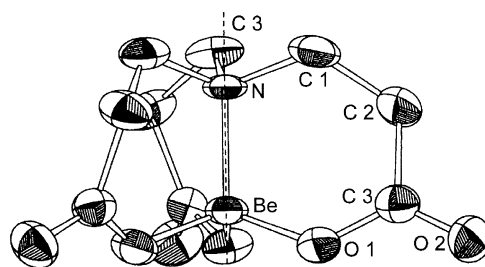


FIG. 23. Molecular structure of the nitrilo-tripropionato complex anion $[\text{Be}(\text{ntp})]^-$. Reproduced with permission from Ref. (249). Copyright 1995, American Chemical Society.

G. PHOSPHONATE LIGANDS

Complexes of beryllium with phosphonate ligands have been extensively researched, mainly by potentiometry. The ligands investigated are as follows: methylphosphonate (259, 260); chloromethylphosphonate (259); 2-aminopropane-1-phosphonate (259); methylenediphosphonate (130, 260, 261); hexamethylenediphosphonate (259); 1-hydroxyethane-1,1-diphosphonate (261); 1,1-dimethyl-1-amino-methylphosphonate (262); phosphonoacetate (260); amino(phenyl)-methylenediphosphonate (262); *N*-(phosphonomethyl)iminodiacetate (263).

Other ligands include the following:

Analogues of the amino-carboxylate ligands with phosphonate replacing one or more carboxylate groups; 1,2-diaminoethane-*N,N'*-dimethylphosphonate (259, 264), 1,2-

TABLE XV

STABILITY CONSTANTS FOR SOME BERYLLIUM(II) COMPLEXES
DETERMINED BY NMR SPECTROSCOPY^a

Complexing agent	$\log K_1$	$\log K_2$	$\log \beta_2$
Chromotropic acid	16.2	12.0	28.2
Tiron	12.2	9.3	21.5
5-Sulfosalicylic acid	11.2	8.5	19.7
5-Nitrosalicylic acid	10.1	8.0	18.1
3-Hydroxy-1,2-dimethylpyridyn-4-one	8.7	7.4	16.1
1-Ethyl-3-hydroxy-2-methylpyridyn-4-one	8.5	7.3	15.8
3-Hydroxy-2-methylpyridyn-4-one	8.4	7.2	15.6
3,5-Dinitrosalicylic acid	7.8	5.5	13.3

^a Taken from Ref. (169); $C_{\text{Be}} = 0.01 \text{ M}$, $C_{\text{L}} = 0.03 \text{ M}$.

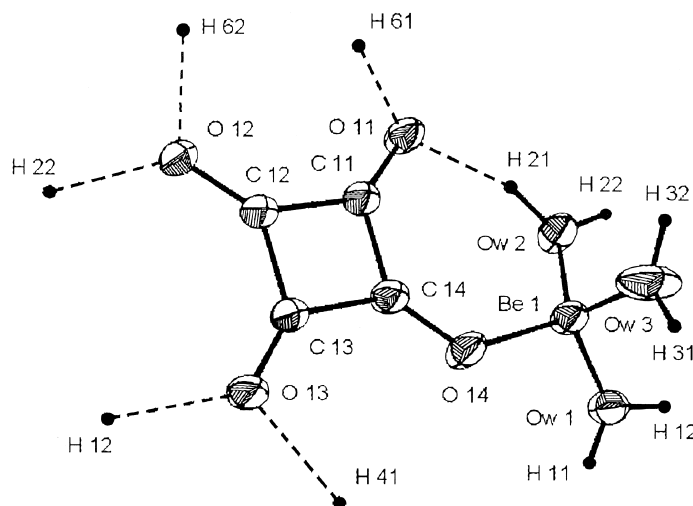


FIG. 24. Molecular structure of the squarato complex $\text{Be}(\text{C}_4\text{O}_4) \cdot 3\text{H}_2\text{O}$. Reproduced with permission from Ref. (42). Copyright 1990, Verlag der Zeitschrift für Naturforschung.

diaminoethane- N,N' -bis(acetate)- N,N' -bis(methylphosphonate) (265), 1,2-diaminoethane- N,N' -bis(*i*-propylphosphonate) (265), 1,5-diaminopentane- N,N' -bis(*i*-propylphosphonate) (265), oxy-bis(ethyleneimino(dimethyl)methylphosphonate) (265), thio-bis(ethyleneimino(dimethyl)methylphosphonate) (265)

Derivatives of polyazamacrocycles: 1,4,7-triazacyclononane- N,N',N'' -tris(methylphosphonate) (266), 1,4,7-tris(beta-dioxaphosphorylethyl)-1,4,7-triazacyclononane (267), 1,4,7,10-tetraazacyclododecane- N,N',N'',N''' -tetra(methylphosphonate) (266), 1,4,7,10-tetraazacyclododecane-1,4,7,10-tetraethylphosphonate (268)

Derivatives of 2-(hydroxyphenyl) methylphosphonate (269, 270).

The results are sparse and in some cases inconsistent both in regard to the stoichiometry of the species formed and in relation to the values of the stability constants. Some results from a systematic study of simple phosphonates (260) are given in Table XVI together with data relating to malonate complexes for comparison purposes.

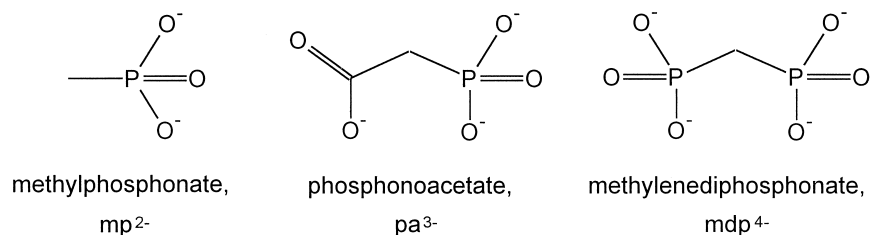


TABLE XVI

DECIMAL LOGARITHMS OF THE FORMATION CONSTANTS OF BERYLLIUM COMPLEXES WITH LIGANDS CONTAINING PHOSPHONATO GROUPS^{a,b}

Reaction ^c	Phosphonoacetate (L ³⁻)	Methylenediphosphonate (L ⁴⁻)	Methylphosphonate (L ²⁻)	Malonate (L ²⁻)
Be + L → BeL	9.24(1)	13.7(1)	6.17(3)	5.36(2)
BeL + L → BeL ₂	5.74(2)	7.66(7)	5.36(8)	3.85(1)
BeL + H → BeHL	3.36(1)	5.04(5)	3.3(1)	
BeHL + H → BeH ₂ L		2.6(1)		
BeL ₂ + H → BeHL ₂	5.05(6)	6.3(1)		
BeHL ₂ + H → BeH ₃ L ₂	≈3	6.5(2)		
Be + HL → BeHL	4.53(1)	8.3(1)		
Be + H ₂ L → BeH ₂ L		4.0(2)	2.0(1)	
Be + 2H ₂ L → Be(H ₂ L) ₂		7.6(2)		
Be ₃ (OH) ₃ + L → Be ₃ (OH) ₃ L	7.2(3)			5.26(7)
Be ₃ (OH) ₃ + 3L → Be ₃ (OH) ₃ L ₃	20.86(3)			12.84(6)

^a 298 K, 0.5 M NaClO₄; data from Ref. (259).

^b Values in parentheses are standard deviations on the last significant figure.

^c The charges of the species have been omitted for simplicity.

Previous workers (130, 259) had used a model in which the only complexes formed were BeL and Be₂L₂ for L = mp; BeHL³⁻ and Be₂L²⁻ for L = mdp. The discrepancy between the old results and the new ones may be traced to the influence of two factors: incorrect allowance made for hydrolysis and unsophisticated methods of calculation, both of which are characteristic of the time when the old work was done. In any case there is no evidence in the recent work for the presence of dimeric species.

The stability of the complexes increases along the ligand series malonate < methylphosphonate < phosphonoacetate < methylenediphosphonate. Phosphonate ligands form stronger complexes than carboxylate ligands. Indeed, the formation of a complex Be(mp) shows that the phosphonate ligand is capable of replacing a coordinated water molecule from the first coordination sphere even without the assistance of the chelate effect. The methylenediphosphonato complexes are much stronger than the malonato complexes where the same chelate effect should be operative.

The superior coordinating capacity of phosphonate over carboxylate is illustrated in the ⁹Be NMR spectra in Fig. 25 (260). The similarity of the spectra obtained by reaction of BeSO₄ and methylphosphonic acid or phosphonacetic acid indicates that the carboxylate group is not bound to the beryllium under these experimental conditions. It should be noted that substitution of a water molecule by a phosphonate ligand causes the ⁹Be resonance to move upfield when it co-ordinates, as does the fluoride ion (271), the only other monodenate ligand

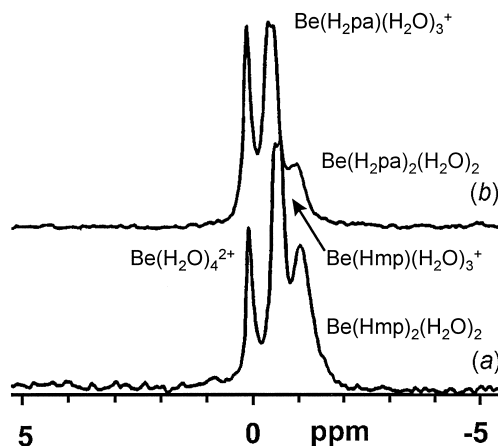


FIG. 25. ^9Be NMR spectra (H_2O , 293 K) of the systems BeSO_4 -methylphosphonic acid (H_2mp), 1/4 (a) and beryllium(II)-phosphonacetic acid (H_3pa), 1/2 (b); $C_{\text{Be}} = 0.1$ M (260).

apart from hydroxide that is capable of replacing a water molecule from $[\text{Be}(\text{H}_2\text{O})_4]^{2+}$ (117).

The partially protonated phosphonate group, $(\text{RPO}_3\text{H})^-$ also forms complexes whose stability increases in the same series, methylphosphonate < phosphonoacetate < methylenediphosphonate. When it comes to complexes of hydrolysis products, phosphonoacetate is the only ligand to form species of the type $\text{Be}_3(\text{OH})_3\text{L}$ and $\text{Be}_3(\text{OH})_3\text{L}_3$. The other phosphonates form such stable complexes that in effect hydrolysis is suppressed. Nowhere is this more evident than with methylenediphosphonate complexes, which are so stable as to suppress the precipitation of $\text{Be}(\text{OH})_2$ under alkaline conditions. A typical speciation diagram for this ligand is shown in Fig. 26 together with ^9Be NMR spectra taken at different pH values. The assignments shown on the figure are consistent with the predominant species in the different pH regions. Clearly the chemical shift of such species are rather similar so that successive deprotonation of the ligand causes the resonance to move to slightly lower field.

Attempts to crystallize a phosphonate complex invariably led to the formation of glassy materials. For example, a solid compound was obtained that analyzed as $\text{K}_2\text{Be}(\text{H}_2\text{mdp})_2 \cdot 2\text{H}_2\text{O}$. Electrospray mass spectrometry spectra of this product confirm the stoichiometry; the most abundant peaks corresponded to the formulas $[\text{Be}(\text{H}_2\text{mdp})_2]^{2-}$ in the negative ion ESMS spectrum and $\{\text{K}_3[\text{Be}(\text{H}_2\text{mdp})]\}^+$ in the positive ion ESMS spectrum (260).

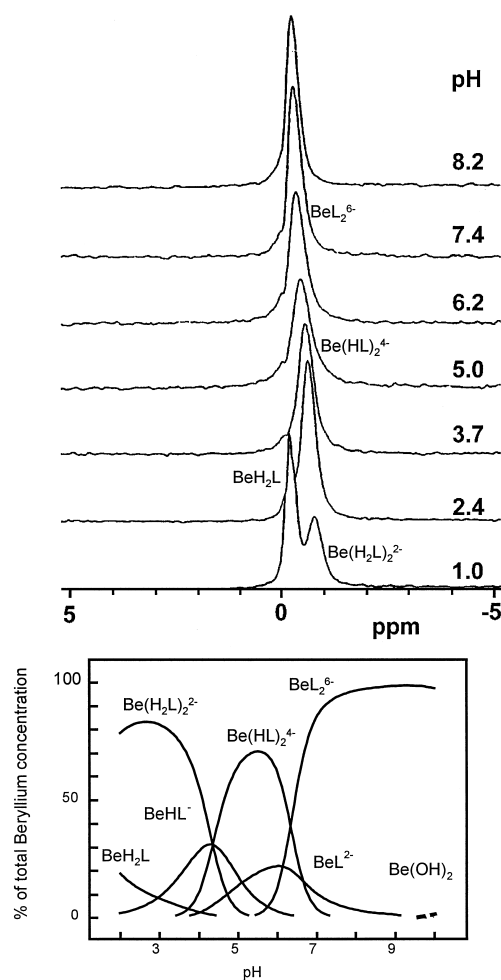
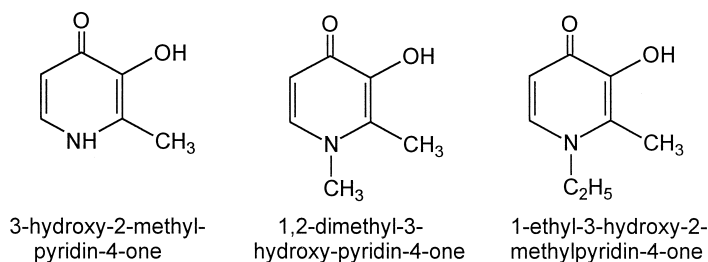


FIG. 26. ^9Be NMR spectra (H_2O , 293 K) and calculated distribution diagram for the system BeSO_4 –methylenediphosphonate ($C_{\text{Be}} = 0.1 \text{ M}$, metal to ligand molar ratio 1/3) (260).

H. OTHER ORGANIC LIGANDS

The interaction of beryllium with ligands derived from pyrone (272), pyridone (273), and pyrimidinedione (274, 275) have long aroused interest in view of the successful use of these ligands in the treatment of metal poisoning.



Evans and Wong determined some related equilibrium constants by ^1H and ^9Be NMR spectroscopy (170). The values of the equilibrium constants obtained by this method, given in Table XV, are in good agreement with those that had been obtained previously (183, 184, 188). This investigation was made possible because three conditions were satisfied: (i) the ligands form complexes of the type BeL and BeL_2 that are sufficiently strong to suppress hydrolysis; (ii) chemical exchange between the various species is sufficiently slow that separate signals are observed for each species; (iii) the signals from each species do not overlap. Figure 27 illustrates the spectra obtained with the ligand 1,2-dimethyl-3-hydroxypyridin-4-one.

Numerous other complexes of beryllium with organic ligands such as alloxides (276–280), β -diketonates (90, 281–297), Schiff bases (64, 298–301), thiols (302), pyridines (303), bipyridyl (304), phthalocyanine (305), hydroxyquinolines (306, 307), tropolones (308, 309), pyrazolylborates, (94, 310), phosphinates (311), hydrazides (312), phenylhydrazonocarboxylates (313), dinaphthofuchsonedicarboxylates (314),

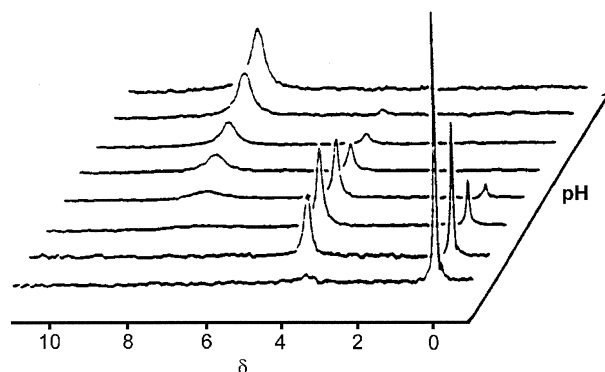


FIG. 27. ^9Be NMR spectra for the system beryllium(II)–1,2-dimethyl-3-hydroxypyridin-4-one (HL), pH range between 2 and 8. The $[\text{Be}(\text{H}_2\text{O})_4]^{2+}$ ion is taken as reference ($\delta = 0$); BeL^+ occurs at δ ca. 4 and BeL_2 occurs at ca. 7.5 ppm (38.0 MHz, H_2O). Reproduced with permission from Ref. (170). Copyright 1992, The Royal Society of Chemistry.

and triphenylmethane dyes (315), are known. These complexes, with few exceptions insoluble in water, are mainly of interest for analytical purposes.

The formation of complexes with ATP was suggested on the basis of ^{31}P NMR spectra (316).

VII. Conclusions

Complexes of the beryllium ion are always 4-coordinate with, at most, minor deviations from regular tetrahedral geometry. The tetra-aqua ion is a very stable entity and substitution of one or more water molecules by monodentate ligands is not thermodynamically favorable except with fluoride, hydroxide, and phosphonate ligands. The aqueous solution chemistry of this ion is dominated by the ease of hydrolysis with the formation, principally, of the hydroxo-bridged species $[\text{Be}_3(\text{OH})_3(\text{H}_2\text{O})_6]^{3+}$. Complex formation, then, is a process in which the ligand is usually competing with the hydrolysis reaction since the aqua-ion is present only in strongly acid conditions (pH less than ca. 3) where many ligands are protonated. Neglecting to take hydrolysis into account in the determination of equilibrium constants has been the cause of many spurious values being reported up to the 1960s and even more recently.

The only monodentate ligands that can compete with hydrolysis are fluoride and phosphonates. Chelating ligands can form stable complexes with beryllium by virtue of the chelate effect. The most stable of these use oxygen donor atoms, but nitrogen coordination, although less favorable, can occur. The most stable chelate complexes are those with six-membered rings. This results from both the requirement of beryllium to be tetrahedral and the steric requirements of the ligands. The strongest known bidentate ligand is the anion of chromotropic acid ($\log \beta_2 = 28.2$). This is followed by other dihydroxyaromatic ligands, e.g., tiron ($\log \beta_2 = 22.6$), and hydroxycarboxylate ligands such as salicylate ($\log \beta_2 = 22.6$). Bidentate phosphonate ligands (e.g., methylenediphosphonate, $\log \beta_2 = 21.4$) and dicarboxylate ligands follow in the stability sequence, but it seems that amino acids do not form strong complexes.

HEALTH AND SAFETY ASPECTS

Although health and safety (317) and biochemical aspects (17) of beryllium are beyond the scope of this review, some reference must be made to toxicity hazards. Above all, **inhalation of any beryllium-**

containing compound must be strictly avoided. It is probable that any substance inhaled will, at the pH of biological fluids in the lungs, be converted into insoluble beryllium hydroxide. Microcrystals of $\text{Be}(\text{OH})_2$ will remain lodged in the lungs indefinitely as there is no naturally occurring substance that can mobilize them by dissolution and transport. It is the presence of these foreign bodies in the lungs that causes chronic beryllium disease, which is cumulative and has a delayed onset. Therefore, stringent precautions must be taken to avoid inhalation of dust containing a beryllium compound. The combination of a well-ventilated fume hood and careful cleaning of any spillages should provide adequate protection for workers in coordination chemistry.

There is little indication that oral ingestion of beryllium compounds is a serious hazard. Presumably this is because no absorption occurs in the low-pH region of the stomach and in the higher pH region of the intestine; where absorption could occur, the beryllium is precipitated as hydroxide. Beryllium compounds can enter the body through lesions in the skin leading to ulceration due to the formation of the hydroxide in tissues under the skin. Therefore, it would be prudent always to wear gloves when handling beryllium compounds.

There is little hazard to the aqueous environment, as beryllium compounds are scarcely soluble in the pH range of natural waters.

ACKNOWLEDGMENTS

The authors thank the EU (HCM program "Metals and Environmental Problems" 1995–1998, Grant ERBCHRHX-CT94-0632) and the *Ministero dell'Ambiente* (Italy, Contract PR/1/C) for financial support.

REFERENCES

1. Cunningham, L. D. "Beryllium," U.S. Geological Survey—Minerals Information; <http://minerals.er.usgs.gov/minerals/pubs/commodity/beryllium/>; Reston, VA 20192 USA, 1997.
2. Skilleter, D. N. *Chem. Brit.* **1990**, 26, 26.
3. Thomas, M.; Aldridge, W. N. *Biochem. J.* **1966**, 98, 94.
4. Silber, P. In "Nouveau Traité de Chimie Minérale"; Pascal, P., Ed.; Masson: Paris, **1958**; Vol. 4, 7–134.
5. Darwin, G. E.; Buddery, J. H. "Beryllium"; Butterworths Scientific: New York, 1960.
6. Everest, D. A. "The Chemistry of Beryllium"; Elsevier: Amsterdam, 1964.
7. Bertin, F.; Thomas, G. *Bull. Soc. Chim. Fr.* **1971**, 3467.

8. Sillén, L. G.; Martell, A. E. "Stability Constants of Metal-Ion Complexes"; Spec. Publ. No. 25; Chemical Society: London, 1971.
9. Bell, N. A. In "Advances in Inorganic Chemistry and Radiochemistry"; Emeléus, H. J. and Sharpe, A. G., Eds.; Academic Press: New York, 1972; Vol. 14, 255-332.
10. Baes Jr., C. F.; Mesmer, R. E. "The Hydrolysis of Cations"; John Wiley & Sons: New York, 1976.
11. Smith, R. M.; Martell, A. E. "Critical Stability Constants"; Plenum: New York, 1977.
12. Högfeltdt, E. "Stability Constants of Metal-Ion Complexes"; Pergamon: Oxford, UK, 1982.
13. Seidel, A. In "Gmelin Handbook of Inorganic Chemistry"; Suppl. Bd. Al; Springer: Berlin, 1986.
14. Hertz, R. K. *ASTM Spec. Tech. Publ.* **1987**, 944 (*Chem. Anal. Met.*), 74, CA 107:69675.
15. Akitt, J. W. In "Multinuclear NMR"; Mason, J., Ed.; Plenum Press: New York, 1987, 189-220.
16. Schmidbaur, H. In "Gmelin Handbook of Inorganic Chemistry"; Springer: Berlin, 1987, Teil 1.
17. Rossman, M. D.; Preuss, O. P.; Powers, M. B. "Beryllium—Biomedical and Environmental Aspects"; Williams and Wilkins: Baltimore, Maryland, 1991.
18. Kumberger, O.; Schmidbaur, H. *Chem. Unserer Zeit* **1993**, 6, 310.
19. Rees Jr, W. S. In "Encyclopedia of Inorganic Chemistry"; King, R. B., Ed.; John Wiley & Sons: New York, 1994; Vol. 1, 67-87.
20. Wong, C. Y.; Woollins, J. D. *Coord. Chem. Rev.* **1994**, 130, 243.
21. Bell, N. A. In "Comprehensive Organometallic Chemistry"; Abel, E. W., Stone, F. G. A. and Wilkinson, G., Ed.; Pergamon Press: Oxford, 1995; Vol. 1, 35-56.
22. Mederos, A.; Dominguez, S.; Chinea, E.; Brito, F.; Midollini, S.; Vacca, A. *Bol. Soc. Chil. Quim.* **1997**, 42, 281.
23. Smith, R. M.; Martell, A. E. "NIST Critically Selected Stability Constants of Metal Complexes Database"; U.S. Department of Commerce, National Institute of Standards and Technology: Gaithersburg, MD (USA), 1997.
24. Pettit, L. D.; Powell, H. K. J. "IUPAC Stability Constants Database"; Academic Software, 1997.
25. Fratiello, A.; Lee, R. E.; Nishida, V. M.; Shuster, R. E. *J. Chem. Phys.* **1968**, 48, 3705.
26. Fratiello, A.; Davis, D. D.; Peak, S.; Shuster, R. E. *Inorg. Chem.* **1971**, 10, 1627.
27. Akitt, J. W.; Duncan, R. H. *J. Chem. Soc. Faraday I* **1980**, 76, 2212.
28. Akitt, J. W.; Elders, J. M. *Bull. Soc. Chim. Fr.* **1988**, 466.
29. Connick, R. E.; Fiat, D. N. *J. Chem. Phys.* **1963**, 39, 1349.
30. Yamaguchi, T.; Ohtaki, H.; Spohr, E.; Palincas, G.; Heinzinger, K.; Probst, M. M. *Z. Naturforsch* **1986**, 41a, 1175.
31. Kulikova, A. V.; Kopylova, E. A.; Kolenkova, M. A. *Russ. J. Inorg. Chem.* **1984**, 965.
32. Burgess, J. "Metal Ions in Solution"; Ellis Horwood Limited: Chichester, 1978.
33. Lincoln, S. F.; Merbach, A. E. In "Advances in Inorganic Chemistry"; Sykes, A. G., Ed.; Academic Press: New York, 1995; Vol. 42, 1-88, and references therein.
34. Hao, L.; Lu, R.; Leaist, D. G. *J. Solution Chem.* **1996**, 25, 231.
35. Bock, C. W.; Glusker, J. P. *Inorg. Chem.* **1993**, 32, 1242.
36. Bock, C. W.; Katz, A. K.; Glusker, J. P. *J. Am. Chem. Soc.* **1995**, 117, 3754.
37. Marx, D.; Hutter, J.; Parrinello, M. *Chem. Phys. Lett.* **1995**, 241, 457.
38. Marx, D.; Fois, E. S.; Parrinello, M. *Int. J. Quantum Chem.* **1996**, 57, 655.

39. Marx, D.; Sprik, M.; Parrinello, M. *Chem. Phys. Lett.* **1997**, 273, 360.
40. Dance, I. G.; Freeman, H. C. *Acta Crystallogr.* **1969**, B25, 304.
41. Sikka, S. K.; Chidambaram, R. *Acta Crystallogr.* **1969**, B25, 310.
42. Robl, C.; Kinkeldey, D. *Z. Naturforsch.* **1990**, 45b, 931.
43. Lutz, H. D.; Lange, N.; Maneva, M.; Georgiev, M. *Z. Anorg. Allg. Chem.* **1991**, 594, 77.
44. Ley, H. Z. *Phys. Chem.* **1899**, 30, 193.
45. Wood, J. K. *J. Chem. Soc.* **1910**, 97, 878.
46. Bleyer, B.; Kaufmann, S. *Z. Anorg. Chem.* **1913**, 82, 71.
47. Prytz, M. *Z. Anorg. Allg. Chem.* **1929**, 180, 355.
48. Prytz, M. *Z. Anorg. Allg. Chem.* **1931**, 197, 103.
49. Bjerrum, J. "Metal Ammine Formation in Aqueous Solution"; P. Haase and Son: Copenhagen, 1941.
50. Mattock, G. *J. Am. Chem. Soc.* **1954**, 76, 4835.
51. Korenman, I. M.; Frum, F. S.; Tsygankova, G. A. *J. Gen. Chem. USSR* **1956**, 26, 1945.
52. Gilbert, R. A.; Garrett, A. B. *J. Am. Chem. Soc.* **1956**, 78, 5501.
53. Schindler, P.; Garrett, A. B. *Helv. Chim. Acta.* **1960**, 43, 2176.
54. Kakihana, H.; Sillén, L. G. *Acta Chem. Scand.* **1956**, 10, 985.
55. Adamovich, L. P.; Shupenko, G. S. *Ukr. Khim. Zh.* **1959**, 25, 155.
56. Kovalenko, P. N.; Geiderovich, O. I. *Zh. Neorg. Khim.* **1959**, 4, 1974.
57. Carell, B.; Olin, Å. *Acta Chem. Scand.* **1961**, 15, 1875.
58. Carell, B.; Olin, Å. *Acta Chem. Scand.* **1962**, 16, 2357.
59. Schwarzenbach, G. *Pure Appl. Chem.* **1962**, 5, 377.
60. Feitknecht, W.; Schindler, P. *Pure Appl. Chem.* **1963**, 6, 130.
61. Hietanen, S.; Sillén, L. G. *Acta Chem. Scand.* **1964**, 18, 1015.
62. Wenger, H. Dissertation, Eidg. Tech. Hoch., Zurich; **1964**.
63. Bertin, F.; Thomas, G.; Merlin, J. C. *Compt. Rend.*, **1965**, 260, 1670.
64. Green, R. W.; Alexander, P. W. *Aust. J. Chem.* **1965**, 18, 651.
65. Bertin, F.; Thomas, G.; Merlin, J. C. *Bull. Soc. Chim. Fr.* **1967**, 2393.
66. Mesmer, R. E.; Baes, J. C. F. *Inorg. Chem.* **1967**, 6, 1951.
67. Ohtaki, H. *Inorg. Chem.* **1967**, 6, 808.
68. Ohtaki, H.; Kato, H. *Inorg. Chem.* **1967**, 6, 1935.
69. Lanza, E.; Carpeni, G. *Electrochim. Acta* **1968**, 13, 519.
70. Paris, M.; Gregoire, C. *Anal. Chim. Acta* **1968**, 42, 439.
71. Shevchenko, F. D.; Kuzina, L. A.; Vysotskaya, G. A. *Soviet. Progr. Chem. (Ukr. Khim. Zh)* **1968**, 34, 75.
72. Lanza, E. *Rev. Chim. Miner.* **1969**, 6, 653.
73. Schwarzenbach, G.; Wenger, H. *Helv. Chim. Acta* **1969**, 52, 644.
74. Kakihana, H.; Maeda, M. *Bull. Chem. Soc. Japan* **1970**, 43, 109.
75. Civatta, L.; Grimaldi, M. *Gazz. Chim. Ital.* **1973**, 103, 731.
76. Vanni, A.; Gennaro, M. C.; Ostacoli, G. *J. Inorg. Nucl. Chem.* **1975**, 37, 1443.
77. Tsukuda, H.; Kawai, T.; Maeda, M.; Ohtaki, H. *Bull. Chem. Soc. Japan* **1975**, 48, 691.
78. Mitskevich, B. F.; Samchuk, A. I. *Geokhimiya* **1978**, 9, 1419.
79. Brown, P. L.; Ellis, J.; Sylva, R. N. *J. Chem. Soc. Dalton Trans.* **1983**, 2001.
80. Bruno, J. *J. Chem. Soc. Dalton Trans.* **1987**, 2431.
81. Bruno, J.; Grenthe, I.; Muñoz, M. *J. Chem. Soc. Dalton Trans.* **1987**, 2445.
82. Mederos, A.; Dominguez, S.; Morales, M. J.; Brito, F.; China, E. *Polyhedron* **1987**, 6, 303.

83. Maeda, M.; Murata, Y.; Ito, K. *J. Chem. Soc. Dalton Trans.* **1987**, 1853.
84. Chineza, E.; Domínguez, S.; Mederos, A.; Brito, F.; Sánchez, A.; Ienco, A.; Vacca, A. *Main Group Metal Chem.* **1997**, *20*, 11.
85. Alderighi, L.; Bianchi, A.; Mederos, A.; Midollini, S.; Rodriguez, A.; Vacca, A. *Eur. J. Inorg. Chem.* **1998**, 1209.
86. Pâris, M. R.; Gregoire, C. *Anal. Chim. Acta* **1968**, *42*, 431.
87. Sillén, L. G.; Warnquist, B. *Ark. Kemi* **1969**, 315.
88. Cecconi, F.; Ghilardi, C. A.; Midollini, S.; Orlandini, A.; Mederos, A. *Inorg. Chem.* **1998**, *37*, 146.
89. Cecconi, F.; Ghilardi, C. A.; Midollini, S.; Orlandini, A.; Mederos, A. *Inorg. Chem.* **1998**, *37*, 146.
90. Green, R. W.; Alexander, P. W. *J. Phys. Chem.* **1963**, *67*, 905.
91. Schmidbaur, H.; Schmidt, M.; Schier, A.; Riede, J.; Tamm, T.; Pyykko, P. *J. Am. Chem. Soc.* **1998**, *120*, 2967.
92. Faure, R.; Bertin, F.; Loiseleur, H.; Thomas-David, G. *Acta Cryst.* **1974**, *B30*, 462.
93. Sohrin, Y.; Kokusen, H.; Kihara, S.; Matsui, M.; Hata, Y.; Kushi, Y.; Shiro, M. *J. Am. Chem. Soc.* **1993**, *115*, 4128.
94. Sohrin, Y.; Matsui, M.; Hata, Y.; Hasegawa, H.; Kokusen, H. *Inorg. Chem.* **1994**, *33*, 4376.
95. Barbaro, P.; Cecconi, F.; Ghilardi, C. A.; Midollini, S.; Orlandini, A.; Alderighi, L.; Peters, D.; Vacca, A.; Chineza, E.; Mederos, A. *Inorg. Chim. Acta* **1997**, *262*, 187.
96. Everest, D. A.; Mercer, R. A.; Miller, R. P.; Milward, G. L. *J. Inorg. Nucl. Chem.* **1962**, *24*, 525.
97. Scholder, R.; Hund, H.; Schwarz, H. Z. *Z. Anorg. Allg. Chem.* **1968**, *361*, 284.
98. Schmidt, M.; Schier, A.; Riede, J.; Schmidbaur, H. *Inorg. Chem.* **1998**, *37*, 3452.
99. Ishiguro, S.; Ohtaki, H. *Bull. Soc. Chim. Japan* **1979**, *52*, 3198.
100. Fricke, R.; Humme, H. *Z. Anorg. Chem.* **1929**, *178*, 401.
101. Stahl, R.; Jung, C.; Lutz, H. D.; Kockelmann, W.; Jacobs, H. Z. *Anorg. Allg. Chem.* **1998**, *624*, 1130.
102. Lutz, H. D.; Jung, C.; Mortel, R.; Jacobs, H.; Stahl, R. *Spectroc. Acta Pt. A—Molec. Biomolec. Spectr.* **1998**, *54*, 893.
103. Tananaev, I. V.; Deichman, E. N. *Izv. Akad. Nauk SSSR, Otd. Khim.* **1949**, 144.
104. Kleiner, K. E. *Zhur. Obshch. Khim.*, **1951**, *21*, 18.
105. Yates, L. M., Thesis, Washington State College, Washington, 1955.
106. Babko, A. K.; Shimadina, L. *Zh. Neorg. Khim.* **1959**, *4*, 1060.
107. Tananaev, I. V.; Vinogradova, A. D. *Zh. Neorg. Khim.* **1960**, *5*, 321.
108. Hardy, C. J.; Greenfield, B. F.; Scargill, D. *J. Chem. Soc.* **1961**, 174.
109. Talipov, S.; Podgornova, V.; Zinina, G. *Uzbeksk. Khim. Zhur.* **1961**, *4*, 11.
110. Buslaev, Y. A.; Gustyakova, M. P. *Zhur. Neorg. Khim.* **1965**, *10*, 1524.
111. Presnyakova, O. E.; Prishchepo, R. S. *Zh. Neorg. Khim.* **1966**, *11*, 1436.
112. Ahrland, S. *Helv. Chim. Acta* **1967**, *50*, 306.
113. Feeney, J.; Haque, R.; Reeves, L. W.; Yue, C. P.; J. Feeney, R. H., L. W. Reeves, and C. P. Yue, *Canad. J. Chem.*, 1968, *46*, 1389 *Can. J. Chem.* **1968**, *46*, 1389.
114. Hogben, M.; Radley, K.; Reeves, L. *Can. J. Chem.* **1970**, *48*, 2960.
115. Gordienko, V. I.; Mikhailyuk, Y. I. *Zh. Anal. Khim.* **1970**, *25*, 2267.
116. Mesmer, R. E.; Baes Jr., C. F. *Inorg. Chem.* **1969**, *8*, 618.
117. Anttila, R.; Grenthe, I.; Glaser, J.; Bruno, J.; Lagerman, B. *Acta Chem. Scand.* **1991**, *45*, 423.
118. Kolosova, I. F.; Belyavskaya, T. A. *Vest. Mosk Univ., Khim.* **1963**, *18(1)*, 52.
119. Morris, D. F. C.; Jones, M. W. *J. Inorg. Nucl. Chem.* **1965**, *27*, 2454.

120. Sekine, T.; Komatsu, Y.; Sakairi, M. *Bull. Chem. Soc. Jpn.* **1971**, *44*, 1480.
121. Pachkaeva, T.; Tamm, N. S.; Novoselova, A. V. *Zhur. Neorg. Khim.* **1971**, *16*, 219(E:113).
122. Belyavskaya, T. A.; Kolosova, I. F. *Vestn. Mosk. Univ., Ser. 2: Khim.* **1962**, *25*, 55.
123. Kohler, G.; Wendt, H. *Ber. Buns. Phys. Chem.* **1966**, *70*, 674.
124. Sekine, T.; Sakairi, M. *Bull. Chem. Soc. Jpn.* **1967**, *40*, 261.
125. Prasad, B. *J. Indian Chem. Soc.* **1968**, *45*, 1037.
126. Knoche, W.; Firth, C.; Hess, D. *Adv. Mol. Relax. Proc.* **1974**, *6*, 1.
127. Ripan, R.; Vericeanu, G. *Stud. Univ. Babes-Bolyai* **1968**, *13*, 31.
128. Chukhlantsev, V. G.; Alyamovskaya, K. V. *Izv. Vyssh. Ucheb. Zaved., Khim.* **1961**, *4*, 359.
129. Ciavatta, L.; Iuliano, M.; Porto, R. *Ann. Chim. (Rome)* **1997**, *87*, 375.
130. Dyatlova, N. M.; Medyntsev, V. V.; Medved, T. Y.; Kabachnik, M. I. *J. Gen. Chem. USSR (Engl. Transl.)* **1968**, *38*, 1030.
131. Anderegg, G. *Helv. Chim. Acta* **1965**, *48*, 1712.
132. Bruno, J.; Grenthe, I.; Sandström, M.; Ferri, D. *J. Chem. Soc. Dalton Trans.* **1987**, 2439.
133. Baldwin, W. G.; Stranks, D. R. *Aust. J. Chem.* **1968**, *21*, 2161.
134. Biernann, W.; McCorkell, R. *Can. J. Chem.* **1967**, *45*, 2846.
135. Gruenewald, B.; Knoche, W.; Rees, N. H. *J. Chem. Soc. Dalton* **1976**, 2338.
136. Bamberger, C. E.; Suner, A. *Inorg. Nucl. Chem. Letters* **1973**, *9*, 1005.
137. Tedesco, P. H.; De Rumi, V. B. *J. Inorg. Nucl. Chem.* **1975**, *37*, 1833.
138. Bhattacharya, A. K., Personal communication to Martell, A. E., reported in "Stability Constants."
139. Pedersen, K. *Acta Chem. Scand.* **1949**, *3*, 676.
140. Marvel, C. S.; Martin, M. M. *J. Am. Chem. Soc.* **1958**, *80*, 619.
141. Cardwell, T. J.; Carter, M. R. L. *J. Inorg. Nucl. Chem.* **1977**, *39*, 2139.
142. Moeller, T. *Inorg. Synth.* **1950**, *3*, 4, and references therein.
143. Urbain, G.; Lacombe, H. C. R. *Seances Acad. Sci.* **1901**, *133*, 874.
144. Bragg, W. H.; Morgan, G. T. *Proc. R. Soc. London, A* **1923**, *104*, 437.
145. Addison, C. C.; Walker, A. *Proc. Chem. Soc.* **1961**, 242.
146. Tuseev, N. I.; Sipachev, V. A.; Galimzyanov, R. F.; Golubinskii, A. V.; Zasorin, E. Z.; Spiridonov, V. P. *J. Mol. Struct.* **1984**, *125*, 277.
147. de Bruin, H. J.; Kairaitis, D.; Temple, R. B. *Aust. J. Chem.* **1962**, *15*, 457.
148. Starý, J. *Anal. Chim. Acta* **1963**, *28*, 132.
149. Athavale, V. T.; Mahadevan, N.; Mathur, P. K.; Sathe, R. M. *J. Inorg. Nucl. Chem.* **1967**, *29*, 1947.
150. Couturier, Y.; Faucherre, J. *Bull. Soc. Chim. Fr.* **1970**, 1323.
151. Votava, J.; Bartusek, M. *Collect. Czech. Chem. Commun.* **1975**, *40*, 2050.
152. Duc, G.; Bertin, F.; Thomas-David, G. *Bull. Soc. Chim. Fr.* **1977**, 196.
153. Jaber, M.; Bertin, F.; Thomas-David, G. *Can. J. Chem.* **1978**, *56*, 777.
154. Gruenewald, B.; Knoche, W. *J. Chem. Soc. Dalton Trans.* **1978**, 1221.
155. Tedesco, P. H.; Gonzales Quintana, J. *J. Inorg. Nucl. Chem.* **1974**, *36*, 2628.
156. Duc, G.; Bertin, F.; Thomas-David, G. *Bull. Soc. Chim. Fr.* **1977**, 645.
157. Jaber, M.; Bertin, F.; Thomas-David, G. *Bull. Soc. Chim. Fr.* **1988**, 470.
158. Duc, G.; Thomas, G. *Bull. Soc. Chim. Fr.* **1972**, 4439.
159. Singh, A.; Dubey, S. E. A. *Indian J. Chem.* **1979**, *17A*, 623.
160. Schubert, J.; Lindenbaum, A. *J. Biol. Chem.* **1954**, *208*, 359.
161. Mukherji, A. K.; Dey, A. K. *J. Inorg. Nucl. Chem.* **1958**, *6*, 314.
162. Vanni, A.; Gennaro, M. C. *Annali Chim.* **1974**, *64*, 397.

163. Duc, G.; Bertin, F.; Thomas-David, G. *Bull. Soc. Chim. Fr.* **1975**, 495.
164. Nayan, R.; Dey, A. K. *Z. Naturforsch.* **1970**, B25, 1453.
165. Grewal, S.; Sekhon, B. S.; Chopra, S. L. *Thermochim. Acta* **1975**, 11, 315.
166. Sandhu, S.; Kumaria, J.; Sandhu, R. *Indian J. Chem.* **1976**, 14A, 817.
167. Alderighi, L.; Cecconi, F.; Ghilardi, C.; Mederos, A.; Midollini, S.; Orlandini, A.; Vacca, A. *Polyhedron*, **1999**, 18, 3305.
168. Jaber, M.; Thomas-David, G. *Bull. Soc. Chim. Fr.* **1985**, 644.
169. Schmidt, M.; Bauer, A.; Schier, A.; Schmidbaur, H. *Z. Naturforsch.* **1998**, 53b, 727.
170. Evans, D. F.; Wong, C. Y. *J. Chem. Soc. Dalton Trans.* **1992**, 2009.
171. Schmidt, M.; Bauer, A.; Schmidbaur, H. *Inorg. Chem.* **1997**, 36, 2040.
172. Belyavskaya, T. A.; Kolosova, I. F. *Zh. Neorg. Khim.* **1965**, 10, 236 (441).
173. Joshi, J. D.; Bhattacharya, P. K. *Indian J. Chem.* **1975**, 13, 88.
174. Piispanen, J.; Lajunen, L. H. *J. Acta Chem. Scand.* **1996**, 50, 1074.
175. Duc, G.; Thomas-David, G. *Bull. Soc. Chim. Fr.* **1980**, 1, 169.
176. Kolosova, I. F.; Belyavskaya, T. A. *Zh. Neorg. Khim.* **1965**, 10, 764.
177. Maslowska, J.; Owczarek, A. *Pol. J. Chem.* **1988**, 62, 75.
178. Duc, G.; Thomas-David, G. *Bull. Soc. Chim. Fr.* **1979**, I, 163.
179. Feldman, I.; Toribara, T. Y.; Havill, J. R.; Neuman, W. F. *J. Am. Chem. Soc.* **1955**, 77, 878.
180. Patnaik, R.; Pani, S. *J. Indian Chem. Soc.* **1961**, 38, 896.
181. Rosenheim, A.; Lehmann, F. *Liebigs Ann. Chem.* **1924**, 440, 153.
182. Kumberger, O.; Riede, J.; Schmidbaur, H. *Z. Naturforsch.* **1992**, 47b, 1717.
183. Banks, C. V.; Singh, R. S. *J. Am. Chem. Soc.* **1959**, 81, 6159–6163.
184. Banks, C. V.; Singh, R. S. *J. Inorg. Nucl. Chem.* **1960**, 15, 125.
185. Agarwal, R. P.; Mehrotra, R. C. *J. Less Common Metals* **1961**, 3, 398.
186. Das, R. C.; Aditya, S. *J. Indian Chem. Soc.* **1961**, 38, 19.
187. Das, R. C.; Aditya, S. *J. Indian Chem. Soc.* **1964**, 41, 765.
188. Bartusek, M.; Zelinka, J. *Collect. Czech. Chem. Commun.* **1967**, 32, 992.
189. Adamovich, L. P.; van Nyan, V. *Zh. Anal. Khim.* **1968**, 23, 994.
190. Dube, S. S.; Dhindsa, S. S. *Z. Naturforsch.* **1969**, 24b, 967.
191. Dube, S. S.; Dhindsa, S. S. *Z. Naturforsch.* **1969**, 24b, 1234.
192. Vartak, D.; Menon, K. *J. Inorg. Nucl. Chem.* **1971**, 33, 1003.
193. Chattopadhyaya, M. C.; Singh, R. S. *Anal. Chim. Acta* **1974**, 70, 49.
194. Saarinen, H.; Raikas, T.; Lajunen, L. *Finn. Chem. Lett.* **1974**, 109.
195. Abbasi, S. A.; Bhat, B. G.; Singh, R. S. *Indian J. Chem.* **1976**, 14B, 718.
196. Lajunen, L. H. *J. Ann. Acad. Sci. Fenn. Ser. A2* **1976**, 179, 62.
197. Jain, U.; Kumari, V.; Sharma, R. C.; Chaturvedi, G. K. *J. Chim. Phys.* **1977**, 74, 1038.
198. Saarinen, H.; Lajunen, L.; Isoluoma, P. *Finn. Chem. Lett.* **1977**, 66.
199. Lajunen, L. H. J.; Karvo, M. *Anal. Chim. Acta* **1978**, 97, 423.
200. Lajunen, L. H. J.; Tikanmaki, M. *Acta Univ. Ouluensis, Ser. A* **1978**, 74, 21.
201. Sharma, R. C.; Dhindsa, S. S.; Bhargava, D. N. *Monatsh. Chem.* **1978**, 109, 179.
202. Lajunen, L. H. J.; Karvo, M.; Tikanmaki, M. *Finn. Chem. Lett.* **1979**, 45.
203. Lajunen, L. H. J.; Kostama, A.; Karvo, M. *Acta Chem. Scand., Ser. A* **1979**, A33, 681.
204. Lajunen, L.; Tikanmaki, M. *Acta Univ. Oulu* **1979**, A74, 20s.
205. Abbasi, S. A. *J. Indian Chem. Soc.* **1984**, 61, 125.
206. Budesinsky, B.; West, T. S. *Anal. Chim. Acta* **1968**, 42, 455.
207. Sathe, R.; Shetty, S. *J. Inorg. Nucl. Chem.* **1970**, 32, 1383.
208. Saarinen, H.; Raikas, T.; Rauala, A. *Finn. Chem. Lett.* **1974**, 104.

209. Sandhu, R.; Singh, K. *Thermochim. Acta* **1976**, *17*, 325.
210. Lajunen, L. H. J. *Finn. Chem. Lett.* **1978**, 129.
211. Lajunen, L. H. J.; Tikanmaki, M. *Finn. Chem. Lett.* **1978**, 96.
212. Lajunen, L. H. J.; Hiljanen, T. *Acta Univ. Ouluensis, Ser. A* **1980**, *105*, 18.
213. Lajunen, L. H. J.; Seppanen, M. T.; Nurmesniemi, H.; Leskela, M. *Oulun Yliopiston Kem. Laitoksen Raporttisar.* **1981**, *8*, 10.
214. Lajunen, L. H. J.; Kopsa-Moilanen, V. *Finn. Chem. Lett.* **1982**, 6.
215. Lajunen, L. H. J. *J. Indian Chem. Soc.* **1982**, *59*, 1238.
216. Schmidbaur, H.; Kumberger, O.; Riede, J. *Inorg. Chem.* **1991**, *30*, 3101.
217. Schmidbaur, H.; Kumberger, O. *Chem. Ber.* **1993**, *126*, 3.
218. Manoussakis, G.; Karayannidis, P.; Tsipis, C. *Chem. Chron.* **1972**, *1*, 14.
219. Perkins, D. J. *Biochem. J.* **1952**, *51*, 487.
220. Duc, G.; Bertin, F.; Thomas-David, G. *Bull. Soc. Chim. Fr.* **1974**, 793.
221. Ghandour, M. A.; Azab, H. A.; Hassan, A.; Ali, A. M. *Polyhedron* **1989**, *8*, 189.
222. Perkins, D. J. *Biochem. J.* **1953**, *55*, 649.
223. Singh, M. K.; Srivastava, M. K. *J. Inorg. Nucl. Chem.* **1972**, *34*, 567.
224. Singh, M. K.; Srivastava, M. K. *J. Inorg. Nucl. Chem.* **1972**, *34*, 2067.
225. Singh, M. K.; Srivastava, M. K. *J. Inorg. Nucl. Chem.* **1972**, *34*, 2081.
226. Mederos, A.; Medina, E.; Colomer, A.; Brito, F. *Polyhedron* **1989**, *8*, 2017.
227. Singh, S.; Rani, B.; Yadava, K. *Chem. Scr.* **1986**, *26*, 363.
228. Chawla, I. D.; Andrews, A. C. *J. Inorg. Nucl. Chem.* **1970**, *32*, 91.
229. Duc, G.; Bertin, F.; Thomas-David, G. *Bull. Soc. Chim. Fr.* **1976**, 414.
230. Singh, S.; Radna Pani, B.; Vyas, M.; Yadava, K. *Pol. J. Chem.* **1985**, *59*, 1021.
231. Srivastava, J. P. N.; Srivastava, M. N. *Indian J. Chem.* **1976**, *14A*, 818.
232. Krishnan, k.; Plane, R. A. *Inorg. Chem.* **1967**, *6*, 55.
233. Izatt, R. M.; Fernelius, W. C.; Block, B. P. *J. Phys. Chem.* **1955**, *59*, 80.
234. Srivastava, S. *J. Proc. Inst. Chem. India* **1967**, *39*, 173.
235. Alderighi, L.; Gans, P.; Midollini, S.; Vacca, A. Unpublished results.
236. Bertin, F.; Thomas, G. *Bull. Soc. Chim. Fr.* **1968**, 1255.
237. Chawla, I. D.; Andrews, A. C. *J. Inorg. Nucl. Chem.* **1969**, *31*, 3809.
238. Hakkinen, P.; Lajunen, K. *Finn. Chem. Lett.* **1987**, *14*, 7.
239. Dubey, S. N.; Singh, A.; Puri, D. M. *J. Inorg. Nucl. Chem.* **1981**, *43*, 407.
240. da Silva, J. J. R. F.; Abreu Vaz, M. C. T. *J. Inorg. Nucl. Chem.* **1977**, *39*, 613.
241. Irving, H.; da Silva, J. J. R. F. *J. Chem. Soc.* **1963**, 458.
242. Irving, H.; da Silva, J. J. R. F. *J. Chem. Soc.* **1963**, 448.
243. Irving, H.; da Silva, J. J. R. F. *J. Chem. Soc.* **1963**, 3308.
244. Mederos, A.; Domínguez, S.; Medina, A. M.; Brito, F.; China, E.; Bazdikian, K. *Polyhedron* **1987**, *6*, 1365.
245. Starostin, V. V.; Spitsyn, V. I.; Silina, G. F. *Zhur. Neorg. Khim.* **1963**, *8*, 335 (660).
246. Bamberger, C.; Laguna, F. *J. Inorg. Nucl. Chem.* **1966**, *28*, 1067.
247. Bamberger, C. E.; Botbol, J. *J. Inorg. Nucl. Chem.* **1970**, *32*, 1569.
248. Mederos, A.; Felipe, J. M.; Hernández-Padilla, M.; Brito, F.; China, E.; Bazdikian, K. *J. Coord. Chem.* **1986**, *14*, 277.
249. China, E.; Domínguez, S.; Mederos, A.; Brito, F.; Arrieta, J. M.; Sanchez, A.; Germain, G. *Inorg. Chem.* **1995**, *34*, 1579.
250. Nakasuka, N.; Sawaragi, M.; Matsumura, K.; Tana, M. *Bull. Chem. Soc. Jpn.* **1992**, *65*, 1722.
251. Dubey, S. N.; Mehrotra, R. C. *J. Less Common Met.* **1964**, *7*, 169.
252. Basargin, N. N.; Rozovskii, Y. G.; Socolova, L. D.; Kurbanova, L. M. *Zh. Neorg. Khim.* **1981**, *26*, 2042.

253. Basinger, M. A.; Johnson, J. E.; Burke, L. T.; Jones, M. N. *Res. Commun. Chem. Pathol. Pharmacol.* **1982**, 36, 519.
254. Hakkinen, P. *Finn. Chem. Lett.* **1984**, 151.
255. Hakkinen, P. *Finn. Chem. Lett.* **1986**, 13, 53.
256. Hakkinen, P. *Finn. Chem. Lett.* **1987**, 14, 15.
257. Kumberger, O.; Riede, J.; Schmidbaur, H. *Chem. Ber.* **1992**, 125, 2701.
258. Klüfers, P.; Mayer, P.; Schuhmacher, J. Z. *Anorg. Allg. Chem.* **1995**, 621, 1373.
259. Dyatlova, N. M.; Medyntsev, V. V.; Medved, T. Y.; Kabachnik, M. I. *J. Gen. Chem. USSR (Engl. Transl.)* **1968**, 38, 1025.
260. Alderighi, L.; Vacca, A.; Cecconi, F.; Midollini, S.; Chinea, E.; Domínguez, S.; Valle, A.; Dakternieks, D.; Duthie, A. *Inorg. Chim. Acta* **1999**, 285, 39.
261. Kabachnik, M. I.; Lastovskii, R. P.; Medved, T. Y.; Medyntsev, V. V.; Kolpakova, I. D.; Dyatlova, N. M. *Dokl. Akad. Nauk SSSR* **1967**, 177(3), **582**.
262. Dyatlova, N. M.; Medyntsev, V. V.; Balashova, T. M.; Medved, T. Y.; Kabachnik, M. I. *Zh. Obshch. Khim.* **1969**, 39(2), 329.
263. Voronezhova, N. I.; Rudyak, Y. V.; Dyatlova, N. M.; Grigor'ev, A. I. *Koord. Khim.* **1980**, 6, 991.
264. Dyatlova, N. M.; Kabachnik, M. I.; Medved, T. Y.; Rudomino, M. V.; Belugin, Y. F. *Proc. Acad. Sci. (USSR)* **1965**, 161, 307 (607).
265. Dyatlova, N. M.; Medyntsev, V. V.; Medved, T. Y.; Kabachnik, M. I. *J. Gen. Chem. USSR (Engl. Transl.)* **1968**, 38, 1035.
266. Medved, T. Y.; Kabachnik, M. I.; Bel'skii, F. I.; Pisareva, S. A. *Izv. Akad. Nauk SSSR, Ser. Khim.* **1988**, 9, 2103.
267. Medved, T. Y.; Kabachnik, M. I.; Goryunova, I. B.; Shcherbakov, B. K.; Belskii, F. I.; Petrovskii, P. V.; Polikarpov, Y. M. *Izv. Akad. Nauk SSSR, Ser. Khim.* **1988**, 9, 2107.
268. Polikarpov, Y. M.; Belskii, F. I.; Pisareva, S. A.; Kabachnik, M. I. *Izv. Akad. Nauk SSSR, Ser. Khim.* **1989**, 9, 2112.
269. Siepak, J. *Pol. J. Chem.* **1985**, 59, 955.
270. Siepak, J. *Pol. J. Chem.* **1985**, 59, 651.
271. Kotz, J. C.; Schaffer, R.; Clouse, A. *Inorg. Chem.* **1967**, 6, 620.
272. Kido, H.; Fernelius, W.; Haas, C. *Pennsylvania. State Univ., Contract No. AT(30-1)-907*, **1960**.
273. Goel, D. P.; Dutt, Y.; Singh, R. P. *J. Inorg. Nucl. Chem.* **1970**, 32, 3119.
274. Maslowska, J.; Dorabalski, A. *Pol. J. Chem.* **1983**, 57, 1089.
275. Srivastava, R. C.; Srivastava, M. N. *J. Inorg. Nucl. Chem.* **1978**, 40, 1439.
276. Coates, G. E.; Fishwick, A. H. *J. Chem. Soc. (A)* **1968**, 477.
277. Andersen, R. A.; Coates, G. E. *J. Chem. Soc., Dalton Trans.* **1972**, 2153.
278. Bell, N. A.; Shearer, H. M. M.; Twiss, J. *Acta Crystallogr., Sect. C* **1984**, 40, 610.
279. Bell, N. A.; Shearer, H. M. M.; Twiss, J. *Acta Crystallogr., Sect. C* **1984**, 40, 605.
280. Aggarwal, M.; Mehrotra, R. C. *Synth. React. Inorg. Metal-Org. Chem.* **1984**, 14, 139.
281. van Uitert, L.; Fernelius, W.; Douglas, B. *J. Am. Chem. Soc.*, **1953**, 75, 457.
282. van Uitert, L.; Fernelius, W.; Douglas, B. *J. Am. Chem. Soc.* **1953**, 75, 2739.
283. van Uitert, L.; Fernelius, W.; Douglas, B. *J. Am. Chem. Soc.*, **1953**, 75, 2736.
284. Izatt, R. M.; Haas, C. G.; Block, B. P. J.; Fernelius, W. C. *J. Phys. Chem.* **1954**, 58, 1133.
285. Bryant, B.; Fernelius, W. *J. Am. Chem. Soc.* **1954**, 76, 1696.
286. Izatt, R. M.; Fernelius, W. C.; Block, B. P. *J. Phys. Chem.* **1955**, 59, 235.
287. Kluiber, R. W.; Lewis, J. W. *J. Am. Chem. Soc.* **1960**, 82, 5777.
288. Martin, D.; Janusonis, G.; Martin, B. *J. Am. Chem. Soc.* **1961**, 83, 73.

289. Martin, D.; Martin, B. *Inorg. Chem.* **1962**, *1*, 404.
290. Uhlemann, E.; Frank, E. *Z. Anorg. Chem.* **1965**, *340*, 319.
291. Chawla, I. D.; Spillert, C. R. *J. Inorg. Nucl. Chem.* **1968**, *30*, 2717.
292. Rudenko, N. P.; Sevast'yanov, A. I.; Lanskaya, N. G. *Zh. Neorg. Khim.* **1968**, *13*, 1566.
293. Moiseeva, L.; Kuznetsova, N. *Zh. Anal. Khim.* **1971**, *26(11)*, 2090.
294. Jablonski, Z.; Wasag, T.; Millo, S. *Rocz. Chem.* **1976**, *50*, 1467.
295. Irving, R. J.; Ribeiro da Silva, M. A. V. *J. Chem. Soc. Dalton Trans.* **1977**, 413.
296. Starý, J.; Liljenzin, J. O. *Pure Appl. Chem.* **1982**, *54*, 2557.
297. Ribeiro da Silva, M. A. V.; Reis, A. M. M. V. *J. Chem. Thermodyn.* **1983**, *15*, 957.
298. Green, R. W.; Alexander, P. W. *Aust. J. Chem.* **1965**, *18*, 1297.
299. Green, R. W.; Alexander, P. W. *Aust. J. Chem.* **1965**, *18*, 329.
300. Green, R. W.; Sleet, R. *Aust. J. Chem.* **1966**, *19*, 2101.
301. Ceconi, F.; China, E.; Ghilardi, C. A.; Midollini, S.; Orlandini, A. *Inorg. Chim. Acta* **1997**, *260*, 77.
302. Saxena, R. S.; Scheelwant, S. S. *Monatsh. Chem.* **1975**, *106*, 1081.
303. Relan, P. S.; Bhattacharya, P. K. *J. Indian Chem. Soc.* **1967**, *44*, 536.
304. Coates, G. E.; Green, S. I. E. *J. Chem. Soc.* **1962**, 3340.
305. Rudenko, N. P.; Sevast'yanov, A. I. *Zh. Neorg. Khim.* **1968**, *13*, 184.
306. Barrett, P. A.; Dent, C. E.; Linstead, R. P. *J. Chem. Soc.* **1936**, 1719.
307. Linstead, R. P.; Robertson, J. M. *J. Chem. Soc.* **1936**, 1736.
308. Bryant, B.; Fernelius, W. *J. Am. Chem. Soc.* **1954**, *76*, 4864.
309. Hirai, M.; Oka, Y. *Bull. Chem. Soc. Jpn.* **1970**, *43*, 778.
310. Han, R.; Parkin, G. *Inorg. Chem.* **1992**, *31*, 983.
311. Gemiti, F.; Giancotti, V.; Ripamonti, A. *J. Chem. Soc. (A)* **1968**, 763.
312. Grewal, S.; Sekhon, B. S.; Pannu, B. S.; Chopra, S. L. *Indian J. Chem.* **1975**, *13*, 623.
313. Rao, D. M.; Ramaiah, E. K.; Ram, K. *Proc. Natl. Acad. Sci., India, Sect. A* **1995**, *65*, 403.
314. Adamovich, L. P.; Mirnaya, A. P.; Khukhryanskaya, A. K. *Zh. Anal. Khim.* **1969**, *12(24)*, 1816.
315. Hayashi, K.; Sasaki, Y.; Tagashira, S.; Kosaka, E. *Anal. Chem. (USA)* **1986**, *58*, 1444.
316. Bock, J. L.; Ash, D. E. *J. Inorg. Biochem.* **1980**, *13*, 105.
317. "Encyclopedia of Occupational Health and Safety"; Parmeggiani, L. (Ed.); 3rd ed.; International Labour Organization: Geneva, 1983; Vol. 1.

GROUP 2 ELEMENT PRECURSORS FOR THE CHEMICAL VAPOR DEPOSITION OF ELECTRONIC MATERIALS

JASON S. MATTHEWS*[†] AND WILLIAM S. REES JR.*^{†‡}

*School of Chemistry and Biochemistry, [†]Molecular Design Institute, [‡]School of Materials
Science and Engineering, Georgia Institute of Technology, Atlanta, GA 30332-0400

Chemical vapor deposition (CVD) is defined as the preparation of a solid coating from a gaseous precursor by means of a chemical transformation (*1*). The use of chemical vapor distinguishes CVD from physical deposition methods, such as sputtering and evaporation, thus imparting versatility to the deposition technique (*2*). CVD has become the method of choice in the growth of thin films over a very large substrate area. The benefits of the method include non-line-of-sight, high throughput, low cost per unit, and uniform thickness and elemental composition coverage. There exist several different methods of CVD, including, but not limited to, metalorganic vapor phase epitaxy (MOVPE) (*3–6*), plasma enhanced chemical vapor deposition (PECVD) (*7, 8*), photo CVD (*9*), low pressure chemical vapor deposition (LPCVD) (*10, 11*), combustion chemical vapor deposition (*12*), and aerosol assisted chemical vapor deposition (*13, 14*). Each of these methods has their benefits and drawbacks, and additionally, their use is highly dependent upon the size, as well as the complexity, of the device being prepared (*15*).

Independent of the CVD system, certain constants must be adhered to. The precursor is one of the most important components of the CVD system and is often referred to as the source. The first step in the CVD process is vaporization of the precursor, if it does not already exist as a gas at ambient conditions. The precursor should have sufficient vapor pressure, at least 100 mtorr at delivery temperature, to achieve reasonable deposition rates (*16*). Ambient temperature liquids are preferred to solids, since it is easier to maintain a constant flux of the precursor in the vapor phase. This is due to the fact that liquids rapidly reestablish equilibrium upon removal of vapors,

whereas solids tend to require longer periods because of their significantly smaller surface area (1). The precursor should also be thermally stable in the solid as well as the vapor phase up to the delivery temperature. This prevents premature decomposition from occurring at the source, or in the lines leading to the substrate. In order to give a film with the desired composition, morphology, and purity, the precursor must undergo controlled thermal decomposition at substrate temperatures. It is therefore necessary to find a precursor that is thermally stable at source temperatures but decomposable at substrate temperatures. Precursors usually take the form of a metalorganic or organometallic compound, with the metal being a major component of the desired film. The properties of the material being grown are highly dependent upon the purity as well as the chemical make-up and decomposition pathway of the precursor (17). Poor decomposition pathways can lead to the incorporation of undesired elements into the thin film, necessitating the use of various postdeposition annealing processes.

Precursors are used in chemical vapor deposition to prepare materials that can be separated into two categories, specifically metals and nonmetals. CVD of metals have broad sweeping applications in the silicon-based microelectronics industry, and research in this area had been fed by the increasing demand for performance, size reduction, and speed in the circuits of electronic devices. Increasing the speed of integrated circuits can be accomplished by reducing the size of the device. Early integrated circuits had one interconnect level because of the relatively small number of devices that had to be connected. However, the reduction in device size led to an increase in the number of devices on a single chip, which did not leave enough room for interconnect lines. Solving this problem was accomplished via the use of multilevel structures that allow for flexibility in interconnect routing by increasing the effective surface area for metallization. The more complex features of the multilevel structures have raised several concerns about the reliability and performance of the metal interconnects. These concerns are directly related to the resistance of the type of metal being used for the interconnect (17, 18). Metals with low resistivities are ideal for use as interconnects, since they reduce RC delays and IR voltage drops, thereby increasing device performance. Aluminum has an extremely low resistivity; however, its deposition has been limited to PVD techniques such as sputtering, which results in nonconformal coverage of the substrate. Tungsten, which can be deposited via CVD, has stepped up to replace aluminum in several interconnect schemes. The process is carried out by silane or

hydrogen reduction of tungsten hexafluoride, after a selective self-limiting reduction by Si (19). Copper may serve as a better replacement for aluminum, since it has a lower resistivity than either tungsten or aluminum. This would allow for an increase in the operating frequency of the device, as well as the use of higher current densities. These interconnect devices are all made up of materials that are referred to as conductors. One property of these materials is that they show a decrease in conductivity with an increase in temperature. For semiconductors the inverse is true.

Semiconductors are defined as materials that contain a relatively small number of current carriers when compared to metal conductors (20). Semiconductors are hybrids of insulators and conductors in that the separation between their valence and conduction band is not as large as that of an insulator, nor is there any overlap as is exhibited in conductors. As mentioned earlier, an intrinsic property of semiconductors is that an increase in conductivity is observed in conjunction with an increase in temperature. This phenomenon does not occur in conductors; instead, a thermally induced scattering of carrier electrons lowers the conductivity of the material. Scattering of electrons also occurs in semiconductors; however, the increase in temperature allows for the thermal promotion of electrons from the valence to the conduction band, which increases the conductivity of the material. Materials with band gaps residing in the visible region have applications in solar cells and thin film electroluminescent (TFEL) displays, whereas those in the infrared region can be used in thermal imaging technology. In addition to differing band gaps, semiconductors can have direct and indirect band-gap transitions. Semiconductors such as silicon and germanium are indirect band-gap materials and are useless in devices where fast and efficient generation of conducting species is required. Direct band-gap materials such as GaAs and CdS are more useful for lasers and other optoelectronic devices. Two important classes of semiconductors are the III–V, GaAs and InP, and the II–VI, CdS and ZnSe, materials. Applications of the III–V materials can be found in LEDs, semiconductors for use in optoelectronic devices, solar cells, and LDs. Current CD-ROM devices are red laser-based. The use of a blue laser would allow for the storage of about five times more information per unit area than is observed with the current red laser technology. The II–VI materials also have uses in solar cells, TFELs, and LEDs; additional applications are found in the area of blue phosphors, infrared detectors, and thermal imaging systems.

Superconductors are defined as a class of materials that have zero

electrical resistance. This phenomenon was first observed at the turn of the century when elemental mercury was cooled to 4 K, T_c (the temperature at which superconductivity is observed), with liquid helium. In 1957 Bardeen–Cooper–Schreiffer (BCS) theory was developed to explain the phenomena of superconductivity. Based on this theory, it was believed that a T_c higher than 30 K was unattainable. In 1986, Bednorz and Mueller observed superconductivity at temperatures greater than 30 K in complex oxides of copper. The following year researchers discovered superconductors with T_c values as high as 95 K. This was considered to be a major breakthrough, since these materials could now operate at temperatures higher than the boiling point of liquid nitrogen (77 K), which is readily available and relatively inexpensive, compared to liquid helium. It was possible to envisage these materials being applied to transmission lines, motors, and microelectronics. In addition to the critical temperature (T_c), other important values include the critical current (I_c), the current at which superconductivity is suppressed, which when normalized to the cross-sectional gives the critical current density (J_c). The critical field (H_c), the threshold value at which an applied magnetic field destroys superconductivity, also plays an important role in the usefulness of the material. For microwave applications at frequencies of 1–15 GHz, R_s , nonzero surface resistance, is the dominant figure of merit (21). This parameter varies as a function of temperature, frequency, and film quality. In addition to exhibiting zero resistance at the critical temperature, superconductors also behave as perfect diamagnets, expelling all magnetic flux from their interior, a phenomenon known as the Meissner effect.

The unique properties exhibited by superconductors allow for numerous revolutionary applications. These applications are separated into three different categories: large-scale applications, low-field applications, and superconducting electronics applications. Large-scale applications include high-field superconducting magnets that can be used in nuclear magnetic resonance (NMR), magnetic resonance imaging (MRI), and magnetically levitated (MAGLEV) trains. Low-field applications are evidenced in superconducting transmission lines, which have been tested at Brookhaven National Laboratories. The successful prototype three-phase, 1000 MVA ac transmission line used a conductor cable constructed from a Nb_3Sn (LTS) tape mounted on an aluminum stabilizer. The results showed that YBCO (HTS) materials would allow for commercialization of this application if the 60 Hz loss experienced in these materials could be overcome (22). Superconducting electronics applications include digital-to-analog convert-

ers, single flux quantum shift resisters, neural networks, superconducting quantum interference devices (SQUIDs), voltage standards, bolometric detectors, superconducting field effect transistors, and passive microwave devices. The SQUID is the most widely used superconducting electronic device. It is the most sensitive sensor for magnetic flux and it can be used for any physical quantity that can be transduced to a change in magnetic flux, such as electrical current, voltage, or position. Applications include biomagnetometry, geophysical, astronomical, and material sciences.

The conductors, semiconductors, and superconductors that have been discussed are materials that can be prepared via some type of CVD process. In order to prepare each material, a precursor is required. The precursor chemistry of these materials is based heavily on organometallic and inorganic chemistry. Numerous ligand platforms have been investigated for use in the preparation of suitable CVD precursors.

The alkoxide chemistry of group 2 metals is as rich as it is diverse. A significant amount of the research conducted in this area has been directed toward the reduction of intermolecular interactions and the preparation of volatile monomeric compounds. Group 2 metal alkoxides can be easily prepared from the corresponding alcohol. The reaction, depending on the alcohol, can be carried out by combining the group 2 metal with the appropriate alcohol. In certain cases, it is necessary to carry out the reaction in the presence of liquid ammonia or ethanol. This method makes use of the intermediate metal amide or metal alkoxide and proceeds via ligand exchange. The heavy group 2 compounds of the simple monoanionic alkoxides, such as methoxide and ethoxide, exist as polymers in the solid state (23). These compounds exist as polymers, since each ligand is monodentate. This observation is in line with Bradley's classic structural theory, which states that metal alkoxides will adopt the smallest degree of aggregation that permits the metal atoms to attain their preferred coordination numbers (24). An excellent example of Bradley's theory is observed when a bidentate alkoxide is used as the ligand. The product that is obtained from the reaction of calcium filings with 2 equiv of 2-methoxyethanol (25) contains three 6-coordinate and six 7-coordinate calcium atoms for an average coordination number of 6.67 (Fig. 1). Unlike nonmolecular analogues, this compound is soluble in nondonor solvents. Soluble and volatile alkoxides of the heavy group 2 elements may be useful in the preparation of sol-gel and CVD precursors. Several research groups have investigated an extension of this motif in an attempt to further reduce the molecularity of group 2 alkoxides.

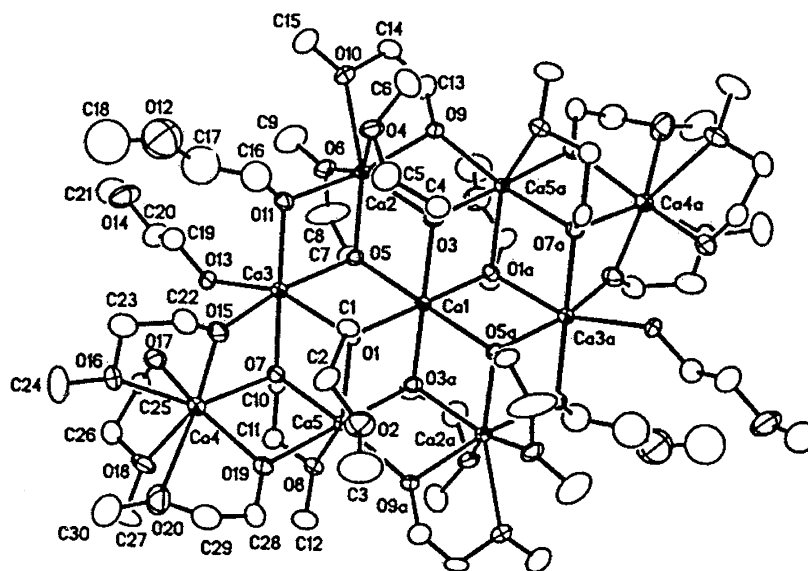


FIG. 1. ORTEP of $\text{Ca}_9(\text{OCH}_2\text{CH}_2\text{OMe})_{18}(\text{HOCH}_2\text{CH}_2\text{OMe})_2$.

Using a tetradentate ligand, Rees and Moreno have proposed the first example of a monomeric barium bis-alkoxide (26). The proposed solution structure (Fig. 2) was determined based on cryoscopic and spectroscopic data. One notable characteristic of this monomeric barium alkoxide is that it is an ambient temperature liquid. Although the compound exists as a monomer in the solution state, oligomeric species prevail in the absence of solvent. This phenomenon has been ob-

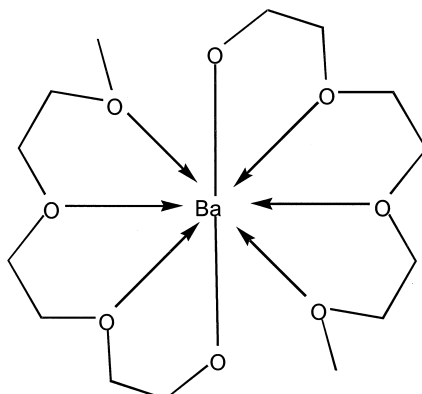


FIG. 2. The proposed solution structure as determined by cryoscopic measurements.

served in the megacuster calcium compound isolated by Buhro *et al.* (25), who reported that the compound dissociated into "fragments" in the presence of cold benzene.

The theme of coordinatively saturating the metal center of heavy group 2 elements has yielded molecular compounds; however, their volatility and vapor phase stability are insufficient for CVD. The widely employed concept of using steric bulk to shield reactive molecular centers has also met with very little success in the area of CVD precursors. Sterically demanding aryloxides have been investigated for use with group 2 metals. The simplest example of the group 2 aryloxides is prepared by reacting strontium metal with phenol in THF at reflux. Crystallization of the product affords a tetramer with two different strontium environments (27), six molecules of THF, and two neutral ligands (Fig. 3). The reaction of 2,6-di-*tert*-butyl,4-methylphenol with strontium metal in THF gives the tetrahydrofuranate adduct. Refluxing the isolated product in toluene at 80°C and 10^{-2} torr affords the corresponding homoleptic derivative as determined by NMR analysis (28). The reaction of 2,4,6-tri-*tert*-butyl phenol with strontium in liquid ammonia has been reported to produce a heteroleptic monomeric compound following its reaction with Lewis bases, according to X-ray analysis (29) (Fig. 4). The ammonia adduct is initially obtained and is readily converted to the homoleptic dimer by

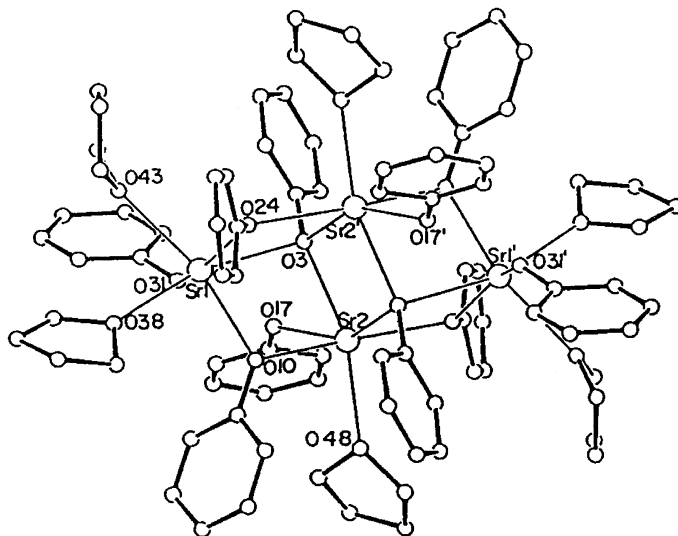
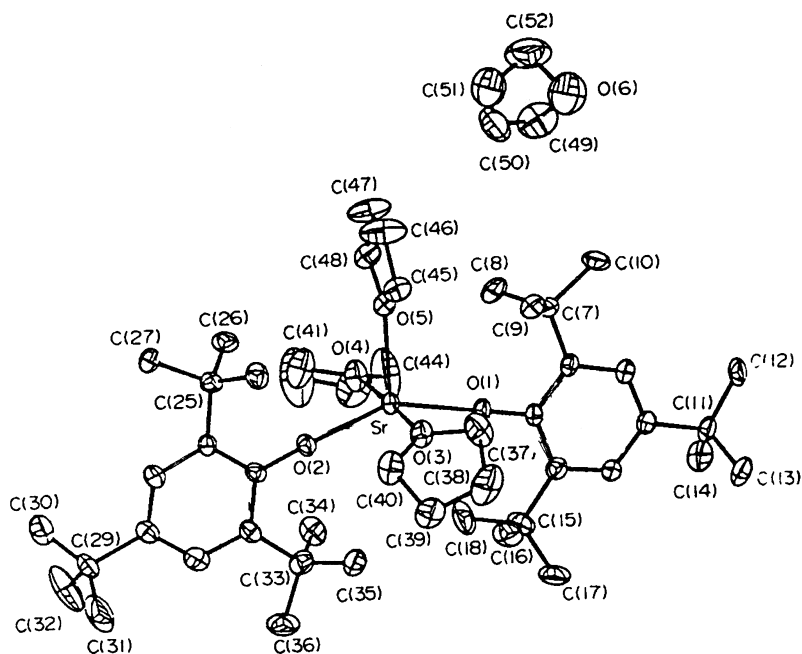


FIG. 3. ORTEP of $\text{Sr}_4(\text{OPh})_2(\text{PhOH})_2(\text{THF})_6$.

FIG. 4. SNOOPI drawing of $[\text{Sr}(\text{OC}_6\text{H}_2\text{Bu}^t)_2(\text{THF})_3] \cdot 0.5 \text{ THF}$.

refluxing in toluene at 10^{-2} torr for 30 minutes. When 2,6-di-*t*-butyl-4-methylphenol is reacted with highly reactive calcium or barium in THF, it is possible to isolate the metal phenoxide with coordinating THF molecules (30). The calcium analogue exists as a heteroleptic monomer with three THF molecules (Fig. 5); the barium analogue contains four THF molecules. Removal of the coordinating solvent molecules in the calcium compound can be accomplished by heating at 80°C and 10^{-2} torr. Structurally characterized barium aryloxides also incorporate coordinating solvents in order to coordinatively saturate the metal center (31–33). The reversible coordination mode of the solvent molecules would result in nonintact sublimation of the CVD precursor. Upon losing solvent molecules, the compound would likely aggregate to form a highly involatile oligomer, rendering it useless as a CVD precursor. Homoleptic monomeric alkoxides are very rare. The use of tritox, a sterically demanding ligand, to prepare calcium compounds results in an unstable aggregate that decomposes to form the trimer of calcium ditox (Fig. 6). The use of intramolecular Lewis bases to coordinatively saturate the metal center of heavy group 2 metals has had very little success. Hermann decided to com-

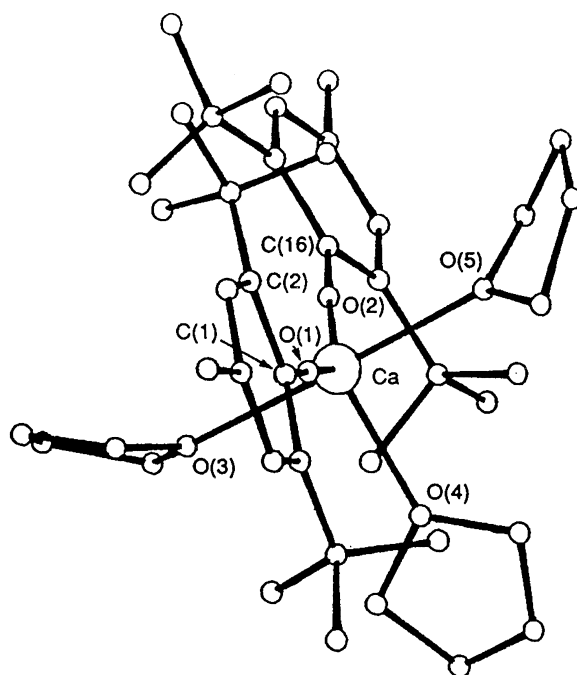


FIG. 5. X-ray structure of $[\text{Ca}(\text{OAr})_2(\text{thf})_3]$ [Ar = C₆H₂But-2,6-Me].

bine the approach of steric bulk and donor functionality to prepare homoleptic, volatile group 2 alkoxides that are stable in the vapor phase (Fig. 7) (34).

The organometallic chemistry of the lighter alkaline earth metals has been extensively investigated. Much of the chemistry has focused on the preparation of organomagnesium reagents. The organometallic chemistry of the heavier group 2 elements (calcium, strontium, and barium) has not been extensively investigated, with the majority of

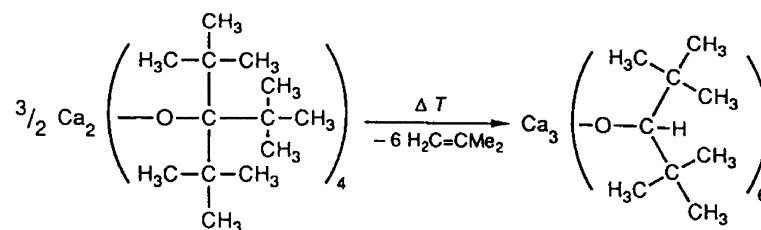


FIG. 6. Decomposition to calcium ditox.

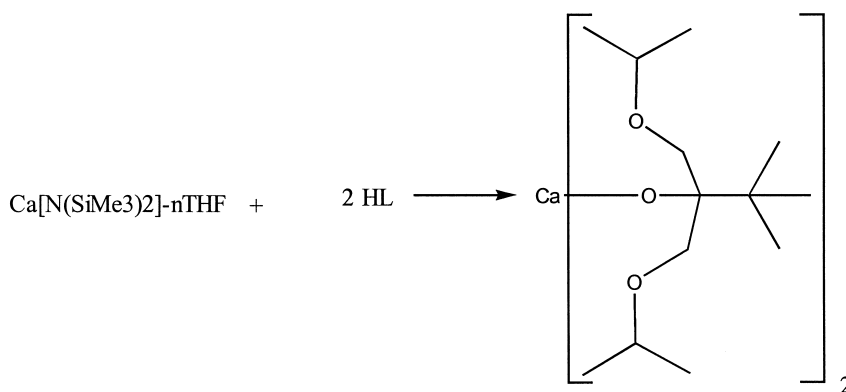


FIG. 7. Hermann's monomeric calcium alkoxide.

the known compounds making use of the cyclopentadienide ligand platform. These compounds are volatile and can be sublimed under reduced pressure at temperatures ranging from 260 to 440°C, with calcium being the most volatile and barium the least volatile (35). The base free decamethyl metallocene compounds are not soluble in hydrocarbon solvents because of their quasi-polymeric solid-state structures (Fig. 8) (36). Structural similarities can be found between the alkaline earth compounds and divalent lanthanide compounds, with calcium being similar in size to Yb^{II} and Sr being similar to Eu^{II} (37).

There have been several efforts geared toward reducing the oligomeric nature of the group 2 metallocene compounds. Reduction of the nuclearity has been accomplished via the use of sterically demanding cyclopentadienides and intermolecular Lewis bases (38–40). Hanusa and Williams have used bidentate amines to coordinatively saturate

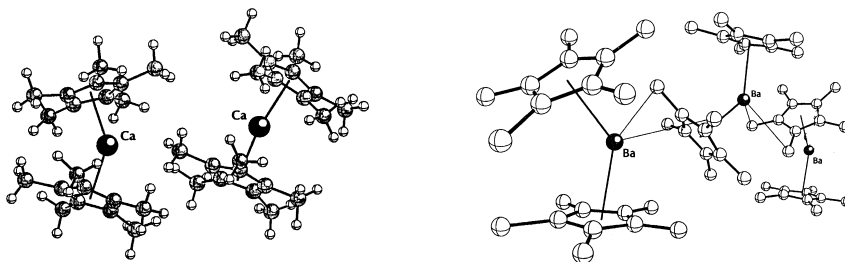


FIG. 8. ORTEP plots of the quasi-polymeric base-free calcium and barium metallocenes.

the group 2 metallocene compounds (41). X-ray crystallographic data of the pentamethyl cyclopentadieneide pyrazine barium compound reveal a dimeric structure (Fig. 9). It is believed that the calcium analogue also exists as a dimer in the solid state. A monomeric calcium relative is shown in Figure 10. UV-vis data of these compounds show that the pyrazine is coordinated to the metal center in a reversible fashion, leading to the conclusion that the pyrazine is weakly coordinated to the metal center. Efforts have been made to combat this problem via the use of intramolecular Lewis base-stabilization. This was accomplished by tethering an ether or amine containing alkyl group directly to the cyclopentadieneide ligand (42–44). The intramolecular Lewis base-stabilized cyclopentadieneides also suffer from thermal instability. NMR data suggest that the Lewis bases are coordinating in a reversible fashion. The base free analogues of the previously discussed compounds exist as monomers in the solid state and are easily synthesized in diethyl ether or THF. The product is isolated as the Lewis base adduct, with the base free derivative being obtained after distillation or sublimation (45). It is important to note that the intermolecular Lewis base is more labile in the case of barium than in the case of calcium. This is due in part to the larger ionic radius of barium that results in lower charge density; hence, it is a weaker Lewis acid than calcium. In addition to having poor vapor pressures, the group 2 metallocenes have been shown to incorporate a significant amount of carbon into the thin film during the CVD process (46). Carbon incorporation greatly decreases the performance of electronic materials and diminishes their utility. Much of the effort to prepare group 2 CVD precursors makes use of alternate ligand platforms.

Alkaline-earth amides of group 2 elements from Be to Ba have been synthesized and structurally characterized. Primary amides can be

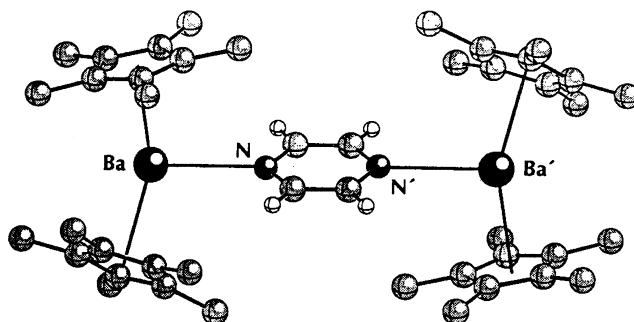
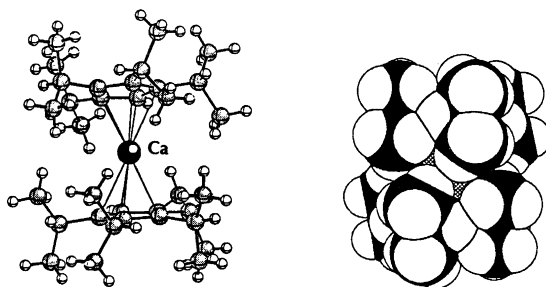


FIG. 9. Structure of the $[\text{Cp}^*_2\text{Ba}]_2(\mu\text{-NC}_6\text{H}_4\text{N})$ dimer.

FIG. 10. ORTEP and space filling model of $[(i\text{-Pr})_4\text{C}_5\text{H}]_2\text{Ca}$.

prepared via the reaction of liquid ammonia with the metal of choice. These primary metal amides are nonmolecular species (47). Replacement of the hydrogen atoms located on each nitrogen with the bulky trimethylsilyl group to afford the bis-trimethylsilylamido ligand allows for the formation of molecular species (48, 49) (Table I). The base free derivatives, with the exception of Be, are dimeric in the solid state. The incorporation of two molecules of THF allows for the stabilization of monomeric species (50). The remainder of the alkaline earth amide chemistry centers around magnesium for the preparation of magnesium doped group 13 nitrides. These materials are among the leading candidates for the fabrication of stable high-luminosity blue and green photonic devices (51). Magnesium amide compounds are found to exist in coordination environments that include 2 and range from 4 to 10 (52). Though the amide chemistry has been ex-

TABLE I

STRUCTURES OF ALKALINE-EARTH
BIS(TRIMETHYLSILYL)AMIDES AND ADDUCTS

Complex	CN	Nuclearity
$\text{Be}[\text{N}(\text{SiMe}_3)_2]_2$	2	Monomeric
$\{\text{Mg}[\text{N}(\text{SiMe}_3)_2]_2\}_2$	3	Dimeric
$\{\text{Mg}[\text{N}(\text{SiMe}_3)_2]_2(\text{THF})_2\}$	4	Monomeric
$\{\text{Ca}[\text{N}(\text{SiMe}_3)_2]_2\}_2$	3	Dimeric
$\text{Ca}[\text{N}(\text{SiMe}_3)_2]_2(\text{DME})$	4	Monomeric
$\{\text{Sr}[\text{N}(\text{SiMe}_3)_2]_2\}_2$	3	Dimeric
$\text{Sr}[\text{N}(\text{SiMe}_3)_2]_2(\text{DME})_2$	4	Monomeric
$\text{Sr}[\text{N}(\text{SiMe}_3)_2]_2(\text{dioxane})_2$	4	1-D polymer
$\{\text{Ba}[\text{N}(\text{SiMe}_3)_2]_2\}_2$	3	Dimeric
$\{\text{Ba}[\text{N}(\text{SiMe}_3)_2]_2(\text{THF})\}_2$	4	Dimeric
$\text{Ba}[\text{N}(\text{SiMe}_3)_2]_2(\text{THF})_2$	4	Monomeric

tremely successful for the preparation of magnesium CVD precursors, results with the heavier congeners are not as promising. The lack of success arises from the difference in ionic radius as one descends from magnesium to calcium, strontium, and barium. Magnesium has an ionic radius that ranges from 57 to 72 pm and is therefore well suited for the monoanionic monodentate amide ligand. The heavier group 2 elements have ionic radii that range from 100 to 142 pm and therefore require a more sterically demanding coordination environment. The monoanionic bidentate β -diketonate ligand is better suited for the heavy group 2 elements. The ligand forms a "quasiaromatic" six-membered ring containing the metal atom. Sievers (53) demonstrated that it was possible to separate various metal β -diketonates in the vapor phase, thus showing their volatility and vapor phase stability. The β -diketonate of choice for use in the preparation of volatile group 2 CVD precursors is 2,2,6,6-tetramethylheptanedionate. The ligand makes use of two sterically demanding *t*-butyl groups to aid in the encapsulation of the metal center. Acetylacetonato derivatives tend to leave the metal center unprotected against intermolecular interactions, hence allowing for the formation of oligomeric or polymeric compounds. Magnesium bis-tetramethylheptanedionate has been synthesized by Drake and co-workers via the reaction of magnesium ethoxide with the β -diketone (54). The isolated compound was not structurally characterized; however, the authors propose a base free oligomer. TGA analysis of the compound shows a two step process that is indicative of a heteroleptic compound (Fig. 11). Rees and co-workers (55) have isolated and structurally characterized the bis-etherate analogue of the magnesium β -diketonate (Fig. 12). In addi-

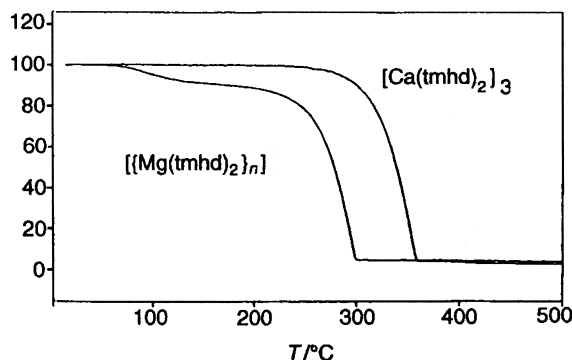


FIG. 11. TGA plots of the magnesium and calcium tmhd compounds prepared by Drake (54).

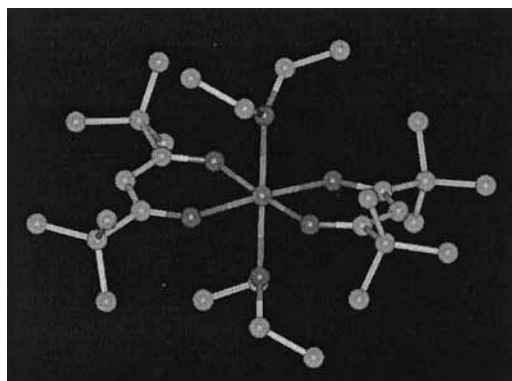


FIG. 12. X-ray crystal structure of magnesium Mg tmhd bis-etherate.

tion, the TGA analysis (Fig. 13) of the base free derivative calls into question the data presented by Drake and co-workers. The calcium bis-tetramethylheptanedionate was also synthesized by Drake; in addition, the compound was structurally characterized (Fig. 14). The solid-state structure of the calcium compound reveals a trimer containing two terminal and four bridging β -diketonates. TGA analysis

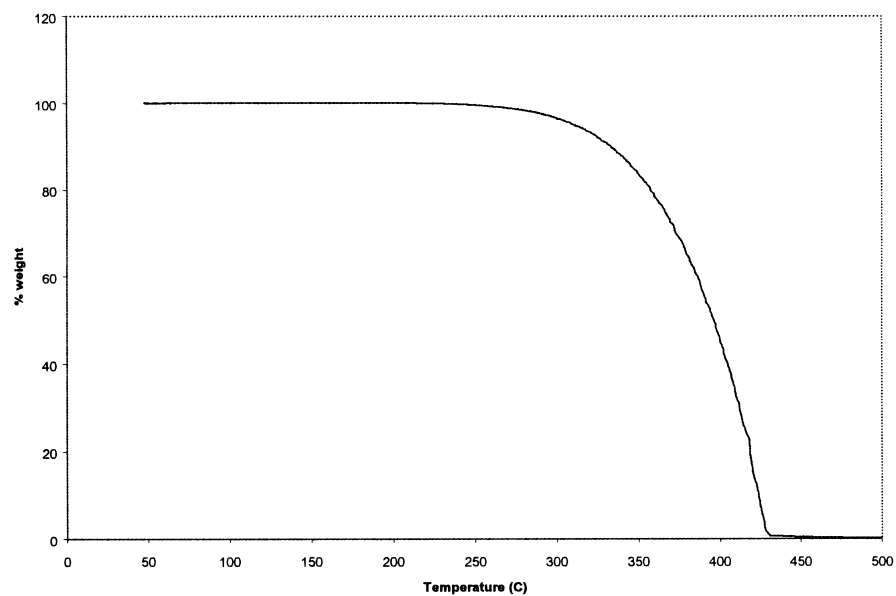


FIG. 13. TGA plot of base free $\text{Mg}(\text{tmhd})_2$ by Rees (55).

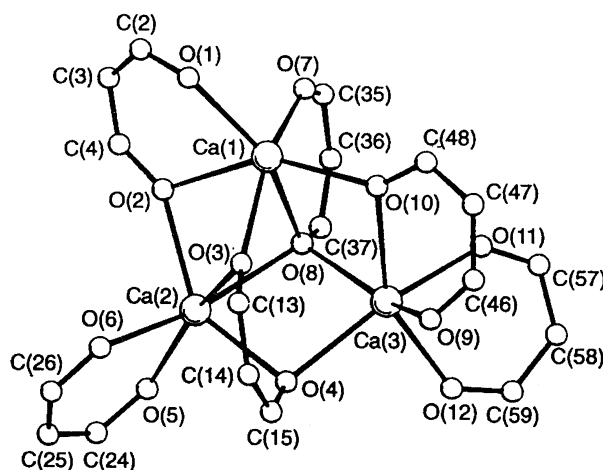


FIG. 14. Molecular structure of $[\text{Ca}_2(\text{tmhd})_3]$; the *tert*-butyl groups have been omitted.

of the compound shows that it is volatile and stable in the vapor phase. The strontium analogue also exists as a trimer in the solid state with three terminal ligands and three bridging ligands in addition to one neutral β -diketone (56). The barium bis-tetramethylheptanedionate has been synthesized and structurally characterized by both Drake and Trojanov (57). The compound exists as a tetramer in the solid state and sublimes intact at approximately 400°C; however, there have been reports that the compound is unstable at high temperatures for prolonged periods of time. The observed decomposition is most likely due to the high source temperatures that are necessary to volatilize the precursor and prevent condensation at the source during the CVD process. Several efforts have been made to reduce the oligomeric character of the β -diketones, including incorporation of an intermolecular Lewis base as well as use of fluorinated ligands (Fig. 15). The barium hfac and tfac derivatives behave similarly to the tmhd analogue, decomposing at temperatures that are slightly above their sublimation temperatures (58, 59). Group 2 analogues of Hdffd, Htdfnd, and Hfod (60) are highly volatile; they all sublime below 220°C and exhibit good thermal stability. Films grown from the fluorinated precursors contain significant amounts of metal fluoride that cannot be completely removed via postdeposition hydrolysis. The postdeposition washes and residual fluoride greatly affect the fabrication of the electronic materials since they demand epitaxial material (61). The use of intermolecular Lewis bases, specifically tetraglyme, in

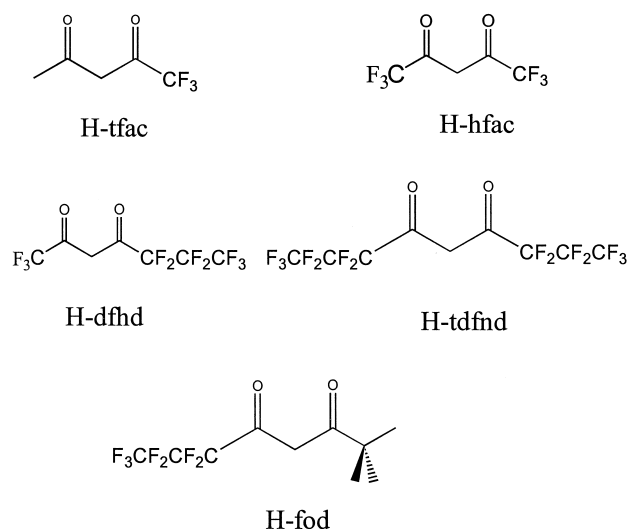


FIG. 15. Fluorinated ligands that are used in the preparation of volatile group 2 CVD precursors.

combination with β -diketones produces thermally unstable compounds. This observation arises from the weak interaction that exists between the tetraglyme and the metal center. Tuning the Lewis acidity of the metal center via the use of fluorinated β -diketones affords a more stable interaction between the tetraglyme and the metal. Barium bis-hexafluoroacetylacetonato (Fig. 16) sublimates intact, which is

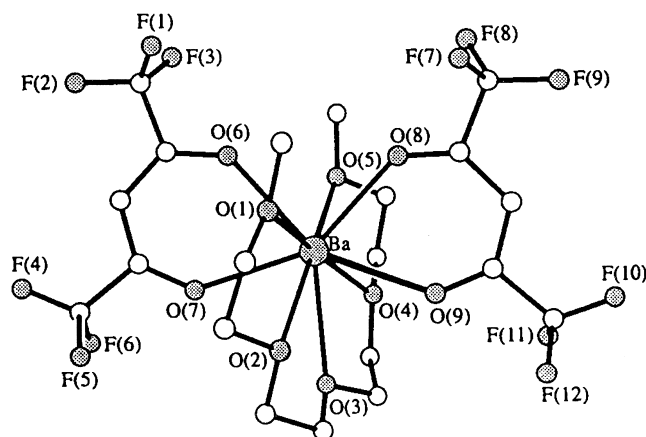


FIG. 16. Molecular structure of $\text{Ba}(\text{hfac})_2 \cdot [\text{Me}_3\text{O}(\text{CH}_2\text{CH}_2\text{O})_4\text{-Me}]$.

in sharp contrast to the nonfluorinated analogue. The thermal stability of the complex is believed to arise from the weakened interaction between the β -diketonate oxygen and the metal itself, which arises from the fact that the fluorine atoms are pulling electron density away from the oxygen atoms. This leaves the metal in an extremely high state of electron deficiency, hence allowing for a stronger interaction between the tetraglyme oxygen and the metal. This theory has been supported by X-ray crystallographic data, which clearly indicate the formation of longer β -diketonate oxygen-metal interatomic distances and a strong tetraglyme oxygen-metal interaction (62).

The poor performance of the intermolecular stabilized β -diketonates and fluorinated ligands resulted in the investigation of intramolecular Lewis base-stabilized complexes. Rees and co-workers have successfully synthesized the first example of a β -diketonate ligand containing an intramolecular Lewis base (63). The ligand contains a methoxy moiety that is tethered to the diketone backbone via a propyl group. The barium derivative was isolated as a liquid and determined to be monomeric based on solution cryoscopic data. Other investigation, in the area of intramolecular Lewis base-stabilized compounds, have been carried out by Marks and co-workers. Modification of the β -diketonate ligand via the attachment of a polyether monoamine to afford a β -ketoiminate ligand was carried out by Marks. The idea behind synthesizing the β -ketoiminate ligand arose from the strategy of saturating the metal coordination sphere with sterically encumbered nonpolar or coordinating ligands. This reduces the lattice cohesive energies, hence limiting molecular oligomerization (64, 65). Several different ligands were synthesized via the modification of R and R' (Fig. 17). The two monoether derivatives were determined to exist as dimers while the remaining four were monomeric (Fig. 18). These compounds were volatile and could be sublimed at reduced pressure (10^{-3}

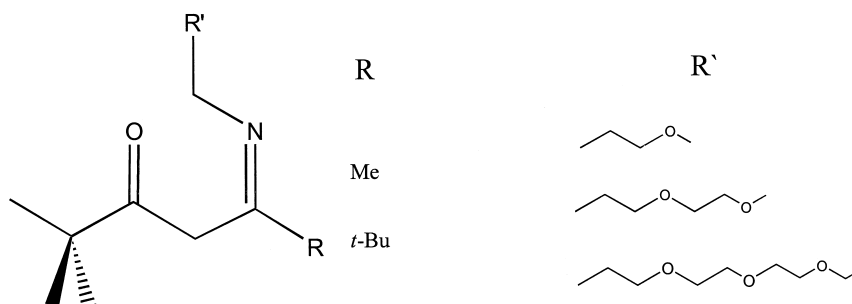


FIG. 17. Ether containing β -ketoiminates synthesized by Marks and co-workers.

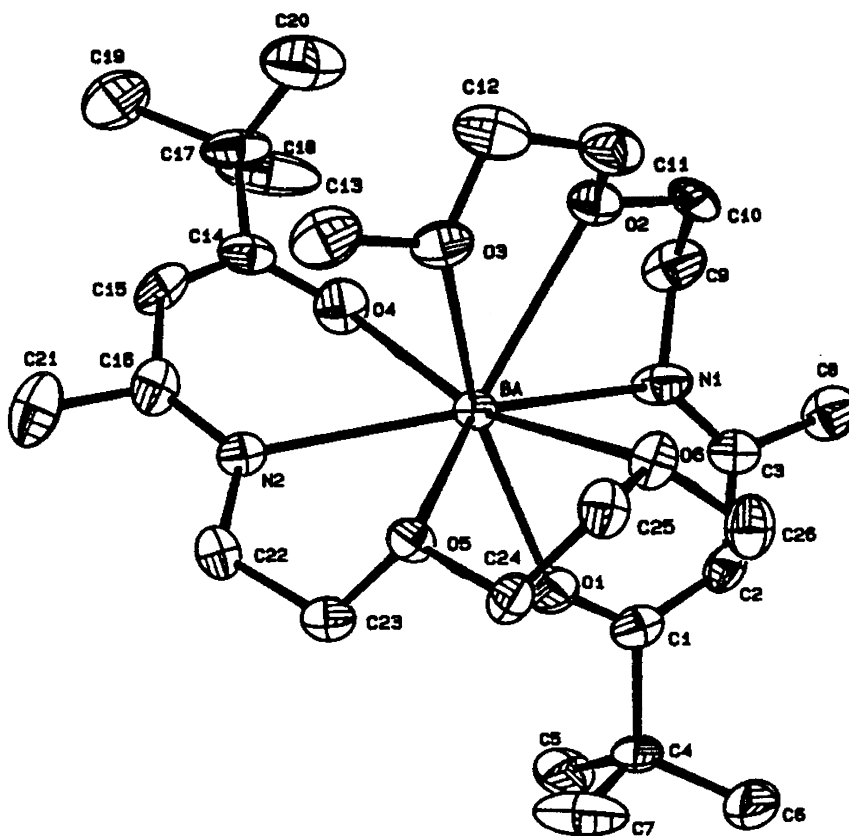


FIG. 18. ORTEP of the β -ketoiminate complex, Ba(diki)_2 .

torr) with minimal decomposition. Marks has used barium bis- β -ketoiminates to grow BaPbO_3 thin films, thus showing the efficacy of β -ketoiminates as ligands for use in the preparation of CVD precursors.

REFERENCES

1. Rees, W. S., Jr. "CVD of Non-Metals," VCH: Weinheim, **1996**.
2. Jensen, K. F. In "Microelectronics Processing, Chemical Engineering Aspects"; Hess, D. W., and Jensen, K. F., Eds.; ACS Advances in Chemistry Series 23; American Chemical Society: Washington, DC, 1989; pp. 200–206.
3. Wu, J.; Yaguchi, H.; Onabe, K. *Appl. Phys. Lett.* **1998**, *2*, 193.
4. Yasuda, K.; Kojima, K.; Mori, K.; Kubota, Y.; Nimura, T.; Inukai, F.; Asai, Y. *J. Elect. Matl.* **1998**, *6*, 527.

5. Mitra, P.; Case, F. C.; Reine, M. B. *J. Elect. Matl.* **1998**, 6, 510.
6. Nonogaki, Y.; Iguchi, T.; Fuchi, S.; Fujiwara, Y.; Takeda, Y. *Appl. Surf. Sci.* **1998**, 130–132, 724.
7. Durrant, S. F.; Bica De Morales, M. A. *J. Polymer Sci. B* **1998**, 36, 1881.
8. Foxon, C. T.; Hughes, O. H. *J. Matl. Sci.: Matls. in Elec.* **1998**, 9, 227.
9. Wankerl, A.; Emerson, D. T.; Cook, M. J.; Shealy, J. R. *J. Cryst. Growth* **1998**, 191, 8.
10. Erkov, V. G.; Devyatova, S. F.; Golod, I. A.; Timofeeva, G. V.; Pokrovskii, L. D. *Russian Microelectronics* **1998**, 3, 183.
11. Izena, A.; Sakuraba, M.; Matsuura, T.; Murota, J. *J. Cryst. Growth* **1998**, 188, 131.
12. Hwang, T. J.; Hendrick, M. R.; Shao, H.; Hornis, H. G.; Hunt, A. T. *Matls. Sci. and Eng.* **1998**, A244, 91.
13. Nyman, M.; Jenkins, K.; Hampden-Smith, M. J.; Kodas, T. T.; Duesler, E. N. *Chem. Mater.* **1998**, 10, 914.
14. Hubert-Pfalzgraf, L. G.; Guillon, H. *Appl. Organomet. Chem.* **1998**, 12, 221.
15. Jones, A. C.; O'Brien, P. "CVD of Compound Semiconductors. Precursor Synthesis, Development and Applications," VCH: Weinheim, 1996.
16. Interrante, L. V.; Hampden-Smith, M. J. "Chemistry of Advanced Materials"; Wiley-VCH; Weinheim, **1998**.
17. Moore, G. E. "International Electron Devices Meeting," Washington, DC, Dec. 1975, p. 11; Keyes, R. W. *IEEE Trans. Electron Devices* **1979**, ED-26, 271.
18. Saraswatt, K. C.; Mohammadi, F. *IEEE Trans. Electron Devices*, **1982**, ED-29, 645; Brews, J. R. *IEEE Trans. Electron Devices* **1986**, ED-33, 1356; Chaudary, P. J. *J. Appl. Phys.* **1974**, 45, 4339; Penney, R. V. *J. Phys. Chem. Solids* **1964**, 25, 335.
19. McConica, C. M.; Krishnamani, K. J. *J. Electrochem. Soc.* **1986**, 133, 2542; Singer, P. H. *Semicond. Int.* **1990**, March, 45.
20. Dennard, R. H.; Gaensslen, F. H.; Yu, H.; Rideout, V. L.; Bassows, E.; LeBlank, A. R. *IEEE J. Solid-State Circuits* **1974**, SC-9, 256.
21. Cracknell, D. J. *GEC J. Res.* **1992**, 9, 155.
22. Geballe, T. H.; Hulm, J. K. *Science* **1988**, 239, 367.
23. Bradley, D. C.; Mehrotra, R. C.; Gaul, D. P. "Metal Alkoxides"; Academic Press: New York, **1978**, 411.
24. Bradley, D. C. *Chem. Rev.* **1989**, 89, 1317.
25. Goel, S. C.; Matchett, M. A.; Chiang, M. Y.; Buhro, W. E. *J. Am. Chem. Soc.* **1991**, 113, 1844.
26. Rees, W. S.; Jr.; Moreno, D. A. *J. Chem. Soc., Chem Commun.* **1991**, 24, 1759.
27. Drake, S. R.; Streib, W. E.; Chisholm, M. H.; Caulton, K. G. *Inorg. Chem* **1990**, 29, 2708.
28. Cloke, F. G. N.; Hitchcock, P. B.; Lappert, M. F.; Lawless, G. A.; Royo, B. *J. Chem. Soc. Chem. Commun.* **1991**, 724.
29. Drake, S. R.; Otway, D. J.; Hursthouse, M. B.; Abdul Malik, K. M. *Polyhedron* **1992**, 11, 1995.
30. Hitchcock, P. B.; Lappert, M. F.; Lawless, G. A.; Royo, B. *J. Chem. Soc. Chem Commun.* **1990**, 1141.
31. Caulton, K. G.; Chisholm, M. H.; Drake, S. R.; Folting, K. *Inorg. Chem.* **1991**, 30, 1500.
32. Caulton, K. G.; Chisholm, M. H.; Drake, S. R.; Folting, K. *J. Chem. Soc. Chem. Commun.* **1990**, 1349.
33. Caulton, K. G.; Chisholm, M. H.; Drake, S. R.; Streib, W. E. *Angew. Chem.* **1990**, 102, 1492.

34. Hermann, W. A.; Huber, N. W.; Priermeier, T. *Angew. Chem. Int. Ed. Engl.* **1994**, *33*, 105.
35. Zenger, R.; Stucky, G. D. *J. Organometallic Chem.* **1974**, *80*, 7.
36. Williams, R. A.; Hanusa, T. P.; Huffman, J. C. *J. Chem. Soc. Chem. Commun.* **1988**, 1045.
37. Shannon, R. D. *Acta Cryst.* **1976**, *32A*, 751.
38. Burns, C. J.; Andersen, R. A. *J. Organomet. Chem.* **1987**, *325*, 31.
39. Gardiner, M. G.; Raston, C. L.; Kennard, C. H. L. *Organometallics* **1991**, *10*, 3680.
40. Williams, R. A.; Tesh, K. F.; Hanusa, T. P. *J. Am. Chem. Soc.* **1991**, *113*, 4843.
41. Williams, R. A.; Hanusa, T. P. *J. Organomet. Chem. Soc.* **1992**, *429*, 143.
42. Rees, W. S. Jr.; Lay, U.; Dippel, K. A. *J. Organomet. Chem.* **1994**, *483*, 27.
43. Jutzi, P.; Siemeling, U. *J. Organomet. Chem.* **1995**, *500*, 175; du Plooy, K. E.; Moll, U.; Wocadlo, S.; Massa, W.; Okuda, J. *Organometallics* **1995**, *14*, 3129.
44. Hanusa, T. P. *Polyhedron* **1990**, *11*, 1345.
45. Williams, R. A.; Hanusa, T. P.; Huffman, J. C. *Organometallics* **1990**, *9*, 1128.
46. Greenwald, A. C.; Rees, W. S.; Lay, U. W. *Mater. Res. Soc. Proc.* **301**, 1997.
47. Wells, A. F. "Structural Inorganic Chemistry," 5th ed. 1984.
48. Hanusa, T. P. *Chem. Rev.* **1993**, *93*, 1023.
49. Vaartstra, B. A.; Huffman, J. C.; Streib, W. E.; Caulton, K. G. *Inorg. Chem.* **1991**, *30*, 121.
50. Bradley, D. C.; Hursthouse, M. B.; Ibrahim, A. A.; Abdul Malik, K. M.; Motevalli, M.; Moseler, R.; Powell, H.; Runnacles, J. D.; Sullivan, A. C. *Polyhedron* **1960**, *9*, 2959.
51. Mohamad, S. N.; Salvador, A. A.; Morkoc, H. *Proc. IEEE* **1995**, *83*, 1306; Mohamad, S. N.; Morkoc, H. *Science* **1995**, *2678*, 51.
52. Holloway, C. E.; Melnik, M. J. *Organometallic Chem.* **1994**, *465*, 1.
53. Moshier, R. W.; Sievers, R. E. "Gas Chromatography of Metal Chelates," Pergamon Press: Oxford, 1965.
54. Arunasalam, V.-Cumarán.; Drake, S. R.; Hursthouse, M. B.; Hursthouse, K. M.; Abdul Malik, K. M.; Miller, S. A. S.; Mingos, D. M. P. *J. Chem. Soc. Dalton Trans.* **1996**, 2435.
55. Flanagan, J. S.; Luten, H. A.; Rees, W. S., Jr. In preparation.
56. Drake, S. R.; Hursthouse, M. B.; Abdul Malik, K. M.; Otway D. J. *J. Chem. Soc. Dalton Trans.* **1993**, 2883.
57. Drozdoyv, A. A.; Trojanov, S. I. *Polyhedron* **1992**, *11*, 2877.
58. Purdy, A. P.; Berry, A. D.; Holm, R. T.; Fatemi, M.; Gskill, K. K. *Inorg. Chem.* **1989**, *28*, 2799.
59. Shinohara, K.; Munahata, F.; Yamanaha, M. *Jpn. J. Appl. Phys.* **1988**, *27*, L1683.
60. Thompson, S. C.; Cole-Hamilton, D. J.; Gilliland, D. D.; Hitchman, M. L.; Barnes, J. C. *Adv. Mater. Optics Electron.* **1992**, *1*, 81.
61. Richards, B. C.; Cook, S. L.; Pinch, D. L.; Andrews, G. W.; Lengeling, G.; Schulte, B.; Jurgensen, H.; Shen, Y. Q.; Vase, P.; Freltoft, T.; Spee, C. I. M. A.; Linden, J. L.; Hitchman, M. L.; Shamlan, S. H.; Brown, A., *Physica C* **1995**, *252*, 229.
62. Timmer, K.; Spee, K. I. M. A.; Mackor, A.; Meinema, H. A.; Spek, A. L.; v. d. Sluis, P. *Inorg. Chem. Acta* **1991**, *69*, 2418.
63. Rees, W. S., Jr.; Caballero, C. R.; Hesse, W. *Angew. Chem. Int. Ed. Engl.* **1992**, *6*, 735.
64. Schulz, D. L.; Hinds, B. J.; Stem, C. L.; Marks, T. J. *Inorg. Chem.* **1993**, *32*, 249.
65. Schulz, D. L.; Hinds, B. J.; Neumayer, D. A.; Stern, C. L.; Marks, T. J. *Chem. Mater.* **1993**, *5*, 1605.

MOLECULAR, COMPLEX IONIC, AND SOLID STATE PON COMPOUNDS

ROGER MARCHAND,* WOLFGANG SCHNICK,[†] and NORBERT STOCK[‡]

*Laboratoire des Verres et Ceramiques, UMR CNRS 6512, Universite de Rennes 1, Campus de Beaulieu, CS 74 205, F-35042 Rennes Cedex (France); [†]Institute for Inorganic Chemistry, University of Munich, D-81377 Munich (Germany); [‡]Material Research Laboratory, University of California, Santa Barbara, California 93106

- I. Introduction
- II. Molecular PON Compounds
 - A. Introduction
 - B. Crystal Structures
- III. Acyclic Molecular Ionic PON Compounds
 - A. Introduction
 - B. Crystal Structures
- IV. Cyclic PON Compounds
 - A. Introduction
 - B. Conformation of Tri- and Tetrametaphosphimate Ions
 - C. Tri- and Tetrametaphosphimates
 - D. Phosphimatometallates
- V. Solid-State PON Compounds
 - A. Introduction, General Considerations
 - B. The Phosphorus Oxynitride PON
 - C. The Oxynitride P_4N_6O
 - D. The PON Sodalites
 - E. The $M_3M^{III}P_3O_9N$ and $M_2M^{II}P_3O_9N$ Series
 - F. The $Cs_3M^{II}_2P_6O_{17}N$ Series
 - G. The $M_2M^{II}P_3O_8N$ Series
 - H. The Na-P-O-N System
 - I. Other Systems/X-Ray Amorphous Metallophosphate Oxynitrides
- VI. Conclusion
- References

I. Introduction

The crystal chemistry of oxophosphates (1) and nitridophosphates (2) has been investigated extensively. In contrast to this, few crystal-

lographic data about nitridooxophosphates, which can be seen as the link between these two end members, have been available until recently.

Nevertheless, nitridooxophosphate glasses have been of interest in the past because of the improvement in physical properties such as hardness and refractive index when nitrogen is incorporated into phosphate glasses (3–7). These changes can be attributed to the substitution of divalent oxygen by trivalent nitrogen thus producing a more tightly linked glass network. The replacement of oxygen by nitrogen leads to different kinds of $P(N, O)_4$ tetrahedra PO_3N , PO_2N_2 , PON_3 , and PN_4 which can be characterized by XPS, NMR, and vibrational spectroscopy (8–10).

Another field of investigation is the use of metal nitridooxophosphates such as AlPON (11) or ZrPON (12) as catalysts. The incorporation of nitrogen leads to a change in acid–base properties and to improved stability.

The present review is mainly concerned with the crystal chemistry of compounds containing phosphorus(V) bound to oxygen and nitrogen forming $P(N, O)_4$ tetrahedra. Thus, ammonium phosphates will be omitted as well as hydrazine and carbon containing compounds. We will focus on the structure of molecular, molecular ionic, and condensed PON compounds. Some aspects of these compounds have been summarized in the literature in the past (13–16).

II. Molecular PON Compounds

A. INTRODUCTION

Although the chemistry of alkylamino PON compounds has been intensively investigated, only two non-carbon-containing compounds, $OP(NH_2)_3$ and $(NH_2)_3(O)PNP(NH_2)_3$, have been described in detail. These two compounds have been obtained by ammonolysis of the corresponding chloro compounds, $OPCl_3$ (17) and $Cl_2P(O)NPCl_3$ (18), at $-78^\circ C$. Furthermore, $OP(NH_2)_3$ as well as $(NH_2)_3(O)PNP(NH_2)_3$ have been observed as decomposition products of phosphazenes during hydrolysis (19). Both compounds are air sensitive and must be stored under inert conditions to prevent hydrolysis. Their use in the synthesis of condensed PON compounds has also been shown. Thus, the phosphorus(V) oxynitride PON and PON sodalites can be obtained (Sections V,B and V,D). In addition, the adduct $(NH_2)_3(O)PNP(NH_2)_3 \cdot NH_4Cl$ has been observed as a microcrystalline powder (18).

B. CRYSTAL STRUCTURES

The crystal structures of $\text{OP}(\text{NH}_2)_3$ ($P2_1/c$, $a = 840(2)$, $b = 877(2)$, $c = 542(1)$ pm, $\beta = 95.4(1)^\circ$, $Z = 4$) and $(\text{NH}_2)_3(\text{O})\text{PNP}(\text{NH}_2)_3$ ($P2_1/c$, $a = 1462.8(3)$, $b = 944.8(2)$, $c = 1026.9(2)$ pm, $\beta = 110.7(1)^\circ$, $Z = 8$) have been reported (18, 20). An important feature in both structures is the formation of a network by $\text{N}-\text{H}\cdots\text{N}$ and $\text{N}-\text{H}\cdots\text{O}$ hydrogen bonds. In both compounds, each O atom forms four $\text{N}-\text{H}\cdots\text{O}$ hydrogen bonds. In $(\text{NH}_2)_3(\text{O})\text{PNP}(\text{NH}_2)_3$ two crystallographically unique molecules are found that form a three-dimensional network by intermolecular hydrogen bonding interactions ($\text{N}-\text{H}\cdots\text{N} \geq 313$ pm, $\text{N}-\text{H}\cdots\text{O} \geq 293$ pm). The average P–O bond length (150 pm) is comparable to the one in $\text{OP}(\text{NH}_2)_3$ (151 pm) or (H_3PO_4) (152 pm), but it is longer than in OPCl_3 (145 pm) and $\text{Cl}_2(\text{O})\text{PNP}(\text{NH}_2)_3$ (21) (145.4 pm). This can be explained by the presence of hydrogen bonds.

The P– NH_2 bond lengths in $(\text{NH}_2)_3(\text{O})\text{PNP}(\text{NH}_2)_3$ of amino groups in the vicinity of the O atom are slightly longer than the others. This situation is in accordance to the observations in $\text{OP}(\text{NH}_2)_3$ and $\text{P}(\text{NH}_2)_4^+$ compounds (20, 22, 23). In agreement with the written formula $(\text{NH}_2)_3(\text{O})\text{P}-\text{N}=\text{P}(\text{NH}_2)_3$, different P–N bond lengths to the bridging N atom are found.

III. Acyclic Molecular Ionic PON Compounds

A. INTRODUCTION

The formal stepwise exchange of the isoelectronic groups OH^- by NH_2^- in phosphates leads to the series H_3PO_4 , $\text{H}_2\text{PO}_3\text{NH}_2$, $\text{HPO}_2(\text{NH}_2)_2$, $\text{OP}(\text{NH}_2)_3$. Further exchange of O^{2-} by NH^{2-} leads to the tetraaminophosphonium ions $\text{P}(\text{NH}_2)_4^+$, which have only recently been characterized (22, 23). Corresponding to the formal substitution of OH^- by NH_2^- in phosphates, in polyphosphates bridging O^{2-} can be formally replaced by NH^{2-} , leading to polyimidophosphates. Furthermore, the formal replacement of terminal OH^- groups by NH_2^- groups leads to polyamidoimidophosphates.

Only two monoamidophosphates (phosphoroamidates), KHPO_3NH_2 (24–26) and $\text{NaHPO}_3\text{NH}_2$ (27, 28), and the two diamidophosphates (phosphorodiamidates) $\text{AgPO}_2(\text{NH}_2)_2$ (29) and $\text{CsPO}_2(\text{NH}_2)_2$ (30) have been structurally characterized by X-ray crystallography (Table I), but the synthesis and characterization of others have been published. Thus, the monoamidophosphates $\text{H}_2\text{PO}_3\text{NH}_2$ (26), $\text{H}_2\text{PO}_3\text{NH}_2 \cdot \text{H}_2\text{O}$

TABLE I

CRYSTALLOGRAPHIC DATA FOR ACYCLIC MOLECULAR-IONIC PON COMPOUNDS

Compound	a [pm], α [°]	b [pm], β [°]	c [pm], γ [°]	SG	Z	Ref.
$\text{NaHPO}_3\text{NH}_2$	577.3(3), 90	577.3(3), 90	603.1(3), 120	$P6_3$	2	27, 28
KHPO_3NH_2	614.3(2), 90	687.2(1), 89.25(2)	1028.8(1), 90	$P2_1/n$	4	24
$\text{AgPO}_2(\text{NH}_2)_2$	577.43(9), 90	577.43(9), 90	1035.5(2), 120	$P3_121$	3	29
$\text{Na}_4\text{PO}_3\text{NHPO}_3 \cdot 10\text{H}_2\text{O}$	1706.9(7), 90	690.5(5), 110.34(4)	475.2(12), 90	$C2/c$	4	54, 55
$\text{K}_4\text{P}_3(\text{NH}_2)\text{O}_9 \cdot 4\text{H}_2\text{O}$	608(2), 95.9(5)	1006(3), 91.7(5)	1272(4), 107.1(5)	$P1$	2	53

(26), $\text{NH}_4\text{HPO}_3\text{NH}_2$ (31), $\text{AgHPO}_3\text{NH}_2$ (25), $\text{Ag}_2\text{PO}_3\text{NH}_2$ (25), $\text{Na}_2\text{PO}_3\text{NH}_2 \cdot 6\text{H}_2\text{O}$ (32), $\text{MgPO}_3\text{NH}_2 \cdot 7\text{H}_2\text{O}$ (25), and $\text{Ba}[\text{HPO}_3(\text{NH}_2)_2] \cdot 2\text{H}_2\text{O}$ (25) and the diamidophosphates $\text{HPO}_2(\text{NH}_2)_2$ (33), $\text{NH}_4\text{PO}_2(\text{NH}_2)_2$ (34, 35), $\text{Mg}[\text{O}_2\text{P}(\text{NH}_2)_2]_2 \cdot 6\text{H}_2\text{O}$ (36), $\text{Ca}[\text{O}_2\text{P}(\text{NH}_2)_2]_2 \cdot 2\text{H}_2\text{O}$ (36), and $\text{NaPO}_2(\text{NH}_2)_2 \cdot 5\text{H}_2\text{O}$ (37) are known. The interest in these compounds is based on their properties as flame retardants (38) or fertilizers (39). Furthermore, their pyrolysis and their use in the formation of oligo- and polyimidophosphates have been investigated (37, 40). Because of the potential use of these polyimidophosphates as fertilizers, their formation (41–48) as well as their decomposition (49–51) under aqueous conditions as well as by solid state reactions was investigated. A few oligo-imido/amidophosphates have been obtained, e.g., $\text{Na}_5\text{P}_3(\text{NH}_2)_2\text{O}_8 \cdot 6\text{H}_2\text{O}$ (52) and $\text{Rb}_4\text{P}_3(\text{NH}_2)\text{O}_9 \cdot 4\text{H}_2\text{O}$ (53), but only the crystal structures of $\text{Na}_4\text{PO}_3\text{NHPO}_3 \cdot 10\text{H}_2\text{O}$ (54) and $\text{K}_4\text{P}_3(\text{NH}_2)\text{O}_9 \cdot 4\text{H}_2\text{O}$ (53) have been described (Table I). The crystal structures of $(\text{NH}_4)_2\text{P}_2\text{O}_4(\text{NH}_2)_2$ (55), a diamidophosphate(IV), and the amidothiophosphates $\text{NH}_4(\text{POS}(\text{NH}_2)_2)$ (56) and $(\text{NH}_4)_2[\text{PO}_2\text{S}(\text{NH}_2)]$ (57) have been reported but will not be described in detail here.

B. CRYSTAL STRUCTURES

Only the monoamidophosphates $\text{NaHPO}_3\text{NH}_2$ and KHPO_3NH_2 as well as the diamidophosphates $\text{AgPO}_2(\text{NH}_2)_2$ and $\text{CsPO}_2(\text{NH}_2)_2$ have been characterized by X-ray structure determination. In the monoamidophosphates the anions exist as zwitterions $^+\text{NH}_3\text{PO}_3^{2-}$; the phosphorus atom is surrounded tetrahedrally by three oxygen atoms and one nitrogen atom. In the sodium salt each anion is situated on a threefold axis coinciding with the P–N bond direction. The nitrogen atom is linked by hydrogen bonds to three oxygen atoms, each belonging to different anions. Thus, a three-dimensional network is formed. Since nitrogen is also tetrahedrally surrounded and therefore sp^3 hybridized, the P–N bond lengths in monoamidophosphates correspond

to an "ideal" P–N single bond. The recorded P–N bond length in Na NH₃PO₃ is 176.9(10) pm. A more reliable value was obtained by the analysis of the potassium salt KPO₃NH₃, where a P–N bond length of 180.0(4) pm was found. In KNH₃PO₃ each O atom forms one hydrogen bond with a hydrogen of the NH₃ group, forming a three-dimensional network. In the silver diamidophosphate AgPO₂(NH₂)₂ a three-dimensional network of corner-sharing PO₂N₂ tetrahedra and bent AgO₂N₂ squares is formed. The H positions have not been reported. In contrast to the silver compound, in cesium diamidophosphate, CsPO₂(NH₂)₂, the H positions have been located unambiguously. The P atoms as centers of the tetrahedra [PO₂(NH₂)₂][−] form together with Cs ions the motif of a distorted NaCl type. This arrangement contains a three-dimensional framework of N–H···O and N–H···N hydrogen bonds.

In the imidophosphate Na₄PO₃NHPO₃·10H₂O the anion PO₃NHPO₃^{4−} shows similarities to the corresponding pyrophosphate ion in the isomorphous pyrophosphate Na₄P₂O₇·10H₂O. Thus, the P–N–P bond angle (127.2°) and the P–N bond length (168 pm) are remarkably similar to the P–O–P bond angle (128.6°) and bridging P–O bond length (163 pm). The closest intermolecular N–O distances (329.2 and 344.6 pm) as well as the apparently identical hydrogen bonding schemes in the crystal structures of Na₄P₂O₇·10H₂O and Na₄PO₃NHPO₃·10H₂O indicate that the imido hydrogen is blocked from forming N–H···O hydrogen bonds (54). This close similarity was used to explain the similar biological behavior of ATP and the imidophosphate analogue of ATP (54).

In the amidopolyphosphate K₄P₃(NH₂)O₉·4H₂O a triphosphate ion with one OH[−] group formally replaced by NH₂[−] is observed. The anion is bent and therefore does not have the straight arrangement as found in Na₅P₃O₁₀. Since hydrogen positions have not been obtained, the N atom was only localized on behalf of the P–N distance. Hydrogen bonding N–H···O has not been observed. The crystal structure consists of layers of monoamidotriphosphate and potassium ions alternating with layers of water molecules.

IV. Cyclic PON Compounds

A. INTRODUCTION

The polymetaphosphimates comprise the greatest number of structurally investigated PON compounds. These contain anions of the

general composition $(\text{PO}_2\text{NH})_n^-$ with $n = 3, 4$, which have been extensively investigated since they are a good example for tautomerism in inorganic compounds $((\text{P}(\text{OH})\text{ONH})_3 \text{ vs } (\text{P}(\text{OH})_2\text{N})_3$, (Fig. 1). The polymetaphosphimates can be formally deduced from the cyclotri- and cyclotetraphosphoric acid by substitution of all ring oxygens by imido groups. The formal partial substitution of one or two O^{2-} by NH^{2-} in the trimetaphosphimate ion leads to imido- and diimidocyclotriphosphate. They are formed during the hydrolysis of the $(\text{PO}_2\text{NH})_3^{3-}$ ions in aqueous solutions and were mainly characterized by NMR and IR spectroscopy (58–60). In addition to this the synthesis and thermal behavior of sodium monoimidocyclotriphosphate, $\text{Na}_3(\text{P}_3\text{O}_8\text{NH}) \cdot 2\text{H}_2\text{O}$, has been described in detail (61). The chemistry of tri- and tetrametaphosphimic acid as well as their salts was investigated first by Stokes (62–64) at the end of the last century and later by Fiquelmont (65–70). Most often the syntheses of tri- and tetrametaphosphimates start from $(\text{PNCl}_2)_3$ and $(\text{PNCl}_2)_4$, but it has been shown that P_3N_5 is also a possible starting material (71). Thus, syntheses of a large number of tri- and tetrametaphosphimates with main group ions H^+ (72, 73), Na^+ (62, 66, 74–76), K^+ (77), Rb^+ , Cs^+ , NH_4^+ (64, 81), Ca^{2+} (78), Al^{3+} , Ga^{3+} , In^{3+} (79), transition metal ions Ag^+ (80, 81), Fe^{2+} , Fe^{3+} (82), Cu^{2+} (83), Co^{2+} , Ni^{2+} , Zn^{2+} (84, 85), and Cr^{3+} (86), and most lanthanide ions (87–89) have been reported.

The following reactions have been employed in the syntheses of tri- and tetrametaphosphimates. Since most often the compounds are very soluble in water, single crystals were grown by evaporation of the solvent or by diffusion controlled addition of an organic solvent such as acetone, ethanol, or methanol.

1. Hydrolysis of hexachlorocyclotriphosphazene or octachlorocyclotetraphosphazene in the presence of a metal acetate, for example,

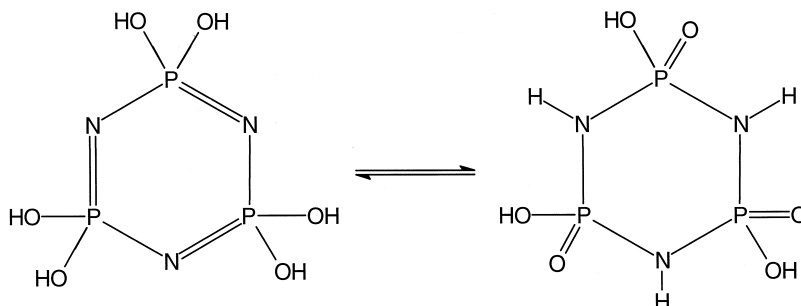


FIG. 1. Tautomeric forms of $(\text{PO}_2\text{NH})_n^-$ ions, here for $n = 3$.

$\text{Na}(\text{OOCCH}_3) \cdot 3\text{H}_2\text{O}$. This led to the formation of $\text{Na}_3(\text{PO}_2\text{NH})_3 \cdot 4\text{H}_2\text{O}$ (90).

2. Reaction of the tri- or tetrametaphosphimic acid with a base or a carbonate, for example, with NH_3 or $[\text{C}(\text{NH}_2)_3]_2\text{CO}_3$. By this method $(\text{NH}_4)_4(\text{PO}_2\text{NH})_4 \cdot 4\text{H}_2\text{O}$ (91) and $(\text{C}(\text{NH}_2)_3)_3(\text{PO}_2\text{NH})_3 \cdot \text{H}_2\text{O}$ (92) were synthesized.

3. Formation of water-soluble polymetaphosphimates by reaction of $\text{Ag}_3(\text{PO}_2\text{NH})_3$ (93) with a halide under formation of silver halide. With the use of $(\text{NH}_4)_2\text{S}$, the ammonium trimetaphosphimate $(\text{NH}_4)_3(\text{PO}_2\text{NH})_3 \cdot \text{H}_2\text{O}$ has been obtained (94).

4. Direct reaction of two salts, where the side product is very soluble. By this method the transition metal polymetaphosphimates, for example, $\text{M}_3[(\text{PO}_2\text{NH})_3]_2 \cdot 14\text{H}_2\text{O}$ ($\text{M} = \text{Zn}, \text{Co}$), can be obtained (95).

5. Crystallization at elevated temperatures (e.g., $\text{Na}_3(\text{PO}_2\text{NH})_3 \cdot \text{H}_2\text{O}$ (96)) or in the presence of additional salts, e.g., for the synthesis of $\beta\text{-Na}_4(\text{PO}_2\text{NH})_4 \cdot 3\text{H}_2\text{O}$.

6. Reaction between P_3N_5 and alkali metal hydroxide monohydrate under ammonothermal conditions. This led to the trimetaphosphimates $\text{K}_3(\text{PO}_2\text{NH})_3$ and $\text{Rb}_3(\text{PO}_2\text{NH})_3$ (71).

Other than a few single-crystal investigations, until recently the tri- and tetrametaphosphimates were mainly characterized by powder diffraction (34) and vibrational spectroscopy. Extensive IR and Raman spectroscopic investigations have been conducted to find out in which of the two tautomeric forms, $(\text{PO}_2\text{NH})_n^{n-}$ or $(\text{P}(\text{OH})\text{ON})_n^{n-}$, the trimetaphosphimate ions exists (97–100). This issue was unambiguously solved by the crystal structure analysis of $\text{Na}_3(\text{PO}_2\text{NH})_3 \cdot 4\text{H}_2\text{O}$, which confirmed the existence of the imido form in the solid state (90).

IR and Raman investigations by Steger *et al.* established the possible ring conformations of tri- and tetrametaphosphimate ions (74, 80, 101–103). Based on these results, interpretations of vibrational spectra (104, 105) as well as calculations of force constants in group III, transition metal, and rare earth tri- and tetrametaphosphimates were performed by Sukova *et al.* by least squares methods (106–110). Furthermore, calculations by the CNDO/2, MNDO, and PM3 methods were made (111–114). In addition, EPR spectra of some trimetaphosphimates were recorded (115). ^{31}P NMR experiments were used to investigate the formation and decomposition of polymetaphosphimates (60, 116–119), as well as for the protonation behavior of mono-, di-, and tri- μ -imido cyclotriphosphates (120). The protonation was also studied potentiometrically (121). ^{27}Al NMR experiments (122, 123)

were used to evaluate the multidentate complexation behavior of $(\text{PO}_2\text{NH})_3^{3-}$ ions.

The complexation of tri- and tetrametaphosphimate ions (124–127) by group III, rare earth (88, 89, 128), and transition metals (125) was studied by Rozanov *et al.* and led to a vast number of new compounds. These were mostly obtained as amorphous or microcrystalline products, and they have not been characterized in detail by X-ray structure analyses.

The formation and decomposition of tri- and tetrametaphosphimate in water in terms of their dependence on time, pH value, and temperature (117–119, 129–135), as well as their thermal stability, have been investigated in detail by various authors (47, 136–139). The mechanism of hydrolysis of halogenocyclophosphazenes and the structure of the products and intermediates was also studied by quantum chemical methods (140). Some of these investigations have also aimed at the application of the polymetaphosphimates as fertilizers (141–145), flame retardants, binders (146), biomaterials (147), or ion exchange materials (148, 149). Furthermore, bicyclophosphazenes of $(\text{PNCl}_2)_4$, i.e., $(\text{Cl}_7\text{N}_4\text{P}_4\text{NH}(\text{CH}_2)_n\text{NHP}_4\text{N}_4\text{Cl}_7)$ with $n = 4, 6, 12$, and their hydrolysis to bicyclotetrametaphosphimates (150, 151) as well as bicyclic trimetaphosphimates have been described in the literature (152).

B. CONFORMATION OF TRI- AND TETRAMETAPHOSPHIMATE IONS

Tri- and tetrametaphosphimate rings can adopt different conformations. Therefore, for detailed characterization and structural comparison of the cyclic six- and eight-membered PN rings of the $(\text{PO}_2\text{NH})_3^{3-}$ and $(\text{PO}_2\text{NH})_4^{4-}$ ions, a conformation analysis is important. The ring conformations can be analyzed for example by evaluation of torsion angles (153, 154), displacement asymmetry parameters (155), or puckering parameters (156) using the results of the single-crystal structure determinations.

The exact description of the ring geometry is given by the sequence of the torsion angles. The sequence of the signs of the torsion angles is characteristic for a given conformation; the absolute values allow a quantitative evaluation. To describe the deviation of a ring conformation from an ideal conformation the use of displacement asymmetry parameters (DAP-values), as shown by Nardelli, is very helpful (155). These DAP-values are dimensionless and describe whether mirror planes and twofold axes are present. The smaller the DAP-values are, the smaller is the deviation from the ideal symmetry.

These two approaches are only straightforward if almost ideal ring conformations are present. In general the rings attain a conformation that can only be precisely described by linear combinations of the ideal ring conformations. For this the puckering parameters have been shown to be especially useful. With the program PARST97 (157) the contribution of each ideal conformation can be obtained by calculating the puckering parameters; there are $N - 3$ parameters for an N -membered ring. The puckering parameters for five-, six-, and eight-membered rings are given in the literature (16, 158). Employing these methods it was found that in trimetaphosphimates the P_3N_3 rings most often adopt a chair conformation. Nevertheless, in very few cases a conformation is found that is a combination of the twist and the boat conformation. The P_4N_4 rings in tetrametaphosphimates exhibit either a saddle or a long chair conformation. Only one example is known where the eight-membered rings attain a crown conformation due to the coordination behavior as a tetradentate ligand. Some conformations of an eight-membered ring (first column) together with the sequence of torsion angles (second column), the present symmetry elements m and 2 (third column), and the puckering parameter (fourth column) are given in Table II.

C. TRI- AND TETRAMETAPHOSPHIMATES

Although tri- and tetrametaphosphimates have been studied extensively, only a few single-crystal structure analyses had been conducted until recently. Tables III and IV, respectively, give a summary of the crystallographic data of all hitherto known structures.

1. Crystal Structures of Trimetaphosphimates

The crystal structure determinations of trimetaphosphimates showed that $N-H \cdots O$ hydrogen bonds between the ring anions play an important role. In most of these salts the $(PO_2NH)_3^{3-}$ rings adopt approximately a chair conformation. In a few cases a conformation is found that is best described as a linear combination of the boat and the twist conformation. Examples of these conformations as well as some structural aspects of trimetaphosphimates are given in Fig. 2.

The acidity of the trimetaphosphimic acid is evident in the crystal structure of $H_3(PO_2NH)_3 \cdot 2H_2O$ (159) where a partial proton transfer to water molecules is observed, leading to the formula $(H_5O_2)H_2(PO_2NH)_3$. The same anion $H_2(PO_2NH)_3^{2-}$ is also found in $H_2(NH_4)(PO_2NH)_3 \cdot CH_3OH$ (159). The anions attain a distorted boat conformation that can be traced back to the low charge of the ring

TABLE II
IDEAL RING CONFORMATIONS IN TETRAMETAPHOSPHIMATES

Conformation	Torsion angles	Symmetry elements	Puckering parameter ^a
Crown			$q_4 \neq 0$
Saddle			$q_2 \neq 0$ $\phi_2 = n(\pi/4)$, $n = 2m$, $m = 0, 1, 2, \dots$
Chair			$q_3 \neq 0$ $\phi_3 = n(\pi/8)$, $n = 0, 1, 2, \dots$
Boat			$q_2 \neq 0$ $\phi_2 = n(\pi/4)$ $n = 2m + 1$, $m = 0, 1, 2, \dots$

^a For the general equation of eight-membered rings (only the values different from zero are given): $z_j = (2/8)^{1/2} q_2 \cos[\phi_2 + 4\pi(j-1)/8] + (2/8)^{1/2} q_3 \cos[\phi_3 + 6\pi(j-1)/8] + 8^{-1/2} q_4 (-1)^{j-1}$.

ion. In contrast to this observation, in $\text{Ag}_3(\text{PO}_2\text{NH})_3$ the ring anions also attain a distorted boat conformation. This distortion could have been caused by metal–nitrogen interactions that are unique in the crystal chemistry of trimetaphosphimates but have been also observed in $\text{Ag}(\text{PO}_2(\text{NH})_2)$ (29).

In all trimetaphosphimates of monovalent cations, the formation of $\text{N-H} \cdots \text{O}$ hydrogen bonds leads to a connection of $(\text{PO}_2\text{NH})_3^{3-}$ ions.

TABLE III

CRYSTALLOGRAPHIC DATA OF TRIMETAPHOSPHIMATES

Compound	a [pm], α [°]	b [pm], β [°]	c [pm], γ [°]	SG	Z	Ref.
$K_3(PO_2NH)_3$	1271.4(2), 90	1271.4(2), 90	1017.9(2), 120	$R3$	6	71, 93
$Ag_3(PO_2NH)_3$	1166.6(1), 90	786.4(1), 106.9(1)	997.8(1), 90	$P2_1/c$	4	93
$Na_3(PO_2NH)_3 \cdot H_2O$	988.0(1), 90	1221.2(1), 104.4(1)	764.6(1), 90	$C2$	4	96
$Na_3(PO_2NH)_3 \cdot 4H_2O$	1697.6(9), 90	783.4(3), 97.1(1)	891.8(6), 90	$P2_1/n$	4	90
$(C(NH_2)_3)_3(PO_2NH)_3 \cdot H_2O$	1565.6(2), 90	1068.3(1), 90	2091.8(2), 90	$Pbca$	8	92
$(NH_4)_3(PO_2NH)_3 \cdot H_2O$	657.1(1), 90	1299.2(1), 102.1(1)	692.4(1), 90	$P2_1$	2	94
$Rb_3(PO_2NH)_3$	1299.71(5), 90	1299.71(5), 90	1054.85(5), 120	$R3$	6	71
$Rh(NH_3)_3(TMP) \cdot 6H_2O$	992.4(1), 90	997.8(1), 90	1267.4(2), 90	$P2_1cn$	4	171
$(NH_4)H_3(PO_2NH)_3 \cdot CH_3OH$	1502.5(3), 90	726.4(1), 90	1925.2(1), 90	$Pbca$	8	159
$H_3(PO_2NH)_3 \cdot 2H_2O$	702.2(1), 90	1400.8(1), 93.3(1)	935.3(2), 90	$P2_1/c$	4	159

The N–H \cdots O hydrogen bonds lead to the formation of pairs of $(PO_2NH)_3^{3-}$ ions in $K_3(PO_2NH)_3$, $Na_3(PO_2NH)_3 \cdot H_2O$, $Rb_3(PO_2NH)_3$, and $(C(NH_2)_3)_3(PO_2NH)_3 \cdot H_2O$ where up to six hydrogen bonds are formed. In contrast to the Na^+ , Rb^+ , and K^+ salts, where pairs of $(PO_2NH)_3^{3-}$ ions are formed by six hydrogen bonds, only four were observed in $(C(NH_2)_3)_3(PO_2NH)_3 \cdot H_2O$. Whereas isolated pairs held together by the metal ions are found in the potassium and the rubidium salts, these pairs are connected to columns in the sodium salt and to sheets in the guanidinium salt via O–H \cdots O hydrogen bonding. The water molecules act as proton donors and acceptors. In $K_3(PO_2NH)_3$ and $Rb_3(PO_2NH)_3$, the pairs of $(PO_2NH)_3^{3-}$ ions are stacked in columns that form a motif of close-packed rods. In $Ag_3(PO_2NH)_3$ the $(PO_2NH)_3^{3-}$ ions form double layers. A three-dimensional network of $(PO_2NH)_3^{3-}$ ions is observed in $(NH_4)_3(PO_2NH)_3 \cdot H_2O$, $H_3(PO_2NH)_3 \cdot 2H_2O$, and $H_2(NH_4)(PO_2NH)_3 \cdot CH_3OH$. The largest amount of water per formula unit in a trimetaphosphimate is found in $Na_3(PO_2NH)_3 \cdot 4H_2O$. Although the $(PO_2NH)_3^{3-}$ ions also attain a chair conformation, in this compound

TABLE IV

CRYSTALLOGRAPHIC DATA OF TETRAMETAPHOSPHIMATES

Compound	a [pm], α [°]	b [pm], β [°]	c [pm], γ [°]	SG	Z	Ref.
$H_4(PO_2NH)_4 \cdot 2H_2O$	1398.0(30), 90	832.0(10), 90	504.0(10), 90	$P2_12_12$	2	160, 161
$Cs_4(PO_2NH)_4 \cdot 6H_2O$	969.3, 90	969.3, 90	1130.6, 90	$P4_2/nmc$	2	163
$K_4(PO_2NH)_4 \cdot 4H_2O$	678.6(2), 90	1037.1(3), 57.9	1433.5(4), 90	$P2_1/c$	2	163
$\beta\text{-}Na_4(PO_2NH)_4 \cdot 3H_2O$	843.6(2), 83, 1(1)	848.5(2), 76.3(1)	994.7(2), 87.5(1)	$P1$	2	164
$\alpha\text{-}Na_4(PO_2NH)_4 \cdot 3H_2O$	1002.7(2), 90	1189.7(2), 104.93(2)	1193.1(2), 90	$P2_1$	4	164
$Na_4(PO_2NH)_4 \cdot 2H_2O$	2225.6(3), 90	513.0(1), 134.21(2)	1566.7(2), 90	$C2/c$	4	164
$(NH_4)_4(PO_2NH)_4 \cdot 4H_2O$	653.0(1), 90	1105.8(1), 92.90(3)	1229.5(1), 90	$P2_1/n$	2	91
$(C(NH_2)_3)_4(PO_2NH)_4 \cdot 4H_2$	1739.6(1), 90	1084.2(1), 90	1335.0(1), 90	$Pbcn$	4	92

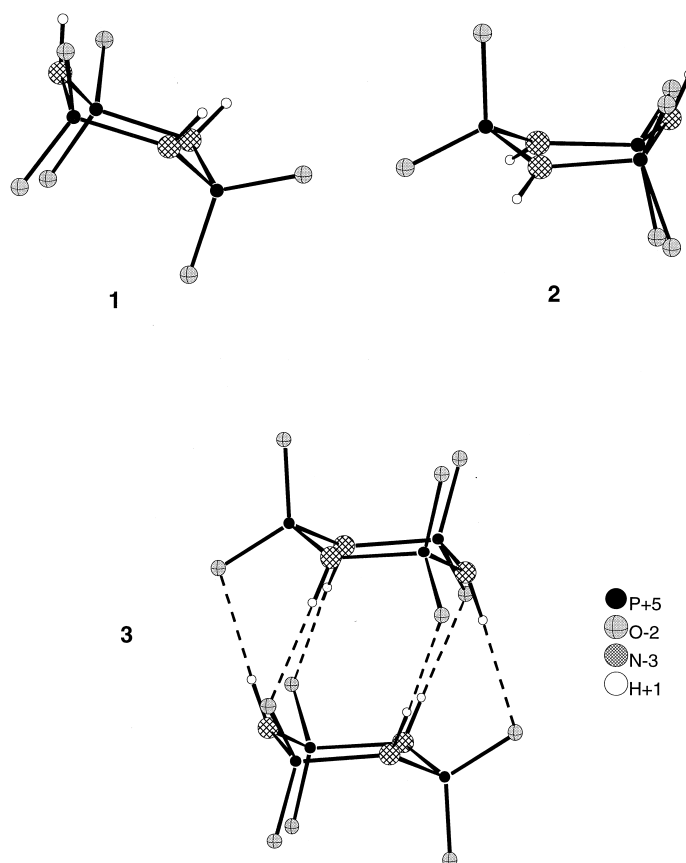


FIG. 2. Examples of the chair (1) and the distorted boat (2) conformation as well as pairs of trimetaphosphimate ions connected by N-H...O hydrogen bonds (3).

they are held together only by two N-H...O hydrogen bonds because of the large contribution of H₂O molecules to the hydrogen bonding.

2. Crystal Structures of Tetrametaphosphimates

The crystal structure determinations of tetrametaphosphimates showed that N-H...O hydrogen bonds between the ring anions play an important structure directing role. The $(\text{PO}_2\text{NH})_4^{4-}$ rings adopt approximately a chair, boat, or saddle conformation. Examples for conformations in $(\text{PO}_2\text{NH})_4^{4-}$ ions as well as some structural aspects of tetrametaphosphimates are given in Fig. 3.

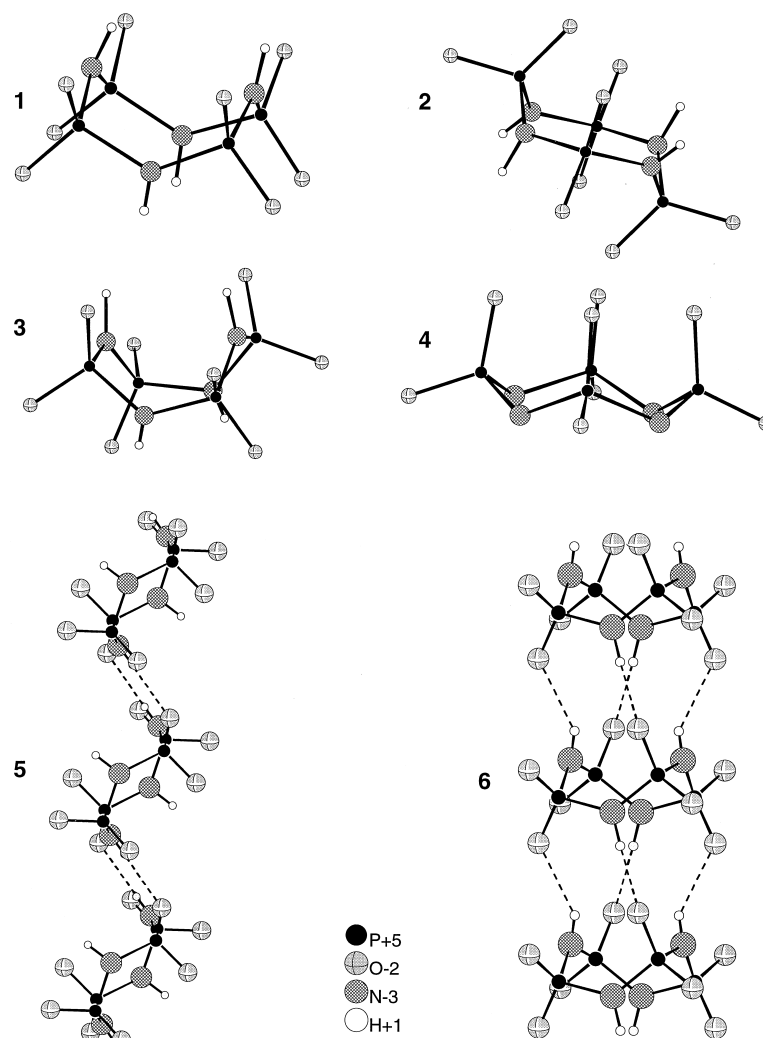


FIG. 3. Examples for conformations in $(\text{PO}_2\text{NH})_4^{4-}$ ions (**1**, saddle; **2**, chair; **3**, distorted boat; **4**, crown) as well as some structural aspects (formation of "strings" (**5**) and of columns (**6**) by N-H...O hydrogen bonding) of tetrametaphosphimates.

In $\text{H}_4(\text{PO}_2\text{NH})_4 \cdot 2\text{H}_2\text{O}$ the anion exhibits a significant distorted boat conformation (*160, 161*). Because of the acidic properties of tetrametaphosphimic acid dihydrate, two protons are transferred to the two water molecules. Thus, the compound is better written as $(\text{H}_3\text{O})_2\text{H}_2$

$(\text{PO}_2\text{NH})_4$. In the crystal the anions are connected to columns via $\text{N}-\text{H}\cdots\text{O}$ hydrogen bonds that are interconnected by $\text{O}-\text{H}\cdots\text{O}$ hydrogen bonds. Preliminary structural data on $\text{K}_2\text{H}_2(\text{PO}_2\text{NH})_4$, $\text{Rb}_2\text{H}_2(\text{PO}_2\text{NH})_4$, and $(\text{NH}_4)_2\text{H}_2(\text{PO}_2\text{NH})_4$ show that these salts are isomorphous to the acid dihydrate, with the cations presumably having the same positions as the water molecules (162). In $\text{Cs}_4(\text{PO}_2\text{NH})_4 \cdot 6\text{H}_2\text{O}$ (163), isolated tetrametaphosphimate ions with the exact symmetry $42m$ of the ideal saddle conformation are observed. They are not connected to each other via $\text{N}-\text{H}\cdots\text{O}$ hydrogen bonds which can be put down to the high water content. A reduced water content in $\alpha\text{-Na}_4(\text{PO}_2\text{NH})_4 \cdot 3\text{H}_2\text{O}$ and $\beta\text{-Na}_4(\text{PO}_2\text{NH})_4 \cdot 3\text{H}_2\text{O}$ (164) leads to a small distortion of the $(\text{PO}_2\text{NH})_4^{4-}$ ion from the ideal symmetry and to the connection of the ring anions by hydrogen bonding forming columns of staggered pairs of $(\text{PO}_2\text{NH})_4^{4-}$ ions. In $\text{Na}_4(\text{PO}_2\text{NH})_4 \cdot 2\text{H}_2\text{O}$ (164) even less water per formula unit is present, leading to an even stronger distortion of the anions. These form straight columns of $(\text{PO}_2\text{NH})_4^{4-}$ ions with eight via $\text{N}-\text{H}\cdots\text{O}$ hydrogen bonds. In $(\text{NH}_4)_4(\text{PO}_2\text{NH})_4 \cdot 4\text{H}_2\text{O}$, $[\text{C}(\text{NH}_2)_3]_4(\text{PO}_2\text{NH})_4 \cdot 4\text{H}_2\text{O}$, and $\text{K}_4(\text{PO}_2\text{NH})_4 \cdot 4\text{H}_2\text{O}$, the anions adopt the chair conformation (91, 92, 163). $\text{N}-\text{H}\cdots\text{O}$ hydrogen bonding leads in these compounds to the formation of strings of $(\text{PO}_2\text{NH})_4^{4-}$ ions.

D. PHOSPHIMATOMETALLATES

1. Introduction

Tri- and tetrametaphosphimates can act as polydentate ions. In principle, coordination by both nitrogen and oxygen is possible, but as seen in the salts of monovalent cations, almost exclusively coordination via oxygen is expected. Thus, the anions can act as polydentate and/or bridging ligands. The trimetaphosphimate ion can act in various ways:

- (a) As a monodentate ligand in combination with monovalent ions such as Na^+ , K^+ , Rb^+ , Ag^+ , NH_4^+ , or $\text{C}(\text{NH}_2)_3^+$
- (b) As a bridging ligand with divalent ions Cu^{2+} , Co^{2+} , Zn^{2+} in $\text{Na}_4\{\text{Cu}[(\text{PO}_2\text{NH})_3]_2\} \cdot 10\text{H}_2\text{O}$ (165), $\text{Na}\{\text{M}[(\text{PO}_2\text{NH})_3]\} \cdot 7\text{H}_2\text{O}$ (166) ($\text{M} = \text{Zn}, \text{Co}$)
- (c) As a tridentate ligand with Ga^{3+} in $\text{Na}_3\{\text{Ga}[(\text{PO}_2\text{NH})_3]_2\} \cdot 12\text{H}_2\text{O}$ (167–169), with Co^{2+} , Zn^{2+} in $\text{Na}_4\{\text{M}[(\text{PO}_2\text{NH})_3]_2\} \cdot 12\text{H}_2\text{O}$ (16, 70), with Rh^{3+} in $\text{Rh}(\text{NH}_3)_3(\text{PO}_2\text{NH})_3 \cdot 6\text{H}_2\text{O}$ (171), with Hf^{2+} , Zr^{2+} in $\text{Na}_4\{\text{M}_4(\mu_2\text{-O})(\mu\text{-OH})_6[(\text{PO}_2\text{NH})_4]_4\} \cdot 18\text{H}_2\text{O}$ and $\text{Na}_4\{\text{M}_4(\mu_2\text{-O})(\mu\text{-OH})_6[(\text{PO}_2\text{NH})_4]_4\} \cdot 21\text{H}_2\text{O}$ (172)
- (d) As a polydentate as well as a bridging ligand in $\text{M}_3[(\text{PO}_2\text{NH})_3]_2 \cdot 14\text{H}_2\text{O}$ ($\text{M} = \text{Zn}, \text{Co}$) and $\text{K}_{1.3}(\text{NH}_4)_{1.7}\{\text{Pr}[(\text{PO}_2\text{NH})_3]_2\} \cdot 8\text{H}_2\text{O}$ (173)

Only one crystal structure of a tetrametaphosphimato metallate— $\text{K}_4\text{H}\{\text{Tm}[(\text{PO}_2\text{NH})_4]_2\} \cdot 18\text{H}_2\text{O}$ —is described in the literature, but no atomic positions were published (174, 175). In this compound two $(\text{PO}_2\text{NH})_4^{4-}$ ions in the crown conformation act as tetradentate ligands forming isolated $\{\text{Tm}[(\text{PO}_2\text{NH})_4]_2\}^{5-}$ complex anions (Fig. 4, 2).

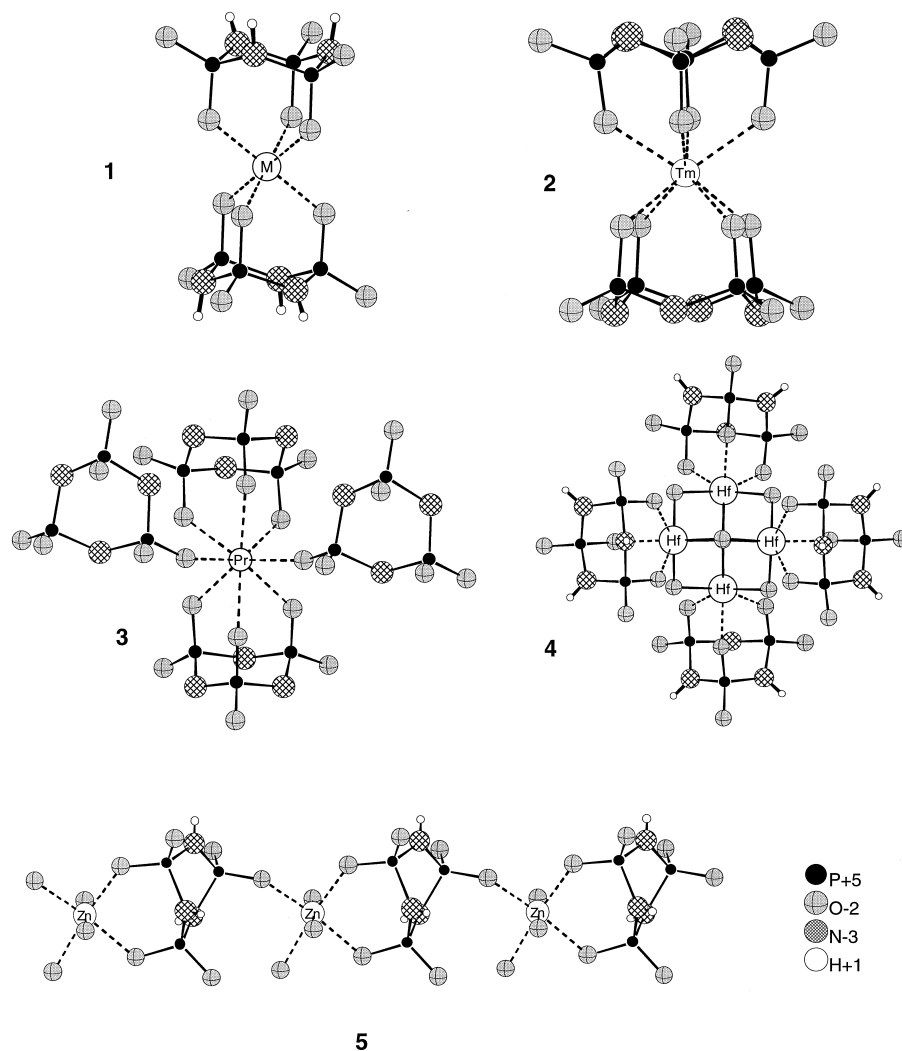


FIG. 4. Structural possibilities in trimetaphosphimatometallates.

Table V gives a summary of the crystallographic data of all hitherto known structures of trimetaphosphimatometallates.

2. Crystal Structures of Trimetaphosphimatometallates

In the following the compounds will be described, depending on the degree of condensation of the metal and trimetaphosphimate ions. Up to now phosphimatometallates with isolated and chainlike (single and double chains) units as well as a layered compound have been described. These structural possibilities are shown in Fig. 4.

Isolated entities are observed in $\text{Na}_3\{\text{Ga}[(\text{PO}_2\text{NH})_{3,12}]\} \cdot 12\text{H}_2\text{O}$, $\text{Na}_4\{\text{M}[(\text{PO}_2\text{NH})_{3,12}] \cdot 12\text{H}_2\text{O}$ ($\text{M} = \text{Co}, \text{Zn}$) with $\{\text{Ga}[(\text{PO}_2\text{NH})_{3,12}]\}^{3-}$ and $\{\text{M}[(\text{PO}_2\text{NH})_{3,12}]\}^{4-}$ ions where Ga^{3+} , Zn^{2+} , and Co^{2+} are octahedrally surrounded by oxygen (Fig. 4, 1). The trimetaphosphimate groups are tridentate ligands attaining the chair conformation. In $\text{Na}_4\{\text{Cu}[(\text{PO}_2\text{NH})_{3,12}] \cdot 10\text{H}_2\text{O}$ complex, centrosymmetric anions $\{\text{Cu}[(\text{PO}_2\text{NH})_{3,12}] \cdot 2\text{H}_2\text{O}\}^{4-}$ are formed in which the trimetaphosphimate ligands act as bidentate end-on ligands connected to the metal by only two oxygen atoms each. The coordination sphere of the copper ion is completed by the coordination of two H_2O molecules forming a considerable distorted CuO_6 octahedron. The characteristic central structural feature of the four trimetaphosphimato zirconate and hafnate compounds $\text{Na}_4\{\text{M}_4(\mu_4\text{-O})(\mu\text{-OH})_6[(\text{PO}_2\text{NH})_{4,14}]\} \cdot 18\text{H}_2\text{O}$, $\text{Na}_4\{\text{M}_4(\mu_4\text{-O})(\mu\text{-OH})_6[(\text{PO}_2\text{NH})_{4,14}]\} \cdot 21\text{H}_2\text{O}$, $\text{M} = \text{Hf}, \text{Zr}$ are the complex tetranuclear anions $\{\text{M}_4(\mu_4\text{-O})(\mu\text{-OH})_6[(\text{PO}_2\text{NH})_{4,14}]\}^{4-}$ with $\text{M} = \text{Zr}$ or Hf (172) (Fig. 4, 4). The anions consist of five corner sharing adamantanoid cages. The central cage $\{\text{M}_4(\mu_4\text{-O})(\mu\text{-OH})_6\}^{18+}$ exhibits a tetracoordinated oxygen in

TABLE V

CRYSTALLOGRAPHIC DATA OF TRIMETAPHOSPHIMATOMETALLATES

Compound	a [pm], α [°]	b [pm], β [°]	c [pm], γ [°]	SG	Z	Ref.
$\text{Zn}_3[(\text{PO}_2\text{NH})_{3,12}] \cdot 14\text{H}_2\text{O}$	743.7(2), 102.7(1)	955.9(2), 90.5(1)	980.1(2), 100.1(1)	$P1$	1	95
$\text{Co}_3[(\text{PO}_2\text{NH})_{3,12}] \cdot 14\text{H}_2\text{O}$	744.3(1), 102.2(2)	955.2(2), 90.0(1)	985.8(2), 99.3(21)	$P1$	1	95
$\text{Na}_4\{\text{Hf}_4(\mu_4\text{-O})(\mu\text{-OH})_6\text{TMP}_4\} \cdot 18\text{H}_2\text{O}$	2267.8(3), 90	2267.8(3), 90	2267.8(3), 90	$Pa3$	8	172
$\text{Na}_4\{\text{Hf}_4(\mu_4\text{-O})(\mu\text{-OH})_6\text{TMP}_4\} \cdot 21\text{H}_2\text{O}$	1435.0(2), 90	1435.0(2), 90	5034.8(10), 120	$R3$	6	172
$\text{Na}_4\{\text{Zr}_4(\mu_4\text{-O})(\mu\text{-OH})_6\text{TMP}_4\} \cdot 18\text{H}_2\text{O}$	2269.3(3), 90	2269.3(3), 90	2269.3(3), 90	$Pa3$	8	172
$\text{Na}_4\{\text{Zr}_4(\mu_4\text{-O})(\mu\text{-OH})_6\text{TMP}_4\} \cdot 21\text{H}_2\text{O}$	1430.3(2), 90	1430.3(2), 90	5028.4(10), 120	$R3$	6	172
$\text{Na}_4\{\text{Zn}[(\text{PO}_2\text{NH})_{3,12}] \cdot 12\text{H}_2\text{O}$	888.3(1), 90	1899.4(1), 104.54(1)	1712.6(2), 90	$C2/c$	4	16, 170
$\text{Na}_4\{\text{Co}[(\text{PO}_2\text{NH})_{3,12}] \cdot 12\text{H}_2\text{O}$	888.1(1), 90	1901.8(2), 104.59(1)	1711.2(1), 90	$C2/c$	4	16, 170
$\text{Na}_4\{\text{Cu}[(\text{PO}_2\text{NH})_{3,12}] \cdot 10\text{H}_2\text{O}$	912.5(2), 66.9(1)	942.7(2), 108.7(1)	965.4(2), 109.4(1)	$P1$	1	165
$\text{Na}_3\{\text{Ga}[(\text{PO}_2\text{NH})_{3,12}] \cdot 12\text{H}_2\text{O}$	872.9(5), 97.8(1)	990.2(5), 87.9(1)	871.6(5), 93.5(1)	$P1$	2	167–169
$\text{Na}[\text{Zn}(\text{PO}_2\text{NH})_{3,12}] \cdot 7\text{H}_2\text{O}$	1020.9(3), 116.0(1)	925.6(2), 97.7(1)	953.9(2), 103.2(1)	$P1$	2	166
$\text{Na}[\text{CO}(\text{PO}_2\text{NH})_{3,12}] \cdot 7\text{H}_2\text{O}$	1020.7(3), 116.0(1)	925.3(2), 97.6(1)	953.0(2), 103.2(1)	$P1$	2	166
$\text{K}_{1,7}(\text{NH}_4)_{1,7}[\text{Pr}[(\text{PO}_2\text{NH})_{3,12}] \cdot 8\text{H}_2\text{O}$	2562.3(8), 90	1057.7(3), 90	863.2(2), 90	$Pna2$	4	173

the center and the other cages are formed by the trimetaphosphimate ions acting as tridentate ligands coordinating Hf or Zr.

The structure of $\text{Na}\{\text{M}(\text{PO}_2\text{NH})_3\} \cdot 7\text{H}_2\text{O}$ ($\text{M} = \text{Zn}, \text{Co}$) is constructed of polymeric chain anions of the empirical composition $\{\text{M}(\text{PO}_2\text{NH})_3 \cdot 3\text{H}_2\text{O}\}^-$. The $(\text{PO}_2\text{NH})_3^{3-}$ ion acts as a tridentate ligand coordinating to two different metal ions, forming two M–O bonds with one of the metal ions and one with the other (166) (Fig. 4, 5). The anion attains a distorted ring conformation. The octahedral coordination of the metal ions is completed by H_2O molecules. In $\text{M}_3[(\text{PO}_2\text{NH})_3]_2 \cdot 14\text{H}_2\text{O}$ ($\text{M} = \text{Zn}, \text{Co}$) the same kinds of chains are observed (95). Whereas in $\text{Na}\{\text{M}(\text{PO}_2\text{NH})_3\} \cdot 7\text{H}_2\text{O}$ (166) charge balance is reached by incorporation of sodium ions, in $\text{M}_3[(\text{PO}_2\text{NH})_3]_2 \cdot 14\text{H}_2\text{O}$ ($\text{M} = \text{Zn}, \text{Co}$) two chains at a time are connected by M^{2+} ions, thus forming double chains.

The only known trimetaphosphimatometallate with a layered structure is $\text{K}_{1.3}(\text{NH}_4)_{1.7}\{\text{Pr}[(\text{PO}_2\text{NH})_3]_2\} \cdot 8\text{H}_2\text{O}$. The coordination polyhedron of the Pr^{3+} ion is a distorted dodecahedron that is formed by the oxygen atoms of two trimetaphosphimate ligands, one of which is a tridentate terminal and the other a pentadentate bridging ligand (Fig. 4, 3). The second $(\text{PO}_2\text{NH})_3^{3-}$ ligand has two different functions. The first is the coordination as a tridentate chelating ligand and the second the connection of three Pr^{3+} ions by using two more oxygen atoms to bind two other cations, thus forming trimetaphosphimate praseodymium layers. The trimetaphosphimate rings have a chair conformation. The difference of the coordination of the lanthanide ion compared to transition-metal ions can be ascribed to the size of the ions and the relatively high polarity of the rare-earth ligand bond. This favors the highly electrostatic bonding of the rare-earth ion to the oxygen atoms of the anionic ligand rather than coordination of water to the cation.

V. Solid-State PON Compounds

A. INTRODUCTION, GENERAL CONSIDERATIONS

The solids considered in this section are phosphorus oxynitrides and nitridooxophosphates. They are pentavalent phosphorus(V) compounds and correspond to a partial substitution of nitrogen, under the nitride form N^{3-} , for oxygen O^{2-} within PO_4 tetrahedra, resulting in the formation of mixed $\text{P}(\text{O}, \text{N})_4$ tetrahedra.

Various categories of compounds are concerned that differ from each other in particular in their crystallization states. Crystalline

compounds will be essentially reported here because of their better structural characterization. However, X-ray amorphous PON and nitridooxophosphates have been also synthesized, for example as high surface area fine powders or as glass phases. In this latter case, the phosphorus oxynitride glasses, it has been shown (176, 177) by ^{31}P MAS NMR that several types of phosphorus-centered tetrahedra are able to coexist: PO_4 , PO_3N , and PO_2N_2 . PON_3 tetrahedra are also known, the only examples to date being given by the oxynitride P_4ON_6 where they coexist with PN_4 tetrahedra (178) and the PON sodalites $\text{M}_{8-m}\text{H}_m[\text{P}_{12}\text{N}_{18}\text{O}_6]\text{X}_2$ with $\text{M} = \text{Cu}^+$, Li^+ ; $\text{X} = \text{Cl}^-$, Br^- , I^- (179).

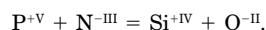
All those solid-state PON compounds are formed by an arrangement of corner-sharing tetrahedra, apart from P_4ON_6 , in which the PN_4 tetrahedra are also edge-sharing (178). This structural motif also occurs in P_3N_5 and HP_4N_7 (180–183). Therefore, they are directly comparable to purely oxygenated phosphate-type compounds and also to silicates or aluminosilicates whose crystal chemistry shows close similarities with that of phosphates. However, nitrogen can bring to the anionic network something more than just its higher negative formal charge and thus play a particular role in the structure as, unlike oxygen, it has the possibility of being threefold coordinated by phosphorus. The simultaneous presence of two kinds of nitrogen atoms, either bridging between two P atoms ($-\text{N}=\text{}$) or bridging between three P atoms ($-\text{N}<\text{}$), has been clearly demonstrated by XPS in phosphorus oxynitride glass compositions (184).

When, in crystalline compounds, nitrogen and oxygen atoms are twofold coordinated by phosphorus, an important question arises concerning their possibility of being structurally ordered. Neutron diffraction is essential here, as the X-ray scattering factors of O and N are not sufficiently different to permit the two atoms to be distinguished. In contrast, the neutron scattering length of nitrogen, 0.94×10^{-12} cm, is significantly larger than that of oxygen, 0.575×10^{-12} cm, thus making it possible to determine whether the anion sublattice is ordered.

Following ternary phosphorus oxynitrides, which involve only phosphorus as a cationic element, quaternary and higher oxynitrides will be described. A number of other solid-state PON compounds are under study and, when considering the richness of the phosphate crystal chemistry and the additional degree of freedom given by the presence of nitrogen, it is very probable that many new nitridooxophosphate compositions will be found in the near future.

B. THE PHOSPHORUS OXYNITRIDE PON

It is well known that, as previously mentioned, close structural relationships exist between phosphates and silicates, as the crystal chemistry of both families is based upon similar XO_4 tetrahedral networks. The introduction of nitrogen within the PO_4 tetrahedra further increases the similarities when the cross-substitution is considered:



The phosphorus oxynitride PON is a typical illustration, as its formula is derived from SiO_2 . Thus, the isoelectronic mixed-anion silica analogue should normally exhibit a crystal structure closely related to that of SiO_2 , which displays a complex P - T phase diagram. SiO_2 has a rich variety of low-pressure structures as a result of the many ways in which the easily moving tetrahedra can be linked to form extended corner-sharing arrays. Therefore, several polymorphs could also be expected for PON. A structural analogy with SiO_2 implies that nitrogen and oxygen are two-coordinated atoms, in other words, that the structures are based on networks of corner-sharing PO_2N_2 tetrahedra. Note the theoretical, but unverified, possibility of PON adopting a completely different crystal structure involving PON_3 tetrahedra in which all the nitrogen atoms would be three-coordinated while the oxygen atom would be nonbridging (185).

1. Synthesis

Although a chemical substance with the PON formulation was reported as early as 1846 (186), this phosphorus oxynitride was not well known for a long time. That is essentially due to some difficulty in its preparation and to the X-ray amorphous character of the commonly obtained powders.

Various methods of synthesis have been described. PON can be obtained by the thermal decomposition under vacuum of triamide $\text{PO}(\text{NH}_2)_3$, which results from ammonolysis of oxychloride POCl_3 (187, 188). The main disadvantage of this method is the moisture-sensitive character of the precursors, in particular POCl_3 . A second method consists of reacting ammonia at about 700°C with a phosphorus derivative such as P_4O_{10} , or better $\text{NH}_4\text{H}_2\text{PO}_4$ (8, 189, 190). It leads to PON after several heatings with intermediate grinding. The reaction between urea $\text{OC}(\text{NH}_2)_2$, melamine $(\text{NCNH}_2)_3$ or guanamine (2,4-diamino-6-alkyl-1,3,5 triazine), and phosphoric acids, ammonium phos-

phates, P_4O_{10} , or urea phosphates has been also described as a preparation process (191). For example:



The resulting product has a low apparent density. Other synthesis techniques have been reported (192), mainly the reaction of a stoichiometric mixture of P_3N_5 and P_4O_{10} , heated at 780°C for 48 h, which directly results in a crystalline powder (193). Crystallization of X-ray amorphous PON produced using the other preparation methods is obtained after heating the powder in an evacuated quartz ampoule at 700–800°C for several days.

2. Cristobalite-Type PON

At ambient conditions, PON adopts a cristobalite-type structure, metastable in SiO_2 . It crystallizes in the β -cristobalite phase, the high-temperature phase observed at ambient pressure for silica. The crystal structures of the two compounds are very similar. Whereas cristobalite silica crystallizes in the cubic $Fd\bar{3}m$ space group, cristobalite PON crystallizes in the tetragonal $P\bar{4}$ space group (8) with the nitrogen and oxygen atoms randomly distributed between the two anionic sites as shown by neutron diffraction experiments (Fig. 5); however, the atomic positions in PON deviate from those found in silica by only a few standard deviations. The unit cell parameters are $a = 462.66(1)$ and $c = 700.37(3)$ pm ($c/a = 1.514$) with $Z = 4$. Note that a refinement by neutron diffraction at the ISIS spallation source (194) prefers finally the more symmetrical $I\bar{4}2d$ space group, which was for a long time the space group attributed to silica (with $c/a = \sqrt{2}$).

The behavior of cristobalite PON has been studied as a function of pressure. No *in situ* evidence for pressure-induced amorphization was noticed. Whereas cristobalite SiO_2 displays four crystalline phases up to 50 GPa (195), PON remains in a cristobalite phase (193, 196). By using Raman spectroscopy and synchrotron X-ray diffraction, Kingma *et al.* (193, 197) observe a displacive transformation below 20 GPa to a high-pressure cristobalite-related structure, which then remains stable to at least 70 GPa. The high value of the calculated bulk modulus (71 GPa) (196) is indicative of the remarkable stiffness of the phase.

3. Quartz-Type PON

The analogy between PON and SiO_2 has been further illustrated by the fact that under high pressure/high temperature conditions (4.5

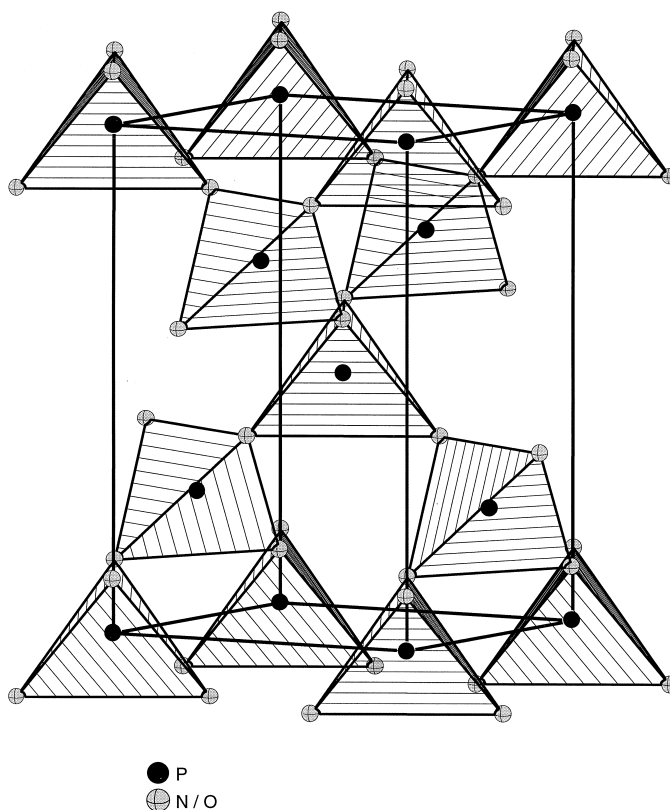


FIG. 5. Arrangement of the PO_2N_2 tetrahedra in the β -cristobalite PON phase (8).

GPa, 700°C) cristobalite PON is transformed into an α -quartz-type modification (198, 199) that is the ambient-pressure, low-temperature phase in silica. The structure at ambient conditions has been refined using time-of-flight neutron powder diffraction data on a quenched sample (200). It is essentially the same as that of α -quartz SiO_2 (trigonal $P3_221$, $Z = 3$), as shown in Table VI, which compares for PON and SiO_2 (201) the unit cell parameters as well as selected distances and angles. Oxygen and nitrogen are completely disordered over the anionic sites. Figure 6 shows the $\text{P}(\text{O}, \text{N})_4$ tetrahedral arrangement.

The behavior of α -quartz PON under pressure has been studied, in particular the pressure dependence of the cell parameters (200, 202). A displacive phase transition to an α -quartz II structure occurs at close to 20 GPa. Progressive and irreversible amorphization is observed above 30 GPa and, above 42 GPa, the product becomes com-

TABLE VI

UNIT CELL PARAMETERS AND SELECTED INTERATOMIC DISTANCES AND ANGLES IN α -QUARTZ PON AND IN THE CORRESPONDING SiO_2 PHASE^a

	PON	SiO_2 (after 201)
a [pm]	475.7(4)	491.37
c [pm]	524.60(2)	540.47
c/a	1.103	1.100
Mean A–X [pm]	157.3	161.0
X–A–X [°], ($\times 2$)	112.2(2)	110.7
X–A–X [°], ($\times 2$)	105.6(2)	108.8
X–A–X	109.6(2)	109.1
X–A–X	109.0(2)	108.8
A–X–A	140.6(1)	143.6

^a A: P or Si; X: (O, N) or O.

pletely amorphous. Such behavior—displacive transformation and amorphization—is very similar to that of α -quartz SiO_2 (195).

As shown in Table VI, the tetrahedra in PON are less regular than in SiO_2 because of the presence of two different anions. The molar volumes of the α -quartz and β -cristobalite phases of PON are compared in Fig. 7, as a function of pressure (200, 203).

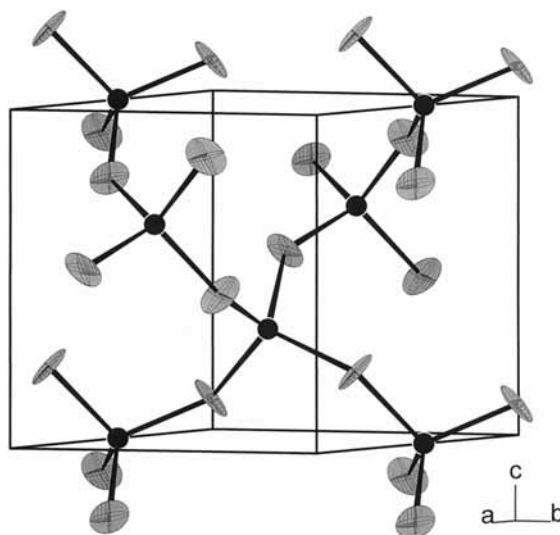


FIG. 6. Perspective view of the α -quartz-type PON structure (200).

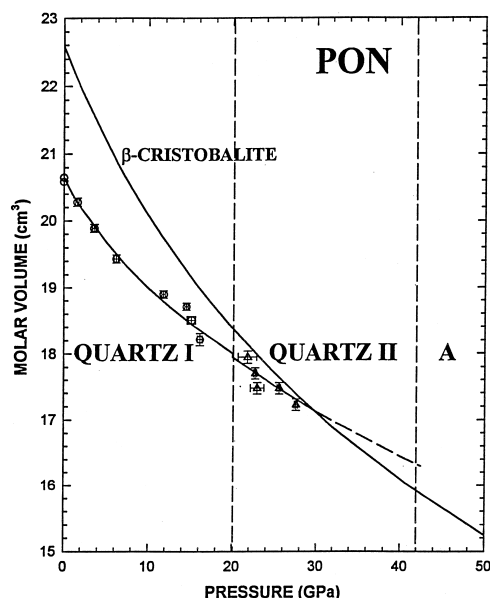


FIG. 7. Molar volumes of quartz and cristobalite polymorphs of PON as a function of pressure (200, 203).

4. Moganite-Type PON

A new polymorph of the phosphorus oxynitride PON has been recovered at ambient pressure by quenching after a treatment at 850°C under a pressure of 2.5 GPa using cristobalite- or quartz-type phases as starting materials (204). It has the same structure as moganite SiO_2 , a polymorph known only since 1976 (205) and the corresponding structure refined in 1992 (206), which occurs as microcrystalline silica fillings of cavities, fissures, and cooling cracks in natural formations, but has never been synthesized up to now. Unlike moganite SiO_2 , which is always found mixed with quartz variety, moganite PON is obtained as a pure and well-crystallized powder. The monoclinic structure (space group $I2/a$, $Z = 12$) has been refined both from an X-ray diffraction pattern (204) and by time-of-flight neutron diffraction (207). The lattice parameters, compared with those of silica, are gathered in Table VII. The crystal structure is based on alternating slabs of left- and right-handed quartz. It is characterized by 4-, 6-, and 8-membered rings of corner-sharing PO_2N_2 tetrahedra (O and N disordered) (207).

TABLE VII

CELL PARAMETERS FOR THE MOGANITE PHASES OF
SiO₂ (204) AND PON (205)

	SiO ₂	PON
<i>a</i> [pm]	875.8(2)	851.9(2)
<i>b</i> [pm]	487.6(1)	474.5(1)
<i>c</i> [pm]	1071.5(2)	1039.7(2)
β [°]	90.08(3)	90.00(1)
<i>V</i> [10 ⁶ pm ³]	457.6	420.3

The occurrence of the moganite-type phase in PON confirms that moganite is really a new structure type in AX₂ compounds. The molar volumes at ambient of the three phases, cristobalite, moganite, and quartz (22.58, 21.05, and 20.64 cm³, respectively) follow the same trend as in silica. The smaller size of the PO₂N₂ tetrahedron relative to that of SiO₄ (cf. Table VI) widens the pressure fields of stability, so that PON appears to be very useful to shed light on the detailed behavior of silica, which is still ill defined.

Note finally that, in spite of several attempts to melt pure PON compositions under very high temperature/high pressure conditions (pressure necessary to prevent any decomposition), the existence of this phosphorus oxynitride as a glass phase has not been established up to the present with certainty (208). However, P–O–N–H glasses, some of them with a low hydrogen content, could be prepared by melting P₄O₁₀ (189, 209) or decomposing ammonium phosphate (189, 210) in an NH₃ atmosphere at around 700°C.

Phosphorus oxynitride, PON, is a useful starting product, as a phosphorus and nitrogen source, to prepare various nitridooxophosphates, in particular phosphorus oxynitride glass compositions (211). Moreover, it shows as a material excellent chemical stability with potential applications in several domains. In microelectronics, for example, PON has been used to form by evaporation insulating films for the passivation of III–V InP substrates and the elaboration of MIS (metal–insulator–semiconductor) structures (190, 212–215). PON could have also valuable properties in flame retardancy (176, 191, 216).

C. THE OXYNITRIDE P₄N₆O

Millers and Vitola (217) have mentioned different crystalline phosphorus oxynitride compositions that are located in between PON and

the binary nitride P_3N_5 , and formulated PON, $x P_3N_5$ ($x \sim 0.5-2$) and P_4ON_6 . To date, only P_4ON_6 has been unambiguously identified. This nitrogen-rich phosphorus oxynitride is prepared starting from a compacted powder sample of crystalline PON (β -cristobalite type) heated in a slow ammonia flow at about 850°C for 30 h (178).

The crystal structure of P_4ON_6 has been solved from both X-ray and neutron powder diffraction data (178). It crystallizes in the orthorhombic space group $Pnnm$ ($Z = 2$) with the unit cell parameters $a = 684.24(1)$, $b = 607.14(2)$, $c = 681.76(1)$ pm. The three-dimensional structure is built up from two types of tetrahedra, PON_3 and PN_4 , in which the two kinds of bridging nitrogen atoms, two-coordinated (N_d) and three-coordinated (N_t), are found. The PON_3 tetrahedra form pairs via bridging oxygen atoms, the nitrogen atoms being, for each, two N_d and one N_t , while the PN_4 tetrahedra contain two N_d and two N_t . The three-coordinated N_t nitrogen atoms connect one PON_3 and two PN_4 tetrahedra. The particular feature of this structure is that the PN_4 tetrahedra are linked in pairs via a joint edge N_t-N_t , which is unique among the structures of phosphate- or silicate-type compounds. Figure 8 shows projections of PON_3 and PN_4 tetrahedra onto the plane (001) and (010), respectively. These tetrahedra are highly distorted, especially the PN_4 ones in which the bond angles range from 83 to 121° , the $P-N_d$ bonds (155 pm) being clearly shorter than the $P-N_t$ ones ($167-169$ pm) because of their π -bond character.

D. THE PON SODALITES

Nitridooxophosphates with a sodalite-like structure have been obtained and characterized by X-ray and neutron powder diffraction as well as ^{31}P MAS NMR spectroscopy (179). These nitridooxophosphates $M_{8-m}H_m[P_{12}N_{18}O_6]X_2$ ($M = \text{Cu}^+$, Li^+ ; $X = \text{Cl}^-$, Br^- , I^-) with a sodalite-like $[P_{12}N_{18}O_6]^{6-}$ framework were synthesized in four different reaction systems ($\text{MX}/\text{HPN}_2/\text{OP}(\text{NH}_2)_3$, $\text{MX}/\text{SP}(\text{NH}_2)_3/\text{OP}(\text{NH}_2)_3$, $\text{Li}_2\text{S}/\text{NH}_4\text{X}/\text{SP}(\text{NH}_2)_3/\text{OP}(\text{NH}_2)_3$). The formation of $\text{Cu}_{4.8}\text{H}_{3.2}[P_{12}N_{18}O_6]\text{Cl}_2$ was elegantly achieved by using CuCl and the molecular precursor $(\text{NH}_2)_2(\text{O})\text{P}-\text{N}=\text{P}(\text{NH}_2)_3$ as starting materials. This precursor already contains the same molar ratio, $\text{P}:\text{O} = 2:1$, found in the PON sodalites. The following PON sodalites were obtained as single-phase microcrystalline products: $\text{Cu}_5\text{H}_3[P_{12}N_{18}O_6]\text{Cl}_{0.1}\text{Br}_{1.9}$, $\text{Li}_{5.4}\text{H}_{2.6}[P_{12}N_{18}O_6]\text{Cl}_{0.1}\text{Br}_{1.9}$, $\text{Li}_{5.7}\text{H}_{2.3}[P_{12}N_{18}O_6]\text{Cl}_{0.2}\text{I}_{1.8}$, $\text{Cu}_{4.8}\text{H}_{3.2}[P_{12}N_{18}O_6]\text{Cl}_2$, $\text{Li}_{5.5}\text{H}_{2.5}[P_{12}N_{18}O_6]\text{Cl}_2$, $\text{Li}_{6.2}\text{H}_{1.8}[P_{12}N_{18}O_6]\text{Br}_2$, and $\text{Li}_{5.8}\text{H}_{2.2}[P_{12}N_{18}O_6]\text{I}_2$. The structure of $\text{Cu}_{4.8}\text{H}_{3.2}[P_{12}N_{18}O_6]\text{Cl}_2$ was refined using neutron and X-ray powder diffraction data, and the structures of $\text{Li}_{5.5}\text{H}_{2.5}[P_{12}N_{18}O_6]\text{Cl}_2$, $\text{Li}_{6.2}\text{H}_{1.8}$

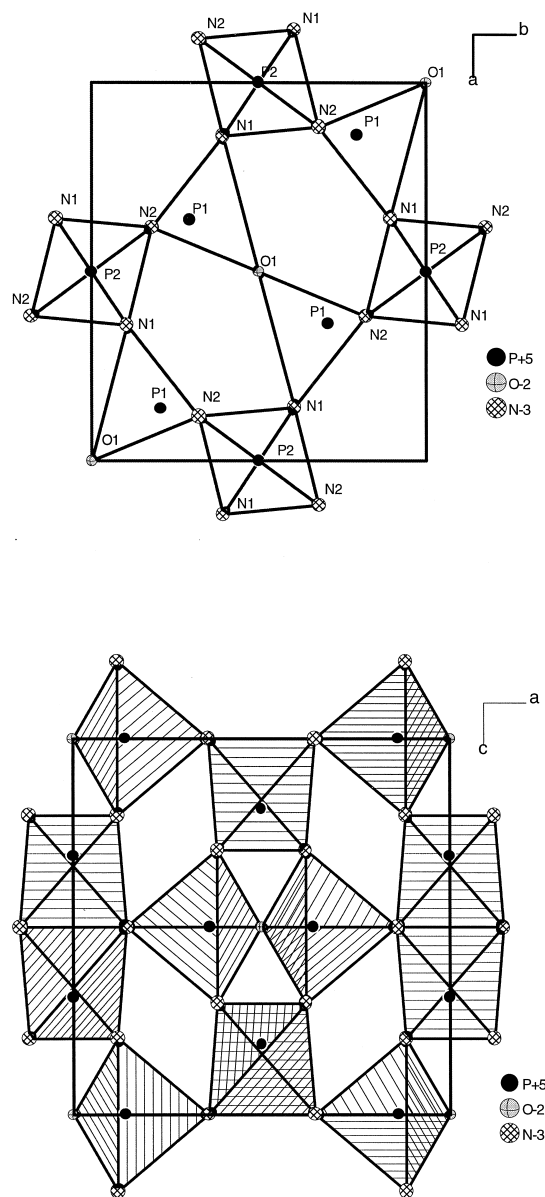


FIG. 8. P_4ON_6 structure (178). Projection of PN_4 and PON_3 tetrahedra onto the plane (001) (above) and onto the plane (010) (below).

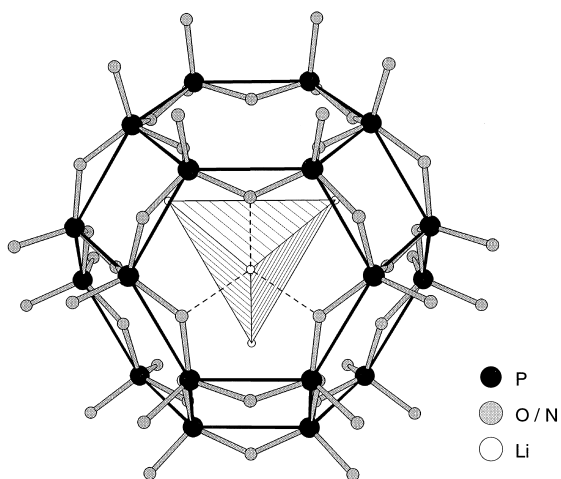


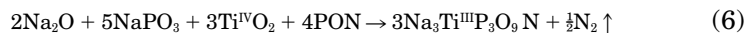
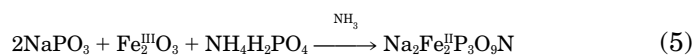
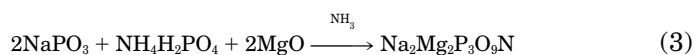
FIG. 9. Section of the crystal structure of the P-O-N sodalites $M_{8-x}H_x[P_{12}N_{18}O_6]Z_2$ ($M = Cu, Li$; $Z = Cl, Br, I$). The β -cage is shown (ZM_4 tetrahedron, M : small white).

$[P_{12}N_{18}O_6]Br_2$, and $Li_{5.8}H_{2.2}[P_{12}N_{18}O_6]I_2$ from X-ray powder diffraction data using the Rietveld method ($I\bar{4}3m$, $a = 820.25(1)$ to $830.81(2)$ pm). As expected, an increase of the cubic lattice constant was found with increasing radius of the halide ions. The three-dimensional framework of the PON sodalites is built up by corner-sharing PON_3 tetrahedra leading to large sodalite cages (β -cages). A β -cage is shown in Fig. 9. In the center of each cage a halide ion is found, which is coordinated by up to four monovalent cations. The cations are bound to three (N, O) atoms and the halide ion. The metal ions are partially replaced by hydrogen, which is covalently bound to the N atoms, thus forming imido groups clearly detectable using IR spectroscopy. The evaluation of the neutron diffraction data showed no evidence of a crystallographic ordering of the N/O atoms. Thus, the O atoms occupy one-fourth of the positions of the N atoms statistically. ^{31}P MAS NMR spectroscopic investigations gave one signal with a isotropic chemical shift of -8.7 ppm. This is in accordance with the presence of no other than PN_3O tetrahedra.

E. THE $M_3M^{III}P_3O_9N$ AND $M_2M^{II}P_3O_9N$ SERIES

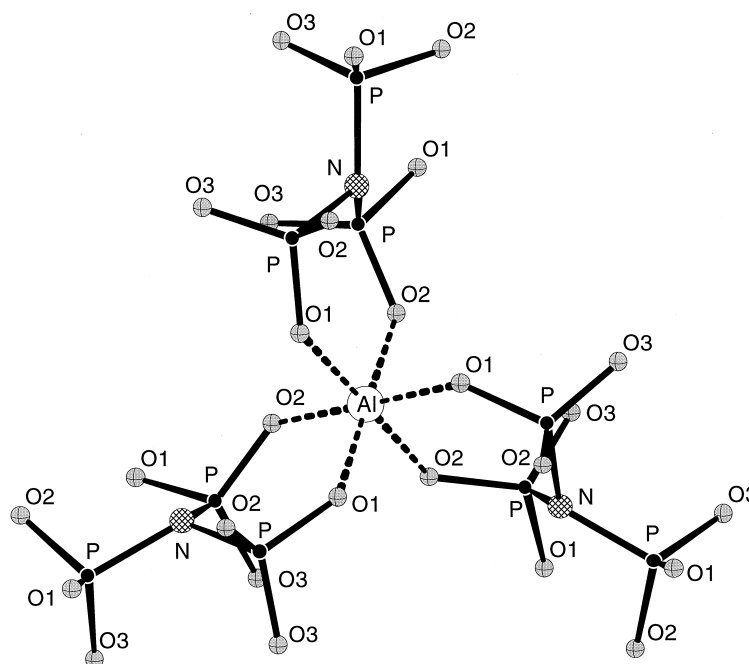
The compounds $Na_3AlP_3O_9N$ and $Na_2Mg_2P_3O_9N$ were the first terms prepared of each of these two isostructural series of nitridooxophosphates (218). Many isotypic compounds and solid solutions have since

been isolated in each series: $M^I M^{III} P_3 O_9 N$ with $M^I = Na, K, (Na, K)$ and $M^{III} = Al, Ga, In, Ti, V, Cr, Mn, Fe, (Al, Cr), (Al, V)$; $M^I M^{II} P_3 O_9 N$ with $M^I = Na$ and $M^{II} = Mg, Mn, Fe, Co$ (219, 220). Versatile preparation methods have been used, involving either gas–solid or solid–solid reactions in the 600–800°C temperature range, the nitrogen source being, for example, ammonia, PON, a binary metal nitride such as AlN, GaN, or TiN, or even $(PNCl_2)_3$ or Na_2NCN . Moreover, the reducing character of NH_3 or the presence of the redox couple N^{3-}/N^0 in the solid starting mixture permits the use of high oxidation state transition metal oxides. Various types of reactions include the following:



All these nitridooxophosphates are of cubic symmetry with a parameter value between ~ 925 (Na/Mg) and ~ 1000 pm (K/In) depending on the M^I/M^{III} cationic couple.

The crystal structure of $Na_3AlP_3O_9N$ has been determined from single-crystal data: space group $P2_13$, $a = 927.4(1)$ pm, $Z = 4$ (221). Nitrogen atoms of PO_3N tetrahedra are threefold coordinated, thus forming discrete $N(PO_3)_3$ groups around aluminum atoms octahedrally surrounded by oxygen atoms. As shown in Fig. 10, each nearly regular AlO_6 octahedron is connected to six tetrahedra, with formation of an $Al[N(PO_3)_3]_3$ entity. These results are in agreement with the ^{27}Al ($\delta_{iso} = 9$ ppm: $Al(OP)_6$) and ^{31}P ($\delta_{iso} = 5$ ppm: PO_3N tetrahedron) MAS NMR observations (9, 220). A ^{23}Na MQ-MAS NMR study, carried out on both $Na_3AlP_3O_9N$ and $Na_2Mg_2P_3O_9N$, has allowed for a precise characterization of the $Na^I + Al^{III} \rightarrow 2 Mg^{II}$ cross-substitution. Among the three independent sodium atoms of the $Na_3AlP_3O_9N$ structure, $Na^I(O_6)(N)$, $Na^{II}(O_6)$, and $Na^{III}(O_6)$, Mg exclusively substitutes the $Na^{II}(O_6)$ atoms that have the least irregular pseudooctahedral environment (9).

FIG. 10. $\text{Al}[\text{N}(\text{PO}_3)_3]_3$ entity in the structure of $\text{Na}_3\text{AlP}_3\text{O}_9\text{N}$ (221).F. THE $\text{Cs}_3\text{M}_2\text{P}_6\text{O}_{17}\text{N}$ SERIES

This series of nitridooxophosphates is illustrated, in particular, by the magnesium derivative, whose crystal structure has been determined on a single crystal (222, 223). $\text{Cs}_3\text{Mg}_2\text{P}_6\text{O}_{17}\text{N}$ crystallizes in the cubic $Pa\bar{3}$ space group with $a = 1223.9(1)$ pm and $Z = 4$, and its structure consists of discrete cyclic arrangements of six $\text{P}(\text{O}, \text{N})_4$ tetrahedra sharing two corners, as shown in Fig. 11, thus forming large $[\text{P}_6\text{O}_{17}\text{N}]^{7-}$ anions. These independent cyclic units are linked together through octahedrally coordinated magnesium atoms (MgO_6), while cesium atoms occupy large cavities of the cyclohexaphosphate network and ensure the electrical neutrality. $\text{Cs}_3\text{Mg}_2\text{P}_6\text{O}_{17}\text{N}$ is a first example of nitridooxocyclohexaphosphate. Nitrogen atoms are bridging (P–N–P) atoms (Fig. 11) and are randomly distributed with oxygen (N:O = 1:5) in the corresponding $24d$ anionic position of the space group.

Isotypic compounds $\text{Cs}_3\text{Fe}_2\text{P}_6\text{O}_{17}\text{N}$ and $\text{Cs}_3\text{Co}_2\text{P}_6\text{O}_{17}\text{N}$ have been obtained with divalent iron or cobalt instead of magnesium. Generally, they were prepared, like the magnesium term, by heating in flowing

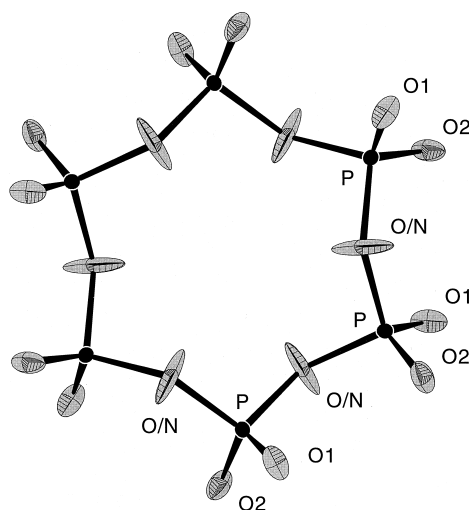


FIG. 11. $(P_6O_{17}N)^{7-}$ cyclic macroanion forming the structural skeleton of $Cs_3Mg_2P_6O_{17}N$ (223).

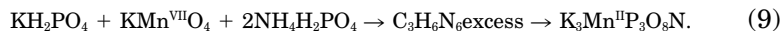
ammonia (but with melamine also used as a nitriding agent) a mixture of $CsPO_3$, $NH_4H_2PO_4$ and the appropriate oxide or carbonate (224).

G. THE $M_2^I M^{II} P_3 O_8 N$ SERIES

Several isotopic compounds of this recently discovered series have been prepared, for $M^I = K$ or Tl and $M^{II} = Mg$, Mn , or Fe (225). However, in the absence of suitable single crystals, the corresponding crystal structure is not yet completely determined. They result from thermal reactions, between 500 and 800°C, of ammonia or other nitriding agents such as melamine or urea, with various mixtures containing $(KPO_3)_n$ (or KH_2PO_4) or Tl_2CO_3 and an oxidic compound of Mg , Mn , or Fe . In the case of the manganese and iron derivatives, the nitrogen-containing starting compound may also act as a reducing agent if the oxidation state of the metal is higher than +2. Examples of reactions are as follows (Eqs. (7)–(9)):



where “ $\text{K}_2\text{Fe}^{\text{III}}\text{P}_3\text{O}_{10}$ ” only refers to a mixture composition obtained in a first step in a muffle furnace, and



PON has been also successfully used as a nitrogen (and phosphorus) source:



These nitridooxophosphates are stable in water and 1 N HCl, which is useful to extract eventual by-products. Their composition has been undoubtedly established by a complete chemical analysis. The XRD powder patterns can be indexed with hexagonal parameters ($Z = 6$) as illustrated for the potassium compounds:

$$\text{K}_2\text{MgP}_3\text{O}_8\text{N}: \quad a = 1016.7(1) \text{ pm} \quad c = 1428.8(1) \text{ pm}$$

$$\text{K}_2\text{MnP}_3\text{O}_8\text{N}: \quad a = 1035(1) \text{ pm} \quad c = 1417(1) \text{ pm}$$

$$\text{K}_2\text{FeP}_3\text{O}_8\text{N}: \quad a = 1025(1) \text{ pm} \quad c = 1418(1) \text{ pm}$$

The general formula of these new oxynitrides $\text{M}_2\text{M}^{\text{I}}(\text{PX}_3)_3$ suggests as for the previous series a cyclophosphate-type structure or a long-chain polyphosphate-type structure, where nitrogen would be structurally equivalent to oxygen.

H. THE Na–P–O–N SYSTEM

Glass compositions as well as crystalline oxynitrides have been isolated in this quaternary system. It is the system where the first nitrated phosphate glasses, of composition $\text{NaPO}_{3-x}\text{N}_{2x/3}$ ($0 < x \leq \sim 1$), were prepared in the early 1980s by melting sodium polyphosphate $\text{Na}(\text{PO}_3)_n$ in flowing ammonia (209, 226). They correspond to a progressive substitution of nitrogen for oxygen within PO_4 tetrahedra. Numerous phosphorus oxynitride glasses have been since studied in various other systems and the structural role of nitrogen is now well understood. As shown by XPS (184), both $-\text{N}<$ and $-\text{N}=\text{}$ nitrogen atoms bonded to three P and two P atoms, respectively, replace bridging ($-\text{O}-$) and nonbridging ($=\text{O}$) oxygen atoms, thus increasing the cross-linking density of the glass network, which results in particular in a significant improvement of the chemical durability of the glasses. The presence of these two types of nitrogen atoms in the Na–P–O–N

glass structure was corroborated by a ^{23}Na NMR study (10) and also by means of Eu^{3+} as a local structural probe (227). All the results show that the sodium atoms are in a purely oxygenated environment.

Several crystalline compositions exist in the Na–P–O–N system. Some of them appear by glass devitrification, but they are preferentially obtained by thermal ammonolysis of sodium phosphates at moderate temperatures (550–600°C) or by reacting these phosphates with PON or nitrogen derivatives of carbonic acid, such as melamine. They are structurally related to each other and have been formulated $\text{Na}_n\text{P}_n\text{O}_{3n-3}\text{N}_2$, where $n = 4, 5$, and 6 (228, 229). Although a structural relationship with amphibole-type silicates has been envisaged, more complicated structures involving both threefold and twofold coordinated nitrogen are probable, if an analogy is made with the structure of corresponding glass compositions.

I. OTHER SYSTEMS/X-RAY AMORPHOUS METALLOPHOSPHATE OXYNITRIDES

A new family of nitridooxophosphates has been characterized in the Al–P–O–N system (230). These oxynitrides were prepared by nitridation under ammonia flow, in the 650–1000°C temperature range, of highly dispersed (200–400 $\text{m}^2 \text{g}^{-1}$) X-ray amorphous aluminophosphate powders ($\text{Al/P} \geq 1$) obtained at low temperature using soft chemistry routes, for example, a sol–gel process (231). Note that the preparation of such a reactive precursor was proved to be essential, as crystalline AlPO_4 does not react with ammonia. The name “ALPON” was applied to all the compositions in the family of nitrated aluminophosphates corresponding to the variation of both phosphorus over aluminum ratio and nitrogen content, and to the general formula $\text{AlP}_{1-a}\text{O}_{4-(3x+5a)/2}\text{N}_x$. The maximum nitrogen enrichment for $a = 0$ leads to the composition AlPON_2 . At nitridation temperatures higher than $\sim 800^\circ\text{C}$, ammonia partially reduces phosphorus P(V) with formation of volatile species so that the oxynitrides prepared under these conditions are phosphorus deficient with respect to the AlPO precursor starting composition. All the nitridooxophosphates, ALPON, are X-ray amorphous powders, and high specific surface areas are kept after nitridation in spite of severe reaction conditions.

A first approach to the ALPON's structure for ($\text{Al/P} = 1$) compositions (232) shows that aluminum and phosphorus atoms are essentially in tetrahedral coordination. Higher nitrogen contents result in chemical shift positions progressively shifted toward higher values, thus confirming the monophasic composition domain. The presence of nitrogen increases the basic character of the high surface area alumi-

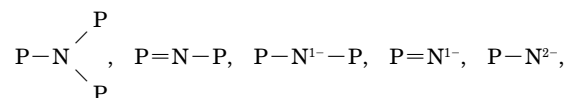
nophosphate oxynitride powders, which are active in Knoevenagel condensations and, as polyfunctional catalyst Ni/AlPON, in the synthesis of methylisobutyl ketone (MIBK) (233). A positive catalytic evaluation in isobutane dehydrogenation has been also carried out for platinum and tin supported AlPON (234).

Similarly, other families of metallophosphates oxynitrides have been studied with catalytic objectives in different M–P–O–N systems (M = Ga, AlGa, AlCr, In, Ti, Zr, ...) (235).

VI. Conclusion

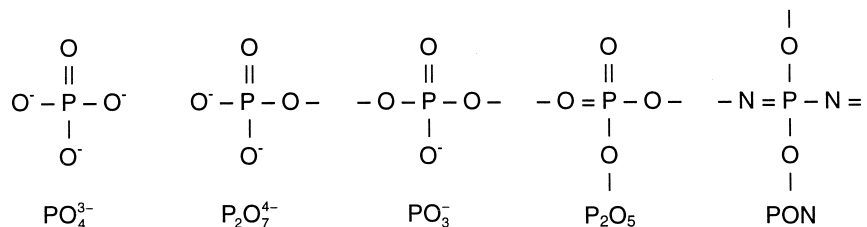
Considerable advances have been made recently, in general, in the study of nitrides, and the same is true, in particular, for compounds containing phosphorus(V)–nitrogen bonds. Among them, solid-state P–O–N compounds can be compared a priori to Si–O compounds (silica, silicates), as the (P–N) couple is isosteric with the (Si–O) couple, and it has been shown that the phosphorus oxynitride PON is clearly a silica analogue. Solid-state P–O–N compounds can also be considered as P–O compounds (phosphates) in which nitrogen has replaced part of the oxygen of the PO₄ tetrahedra. In fact, a structural analogy with silicates or with phosphates is only possible if the nitrogen atoms are bridging between two phosphorus atoms; note that, in all the given examples, they are always randomly distributed with oxygen atoms. However, nitrogen presents also the ability to be bonded to three phosphorus atoms, and this feature largely extends the possibilities for new nitridooxophosphate compositions, as pseudosilicates, as nitrated phosphates, or as compounds with novel crystal structures. Consequently, a great variety of these oxynitrides must be expected in the future.

On the other hand, bridging nitrogen atoms between two or three P atoms constitute the only cases encountered. That would mean that nitrogen never shares any strong bond with another kind of atom, as demonstrated for example in Na₃AlP₃O₉N or in Cs₃Mg₂P₆O₁₇N, where aluminum or magnesium atoms, respectively, have a purely oxygenated octahedral surrounding. The same remark was previously made in NaPON glasses, as indicated earlier, for which it was concluded that among the five theoretical possibilities for nitrogen,



only the two first had to be kept (236).

To conclude, it is pleasant to consider the regular evolution from 0 to 4 of the number of bridging atoms in the following series of phosphate compounds, which is nicely completed by the phosphorus oxynitride PON (237).



REFERENCES

1. Durif, A. "Crystal Chemistry of Condensed Phosphates"; Plenum Press: New York, 1995.
2. Schnick, W. *Angew. Chem. Int. Ed. Engl.* **1993**, *32*, 806.
3. Marchand, R.; Laurent, Y. *Eur. J. Solid State Inorg. Chem.* **1991**, *28*, 57.
4. Grande, T.; Holloway, J. R.; McMillan, P. F.; Angell, C. A. *Nature* **1994**, *369*, 43.
5. Reidmeyer, M. R.; Day, D. E. *J. Am. Ceram. Soc.* **1985**, *68*, 188.
6. Reidmeyer, M. R.; Day, D. E. *J. Non-Cryst. Solids* **1995**, *181*, 201.
7. Pascual, L.; Duran, A. *Mat. Res. Bull.* **1996**, *31*(1), 77.
8. Boukbir, L.; Marchand, R.; Laurent, Y.; Bacher, P.; Roult, G. *Ann. Chim. Fr.* **1989**, *14*, 475.
9. Massiot, D.; Conanec, R.; Feldmann, W.; Marchand, R.; Laurent, Y. *Inorg. Chem.* **1996**, *35*, 4957.
10. Bunker, B. C.; Tallant, D. R.; Balfe, C. F.; Kirkpatrick, R. J.; Turner, G. L.; Reidmeyer, M. R. *J. Am. Ceram. Soc.* **1987**, *70*, 675.
11. Benitez, J. J.; Odriozola, J. A.; Marchand, R.; Laurent, Y.; Grange, P. *J. Chem. Soc. Faraday Trans.* **1995**, *91*(24), 4477.
12. Fripiat, N.; Grange, P. *J. Chem. Soc. Chem. Comm.* **1996**, 1409.
13. Corbridge, D. E. C. "Phosphorus—An Outline of its Chemistry, Biochemistry, and Technology"; Elsevier: Amsterdam, 1990.
14. Hantke, G.; Kirschstein, G.; Senferling, F.; Swass, K. In "Gmelin Handbuch der Anorganischen Chemie, Phosphor Part C", Kotowski, A., Ed.; Verlag Chemie GmbH: Weinheim, 8th Edition, Syst. No. 16, 1965.
15. Panthel, S.; Becke Goehring, M. In "6 und 8 gliedrige Ringsysteme in der P-N Chemie"; Springer-Verlag: Berlin, 1969.
16. Stock, N. Ph.D. Thesis, University of Bayreuth, Germany, 1998.
17. Quimby, O. T. *Inorg. Synth.* **1960**, *6*, 111.
18. Stock, N.; Schnick, W. *Z. Naturforsch.* **1995**, *B51*, 1079.
19. Töpelmann, W.; Thomas, B.; Schadow, H.; Meznik, L. *Z. Chem.* **1984**, *24*, 134.
20. Bullen, G. J.; Stephens, F. S.; Wade, R. J. *J. Chem. Soc. A* **1969**, 1804.
21. Belaj, F. *Acta Crystallogr.* **1993**, *B49*, 254.

22. Schnick, W.; Horstmann, S.; Schmidpeter, A. *Angew. Chem. Int. Ed. Engl.* **1994**, 33, 785; Horstmann, S.; Schnick, W. *Z. Naturforsch.* **1996**, B49, 1381.
23. Horstmann, S.; Schnick, W. *Z. Naturforsch.* **1996**, B51, 127.
24. Cameron, T. S.; Chan, C.; Chute, W. J. *Acta Crystallogr.* **1980**, B36, 2391.
25. Stokes, N. H. *Am. Chem. J.* **1893**, 15, 198.
26. Klement, R.; Brecht, K.-R. *Z. Anorg. Allg. Chem.* **1947**, 254, 217.
27. Cruickshank, D. W. J. *Acta Crystallogr.* **1964**, 17, 671.
28. Hobbs, E.; Corbridge, D. E. C.; Raistrick, B. *Acta Crystallogr.* **1953**, 6, 621.
29. Gilles, M.; Weber, R.; Bergerhoff, G. *Z. Kristallogr.* **1993**, 203, 305.
30. Jacobs, H.; Nymwegen, R. *Z. Anorg. Allg. Chem.* **1997**, 623, 849.
31. Seel, F.; Klein, N. *Z. Naturforsch.* **1983**, B37, 804.
32. Takenaka, A.; Yamanaka, S.; Hattori, M. *Bull. Chem. Soc. Jpn.* **1993**, 66(9), 2762.
33. Stokes, H. N. *Am. Chem. J.* **1894**, 16, 123.
34. Herzog, A. H.; Nielsen, M. L. *Anal. Chem.* **1958**, 30, 1490.
35. Nymwegen, R. Ph.D. Thesis, University of Dortmund, Germany, 1997.
36. Sato, S.; Takayanagi, T.; Watanabe, M. *Bull. Chem. Soc. Jpn.* **1989**, 62(1), 267.
37. Watanabe, M.; Sato, S. *J. Mater. Sci.* **1986**, 21, 2623.
38. Nachbur, H.; Rohringer, P. German Patent No. 2,620,643, 1976.
39. Bednarek, W. *Pol. J. Soil Sci.* **1989**, 22(1), 87.
40. Shimasaki, C.; Oono, Y.; Takai, F.; Shoji, M.; Yoshizawa, M. *Nippon Kagaku Kaishi* **1982**, 3, 376.
41. Gard, D. R. U.S. Patent No. 4,956,163, 1990.
42. Gard, D. R. U.S. Patent No. 4,946,662, 1990.
43. Shimasaki, C.; Ookawa, S.; Ishizaka, R. *Bull. Chem. Soc. Jpn.* **1985**, 58(2), 592.
44. Kozmina, M. L.; Grishina, E. F.; Volkovich, S. I.; Kubasova, L. V. *Vestn. Mosk. Univ., Ser. 2: Khim.* **1978**, 19(5), 611.
45. Bennett, B. G.; Holmes, W. S. German Patent No. 2,238,550, 1974.
46. Kadic, K. Czechoslovakian Patent No. 142,521, 1971.
47. Feldmann, W. *Z. Chem.* **1983**, 23, 139.
48. Riesel, L.; Somieski, R. *Z. Anorg. Allg. Chem.* **1975**, 412(3), 246.
49. Toepelmann, W.; Kroschwitz, H.; Schroeter, D.; Patzig, D.; Lehmann, H. A. *Z. Chem.* **1979**, 19(8), 273.
50. Meznik, L.; Kouril, M. *Chem. Zvesti* **1968**, 22(8), 618.
51. Wanek, W.; Thilo, E. *Z. Chem.* **1967**, 7, 108.
52. Watanabe, M.; Hinatase, M.; Sakurai, M.; Sato, S. *Gypsum Lime* **1991**, 232, 146.
53. Hilmer, W. *Acta Crystallogr.* **1965**, 19, 362.
54. Larsen, M. L.; Willett, R. D. (a) *Acta Crystallogr.* **1974**, B30, 522; (b) *Science* **1969**, 166, 1510.
55. Sheldrick, W. S. *Z. Anorg. Allg. Chem.* **1974**, 408, 175.
56. Mootz, D.; Look, W.; Sassmannshausen, G. *Z. Anorg. Allg. Chem.* **1968**, 358, 282.
57. Mootz, D.; Goldmann, J. *Acta Crystallogr.* **1969**, B25, 1256.
58. Wanek, W.; Novobilsky, V.; Thilo, E. *Z. Chem.* **1967**, 7(3), 109.
59. Narath, A.; Lohman, F. H.; Quimby, O. T. *J. Am. Chem. Soc.* **1956**, 78, 4493.
60. Nielsen, M. L.; Pustinger, J. V. *J. Phys. Chem.* **1964**, 68, 152.
61. Sakurai, M.; Watanabe, M. *J. Mater. Sci.* **1994**, 29(18), 4897.
62. Stokes, H. N. *Am. Chem. J.* **1895**, 17, 275.
63. Stokes, H. N. *Am. Chem. J.* **1896**, 18, 629.
64. Stokes, H. N. *Am. Chem. J.* **1896**, 18, 780.
65. De Ficquelmont, A. M. *Comptes Rendus* **1936**, 200, 1045.
66. De Ficquelmont, A. M. *Ann. Chim.* **1939**, 12, 169.

67. De Ficquelmont, A. M. *Comptes Rendus* **1936**, 202, 423.
68. De Ficquelmont, A. M. *Comptes Rendus* **1936**, 202, 848.
69. De Ficquelmont, A. M. *Comptes Rendus* **1940**, 211, 590.
70. Moureu, H.; De Ficquelmont, A. M. *Comptes Rendus* **1934**, 198, 1417.
71. Jacobs, H.; Nymwegen, R. Z. *Anorg. Allg. Chem.* **1998**, 624(2), 199.
72. Janik, B.; Zeszutko, W. *Zh. Obshch. Khim.* **1973**, 43(2), 274.
73. Nikolaev, A. F.; Dreiman, N. A.; Zyryanova, T. A. *Zh. Obshch. Khim.* **1970**, 40(4), 937.
74. Steger, E.; Lunkwitz, K. Z. *Anorg. Allg. Chem.* **1961**, 313, 262.
75. Sakurai, M.; Watanabe, M. *Bull. Chem. Soc. Jpn.* **1994**, 67(4), 1029.
76. Meznik, L.; Toepelmann, W. Z. *Chem.* **1978**, 18(6), 232.
77. Nielsen, M. L.; Morrow, T. J. *Inorg. Synth.* **1960**, 6, 97.
78. Radosavljevic, S. D.; Sasic, J. S. Z. *Anorg. Allg. Chem.* **1972**, 387(2), 271.
79. Rozanov, I. A.; Berdnikov, V. R.; Sokol, V. I.; Butman, L. A. *Izv. Akad. Nauk SSSR, Neorg. Mater.* **1973**, 9(1), 152.
80. Steger, E.; Lunkwitz, K. Z. *Anorg. Allg. Chem.* **1961**, 313, 271.
81. Nielsen, M. L.; Nielsen, W. W. *Microchem. J. (New York)* **1959**, 3, 83.
82. Rozanov, I. A.; Medvedeva, L. Ya.; Beresnev, E. N. *Zh. Neorg. Khim.* **1978**, 23(8), 2259.
83. Rozanov, I. A.; Medvedeva, L. Ya.; Beresnev, E. N.; Sokol, V. I. *Koord. Khim.* **1978**, 4(5), 684.
84. Rozanov, I. A.; Medvedeva, L. Ya.; Beresnev, E. N.; Sokolov, Yu. A.; Sokol, V. I. *Zh. Neorg. Khim.* **1981**, 26(3), 668.
85. Rozanov, I. A.; Medvedeva, L. Ya.; Beresnev, E. N.; Murashov, D. A. *Zh. Neorg. Khim.* **1983**, 28(2), 427.
86. Rozanov, I. A.; Medvedeva, L. Ya.; Beresnev, E. N. *Koord. Khim.* **1976**, 2(11), 1471.
87. Sokol, V. I.; Rozanov, I. A.; Murashov, D. A. *Zh. Khim.* **1978**, Abstr. No. 19V65.
88. Rozanov, I. A.; Murashov, D. A.; Berdnikov, V. R.; Beresnev, E. N., *Dokl. Akad. Nauk SSSR* **1977**, 234(1), 83.
89. Rozanov, I. A.; Berdnikov, V. R.; Tananaev, I. V.; Cheltsov, P. A. *Dokl. Akad. Nauk SSSR* **1971**, 201(4), 872.
90. Olthof, R.; Migchelsen, T.; Vos, A. *Acta Crystallogr.* **1965**, 19, 596.
91. Stock, N.; Schnick, W. *Acta Crystallogr.* **1998**, C54, 171.
92. Stock, N.; Jürgens, B.; Schnick, W. Z. *Naturforsch.* **1998**, B53, 1115.
93. Stock, N.; Schnick, W. Z. *Naturforsch.* **1997**, 52, 251.
94. Stock, N.; Schnick, W. *Acta Crystallogr.* **1996**, C52, 2645.
95. Stock, N.; Irran, E.; Schnick, W. Z. *Allg. Anorg. Chem.* **1999**, 625, 555.
96. Stock, N.; Schnick, W. *Acta Crystallogr.* **1997**, C53, 532.
97. Pustinger, J. V.; Cave, W. T.; Nielsen, M. L. *Spectrochim. Acta* **1959**, 11, 909.
98. Corbridge, D. E. C.; Lowe, E. J. *J. Chem. Soc.* **1954**, 4555.
99. Lunkwitz, K.; Steger, E. Z. *Anorg. Allg. Chem.* **1968**, 358(3–4), 111.
100. Steger, E.; Lunkwitz, K. *J. Mol. Struct.* **1969**, 3(1–2), 67.
101. Lunkwitz, K.; Steger, E. *Spectrochim. Acta, Part A* **1967**, 23(10), 2593.
102. Steger, E.; Lunkwitz, K. Z. *Anorg. Allg. Chem.* **1962**, 316, 293.
103. Lunkwitz, K. Ph.D. Thesis, Universität Dresden, 1965.
104. Kharitonov, Yu. Ya.; Rozanov, I. A.; Berdnikov, V. R.; Tananaev, I. V. *Izv. Akad. Nauk SSSR, Neorg. Mater.* **1974**, 10(7), 1314.
105. Sukova, L. M.; Petrov, K. I. *Zh. Neorg. Khim.* **1982**, 27(7), 1682.

106. Sukova, L. M.; Berdnikov, V. R.; Petrov, K. I.; Rozanov, I. A.; Novitskii, G. G. *Koord. Khim.* **1980**, 6(4), 519.
107. Sukova, L. M.; Kondratov, O. I.; Petrov, K. I.; Rozanov, I. A.; Novitskii, G. G. *Zh. Neorg. Khim.* **1979**, 24(9), 2444.
108. Sukova, L. M.; Petrov, K. I.; Rozanov, I. A.; Murashov, D. A. *Zh. Neorg. Khim.* **1979**, 24(9), 2396.
109. Sukova, L. M.; Kondratov, O. I.; Petrov, K. I.; Rozanov, I. A.; Novitskii, G. G. *Zh. Neorg. Khim.* **1979**, 24, 2718.
110. Sukova, L. M.; Kondratov, O. I.; Petrov, K. I.; Rozanov, I. A. *Koord. Khim.* **1977**, 3(7), 1096.
111. Rozanov, I. A.; Alekseiko, L. N.; Gloriozov, I. P.; Mamaev, V. M.; Ustynyuk, Yu. A. *Koord. Khim.* **1982**, 8(12), 1615.
112. Rozanov, I. A.; Alekseiko, L. N.; Gloriozov, I. P.; Rezvova, T. V.; Ustynyuk, Yu. A.; Mamaev, V. M. *Koord. Khim.* **1982**, 8(7), 880.
113. Rozanov, I. A.; Alekseiko, L. N.; Gloriozov, I. P.; Mamaev, V. M.; Ustynyuk, Yu. A. *Vestn. Mosk. Univ., Ser. 2: Khim.* **1983**, 24(2), 195.
114. Alekseiko, L. N.; Gorchakov, V. V.; Ivanov, Yu. V.; Murashov, D. A.; Rozanov, I. A. *Zh. Neorg. Khim.* **1989**, 34(9), 2212.
115. Sukova, L. M.; Kondratov, O. I.; Miroshnichenko, I. V.; Petrov, K. I.; Rozanov, I. A. *Koord. Khim.* **1978**, 4(1), 64.
116. Murray, M.; Boulajoun, I. *Phosphorus Res. Bull.* **1996**, 6, 155.
117. Toepelmann, W.; Thomas, B.; Lehmann, H. A.; Meznik, L.; Novosad, J.; Dostal, K. *Collect. Czech. Chem. Commun.* **1981**, 46(1), 173.
118. Toepelmann, W.; Thomas, B.; Meznik, L. *Z. Chem.* **1979**, 19(12), 445.
119. Meznik, L.; Novosad, J.; Dostal, K. *Collect. Czech. Chem. Commun.* **1978**, 43(11), 2846.
120. Miyajima, T.; Maki, H.; Sakurai, M.; Watanabe, M. *Phosphorus Res. Bull.* **1995**, 5, 155.
121. Miyajima, T.; Maki, H.; Sakurai, M.; Watanabe, M. *Phosphorus Res. Bull.* **1995**, 5, 149.
122. Maki, H.; Miyajima, T. *Phosphorus Lett.* **1997**, 29, 14.
123. Maki, H.; Miyajima, T.; Ishiguro, S.-I.; Nariai, H.; Motooka, I.; Sakurai, M.; Watanabe, M. *Phosphorus Res. Bull.* **1996**, 6, 9.
124. Rozanov, I. A.; Murashov, D. A. *Zh. Khim.* **1988**, Abstr. No. 16V36.
125. Rozanov, I. A.; Beresnev, E. N.; Madyuskina, L. L.; Medvedeva, L. Ya. *Zh. Neorg. Khim.* **1983**, 28(8), 2137.
126. Porai-Koshits, M. A.; Sokol, V. I.; Rozanov, I. A. *Zh. Khim.* **1978**, Abstr. No. 19V178.
127. Miyajima, T.; Maki, H.; Sakurai, M.; Sato, S.; Watanabe, M. *Phosphorus Res. Bull.* **1993**, 3, 31.
128. Rozanov, I. A.; Murashov, D. A.; Berdnikov, V. R.; Beresnev, E. N. *Koord. Khim.* **1979**, 5(9), 1319.
129. Quimby, O. T.; Narath, A.; Lohman, F. H. *J. Am. Soc.* **1960**, 82, 1099.
130. Shen, C. Y.; Morgan, F. W. In "Environment Phosphorus Handbook"; Griffith, E. J., Ed.; Wiley: New York, 1973, 241–263.
131. Kobayashi, E. *Bull. Chem. Soc. Jpn.* **1976**, 49(12), 3524.
132. Kobayashi, E. *Chem. Lett.* **1976**, 479.
133. Klement, R.; Biberacher, G. *Z. Anorg. Allg. Chem.* **1956**, 283, 246.
134. Wanek, W.; Thilo, E. *Collect. Czech. Chem. Commun.* **1970**, 35(9), 2712.
135. Wanek, W.; Thilo, E. *Z. Chem.* **1967**, 7(3), 108.

136. Sakurai, M.; Watanabe, M. *Gypsum Lime* **1994**, 250, 164.
137. Belyakov, V. N.; Bortun, A. I. *Ukr. Khim. Zh. (Russ. Ed.)* **1985**, 51(10), 1105.
138. Belyakov, V. N.; Bortun, A. I. *Ukr. Khim. Zh. (Russ. Ed.)* **1983**, 49(11), 1127.
139. Sakurai, M.; Watanabe, M. *Phos. Res. Bull.* **1993**, 3, 55.
140. Alekseiiko, L. N.; Gorchakov, V. V.; Ivanov, Yu. V.; Murashov, D. A.; Rozanov, I. A. *Zh. Neorg. Khim.* **1989**, 34(8), 1958.
141. Fiedler, H. J.; Mai, H.; Seyfarth, W.; Riesel, L.; Schadow, H.; Koehler, H. East German Patent No. 105,000, 1974.
142. Wakefield, Z. T.; Allen, S. E.; McCullough, J. F.; Sheridan, R. C.; Kohler, J. J. *J. Agr. Food Chem.* **1971**, 19(1), 99.
143. Fiedler, H. J.; Mai, H.; Seyfarth, W. *Zentralbl. Bakteriell., Parasitenkd., Infektionskr. Hyg., Abst. 2* **1974**, 129(7), 651.
144. Dick, W. A.; Tabatabai, M. A. *Geoderma* **1978**, 21(3), 175.
145. Minar, J.; Honza, J.; Kouril, M. *Scr. Fac. Sci. Nat. Univ. Purkynianae Brun.* **1987**, 17(3-4), 143.
146. Zyryanova, T. A.; Sheshina, G. M. SU Patent No. 313,836, 1971.
147. Bertoluzza, A.; Fagnano, C.; Francioso, O.; Vasina, M. In "Spectrosc. Biol. Mol., 6th Eur. Conf."; Merlin, J. C.; Turrell, S.; Huvenne, J. P., Eds.; Kluwer: Dordrecht, Netherlands, 1995; pp. 515-516.
148. Kvashenko, A. P.; Belyakov, V. N.; Strelko, V. V. *Ukr. Khim. Zh. (Russ. Ed.)* **1985**, 51(1), 29.
149. Belyakov, V. N.; Bortun, A. I. *Ukr. Khim. Zh.* **1985**, 51, 1105.
150. Medvedeva, L. Ya.; Murashov, D. A.; Rozanov, I. A. *Russ. J. Coord. Chem.* **1997**, 23(10), 748.
151. Rozanov, I. A.; Murashov, D. A.; Moiseev, V. I.; Medvedeva, L. Ya. *Zh. Neorg. Khim.* **1993**, 38(5), 764.
152. Murashov, D. A.; Rozanov, I. A.; Moliseev, V. I.; Prytkov, S. E. *Koord. Khim.* **1991**, 17(3), 308.
153. Zschunke, A. "Molekülstruktur"; Spektrum Akademischer Verlag: Heidelberg, 1993.
154. Bucourt, R. *Topics in Stereochemistry* **1975**, 8, 159.
155. Nardelli, M. *Acta Crystallogr.* **1983**, C39, 1141.
156. Cremer, D.; Pople, J. A. *J. Am. Chem. Soc.* **1975**, 97, 1354.
157. Nardelli, M. PARST97, University of Parma, 1997.
158. Gilli, G. In "Fundamentals of Crystallography"; Giacovazzo, C., Ed.; 1st edition; Oxford University Press: Oxford, 1992; p. 495.
159. Attig, R.; Mootz, D. *Z. Anorg. Allg. Chem.* **1976**, 419, 139.
160. Attig, R.; Mootz, D. *Acta Crystallogr.* **1977**, B33, 605.
161. Mighelsen, T.; Olthof, R.; Vos, A. *Acta Crystallogr.* **1965**, 19, 603.
162. Corbridge, D. E. C. *Acta Crystallogr.* **1953**, 6, 104.
163. Berking, B.; Mootz, D. *Acta Crystallogr.* **1971**, B27, 740.
164. Stock, N.; Schmalz, H.; Schnick, W. *Z. Anorg. Allg. Chem.* **1998**, 624, 1777.
165. Sokol, V. I.; Medvedeva, L. Ya.; Butman, L. A.; Rozanov, I. A. *Koord. Khim.* **1976**, 2(4), 576.
166. Sokol, V. I.; Medvedeva, L. Ya.; Beresnev, E. N.; Rozanov, I. A.; Butman, L. A. *Koord. Khim.* **1978**, 4(6), 949.
167. Butman, L. A.; Rozanov, P. A.; Berdnikov, V. R.; Porai-Koshits, M. A.; Sokol, V. I. *Koord. Khim.* **1975**, 1, 429.
168. Sokol, V. I.; Porai-Koshits, M. A.; Butman, L. A. *Proc. Semin. Crystallochem. Coord. Metallorganic Compounds*, Bratislava (Czechoslovakia), 1973.

169. Sokol, V. I.; Porai-Koshits, M. A.; Butman, L. A.; Rozanov, I. A.; Berdnikov, V. R. *Izv. Akad. Nauk SSSR, Ser. Khim.* **1974**, 485.
170. Rozanov, I. A.; Medvedeva, L. Y.; Sokol, V. I. *Zh. Neorg. Khim.* **1981**, 26, 668.
171. Shubochkin, L. K.; Popov, O. V.; Shubochkina, E. F.; Sokol, V. I.; Rozanov, I. A.; Butman, L. A. *Koord. Khim.* **1977**, 3(6), 902.
172. Stock, N.; Herrendorf, W.; Beck, J.; Schnick, W. *Eur. J. Inorg. Chem.* **1998**, 469.
173. Sokol, V. I.; Porai-Koshits, M. A.; Berdnikov, V. R.; Rozanov, I. A.; Butman, L. A. *Koord. Khim.* **1979**, 5, 1093.
174. Sokol, V. I.; Porai-Koshits, M. A.; Murashev, D. A.; Sadikov, G. G. *Koord. Khim.* **1982**, 8, 1408.
175. Sokol, V. I.; Murashov, D. A.; Rozanov, I. A.; Porai-Koshits, M. A.; Nikolaev, V. P.; Butman, L. A. *Zh. Neorg. Khim.* **1979**, 24(12), 3385.
176. Le Sauze, A. Ph.D. Thesis, Univ. Rennes (France) 1998.
177. Le Sauze, A.; Montagne, L.; Palavit, G.; Fayon, F.; Marchand, R. Proc. 15th Univ. Conf. on Glass Science, Univ. Missouri—Rolla (USA) 1999. *J. Non-Cryst. Solids*, **1999**, in press.
178. Ronis, J.; Bondars, B.; Vitola, A.; Millers, T.; Schneider, J.; Frey, F. *J. Solid State Chem.* **1995**, 115, 265.
179. Stock, N.; Irran, E.; Schnick, W. *Chem. Eur. J.* **1998**, 4, 1822.
180. Horstmann, H.; Irran, E.; Schnick, W. *Angew. Chem. Int. Ed. Engl.* **1997**, 36, 1873.
181. Horstmann, S.; Irran, E.; Schnick, W. *Z. Anorg. Allg. Chem.* **1998**, 624, 620.
182. Horstmann, S.; Irran, E.; Schnick, W. *Angew. Chem. Int. Ed. Engl.* **1997**, 36, 1992.
183. Horstmann, S.; E Irran, E.; Schnick, W. *Z. Anorg. Allg. Chem.* **1988**, 624, 221.
184. Marchand, R.; Agliz, D.; Boukbir, L.; Quémerais, A. *J. Non-Cryst. Solids* **1988**, 103, 35.
185. Guéguen, E. Ph.D. Thesis, Univ. Rennes (France) 1994.
186. Gerhardt, M. *Comptes Rendus* **1846**, 22, 858; *Ann. Chim. Phys.* **1846**, 18, 188.
187. Wetroff, G. *Comptes Rendus* **1937**, 205, 668.
188. Klement, R.; Koch, O. *Chem. Ber.* **1954**, 87, 333.
189. Boukbir, L. Ph.D. Thesis, Univ. Rennes (France) 1987.
190. Marchand, R.; Laurent, Y.; Favennec, P.-N. French Patent No. 87-08962, 1987.
191. Sommer, K. German Patents No. 23 17 282.9 and 23 55 575.1, 1973.
192. Coffman, P. R. Ph.D. Thesis, Arizona State Univ. (USA), 1996.
193. Kingma, K. J.; Gerald Pacalo, R. E.; McMillan, P. F. *Eur. J. Solid State Inorg. Chem.* **1997**, 34, 679.
194. Haines, J. *et al.*, to be published.
195. Kingma, K. J.; Hemley, R. J.; Mao, H. K.; Veblen, D. R. *Phys. Rev. Lett.* **1993**, 70, 3927.
196. Léger, J.-M.; Haines, J.; De Oliveira, L. S.; Chateau, C.; Le Sauze, A.; Marchand, R. *J. Phys.: Condens. Matter* **1996**, 8, L773.
197. Kingma, K. J.; Pacalo, R. E. G.; McMillan, P. F. In "High Pressure-Temperature Research: Properties of Earth and Planetary Materials"; Manghnani, M. H.; Yagi, T., Eds.; Terra Scientific: Tokyo, AGU: Washington, DC, 1997.
198. Millers, T.; Vitola, A.; Vilks, Yu.; Bondars, B.; Davidenko, V. *Izv. Akad. Nauk Latv. SSR, Ser. Khim.* **1981**, 6, 748.
199. Bondars, B.; Millers, T.; Vitola, A.; Vilks, Yu. *Izv. Akad. Nauk Latv. SSR, Ser. Khim.* **1982**, 4, 498.
200. Léger, J.-M.; Haines, J.; De Oliveira, L. S.; Chateau, C.; Le Sauze, A.; Marchand, R.; Hull, S. *J. Phys. Chem. Solids* **1999**, 60, 145.

201. Hazen, R. M.; Finger, L. W.; Hemley, R. J.; Mao, H. K. *Solid State Commun.* **1989**, *72*, 507.
202. Léger, J.-M.; Haines, J.; De Oliveira, L. S.; Chateau, C.; Le Sauze, A.; Marchand, R. *C.R. Acad. Sci. Paris* **1998**, *1*, Ser. IIc, 237.
203. Le Sauze, A.; Haines, J.; Chateau, C.; Léger, J.-M.; Marchand, R. Proc. Int. Symp. on Nitrides II, Limerick (Ireland), 1998.
204. Chateau, C.; Haines, J.; Léger, J.-M.; Le Sauze, A.; Marchand, R. *Am. Mineral.* **1999**, *84*, 207.
205. Flörke, O. W.; Jones, J. B.; Schmincke, H.-U. *Zeit. Krist.* **1976**, *143*, 156.
206. Miehe, G.; Graetsch, H. *Eur. J. Mineral.* **1992**, *4*, 693.
207. Haines, J.; Chateau, C.; Léger, J.-M.; Le Sauze, A.; Diot, N.; Marchand, R.; Hull, S. *Acta Crystallogr.*, **1999**, *B55*, 677.
208. Marchand, R. Private communication, 1999.
209. Marchand, R. *J. Non-Cryst. Solids* **1983**, *56*, 173.
210. Brow, R. K.; Peng, Y. B.; Day, D. E. *J. Non-Cryst. Solids* **1990**, *126*, 231.
211. Boukbir, L.; Marchand, R. *Rev. Chim. Minér.* **1986**, *23*, 343.
212. Dang Tran Quan; Le Bloa, A.; Hbib, H.; Bonnaud, O.; Meinel, J.; Quémerais, A.; Marchand, R. *Rev. Phys. Appl.* **1989**, *24*, 545.
213. Dang Tran Quan; Hbib, H. *J. Solid-St. Electron.* **1993**, *36*(3), 339.
214. Hbib, H.; Bonnaud, O.; Quémerais, A.; Gauneau, M.; Adam, J.-L.; Marchand, R. *J. Phys. III France* **1996**, *6*, 1489.
215. Hbib, H.; Bonnaud, O.; Gauneau, M.; Hamedi, L.; Marchand, R.; Quémerais, A. *Thin Solid Films* **1997**, *310*, 1.
216. Tacke, P.; Neuray, D.; Michael, D. U.S. Patent No. 4,177,185, 1979.
217. Millers, T.; Vitola, A. "Inorganic Compounds of Phosphorus with Nitrogen"; Zinatne: Riga, 1986.
218. Feldmann, W. *Z. Chem.* **1987**, *27*, 100.
219. Feldmann, W. *Z. Chem.* **1987**, *27*, 182.
220. Conanec, R.; Feldmann, W.; Marchand, R.; Laurent, Y. *J. Solid State Chem.* **1996**, *121*, 418.
221. Conanec, R.; L'Haridon, P.; Feldmann, W.; Marchand, R.; Laurent, Y. *Eur. J. Solid State Inorg. Chem.* **1994**, *31*, 13.
222. Peltier-Baron, V.; Feldmann, W.; L'Haridon, P.; Deniard, P.; Brec, R.; Marchand, R. Proc. Int. Symp. on Nitrides II, Limerick (Ireland), 1998.
223. Feldmann, W.; L'Haridon, P.; Marchand, R. *J. Solid State Chem.*, in press.
224. Marchand, R.; L'Haridon, P.; Feldmann, W. Proc. Third. Int. Symp. Inorganic Phosphate Materials, Lille (France), 1999.
225. Feldmann, W.; Conanec, R.; L'Haridon, P.; Marchand, R. Proc. Int. Symp. on Nitrides, Saint-Malo (France), 1996.
226. Marchand, R. *C.R. Acad. Sc. Paris* **1982**, *294*, 91.
227. Boukbir, L.; Marchand, R.; Laurent, Y.; Zhang Jin Chao; Parent, C.; Le Flem, G. *J. Solid State Chem.* **1990**, *87*, 423.
228. Marchand, R.; Feldmann, W.; Guéguen, E. Proc. GDCh Haupttagung, Hamburg (Germany), 1993.
229. Feldmann, W. *Phosphorus, Sulfur and Silicon* **1990**, *51/52*, 141.
230. Conanec, R.; Marchand, R.; Laurent, Y. *High Temp. Chem. Processes* **1992**, *1*, 157.
231. Kearby, K. Proc. 2nd Congr. Catal. Paris, Technip, 1961, 397.
232. Conanec, R. Ph.D. Thesis, Univ. Rennes (France), 1994.
233. Grange, P.; Bastians, P.; Conanec, R.; Marchand, R.; Laurent, Y.; Gandia, L. M.; Montes, M.; Fernandez, J.; Odriozola, J. A. *Stud Surf. Sci. Catal.* **1995**, *91*, 381.

- 234. Massinon, A.; Guéguen, E.; Conanec, R.; Marchand, R.; Laurent, Y.; Grange, P. *Stud. Surf. Sci. Catal.* **1996**, *101*, 77.
- 235. Peltier, V.; Conanec, R.; Marchand, R.; Laurent, Y.; Fripiat, N.; Guéguen, E.; Bastians, P.; Grange, P.; Razafindrakoto, J. French Patent No. 96-00533, 1996.
- 236. Marchand, R.; Laurent, Y.; Quéméraires, A. *Rivista della Staz. Sper. Vetro* **1990**, *5*, 101.
- 237. Le Beuze, A.; Lissilour, R.; Quéméraires, A.; Agliz, D.; Marchand, R.; Chermette, H. *Phys. Rev. B* **1989**, *39(15)*, 11055.

MOLECULAR CLUSTERS OF DIMETALATED PRIMARY PHOSPHANES AND ARSANES

MATTHIAS DRIESS

Lehrstuhl für Anorganische Chemie I: Molekül- und Koordinationschemie
Fakultät für Chemie der Ruhr-Universität Bochum, D-44801 Bochum, Germany

- I. Introduction
 - A. Aim and Scope
 - B. Electronic Features and Structural Principles of Molecular Main Group Metal Pnictides
 - C. Structure–Reactivity Relationships in Pnictide Chemistry
- II. Dilithiation and Disodiation of Primary Phosphanes and Arsanes
 - A. Synthesis and Complexation of Dilithium Derivatives
 - B. Synthesis of Lithium-Rich Mixed-Valent Clusters
 - C. Disodium Derivatives and a Tetrasodium Dication Cluster
 - D. X-Ray Structures
 - E. NMR Spectroscopic and Cryoscopic Measurements
 - F. Reactivity
- III. Dicopper Phosphandiides
 - A. Synthesis
 - B. X-Ray Structure
- IV. Magnesium Phosphandiides
 - A. Synthesis of a Solvent-Free Derivative
 - B. Synthesis of a Solvated Derivative
 - C. X-Ray Structures
- V. Tin(II) Metalated Phosphandiides
 - A. Synthesis
 - B. NMR Spectroscopic Characterization
 - C. Molecular Structures
- VI. Aluminum, Gallium, and Indium Phosphandiides and Arsandiides
 - A. Synthesis
 - B. NMR Spectroscopic Characterization
 - C. X-Ray Structures
- VII. Mixed-Metalated Phosphandiides and Arsandiides
 - A. Synthesis of Li/Al-Mixed Derivatives
 - B. Synthesis of Li/Sn-, Li/Sb- and Ca/Sn-Mixed Clusters
 - C. Dynamic Processes in Solution
 - D. X-Ray Structures
- VIII. Conclusion
- References

I. Introduction

A. AIM AND SCOPE

Metalated compounds of the main Group 5 elements (pnictogens) play an important role in organometallic synthesis. Especially lithium derivatives deserve attention as key reagents for many pnictide transformations and acid–base reactions. However, while metalated amides have been best investigated in terms of structure–reactivity relationships, which has been documented in an excellent review (1), the respective structural and reactivity aspects for the heavier congeners are much less explored. In fact, molecular monometalated phosphanides and arsanides are valuable nucleophilic phosphorus and arsenic transfer reagents for the introduction of phosphaneyl and arsaneyl groups into diversely functionalized systems, but knowledge of their structure–selectivity properties seems relatively scarce (2). Not only that, the first structural insight into the chemistry of molecular dimetalated primary phosphanes and arsanes was not developed until 1996, when the first structures of dilithium derivatives of primary phosphanes and arsanes were reported (3). That this fairly young class of compounds is of considerable interest cannot be denied: Molecular dimetalated phosphanes and arsanes are one of the most reactive nucleophilic phosphorus and arsenic transfer reagents, which, however, are usually obtained in the form of amorphous and insoluble solids (4–7). Their tendency to aggregate lies between that of monometalated derivatives and typical solid state structures of binary main group metal pnictides (e.g., Li_3P) (2, 8). Thus, they can be regarded as intermediates between molecular clusters and typical solid-state compounds in the pnictide series. This review summarizes mainly structural features observed so far for metal-rich, molecular pnictide clusters, containing metal atoms of Groups 1, 2, 3, and 4. Soluble, discrete cluster compounds of the phosphandiide and arsanidiide series are of interest, since they also represent a new class of “container molecules” that can adopt a large variety of cluster shapes. The discovery of spherical molecular host compounds, which easily form inclusion compounds, represents one of the promising topics in supramolecular chemistry. Some fascinating aspects and challenges in how to design shapes and functions of globular clusters have been explained in a recent detailed review (9).

B. ELECTRONIC FEATURES AND STRUCTURAL PRINCIPLES OF MOLECULAR MAIN GROUP METAL PNICTIDES

The ionic character of main group metal–pnictogen bonds with alkali and alkaline earth metals (Groups 1, 2) is relatively large (>90%) because of the huge differences in electronegativities, whereas Group 3 and 4 metals possess more covalent properties. The presence of lone pair electrons at the pnictogen atom adjacent to coordinatively unsaturated metal center in monomeric metalated amines and their homologues strongly favors intermolecular head-to-tail oligomerization to give molecular aggregates. Such clustering is typically seen if electron precise and electron deficient centers are present in a molecule at the same time. While the ionicity of Group 1 and 2 amides, phosphanides, and their congeners primarily determines their structural chemistry, the oligomeric structures of molecular Group 3 and 4 pnictide compounds are more influenced by steric demand of the substituents and

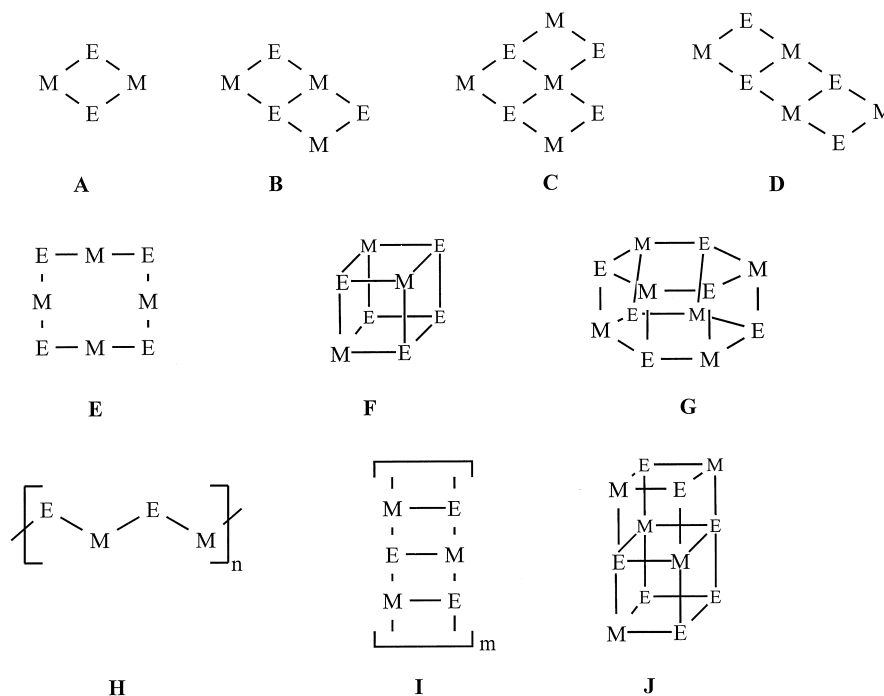


FIG. 1. Structural motifs of metal pnictides: two- and three-dimensional (ladder-like aggregation).

strain effects. The resulting aggregates adopt the different types of cluster structures **A–J** depending on the nature of the metal (atom/ion size, partial charge, polarizability), steric demands of the substituents, and solvation of the metal centers, which has also been seen for other metal–heteroatom associates (Fig. 1) (2). Extensive theoretical studies of aggregates of lithium compounds, which represent the most basic reagents in synthetic chemistry, bear witness to the importance of steric and electronic effects (e.g., nature of the pnictogen atom, solvation effects) (10).

Hitherto no monometalated molecular pnictide exists without solvation of the main group metal atom. Therefore, the monomeric species **L** (Fig. 2) can only be stabilized if the Li ion has its coordination sphere enlarged through donor solvation. More importantly, the lithium phosphanides of the type **K** undergo oligomerization processes to form dimer, tetramer, hexamer, or polymeric assemblies **M–Q** (Fig. 2), which dissociate in solution more easily than related amides (2, 11, 12).

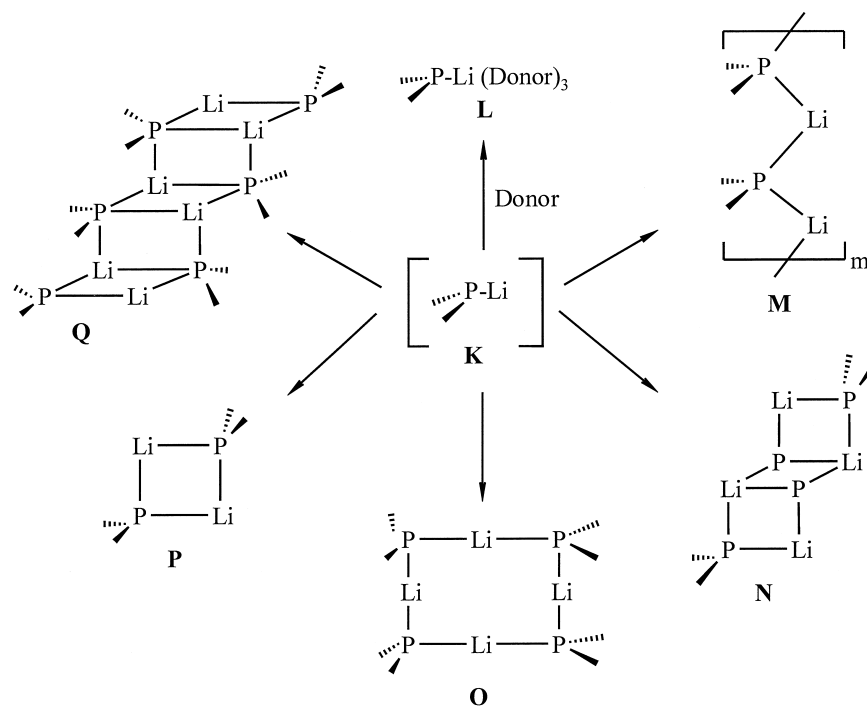
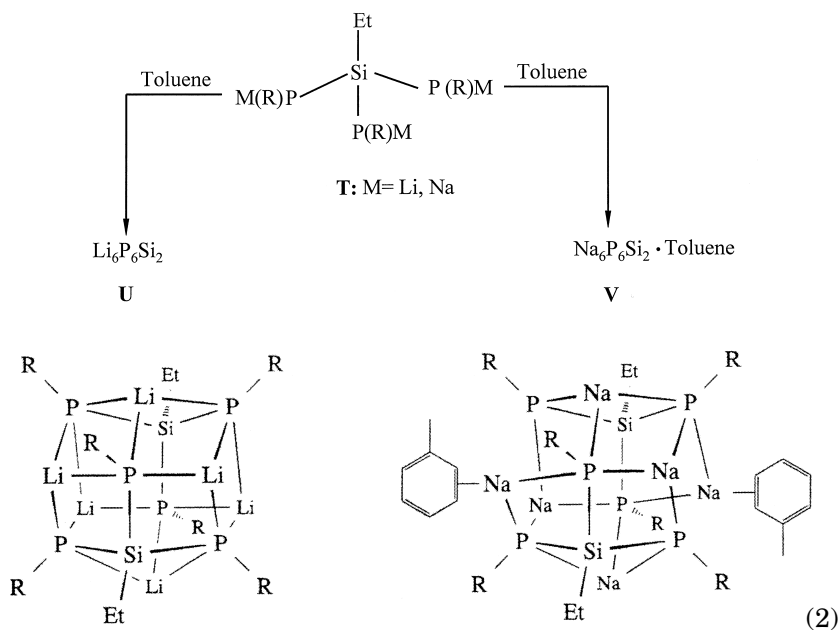
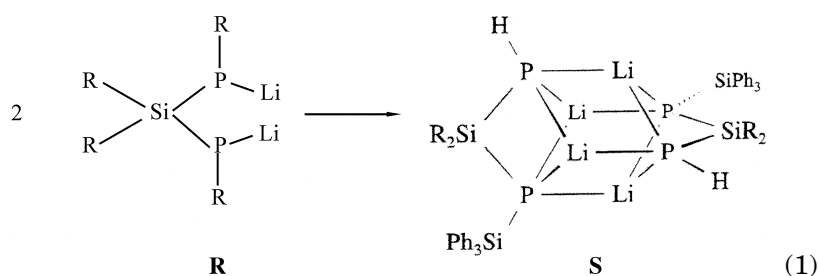


FIG. 2. Oligomerization products **L–Q** depending on donor solvation and size of the PR_2 groups in **K**.

The aggregates of the type **N** and **Q** possess ladder-like, two-dimensional structures whose size is strongly dependent on the degree of solvation of the lithium center and the steric demand of the silyl group. Because of the lipophilicity of the trimethylsilyl ligands and other organosubstituted silyl groups, the degree of association and the solubility of the resulting clusters can be controlled in various ways. For topological reasons, self-assembly processes lead in the case of bis- and tris(lithium pnictide-yl) silanes to aggregates which adopt *per se* three-dimensional ladder-like skeletons. Of particular interest seems the dimerization of **R** and **T**, which furnished the clusters **S**, **U**, and **V**, respectively, having a rhombododecahedral framework (13):



A cluster framework such as that seen in **U** has also been observed for its heavier homologues (14). Apparently, the latter topology is the result of a close packing of anionic pnictide moieties with alkali metal ions that maximizes ionic interactions. The topology of the rhombododecahedral $\text{Li}_6\text{P}_6\text{Si}_2$ framework in **U** has been simply described as a P_6 octahedron representing the anionic partial structure, of which the triangular faces are capped by two μ_3 -RSi moieties and six μ_3 -Li ions as "counterion" partial structure (Fig. 3).

As expected, three-dimensional aggregates, possessing ladder-like closed structures, have also been formed for dimetalated amines, phosphanes, and their congeners. However, only one dilithium derivative of a primary amine could be structurally elucidated thus far: The dilithium azandiide of α -naphthylamine furnishes in Et_2O the decameric form **W**, which consists of a $\text{N}_{10}\text{Li}_{14}$ cluster framework (Fig. 4) (15). The latter framework can be described as composed of two face-fused rhombododecahedra that coordinate to the remaining six exohedral $\text{Li}(\text{OEt}_2)$ groups. This clearly demonstrates that the "oligomer-laddering" model is retained as a basic structural principle even for multivalent molecular pnictides.

C. STRUCTURE-REACTIVITY RELATIONSHIPS IN PNICTIDE CHEMISTRY

It has been expected that reactivity of metalated pnictides is strongly dependent on the degree of association. One consequence is that the basicity of amides has been correlated with the grade of association by means of extensive ^7Li and ^{15}N NMR investigations (16, 17). In contrast, knowledge of structure-reactivity relationships for

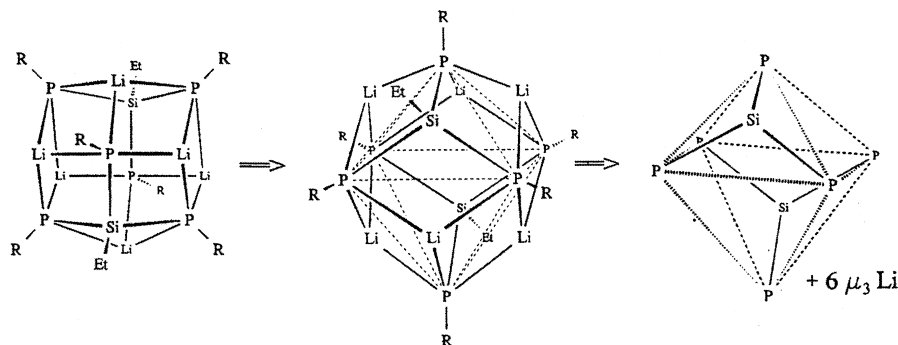


FIG. 3. Topological description of the $\text{Li}_6\text{P}_6\text{Si}_2$ rhombododecahedron face-capped P_6 octahedron.

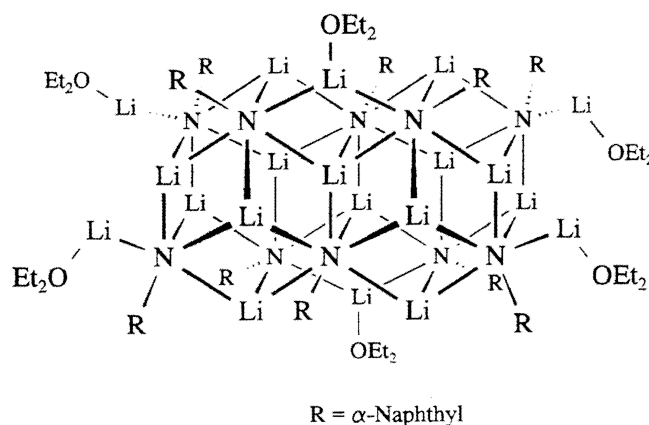


FIG. 4. $N_{10}Li_{14}$ framework of the $(RNLi_2)_{10}(Et_2O)_6$ cluster **W**.

phosphanides and arsanides is scarce. Only a few $^{6/7}Li$ and ^{31}P NMR investigations have been undertaken in order to ascertain the dissociation behavior of simple lithium phosphanides (18), but neither a quantitative correlation with their reactivity nor investigations on Li-As dissociation for lithium arsanides have been reported thus far.

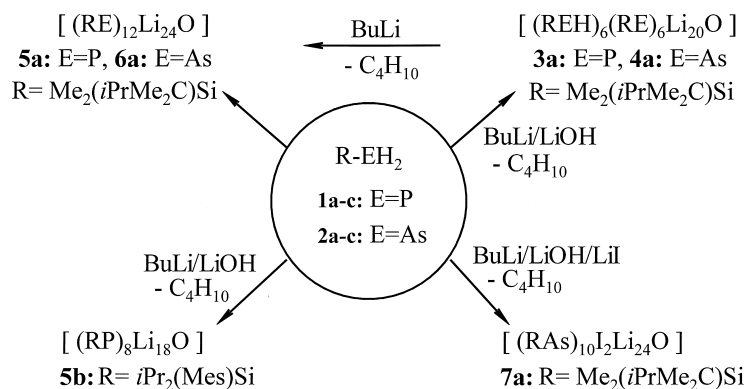
II. Dilithiation and Disodiation of Primary Phosphanes and Arsanes

The considerably strong tendency of dimetalated Group 1 metal derivatives of primary phosphanes and arsanes has been hampered by the lack of isolable crystalline material. Thus, dilithiation of the organophosphanes RPH_2 ($R = Ph$, cyclohexyl) with $PhLi$ in Et_2O or other polar solvents has led to amorphous and insoluble $RPLi_2$ (4). Similarly, the same reaction with more lipophilic substituted phosphanes such as $MesPH_2$ ($Mes = 2,4,6-Me_3C_6H_2$) (19) or Mes^*PH_2 ($Mes^* = 2,4,6-tBu_3C_6H_2$) (20) has also given unsatisfactory results. Only the employment of triorganosilyl groups at phosphorus and arsenic in respective silylphosphanes and silylarsanes solved this problem because of the stronger E-H acidity ($E = P, As$) as well as the higher solubility of the dimetalated derivatives in hydrocarbon and ethereal solvents (3). However, only the corresponding complexes with Li_2O (Li_2O inclusion compounds) and redox reactions under partial H_2 elimination have been isolated. The latter led, for first time, to mixed-valent lithium-rich pnictides (21).

A. SYNTHESIS AND COMPLEXATION OF DILITHIUM DERIVATIVES

Dilithiated primary phosphanes could only be isolated in a reproducible crystalline form if the lithiation of the phosphane with BuLi (ratio of 1:2) in toluene was carried out in the presence of a trace amount of LiOH (3). This is evident by the respective transformation of the silylphosphanes **1**, which furnished, depending on the steric demand of the silyl group, a dodecameric or an octameric associate (Scheme 1). Thus, reaction of **1a** with BuLi in the molar ratio of 1:2 led to the globular, Li₂O-filled cluster **5a**, whereas metalation of the bulkier substituted phosphane **1b** gave the Li₂O-filled octamer **5b**.

It seems clear that LiOH/Li₂O serves as template during the formation of the closed clusters. This has been corroborated by the partial lithiation of **1a** with BuLi in the molar ratio of 2:3, which furnished colorless crystals of the intermediate **3a**. Complete lithiation of **3a** led to yellow crystals of **5a** in 86% yield (Scheme 1) (21). The analogous intermediate **4a** has been accessible in the same procedure, starting from the corresponding arsane **2a**, and its complete lithiation furnished the cluster **6a** in 82% yield in the form of orange-yellow crystals that are isotypic with **5a**. Interestingly, dilithiation of the arsane **2a** with BuLi in the presence of little LiOH and molar excess of LiI formed the unusual decameric arsandiide cluster **7a** (Scheme 1) in moderate yield, which possesses a shell-like framework as the derivatives **5** and **6**, but the icosahedral anionic arsandiide shell has been completed by two iodide centers (see Section II,D). The extremely congested silylphosphane **1d** could not be transformed in the presence of



SCHEME 1. Synthesis of the lithium-rich clusters **3a–6a**, **5b**, and **7a**, starting from the primary silylphosphanes **1a–1c**, and **2a–2e**.

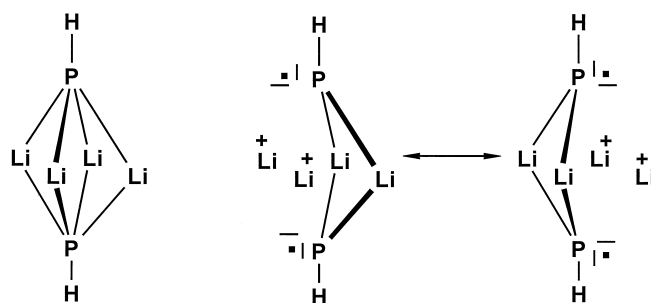
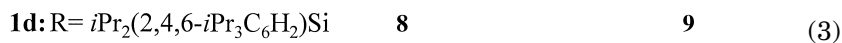
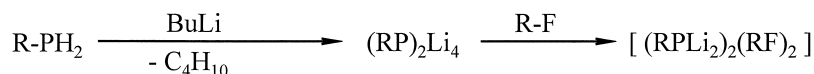


FIG. 5. *Ab initio* optimized structure of $(\text{HPLi}_2)_2$ and its NBO-Lewis resonance structure.

LiOH to a crystalline, Li_2O -containing dilithium derivative. However, the dilithiation of **1d** under rigorous exclusion of donors led to the donor-free dimer **8**, whose composition has been determined by cryoscopy, and its constitution has merely been corroborated by NMR spectroscopy. However, its synthesis in the presence of the bulky triorgano-fluorosilane $i\text{Pr}_2(2,4,6-i\text{Pr}_3\text{C}_6\text{H}_2)\text{SiF}$ formed the corresponding complex **9**, which adopts a ladder-like structure (Eq. 3) as proven by X-ray crystallography (22).

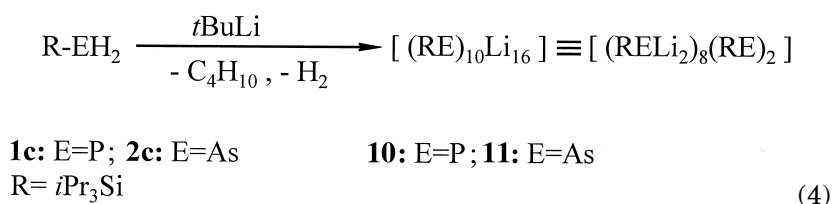


Ab initio calculations (MP2/6-31G*) of the parent compound of **8** revealed that the most stable arrangement of the dimer adopts D_{4h} symmetry (Fig. 5). Interestingly, the four Li ions and the two phosphorus centers constitute an octahedral skeleton with relatively short Li–Li and Li–P distances of 2.645 and 2.458 Å, respectively. Charge analysis (22) undoubtedly supports the electrostatic bonding model for this system because of the high net charges of the natural atomic orbitals (NBO) at Li (+0.768) and P (−1.583), while NBO-Lewis resonance structures support stabilization through delocalization (Fig. 5).

B. SYNTHESIS OF LITHIUM-DEFICIENT MIXED-VALENT CLUSTERS

Reaction of the phosphane **1a** and the arsane **2a** with freshly sublimed *t*BuLi in the molar ratio of 1:2 in toluene as solvent at -80°C

led to yellow, octahedral crystals of the decameric clusters **10** and **11** in 75 and 68% yield, respectively (Eq. 4) (21). Remarkably, molecular hydrogen has been evolved concomitantly, implying the occurrence of a redox reaction during the lithiation. Indeed, **8** and **9** represent lithium-poor, mixed-valent phosphandiide and arsandiide clusters, having a Li:E ratio (E = P, As) of only 1.6:1. No remaining E–H bonds are left in **8** and **9**, which has subsequently been proven by ^1H NMR and IR spectroscopy. It is also noteworthy that the same clusters have been formed if **1a** and **2a** have been added in molar deficiency to the solution of *t*BuLi in toluene at -80°C . Apparently the formation of a closed cluster framework is favored, leading to an E–H activation of the endothermic E–H bonds (23) and reductive H_2 elimination during the lithiation process.

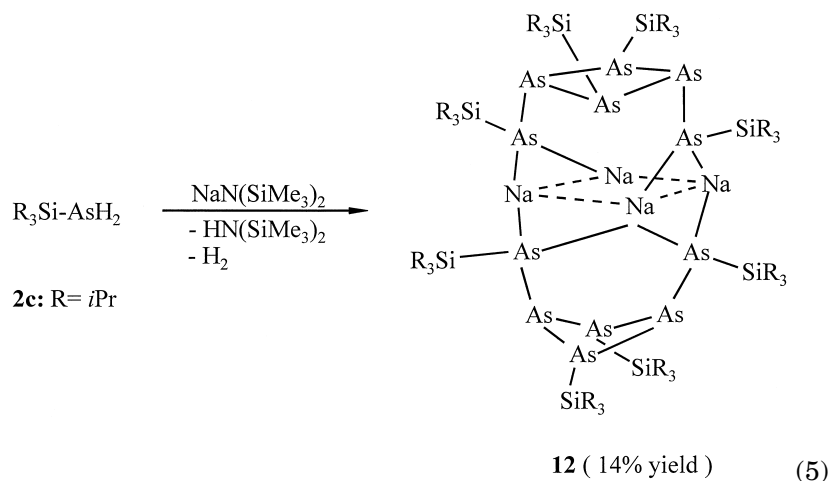


The electrostatically favored cation (Li) and anion (RE) arrangement implies the presence of two different E-, Si- and Li sorts, which has been established by solution and solid-state NMR spectroscopy. The electronic structures of the mixed-valent pnictides **10** and **11** have been simply described as electron-deficient clusters with delocalized framework electrons. Formally the latter consist of two low-valent “anediyl” moieties RE: and eight “andiides” $(\text{RE})^{2-}$ (E = P, As). The relatively large E–E distances of $>4 \text{ \AA}$ exclude the occurrence of localized E–E bonds. However, delocalization of the cluster valence electrons is achieved without Li–Li bonds via Li-mediated multiple bonding. Evidence for this has been seen in the NMR spectra (^{31}P , ^7Li , ^{29}Si), which are in accordance with the electron delocalization model (see later discussion).

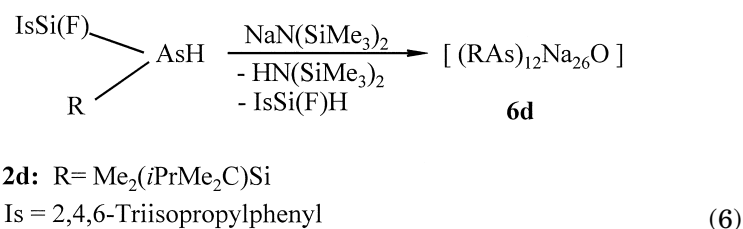
C. DISODIUM DERIVATIVES AND A TETRASODIUM DICATION CLUSTER

The synthesis of crystalline disodium derivatives of primary phosphanes and arsanes turned out to be more difficult than that of dilithium compounds. The reaction of $\text{NaN}(\text{SiMe}_3)_2$ with **2c** led, as in its lithiation with *t*BuLi, under redox reaction (H_2 elimination, As–As bond formation) to the Na_2As_6 dimer **12** (Eq. 5). The latter has been

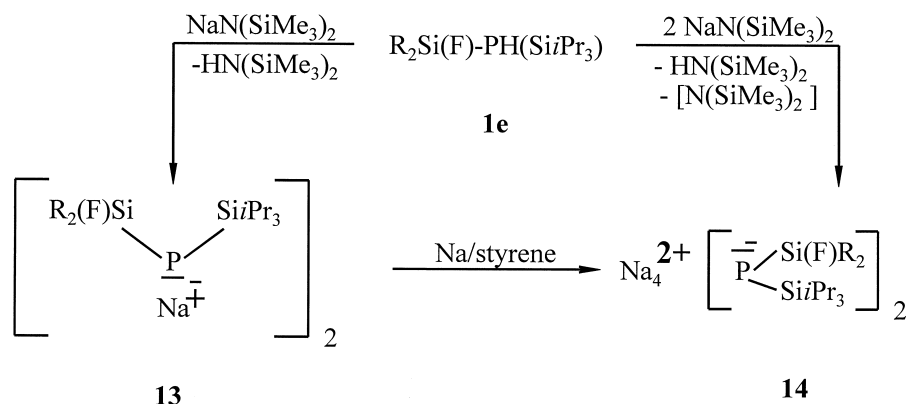
isolated in the form of dark red crystals, which are the only isolable product of this reaction, in ca. 14% yield (**24**).



The strong tendency of silylarsanes to undergo redox reactions with basic and nucleophilic reagents seems to be responsible for the reaction of sterically congested silyl(fluorosilyl)arsane **2d** with $\text{NaN}(\text{SiMe}_3)_2$ in toluene over several days, which led to the **6a** analogue dodecameric disodium salt **6d** (Eq. 6) (25). The latter contains one molecule of Na_2O that is incorporated in the void of the dodecamer, giving a distorted $[\text{Na}_6\text{O}]^{4+}$ core (see Section II,D).



In contrast, the same reaction between the bulkily substituted silyl(fluorosilyl)phosphane **1e** with $\text{NaN}(\text{SiMe}_3)_2$ underwent, surprisingly, a different course (Scheme 2). Its transformation in the molar ratio of 1:1 in toluene as solvent furnished the dimer **13**, whereas **1d** can only be completely converted to **13** if 2 molar equiv sodium amide have been employed, because of the initial formation of heteroaggregate intermediates (26). Excess of sodium amide has been recovered by

SCHEME 2. Synthesis of dimeric **13** and the Na_4^{2+} salt **14**.

fractional crystallization. However, if the reaction is performed at 60°C during prolonged reaction time (**2d**), the unusual complex **14** is furnished as a side product in 8% yield (Scheme 2) (27).

Compound **14** is diamagnetic and represents the first tetrasodium-dication cluster that is stabilized by two sterically congested silyl(fluorosilyl)phosphanide counterions (see Section II,D). It has been also independently synthesized through sodium consumption of **13** in the presence of styrene as catalyst in 24% yield. The electron reservoir of the Na_4^{2+} cluster can serve for reduction processes, that is, it reduces Me_3SiCl to hexamethyldisilane (see Section II,F). The fact that **14** is intensely yellow, and not red or blue as observed for Na-loaded zeolites (28), suggests that the residual metal electrons are probably much less delocalized.

D. X-RAY STRUCTURES

Instead of giving a comprehensive summary on M–E and E–E distances ($\text{M} = \text{Li}, \text{Na}$; $\text{E} = \text{P}, \text{As}$) for the compounds discussed earlier, this section mainly presents considerable structural features. A comprehensive discussion of the characteristic structural aspects of main group metalated phosphanes and arsanes has been published in an excellent review (2).

1. Li_2O -, Na_2O -, and Fluoride-Complexed Clusters

The Li_2O -filled dodecameric clusters **5a** and **6a** are isotypic and crystallize in the monoclinic space group $P2_1/n$. Their structures are topologically best described as ionogenic aggregates formed by three

closed (platonic) shells that are covered by lipophilic triorganosilyl groups (Fig. 6) (3, 21). The E-centers ($E = \text{P}, \text{As}$) form a slightly distorted E_{12} icosahedron, in which each of the 20 triangular faces is capped by a Li center. The 20 Li centers thereby adopt a pentagondodecahedron as dual polyhedron with approximately I_h point symmetry.

The remaining four Li centers are located in the void of the interpenetrating double shells ($E_{12}\text{Li}_{20}$) $^{4-}$ (diameter ca. 8 Å). These Li centers are complexed by an encapsulated Li_2O molecule leading to the formation of a $[\text{Li}_6\text{O}]^{4+}$ octahedral core. This core has approximately O_h symmetry and is tilted with respect to the orientation of the E_{12} icosahedron. Interestingly, a C_3 axis of the octahedron coincides with a C_3 axis of the Li_{20} shell (Fig. 6). Sixfold coordination of O^{2-} by metal ions in molecular compounds is relatively rare (29–31). The Li centers of the inner Li_6O core are, as expected, still coordinated to E centers in close proximity. Therefore, their coordination numbers are 4 and 3, whereas the “external” 20 Li centers are three-coordinated. The averaged Li–O distances in **5a** and **6a** (1.86, 1.87 Å) are practically identical and unremarkable. The related aggregates **3a** and **4a** crystallize triclinic in the space group $P\bar{1}$ (21). Although the incompletely lithiated clusters **3a** and **4a** have a shell structure analogous to that of **5a** and **6a** (Fig. 7), they merely possess an Li_2O core. The Li centers of the latter are still coordinated to three nearby E centers, that is, they are four-coordinated. In contrast, the “external” 18 Li centers are three-coordinate and this leads to differently coordinated E atoms with coordination numbers of 5, 6, and 7.

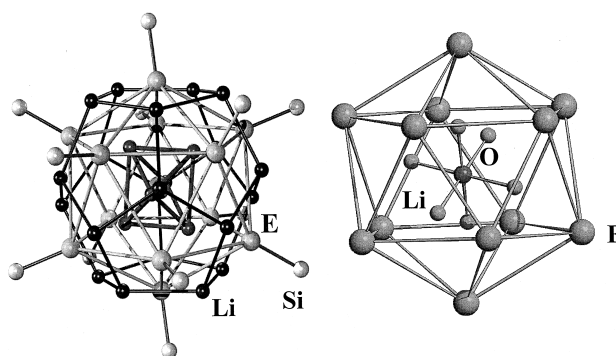


FIG. 6. (Left) Representation of the shell-like form of **5a** and **6a** in the crystal (without the organic groups). (Right) Connection of the Li_6O octahedron with the E-centers ($E = \text{P}, \text{As}$). [Reprinted with permission from (3). Copyright 1996, Wiley-VCH.]

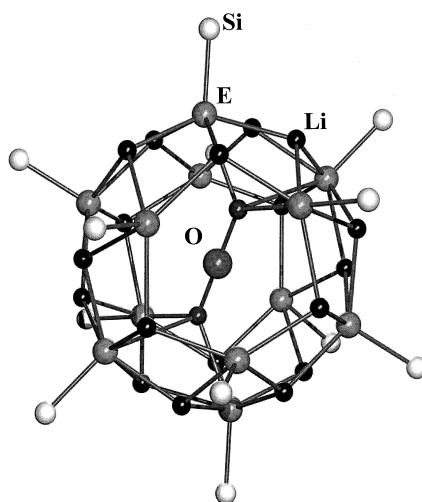


FIG. 7. Representation of the wheel-like clusters **3a** and **4a** in solid state (without the organic groups).

The “open” clusters **3a** and **4a** consists of a three-dimensional, wheel-like $E_{12}Li_{18}$ ladder framework whereby the Li_2O molecule in its void may be regarded as a “stabilizing axis” of the wheel. The remaining E–H hydrogen atoms are probably located on E atoms of the hexagonal E_3Li_3 holes. Even larger triorganosilyl groups at phosphorus lead to aggregates with a smaller degree of association, as shown for the octameric phosphandiide cluster **5b** (Fig. 8) (3). It crystallizes

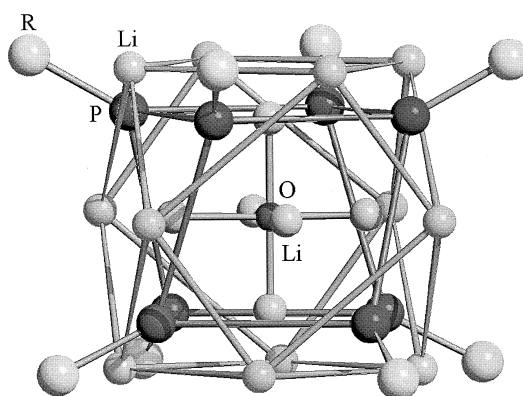


FIG. 8. Representation of the shell-like form of **5b**. For clarity, the silyl groups have been omitted. [Reprinted with permission from (3). Copyright 1996, Wiley-VCH.]

tetragonal in the space group $P4/n$ and consists of three ionic shells. The eight P atoms of the anionic shell comprise a strongly distorted cube, which is surrounded by a Li_{12} unit that additionally surrounds a Li_6O octahedron. The Li–O distances (1.81–1.90(2) Å) are, as expected, significantly shorter than in solid Li_2O (1.98 Å).

The Li centers of the Li_{12} unit are located on the edges of the P_8 framework, whereas the Li centers of the Li_6O core are each located over a face. This situation led to different coordination numbers (2 vs 4) for the two types of Li centers, implying much shorter Li–P bonds for the “external” ones (Δ ca. 0.2 Å). That some of the 12 As centers of the anionic icosahedral partial structure in **6a** can be replaced by other anions has only recently been demonstrated (32). Thus, **7a** crystallizes in the monoclinic space group $P2_1/n$ and possesses a slightly distorted anionic icosahedral framework, which is identical to that observed for **6a**, but two of the $(\text{AsR})^{2-}$ units are replaced by iodide centers (Fig. 9).

The O^{2-} center of the encapsulated Li_2O is only square-planar coordinated because of the lower lithium content. However, the four Li centers of the Li_4O core are disordered. This disordering of the metal-coordinated O^{2-} center has also been seen in the case of the first dodecameric disodium arsandiide– Na_2O complex (Fig. 10) (25). Whereas the positions of the “outer” Na centers have been precisely located, the six “inner” Na centers can adopt 20 equivalent sites. This is probably due to the larger void of the $\text{As}_{12}\text{Na}_{20}$ double shells. However, the origin of this disorder (static and/or dynamic) is not yet known.

The dilithium phosphandiide dimer **9** is complexed by two molecules of a fluorosilane. The complex crystallizes in the monoclinic space group $P2_1/n$. The framework of the aggregate consists of a cen-

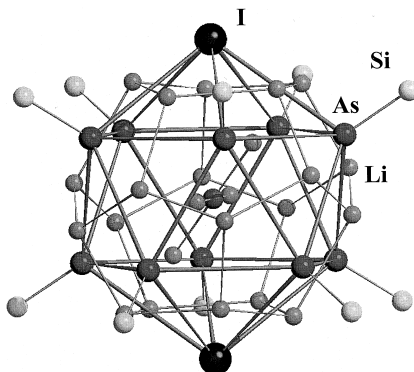


FIG. 9. $\text{As}_{10}\text{I}_2\text{Li}_{24}\text{O}$ -framework of the cluster **7a** in solid state.

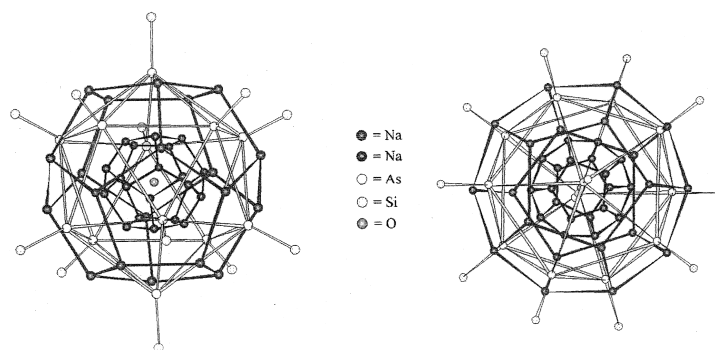


FIG. 10. (Left) Representation of the shell-like form of **6d** in the crystal (without the organic groups). The Na_6O octahedron is disordered. (Right) Side view of **6d**.

trosymmetric dimer with a ladder-like $\text{P}_2\text{Li}_4\text{F}_2$ structure, of which each fluorine atom acts as a bridging donor center toward two Li centers (Fig. 11) (22).

The electronic stabilization of the Li centers is also achieved by Li–H–C and Li–C interactions with methyl groups and π bonds of the

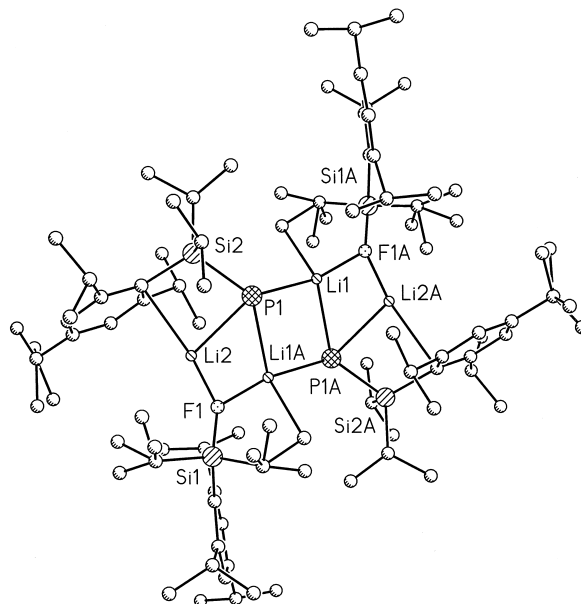


FIG. 11. Molecular structure of the $\text{P}_2\text{Li}_4\text{F}_2$ cluster in **9**. [Reprinted with permission from (22). Copyright 1996, Royal Society of Chemistry.]

aryl groups, respectively, in close proximity. Interestingly, the unusual coordination geometry of the P center, which is mainly due to its steric congestion, suggests that its lone-pair electrons are not involved in the coordination of the Li centers close by. The relatively short Li1–Li2' distance (2.569(9) Å) and the acute Li2–F1–Li1' (90.4(3)°) and Li1'–P1–Li2 angles (58.8(2)°) may explain that the Li centers prefer Li–Li–P three-center–two-electron interactions. However, such a bonding mode is thus far unknown for molecular monolithium pnictide aggregates (1, 2).

2. Mixed-Valent Clusters

The intensely yellow compounds **10** and **11** crystallize in the tetragonal space group $P4/nnc$. The oval $E_{10}Li_{16}$ cluster skeleton ($E = P, As$) is topologically best described as a twofold capped Archimedean antiprism formed by the 10 E atoms, of which each of the 16 triangular faces are occupied by a lithium center (Fig. 12) (21).

Thereby two of the E-centers result in five-coordination, whereas the remaining eight are six-coordinated. However, the respective average Li–E, Si–E, and Li–Li distances are unremarkable with respect to the values in **3a**, **4a**, **5a**, and **6a** (3, 21), and the Li–E distances differ only marginally. Since the relatively large E–E distances (>4 Å) disfavor E–E bonds, the delocalization of the cluster electrons is achieved through Li-mediated multiple center bonds without the involvement of direct Li–Li bonds. Evidence for the latter is seen in

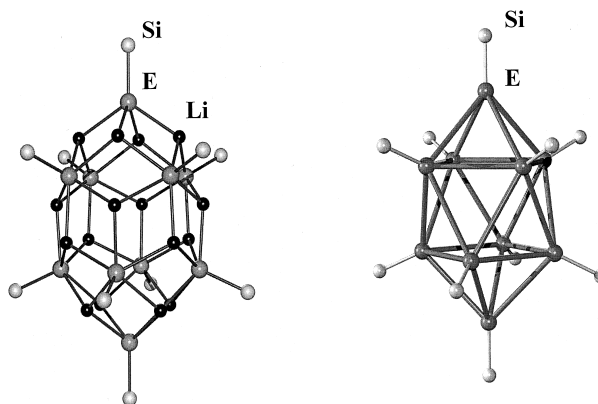


FIG. 12. (Left) Molecular structure of the mixed-valent cluster **10** and **11** in the crystal. (Right) Representation of the E_{10} -dicapped-Archimedean antiprism as anionic partial structure in **10** and **11** ($E = P, As$). For clarity the organic groups of the silyl groups have been omitted.

the unremarkable ^7Li chemical shifts in the CP/MAS ^7Li solid state NMR spectrum (see Section II,E).

3. The Dimeric $\text{Na}_4\text{As}_{12}$ Cluster **12** and the Tetrasodium-Dication Cluster in **14**

Compound **12** represents the first aggregate of a solvent-free sodium polyarsanide that has been elucidated by X-ray diffraction analysis (Fig. 13) (24).

The centrosymmetric dimer consists of four sodium centers that are embedded between the two $(\text{As}_6)^{2-}$ ligands. Interestingly, the unusual two-coordinated Na ions are only bonded to the anionic, exocyclic arsanyl As centers of the cyclotetraarsane-1,4-bis(silylarsanideyl) ligands $[(\text{As}_6)^{2-}]$. The slightly different As–As distances of 2.36 and 2.39 Å are unremarkable and the large Na–Na distances of 3.6–3.8 Å are mainly due to repulsive electrostatic interactions. In contrast, Na–Na bonds are present in the case of the tetrasodium salt **14**. The latter crystallizes in the monoclinic space group $P2_1/n$. The centrosymmetric molecule comprises a rhomboidally distorted planar Na_4 cycle that is the most interesting part of the aggregate (Fig. 14) (27).

The Na–Na distances of 3.076(3) (Na1–Na2) and 3.202(3) Å (Na1–Na1') reflect Na–Na bonds (3.82 Å in elemental Na), whereas the Na1–Na2' distance of 3.530(3) Å suggested less attractive interactions. The Na_4 -dication cluster is embedded between two silyl(fluoro-silyl)phosphanide counterions. The relatively low-coordinated Na centers are remarkably stabilized by the μ_3 -fluorine atoms and by

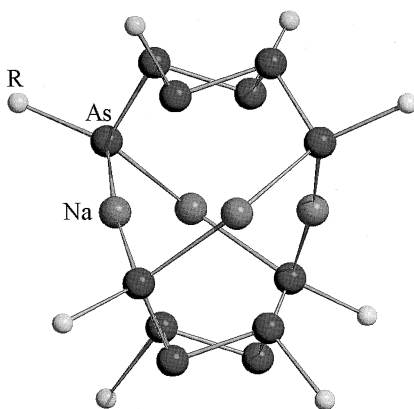


FIG. 13. Molecular structure of **12**. For clarity the organic groups have been omitted.

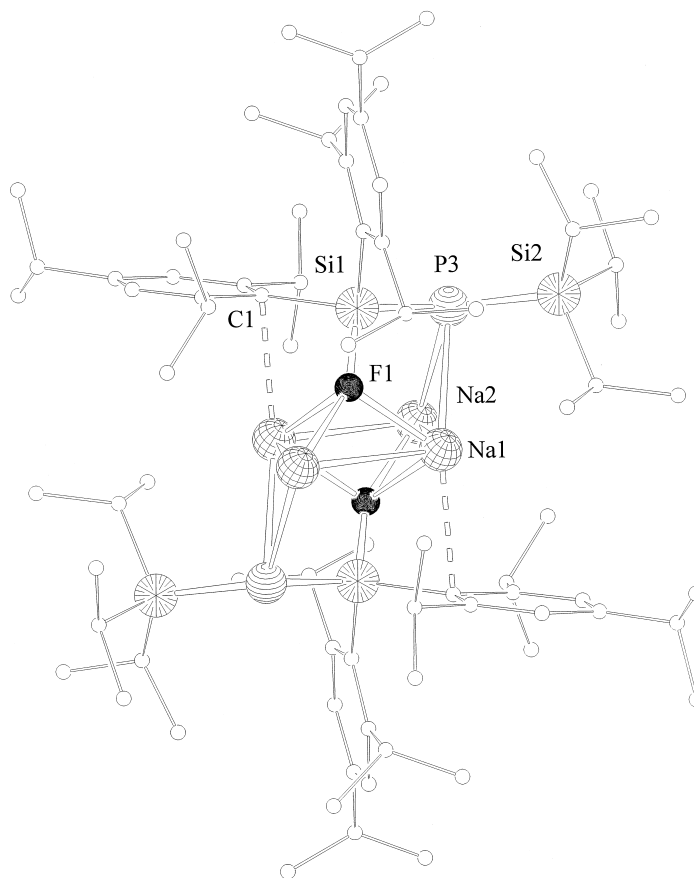


FIG. 14. Molecular structure of the Na_4^{2+} salt **14**. [Reprinted with permission from (27). Copyright 1998, American Chemical Society.]

multiple-center Na–Na–P and *ipso*-C atom interactions. The Na–P distances of 2.911(2) and 2.905(3) Å resemble those values observed for other sodium phosphanides (13, 33, 34).

E. NMR SPECTROSCOPIC AND CRYOSCOPIC MEASUREMENTS

1. Li_2O -, Na_2O -, and Fluoride-Complexed Clusters

The metal pnictides discussed earlier are much more strongly aggregated than those of their monometalated analogues. The latter represent highly flexible systems in solution that undergo fast ion-pair separation processes (2). The multinuclear NMR spectra of the

Li_2O -filled clusters **3a**, **4a**, **5a**, **5b**, and **6a** in toluene or THF (see Table I) suggest that the compounds possess a low tendency for dissociation in solution. The remaining E–H protons (E = P, As) in the incompletely lithiated derivatives **3a** and **4a** are detected in the ^1H NMR spectra (21). Correspondingly, the E–H stretching frequencies for **3a** ($\nu = 1930\text{ cm}^{-1}$) and **4a** ($\nu = 1897\text{ cm}^{-1}$) clearly corroborate the presence of E–H moieties.

The CP/MAS- ^{29}Si solid state NMR spectrum of **6a** proves the presence of six crystallographically (and chemically) different ^{29}Si nuclei, of which two sorts coincide (Fig. 15). It is noteworthy that the ^7Li NMR spectrum of **6a** in solution (Fig. 16) showed the expected distinction of four Li sorts: The two singlets at $\delta = 1.78$ and 1.56 correspond

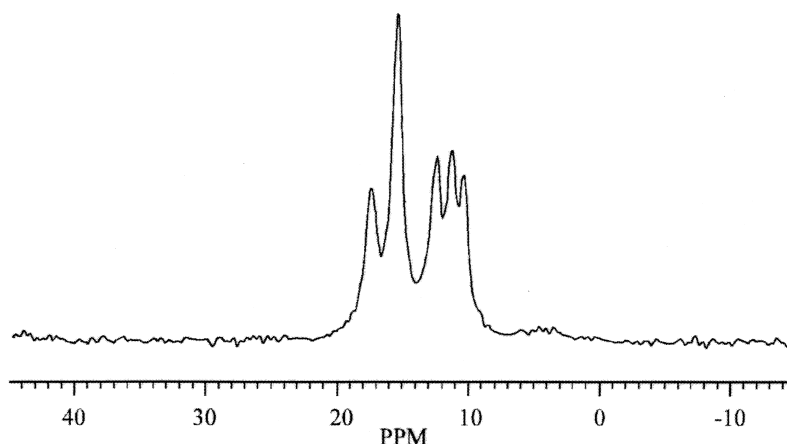
TABLE I

SUMMARY OF SELECTED SOLUTION NMR-SPECTROSCOPIC DATA OF **3a–6a**, **5b**, AND **8–11**
(MULTIPLICITY AND $J[\text{Hz}]$ IN BRACKETS); n.o. = NOT OBSERVED

	$\delta^{29}\text{Si}$	$\delta^{31}\text{P}$	$\delta^7\text{Li}$	$\delta^1\text{H(E-H)}$
3a ^a	n.o.	–301 (d, 152) –362 (br.) –365 (br.)	1.10 (br.) 1.40 (br.) 5.56 (br.)	–1.78 (d, 152)
4a ^a	n.o.	— —	1.05 (br.) 1.61 (br.) 5.21 (br.)	–1.63 (s)
5a ^b	n.o.	–361 (br.) –368 (br.)	2.10 (br.) –0.80 (br.) –1.70 (br.)	—
5b ^b	n.o.	–3.36.9 (br.) –340.1 (br.) –355.9 (br.)	0.9 (br.)	—
6a ^b	17.7 (br.) 11.8 (br.)	—	1.78 (s) 1.55 (s) 0.0 (br.) –1.32 (s)	—
8 ^b	—	–323.2 (br.) –328.6 (br.) –336.6 (br.)	6.4 (br.)	—
9 ^b	—	–307.3 (br.) –319.6 (br.)	5.6 (br.) –4.8 (br.)	—
10 ^b	26.9–28.1 (m)	–366.8 (br.) –368.9 (br.)	1.45 (br.) 1.66 (br.)	—
11 ^b	16.7 (s) 17.5 (s)	—	1.40 (s) 1.68 (s)	—

^a Measured in THF- d_8 .

^b Measured in toluene- d_8 .

FIG. 15. ^{29}Si CP/MAS NMR spectrum of **6a**.

to the Li_{20} shell ("outer" Li centers), whereas the broad signal at $\delta = 0$ and the singlet at $\delta = -1.32$ has been assigned to the "inner" Li centers of the Li_6O core.

Cryoscopic measurements in benzene with different concentrations have demonstrated that the compounds remain undissociated. However, **8** and **9** undergo dissociation in solution as shown by means of NMR and cryoscopic measurements. A relatively strong deshielding of the ^7Li nuclei has been observed for **8** and **9** but also in the case of the incompletely lithiated clusters **3a** and **4a**.

2. Mixed-Valent Clusters

The NMR spectra of **10** and **11** show that the structures are retained in solution (see Table I). Furthermore, the ^{31}P -decoupled CP/MAS- ^{29}Si solid state NMR spectrum of **10** showed two singlets at $\delta = 27.9$ and 29.0 in the ratio of 4:1, whereas the $^7\text{Li}\{^{31}\text{P}\}$ NMR spectrum exhibited two singlets at $\delta = 1.42$ and 1.65 in the expected ratio of 1:1 (35). Cryoscopic measurements have proven that the degree of aggregation of **10** is $n = 8$.

3. The Dimeric $\text{Na}_4\text{As}_{12}$ Cluster **12** and the Tetrasodium-Dication Cluster in **14**

The dimer **12** can only be dissolved in ether solvents, when it undergoes dissociation, as corroborated by cryoscopic measurements and ^{23}Na NMR spectra (24). In contrast, the Na_4 -cluster salt **14** cannot be dissolved in any common organic solvents without decomposition

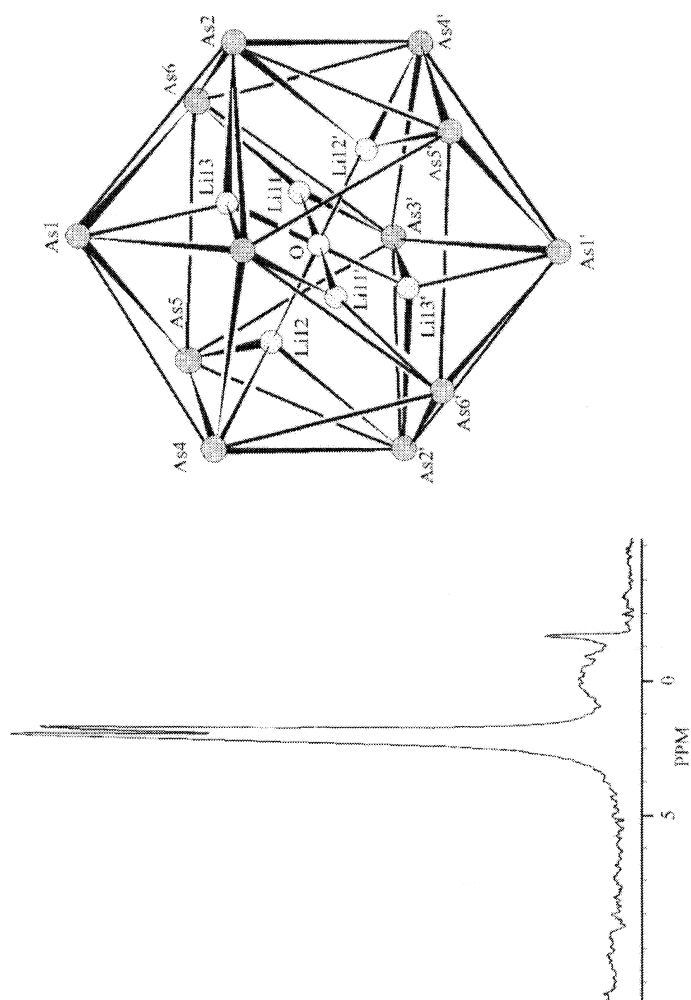


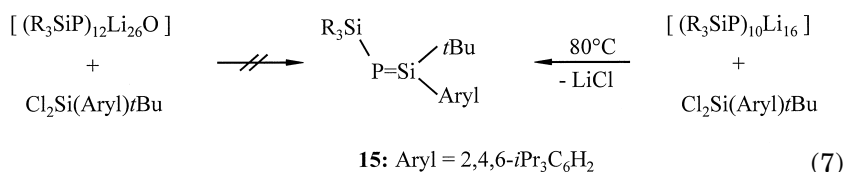
Fig. 16. ^7Li NMR spectrum of **6a** in solution.

(^{31}P and ^{19}F NMR spectroscopy), and attempts to record a CP/MAS solid-state NMR spectrum (^{19}F , ^{31}P , ^{23}Na) failed because of the large line-broadening by the ^{23}Na ions ($I = 3/2$) and strong spin–spin coupling.

F. REACTIVITY

1. Li_2O -Filled Clusters vs Mixed-Valent Clusters

It is instructive to compare the reactivity of the Li_2O -filled alkali metal-rich clusters **5a**, **5b**, and **6a** with that of the related mixed-valent pnictide clusters **10** and **11**, respectively. Since these compounds are highly soluble dilithiated phosphandiide and arsandiide derivatives, they can serve as nucleophilic building blocks in metathesis reactions. A considerable challenge would be their employment as phosphorus and arsenic transfer reagents as demonstrated in the synthesis of metastable phosphasilenes (i.e., compounds with an $\text{Si}=\text{P}$ bond). However, the reactivity of Li_2O -filled vs “empty” mixed-valent clusters toward the bulky substituted dichloro(aryl)-*tert* butylsilanes is remarkably different. In fact, while **5a** reacts with dichloro(isityl)-*tert*-butylsilane (isityl = 2,4,6-*i*- $\text{Pr}_3\text{C}_6\text{H}_2$) in toluene only above 110°C with the formation of several products (no $\text{Si}=\text{P}$ compound was formed), the same reaction with the mixed-valent cluster **10** leads to the desired phosphasilene **15** at 80°C in 55% yield.

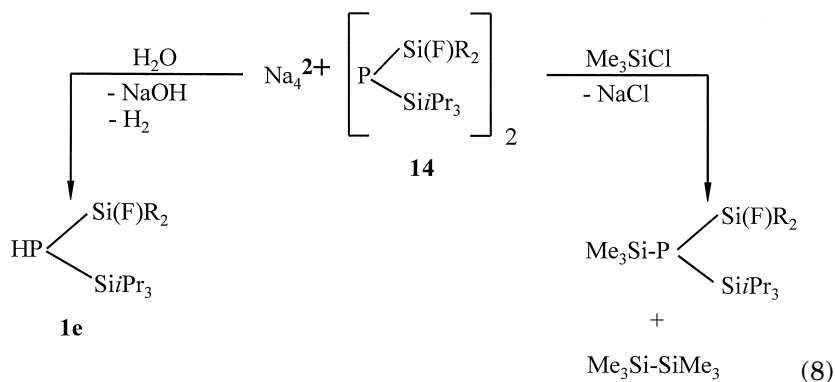


The lower reactivity of **5a** versus **10** reflects the stronger close packing of the anionic and cationic centers than that in the electron deficient cluster **10**. Similar relations have been observed for analogous arsenic compounds (36).

2. Reactivity of the Na_4 -Dication Cluster

Since compound **14** bears two equivalent Na atoms, which can bring about reduction, its reactivity toward Me_3SiCl has been investigated (27). Indeed, the reaction of **14** with 4 molar equivalents of Me_3SiCl furnishes hexamethyldisilane, with reductive Si–Si bond formation, and the corresponding formation of trisilylphosphane (Eq. 8).

Hydrolysis of **14** gives the secondary silyl(fluorosilyl)phosphane **1e**, with evolution of H₂.

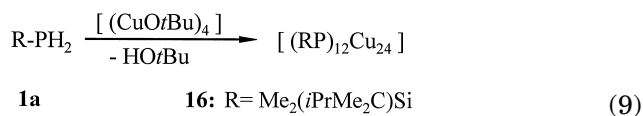


III. Dicopper Phosphandiides

It is a challenge to study dimetalated derivatives of primary phosphanes that possess more covalent metal–phosphorus bonds. This can be achieved through replacement of the alkali metal ions in bimetallic phosphandiides by monovalent coin metal centers.

A. SYNTHESIS

A series of metal-rich, coin-metal containing phosphanediyl clusters (phosphandiides) with additional terminal donor ligands (i.e., triorganophosphanes) have been prepared; only one example of a donor-free dicopper phosphandiide has been reported up to now (37, 38). Thus, the neutral cluster **16** has been prepared by the reaction of the primary phosphane **1a** with CuOtBu in toluene at 60°C and has been isolated in 81% yield in the form of dark red crystals that are only sparingly soluble (39):



The employment of CuOtBu as copper-transfer reagent in this Brønsted acid–base reaction is remarkable. There is no hint of the

formation of a corresponding silyl ether, $R_3SiOtBu$, although the Si–P bond in primary silylphosphanes is usually acid-sensitive. This is probably due to the relatively high P–H acidity of silylphosphanes besides the high steric protection of the Si–P bond in **1a** through its large triorganosilyl group. If the reaction is performed in the presence of LiOH or Cu_2O , no evidence for inclusion or complexation of the oxide is obtained. Thus, the self-assembly process of the formation of Cu_2PR clusters is distinctly different from that of the dialkali metal derivatives, which easily incorporate M_2O ($M = Li, Na$) (see Section II).

B. X-RAY STRUCTURE

The cluster **15**, which crystallizes in the rhombohedral space group $R\bar{3}$, has a remarkably different structure with respect to the structural features of **3a**, **5a**, and **10** (see Section II,D). Although a dodecameric aggregate is present, as is the case for **5a** (21), the cluster framework in **15** does not adopt a globular shape (39). The structure is built up of 24 Cu atoms surrounded by 12 triorganosilylphosphanediyl moieties. The 24-metal-atom cluster consists of three planar Cu_6 rings and two peripheral Cu_3 cycles that all lie parallel to one another (Fig. 17).

The 12 RP fragments cap alternately the Cu_4 faces of the Cu_{24} polyhedron, resulting in fivefold-coordinated phosphorus atoms. This structure resembles that of the recently described $[Cu_{24}(NPh)_{14}]^{4-}$ anionic cluster (40). The Cu–P and Si–P distances are unremarkable. The construction principle of parallel Cu layers to form a metal-like package has also been observed for other Cu clusters (41). The main reason for the different structures of Cu_2PR and Li_2PR clusters is the covalent character of the Cu–P bond, with the additional involvement of favorable Cu–Cu interactions. The latter are probably due to relativistic d^{10} - d^{10} interactions (dispersion-type of interaction) (42, 43).

IV. Magnesium Phosphandiides

Since the Mg–P bond is probably as ionic as the Li–P bond, it is expected that the structural features of their aggregates are very similar. However, structurally characterized magnesium phosphanides are scarce (44–46). Only recently have the first magnesium phosphandiides been prepared and structurally characterized (47, 48).

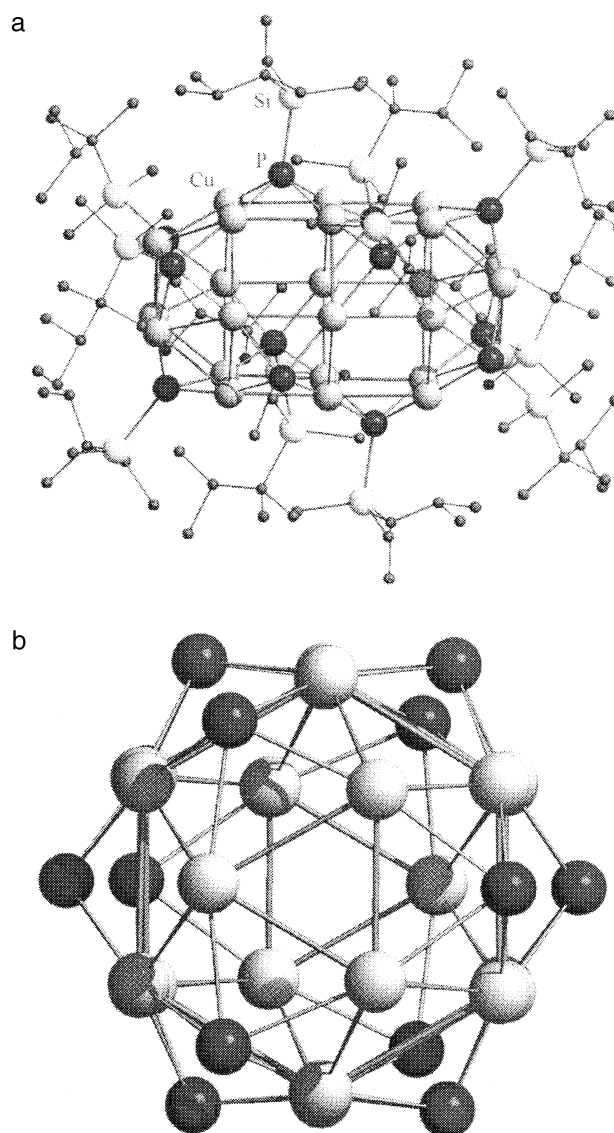
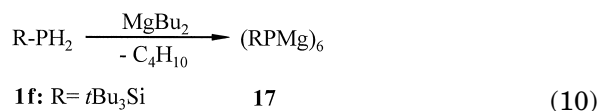


FIG. 17. (a) Structure of **16**. (b) Projection of the $\text{Cu}_{24}\text{P}_{12}$ cluster of **16** along the parallel Cu_3 and Cu_6 rings. [Reprinted with permission from (39). Copyright 1997, Wiley-VCH.]

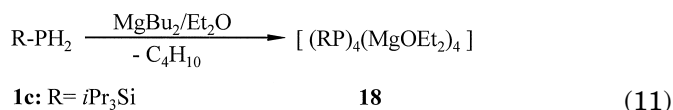
A. SYNTHESIS OF A SOLVENT-FREE DERIVATIVE

Reaction of the primary phosphane $t\text{Bu}_3\text{SiPH}_2$ **1f** with MgBu_2 furnishes the solvent-free hexameric cluster **17** (Eq. 10) (47). Yellow crystals, have been isolated in 39% yield, which are thermochromic. The NMR spectrum, especially the ^{31}P NMR signal at $\delta = -263.8$, suggested that the molecule prefers a high symmetry or dissociates rapidly on the NMR time scale. Since **15** is highly soluble in aromatic hydrocarbons even at low temperature and free of metal oxide, it can thus be regarded as a valuable source of phosphandiide, that is, for nucleophilic RP^{2-} transfer reactions.



B. SYNTHESIS OF A SOLVATED DERIVATIVE

Since the degree of aggregation is dependent on the complexation (solvation) of the metal cations in a molecular ionogenic cluster (cluster degradation), the polarity and donor ability of the solvent play an important role. Thus, the synthesis of magnesium phosphandiides in ether solvents results in the formation of smaller aggregates. This has been shown by the synthesis of the Et_2O -solvated tetrameric magnesium phosphandiide **18**, which is accessible by reaction of **1c** with MgBu_2 in Et_2O (Eq. 11) (48). The colorless crystalline compound, which is highly soluble in aromatic hydrocarbons, has been isolated in 40% yield. Its ^{31}P NMR spectrum revealed a singlet at $\delta = -321.9$, that is, the ^{31}P nuclei are more shielded than those of hexameric, solvent-free **17**. This is probably due to the smaller endocyclic angles at phosphorus in **18**, rather than an electronic effect through the external ether ligands at magnesium.



C. X-RAY STRUCTURES

The solvent-free cluster **17** crystallizes in the monoclinic space group $P2_1/c$ and comprises a hexagonal Mg_6P_6 prism with disordering

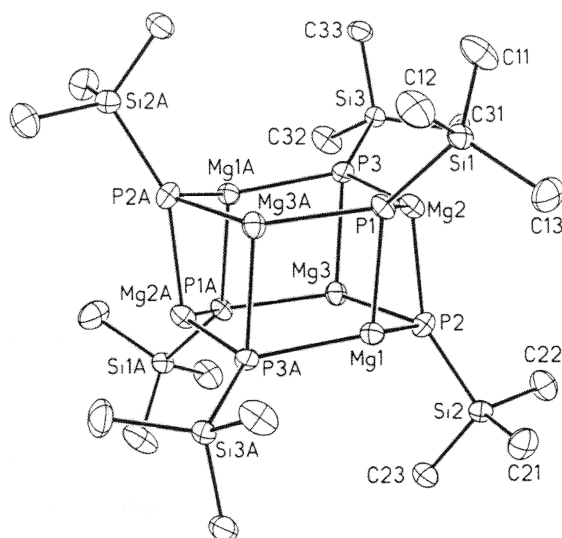


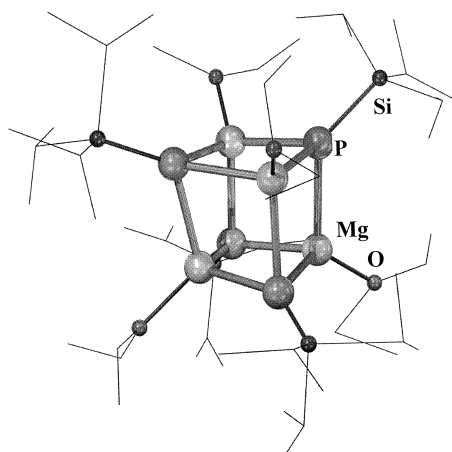
FIG. 18. Molecular structure of **17**. [Reprinted with permission from (47). Copyright 1999, American Chemical Society.]

(Fig. 18) (47). The Mg–P distances within the six-membered Mg_3P_3 cycles (2.47 to 2.51 Å) are different from those distances between the Mg_3P_3 cycles (2.50 to 2.59 Å). The endocyclic angles at magnesium are 127.7, 127.2, and 133.9° within the six-membered Mg_3P_3 ring and lie between 100.5 and 102.7° for the angles within the Mg_2P_2 cycles. The tetrameric phosphandiide **18** crystallizes in the space group $C2/c$. The Mg_4P_4 cubane-like cluster is strongly distorted because of electrostatic repulsions between identically charged centers (Fig. 19) (48).

The average value of the Mg–P distance of 2.53 Å resembles that of **17** and of other related magnesium phosphanides (47). However, the endocyclic angles at phosphorus (average 81.3°) are much smaller than that values in **17**.

V. Tin(II) Metalated Phosphandiides

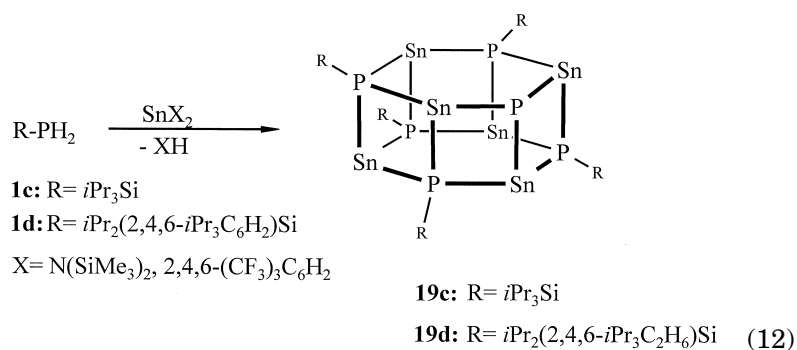
In contrast to magnesium phosphandiides, analogous tin(II) derivatives possess more covalent metal–phosphorus bonds. This basic difference is also apparent for dilithium versus dicopper(I) phosphandiides (see Section II and III). It is, therefore, interesting to assess the structural and electronic features of such species in a similar way. To date, only three tin(II) phosphandiide derivatives have been prepared

FIG. 19. Molecular structure of **18**.

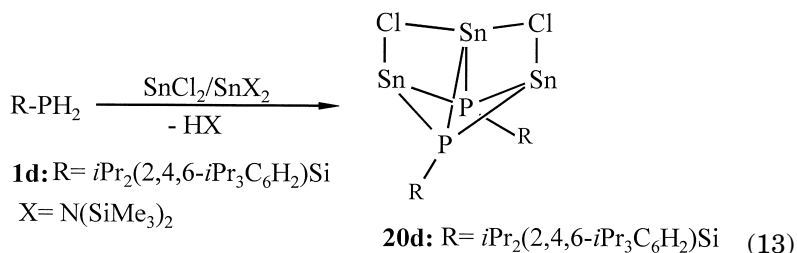
(39, 49). They are promising precursors for phosphandiide transmetalation reactions (tin–metal exchange), that is, for the synthesis of other types of bimetallic phosphandiides.

A. SYNTHESIS

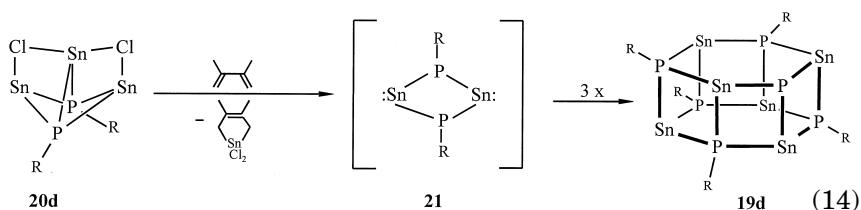
The Sn_6P_6 cages **19c** and **19d** are accessible by two different Brønsted acid–base reaction pathways: Reaction of **1c** and **1d**, respectively, with two different stannanediyl derivatives furnished in 80–89% yield red-black crystals of the aggregates (Eq. 12) (39). The tin(II) phosphandiides are somewhat related to the previously described oligomeric bis (phosphaneyl) stannanediyls of the type $(\text{R}_2\text{P})_2\text{Sn}$, which easily form intermolecular aggregates (50, 51) or remain monomeric, if the phosphorus atoms bear very crowded organosilyl substituents (52).



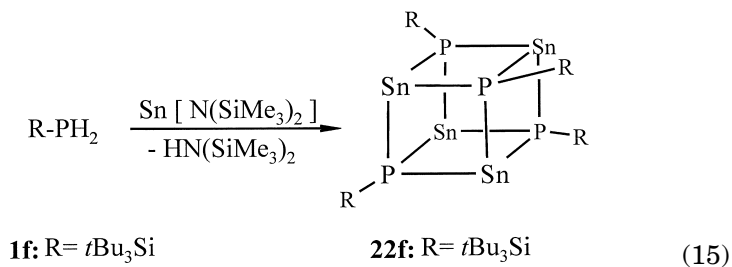
The unusual $\text{Sn}_3\text{P}_2\text{Cl}_2$ cluster **20d** has been isolated in 44% yield in the form of yellow crystals (Eq. 13) (39), simply by the same reaction of **1d** with the stannanediyls but in the presence of SnCl_2 . **20d** represents formally an adduct of the cyclic bis(stannanediyl) phosphandiide **21** and SnCl_2 , which coordinate to each other upon their complementary Lewis acid/Lewis base sites.



The transient $(\text{RPSn})_2$ **21**, which possibly represents a reactive intermediate during the synthesis of the hexameric Sn_6P_6 clusters **19c** and **19d**, has been trapped by the transformation of **20d** in the presence of 2,3-dimethylbuta-1,3-diene, which solely gave **19d** and the corresponding 1*H*-1,1,-dichlorostannol (Eq. 14).



The first Sn_4P_4 cube **22f** has been prepared in an analogous procedure, starting from the very bulky silylphosphane and Lappert's stannanediyl (Eq. 15) (49), which has been isolated in the form of dark red crystals in 95% yield.



B. NMR SPECTROSCOPIC CHARACTERIZATION

The tin(II) phosphandiides **19c**, **19d**, and **22f** show, with exception of the SnCl_2 -adduct **20d**, unusual high-field positions of the ^{31}P NMR singlet signals (Table II). However, the relatively small $^1J(\text{P}, \text{Sn})$ coupling constants also reflect considerable electronic features. DFT calculations of the parent compound $\text{H}_6\text{Sn}_6\text{P}_6$ revealed that spin-orbital coupling has a strong influence on the ^{31}P chemical shift (39).

Thus, DFT-IGLO calculations of the ^{31}P chemical shift without spin-orbital corrections yielded a value of $\delta = -274$, whereas additional spin-orbital correction leads to a further high-field shift (-80) to $\delta = -354$. Remarkably, the calculation of the ^{31}P chemical shift of the parent compound of **20d**, $\text{H}_2\text{P}_2\text{Sn}_3\text{Cl}_2$, gave a value of $\delta = -52$ with a spin-orbital contribution of only -22 . The low spin-orbital contribution for **19c**, **19d**, and **22f** vs **20d** is probably due to the different strength of the contribution of the $3s$ orbital of phosphorus to the Sn-P bonds.

C. MOLECULAR STRUCTURES

The Sn_6P_6 cluster **19c** crystallizes in the triclinic space group $P\bar{1}$. It forms a distorted hexagonal Sn_6P_6 prism with three-coordinated Sn and four-coordinated P atoms (Fig. 20) (39), that is, the structure is topologically identical with that of solvent-free **17** (see Fig. 18).

The averaged Sn-P distances of $2.626(3)$ Å in the Sn_3P_3 plane are only slightly longer than the corresponding Sn-P distances between the two Sn_3P_3 planes ($2.665(3)$ Å). The reluctance of tin(II) to undergo sp -hybridization favors relatively small endocyclic angles at the tin centers (87 – 101°). In contrast, the corresponding endocyclic angles at phosphorus in the Sn_3P_3 arrangement are relatively large (139.1°), whereas those in the Sn_2P_2 moieties are in the range 90.7 to 106.1° . The Sn_4P_4 cubane **22f** crystallizes in the monoclinic space group

TABLE II

LISTING OF $\delta^{31}\text{P}$ NMR DATA AND $^1J(^{31}\text{P}, ^{119}\text{Sn})$
COUPLING CONSTANTS [Hz] FOR **19c**, **19d**, **20d**,
AND **22f**

	$\delta^{31}\text{P}$	$^1J(\text{P}, \text{Sn})$	Ref.
19c	-475.2	708	<i>39</i>
19d	-440.5	793	<i>39</i>
20d	-122.4	1037	<i>39</i>
22f	-452.1	766	<i>49</i>

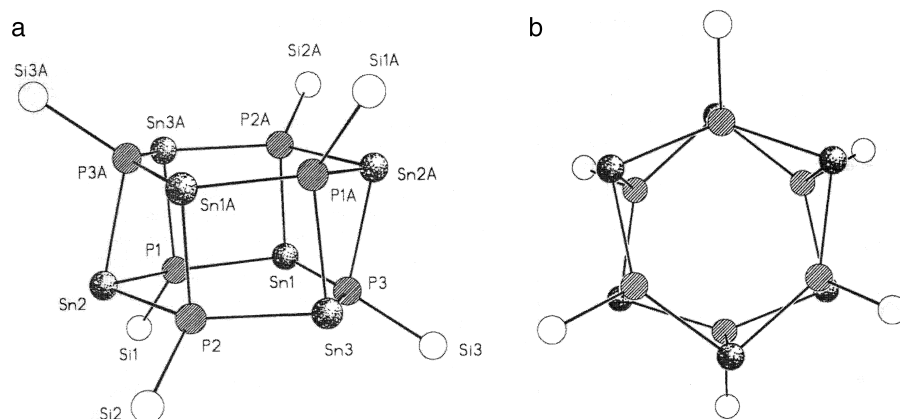


FIG. 20. Molecular structure of **19c**. [Reprinted with permission from (39). Copyright 1997, Wiley-VCH.]

$P2_1/c$ (Fig. 21), possesses Sn–P distances practically identical to those observed in **19c**, and shows relatively small endocyclic P–Sn–P angles (average 82.7°) (49). The corresponding angles at phosphorus are ca. 14° larger.

The SnCl_2 adduct **20d** crystallizes in the monoclinic space group $P2_1/c$ and shows only slight variations in the Sn–P distances (av.

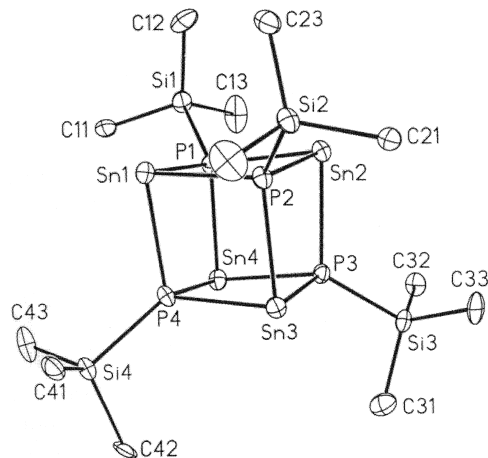


FIG. 21. Molecular structure of **22f**. [Reprinted with permission from (49). Copyright 1998, Wiley-VCH.]

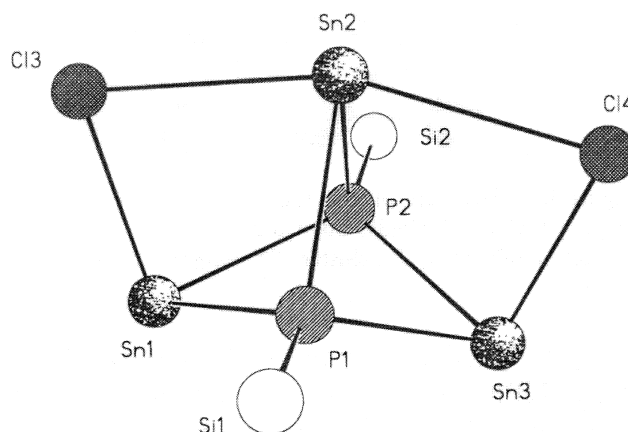


FIG. 22. Molecular structure of **20d**. [Reprinted with permission from (39). Copyright 1997, Wiley-VCH.]

2.622(3) Å); these are practically identical with those in **19c** (Fig. 22) (39).

The Sn–Cl distances in the SnCl₂ dumb-bell as opposite to the Sn(P)–Cl tin centers differ by 0.3 Å, which has been explained by the higher coordination of the SnCl₂ tin atom. Similar complexes between cyclodiazastannanediyls with SnX₂ have been reported (53).

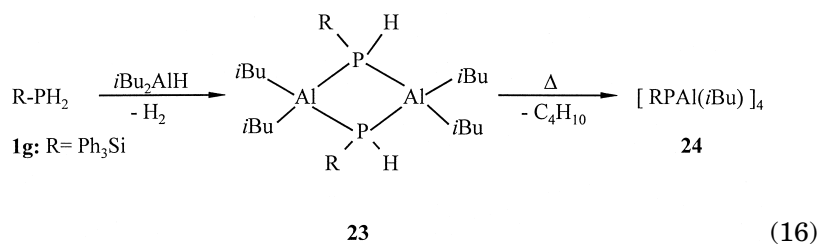
VI. Aluminum, Gallium, and Indium Phosphandiides and Arsandiides

Molecular Group 3–5 compounds are currently of considerable interest for two reasons: (a) they can serve as volatile low molecular weight single-source precursors for the CVD synthesis of binary and multinary group 3/5 semiconductors with remarkable optoelectronic properties (54), or (b) they are potentially useful cocatalysts for the polymerization reactions of unsaturated organic substrates (55, 56). Various strategies have been employed to synthesize well-defined aggregates.

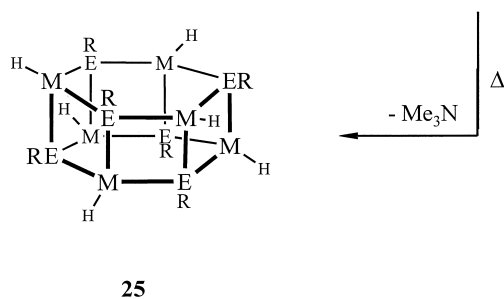
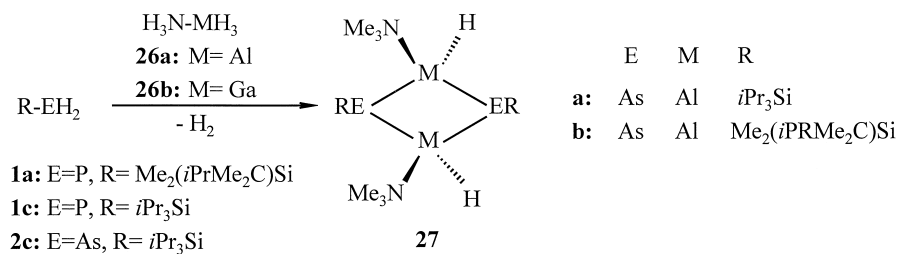
A. SYNTHESIS

A facile method to form M–P and M–As bonds (M = Al, Ga, In) is represented by the reaction of primary phosphanes and arsanes with E–H containing organometal reagents, which takes place with elimination of H₂. Thus, stepwise reaction of *i*Bu₂AlH with the primary

silylphosphane **1g** furnished, via the Al_2P_2 heterocycle **23**, the first Al_4P_4 cubane-like cage **24** (Eq. 16) (57).



The more highly aggregated AlP-, AlAs-, GaP-, and GaAs-clusters **25** have been synthesized by the reaction of the primary silylphos-

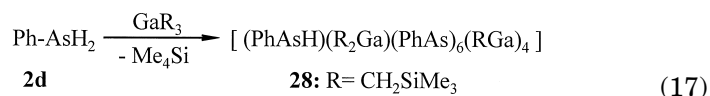


	E	M	R
a:	As	Al	$i\text{Pr}_3\text{Si}$
b:	As	Al	$\text{Me}_2(i\text{PrMe}_2\text{C})\text{Si}$
c:	As	Ga	$i\text{Pr}_3\text{Si}$
d:	P	Al	$i\text{Pr}_3\text{Si}$

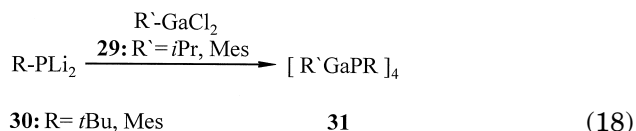
SCHEME 3. Stepwise formation of **25** via **27**.

phanes **1a**, **1c** and silylarsane **2c** with **26a** and **26b**, respectively (Scheme 3) (58).

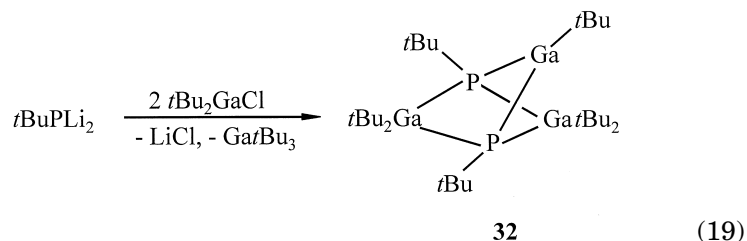
The formation of the hexamers occurs via four-membered E_2M_2 -heterocycles **27** that have been isolated and structurally characterized in the cases of **27a** and **27b**. The Me_3N donor molecules of **27** can be easily cleaved upon heating, which furnished the hexameric Al- and Ga phosphandiides and arsandiides **25** in good yields (58). The unusual Ga_5As_7 cluster **28** has been synthesized through the cyclocondensation reaction of $PhAsH_2$ **2d** with R_3Ga ($R = CH_2SiMe_3$) in the molar ratio of 1:1, which turned out to be a mixed gallium arsanide-arsandiide aggregate (Eq. 17) (59).



Several Ga_4P_4 cube derivatives **31** have been synthesized by salt metathesis reaction, starting from $R'GaCl_2$ **29** and dilithium organophosphandiides **30** (Eq. 18) (57, 60, 61). Their formation occurred via cyclic intermediates, but $Ga=P$ intermediates could not be detected.

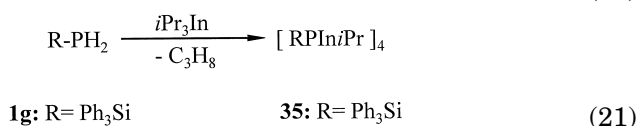
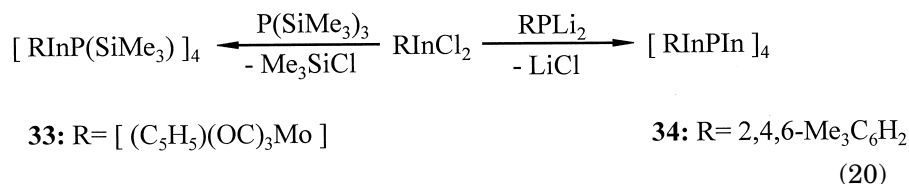


The three-component reaction among $RGaCl_2$ **29**, $GaCl_3$, and $RPLi_2$ **30** ($R = 2,4,6-Me_3C_6H_2$) furnished a Ga_4P_4 cubane with one exocyclic PHR substituent at gallium (61). Another type of gallium phosphandiide has been prepared by reaction of $tBuPLi_2$ with tBu_2GaCl in the molar ratio of 1:2 (Eq. 19) (62).



Related gallium phosphandiides and some sterically congested monomeric digallyl phosphandiides have also been synthesized, and these results have been summarized in a detailed review (63). Molec-

ular indium phosphandiide aggregates are far less well investigated than gallium phosphandiides. Hitherto only three In_4P_4 cuboidal derivatives have been reported (64–66). Thus, reaction of the substituted indium chloride RInCl_2 [$\text{R} = (\text{C}_5\text{H}_5)(\text{OC})_3\text{Mo}$] with $\text{P}(\text{SiMe}_3)_3$ furnished the propellane-like compound **33** (64), whereas salt metathesis of RPLi_2 with RInCl_2 ($\text{R} = 2,4,6\text{-Me}_3\text{C}_6\text{H}_2$) led to **34** (Eq. 20) (65). Furthermore, the In_4P_4 cubane **35** has been prepared, starting from the silylphosphane **1g** and the corresponding triorganoindane (Eq. 21) (66).



B. NMR SPECTROSCOPIC CHARACTERIZATION

An important result of the multinuclear NMR investigations of **23–25**, **27**, **28**, and **31–35** is that the structures, in contrast to aggregates of monometalated secondary phosphanes and arsanes, are retained in solution. Thus, the phosphandiide derivatives here discussed show resonance signals in their ^{31}P NMR spectra that are independent of concentration and temperature (see Table III). The ^{31}P and ^{27}Al NMR chemical shifts of **23–25**, **27**, and **31–35** differ with respect to ring size of the clusters and electronic influences by the substituents at phosphorus and aluminum.

C. X-RAY STRUCTURES

The four-membered Al_2As_2 heterocycle **27a** was the first derivative to be structurally characterized (58). It crystallizes in the triclinic space group $P\bar{1}$. The Al_2As_2 ring is puckered, with pyramidally coordinated As atoms and tetrahedrally surrounded Al centers (Fig. 23). The amine groups at aluminium are *cis*-oriented to each other, which is probably due to the steric demand of the silyl groups. The average

TABLE III
LISTING OF $\delta^{31}\text{P}$ AND $\delta^{27}\text{Al}$ NMR DATA FOR **23–25**, **27**, AND
31–35

	$\delta^{31}\text{P}$	$\delta^{27}\text{Al}$	Ref.
23	–216.8 (anti) –217.6 (syn)	—	57
24	–213	—	57
25a	—	48	58
25b	—	40	58
25d	–277	46	58
27a	—	127	58
27b	—	140	58
31 (<i>i</i> PrGa, <i>Pt</i> Bu)	–12.8	—	60
31 (MesGa, <i>Pt</i> Bu) ^a	1.5	—	60
32	–80	—	62
33	–137.7	—	64
34	–75.5	—	65
35	–168.0	—	66

^a Mes = 2,4,6-Me₃C₆H₂.

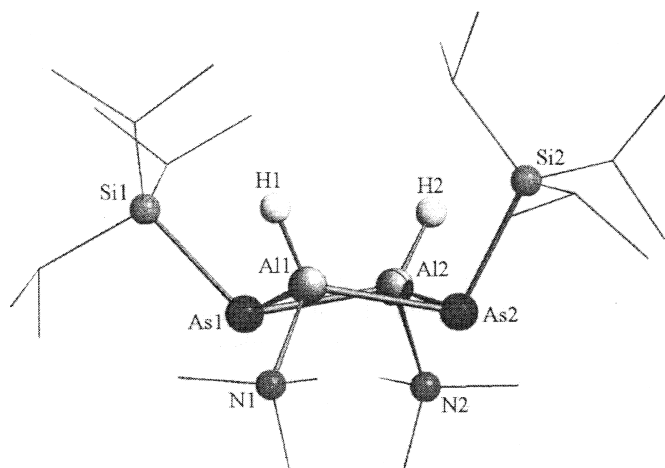


FIG. 23. Molecular structure of **27a**. [Reprinted with permission from (58). Copyright 1998, Wiley-VCH.]

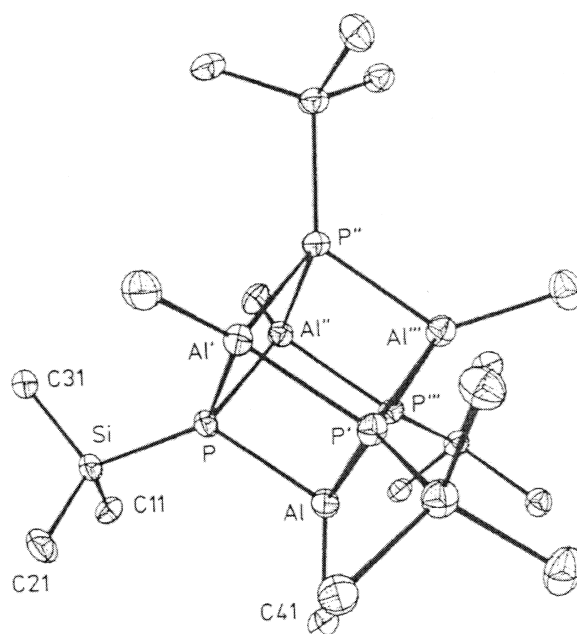


FIG. 24. Molecular structure of **24**. [Reprinted with permission from (57). Copyright 1990, Wiley-VCH.]

Al–As distance (2.447(2) Å) resembles the values in a six-membered Al_3As_3 borazine analogue, although the latter has only three-coordinate Al centers (63). The first Al_4P_4 cube to be structurally characterized was **24** (Fig. 24) (57). The cube is distorted and the Al–P distances (ca. 2.41 Å) are little shorter than that in dimeric Al_2P_2 compounds. The analogous cuboidal-like M_4E_4 cluster (E = P, As; M = Al, Ga, In) **31** and **33–35** possess also distorted arrangements, due to the steric demand of their substituents and high polarity of the E–M bonds.

The hexameric E_3M_3 clusters (M = Al, Ga; E = P, As) **25a**, **25c**, and **25d** comprise hexagonal prismatic E_3M_3 skeletons, as representatively shown for **25a** in Fig. 25 (58). Thus, the cluster core resembles that of the Sn_3P_3 drums **19** (see Fig. 20), and the Al–As distances are only marginally longer than those in **27a**. Apparently, the Al–H bonds are shielded by the bulky silyl groups, which hampered selective substitution reactions at the Al–H bond.

The structure of **32** (62) is remarkable since it possesses, at the same time, three- and four-coordinated Ga centers (Fig. 26), whereas **28** represents the first example of a partially metalated arsane–

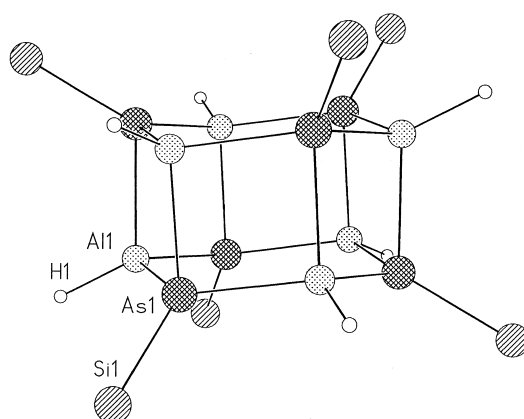


FIG. 25. Molecular structure of **25**. [Reprinted with permission from (58). Copyright 1998, Wiley-VCH.]

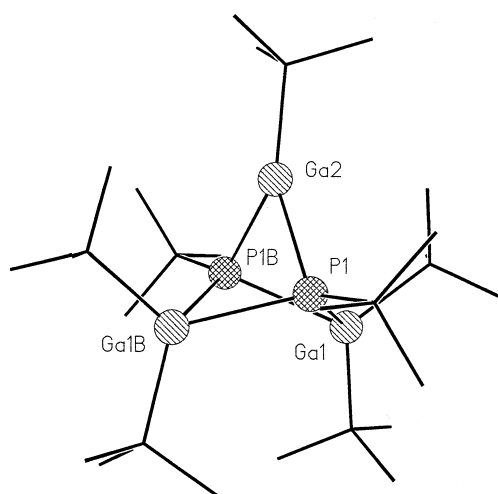


FIG. 26. Molecular structure of **32**. [Reprinted with permission from (62). Copyright 1993, American Chemical Society.]

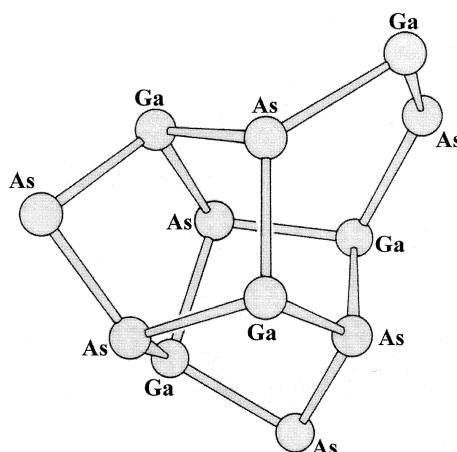


FIG. 27. The GaAs core of compound **28**. [Reprinted with permission from (59). Copyright 1986, Royal Society of Chemistry.]

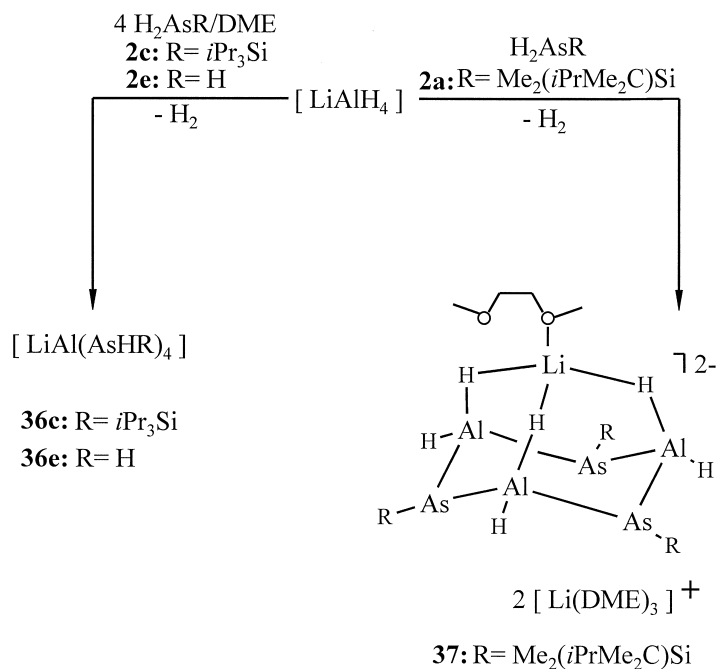
arsandiide cluster $M_x(RAsH)_y(RAs)_z$ with main Group 3 elements (Fig. 27) (59).

VII. Mixed-Metalated Phosphandiides and Arsandiides

The synthesis of mixed-metalated species provides more information about the influence of different metals on the degree of aggregation of phosphandiides and arsandiides, respectively. Not only that, the issue whether “ring-laddering” is still preferred if ionic metal centers (Groups 1, 2) and more covalent metal atoms (Groups 3, 4) are, at the same time, coordinated to RE^{2-} ligands ($E = P, As$) is of particular interest. It is a considerable challenge to tune the reactivity of phosphandiides and their arsenic analogues for selective nucleophilic RE^{2-} transfer reactions.

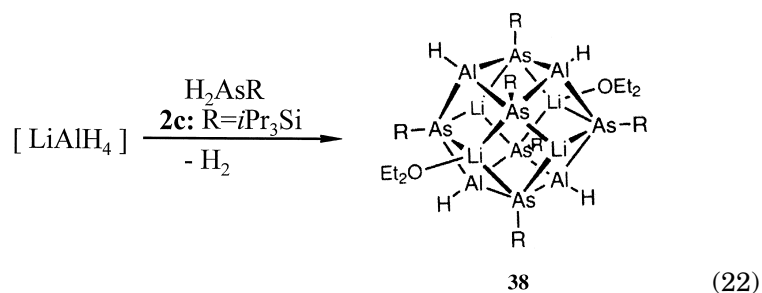
A. SYNTHESIS OF Li/Al-MIXED DERIVATIVES

A convenient route to “andiides,” where Li and Al centers are, at the same time, involved is represented by the reaction of $LiAlH_4$ with primary silylphosphanes and silylarsanes (Scheme 4) (67). However, the outcome of such reactions is dependent on the stoichiometry. The silylarsane **2c** reacts with $LiAlH_4$ in the molar ratio of 4:1 in 1,2-dimethoxyethane, under evolution of H_2 , resulting in the corresponding tetrakis(arsaneyl)-substituted lithium alanate **36c** in quantitative yield. The similar transformation of the arsane **2a** with $LiAlH_4$ in the

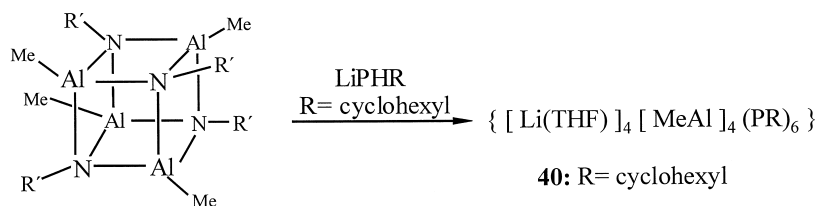
SCHEME 4. Synthesis of the diorganoarsaneyl alanates **36c**, **36e**, and **37**.

molar ratio of 1 : 1 led to the unusual ion-triple **37** in the form of colorless crystals in 81% yield (67).

The reaction of the arsane **2c** with LiAlH_4 in the ratio of 1 : 1 in diethyl ether as solvent led, under H_2 elimination, to the rhombododecahedral $\text{Li}_4\text{Al}_4\text{As}_6$ cluster **38** (Eq. 22) (58). The latter impressively demonstrates the influence of the solvent donor ability on the outcome of the reaction. Remarkably, the introduction of AsH_3 into a solution of LiAlH_4 in DME furnishes the corresponding alanate **36e**, $\text{LiAl}(\text{AsH}_2)_4$, which cleanly decomposes in solution at 25°C over 3–4 days, giving the Zintl ion $(\text{As}_7)^{3-}$ in high yield (67).

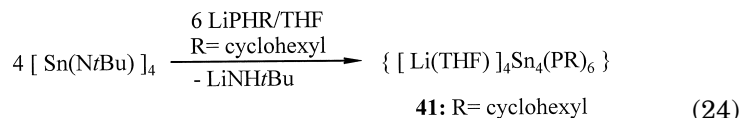


Another method to prepare mixed Li/Al derivatives has been developed by ligand-exchange reactions, starting from the Al_4N_4 cube **39** and LiPHR ($\text{R} = \text{cyclohexyl}$) (68). Thus, the outcome of the latter is the rhombododecahedral $\text{Li}_4\text{Al}_4\text{P}_6$ cluster **40**, which bears exohedral THF donor ligands at the lithium centers (Eq. 23) (68).

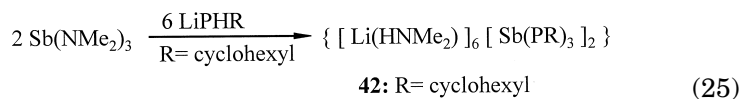


B. SYNTHESIS OF Li/Sn-, Li/Sb-, AND Ca/Sn-MIXED CLUSTERS

The same strategy as for the synthesis of **40** has been employed for the preparation of the Li/Sn-mixed cluster **41**. Thus, replacement of the imido groups in $[\text{Sn}(\text{NtBu})]_4$ with LiPHR ($\text{R} = \text{cyclohexyl}$) in the molar ratio of 4:6 yielded the metallacyclic cage complex **41**, which has a rhombododecahedral $\text{Li}_4\text{Sn}_4\text{P}_6$ core (Eq. 24) (69). The clusters **40** and **41** are isostructural, since the MeAl fragments in **40** have been replaced by the isoelectronic $\text{Sn}(\text{II})$ centers.

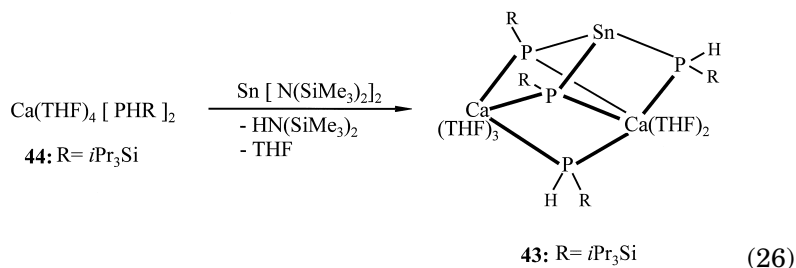


Replacement of the NMe_2 groups in $\text{Sb}(\text{NMe}_2)_3$ by phosphandiide ligands has been achieved by the reaction shown in Eq. (25) (70). Interestingly, all of the HNMe_2 produced by this reaction coordinates to the Li ions in **42**, which leads to a rhombododecahedral $\text{Li}_6\text{Sb}_2\text{P}_6$ skeleton.



The first Ca/Sn-mixed phosphandiide cluster **43** has been prepared by reaction of the calcium phosphanide **44** with $\text{Sn}[\text{N}(\text{SiMe}_3)_2]_2$ in THF

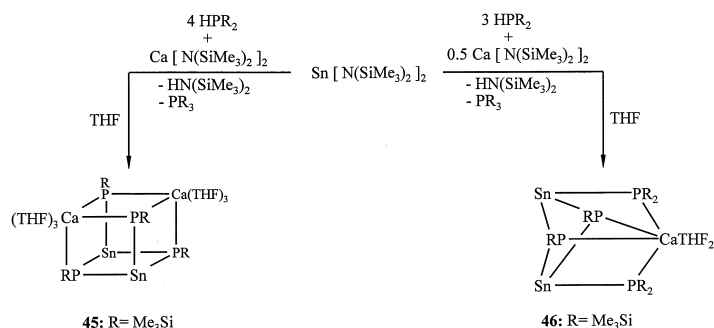
as solvent (Eq. 26) (71). The latter contains both phosphanide and phosphandiide ligands composing a Ca_2SnP_4 skeleton.



Interestingly, the three-component metathesis reaction among $\text{Ca}[\text{N}(\text{SiMe}_3)_2]_2$, $\text{Sn}[\text{N}(\text{SiMe}_3)_2]_2$, and HPR_2 ($\text{R} = i\text{Pr}_3\text{Si}$) in the molar ratio of 1 : 1 : 4 in THF led, under evolution of PR_3 , to the $\text{Ca}_2\text{Sn}_2\text{P}_4$ heterocubane **45**, whereas its reaction in the molar ratio of 1 : 2 : 6 gave the cluster **46**, which comprises a CaSn_2P_4 framework (Scheme 5) (72). The same reaction with barium hexamethyldisilazanide instead of the calcium salt in THF furnished the isostructural BaSn_2P_4 cluster (73), whereas the reaction of the bulkily substituted barium phosphanide $\text{Ba}(\text{PHR})_2$ ($\text{R} = i\text{Pr}_3\text{Si}$) with the stannanediyl $\text{Sn}[\text{N}(\text{SiMe}_3)_2]_2$ (molar ratio of 2 : 3) gave the corresponding BaSn_3P_4 heterocubane, of which the Ba ion is solvated by a toluene ligand in a η^6 -fashion (49).

C. DYNAMIC PROCESSES IN SOLUTION

The presence of both ionic and covalent backbones in the clusters **37**, **38**, **40**, **41**, **42**, and **43** has raised the question whether the structures of the “andiides” remain intact in solution. This is undoubtedly



SCHEME 5. Synthesis of the mixed-Ca/Sn phosphandiide clusters **46** and **47**.

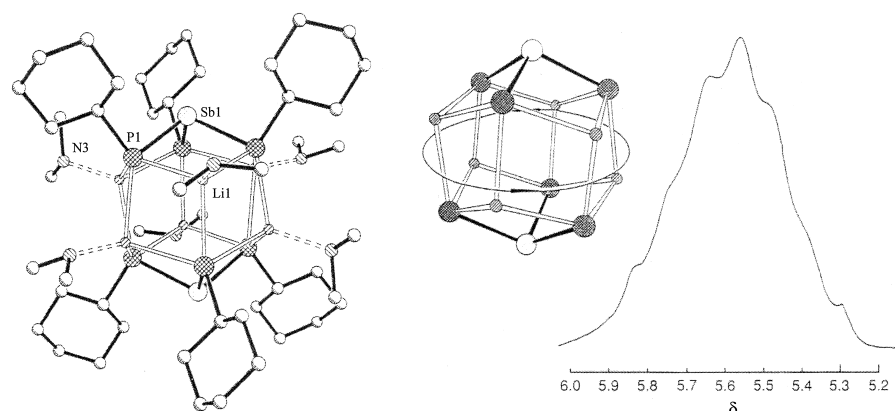


FIG. 28. (Left) Molecular structure of **42** · 2 C₆H₅Me. (Right) Dynamic “carousel” process and the ⁷Li NMR spectrum of **42**. [Reprinted with permission from (70). Copyright 1997, Royal Society of Chemistry.]

not the case. Apparently, this implies some advantages for transmetalation and “andiide” transfer reactions with respect to the undissociated dilithium phosphandiides and arsandiides (see Section I) and related homometallic “andiides” (see Sections III, V, and VI). Thus, the singlet in the ⁷Li NMR spectrum of the tripodal Li complex **37** in THF ($\delta = -3$) clearly indicates fast Li exchange. The rhombododecahedral cores of **38**, **40**, **41**, and **42** are also highly dynamic in solution and show fast ligand exchange of the exohedral donor-solvent molecules. A very interesting dynamic process has been observed in the case of the Li₆Sb₂P₆ cluster compound **42**: Variable-temperature ⁷Li NMR suggests a dynamic “carousel” process of the Li ions around the two intact [Sb(PR)₃]₃⁻ trianions of the core (Fig. 28) (70).

D. X-RAY STRUCTURES

The ion-triple **37** crystallizes in the orthorhombic space group *P*2₁2₁2₁. The dianion in **37** is remarkable, since the hydridic H atoms are evidently better donors toward Li ions than the As centers, and the DME molecule functions rather surprisingly as a monodentate ligand (Fig. 29) (67). The Al–As distances are unremarkable and in the range of other chair-shaped Al₃As₃ frameworks (63).

The topologies of the skeletons in **38** (67), **40** (68), **41** (69), and **42** (70) are identical and represents a distorted rhombododecahedron. The cluster cores of **38** and **40** are shown in Figs. 30 and 31 as repre-

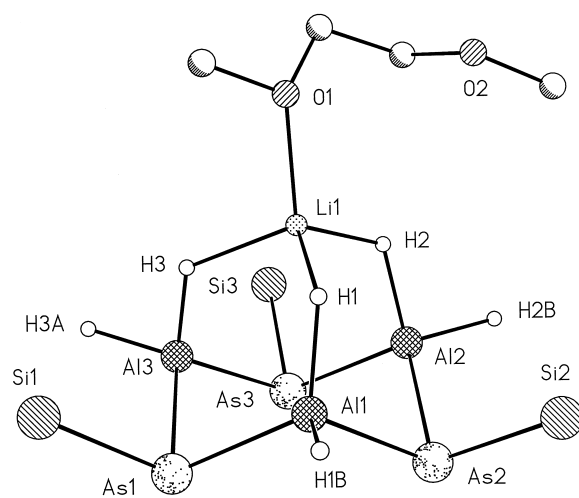


FIG. 29. Molecular structure of the dianion of **37**. [Reprinted with permission from (67). Copyright 1996, Wiley-VCH.]

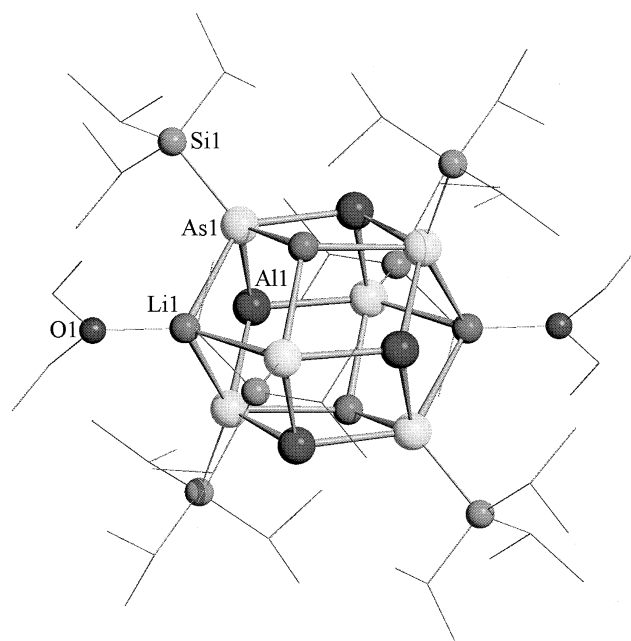


FIG. 30. Molecular structure of **38**. [Reprinted with permission from (58). Copyright 1998, Wiley-VCH.]

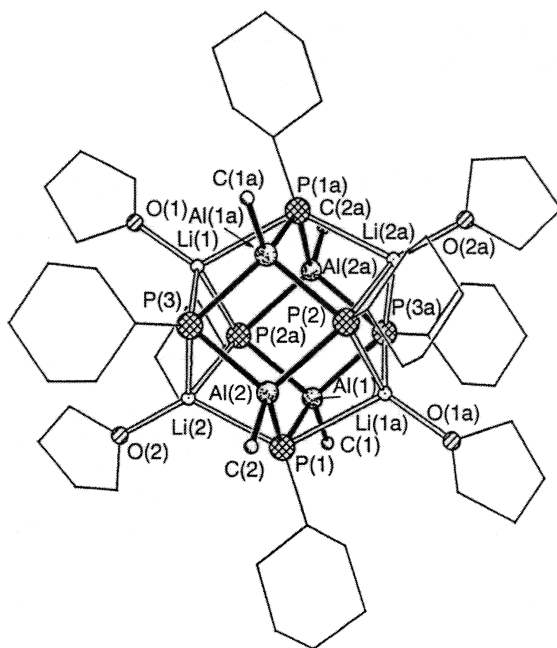


FIG. 31. Molecular structure of **40**. [Reprinted with permission from (68). Copyright 1996, Royal Society of Chemistry.]

sentatives of the series. All Li ions of the compounds are solvated, with the exception of **38**, where only two Li ions coordinate to solvent molecules (Et_2O).

The Ca/Sn-mixed metalated phosphanide-phosphandiide cluster **43** crystallizes in the triclinic space group $P\bar{1}$ (71). It consists of a trigonal Ca_2SnP_2 bipyramid, where the phosphandiide P centers serve as μ_3 -bridging centers to the metals. The two phosphanide ligands, however, are μ -bridging between two Ca and Ca/Sn centers (Fig. 32). Both Ca ions are octahedrally coordinated.

VIII. Conclusion

In summary, the solubility and the degree of aggregation of dimetalated phosphanes and arsanes can be controlled by employing appropriate lipophilic substituents at phosphorus and arsenic. Triorganosilyl substituents fulfill this requirement especially well. The tendency

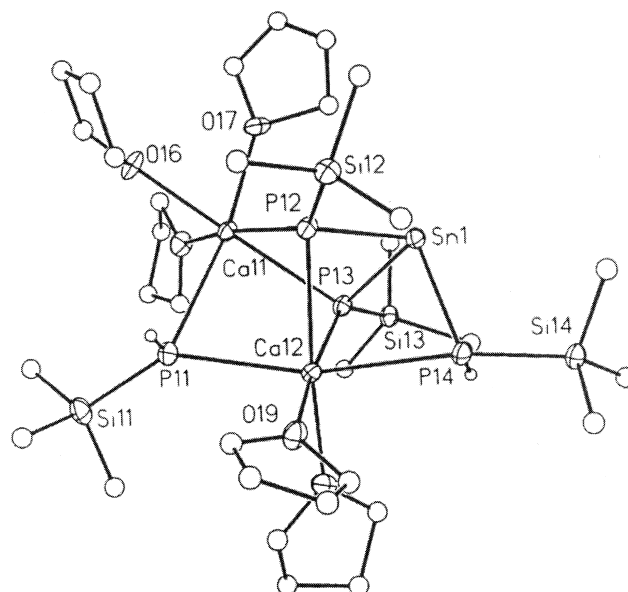


FIG. 32. Molecular structure of **43**. [Reprinted with permission from (71). Copyright 1996, Elsevier Sciences S. A.]

of such clusters to undergo dissociation in solution is crucial for their reactivity, which is particularly important for “andiide” transfer reactions with electrophiles. However, the tendency for dissociation is determined not only by the metal–pnictogen bond polarity, but also by the ability of the aggregates to form host–guest complexes. The latter has been obtained for dilithium and disodium “andiides” that easily accommodate M_2O ($M = Li, Na$) in their voids. Thus, this issue provides also model compounds for the study of nucleation processes of ionic materials. With the exception of the coin-metal phosphandiides, the structural principle of aggregation is mainly based on the model of three-dimensional ring-laddering, leading to globular or oval cluster frameworks. Promising building blocks for $(RE)^{2-}$ transfer reactions ($E = P, As$) represent mixed-metalated derivatives containing p -block metals ($Sn(II), Sb(III)$ etc.), which support metal exchange. Furthermore, employment of metalated primary phosphanes and arsanes as single-source precursors for the synthesis of binary and multinary metastable solids, i.e., for the preparation of optoelectronic materials, is of considerable interest.

ACKNOWLEDGMENTS

The author is indebted to his fellow workers Drs. S. Rell, K. Merz, S. Martin, H. Pritzkow, S. Kuntz, and Dipl. Chem. U. Hoffmanns. Financial support from the Deutsche Forschungsgemeinschaft, the Fonds der Chemischen Industrie, and the Ministerium für Wissenschaft und Forschung, Nordrhein-Westfalen (Germany), is gratefully acknowledged.

REFERENCES

1. Pauer, F.; Power, P. P. "Lithium Compounds of the Main Group 5 Elements." In "Lithium Chemistry: A Theoretical and Experimental Overview," Sapse, A.-M.; Schleyer, P.v.R., Eds.; Wiley: New York, 1995; pp. 324–361.
2. Pauer, F.; Power, P. P. "Structure of lithium salts of heteroatom compounds." In "Lithium Chemistry: A Theoretical and Experimental Overview," Sapse, A.-M.; Schleyer, P.v.R., Eds.; Wiley: New York, 1995; pp. 361–373.
3. Driess, M.; Pritzkow, H.; Martin, S.; Rell, S.; Fenske, D.; Baum, G. *Angew. Chem. Int. Ed. Engl.* **1996**, *35*, 986.
4. Issleib, K.; Tzschach, A. *Chem. Ber.* **1959**, *92*, 1118.
5. Parshall, G. W.; Lindsey, R. V. *J. Am. Chem. Soc.* **1959**, *81*, 6273.
6. Fritz, G.; Schäfer, H.; Hölderich, W. Z. *Anorg. Allg. Chem.* **1974**, *407*, 266.
7. Appel, R.; Geisler, K. *J. Organomet. Chem.* **1976**, *112*, 61.
8. v. Schnering, H.; Hönl, W. *Chem. Rev.* **1988**, *88*, 243.
9. Atwood, J. L.; MacGillivray, L. R. *Angew. Chem. Int. Ed. Engl.* **1999**, *38*, 1018.
10. Sapse, A.-M.; Jain, D. C.; Raghavachari, K. "Theoretical studies of aggregates of lithium compounds." In "Lithium Chemistry: A Theoretical and Experimental Overview" Sapse, A.-M.; Schleyer, P.v.R., Eds.; Wiley: New York, 1995; pp. 45–65.
11. Becker, G.; Eschbach, B.; Käshammer, D.; Mundt, O. Z. *Anorg. Allg. Chem.* **1994**, *620*, 29.
12. Driess, M.; Pritzkow, H. Z. *Anorg. Allg. Chem.* **1996**, *622*, 1524.
13. Driess, M.; Huttner, G.; Knopf, N.; Pritzkow, H.; Zsolnai, L. *Angew. Chem. Int. Ed. Engl.* **1995**, *34*, 316.
14. Zsolnai, L.; Huttner, G.; Driess, M. *Angew. Chem. Int. Ed. Engl.* **1993**, *32*, 1439.
15. Armstrong, D. R.; Barr, D.; Clegg, W.; Drake, S. R.; Singer, R. J.; Snaith, R.; Stalke, D.; Wright, D. S. *Angew. Chem. Int. Ed. Engl.* **1991**, *30*, 1707.
16. Gilchrist, J. H.; Harrison, A. T.; Fuller, D. J.; Collum, D. B. *J. Am. Chem. Soc.* **1990**, *112*, 4069.
17. Lucht, B. L.; Collum, D. B. *J. Am. Chem. Soc.* **1996**, *118*, 3529.
18. (a) Colquhoun, I. J.; McFarlane, H. C. E.; McFarlane, W. *Phosphorus Sulfur* **1983**, *18*, 61; (b) Zschunke, A.; Riemer, M.; Schmidt, H.; Issleib, K. *Phosphorus Sulfur* **1983**, *17*, 237.
19. Niedieck, K.; Neumüller, B. Z. *Anorg. Allg. Chem.* **1993**, *619*, 385.
20. Cowley, A. H.; Kilduff, J. E.; Newman, T. H.; Pakulski, M. *J. Am. Chem. Soc.* **1982**, *104*, 5820.
21. Driess, M.; Hoffmanns, U.; Martin, S.; Merz, K.; Pritzkow, H. *Angew. Chem. Int. Ed. Engl.* **1999**, *38*, 2733.
22. Driess, M.; Rell, S.; Pritzkow, H.; Janoschek, R. *Chem. Commun.* **1996**, 305.

23. Hollemann-Wiberg, "Lehrbuch der Anorganischen Chemie"; de Gruyter: Berlin, 100th edition; p. 277, Table 35.
24. Driess, M.; Martin, S.; Pritzkow, H. Unpublished.
25. Driess, M.; Skipinski, M.; Baum G.; Fenske, D. Unpublished.
26. Driess, M.; Pritzkow, H.; Skipinski, M.; Winkler, U. *Organometallics* 1997, **16**, 5108.
27. Driess, M.; Pritzkow, H.; Skipinski, M.; Winkler, U. *J. Am. Chem. Soc.* 1998, **120**, 10774.
28. Edwards, P. P.; Anderson, P. A.; Thomas, J. M. *Acc. Chem. Res.* **1996**, **29**, 23.
29. Gais, H.-J.; Vollhardt, J.; Gunther, H.; Moskau, D.; Lindner, H. J.; Braun, S. *J. Am. Chem. Soc.* 1988, **110**, 978.
30. Chivers, T.; Downard, A.; Yap G. P. A. *J. Chem. Soc., Dalton Trans.* 1998, 2603.
31. Kennedy, A. R.; Mulvey, R. E.; Rowlings, R. B. *Angew. Chem. Int. Ed. Engl.* 1998, **37**, 3180.
32. Driess, M.; Kuntz, S.; Merz, K. Unpublished.
33. Adrianarison, M.; Stalke, D.; Klingebiel, U. *Chem. Ber.* 1990, **123**, 71.
34. Koutsantonis, G. A.; Andrews, P. C.; Raston, C. L. *J. Chem. Soc., Chem. Commun.* 1995, 47.
35. Driess, M.; Schaller, T.; Sebald, A. *Solid State Nucl. Magn. Reson.* **1997**, **9**, 219.
36. Driess, M. *Pure Appl. Chem.* **1999**, **71**, 437.
37. Fenske, D.; Simon, F. *Angew. Chem. Int. Ed. Engl.* 1997, **109**, 240.
38. Schmid, G., Ed. "Overview: Clusters and Colloids-From Theory to Applications" VCH: Weinheim, 1994.
39. Driess, M.; Martin, S.; Merz, K.; Pintchouk, V.; Pritzkow, H.; Griitzmacher, H.; Kaupp, M. *Angew. Chem. Int. Ed. Engl.* **1997**, **36**, 1894.
40. Decker, A.; Fenske, D.; Maczekt, K. *Angew. Chem. Int. Ed. Engl.* **1996**, **35**, 2863.
41. Fenske, D.; Ohmer, J.; Hachgenein, J.; Merzweiler, K. *Angew. Chem. Int. Ed. Engl.* **1988**, **27**, 1277.
42. Pykkö, P. *Chem. Rev.* **1997**, **97**, 597.
43. Driess, M.; Faulhaber, M.; Merz, K. *Chem. Commun.* 1998, 1887.
44. Hey, E.; Engelhardt, L.; Raston, C. L.; White, A. H. *Angew. Chem. Int. Ed. Engl.* 1987, **26**, 81.
45. Westerhausen, M.; Pfitzner, A. *J. Organomet. Chem.* **1995**, **487**, 187.
46. Westerhausen, M.; Digeser, M. H.; Wienecke, B.; Nöth, H.; Knizek, J. *Eur. Z. Inorg. Chem.* 1998, **120**, 6722.
47. Westerhausen, M.; Krofta, M.; Pfitzner, A. *Inorg. Chem.* **1999**, **38**, 598.
48. Driess, M.; Kuntz, S.; Merz, K. Unpublished.
49. Westerhausen, M.; Krofta, M.; Wiberg, N.; Knizek, J.; Nöth, H.; Pfitzner, A. *Z. Naturforsch.* **1998**, **53B**, 1489.
50. du Mont, W.-W.; Kroth, H.-J. *Angew. Chem.* **1977**, **89**, 832.
51. Goel, S. C.; Chiang, M. Y.; Rauscher, D. J.; Buhro, W. E. *J. Am. Chem. Soc.* 1993, **115**, 160.
52. Driess, M.; Janoschek, R.; Pritzkow, H.; Rell, S.; Winkler, U. *Angew. Chem. Int. Ed. Engl.* **1995**, **34**, 1614.
53. Veith, M.; Huch, V.; Lisowsky, R.; Hobein, P. Z. *Anorg. Allg. Chem.* 1989, **569**, 43.
54. Hitchman, M. L.; Jensen, K. F. "Chemical vapor deposition-An overview." In "Chemical Vapor Deposition: Principles and Applications," Hitchman, M. L.; Jensen, K. F., Eds.; Academic Press: San Diego, 1993.
55. Koide, Y.; Bott, S. G.; Barron, A. R. *Organometallics* **1996**, **15**, 2213.
56. Koide, Y.; Barron, A. R. *Macromolecules* 1996, **29**, 1110.

57. Cowley, A. H.; Jones, R. A.; Mardones, M. A.; Atwood, J. L.; Bott, S. G. *Angew. Chem. Int. Ed. Engl.* **1990**, *29*, 1409.
58. Driess, M.; Kuntz, S.; Merz, K.; Pritzkow, H. *Chem. Eur. J.* **1998**, *4*, 1628.
59. Wells, R. L.; Prudy, A.; McPhail, A. T.; Pitt, C. G. *J. Chem. Soc., Chem. Commun.* 1936, 487.
60. Niediek, K.; Neumiiller, B. *Chem. Ber.* **1994**, *127*, 67.
61. Niediek, K.; Neumüller, B. *Z. Anorg. Allg. Chem.* **1995**, *621*, 889.
62. Petrie, M. A.; Power, P. P. *Organometallics* 1993, *12*, 1592.
63. Brothers, P. J.; Power, P. P. *Adv. Organomet. Chem.* **1996**, *39*, 30.
64. App, U.; Merzweiler, K. *Z. Anorg. Allg. Chem.* **1995**, *621*, 1731.
65. Werner, B.; Neumiiller, B. *Organometallics* **1996**, *15*, 4258.
66. Atwood, D. A.; Cowley, A. H.; Jones, R. A.; Mardones, M. A. *J. Organomet. Chem.* 1993, 449, C1.
67. Driess, M.; Merz, K.; Pritzkow, H.; Janoschek, R. *Angew. Chem. Int. Ed. Engl.* **1996**, *35*, 2507.
68. Allan, R. E.; Beswick, M. A.; Raithby, P. R.; Steiner, A.; Wright, D. S. *J. Chem. Soc., Dalton Trans.* **1996**, 4153.
69. Allan, R. E.; Beswick, M. A.; Cromhout, N. L.; Paver, M. A.; Raithby, P. R.; Steiner, A.; Wright, D. S. *Chem. Commun.* **1996**, 1501.
70. Beswick, M. A.; Goodman, J. M.; Harmer, C. N.; Hopkins, A. D.; Paver, M. A.; Raithby, P. R.; Wheatley, A. E. H.; Wright, D. S. *Chem. Commun.* **1997**, 1879.
71. Westerhausen, M.; Löw, R.; Schwarz, W. *J. Organomet. Chem.* 1996, 513, 213.
72. Westerhausen, M.; Schwarz, W. *Z. Anorg. Allg. Chem.* 1996, 622, 903.
73. Westerhausen, M.; Hausen, H. D.; Schwarz, W. *Z. Anorg. Allg. Chem.* 1995, 621, 877.

COORDINATION COMPLEXES OF BISMUTH(III) INVOLVING ORGANIC LIGANDS WITH PNICTOGEN OR CHALCOGEN DONORS

GLEN G. BRIAND and NEIL BURFORD

Department of Chemistry, Dalhousie University, Halifax, Nova Scotia B3H 4J3, Canada

- I. Introduction and Scope
 - A. Abbreviations
- II. Alkoxides, Thiolates, and Selenolates
 - A. Alkoxides
 - B. Thiolates
 - C. Selenolates
- III. Carboxylates, Thiocarboxylates, Dithiocarboxylates, and Diselenocarboxylates
 - A. Carboxylates
 - B. Thiocarboxylates
 - C. Dithiocarboxylates, Dithiocarbamates, and Dithioxanthates
 - D. Diselenocarboxylates (Diselenocarbamates)
- IV. Ethers and Thioethers
 - A. Ethers
 - B. Thioethers
- V. Ketones and Thiones
- VI. Amides
- VII. Amines, Phosphines, and Arsines
 - A. Amines
 - B. Phosphines
 - C. Arsines
- VIII. Nonsymmetric Bifunctional and Multifunctional Ligands
 - A. Hydroxy- and Alkoxide Carboxylates
 - B. Ketoalkoxides
 - C. Amino-, Imino-, and Azathiolates
 - D. Hydroxy-, Alkoxide, Ether, and Ketothiolates
 - E. Thiolatocarboxylates
 - F. Aminocarboxylates
 - G. Hydroxyamines and Aminoalkoxides
- IX. Conclusions
- References

I. Introduction and Scope

The development of bismuth chemistry must be considered in its infancy, despite a long history of medicinal applications (1–4) and more recent interest in materials exhibiting high-temperature superconductivity (5, 6). High and variable coordination numbers are responsible for a diverse structural chemistry. Traditional covalent bonding reminiscent of nonmetals is supplemented by coordinative interactions typical of transition metals, where the large atomic radius and orbital availability allows for coordination numbers as high as 9 or 10. The redox chemistry is restricted by the inert pair effect, but this imposes interesting structural features that have prompted unusual bonding models (7). In this article, we overview the structural diversity demonstrated by complexes of bismuth(III) with organic-based ligands involving the elements of Groups 15 (pnictogens) and 16 (chalcogens) as donor sites, recognizing the potential for tailoring structure and reactivity by manipulation of the organic moiety. Although most complexes of bismuth obey standard valence guidelines, the high and variable coordination numbers accessible to bismuth are responsible for interesting and unpredictable structural arrangements. Certain aspects of this chemistry have been reviewed in other contexts, including general chemistry (8), medicinal chemistry (3, 9), and antimicrobial activity (10). This discussion is restricted to compounds that are in most instances molecular so that the generally polymeric binary and tertiary inorganic compounds of bismuth are not included. Also omitted is the organochemistry of bismuth, which has been extensively reviewed by Doak and Freedman (11–14).

The formulas of well-defined bismuth compounds are presented here in table format to outline the type and extent of characterization data available for each, enabling assessment of the significance and relevance of the observations with regard to synthesis and reactivity. For example, complexes that are isolated in low yield, or for which a yield is not reported, do not warrant extensive discussion of the synthetic approach or a balanced equation for the reaction. Some of the structural features are described in detail to illustrate the novelty or generality of a particular arrangement. Collectively, the data provide important insights for the chemistry of bismuth and are applicable to the chemistry of other heavy elements. The review is structured in terms of the functional group that represents the donor site of the ligand, and these are illustrated in Chart 1, listing only those types of ligand for which bismuth complexes have been identified. Line drawings are provided for structures of complexes that are more complicated than the empiri-

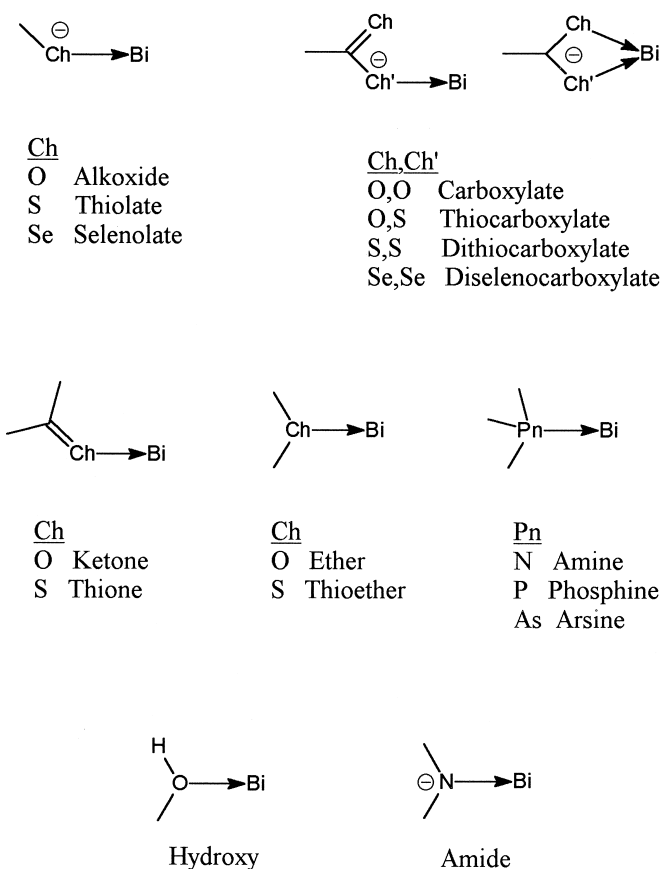


CHART 1. Functional groups with chalcogen or pnictogen sites as donors to bismuth.

cal formula indicates and are abbreviated in certain cases for clarity. Structures are drawn to illustrate connectivity only, as Lewis drawings or other representations of bonding are not meaningful or are misleading. Ligands are often abbreviated in these drawings to focus attention on the coordination environment of bismuth.

A. ABBREVIATIONS

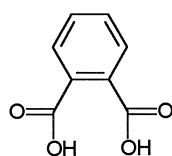
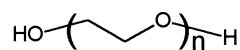
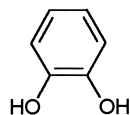
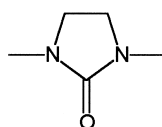
Habt	2-aminobenzenethiol
Hacac	acetylacetone
Hacd ³³	2-aminocyclopent-1-ene-1-dithiocarboxylic acid

Hamp ^{§3}	6-amino-8-mercaptapurinium
aptu ^{§3}	1-allyl-3-(2-pyridyl)thiourea-S
avg.	average bond distance/angle
Hbdmap	1,3-(dimethylamino)-2-propanol
bipy	bipyridyl
Hbta ^{§7}	bis(<i>tert</i> -butylketoethyl)amine
bit ^{§3}	benzimidazol-2(3 <i>H</i>)-thione
H ₂ cat ^{§2}	catechol
cfl ^{§7}	<i>p</i> -chlorobenzoyl-2-furaldehydohydrazine
H ₄ cit	citric acid
cmpnd	compound
cond	conductivity measurements
<i>m</i> -crown- <i>n</i> ^{§2}	cyclic crown ethers (<i>m</i> = atoms in the heterocycle, 12, 15, 18; <i>n</i> = number of oxygen atoms, 4, 5, 6)
cyclen ^{§4}	1,4,7,10-tetraazacyclododecane
H ₄ cydta ^{§6}	<i>trans</i> -cyclohexane-1,2-diaminotetraacetic acid
H ₄ cydtpa ^{§6}	<i>N</i> -(2-aminoethyl)- <i>trans</i> -1,2-diaminocyclohexane- <i>N,N',N''</i> -pentaacetic acid
H ₂ dapt ^{§7}	2,6-diacetylpyridine bis(2-thenoylhydrazone)
H ₂ dapts ^{§5}	2,6-diacetylpyridine bis(thiosemicarbazone)
Hdbt ^{§5}	2,6-dimethoxybenzenethiol
deimdt ^{§3}	<i>N,N'</i> -diethylimidazolidine-2-thione-S
dmf	dimethylformamide
dmpe	bis(dimethylphosphino)ethane
dmpu ^{§2}	<i>N,N'</i> -dimethylpropyleneurea
dmsO	dimethylsulfoxide
dpe	diphenylphosphinoethane
dpm	dipivaloylmethane
H ₂ dpmd ^{§7}	di-2-pyridylmethanediol
dppe	bis(diphenylphosphino)ethane
dppm	bis(diphenylphosphino)methane
dqp ^{§4}	2,6-bis(2'-quinolyl)pyridine
dtcR ₂ ^{§3}	dithiocarbamate
H ₈ dtpa ^{§6}	diethylenediaminepentaacetic acid
dtxR ^{§3}	dithioxanthates
H ₂ dz ^{§5}	3-mercapto-1,5-diphenylformazan (dithizone)
EA	elemental/chemical analysis
Heacd ^{§3}	2-ethylaminocyclopent-1-ene-1-dithiocarboxylic acid
H ₄ edta ^{§6}	ethylenediaminetetraacetic acid
etu ^{§3}	imidazolidine-2-thione
Hemal ^{§2}	ethylmaltol (2-ethyl-3-hydroxy-4 <i>H</i> -pyran-4-one)
H ₂ eon ^{§2}	polyethylene glycol (<i>n</i> = 3,4,5,6)
H ₄ gal	gallic acid
GED	gas electron diffraction
hex	hexane
hmpa	hexamethylphosphoramide
IR	infrared spectroscopy; mid- (MIR); far- (FIR)
H ₂ lac	lactic acid

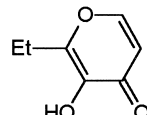
§ The parent acids of the more complicated anionic ligands and many of the neutral ligands are illustrated in Charts 2–7 (labelled as §# in abbreviations IA).

mag	magnetic susceptibility
H ₃ mal	malic acid
Me ₃ [9]aneN ₃ ^{§4}	1,4,7-trimethyl-1,4,7-triazacyclononane
Hmmq ^{§5}	2-methyl-8-mercaptoquinolinate
mnt ^{§3}	maleonitriledithiolate
mp	melting/decomposition (d) point; sublimation point
MS	mass spectrometry
H ₂ mpa ^{§5}	2-mercaptopropionic acid
H ₃ mpa ^{§5}	3-mercaptopropionic acid
MW	molecular weight measurement
NMR	nuclear magnetic resonance spectroscopy
H ₃ nta ^{§6}	nitriloacetic acid
H ₄ oedta ^{§6}	<i>N</i> -hydroxyethylethylenediaminetriacetic acid
H ₃ onda ^{§6}	<i>N</i> -hydroxyethylnitrilodiacetic acid
Hpaphy ^{§4}	pyridine-2-aldehyde-2'-pyridylhydrazone
H ₂ pc ^{§4}	phthalocyanine
pbda ^{§4}	<i>o</i> -phenylenebis(dimethylarsine)
H ₂ pdc ^{§6}	pyridine-2,6-dicarboxylic acid
pen ^{§5}	D-(–)-penicillaminato- <i>O,S,N</i>
phen	phenanthroline
H ₂ phthal ^{§2}	phthalic acid
Hpmq ^{§5}	2-phenyl-8-mercaptoquinolinate
pol	polarography
pot	potentiometry
pptu ^{§3}	1-phenyl-3-(2-pyridyl)-2-thiourea
pyr	pyridine
Hqui ^{§6}	quinaldic acid
Raman	Raman spectroscopy; resonance Raman spectroscopy
H ₃ saltren ^{§7}	[2,2',2''-nitrilotris(ethane-2,1-diylnitrilomethylidyne)]trisphenol
sol	solubility studies
H ₄ tar	tartaric acid
tdt	toluenedithiolate
ted	<i>N,N,N',N'</i> -tetraethylethylenediamine
terpy ^{§4}	2,2':6'2''-terpyridine
H ₂ tga ^{§5}	mercaptoacetic acid
thf	tetrahydrofuran
thpt ^{§3}	3,4,5,6-tetrahydropyrimidine-2(1 <i>H</i>)-thione
tm ^{§3}	hydrotris(methylimidazolyl)borate
tol	toluene
tp	hydrotris(pyrazolyl)borate
tpta ^{§4}	2,4,6-tris(2'-pyridyl)-1,3, triazine
Htr ^{§2}	tropolone
H ₂ tsal ^{§5}	thiosalicylic acid
HtscR ₁ R ₂ ^{§5}	thiosemicarbazones
H ₆ ttha ^{§6}	triethylenetetraminehexaacetic acid
tu ^{§3}	thiourea
UV	UV-visible spectroscopy; near infrared spectroscopy
X-ray	X-ray crystallographic studies

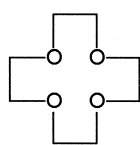
[§] The parent acids of the more complicated anionic ligands and many of the neutral ligands are illustrated in Charts 2–7 (labelled as §# in abbreviations IA).

H₂phthaln = 3, H₂eo3n = 4, H₂eo4n = 5, H₂eo5n = 6, H₂eo6H₂cat

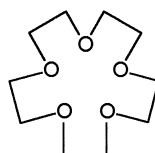
dmpu



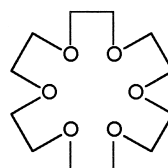
Hemal



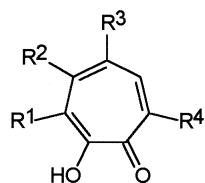
12-crown-4



15-crown-5



18-crown-6



Htr

R¹ = H, Me, Br, CH₂OHR² = H, Me, Et, iPr, benzoR³ = H, Me, NO₂, CHO, Br, CH₂OHR⁴ = H, Me, Br, CH₂OH

CHART 2. Carboxylate, ether, and ketone derivatives used as ligands on bismuth.

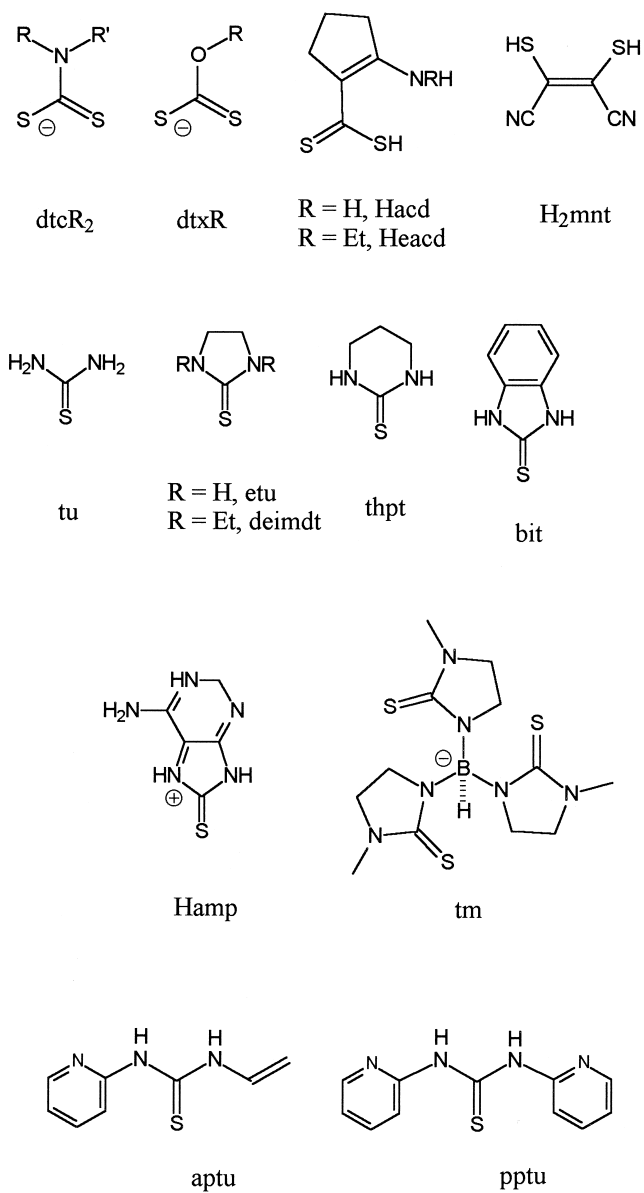
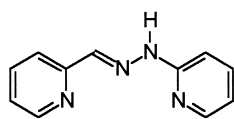
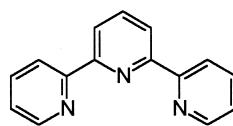


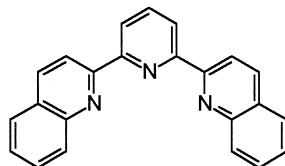
CHART 3. Sulfur donor derivatives used as ligands on bismuth.



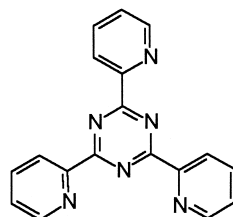
Hpaphy



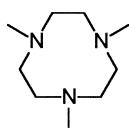
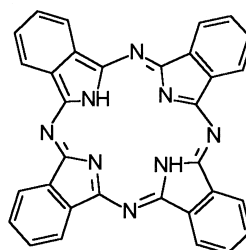
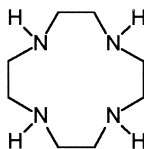
terpy



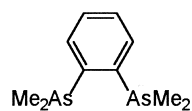
dqp



tpta

Me₃[9]aneN₃H₂pc

cyclen



pbda

CHART 4. Polyimines and -amines used as ligands on bismuth.

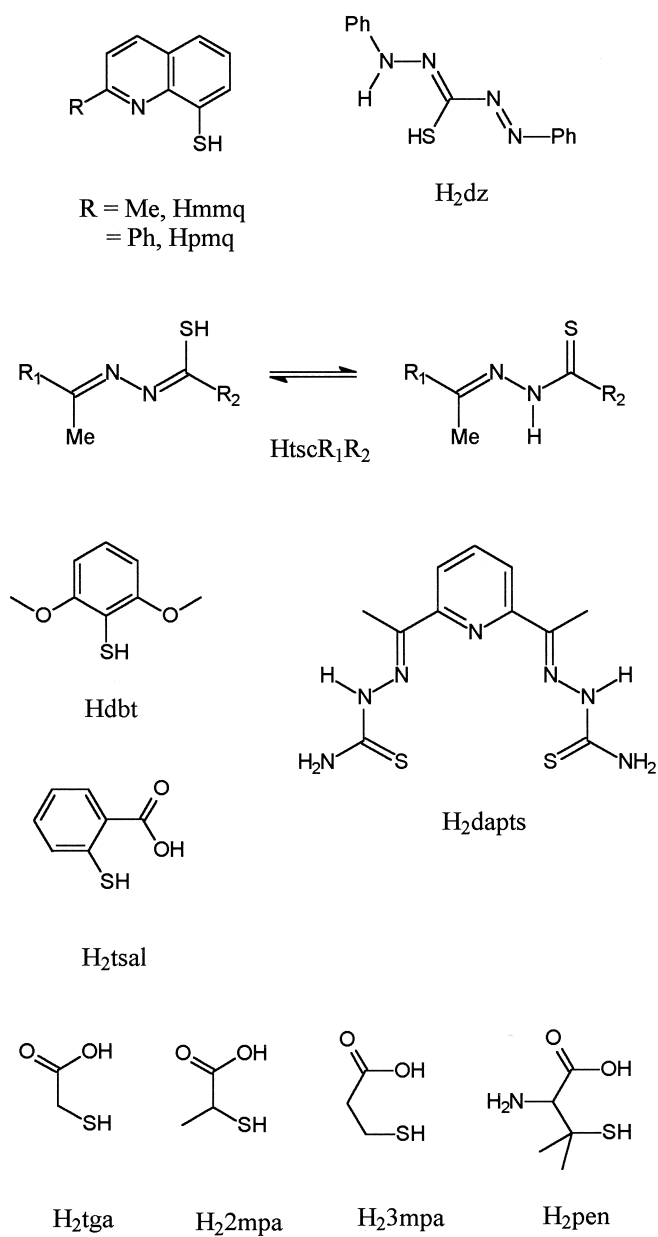


CHART 5. Multifunctional ligands for bismuth with sulfur donors.

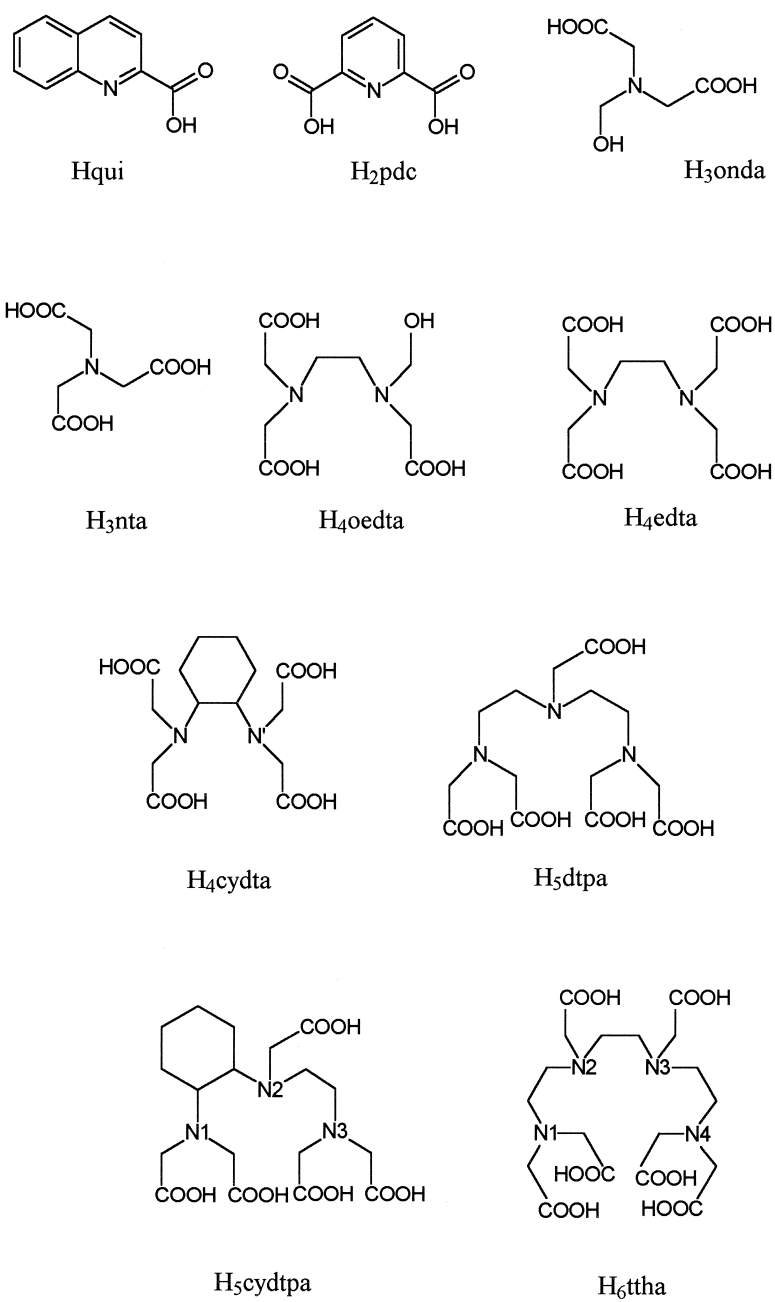


CHART 6. Aminocarboxylic acids used as ligands on bismuth.

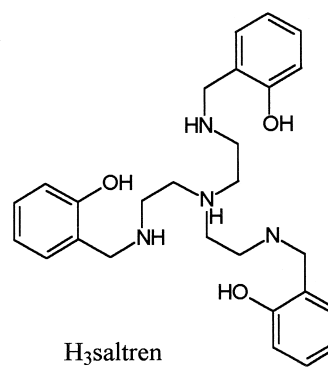
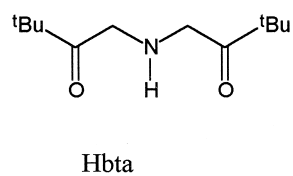
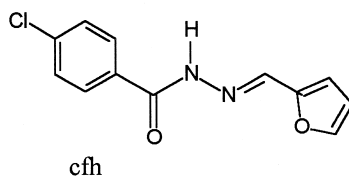
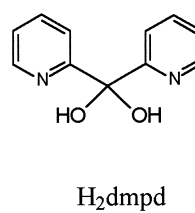
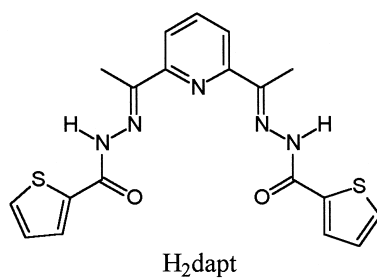
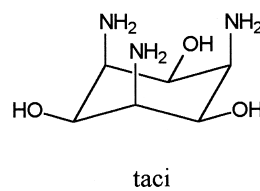
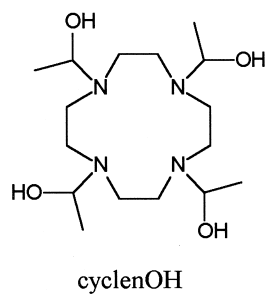


CHART 7. Hydroxyamines as ligands on bismuth.

II. Alkoxides, Thiolates, and Selenolates

Bismuth complexes of the prototypical general formula $\text{Bi}(\text{ER})_3$ have been extensively studied and numerous isolated examples are reported for $\text{E} = \text{O}$ and S . X-ray crystallographic studies reveal a variety of structural arrangements, with most involving multiple secondary inter- and/or intramolecular interactions. Most common are dimeric structures or polymeric arrays resulting from the ligand engaging more than one bismuth center and behaving as a bridging unit. Examples of cluster structures are also observed for certain alkoxide derivatives. Numerous chelate complexes have been isolated with dithiolate ligands, and although related bridging features are evident, the polymeric structures are less common and are dislocated by the tethering nature of the bifunctional anionic ligand.

A. ALKOXIDES

Monomeric arrangements are rare for alkoxide complexes of bismuth and require excess anionic ligands or bulky substituents. Otherwise the alkoxide ligands typically impose dimerization or multinuclear clustering, which are expressed in a variety of currently unusual structural arrangements (Table I).

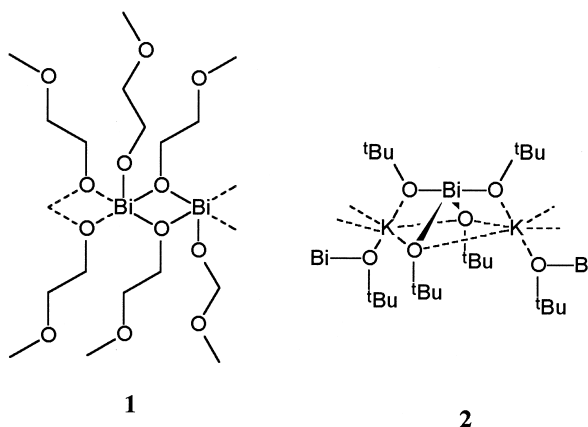
Bismuth alkoxides are most conveniently prepared by the reaction of a bismuth halide with an alkali metal alkoxides in benzene or thf under reflux conditions (15). Most exhibit low solubility in common organic solvents, but sublime under reduced pressure. Although incomplete, X-ray diffraction studies on $[\text{BiO}(\text{tBu})_3]_\infty$ (17) show a linear arrangement of metal atoms, and electron diffraction studies indicate a trigonal pyramidal structure in the gas phase (18). $[\text{Bi}_2(\mu_2, \eta^1\text{-OC}_2\text{H}_4\text{OMe})_4(\eta^1\text{-OC}_2\text{H}_4\text{OMe})_2]_\infty$ (20) is unusually soluble, even in organic solvents such as pentane, and the crystal structure (19–21) reveals asymmetric dimeric units, linked into one-dimensional polymeric chains through bridging equatorial alkoxide ligands **1**, with apical sites alternating in an up–down fashion. A distorted square pyramidal environment can be assigned for bismuth, composed of four basal bridging alkoxide oxygen atoms [$\text{Bi}-\text{O}$ 2.200(7)–2.573(6) Å] and a terminal alkoxide oxygen atom [$\text{Bi}-\text{O}$ 2.071(6) and 2.114(6) Å], but long contacts impose a pseudo octa-coordination for one bismuth center and hepta-coordination for the other. Solution NMR spectra indicate equilibria between various oligomers and/or isomers, and molecular weight measurements in benzene suggest a preference for the dimeric species (20). Alcoholysis of $\text{Bi}(\text{NMe}_2)_3$ allows

TABLE I
ANALYTICAL DATA FOR BISMUTH ALKOXIDE COMPLEXES

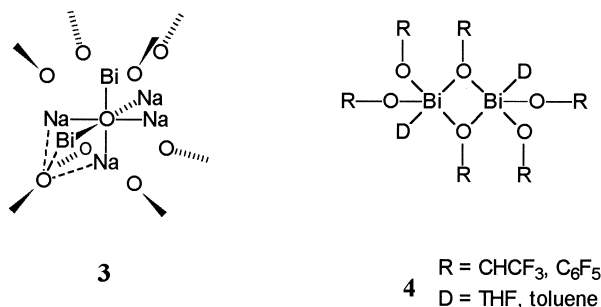
Empirical formula	X-ray structure #	Yield (%)	mp	EA	sol	IR	NMR	MS	GED	MW	TGA	Ref.
Bi(OMe) ₃		93	—	x	x	—	—	—	—	—	—	15
Bi(OEt) ₃		86–90	x	x	x	x	x	—	—	—	—	15, 16
Bi(O ⁱ Pr) ₃		80	x	x	x	—	x	—	—	—	—	15
Bi(O ⁱ Bu) ₃	x	41–80	x	x	x	x	x	x	x	—	—	17, 18
Bi(OC ₂ H ₅ OMe) ₃	1	ca50–89	x	x	x	x	x	—	—	x	—	19–21
Bi(OC ₂ H ₄ NMe ₂) ₃		50–80	x	x	—	—	x	—	—	—	—	21
Bi(OCHMeCH ₂ NMe ₂) ₃		50–80	x	x	—	—	x	—	—	—	—	21
Bi(OCMe ₂ Et) ₃		50–80	x	x	—	—	x	—	—	—	—	8
Bi(OC ₆ H ₃ Me ₂ -2,6) ₃	x	80	—	—	—	—	x	—	—	—	—	22
Bi(dpm) ₃		—	x	x	—	x	x	x	—	—	—	20
KBi(O ⁱ Bu) ₄	2	37	x	x	—	—	x	—	—	—	—	17
Na ₄ Bi ₂ O(O ⁱ Bu) ₈	3	15	x	—	—	—	x	—	—	—	—	17
Bi[OC(CF ₃) ₃] ₃		93	—	x	—	x	x	—	—	—	—	23
Bi[OCH(CF ₃) ₂] ₃ (thf) ₂	4	39	—	—	x	x	x	—	—	—	x	24
Bi(OC ₆ F ₅) ₃ (tol) ₂ [tol] ₂	4	51	—	—	x	x	x	—	—	—	—	24
Bi(OC ₆ F ₅) ₃ (tol) ₂	4	—	—	—	x	—	x	—	—	—	x	24
Bi(OC ₆ F ₅) ₃ (thf) ₂ [hex] ₂	4	—	—	—	—	—	—	—	—	—	—	24
Bi(OC ₆ F ₅) ₃ (thf) ₂	4	—	—	—	—	x	—	—	—	—	—	24
Bi ₂ O ₇ (OC ₆ F ₅) ₂ [Bi(OC ₆ F ₅) ₄] ₂ [tol] ₂	5	—	—	—	—	—	—	—	—	—	—	25
Bi ₂ O ₇ (OC ₆ F ₅) ₂ [Bi(OC ₆ F ₅) ₄] ₂ [thf] ₂	5	—	—	—	—	—	—	—	—	—	—	25
Na ₄ Bi ₂ O(OC ₆ F ₅) ₈	3	72	—	x	—	x	x	—	—	—	—	26
NaBi(OC ₆ F ₅) ₄	6	72	—	x	—	x	x	—	—	—	—	26
[Bi ₂ (μ ₃ -O) ₂ (μ-OC ₆ H ₃ Me ₂ -2,6) ₂] (OC ₆ H ₃ Me ₂ -2,6) ₂]	7	23	—	x	—	—	x	—	—	—	—	27
BiCl ₂ (thf)(μ-OAr) ₂ Ar = OC ₆ H ₃ Me ₂ -2,6 and OC ₆ H ₃ Me ₂ -2,4,6,2,6	8	20/19	—	x	—	—	—	—	—	—	—	28
[NMe ₄][Bi(OC ₆ H ₃ Me ₂ -2,6) ₃ Cl]	9	—	—	—	—	—	x	—	—	—	—	28
[PPh ₄][BiBr(OC ₆ H ₃ Me ₂ -2,4,6) ₂ Br]	—	—	—	—	—	—	x	—	—	—	—	28
[PPh ₄][BiBr ₂ (OC ₆ H ₃ Me ₂ -2,4,6) ₂ (μ-Br) ₂]	10	—	—	—	—	—	x	—	—	—	—	28
[PPh ₄] ₂ [BiBr ₂ (OC ₆ H ₃ Me ₂ -2,6) ₃]	—	—	—	x	—	—	x	—	—	—	—	28
Bi ₂ (OCH ₂ CH ₂ O) ₃	11	—	—	x	—	x	—	—	—	—	—	29
[NH ₄][Bi(cat) ₂]	12	—	—	x	—	—	—	—	—	—	—	30

for further derivatization of Bi(OR)₃ (R = CH₂CH₂NMe₂, CHMeCH₂NMe₂, or CMe₂Et) (21).

Bi(OC₆H₃Me₂-2,6)₃ is molecular in the solid state, with a distorted trigonal pyramidal geometry for bismuth, and the ligands twisted away from the fourth coordination site [avg. O–Bi–O 92(2)°] suggesting a stereochemically active lone pair (22). Bi(dpm)₃ has been spectroscopically characterized and reaction of dpmH with Bi(OⁱBu)₃ is described to give a mixed alkoxide ligand complex [Bi(OⁱBu)₂(dpm)]_n (20). Bi(OⁱBu)₃ also reacts with potassium *t*-butoxide in benzene to give [KBi(OⁱBu)₄] (17) in which bismuth adopts an unusual four coordinate see-saw bonding environment **2** [apical: Bi–O 2.265(8) and 2.285(9); equatorial: 2.061(10) and 2.075(8) Å]. Potassium atoms

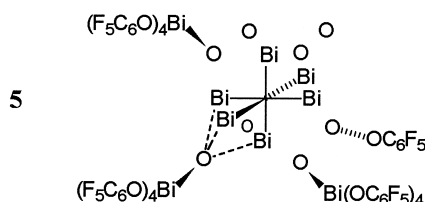


bridge pairs of alkoxide oxygen atoms between monomers to form a one-dimensional polymeric chain. The corresponding reaction with sodium *t*-butoxide gives the oxide-alkoxide cluster compound $[\text{Na}_4\text{Bi}_2\text{O}(\text{O}^t\text{Bu})_8]$, which is disordered in the solid state and is best viewed as an octahedral array of metal atoms encasing a unique oxygen atom, with each face capped by a butoxide **3**. No reaction was observed between $\text{Bi}(\text{O}^t\text{Bu})_3$ and lithium *t*-butoxide.

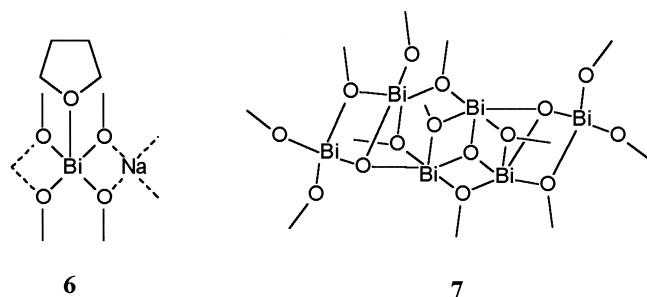


Several examples of fluorinated alkoxides and aryloxides have been prepared by a variety of methods, including the oxidative addition reaction of Bi metal with excess $(\text{CF}_3)_3\text{COCl}$ to give $[\text{Bi}\{\text{OC}(\text{CF}_3)_3\}_3]$ (**23**). Reaction of $\text{NaOCH}(\text{CF}_3)_2$ with BiCl_3 in a 3:1 ratio in thf gives $[\text{Bi}\{\text{OCH}(\text{CF}_3)_2\}_2\{\mu\text{-OCH}(\text{CF}_3)_2\}(\text{thf})_2]$ **4** (**24**, **31**). Derivatives and adducts of OC_6F_5 complexes $[\text{Bi}(\text{OC}_6\text{F}_5)_2(\mu\text{-OC}_6\text{F}_5)]_2$ are prepared from Biph_3 and HOC_6F_5 , and various solvent adducts have been isolated. Solution NMR studies suggest the existence of monomeric units at room temperature and dimeric species at lower temperatures, but

X-ray studies confirm $\text{Bi}_2(\mu\text{-OR})_2$ centrosymmetric dimers **4** in the solid state (24). Terminal alkoxides are generally bound more tightly than bridging units [terminal Bi–O 2.064(7) Å; bridging Bi–O 2.188(7) and 2.688(7) Å]. The bismuth oxide alkoxide cluster compounds $[\text{Bi}_6(\mu_3\text{-O}_7)(\mu_3\text{-OC}_6\text{F}_5)\{\text{Bi}(\text{OC}_6\text{F}_5)_4\}_3(\text{sol})_2] \cdot [\text{sol}]_2$ (sol = thf or toluene) were also isolated as minor products (25). Both structures contain the unusual octahedral $[\text{Bi}_6(\mu_3\text{-O}_7)(\mu_3\text{-OC}_6\text{F}_5)]^{3+}$ cores **5**, which



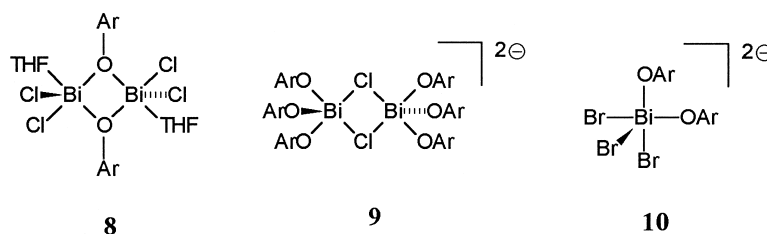
is capped on seven faces by μ_3 -oxide oxygen atoms and on one face by a $\mu_3\text{-OC}_6\text{F}_5$. Three of the μ_3 -oxide oxygen atoms are each bound to a $[\text{Bi}(\text{OC}_6\text{F}_5)_4]^-$ group, with bismuth in a five-coordinate distorted square pyramidal environment. The cluster bismuth atoms have irregular geometries, but similar core bond distances. The reaction of $[\text{Bi}(\text{OC}_6\text{F}_5)_2(\mu\text{-OC}_6\text{F}_5)]_2$ with NaOC_6F_5 gives the perfluorophenyl derivative of **3**, together with $[\text{NaBi}(\text{OC}_6\text{F}_5)_4(\text{thf})]_\infty$, in which the sodium ions contribute to the polymeric array **6** (26).



Reaction of BiPh_3 with 3 equiv of 2,6-dichlorophenol in toluene under reflux conditions gives the oxoalkoxide complex $[\text{Bi}_6(\mu_3\text{O})_3(\mu\text{-OC}_6\text{H}_3\text{Me}_2\text{-2,6})_7(\text{OC}_6\text{H}_3\text{Me}_2\text{-2,6})_5]$, which is solvated with toluene, ether, and the phenol, so that the crystals lose solvent molecules rapidly on removal from the mother liquor (27). The alkoxide bridged hexanuclear unit contains four- and five-coordinate bismuth centers in disphenoidal and square pyramidal geometries **7**. Two four-coordinate bismuth centers are bonded to two alkoxide oxygen atoms, one

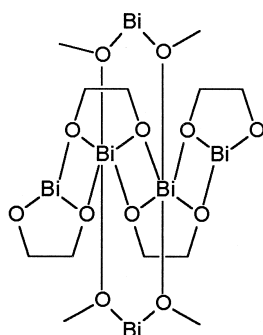
μ_3 -bridging oxide oxygen, and one bridging aryloxide oxygen. Two five-coordinate bismuth centers are bonded to one axial μ_3 -bridging oxide oxygen, and three bridging and one nonbridging aryloxide basal oxygen atoms. The two remaining bismuth centers are bonded to an axial μ_3 -bridging oxide oxygen and three bridging aryloxide and one μ_3 -bridging oxide oxygen atoms.

Partial substitution of halides on bismuth predictably gives alkoxy-bismuth halides, and salts of bismuth anions are obtained by reaction of the alkoxide with an ammonium or phosphonium halide (28). Two isostructural derivatives $[\text{Bi}_2\text{Cl}_4(\text{thf})_2(\mu\text{-OAr})_2]$ ($\text{Ar} = \text{C}_6\text{H}_3\text{Me}_{2,6}$ and $\text{C}_6\text{H}_2\text{Me}_{3-2,4,6}$) are composed of dimeric units residing on a C_2 axis **8**. The bismuth is in a five-coordinate distorted square pyramidal geometry in each case. The apical sites are occupied by terminal

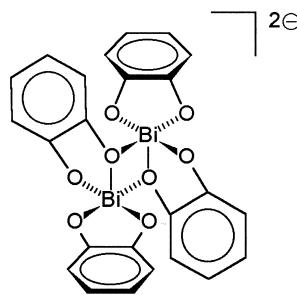


chlorine atoms and a thf molecule. The anionic analogues retain the dimeric structures as illustrated in the structure of $[\text{NMe}_4]_2[\text{Bi}_2(\text{OC}_6\text{H}_3\text{Me}_{2,6})_6(\mu\text{-Cl})_2]$ **9**, but $[\text{PPh}_4]_2[\text{BiBr}_2(\text{OC}_6\text{H}_3\text{Me}_{2,6})_3]$ **10** is a monomeric dianion with bismuth in a distorted square pyramidal environment. The apical site is occupied by an aryloxide oxygen atom [$\text{Bi}-\text{O}$ 2.119(7) Å], while the basal sites are occupied by three bromine atoms [$\text{Bi}-\text{O}$ 2.793(2)–3.1107(12) Å] and one aryloxide oxygen atom [$\text{Bi}-\text{O}$ 2.193(7) Å].

Two chelate alkoxide complexes have been isolated. $\text{Bi}_2(\text{OCH}_2\text{CH}_2\text{O})_3 \cdot 1.5\text{H}_2\text{O}$ was obtained by heating bismuth hydroxide in ethylene glycol at 80°C. The polymeric solid state structure **11** involves hexacoordination for bismuth composed of one chelated ligand and four long contacts to oxygen atoms from neighboring units. $[\text{NH}_4]_2[\text{Bi}_2(\text{cat})_4] \cdot (\text{H}_2\text{Cat})_2 \cdot 2\text{H}_2\text{O}$ was isolated from the reaction of ammonium catecholate with excess bismuth(III) oxide or bismuth (III) carbonate under reflux conditions in water (30). The structure contains the $[\text{Bi}_2(\text{C}_6\text{H}_4\text{O}_2)_4]^{2-}$ anion as a centrosymmetric dimer **12** with a distorted square-pyramidal environment for bismuth. The bis-chelate complexation of bismuth effects a see-saw coordination geometry



11



12

[Bi–O 2.150(3)–2.322(4) Å] with the planes of two perpendicular catechol ligands, and one oxygen imposes a long intermolecular contact [Bi···O 2.653(3) Å].

B. THIOLATES

The favorable bismuth–sulfur bond translates into thermal and hydrolytic stability for the thiolates of bismuth, which are currently more numerous than the alkoxide derivatives (Table II). Various monomeric trithiolates have been identified, and most adopt predictable structural formulas, although the solid-state structures reveal interesting intermolecular and intramolecular interactions.

Prototypical tris(thiolate)bismuth complexes are readily obtained by a wide range of metathesis reactions (including the co-production of mineral acids) because of the high thiophilicity of bismuth. For example, tris(ethylthiolato)bismuth is prepared from the simple reaction of bismuth nitrate with ethanethiol (32). Series of related complexes have been prepared, such as arylthiolates $\text{Bi}(\text{SAr})_3$ ($\text{Ar} = \text{C}_6\text{H}_3\text{Me}_2$ -2,6, $\text{C}_6\text{H}_3\text{Me}_2$ -3,5, $\text{C}_6\text{H}_4\text{Me}$ -4), including derivatives with substantial steric bulk [$\text{Bi}(\text{SC}_6\text{H}_2\text{R}_3$ -2,4,6) $_3$; $\text{R} = \text{Me}$, ^iPr , ^tBu (39)] (38). The compounds are air stable, sublime under reduced pressures, and are soluble in many organic solvents.

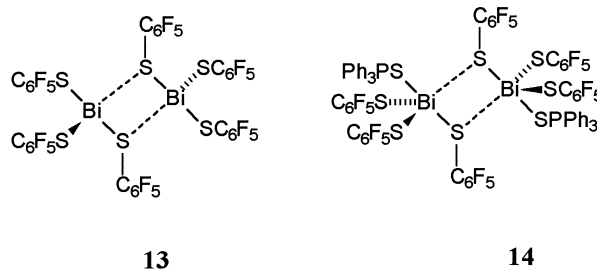
Mass spectrometric studies indicate that smaller molecule derivatives such as $\text{Bi}(\text{SCMe}_3)_3$ are monomeric in the gas phase (33), and the solid-state structure of $\text{Bi}(\text{SC}_6\text{H}_2^t\text{Bu}_3$ -2,4,6) $_3$ reveals a pyramidal environment for bismuth [S–Bi–S 90.3(2) to 104.5(2)°] with uniform Bi–S distances [Bi–S 2.554(7) to 2.569(8) Å]. However, the absence of intermolecular contacts is likely enforced by the steric bulk of the

ANALYTICAL DATA FOR BISMUTH THIOLATE COMPLEXES

Empirical formula	X-ray structure #	Yield (%)	mp	EA	solub (s) pol(p)	IR	Raman	UV	NMR	MS	TGA	Ref.
Bi(SEt) ₃	—	—	x	—	—	—	—	—	—	—	—	32
Bi(S ^t Bu) ₃	—	100	x	x	—	x	—	—	x	x	—	33
Bi(SCH ₂ Ph) ₃	—	C ₆ H ₅ CH ₂ SH/72 C ₆ H ₅ CH ₂ SLi/61	x	—	—	x	—	x	x	—	x	36 34
Bi(SPh) ₃	x	79	x	x	s	x	—	—	—	—	x	35, 36
Bi(SAr) ₃	—	—	—	x	—	—	—	—	x	—	—	37
Ar = C ₆ H ₃ Me ₂ -2,6	—	78	—	—	—	—	—	—	—	—	—	—
Ar = C ₆ H ₂ Me ₃ -3,5	—	49	—	—	—	—	—	—	—	—	—	—
Ar = C ₆ H ₂ M3 ₃ -4	—	62	—	—	—	—	—	—	—	—	—	—
Bi(SC ₆ H ₃ Me ₂ -2,4,6) ₃	—	86	x	x	—	—	—	—	x	—	x	38, 39
Bi(SC ₆ H ₃ Me ^t Pr ₂ -2,4,6) ₃	—	85	x	x	—	—	—	—	x	—	—	38, 39
Bi(SC ₆ H ₃ Me ^t Bu ₂ -2,4,6) ₃	x	86/77	x	x	—	—	—	—	x	—	x	39
Bi(SC ₆ H ₄ F- <i>p</i>) ₃	—	80	x	x	—	—	—	—	—	—	—	40
Bi(SC ₆ F ₅) ₃	13	93/70	x	x	s	x	—	—	x	—	—	36, 37, 41
[Na ₂ (thf) ₄][Bi(SC ₆ F ₅) ₃]	X	—	—	—	—	—	—	—	—	—	—	36
Bi(SC ₆ F ₅) ₃ L _n	—	~50	—	x	—	—	—	—	—	—	—	42
L = SPPH ₃ , <i>n</i> = 1	14	—	—	—	—	—	—	—	—	—	—	—
L = OPPH ₃ , <i>n</i> = 2	x	—	—	—	—	—	—	—	—	—	—	—
L = S=C(NHMe) ₂ , <i>n</i> = 3 L	x	—	—	—	—	—	—	—	—	—	—	—
= hmpa, <i>n</i> = 2	x	—	—	—	—	—	—	—	—	—	—	—
L = dmpu, <i>n</i> = 2	x	—	—	—	—	—	—	—	—	—	—	—
L = NCS[K], <i>n</i> = 1	15	—	—	—	—	—	—	—	—	—	—	—
L = OSPH ₂ , <i>n</i> = 2	—	—	—	—	—	—	—	—	—	—	—	—
L = S=C(NH ₂) ₂ , <i>n</i> = 2	—	—	—	—	—	—	—	—	—	—	—	—
ClBiSCH ₂ CH ₂ S	—	82/82	x	x	—	x	x	—	—	x	—	43, 44
BrBiSCH ₂ CH ₂ S	—	96	x	x	—	x	—	—	—	—	—	43
ClBiS(tol)S	—	86	x	x	—	—	—	—	—	—	—	45
XBisCH ₂ CH ₂ S · 2L	—	85	x	x	—	—	—	—	—	x	—	45
XBis(tol)S · 2L	—	—	—	—	—	—	—	—	—	—	—	—
X = Cl, Br	—	—	—	—	—	—	—	—	—	—	—	—
L = bipy, phen	—	—	—	—	—	—	—	—	—	—	—	—
X = Cl, L = pyr	—	—	—	—	—	—	—	—	—	—	—	—
	16	—	—	—	—	—	—	—	—	—	—	44, 45
ClBiSCH ₂ CH ₂ SCCH ₂ CH ₂ S	17	—/87	x	x	—	x	x	—	—	x	—	44, 46
ClBiSCH ₂ CH ₂ OCH ₂ CH ₂ S	17	~60/92	x	x	—	x	x	—	—	x	—	44, 47
Bi ₂ (tdt) ₃	—	—	—	x	p	—	—	—	—	—	—	48
ClBiS(CH ₂) _n = 3, 4	—	95	x	x	—	x	x	—	—	x	—	44
SCCH ₂ CH ₂ SBiSCH ₂ CH ₂ SBiSCH ₂ CH ₂ S	18	97	x	x	—	x	x	—	—	x	—	44
S(CH ₂) ₂ SBiS(CH ₂) _n	—	92	x	x	—	x	x	—	—	x	—	44
SBiS(CH ₂) _n S	—	—	—	—	—	—	—	—	—	—	—	—
<i>n</i> = 3, 4	—	—	—	—	—	—	—	—	—	—	—	—
SCCH ₂ CH ₂ SCCH ₂ CH ₂ SBiSC	19	67	x	x	—	x	x	—	—	x	—	44
H ₃ CH ₂ SCCH ₂ CH ₂ BiiSCH ₂ C	—	—	—	—	—	—	—	—	—	—	—	—
H ₃ SCCH ₂ CH ₂ S	—	—	—	—	—	—	—	—	—	—	—	—
SCCH ₂ CH ₂ OCH ₂ CH ₂ SBiSC	—	99	x	x	—	x	x	—	—	x	—	44
H ₃ CH ₂ OCH ₂ CH ₂ BiSCH ₂ C	—	—	—	—	—	—	—	—	—	—	—	—
H ₃ OCH ₂ CH ₂ S	—	—	—	—	—	—	—	—	—	—	—	—
[Et ₄ N][Bi(mnt)(X) ₂](X = Cl, Br)	—	—	—	x	p	x	—	—	—	—	—	48
[Et ₄ N] ₂ [Bi ₂ (mnt) ₂ (X) ₂] ₂	—	—	—	—	—	—	—	—	—	—	—	—
[Et ₄ N] ₄ [Bi ₂ (mnt) ₂] ₂	—	—	—	—	—	—	—	—	—	—	—	—
[Ph ₄ As][Bi(mnt) ₂]	20	—	—	—	—	—	—	—	—	—	—	49

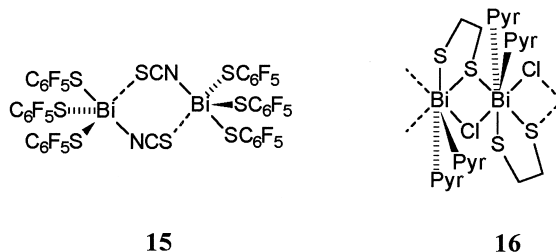
ligand (39), as the pentafluorinated derivative $\text{Bi}(\text{SC}_6\text{F}_5)_3$ (41) adopts a loosely bound dimeric arrangement **13**, with bismuth in a four-coordinate disphenoidal environment (36), composed of three shorter Bi–S distances [Bi–S 2.532(2) and 2.540(2); Bi–S_{bridging} 2.584(2) Å] and one longer bridging sulfur contact [Bi---S_{terminal} 3.323(2) Å].

Reaction of BiCl_3 with 3 equiv NaSC_6F_5 in thf results in the surprising formation of the pentathiolate dianion in $[\text{Na}_2(\text{thf})_4][\text{Bi}(\text{SC}_6\text{F}_5)_5]$ (36). This “overthiolation” is attributed to the greater Lewis acidity of the bismuth center imposed by the electron-withdrawing ability of the fluorinated ligands. The structure of the anion $[\text{Bi}(\text{SC}_6\text{F}_5)_5]^{2-}$ involves bismuth in a square pyramidal geometry [Bi–S_{equatorial} 2.988(9), 2.703(9), 2.889(9), and 2.746(10); Bi–S_{axial} 2.609(10) Å], with the remaining apical site occupied by a long intramolecular bismuth fluorine contact [Bi---F 2.94 Å]. Enhancement of the Lewis acidity is further demonstrated by the range of adducts of the general formula $[\text{Bi}(\text{SC}_6\text{F}_5)_3\text{L}_n]$ (L = SPh_3 , $n = 1$; L = OPPh_3 , $n = 2$; L = $\text{S}=\text{C}(\text{NHMe})_2$, $n = 3$; L = OSPh_2 , $n = 2$; L = $\text{S}=\text{C}(\text{NH}_2)_2$, $n = 2$; L = hmpa, $n = 2$; L = dmpu, $n = 2$; L = $(\text{NCS})^-$ [K(18-crown-6)], $n = 1$) (42). The complexes adopt a range of stoichiometries (1:1, 1:2, and 1:3), and they exhibit a variety of structural arrangements. $\text{Bi}(\text{SC}_6\text{F}_5)_3(\text{SPPPh}_3)$ exists as a centrosymmetric dimer **14** in the solid



state, with bismuth in a square pyramidal geometry. The axial site is occupied by a SC_6F_5 sulfur atom [Bi–S 2.58(1) Å], while the basal sites are occupied by two *cis* sulfur atoms (one terminal and one bridging) of the two remaining SC_6F_5 ligands, the sulfur atom of the SPPPh_3 ligand [Bi–S 3.01(1) Å], and a long contact from a bridging sulfur of the other molecule in the dimer [Bi---S 3.15(1) Å]. The *trans* effect of the SPPPh_3 ligand causes one of the thiolate bond distances to be longer [Bi–S_{bridging} 2.62(2) Å] than the other two in the monomer, while the long contact from the bridging sulfur atom has no effect [Bi–S_{terminal} 2.57(1) Å]. A dimeric structure and square pyramidal geometry

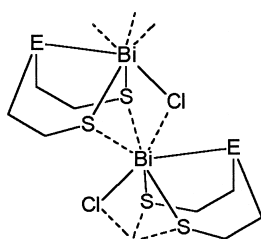
for bismuth is also observed in the anion $[\text{Bi}(\text{SC}_6\text{F}_5)_3(\text{NCS})]$ $[\text{Bi}-\text{S}_{\text{SC}_6\text{F}_5}$ 2.645(2), 2.2.614(2), 2.564(2) Å], but with bridging through the isothiocyanate ligand **15**, which is more tightly held to the monomer



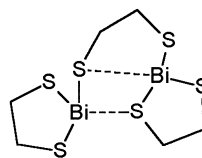
through the nitrogen atom and has a long contact to the neighboring molecule through its sulfur atom $[\text{Bi}-\text{N}$ 2.577(6); $\text{Bi} \cdots \text{S}$ 3.178(2) Å]. A *trans* effect from the NCS ligand is again observed. Penta-coordination of the bismuth center in the bis adducts $[\text{Bi}(\text{SC}_6\text{F}_5)_3(\text{OPPh}_3)_2]$, $[\text{Bi}(\text{SC}_6\text{F}_5)_3(\text{hmpa})_2]$, and $[\text{Bi}(\text{SC}_6\text{F}_5)_3(\text{dmu})_2]$ renders the molecules monomeric. The apical site is again occupied by the sulfur atom of the SC_6F_5 ligand $[\text{Bi}-\text{S}$: 2.588(2); 2.588(1); 2.548(2) Å, respectively], while the basal sites are occupied by two sulfur atoms of two *cis* SC_6F_5 ligands $[\text{Bi}-\text{S}$: 2.613(1) and 2.617(2); 2.626(1) and 2.670(1); 2.574(2) and 2.587(2) Å, respectively] and two oxygen atoms of the donors $[\text{Bi}-\text{O}$ 2.586(6) and 2.627(5); 2.502(3) and 2.547(3); 2.728(5) and 2.645(4) Å, respectively]. A *trans* effect is again evident in the basal $\text{Bi}-\text{S}$ bond distances. A hexacoordinate, near octahedral environment is observed for $[\text{Bi}(\text{SC}_6\text{F}_5)_3(\text{S}=\text{C}(\text{NHMe})_2)_3]$ with a *fac* configuration $[\text{Bi}-\text{S}$ 2.721(2); $\text{Bi}-\text{O}$ 2.946(3) Å]. These VSEPR consistent geometries and *trans* effects are consistent with a model in which the $\text{Bi}-\text{S}$ σ^* orbitals are the acceptor orbitals for the electron pair donation of the adduct ligands.

Dithiols react rapidly and quantitatively with many bismuth halides and salts to effect a dimetathesis reaction, favored by both the dianionic nature of the ligand and chelate structure. The reaction, first recognized by Powell (43, 45), has been exploited to give a series of monocyclic dithiolate complexes (43, 44, 48) with varying ring sizes. Eight-membered heterocycles, referred to as bismocanes **17** (46, 47) are readily obtained using ether or thioether derivatives, which are favored by virtue of the auxiliary cross ring coordinative interactions $\{\text{S}-\text{Bi}$ $[\text{Bi}-\text{S}$ 2.541(6) Å]. In addition, this interaction together with those of two thiolate sulfur atoms contacts $[\text{Bi} \cdots \text{S}$ 3.534(7) Å] and a chlorine $[\text{Bi}-\text{Cl}$ 3.285(6) Å] from a neighboring molecule imposes a seven-coordinate environment for bismuth.

A systematic series of monocyclic chlorobismuthdithiolates have



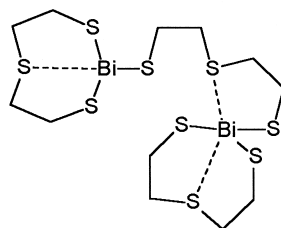
17 E = O, S



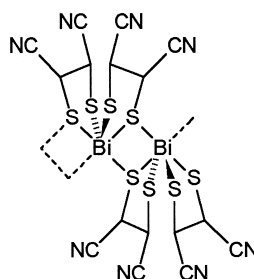
18

been comprehensively characterized and shown to be kinetic products of the metathesis reaction (44). In the presence of sodium nitrate and excess dithiol, the bismuth–chlorine bond is activated and the third remaining metathesis occurs to give “tethered” bicyclic trithiabismuth compounds (44). The general reaction of $\text{Bi}(\text{NO}_3)_3$ with the appropriate ligand in ethanol at a 2:3 ratio also results in a complete metathesis and affords a systematic series of tethered bicyclic compounds. Two derivatives (**18** and **19**) have been crystallographically characterized and involve intermolecular and intramolecular coordinative interactions to bismuth. The most prominent feature in these structures is the formation of five-membered ring motifs.

The dipyrindine complex of the ethanedithiolate derivative $[\text{Bi}-\text{N} \ 2.534(8) \text{ and } 2.592(9) \text{ \AA}]$ has a polymeric solid-state structure **16** involving alternating $\text{Bi}-\text{Cl}$ [$\text{Bi}-\text{Cl} \ 3.111(4) \text{ and } 3.231(5) \text{ \AA}$] and $\text{Bi}-\text{S}$ [$\text{Bi} \cdots \text{S} \ 3.443(5) \text{ \AA}$] intermolecular contacts [cf. intra-ring $\text{Bi}-\text{S} \ 2.545(4) \text{ and } 2.592(9) \text{ \AA}$]. Anionic complexes of bismuth dicyanoethylene-1,2-dithiolates (maleonitriledithiolate = mnt) were isolated as the tetraethylammonium salts (48). The mixed (halide) ligand complexes $[\text{Et}_4\text{N}]_2[\text{Bi}_2(\text{mnt})_2\text{X}_4]$ ($\text{X} = \text{Cl}, \text{Br}$) and $[\text{Et}_4\text{N}]_2[\text{Bi}_2(\text{mnt})_3\text{X}_2]$ ($\text{X} = \text{Cl}, \text{Br}$), as well as the homoleptic complex $[\text{Et}_4\text{N}]_4[\text{Bi}_2(\text{mnt})_5]$, are speculated to be dinuclear species. However, the structure of the tetraphenylarsonium salt $[\text{Ph}_4\text{As}][\text{Bi}(\text{mnt})_2]$ **20** involves an



19



20

infinite polymeric chain (49). Bismuth is six-coordinate and chelated by two dithiolate ligands, one sulfur atom of each ligand bridging adjacent bismuth centers [Bi–S 2.693(7) and 2.664(7); Bi–S_{bridging} 2.746(9) and 2.836(8) Å].

C. SELENOLATES

The aryl-substituted derivatives of [Bi(SeC₆H₂R'₃-2,4,6)₃] (R' = Me, ⁱPr, ^tBu) are the only isolated examples of selenolate complexes. They have been characterized by mp, elemental analysis, NMR spectroscopy, and thermal gravimetric analysis, and the solid-state structure of the isopropyl-substituted derivative reveals a tricoordinate environment for bismuth [Bi–Se 2.630(8)–2.711(8) Å; Se–Bi–Se 92.3(2)–103.3(2)°], imposed by the steric bulk of the ligands (38).

III. Carboxylates, Thiocarboxylates, Dithiocarboxylates, and Diselenocarboxylates

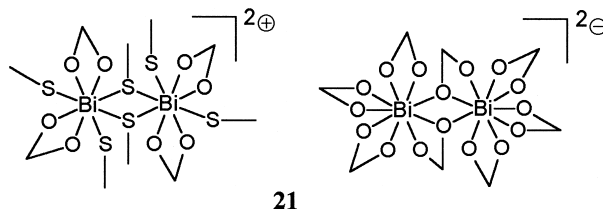
A. CARBOXYLATES

(See Table III.) Bismuth formate Bi(OOCH)₃ is prepared by reacting bismuth oxide with a 40% formic acid solution under reflux conditions (50, 64). The solid-state structure shows three different Bi–O distance ranges [avg. 2.38, 2.52, and 2.77 Å] and all oxygen atoms interacting with bismuth, which occupies a six-coordinate, distorted octahedral environment. The octahedra are linked via the carbon centers re-

TABLE III
ANALYTICAL DATA FOR BISMUTH CARBOXYLATE COMPLEXES

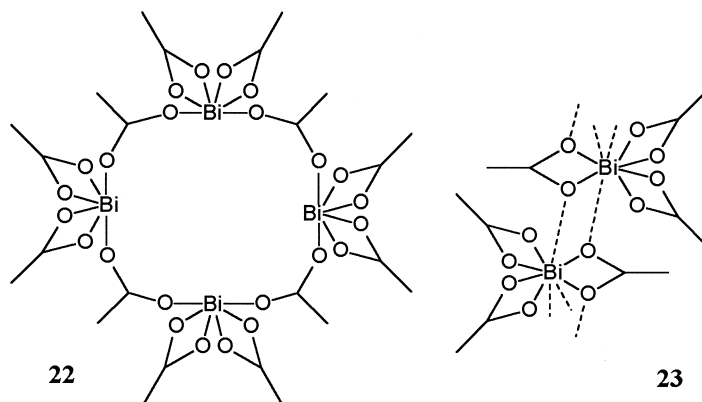
Empirical formula	X-ray structure #	Yield (%)	mp	EA	sol	IR	NMR	MS	Ref.
Bi(OOCH) ₃	x	—	—	—	—	x	—	—	50
K ₂ Bi(OOCH) ₅	x	—	—	—	—	—	—	—	51
Bi(OOCCCH ₃) ₃	x	90	—	x	x	x	—	—	52–54
Bi ₂ (CH ₃ COO) ₆ (tu) ₃ H ₂ O	21	—	—	—	—	—	—	—	55
Bi(CH ₃ COO) ₃ (tu) ₃	x	—	—	—	—	—	—	—	55
Bi(O ₂ CCMe ₂) ₃	22	100	x	x	x	x	x	—	56, 57
Bi(OOCC ₆ H ₅) ₃	23	—	—	x	—	—	—	—	58
BiO(OOCCCH ₃)	x	—	—	x	—	—	—	—	59
Bi(OOCCF ₃) ₃	—	—	x	x	—	x	x	x	60, 61
Bi(OOCCF ₃) ₃ (OOCCF ₃)	x	94	—	—	—	—	—	—	61, 62
NaBi(CF ₃ COO) ₄	—	—	—	x	—	x	—	—	60
[H ₂ teed][Bi(O ₂ CCF ₃) ₃]	x	—	x	x	—	x	—	—	63

sulting in a sheet structure, and an overall trigonal prismatic nine-coordinate environment. Bismuth acetate $\text{Bi}(\text{OOCCH}_3)_3$ has been prepared by the recrystallization of "commercial reagents" from acetic acid solution (53) and by dissolving Bi_2O_3 in hot acetic acid and acetic anhydride (54). It adopts a layered structure (52). Two structurally characterized thiourea adducts of bismuth acetate demonstrate the structural versatility of bismuth (55). $\text{Bi}_2(\text{CH}_3\text{COO})_6(\text{tu})_3\text{H}_2\text{O}$ is ionic and composed of dimeric cations $[\text{Bi}_2(\text{CH}_3\text{COO})_4(\text{tu})_6]^{2+}$ and anions $[\text{Bi}_2(\text{CH}_3\text{COO})_8]^{2-}$ **21**, in which the acetate ligands are principally



bidentate [Bi–O 2.31(1)–2.71(2) Å; Bi–O_{terminal} 2.26(1)–2.65(1); Bi–O_{bridging} 2.78(1) Å], but also effect a bridge in the homoleptic anion. The cation predictably involves bridging thiourea sulfur atoms [Bi–S 2.909(5) and 3.132(5) Å] as well as two terminal thiourea ligands [Bi–S 2.677(5) and 3.152(6) Å]. In contrast, $\text{Bi}(\text{CH}_3\text{COO})_3(\text{tu})_3$ is molecular in the solid state with bismuth in a nine-coordinate environment composed of three bidentate acetate groups [avg. Bi–O 2.509(4) Å] and three thiourea sulfur atoms [avg. Bi–S 3.061(2) Å] in a *fac* arrangement.

Bismuth acetate is susceptible to ligand exchange reactions, and a number of bismuth carboxylate derivatives have been prepared (56). With 2,2-dimethylpropionic acid, a tetrameric complex is obtained $[\text{Bi}(\text{O}_2\text{CCMe}_3)_3]_4$ **22** (57), in which each bismuth center is nine-coordinate and is bound to six 2,2-dimethylpropionate groups in chelate, μ_2 -, and μ_3 -fashion [Bi–O range 2.24–3.16 Å]. The presence of bulkier substituents is responsible for the less polymeric structure, which renders the compound more volatile, and it is crystallized by sublimation. In contrast, the tris(benzoate) complex $\text{Bi}(\text{OOC}_6\text{H}_5)_3$ adopts a one-dimensional polymer **23** involving two unique bismuth centers (58). Nine coordination at each bismuth center is composed of six oxygen atoms from three asymmetrically chelating ligands, each of which also bridges bismuth centers [Bi–O_{nonbridging} 2.198(14)–2.533(16); Bi–O_{bridging} 2.243(14)–2.793(18) Å], and in turn each bismuth center receives a long contact from three ligand oxygen atoms [Bi–O



2.624(16)–3.380(16) Å]. Alkoxide/oxide compounds of the speculated general formula $\text{BiO}(\text{OOCR})$ are formed by dissolving Bi_2O_3 in the carboxylic acid, followed by dilution and distillation of the excess acid (59). The compounds were characterized by elemental analysis and preliminary X-ray diffraction data.

$\text{Bi}(\text{OOC}\text{CF}_3)_3$ and the corresponding tetraacetate salt $\text{Na}[\text{Bi}(\text{OOC}\text{CF}_3)_4]$ are obtained from the reaction of excess trifluoroacetic anhydride with Bi_2O_3 and NaBiO_3 , respectively, under reflux conditions (60), or by metathesis reaction (61). A salt of the dianion $[\text{Bi}(\text{O}_2\text{CCF}_3)_5]^{2-}$ is prepared from BiPh_3 with teed in excess trifluoroacetic acid (63). Bismuth occupies a symmetric 10-coordinate environment involving oxygen atoms of five bidentate trifluoroacetate groups [$\text{Bi}-\text{O}$ 2.44(3)–2.62(2) Å], to give a distorted pentagonal prism. $\text{Bi}(\text{phthal})\text{OH}$ was prepared by reacting Bi_2O_3 with H_2phthal in a 1:2 ratio in acetone under reflux conditions, and the IR spectrum indicates an unsymmetrically bidentate coordination of both carboxylate groups (65).

B. THIOCARBOXYLATES

A series of thiobenzoate derivatives of the general formula $\text{Bi}(\text{SOCC}_6\text{H}_4\text{R})_3$ ($\text{R} = \text{H}$ (66), *o*-Me, *p*-Me) (67) were prepared in high yield from the reaction of Bi_2O_3 with an excess of the appropriate ligand in acetone, and were characterized by melting point, elemental analysis, and IR and NMR spectroscopy (67). For $\text{R} = \text{o-Me}$, the complex is very soluble in organic solvents, enabling crystallization and structure determination, which reveals three chelating thiocarboxylate ligands [$\text{Bi}-\text{S}$ 2.630(3) Å], with relatively long bismuth–oxygen

bond distances [Bi–O 2.752(6) Å] and the three sulfur atoms in a pyramidal *fac* arrangement. Long contacts from the three sulfur atoms of a neighboring molecule [Bi---S 3.498 Å] give a coordination number of 9 for bismuth.

C. DITHIOCARBOXYLATES, DITHIOCARBAMATES AND DITHIOXANTHATES

Numerous complexes of bismuth involving dithiocarbamate (dtcR₂) and/or dithioxanthates (dtxR) ligands are known, (Table IV and Chart 3); however, there are few examples of authentic dithiocarboxylate complexes. Bi(eacd)₃ represents the only structurally characterized example of dithiocarboxylate and adopts a monomeric solid-state structure with bismuth in a six-coordinate distorted trigonal antiprismatic environment [Bi–S_{short} 2.617(2) and 2.647(1); Bi–S_{long} 2.963(2) and 3.108(2) Å], and a closest long bismuth sulfur contact of 3.689 Å (68). Throughout the more extensive series of dithiocarboxylate derivatives (dithiocarbamates and dithioxanthates), complexes are generally homoleptic and adopt predictable formulas. Although there are examples of thio bridging ligands, they are rare, and intermolecular interactions are more obviously formed by halides in the mono- and bis-dithiocarboxylate complexes.

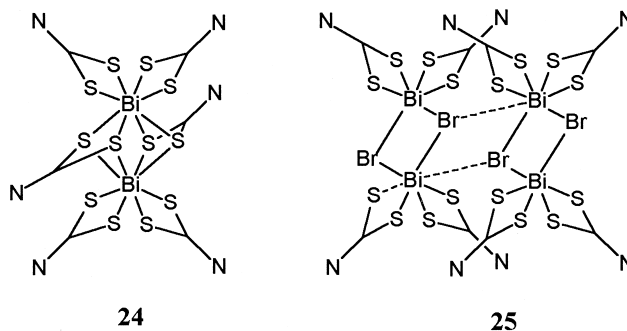
Tris(dithiocarbamate) complexes have been obtained using various synthetic methods, including reaction of bismuth halide with the appropriate amine and carbon disulfide and reactions of bismuth nitrate or bismuth halide with salts of the dithiocarbamate. Bi(dtcEt₂)₃ (69) exists as a weakly bound dimer in the solid state (70, 71), with three chelating dithiocarbamate ligands [Bi–S_{short} 2.595(5)–2.775(5); Bi–S_{long} 2.956(5)–2.964(4) Å] and a long sulfur contact from a neighboring molecule [Bi–S 3.210(4) Å]. A better-established dimer **24** is observed for the ethanol-substituted derivative Bi(dtc{HOCH₂CH₂}₂)₃ (72) which contains bismuth in an eight-coordinate distorted square antiprism bonding environment imposed by four nonbridging sulfur atoms of two asymmetrically bound dithiocarbamate ligands [Bi–S_{short} 2.669(7)–2.729(7); Bi–S_{long} 2.790(7)–2.885(7) Å] and four bridging sulfur atoms [Bi–S 3.076(9)–3.179(9) Å] of two chelating ligands. A weak interaction is responsible for the intermonomer relationship between unique bismuth complexes of Bi(dtc{CH₂CH₂}₂)₃ in the solid state (73). The six- and seven-coordinate environments are generated by three asymmetrically bound dithiocarbamate ligands [Bi–S_{short} 2.612(7)–2.784(7); Bi–S_{long} 2.860(9)–3.017(8) Å], and a long contact from a sulfur atom of one ligand [Bi---S 3.163(6) Å].

TABLE IV

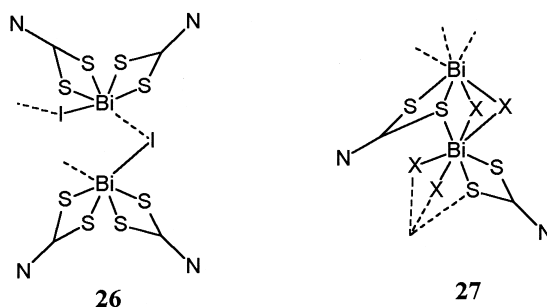
ANALYTICAL DATA FOR DITHIOCARBOXYLATE (DITHIOCARBAMATE AND DITHIOXANTHATE) COMPLEXES OF BISMUTH

Empirical formula	X-ray structure #	Yield (%)	mp	EA	sol	cond	IR	UV	NMR	MS	TGA	CV	MW	Ref.
Bi(eacd) ₃	x	90–98	—	—	—	—	—	—	—	—	—	—	—	68
Bi(dtcEt ₂) ₃	—	63	x	x	x	—	x	—	—	—	x	—	—	69–71
Bi(dtc{HOCH ₂ CH ₂ }) ₃	24	—	—	—	—	—	—	—	—	—	—	x	—	72
Bi(dtc{CH ₃ CH ₂ }) ₃	x	95	—	x	—	—	x	—	—	—	—	—	—	73
Bi(dtcEt ₂) ₂ Br	25	94	x	x	x	x	x	x	x	—	—	—	x	74, 75
Bi(dtcR ₂) ₂ Br(R = ⁱ Bu, CH ₂ C ₆ H ₅)	—	86–84	x	x	x	x	x	x	x	—	—	—	x	74
Bi(dtcR ₂) ₂ Br(R = CH ₂ CH ₃ , (CH ₃) _{2.5})	—	91–95	x	x	x	x	x	x	—	—	—	—	x	74
Bi(dtcEt ₂) ₂ I	26	85	x	x	x	—	x	x	x	x	—	—	x	76
Bi(dtcR ₂) ₂ I(R = ⁱ Bu, CH ₂ C ₆ H ₅)	—	80, 75	x	x	x	—	x	x	x	—	—	—	x	76
Bi(dtc{CH ₃ CH ₂ }) ₂ I(R = (CH ₃) _{2.5})	—	84	x	x	x	—	x	x	—	—	—	—	x	76
Bi(dtc{CH ₃ CH ₂ }) ₂ I	—	88	x	x	x	—	x	x	—	x	—	—	x	76
Bi(dtc{CH ₃ CH ₂ }) ₂ Cl(tu)	x	low	—	x	—	—	x	—	—	—	—	—	—	73
[Bi(dtcR ₂) ₂ (BF ₄) ₂](R = Et, CH ₃ CH ₂ , (CH ₃) _{2.5})	—	~70	x	x	x	x	x	x	x	x	—	—	x	77
Bi(dtcEt ₂)Cl ₂	27	60	x	x	—	—	x	—	x	—	—	—	—	78, 79
Bi(dtcEt ₂)X ₂ (X = ⁸⁰ Br, I)	27	—	x	x	—	—	x	—	—	—	—	—	—	81

[illegible]



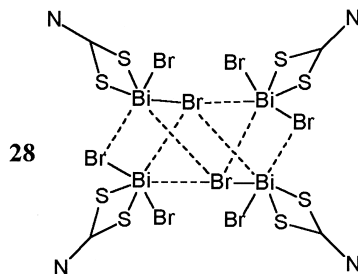
The bromide and iodide complexes $\text{Bi}(\text{dtcR}_2)_2\text{Br}$ ($\text{R} = \text{Et}$, ^iBu , $\text{CH}_2\text{C}_6\text{H}_5$, CH_2CH_2 , $(\text{CH}_2)_{2.5}$; $\text{X} = \text{Br}$ (**74**), $\text{X} = \text{I}$ (**76**)) are prepared from the respective tris(dialkyldithiocarbamate) by stoichiometric addition of bromine or iodine in CCl_4 or CHCl_3 , but the dihalo derivatives have not been obtained. Conductance measurements of the bromo analogues suggest that they are non-electrolytes in nitrobenzene, while molecular weight measurements of all monohalo compounds indicate that they exist as dimers in solution. The spectroscopic data of the iodo complex suggest that dithiocarbamate ligands function as bidentate ligands. $\text{Bi}(\text{dtcEt}_2)_2\text{Br}$ exists as a tetramer-based (**25**) polymeric network in the solid state, with two unique bismuth environments (**75**). Both centers bear four sulfur atoms of two asymmetrically bound dithiocarbamate ligands [$\text{Bi}-\text{S}_{\text{short}}$ 2.669(5) and 2.657(4); $\text{Bi}-\text{S}_{\text{long}}$ 2.719(6) and 2.843(7) Å; $\text{Bi}-\text{S}_{\text{short}}$ 2.641(5) and 2.658(4); $\text{Bi}-\text{S}_{\text{long}}$ 2.716(6) and 2.814(5) Å]. One center additionally binds two *cis* bridging μ_2 - and μ_3 -bromine atoms [$\text{Bi}-\text{S}$ 3.066(2) and 3.004(2) Å, respectively], and the other binds three *fac* bridging μ_2 - and μ_3 -bromine atoms [μ_2 : $\text{Bi}-\text{S}$ 3.104(2); μ_3 : $\text{Bi}-\text{S}$ 3.232(2) and 3.390(3) Å]. The corresponding iodide is a one-dimensional polymer with a $-\text{Bi}-\text{I}-\text{Bi}-\text{I}-$ backbone (**26**) and six-coordinate environment consisting of four sulfur atoms of two dithiocarbamate ligands [$\text{Bi}-\text{S}$ 2.646(4)–2.860(5) Å] and two *cis* bridging μ_2 -iodine atoms [$\text{Bi}-\text{I}$ 3.257(2) and 3.354(1) Å] (**75**). $\text{Bi}(\text{dtc}[\text{CH}_2\text{CH}_2]_2)_2\text{Cl}(\text{tu})$ (**73**) is dimeric, but involves only chlorine bridges, and the dithiocarbamate and thio-urea ligands are terminal, imposing a seven-coordinate environment [$\text{Bi}-\text{S}_{\text{short}}$ 2.624(4) and 2.649(3); $\text{Bi}-\text{S}_{\text{long}}$ 2.805(3) and 2.735(3) Å; $\text{Bi}-\text{Cl}$ 2.911(4) and 3.187(4) Å; $\text{Bi}-\text{S}$ 3.017(4) Å]. The tetrafluoroborate salts $[\text{Bi}(\text{dtcR}_2)_2(\text{BF}_4)]$ ($\text{R} = \text{Et}$, CH_2CH_2 , $(\text{CH}_2)_{2.5}$) are obtained from the reaction with gaseous BF_3 (**77**), and conductivity data suggest that the compounds are univalent electrolytes in nitrobenzene.



Mono-dithiocarbamatedihalo complexes $\text{Bi}(\text{dtcEt}_2)\text{X}_2$ ($\text{X} = \text{Cl}$ (80), Br , I) (78, 81, 95) are isostructural one-dimensional polymers **27** with bismuth in a seven-coordinate environment (79), involving two sulfur atoms of a bidentate dithiocarbamate ligand [Bi–S: 2.594(3) and 2.671(3); 2.599(3), 2.673(3); 2.611(5) and 2.690(5) Å], two pairs of *cis* μ_2 -halogen atoms [Bi–Cl 2.673(3)–3.165(3); Bi–Br 2.820(2)–3.305 (2); Bi–I 3.032(2) and 3.501(2) Å], and a bridging sulfur atom [Bi–S: 378(3); 387(3); 3.462(5) Å]. As isostructural series of somewhat irregularly shaped neutral pentanuclear complexes with the intermediate mono-/bis- empirical formula $[\text{Bi}_5(\text{dtcEt}_2)_8\text{X}_7(\text{dmf})]$ ($\text{X} = \text{Cl}$, Br , I) were obtained on recrystallization of appropriate mono(dithiocarbamate) dihalide from dmf and *n*-butanol (82). Of the three unique bismuth centers, one bears bidentate and bridging dithiocarbamate ligands [Bi–S: 2.60(1)–2.78(1); 2.604(5)–2.800(5); 2.62(1)–2.81(1) Å], a terminal halogen atom [Bi–X: 2.89(1); 3.050(2); 3.278(3) Å], a bridging μ_2 -halogen atom [Bi–X: 3.42(1); 3.515(3); 3.706(4) Å], and a bridging μ_3 -halogen atom [Bi–X: 3.43(1); 3.533(3); 3.680(3) Å]. A second bismuth center is coordinated to two bidentate dithiocarbamate ligands [Bi–S: 2.61(1)–2.77(1); 2.606(6)–2.793(6); 2.63(1)–2.80(1) Å], a bridging μ_2 -halogen atom [Bi–X: 3.04(1); 3.194(3); 3.421(4) Å], and a bridging μ_3 -halogen atom [Bi–X: 3.42(1); 3.469(3); 3.582(3) Å]. A third bismuth center is coordinated to three terminal halogen atoms [Bi–X: 2.68(1)–2.74(1); 2.855(2)–2.862(3); 3.053(3)–3.079(3) Å], two bridging μ_2 -halogen atoms [Bi–X: 2.68(1) and 2.74(1); 2.860(3) and 2.862(3); 3.070(3) and 3.053(3) Å], and one bridging μ_3 -halogen atom [Bi–X: 2.71(1); 2.855(2); 3.079(3) Å].

The ionic materials $[\text{NEt}_4][\text{Bi}(\text{dtcEt}_2)\text{I}_3]$ and $[\text{NEt}_4][\text{Bi}(\text{dtcEt}_2)\text{I}_2\text{Br}]$ were isolated from evaporating solutions of $[\text{Bi}(\text{dtcEt}_2)\text{I}_2]$ and NEt_4X , ($\text{X} = \text{I}$, Br) (83) and adopt halide bridge dimeric structures, with bismuth in a six-coordinate, octahedral environment. The coordination sphere is occupied by a terminal halogen atom [Bi–I 2.965(1); Bi–Br

2.813(2) Å] and a bridging iodine atom in the axial sites [Bi–I 3.190(1); 3.115(2) Å], and two sulfur atoms of a bidentate dithiocarbamate ligand [Bi–S 2.649(3)–2.769(3); 2.649(5)–2.770(6) Å], a terminal iodine atom [Bi–I 3.091(1); 3.006(2) Å], and a bridging iodine atom [Bi–I 3.291(1); 3.244(2) Å] in the equatorial sites. The salt [Hpyr][Bi₄(dtcEt₂)₄Br₁₀] containing a tetranuclear dianion **28** was isolated



from a slowly evaporating solution of Bi(dtcEt₂)Br₂ in pyridine/*n*-butanol (82) and contains a bismuth in a relatively low, five-coordinate environment involving one terminal bromine atom [avg. Bi–Br 2.94(1) Å], three bridging bromine atoms [Bi–Br 3.24(1)–3.34(1) Å], and two sulfur atoms of a bidentate dithiocarbamate ligand [Bi–S 2.68(3)–2.73(3) Å]. A very long contact to the empty site on each bismuth center is evident [avg. Bi---S 3.74(1) Å].

The dithioxanthate ligands predictably behave in a similar fashion to dithiocarbamates. Various derivatives of Bi(dtxR)₃] (R = Me, Et, ⁱPr, C₆H₁₁, CH₂C₆H₅), have been isolated (84, 86, 88). All exhibit intermolecular interactions. Dimers analogous to **24** are observed in most cases (R = Me [Bi–S_{short} 2.596(3)–2.747(3); Bi–S_{long} 2.933(4)–2.998(4) Å; Bi–S 3.405(1) Å] (85); R = ⁱPr [Bi–S_{short} 2.682(2) and 2.825(3); Bi–S_{long} 2.926(2) and 3.175(2); Bi---S 2.842(2) Å] (88, 89), R = C₆H₁₁, CH₂C₆H₅) (90), and a polymer structure derivative of **28** is observed for R = ⁱPr [Bi–S_{short} 2.605(8)–2.828(9); Bi–S_{long} 2.892(9)–2.99(1) Å] (87). In this case, two long sulfur contacts from two neighboring molecules [Bi---S 3.352(8)–3.627(9) Å] give a bismuth–sulfur “ladder”-type polymeric backbone. The bis(dithioxanthate) halides Bi(dtxEt)₂X (X = Cl, Br) are prepared by reacting 2 equiv of Bi(dtxEt)₃ with chlorine or bromine dissolved in CCl₄, or with cupric chloride or bromide in CH₂Cl₂ (91). Spectroscopic data suggest polymeric solid-state structures, while molecular weight measurements suggest that they are monomeric in solution. A tetrakis dithioxanthate [NEt₄][Bi(dtxEt)₄] (92) was isolated from the reaction of Bi(dtxEt)₃ with [NEt₄][dtxEt]

in hot ethanol. (86). The anion is monomeric with bismuth in an eight-coordinate dodecahedral environment [Bi-S_{short} 2.803(11)–2.868(11); Bi-S_{long} 2.940(13)–2.972(10) Å; 2.833(6) and 2.859(9) Å].

Mixed-ligand dithiocarbamate and dithioxanthate complexes Bi(dtcR₂)₂(dtcR'₂) (R,R' = Et, {CH₂CH₂}₂; {CH₂CH₂}₂, Et; Et, CH₂C₆H₅; {CH₂CH₂}₂, CH₂C₆H₅; {CH₂CH₂}_{2.5}, Et; {CH₂CH₂}_{2.5}, CH₂C₆H₅; {CH₂CH₂}₂, CHCH; {CH₂CH₂}_{2.5}, CHCH) are readily prepared by substitution or metathesis (93), and infrared data suggest that dithiocarbamate ligands are more strongly bound than dithioxanthate ligands because of ²⁻S₂C=N⁺ resonance.

D. DISELENOCARBOXYLATES (DISELENOCARBAMATES)

Diselenocarbamate complexes Bi{SeC(Se)N(C₂H₅)₂}₃, (R = CH₂H₅ (96), R = C₄H₉, R = CH₂C₆H₅ (97)) were prepared by reacting BiCl₃, carbon diselenide, and the appropriate dialkylamine (1:3:6) in CCl₄. The compounds are air stable and have been characterized by melting point, elemental analysis, IR, UV, and NMR spectroscopy.

IV. Ethers and Thioethers

A. ETHERS

(See Table V and Chart 2.) The ability of bismuth to routinely access nine-coordinate environment is fundamentally demonstrated by the homoleptic cationic water complex that has been isolated as the triflate salt [Bi(H₂O)₉][SO₃CF₃]₃ from a suspension of Bi₂O₃ in trifluoromethanesulfonic acid anhydride with trifluoromethanesulfonic acid (1:3:6) at 0°C (98). The tricapped trigonal prism environment for bismuth involves occupation of capping and noncapping coordination sites by the oxygen atoms of water molecules [Bi-O_{capping}: 2.448(2); Bi-O_{non-capping}: 2.577(2) Å]. Several tetrahydrofuran (thf) adducts have been isolated as both neutral bismuth halides [BiCl₃(thf)₂ and BiBr₃(thf)₃] (99) and halide-rich anions [Li(thf)₄]₂[Bi₂Cl₈(thf)₂] (100). The structure of BiCl₃(thf)₂ is a one-dimensional polymer, with bismuth in a seven-coordinate pentagonal bipyramidal environment. The apical sites are occupied by a thf oxygen atom [avg. Bi-O 2.621 Å] and a chlorine atom [avg. Bi-Cl 2.502 Å], while the basal sites are occupied by a thf oxygen atom [Bi-O 2.556 Å], two tightly bound *cis* chlorine atoms [Bi-Cl 2.533(2)–2.634(2) Å], and two loosely bound *cis* bridging chlorine atoms [Bi---Cl 3.132(2)–3.372(2) Å]. The shorter Bi-O bond lengths are *trans*

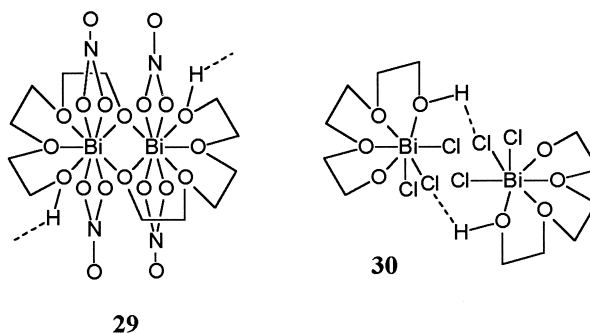
TABLE V
ANALYTICAL DATA FOR BISMUTH ETHER COMPLEXES

Empirical formula	X-ray structure #	Yield (%)	mp	EA	IR	Raman	NMR	Ref.
[Bi(H ₂ O) ₆](SO ₃ CF ₃) ₃	x	81	—	x	x	x	—	98
BiX ₃ (thf) ₂ (X = Cl, Br)	x	—	—	—	—	—	—	99
[Li(thf) ₄] ₂ [Bi ₂ Cl ₆ (thf) ₂]	x	100	x	—	—	—	—	100
Bi(OSiPh ₃) ₃ (thf) ₃	x	—	—	—	x	—	x	20
Bi(NO ₃) ₃ (Heo3)	29	—	x	x	—	—	—	101, 102
Bi(NO ₃) ₃ (Heo4)MeOH	(29) ^a	—	x	x	—	—	—	101
Bi(NO ₃) ₃ (Heo6)	(29)	—	x	x	—	—	—	101
[Bi(NO ₃) ₂ (H ₂ eo5)][Bi(NO ₃) ₂ (eo5)]	x	—	x	x	—	—	—	101
Bi(NO ₃) ₃ (H ₂ O) ₂								
BiX ₃ (H ₂ eo4) (X = Cl Br)	30	—	x	x	—	—	—	102
BiCl ₃ (H ₂ eo5)	(30)	—	x	x	—	—	—	102
[BiI ₂ (H ₂ eo5)][Bi ₂ I ₇](MeOH) ₂	x	—	x	x	—	—	—	102
[BiBr ₂ (H ₂ eo6)][BiBr ₄]	x	—	x	x	—	—	—	102
Bi(NO ₃) ₃ (12-crown-4)	31	—	x	x	—	—	—	101
[Bi(NO ₃) ₃ (H ₂ O) ₃] · (18-crown-6)	32	—	x	x	—	—	—	101
BiCl ₃ (12-crown-4)	(33)	—	—	x	—	—	—	103
BiBr ₂ (12-crown-4)	(33)	—	x	x	—	—	—	102
BiCl ₃ (15-crown-5)	33	—	x	x	x	—	x	102, 108
BiX ₃ (benzo-15-crown-5) (X = Cl Br)	x	—	x	x	—	—	—	102
BiCl ₃ (MeOH)(18-crown-6)	34	—	x	x	—	—	—	102
[BiCl ₂ (18-crown-6)] ₂ Bi ₂ Cl ₆	x	—	—	x	—	—	—	103
[BiBr ₂ (18-crown-6)][BiBr ₄]	x	—	x	x	—	—	—	102
[BiCl ₃ (18-crown-6)][BiCl ₃ (18-crown-6)H ₂ O]	x	—	—	—	—	—	—	104
[BiCl(18-crown-6)(CH ₃ CN) ₂][SbCl ₆] ₂	x	—	—	—	—	—	—	105
[Bi(12-crown-4) ₂](MeCN)[SbCl ₆] ₃	x	—	—	x	x	—	—	106

^a Parentheses refer to a representative structure.

to the longer Bi–Cl bonds. In contrast, an extra thf ligand has access to bismuth in the bromide derivative BiBr₃(thf)₃, so that it is monomeric in the solid state and contains a six-coordinate octahedral bismuth atom. The bromine atoms and thf ligands adopt a *fac* configuration [Bi–Br 2.628(5)–2.685(10) Å; Bi–O 2.600(8)–2.700(7) Å]. The dianion [Bi₂Cl₃(thf)₂]²⁻ is a discrete centrosymmetric dimer, with bismuth in a six-coordinate near-octahedral bonding environment. The axial sites are occupied by a thf oxygen atom [Bi–O 2.594(10) Å] and a chlorine atom [Bi–Cl 2.555(4) Å], while the equatorial sites are occupied by two *cis* bridging chlorine atoms [Bi–Cl 2.902(4) Å] and two terminal chlorine atoms [Bi–Cl 2.573(4) and 2.2.551(3) Å]. A trisiloxide complex Bi(OSiPh₃)₃(thf)₃ has been shown to adopt a solid-state structure similar [Bi–O 2.04 Å; thf; Bi–O 2.95(1) Å] (20) to that observed for the tribromide. Dioxane is speculated to bridge two bismuth trichloride acceptors in a system with the empirical formula [(BiCl₃)₂(diox)₃] based on elemental analysis data (107).

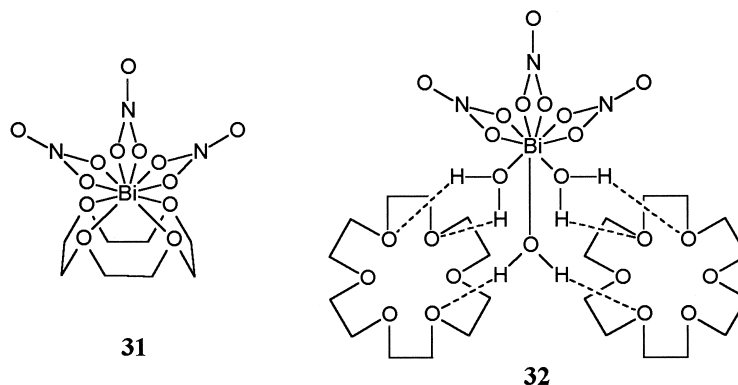
Nitrate anions can be substituted on bismuth nitrate by reaction with polyethylene glycols effecting deprotonation (or ionization) of one end of the ligand chain (101). Centrosymmetric dimers of the general form **29** are observed, with nitrate anions asymmetrically coordinated, staggered, and *trans* to one another [Bi–O 2.240(1)–2.28(2) Å] in [Bi(NO₃)₂(Heo3)]₂, [Bi(NO₃)₂(Heo4)]₂(MeOH)₂, and [Bi(NO₃)₂(Heo6)]₂. Bismuth centers are doubly bridged by alkoxide oxygen atoms [Bi–O 2.20(1)–2.28(1) Å], and most ether oxygen atoms are coordinated to bismuth [Bi–O 2.51(1)–2.98(1) Å]. The protonated terminus of the ligand provides a hydrogen bond to a neighboring dimer. The ionic compound [Bi(NO₃)₂(H₂eo5)][Bi(NO₃)₂(eo5)Bi(NO₃)₃](2H₂O)₂ contains a dianionic ligand in the anion [Bi–O 2.217(9) and 2.29(1) Å] and a neutral ligand in the cation [Bi–O_{ether} 2.43(1)–2.69(1) Å]. The coordination number for bismuth in these compounds is 9 or 10.



Deprotonation of the ligands is not observed for the analogous reactions with bismuth halide complexes (102). Derivatives of BiX₃(H₂eo4) **30** (X = Cl, Br) [avg. Bi–Cl 2.55(3) Å; avg. Bi–Br 2.2.70(2) Å] involve all five oxygen atoms bound to bismuth [Bi–O 2.627(8)–2.901(7) Å], while in BiCl₃(H₂eo5) [avg. Bi–Cl 2.56(3) Å] only five of the six ligand oxygen atoms interact with bismuth [Bi–O 2.73(1)–2.91(1) Å]. In general, bismuth adopts eight-coordinate environments in bicapped trigonal prism geometries. The BiX₃ unit is more susceptible to ligand exchange when X = Br or I, and unusual ionic complexes are observed, including [BiI₂(H₂eo5)][Bi₂I₇].2MeOH and [BiBr₂(H₂eo6)][BiBr₄].

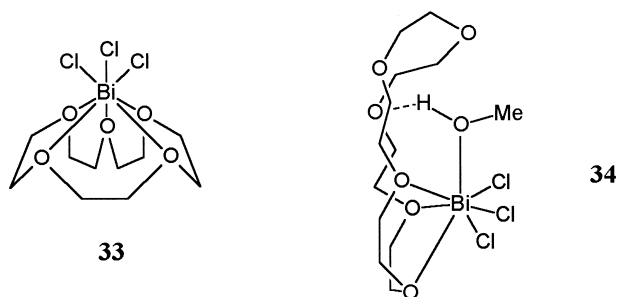
Crown ether complexes of bismuth nitrate were prepared by reacting Bi(NO₃)₃·5H₂O in 3:1 MeCN:MeOH with a stoichiometric amount of the crown ether (101). Bi(NO₃)₃(12-crown-4) has bismuth in a 10-coordinate C_s 4A,6B-expanded dodecahedral geometry **31**, in which all four ether oxygen atoms are bound to the bismuth center

[Bi–O 2.54(1)–2.68(2) Å]. In contrast, the nine-coordinate capped square antiprism geometry for bismuth in $[\text{Bi}(\text{NO}_3)_3(\text{H}_2\text{O})_3] \cdot (18\text{-crown-6})$ does not involve the expected multidentate ether coordination to bismuth, but rather a hydrogen-bonded interaction of the crown ether with the hydrated bismuth center chelated by bidentate nitrate groups [Bi–O 2.38(2)–2.56(2) Å] **32**, implying that the hexado-



nor nature of the crown ether in the presence of three nitrate ligands is overwhelming the maximum coordinate capacity of the bismuth center.

A series of corresponding and related halide crown ether complexes have been isolated, and their ionic or covalent formulas seem to predictably depend on the reaction conditions. The structural observations made for $[\text{BiX}_3(12\text{-crown-4})]$ ($\text{X} = \text{Cl}, \text{Br}$) [avg. Bi–Cl 2.52(1) Å; Bi–O 2.652(8)–2.742(9) Å; avg. Bi–Br 2.72(4) Å] (102, 103), $[\text{BiX}_3(15\text{-crown-5})]$ ($\text{X} = \text{Cl}$ (102, 108) Br) [avg. Bi–Cl 2.54(1) Å; Bi–O 2.77(1)–2.91(1) Å; avg. Bi–Br 2.69(2) Å; Bi–O 2.72(2)–3.00 (4) Å] (103), $\text{BiX}_3(\text{benzo-15-crown-5})$ ($\text{X} = \text{Cl}, \text{Br}$) [avg. Bi–Cl 2.53(2) Å; Bi–O 2.793(9)–2.844(9) Å; avg. Bi–Br 2.68(2) Å; Bi–O 2.80(1)–2.88(1) Å], $\text{BiCl}_3(\text{MeOH})(18\text{-crown-6})$ (103), $[\text{BiCl}_2(18\text{-crown-6})]_2\text{Bi}_2\text{Cl}_8$ (103), $[\text{BiBr}_2(18\text{-crown-6})][\text{BiBr}_4]$ (102), and $[\text{BiCl}_3(18\text{-crown-6})][\text{BiCl}_3(18\text{-crown-6})\text{H}_2\text{O}]$ (104) exhibit similar structural features to those of the corresponding polyethylene glycol halide complexes. The absence of hydrogen-bond donors in the crown ether complexes imposes alternative structural types, including puckering of the crown ether. Although Bi–O interactions are weaker, the pyramidalization of BiX_3 is retained, and symmetric structures are achievable for smaller rings, as represented by **33**. In contrast to the nitrate complex, which was apparently restricted by the hexadonor nature 18-crown-6, the bismuth center of $\text{BiCl}_3(\text{MeOH})(18\text{-crown-6})$ [avg. Bi–Cl 2.54(2) Å] binds



only three adjacent ether oxygen atoms [Bi–O 2.776(7)–2.805(7) Å] and the oxygen of methanol [Bi–O 2.549(9)(9) Å] **34**. In this context, it is interesting to note that the structure of [BiCl₃(18-crown-6)] [BiCl₃(18-crown-6)H₂O] (**104**) contains discrete component molecules. The former (nonhydrated molecule) has the BiCl₃ apex [avg. Bi–Cl 2.495(9) Å] oriented at the center of the crown ether cavity with all six oxygen atoms coordinated to bismuth [Bi–O 2.84(3)–3.16(2) Å], while in the latter, BiCl₃ engages only three of the sites and the pyramid [avg. Bi–Cl 2.51(3) Å] in the hydrated molecule is off-center to the cavity of the crown ether [Bi–O 2.76(2)–2.88(2) Å].

The ionic compounds [BiCl₂(18-crown-6)]₂[Bi₂Cl₈] (**103**) and [BiBr₂(18-crown-6)][BiBr₄] (**102**) show each bismuth bound to two halide atoms [avg. Bi–Cl 2.501(6) Å; avg. Bi–Br 2.666(5) Å] and all six ether oxygen atoms [Bi–O: 2.49(1)–2.66(2) Å; 2.47(2)–2.73(2) Å]. Similar features are evident in a complex involving the smaller crown ether, which has been isolated as an antimonate salt, [BiCl₂(15-crown-5)(CH₃CN)][SbCl₆] [Bi–Cl 2.515(7) and 2.489 Å and Bi–N 2.65(3) Å] (**105**). Acetonitrile adducts of the corresponding dication [BiCl(18-crown-6)(CH₃CN)₂][SbCl₆]₂ (**105**) and trication [Bi(12-crown-4)₂(MeCN)][SbCl₆]₃ (**106**) have also been isolated. The dication has bismuth encompassed by the crown ether and bonded to all ether oxygen atoms, and the chlorine atom [Bi–Cl 2.479(6) Å] and the pair of acetonitrile nitrogen atoms [Bi–N 2.82(2) and 2.86(3) Å] are bound from the opposite side to the crown ether. The trication adopts a sandwich structure in which bismuth is bound to all four oxygen atoms of each crown ether [Bi–O 2.436(5) and 2.545(5) Å]. The acetonitrile nitrogen atom occupies a position between the two ligands [Bi–N 2.650(9) Å].

B. THIOETHERS

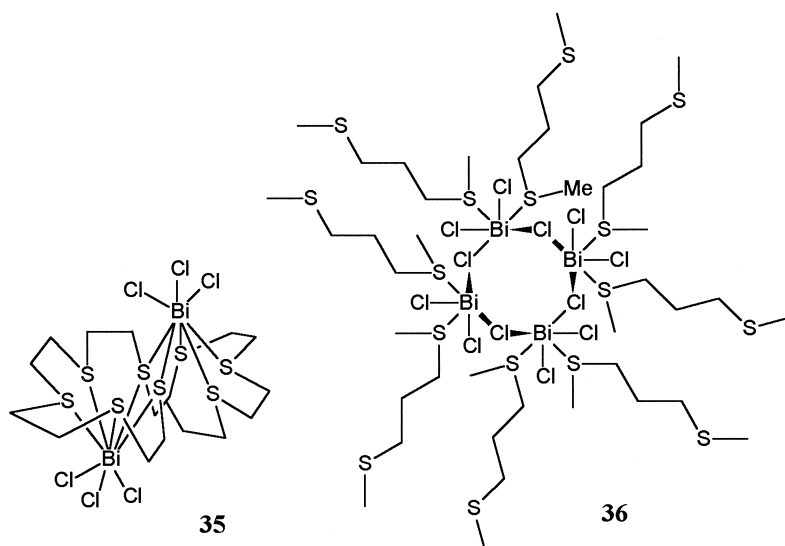
(See Table VI.) Crown thioethers of various sizes ([12]aneS₄ = 1,4,7,10-tetrathiacyclododecane, [15]aneS₅ = 1,4,7,10,13-pentathia-

TABLE VI
 ANALYTICAL DATA FOR BISMUTH THIOETHER COMPLEXES

Empirical formula	X-ray structure #	Yield (%)	mp	EA	IR	UV	NMR	MS	Ref.
BiCl ₃ ([12]aneS ₄)	x	66	x	x	x	x	x	—	109
{BiCl ₃ ([15]aneS ₅) ₂ (MeCN)}	x	82	x	x	x	x	x	—	109
BiCl ₃ ([18]aneS ₆)	x	79	x	x	x	x	x	—	110
(BiCl ₃) ₂ ([24]aneS ₈)	35	72.6	x	x	x	—	—	x	111
BiCl ₃ (MeSCH ₂ CH ₂ CH ₂ SMe)	36	~20	—	x	x	—	—	—	112
[SMe ₃] ₂ [Bi ₂ I ₈ (SMe ₂) ₂]	x	small	—	—	—	—	—	—	113

cyclopentadecane, [18]aneS₆ = 1,4,7,10,13,16-hexathiacyclooctadecane, [24]aneS₈ = 1,4, 7,10,13,16,19,22-octathiacyclotetracosane) form 1:1 complexes with bismuth trichloride that are essentially analogues of the prototypical crown ether complexes described earlier. The solid-state structures observed for BiCl₃([12]aneS₄), {BiCl₃([15]aneS₅)₂/(MeCN) (109) and BiCl₃([18]aneS₆) (110) confirm that all sulfur centers interact with bismuth, although the bonds are weak [avg. Bi–S > 3.0 Å]. Consistently, the three bismuth chlorine bonds are similar to those of the free acid [avg. Bi–Cl 2.571 vs 2.496 Å; Cl–Bi–Cl 92.3 vs 90.9°, respectively]. The larger, more flexible octathioether is able to engage two molecules of bismuth chloride in (BiCl₃)₂([24]aneS₈) (111). Two pentasulfur cradle sites [avg. Bi–S 3.21 (3) Å] are centrosymmetrically related on opposite sides of the thiamacrocyclic, and together with the three chlorine atoms, bismuth is eight-coordinate (**35**).

The only two examples of bismuth complexes involving acyclic thioether ligands are unique. Bismuth chloride forms a 1:1 complex with a dithioether, which adopts a polymeric structure of tetrameric units **36**, [Bi₄Cl₁₂(MeSCH₂CH₂CH₂SMe)₄]_n · nH₂O (112). Bismuth occupies a six-coordinate distorted octahedral environment composed of two *cis* terminal chlorine atoms [Bi–Cl 2.538(7) and 2.533(7) Å], two μ_2 bridging chlorine atoms [Bi–Cl 2.913(7) and 2.969(6) Å], and two sulfur atoms from different bridging thioether ligands [Bi–S 2.857(7) and 2.977(7) Å]. The presence of long-range Bi---Cl contacts [3.268(7) Å] across the Bi₄Cl₄ ring of the tetramer results in a pseudo-cuboidal arrangement. The reaction of bismuth iodide with dimethyl sulfide gives the salt [SMe₃]₂[Bi₂I₈(SMe₂)₂] as a minor product (113). Bismuth occupies a six-coordinate near-octahedral environment, made up of sulfur [Bi–S 3.054(8) Å], three terminal iodine atoms [avg. Bi–I 2.948 Å], and two bridging iodine atoms [Bi–I 3.234(3) and 3.229(3) Å] in a centrosymmetric dimeric unit.



V. Ketones and Thiones

(See Table VII and Chart 3.) $[\text{Bi}(\text{dmpu})_6][\text{Bi}_3\text{I}_{12}]$ represents a unique example of a ketone complex. It was prepared from the reaction of excess dmpu with BiI_3 in thf or toluene and has been characterized by elemental analysis and X-ray crystallography (114). The cation is a classical six-coordinate near-octahedral complex $[\text{Bi}-\text{O} \ 2.312(8) \text{ \AA}; \text{Bi}-\text{O}-\text{C} \ 155.7(8)^\circ]$. Hexacoordinate, near-octahedral complexes are typical for thione ligands as well, but higher coordination numbers are also observed. Pentathiourea and trithiourea complexes are isolated from solutions of $\text{Bi}(\text{NO}_3)_3$ and thiourea (115). A seven-coordinate pentagonal bipyramidal geometry is observed for bismuth in $[\text{Bi}(\text{NO}_3)(\text{tu})_5][\text{NO}_3]_2 \cdot \text{H}_2\text{O}$ by virtue of sulfur atoms in the axial sites $[\text{Bi}-\text{S} \ 2.909(2) \text{ and } 2.767(2) \text{ \AA}]$ and three equatorial sites $[\text{Bi}-\text{S} \ 2.637(2)-2.937(2) \text{ \AA}]$, together with two oxygen atoms of a bidentate nitrate ligand $[\text{Bi}-\text{O} \ 2.814(5) \text{ and } 2.916(5) \text{ \AA}]$. Bismuth is eight-coordinate in $\text{Bi}(\text{NO}_3)_3(\text{tu})_3$ with three thiourea ligands in a facial-type arrangement $[\text{Bi}-\text{S} \ 2.668(3)-2.681(3) \text{ \AA}]$ and the oxygen atoms of one monodentate $[\text{Bi}-\text{O} \ 2.579(9) \text{ \AA}]$ and two asymmetrically bound bidentate nitrate ligands $[\text{Bi}-\text{O} \ 2.66(1)-2.94(1) \text{ \AA}]$.

Two salts involving bismuth complexes as both ions have been structurally characterized (116). $[\text{Bi}_2\text{Cl}_4(\text{tu})_6][\text{BiCl}_5(\text{tu})]$ consists of a binuclear centrosymmetric dication (117), and bismuth adopts a six-

TABLE VII
ANALYTICAL DATA FOR BISMUTH THIONE COMPLEXES

Empirical formula	X-ray structure #	Yield (%)	mp	EA	cond	IR	NMR	Ref.
[Bi(NO ₃)(tu) ₃][NO ₃] ₂ · H ₂ O	x	—	—	—	—	—	—	115
Bi(NO ₃) ₃ (tu) ₃	x	—	—	—	—	—	—	115
[Bi ₂ Cl ₄ (tu) ₆][BiCl ₅ (tu)]	x	—	x	—	—	—	—	116, 117
[Bi(tu) ₆][Bi{(tu) _{1.5} Cl _{1.5} }Cl ₃] ₂	x	—	x	—	—	—	—	116
BiCl ₃ (aptu) ₂	x	—	—	—	—	—	—	118
[Bi(aptu) ₆][NO ₃] ₃	x	—	—	—	—	—	—	118
BiCl ₃ (pptu) ₃	x	—	—	x	—	x	—	119
BiCl ₃ (deimdt) ₂	x	—	—	x	—	x	—	119
BiBr ₃ (etu) ₃	x	—	—	—	—	x	—	120
[Bi(etu) ₆][SO ₄] ₃	x	—	—	—	—	x	—	120
BiCl ₃ (thpt) ₃	x	93.4	x	x	x	x	—	121
BiX ₃ (thpt) ₃ (X = Br, NO ₃)	—	71.2–88.8	x	x	x	x	—	121
BiX ₃ (bit) ₄ · 4H ₂ O (X = Cl, Br, NO ₃), Bi(ClO ₄) ₃ (L = thpt, bit)	—	71.2–88.8	x	x	x	x	—	121
[Hamp] ₃ [BiCl ₅ (Hamp)]Cl · 5H ₂ O [Hamp] ₃ [BiCl ₅ (Hamp)] · 2H ₂ O	x	—	—	x	—	—	—	122
BiCl ₃ [RNHC(S)C(S)NHR] ₂ · Me ₂ CO (R = Me, Et, ⁿ Pr, ⁿ Bu)	—	—	—	x	—	x	—	123
BiCl ₃ [RNHC(S)C(S)NHR] ₂ (R = CH ₂ Ph)	—	—	—	—	—	—	—	123
BiCl ₃ [EtNHC(S)C(S)NHEt] ₂	x	—	—	x	—	x	—	123, 124
Bi(tm)Cl ₂	x	—	—	—	—	—	—	125
[Bi(tm) ₂][Na(tp) ₃] · 4CH ₂ Cl ₂ · ClCH ₂ CH ₂ Cl	x	68	—	x	—	x	x	125

coordinate octahedral geometry in both ions. This is imposed in the cation by three facial sulfur atoms [Bi–S 2.680(6)–2.739(10) Å], a terminal chlorine atom [Bi–Cl 2.677(10) Å], and two bridging chlorine atoms [Bi–Cl 2.934(6)–2.939(6) Å], and the coordination sphere is according to the formula of the anion [Bi–Cl 2.709(6)–2.763(10) Å; Bi–S 2.763(10) Å]. The trication of [Bi(tu)₆][Bi{(tu)_{1.5}Cl_{1.5}}Cl₃]₂ contains a nearly octahedral coordination sphere of sulfur atoms [Bi–S 2.848(4) Å], (116), whereas the anion is disordered [Bi–Cl 2.728(3) Å; Bi–Cl/S 2.714(8) Å], giving a formula of [BiCl₆]^{3–} or BiCl₃(tu)₃.

The asymmetrically substituted thiourea derivative aptu gives a chloride bridged centrosymmetric dimer with bismuth chloride [BiCl₃(aptu)₂]₂, two *cis* terminal sulfur atoms [Bi–S 2.735(6) and 2.786(6) Å], two *cis* terminal chlorine atoms [Bi–Cl 2.503(5) and 2.723(5) Å], and two *cis* bridging chlorine atoms [Bi–Cl 2.894(5) and 3.073(5) Å] (118). Analogous chloride bridging is observed for [BiCl₃(deimdt)₂]₂ with bismuth in a more distorted octahedral environment [Bi–S 2.783(5) and 2.871(4); Bi–Cl_{terminal} 2.558(4) and 2.613(5); Bi–Cl_{bridging} 2.934(5) and 2.807(6) Å] (119). Bismuth nitrate reacts with

aptu to give $[\text{Bi}(\text{aptu})_6][\text{NO}_3]_3$ (118), in which the mononuclear cation is hexacoordinate octahedral complex $[\text{Bi}-\text{S } 2.797(9)-2.808(10) \text{ \AA}]$, analogous to that described for thiourea. The thiourea derivative ligands pptu and etu form meridional octahedral mononuclear complexes $\text{BiCl}_3(\text{pptu})_3$ $[\text{Bi}-\text{S } 2.800(3)-2.872(2) \text{ \AA}; \text{Bi}-\text{Cl } 2.675(2)-2.800(3) \text{ \AA}]$ and $\text{BiBr}_3(\text{etu})_3$ $[\text{Bi}-\text{S } 2.812(5)-2.869(5); \text{Bi}-\text{Br } 2.770(2)-2.881(2) \text{ \AA}]$. A near-octahedral geometry is also evident in the salt $[\text{Bi}(\text{etu})_4]_2[\text{SO}_4]_3$ (120) by virtue of four sulfur atoms $[\text{Bi}-\text{S } 2.665(4)-2.830(4) \text{ \AA}]$ and two *cis* oxygen atoms of two monodentate sulfate groups, which are bound at different distances $[\text{Bi}-\text{O } 2.413(12) \text{ and } 2.716(15) \text{ \AA}]$. A facial configuration is observed in $\text{BiCl}_3(\text{thpt})_3$ $[\text{Bi}-\text{S } 2.741(4)-2.779(4) \text{ \AA}; \text{Bi}-\text{Cl } 2.669(5)-2.784(4) \text{ \AA}]$. Complexes with higher thione substitution have only been spectroscopically characterized, including $[\text{BiX}_3(\text{bit})_4] \cdot 4\text{H}_2\text{O}$ ($\text{X} = \text{Cl}, \text{Br}, \text{NO}_3$) and $[\text{Bi}(\text{ClO}_4)(\text{L})_5]$ ($\text{L} = \text{thpt}, \text{bit}$) (121).

The unusual salts $[\text{Hamp}]_2[\text{BiCl}_5(\text{Hamp})]\text{Cl} \cdot 5\text{H}_2\text{O}$ and $[\text{Hamp}][\text{BiCl}_5(\text{Hamp})] \cdot 2\text{H}_2\text{O}$ involving the protonated (cationic) ligand Hamp were isolated from the reaction of BiCl_3 with $(\text{Hamp})\text{Cl}$ (122). They both contain the $[\text{BiCl}_5(\text{Hamp})]^-$ anion, which is a near-octahedral complex $[\text{Bi}-\text{Cl}: 2.536(6)-2.825(6); 2.576(3)-2.883(3) \text{ \AA}; \text{Bi}-\text{S}: 2.829(5); 2.935(3) \text{ \AA}]$.

Complexes of bismuth chloride with 2 equiv of the *N,N'*-substituted dithioamide ligands of the general formulas $[\text{BiCl}_3\{\text{RNHC}(\text{S})\text{C}(\text{S})\text{NHR}\}_2]$ ($\text{R} = \text{Me}, \text{Et}, ^i\text{Pr}, ^n\text{Bu}, \text{CH}_2\text{Ph}$) likely involve five-membered chelate interactions (123) as demonstrated by the structurally characterized example $[\text{BiCl}_3\{\text{EtNHC}(\text{S})\text{C}(\text{S})\text{NHEt}\}_2] \cdot \text{Me}_2\text{CO}$, which involves a seven-coordinate pentagonal bipyramidal environment for bismuth (124), with chlorine atoms in axial positions $[\text{Bi}-\text{Cl } 2.635(10) \text{ and } 2.717(1) \text{ \AA}]$ and one equatorial $[\text{Bi}-\text{Cl } 2.651(12) \text{ \AA}]$ with four sulfur centers $[\text{Bi}-\text{S } 2.818(13)-3.042(12) \text{ \AA}]$.

The tridentate hydrotris(methimazolyl)borate (tm) ligand forms a neutral dichloro complex $[\text{Bi}(\text{tm})\text{Cl}(\mu\text{-Cl})_2]$ in the reaction of BiCl_3 with 3 equiv of $\text{Na}(\text{tm})$ (125). A typical dichloride bridged $[\text{Bi}-\mu_2\text{-Cl } 2.887(5) \text{ and } 3.009(5) \text{ \AA}]$ dimer is observed in the solid state with near octahedral environment for bismuth and facial configuration of the corresponding three chlorine atoms $[\text{Bi}-\text{Cl } 2.807(5) \text{ \AA}; \text{Bi}-\text{S}(\text{ax}) 2.714(5) \text{ \AA}, (\text{eq}) 2.635(4) \text{ and } 2.687(5) \text{ \AA}]$. In the presence of NaTp , the unusual bis-substituted monocation is formed in the salt $[\text{Bi}(\text{tm})_2][\text{Na}(\text{tp})_2] \cdot 4\text{CH}_2\text{Cl}_2 \cdot \text{ClCH}_2\text{CH}_2\text{Cl}$ (125). The cation involves near-octahedral bismuth "sandwiched" between two tm ligands $[\text{Bi}-\text{S } 2.802(2)-2.806(2) \text{ \AA}]$.

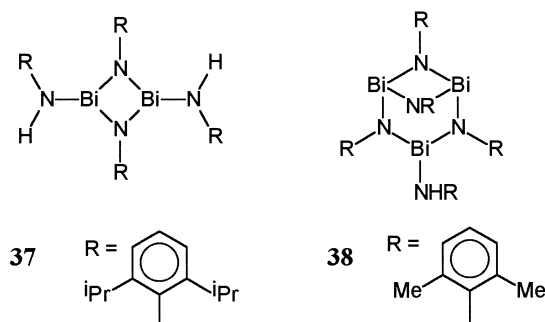
VI. Amides

Bismuth amides (aminobismuthines) (see Table VIII) are rare, but those established examples can be conveniently prepared by the reaction of bismuth trichloride with the aminolithium salt in thf or thf-petroleum ether. The homoleptic derivatives $\text{Bi}(\text{NR}_2)_3$ [$\text{R} = \text{Me}$ (126, 127), Et (126) ^nPr (126), and Ph (128)] are unstable at room temperature in most solvents except thf. $\text{Bi}(\text{NMe}_2)_3$ is volatile, implying the absence of strong intermolecular interactions [shortest intermolecular contacts $\text{Bi} \cdots \text{N}$ 3.192 Å; $\text{Bi} \cdots \text{Bi}$ 3.849 Å], which is confirmed in the solid-state structure (127), revealing a monomeric trigonal pyramidal geometry around the bismuth, also observed for $\text{Bi}(\text{NPh}_2)_3$. The $\text{Bi}-\text{N}$ bond lengths (average $\text{Bi}-\text{N}$ 2.20 Å) (128) can be considered typical, with each nitrogen center trigonal planar. A series of monosilylated amidobismuthines (129) and the corresponding disilylated derivative (130) are spectroscopically characterized.

Incomplete metathesis occurs between bismuth chloride and lithiated diisopropylaniline, giving a dimeric cyclic bismetidine [$(\text{C}_6\text{H}_3^i\text{Pr}_2)\text{NHBiN}(\text{C}_6\text{H}_3^i\text{Pr}_2)_2$] (**37**) (132), independent of reaction conditions. The solid-state structure shows that both the $\text{Bi}-\text{N}_{\text{cyclic}}$ [2.158(4) and 2.174(5) Å] and $\text{Bi}-\text{N}_{\text{acyclic}}$ [2.164(4) and 2.158(4) Å] bonds are equivalent. The geometry at each bismuth is trigonal pyramidal with

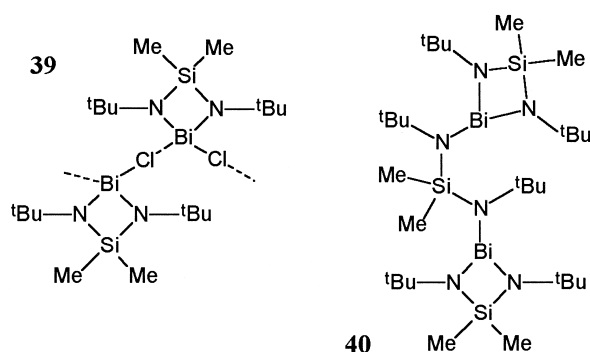
TABLE VIII
ANALYTICAL DATA FOR BISMUTH AMIDE COMPLEXES

Empirical formula	X-ray structure #	Yield (%)	mp	EA	solub	IR	Raman	UV-vis	NMR	MS	MW	Ref.
$\text{Bi}(\text{NMe}_2)_3$	x	20/ca. 6 0	x	x	—	—	—	—	x	—	—	126, 127
$\text{Bi}(\text{NEt}_2)_3$	—	52	x	x	—	—	x	—	x	—	—	126
$\text{Bi}(\text{N}^i\text{Pr}_2)_3$	—	41	x	x	—	—	x	—	x	—	—	126
$\text{Bi}(\text{NPh}_2)_3$	x	30	—	x	x	—	—	—	x	—	—	128
$\text{Bi}[\text{NH}(\text{C}_6\text{H}_2^i\text{Bu}_3)]_3$	—	11	x	x	—	x	x	—	x	—	—	131
$\text{Me}_2\text{Bi}[\text{NMe}(\text{SiMe}_2)]$	—	37.6	x	—	—	—	—	—	x	—	—	129
$\text{MeBi}[\text{NMe}(\text{SiMe}_2)]_2$	—	43	x	—	—	—	—	—	x	—	—	129
$\text{Bi}[\text{NMe}(\text{SiMe}_2)]_3$	—	54	x	x	—	—	—	—	x	—	—	129
$\text{Bi}[\text{N}(\text{SiMe}_2)]_3$	—	30	x	x	—	—	—	—	x	—	—	130
$(\text{C}_6\text{H}_3^i\text{Pr}_2)\text{NH}$ $\text{BiN}(\text{C}_6\text{H}_3^i\text{Pr}_2)$	37	57	x	—	—	x	—	—	x	x	—	132
$[\text{Bi}_3\{\mu\text{-N}-(2,6\text{-Me}_2\text{C}_6\text{H}_3)_4\}\{\text{NH}(2,6\text{-Me}_2\text{C}_6\text{H}_3)\}]$	38	—	—	—	—	—	—	—	—	—	—	27
$[\text{Me}_2\text{Si}(\text{N}^i\text{Bu})_2\text{Bi}]\text{Cl}$	39	60/81	x	x	—	—	—	—	x	x	x	133
$\text{Bi}_2[\text{N}^i\text{Bu})_2\text{SiMe}_2]_3$	40	22	x	x	—	—	—	—	x	x	x	133
$[\text{Me}_2\text{Si}(\text{N}^i\text{Bu})_2\text{Bi}][\text{AlCl}_4]$	x	—	x	x	—	—	—	x	x	x	—	134
$[\text{Me}_2\text{Si}(\text{N}^i\text{Bu})_2\text{Bi}][\text{GaCl}_4]$	—	—	x	x	—	—	—	—	x	x	—	134
$[\text{Me}_2\text{Si}(\text{N}^i\text{Bu})_2\text{Bi}][\text{InCl}_4]$	—	—	x	x	—	—	—	—	x	—	—	134



bond angles from 78.5 (2) to 97.4(2)°, suggesting an exclusive *p* character of the bismuth atom orbitals contributing to the Bi–N bond with the lone electron pair held in the *s* orbital. The unusual bicyclic compound $[\text{Bi}_3(\mu\text{-N}(2,6\text{-Me}_2\text{C}_6\text{H}_3)_4)\{\text{NH}(2,6\text{-Me}_2\text{C}_6\text{H}_3)\}]$ **38** has been isolated with the slightly less sterically encumbering ligand (27). A unique bismuth atom is bound to a terminal exocyclic amido group [Bi–N 2.16(2) Å] and two endocyclic imido nitrogen atoms [avg. Bi–N 2.17 Å]. These are in turn bound to two endocyclic bismuth atoms [Bi–N 2.15(2) and 2.17(2) Å], which are bridged by two endocyclic imido nitrogen atoms [average Bi–N 2.21 Å].

The bis(amino)silabismetidine heterocycle is observed in the compounds $[\text{Me}_2\text{Si}(\text{N}^t\text{Bu})_2\text{Bi}]\text{Cl}$ **39** and $\text{Bi}_2[(\text{N}^t\text{Bu})_2\text{SiMe}_2]_3$ **40** (133). The



former contains bismuth in a four-coordinate see-saw type geometry, with the equatorial sites are occupied by the two ligand nitrogen atoms and short Bi–N bond distances [2.124(9) Å]. The axial sites are occupied by two chlorine atoms [Bi–Cl 2.748(4) Å], forming a one-dimensional polymeric structure. A molecular tethered bicyclic struc-

ture is observed for the latter. Compound **39** reacts with ECl_3 [$\text{E} = \text{Al}, \text{Ga}, \text{or In}$] to give salts of the cation $[\text{Me}_2\text{Si}(\text{N}^t\text{Bu})_2\text{Bi}]^+$ that exhibit similar structural trends (134), but with shorter Bi–N bond distances [2.08(1) and 2.086(9) Å].

VII. Amines, Phosphines, and Arsines

A. AMINES

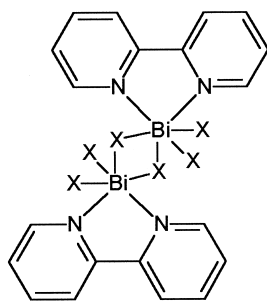
Formation constants for polyamine complexes of the Bi^{3+} cation (Table IX and Chart 4), determined by differential pulse polarography (151, 152), show one of the highest affinities of any metal ion. While the weaker bidentate (e.g., ethylenediamine) or monodentate (e.g., ammonia) ligands do not form stable complexes, demonstrating the significance of the chelate effect, pyridine (py) complexes represent the only monodentate examples and are usually formed by recrystallization of the bismuth-based Lewis acid from pyridine. $[\text{Bi}(\text{S}_2\text{CNEt}_2\text{X}_2(\text{pyr})_3) \cdot \text{pyr}]$ ($\text{X} = \text{Cl or I}$) (135) are isomorphous, consisting of a seven-coordinate, pentagonal bipyramidal bismuth environment. The halide atoms occupy the axial positions, while the dithiocarbamate S atoms, with the pyridine ligands [$\text{X} = \text{Cl}$, Bi–N 2.668(7)–2.794(8) Å; $\text{X} = \text{I}$, Bi–N 2.71(1)–2.86(1) Å] in equatorial positions. The compounds lose pyridine rapidly on exposure to air. $[\text{C}_5\text{H}_6\text{NCSNEt}_2]_2[\text{BiCl}_5(\text{pyr})]$ was isolated as a second product and contains the first example of a structurally characterized anion of the type $[\text{MX}_5(\text{base})]^{2-}$ with six-coordinate pseudo-octahedral environment [Bi–N 2.615(8) Å] (136). The long Bi–N bond is accredited to electronic effects.

The 2,2'-bipyridyl (bipy) adducts $[\text{BiX}_3(\text{bipy})]$ ($\text{X} = \text{Cl}, \text{Br}, \text{I}$) are prepared from combinations of BiX_3 and bipy in acetone (137) and are air stable. Slow cooling of concentrated solutions at various stoichiometries enabled the isolation of a number of important representative complexes (138–140, 145, 153) and provides a systematic assessment of structural features. $[\text{BiI}_3(\text{bipy})]$ (138) is a diiodide bridged dimer **41** involving six-coordinate near-octahedral bismuth centers. The axial sites are occupied by a terminal iodine atom [Bi–I 2.873(3) Å] and a bridging iodine atom [Bi–I 3.330(2) Å]. The equatorial sites are occupied by two nitrogen atoms [2.48(2) and 2.46(1) Å], a terminal iodine atom [Bi–I 2.966(3) Å], and a bridging iodine atom [Bi–I 3.141(2) Å]. Introduction of another donor molecule, as in the dmso adduct (145), imposes a mononuclear unit with the coordination sphere of bismuth occupied by the three iodine atoms in a facial arrangement [Bi–I

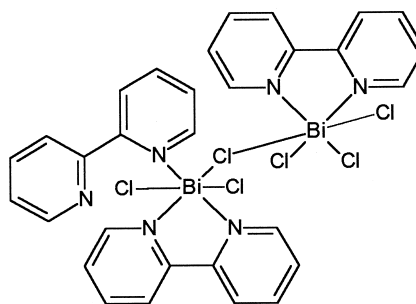
TABLE IX
ANALYTICAL DATA FOR BISMUTH AMINE COMPLEXES

Empirical formula	X-ray structure #	Yield (%)	mp	EA	solub	Cond	IR	Raman	UV	NMR	MS	Ref.
Bi(S ₂ CNEt ₂)X ₃ (py) ₃ · py (X = Cl or I)	x	—	—	—	—	—	—	—	—	—	—	135
[C ₅ H ₅ NCSN ₂ Et ₂][BiCl ₅ (py)]	x	—	—	x	—	—	—	—	—	—	—	136
[BiX ₃ (bipy)](X = Cl, Br, I)	x	—	—	x	—	x	—	—	—	—	—	137
BiI ₃ (bipy)	41	—	x	x	—	x	x	—	—	—	—	137, 138
BiI ₃ (bipy) · dmso	x	—	x	—	—	—	—	—	—	—	—	138
BiBr ₃ (bipy) · MeCN	41	—	x	—	—	—	—	—	—	—	—	138
[bipyH][BiCl ₄ (bipy)]	x	—	x	x	—	—	x	x	—	—	—	139
[bipyH][BiBr ₄ (bipy)]	x	—	—	—	—	—	—	—	—	—	—	139
[bipyH][BiCl ₄ (bipy)] · 1.5MeCN	x	—	x	—	—	—	x	x	—	—	—	139
(BiCl ₃) ₂ (bipy) ₃	42	—	x	—	—	—	x	—	—	—	—	138
(BiX ₃)(bipy) ₂ (X = Br, I)	x	—	x	x	—	—	x	—	—	—	—	140
(Bi(NO ₃) ₃)(bipy) ₂	x	—	x	x	—	—	x	—	—	—	—	141
Bi(S ₂ CNEt ₂)I ₃ (bipy)	x	—	—	—	—	—	—	—	—	—	—	142
[Bi(CNS) ₃ (bipy) ₂] ₂	x	—	x	x	—	—	x	—	—	—	—	143
BiCl ₃ (phen) _{1.33} BiX ₃ (phen)(X = Br, I)	—	—	x	x	x	x	x	—	—	—	x	144
(BiX ₃)(phen)(dmso) ₃ (X = Cl, Br) · 3 dmso	x	—	x	x	—	—	x	x	—	—	—	145
[(phen)BiI ₅ (O-dmso) ₃][(phen)BiI ₄] · 1.5 dmso	x	—	x	x	—	—	—	—	—	—	—	145
(BiBr ₃)(phen)(dmso) ₃ · MeCN	x	—	x	x	—	—	—	—	—	—	—	138
(phen) ₂ BiCl ₃	x	—	x	x	—	—	x	x	—	—	—	140
(phen) ₂ BiBr ₃	x	—	—	—	—	—	—	—	—	—	—	140
(phen) ₂ BiBr ₃ (MeCN) · MeCN	x	—	—	—	—	—	—	—	—	—	—	140
(phen) ₂ BiI ₃ (CH ₂ Cl ₂) · CH ₂ Cl ₂	x	—	x	x	—	—	—	—	—	—	—	140
(phen)(NO ₃) ₂ Bi(μ-OH) ₂ Bi(NO ₃) ₂ (phen)	43	—	x	x	—	—	x	—	—	—	—	141
(phen) ₂ Bi(NO ₃) ₃	x	—	x	x	—	—	x	—	—	—	—	141
BiX ₃ (paphyH) (X = Cl, Br, I)	—	—	x	x	x	x	x	—	—	—	x	144
Bi(CNS) ₃ (paphyH)	—	—	—	x	x	—	x	—	—	—	—	146
Bi(CNS) ₃ (terpy)	—	—	—	x	x	—	x	—	—	—	—	146
Bi(S ₂ CNEt ₂)I ₃ (terpy)	x	—	—	x	—	—	—	—	—	—	—	142
Bi(CNS) ₃ (dqp) Bi(CNS) ₃ (tpta)	—	—	—	x	x	—	x	—	—	—	—	146
(BiCl ₃ · Me ₃ 9)aneN ₃	x	90.3	x	x	—	—	x	—	—	x	—	147, 148
Bi(cyclen)(H ₂ O)(ClO ₄) ₃	x	—	—	x	—	—	—	—	—	—	—	149
[¹⁸ Bu ₄ N][Bi(pc) ₂] [Ph ₃ PNPPh ₃][Bi(pc) ₂]	—	—	—	x	—	—	x	x	x	—	—	150
Bi(pc) ₂ · CH ₂ Cl ₂	x	—	—	x	—	—	x	x	x	—	—	150
Bi(pc) ₂ (Br) _x (1.5 ≤ x ≤ 2.5)	—	—	—	—	—	—	x	x	x	—	—	150

2.913(4) and 3.011(3) Å], the two nitrogen atoms of the bipy ligand [Bi–N 2.56(2) Å], and the oxygen atom of the dmso ligand [Bi–O 2.53(2) Å]. Interestingly, the acetonitrile adduct of BiBr₃(bipy) (*138*) has the same dimeric structure **41** with lattice MeCN molecules [axial: Bi–Br_{terminal} 2.681(1) Å; Bi–Br_{bridging} 3.032(2) Å; equatorial: Bi–Br_{terminal} 2.779(2) Å; Bi–Br_{bridging} 2.95(1) Å; Bi–N 2.51(1) and 2.423(8) Å]. Salts of the general formula [bipyH][BiX₄(bipy)] (X = Cl, Br) (*139*) contain monomeric, anionic near-octahedral bismuth complexes [Bi–Cl 2.681(6) and 2.678(5) Å; Bi–Br 2.824(4) and 2.804(4) Å; Bi–N_{cl}



41



42

2.50(1); Bi–N_{Br} 2.45(3) Å]. (BiCl₃)₂(bipy)₃ **42** involves a similar bridging arrangement in the solid state with two different bismuth centers (138). One occupies a seven-coordinate environment composed of four nitrogen atoms [Bi–N 2.58(2) and 2.52(3) Å; 2.71(3) and 2.65(3) Å], two terminal chlorine atoms [Bi–Cl 2.62(1) and 2.574(8) Å], and a bridging chlorine atom *trans* to a terminal chlorine atom [Bi–Cl 2.872(8) Å]. The second bismuth center occupies a six-coordinate, near-octahedral environment imposed by three terminal chlorine atoms in a facial arrangement [Bi–Cl 2.63(9), 2.63(1), and 2.539(9) Å], the bridging chlorine atom *trans* to a terminal chlorine atom [Bi–Cl 2.973(8) Å], and the two nitrogen atoms [Bi–N 2.51(3) and 2.55(3) Å].

The 1:2 adducts (BiX₃)(bipy)₂ (X = Br, I) (140) adopt a predictable seven-coordinate distorted pentagonal pyramidal environment. The axial sites are occupied by two halide atoms [Bi–Br 2.818(3) and 2.903(3) Å; Bi–I 3.304(2) and 3.127(3) Å], while the equatorial sites are occupied by a halide atom [Bi–Br 2.753(4) Å; Bi–I 2.973(3) Å], and four nitrogen atoms [Bi–N_{Br} 2.60(2) and 2.53(2), 2.59(2) and 2.65(3) Å; Bi–N_I 2.58(2) and 2.61(2) Å; 2.66(2) and 2.71(3) Å]. The nitrate derivative (Bi(NO₃)₃)(bipy)₂ was recrystallized from a dmso solution (141) and a 10-coordinate, near-sphenocoronal environment occupied by four nitrogen atoms [average Bi–N 2.489(3) Å] and three relatively symmetrically bound bidentate nitrate ligands [Bi–O 2.613(3), 2.678(3), and 2.673(3) Å], all in a *cis* arrangement.

A dithiocarbamate complex Bi(S₂CNEt₂)I₂(bipy), prepared from [Bi(S₂CNEt₂)I₂] with a fivefold excess of bipy (142), exists as an iodide bridged dimer reminiscent of **41**. The central bismuth atom is seven-coordinate with a pseudo-pentagonal-bipyramidal geometry occupied by a terminal I atom and a bipy nitrogen atom [Bi–N 2.56(1) Å] in

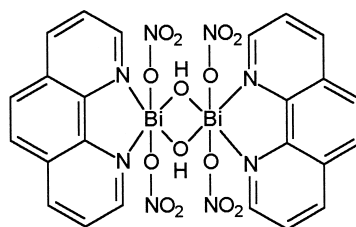
the axial positions, and the sulfur atoms, the N atom [Bi–N 2.61(1) Å], and two bridging I atoms in the equatorial sites. The bond distances to the bridging iodine atoms are exceptionally long [Bi–I 3.501(2) and 3.250(2) Å]. [Bi(CNS)₂(bipy)₂]₂ is obtained from a methanolic solution of NH₄NCS, Bi(NO₃)₃ · 5H₂O and bipy (143). Eight-coordinate geometry is imposed by seven nitrogen atoms, four from two unequally bound bipy ligands [Bi–N 2.542(8) and 2.553(7) Å; 2.620(7) and 2.624(5) Å] and three from thiocyanate groups. The eighth site is occupied by a thiocyanate sulfur atom of an adjacent group, which acts as a bridge to form a centrosymmetric dimer. The irregular geometry around the bismuth atom contains no regular gaps in the coordination sphere, suggesting a non–stereochemically active lone pair. The angles at the metal for each of the bipy ligands [62.6(2) and 63.4(2)°] are the smallest in the complex as a result of the bite and symmetric chelation of the ligands. The longest Bi–N bond [2.648(9) Å] is that of the bridging thiocyanate group, while the remaining two Bi–N bond distances to the terminal thiocyanate groups are shorter [2.453(8) and 2.408(9) Å], corresponding to strong interactions. Eight-coordination is rare for bismuth but has been seen for bismuth thiophosphate.

1,10-Phenanthroline (phen) adducts of bismuth are numerous. Halide complexes BiCl₃(phen)_{1.33} and BiX₃(phen) (X = Br, I) are prepared by mixing methanolic solutions of the appropriate bismuth halide and phen (144). The relatively high melting points, the low solubilities, and the IR spectra suggest the presence of bridging halide atoms, while the absence of a molecular ion in the EI mass spectra suggests a weak complex. A systematic structural study of bismuth halide phen adducts, similar to that for bipy adducts described above, has been reported (138, 140, 145, 153). (BiX₃)(phen)(dmsO)₃ (X = Cl, Br, I) (145) generally involve seven-coordinate bismuth in a regular pentagonal bipyramidal geometry. The axial sites are occupied by two halogen atoms [Bi–Cl 2.636(3) and 2.682(3) Å; Bi–Br 2.784(1) and 2.8510(8) Å], while the equatorial sites are occupied by a halogen atom [Bi–Cl 2.740(3) Å; Bi–Br 2.875(1) Å], two *cis* oxygen atoms of dmsO molecules [Bi–O_{ce} 2.501(8) and 2.560(9) Å; Bi–O_{Br} 2.513(5) and 2.552(6) Å], and two nitrogen atoms of a chelating phen ligand [Bi–N_{ce} 2.514(8) and 2.578(7) Å; 2.541(6) and 2.600(6) Å]. The third dmsO molecule is uncoordinated in a lattice site. (BiI₃)(phen)(dmsO)₃ · 1.5 dmsO is ionic, as if disproportionated in the solid state. The [(phen)BiI₂(O-dmsO)₃]⁺ cation is composed of a seven-coordinate bismuth center in a pentagonal bipyramidal geometry. The axial sites are occupied by two iodine atoms [Bi–I 3.064(3) and 2.952(3) Å], while the equatorial sites are occupied

by oxygen atoms [Bi–O 2.46(1) and 2.59(3) Å] and two nitrogen atoms [Bi–N 2.53(2) Å]. The six-coordinate near-octahedral anion [(phen)BiI₄][−] has two iodine atoms in the axial sites [Bi–I 3.007(3) and 3.089(3) Å], and two iodine atoms [Bi–I 3.033(2) Å] and two phen nitrogen atoms [Bi–N 2.52(2) Å] in the equatorial sites. The acetonitrile solvate of the bromide adduct (BiBr₃)(phen)(dmsO)₃·MeCN (*138*) is isomorphous with the bipy analogue [axial: Bi–Br_{terminal} 2.697(3); Bi–Br_{bridging} 3.018(3) Å; equatorial: Bi–Br_{bridging} 2.991(2) Å; Bi–Br_{terminal} 2.737(2) Å; Bi–N 2.53(1) and 2.43(1) Å].

The 1:2 bismuth chloride and bromide phen adducts [(phen)₂BiX₃] (X = Cl, Br), as well as the solvated bromide and iodide adducts [(phen)₂BiBr₃(MeCN)]·MeCN and [(phen)₂BiI₃(CH₂Cl₂)]·CH₂Cl₂ (*140*), have similar pentagonal bipyramidal structures to those of the 1:2 bismuth bromine and iodine bipy adducts [Bi–Cl_{axial} 2.593(9) and 2.741(8); Bi–Cl_{equatorial} 2.650(6); Bi–N 2.56(2) and 2.46(2), 2.69(2) and 2.71(2) Å; Bi–Br_{axial} 2.78(1) and 2.85(1); Bi–Br_{equatorial} 2.79(1); Bi–N 2.64(6) and 2.39(5), 2.68(7) and 2.83(4) Å; Bi–Br_{axial} 2.836(4) and 2.859(4); Bi–Br_{equatorial} 2.795(4); Bi–N 2.58(3) and 2.50(2), 2.67(3) and 2.70(3) Å; Bi–I_{axial} 3.035(2) and 3.103(2); Bi–I_{equatorial} 3.002(2); Bi–N 2.52(2) and 2.53(1), 2.71(2) and 2.73(2) Å]. The solvent molecules occupy lattice sites.

Two nitrate complexes have been crystallized from 1:1 and 1:2 dmsO solutions of Bi(NO₃)₃·5H₂O and phen, respectively (*141*). While (phen)₂Bi(NO₃)₃ is structurally analogous to the bipy derivative [average Bi–N 2.51(1); Bi–O 2.60(1), 2.62(1) and 2.65(1) Å], (phen)(NO₃)₂Bi(μ-OH)₂Bi(NO₃)₂(phen) is a hydroxide bridged dimer **43** involving

**43**

eight-coordinate bismuth occupied by the oxygen atoms of two asymmetrically bound bidentate nitrate ligands [Bi–O 2.826(4) and 2.650(4) Å; 2.766(4) and 2.685(4) Å], two phen nitrogen atoms [Bi–N 2.426(4) and 2.539(4) Å], and two oxygen atoms of bridging hydroxy groups [Bi–O 2.214(3) and 2.232(3) Å].

The distinct N–H IR stretching frequency of Hpaphy is a probe of its behavior as a neutral tridentate ligand, which is analogous to phen. The halide $\text{BiX}_3(\text{Hpaphy})$ ($\text{X} = \text{Cl}, \text{Br}, \text{I}$) (144) and thiocyanate $\text{Bi}(\text{CNS})_3(\text{Hpaphy})$ complexes (146) are stable in air, and the IR spectra and low solubility suggest a bridging polynuclear bismuth-thiocyano structure. Similar observations and speculations are made for $\text{Bi}(\text{CNS})_3(\text{terpy})$ (146). $\text{Bi}(\text{S}_2\text{CNEt}_2)_2\text{I}_2(\text{terpy})$ was prepared from an *n*-butanol solution of $\text{Bi}(\text{S}_2\text{CNEt}_2)_2\text{I}_2$ with excess terpy (142) and exists as a monomer in the solid state, with a seven-coordinate, pentagonal–bipyramidal environment for bismuth. Iodine atoms occupy the axial sites, and a drastic distortion in the terpy ligand sites enforces weak Bi–N bonds [Bi–N 2.61(2), 2.63(2), and 2.61(2) Å]. Other derivatives of pyridine form analogous adducts with bismuth thiocyanate, $\text{Bi}(\text{CNS})_3(\text{dqp})$, and $\text{Bi}(\text{CNS})_3(\text{tpta})$ (146).

A facial octahedral configuration is observed for $\text{BiCl}_3(\text{Me}_3[9]\text{aneN}_3)$ (147) [Bi–Cl 2.643(8), 2.665(5), and 2.656(8) Å; Bi–N 2.44(3), 2.45(2), and 2.47(2) Å] enforced by the endotridenate ligand (148). This half sandwich structure also exists in solution (^1H and ^{13}C NMR) and is similar to the eight-coordinate bismuth environment of $\text{Bi}(\text{cyclen})(\text{H}_2\text{O})(\text{ClO}_4)_3$ (149), which is prepared by dissolving Bi_2O_3 and cyclen in 70% HClO_4 [avg. Bi–N 2.39 Å].

Salts of the anion $[\text{Bi}(\text{pc}^{2-})_2]^-$ were synthesized by reacting $\text{BiO}(\text{NO}_3)$ with molten 1,2-dicyanobenzene in the presence of potassium methylate, and isolated as salts of $[\text{nBu}_4\text{N}]^+$ or $[\text{Ph}_3\text{PNPPh}_3]^+$ (150). Anodic oxidation gave the mixed-valence paramagnetic compound $[\text{Bi}(\text{pc})_2] \cdot \text{CH}_2\text{Cl}_2$, which involves bismuth sandwiched between the cavities of two pc ligands, resulting in an eight-coordinate square antiprismatic geometry around bismuth. The average Bi– N_{iso} bond length to the slightly distorted Pc ligands is 2.467 Å. Oxidation with bromine gives $[\text{Bi}(\text{pc}^-)_2]\text{Br}_x$ ($1.5 \leq x \leq 2.5$).

B. PHOSPHINES

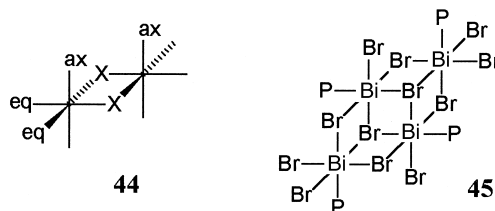
The limited number of isolated bismuth phosphine complexes (Table X) are dimeric in most cases, by virtue of halide bridges, often as centrosymmetric edge-sharing bioctahedra 44. They are generally prepared by the reaction of the bismuth halide with the neutral phosphine, and most examples have been definitively structurally characterized. $\text{Bi}_2\text{Br}_6(\text{PMe}_2\text{Ph})_2(\text{OPMe}_2\text{Ph})_2$ [Bi–P 2.725(2) Å] contains a phosphine oxide ligand [Bi–O 2.371(6) Å] that results from partial oxidation during reaction and occupies an apical site together with a bromine atom [Bi–Br 2.788(1) Å] (154). The *cis* bridging bromine

TABLE X
ANALYTICAL DATA FOR BISMUTH PHOSPHINE COMPLEXES

Empirical formula	X-ray structure #	Yield (%)	mp	EA	Sol	Cond	IR	NMR	MS	Ref.
BiBr ₇ (PMe ₃ Ph)(OPMe ₂ Ph)	44	—	—	x	—	—	—	—	—	154
BiBr ₇ (PMe ₃)	44	12	—	x	—	—	—	x	—	155
[PMe ₃ H][Bi ₂ Br ₇ (PMe ₃) ₂](MeCN) ₂	44	26	—	—	—	—	—	x	—	156
[PMe ₃ H][Bi ₂ I ₇ (PMe ₃) ₂](MeCN) ₂	44	—	—	—	—	—	—	x	—	156
[PPh ₄][BiI ₄ (PMe ₂ Ph) ₂]	x	53	—	x	—	—	—	—	—	157
BiBr ₇ (PEt ₃)	45	44	—	x	—	—	—	—	—	155
BiBr ₇ (dmpe)	x	86(pdr) 75(crs)	—	x	—	—	—	—	—	155
BiCl ₃ (dppm)	46	71	x	x	—	—	x	x	—	158
BiCl ₃ (dppe)	44	63	x	x	—	—	x	x	—	158
Bi ₂ Cl ₆ (dppe) ₂	47	63	x	x	—	—	x	x	—	158
BiX ₃ (dpe) (X = Cl, Br, I)	—	—	x	x	x	x	x	—	x	144

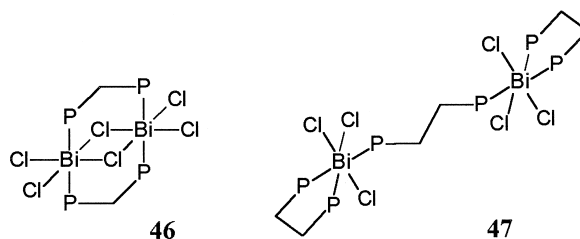
atoms [Bi–Br 3.362(1) and 2.926(1) Å], a terminal bromine atom [Bi–Br 2.741(1) Å], and the phosphorus atom accommodate the equatorial sites [Bi–P 2.725(2) Å]. In Bi₂Br₆(PMe₃)₄, the phosphine ligands occupy axial (ax) and equatorial (eq) positions [Bi–P 2.866(3) and 2.714(2); Bi–Br_{axial} 2.916(1); Bi–Br_{bridging} 2.875(1) and 3.403(1); (equatorial) Bi–Br_{terminal} 2.774(1) Å], but the ³¹P solution NMR spectra shows a single phosphine signal indicating a fluxional process or intermolecular exchange (155).

The salts [PMe₃H][Bi₂X₇(PMe₃)₂](MeCN)₂ (X = Br, I) contain centrosymmetric ‘edge-shared’ bioctahedral anions possessing phosphines in axial sites [Bi–P 2.762(3); (equatorial) Bi–Br_{bridging} 2.988(1); Bi–Br_{terminal} 2.747(1) Å], and the corresponding (*trans*) axial bromine atom [Bi–Br 3.103(1) Å] interacts (bridges) with the next dimer, to give a polymeric solid-state structure (156). The anion of [PPh₄][BiI₄(PMe₂Ph)₂] is uniquely monomeric with a six-coordinate, near-octahedral environment for bismuth composed of *cis* phosphorus atoms at relatively long bond distances [3.005(2) and 2.981(2) Å] and four iodine atoms of similar bond distance [avg. Bi–I 3.048 Å] (151). A tetrameric structure **45** is observed for Bi₄Br₁₂(PEt₃)₄ in which the



six-coordinate near-octahedral subunits [Bi-P 2.733(6), 2.747(7) Å; Bi-Br 2.694(3), 2.691(3), 2.701(3) Å] are bound by bridging μ_2 -bromine atoms [Bi-Br 2.776(3)–3.302(3); 3.112(3)–3.313(4) Å] and μ_3 -bromine atoms [Bi-Br 3.058(3) Å] (155). This may be viewed as two linked 'edge-shared' bioctahedral units.

Diphosphine ligands (dmpe, dppm, dppe) are observed in both chelating and bridging capacities, with the recurring centrosymmetric edge-shared bioctahedral structure imposed by halide bridging **44**. $\text{Bi}_2\text{Br}_6(\text{dmpe})_2$ [(axial) Bi-P 2.791(7); Bi-Br 2.992(3); (equatorial) Bi-P 2.678(8); Bi-Br_{terminal} 2.788(3); Bi-Br_{bridging} 2.887(3) and 3.345(3) Å] (155) and $[\text{Bi}_2\text{Cl}_6(\text{dppe})_2]$ (one of two structurally unique molecules in the structure) [(axial) Bi-P 2.956(10); Bi-Cl 2.470(11); (equatorial) Bi-P 2.699(8); Bi-Cl_{terminal} 2.409(9); Bi-Cl_{bridging} 2.619(9) and 2.945(9) Å] (158) involve terminal chelate diphosphines occupying *cis* axial and equatorial sites. $[\text{Bi}_2\text{Cl}_6(\text{dppm})_2][\text{Bi-P } 2.872(3) \text{ and } 3.090(3); \text{Bi-Cl}_{\text{bridging}} 2.808(4) \text{ and } 2.820(3); \text{Bi-Cl}_{\text{terminal}} 2.475(3) \text{ and } 2.530(4) \text{ Å}]$ is a centrosymmetric dimer involving both halide and diphosphine bridges **46** (158). $[\text{Bi}_2\text{Cl}_6(\text{dppe})_3]$ is crystallized with $[\text{Bi}_2\text{Cl}_6(\text{dppe})_2]$, and contains two octahedral sites $\text{BiCl}_3(\text{dppe})$ linked by a single tethering



dppe molecule **47** [Bi-Cl 2.514(8)–2.555(9) Å; Bi-P_{chelate} 2.654(8), 2.916(6); Bi-P_{bridge} 2.973(9) Å] (158). Complex vibrational spectra have been obtained for $\text{BiCl}_3(\text{dpe})_{1.5}$, $\text{BiBr}_3(\text{dpe})$, and $\text{BiI}_3(\text{dpe})$ indicating the formation of dimeric structures (144).

Bismuth phosphine complexes represent a substantial component of the established phosphine complexes of heavier *p*-block elements, and an excellent overview has presented an important bonding model for these systems (7). The observed structures are considered as trigonal-pyramidal BiX_3 units with three secondary *trans* bonds. If the acceptor orbitals are the Bi-X σ^* orbitals, this *trans* arrangement is expected, as the relationship between the *trans* X-Bi-P bond distances. The shortest Bi-P distance [2.7614(2) vs 2.866(3) Å] is *trans* to the longer Bi-Br distance [3.403(1) vs 2.9916(1) Å], as the only arrangement that will allow the phosphine ligands to occupy *trans*

positions with respect to the most electronegative ligands while maintaining the trigonal-pyramidal BiX_3 unit.

C. ARSINES

The only isolated arsine complexes of bismuth $\text{BiX}_3(\text{pbda})$ (see Chart 4) (Cl, Br, I) are prepared from the reaction of stoichiometric amounts of $\text{Bi}(\text{NO}_3)_3 \cdot 5\text{H}_2\text{O}$ and pbda in dilute hydrochloric acid, hydrobromic acid, and a hydrochloric acid/KI solution, respectively (159). Conductivity and molecular weight determinations in nitrobenzene suggest that the complexes are nonelectrolytes and monomeric.

VIII. Nonsymmetric Bifunctional and Multifunctional Ligands

The characteristics of bismuth complexes involving ligands possessing more than one equivalent donor site are discussed throughout Sections III–VII and are generally consistent with the coordination chemistry of most metals, with the ligands functioning in both multidentate and bridging capacities. Complexes involving ligands with different types of donor sites represent an extensive component of the established chemistry of bismuth and predictably present more extensive and diverse features of structure, stability, and reactivity. The complexes are presented here according to the combinations of donor types within the ligand.

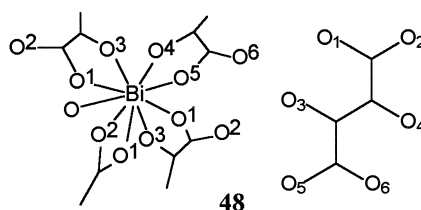
A. HYDROXY- AND ALKOXIDE CARBOXYLATES

As illustrated in Sections III, IV, and V, complexes involving oxygen-based ligands have been extensively studied, including substantial efforts with bifunctional and multifunctional ligands. However, the lability of the Bi–O interaction is naturally sensitive to the basicity of the donors and reactions involving multifunctional ligands are very dependent on reaction conditions. This together with the versatility or flexibility of the ligand backbone results in structural variability in terms of chelation and bridging, so that complexes are difficult to isolate from complicated mixtures. Consequently, the limited number of isolated compounds do not yet represent or define the chemistry of these complexes. Moreover, the formulas are sometimes speculatively assigned on the basis of minimal or incomplete experimental data.

Mixtures of bismuth nitrate or hydroxide with common hydroxycarboxylic acids (gallic, H_4gal ; tartaric, H_4tar ; lactic, H_2lac ; malic, H_3mal ;

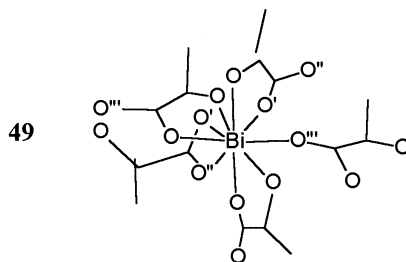
and citric, H_4cit) have been used in a wide range of medicinal capacities since 1900 (4), which has prompted extensive efforts to characterize the complexes isolated from such solutions. However, there are relatively few reports of elemental analysis data and X-ray crystallographic studies, and factors such as ligand stoichiometry or derivatization have not been systematically determined.

Solid-state structures of two bismuth tartrate complexes reveal a similar asymmetric unit composed of two tartrate ligands on a bismuth center and are distinguished by replacement of a proton in $Bi(H_3tar)(H_2tar) \cdot 3H_2O$ (160) with by an ammonium ion in $NH_4[Bi(H_2tar)_2(H_2O)] \cdot H_2O$ (161). The nine-coordinate bismuth environments in each structure are very similar, as illustrated in **48**, respectively,

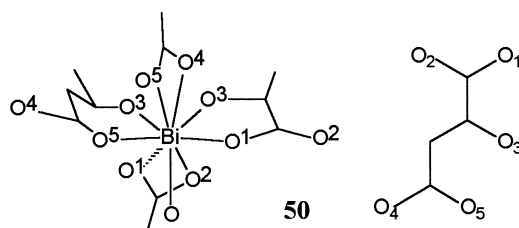


and involve bidentate interactions with three alkoxide/carboxylate (five-membered ring) and one carboxylate (four-membered) of four different tartrate ligands. Consequently, bismuth centers are bridged by the ligands to give coordination polymeric arrays supplemented by hydrogen bonding between ligands and with water.

Although $Bi(Hlac)_3$ is formally homoleptic, two lactate ligands are bound more tightly [$Bi-O_{\text{carboxylate}}$ 2.205(7) Å, $Bi-O_{\text{hydroxy}}$ 2.474(8) Å; $Bi-O_{\text{carboxylate}}$ 2.364(8) Å, $Bi-O_{\text{hydroxy}}$ 2.457(9) Å] than the third [$Bi-O_{\text{carboxylate}}$ 2.628(9) Å, $Bi-O_{\text{hydroxy}}$ 2.800(1) Å], which bridges a second bismuth center via a bidentate carboxylate interaction (162). A carboxylate oxygen interacts with a third bismuth center, giving bismuth a total coordination number of 9 (**49**) and resulting in a complex three-dimensional network.



The structure of $\text{Bi}(\text{mal}) \cdot \text{H}_2\text{O}$ (*160*) involves bismuth coordinated by four malate ligands in three different bidentate fashions **50**, an al-



koxide [2.244(6) Å]/ α -carboxylate [2.407(8) Å] five-membered ring, an alkoxide [2.255(6) Å]/ β -carboxylate [2.571(9) Å] six-membered ring, and two carboxylate [α -2.959(9) and 2.553(8) Å; β -2.351(9) and 3.233(9) Å] four-membered rings. A water molecule [$\text{Bi}-\text{O}_{\text{water}}$ 2.80(1) Å] completes the coordination sphere for a total coordination number of 9 and a highly coordinated polymeric network.

Widespread medicinal use of “colloidal bismuth subcitrate” (CBS) has prompted extensive studies of bismuth compounds involving the citrate anion. Bismuth citrate is essentially insoluble in water, but a dramatic increase in solubility with increasing pH has been exploited as a bio-ready source of soluble bismuth, a material referred to as CBS. Formulation of these solutions is complicated by the variability of the bismuth:anion stoichiometry, the presence of potassium and/or ammonium cations, the susceptibility of bismuth to oxygenation to $\text{Bi}=\text{O}$, and the incorporation of water in isolated solids. Consequently, a variety of formulas are classified in the literature as CBS. Solids isolated from various, often ill-defined combinations of bismuth citrate, citric acid, potassium hydroxide, or ammonium hydroxide have been assigned formulas on the basis of elemental analysis data or by determination of water and ammonia content, but are of low significance in the absence of complementary data other than thermal analysis (*163*), infrared spectroscopy (*163*), or NMR spectroscopy (*164*). In this context, the Merck index lists the chemical formula of CBS as $\text{K}_3(\text{NH}_4)_2\text{Bi}_6\text{O}_3(\text{OH})_5(\text{C}_6\text{H}_5\text{O}_7)_4$ in the 11th edition (*165*), but in the most recent edition provides a less precise name, “tripotassium dicitrato bismuthate” (*166*).

More definitive formulas are available from eight X-ray crystallographic reports, as listed in Table XI, which reveals closely related structures by virtue of potassium and ammonium cations being essentially interchangeable. Most are constructed from a complex of Bi^{3+}

TABLE XI
X-RAY CRYSTALLOGRAPHIC DATA FOR SOLIDS DESCRIBED AS "COLLOIDAL BISMUTH
SUBCITRATE" ($\text{Hcit} = [\text{CO}_2\text{CH}_2\text{C}(\text{OH})(\text{CO}_2)\text{CH}_2\text{CO}_2]^{3-}$)

Formula	Space group	Cell parameters a, b, c, β	Ref.
$\text{KBi}(\text{cit})(\text{H}_2\text{O})_3$	$P2_1/n$	10.924, 15.280, 14.967, 105.48	167
$\text{K}_{0.5}(\text{NH}_4)_{0.5}\text{Bi}(\text{cit})(\text{H}_2\text{O})_3$	$P2_1/n$	10.923, 15.424, 15.037, 105.67	168
$\text{NH}_4\text{Bi}(\text{cit})(\text{H}_2\text{O})_2$	$C2/c$	16.805, 12.544, 10.401, 91.27	169
$\text{K}_{0.5}(\text{NH}_4)_{0.5}\text{Bi}(\text{cit})(\text{H}_2\text{O})_2$	$C2/c$	16.860, 12.395, 10.328, 91.79	168
$\text{Na}_2[\text{Bi}(\text{cit})_2](\text{H}_2\text{O})_7$	$C2/c$	15.723, 13.899, 10.423, 94.39	164
$\text{K}_{4.75}(\text{NH}_4)_{0.25}[\text{Bi}(\text{cit})_2](\text{Hcit})(\text{H}_2\text{O})_{13}$	$P-1$	11.801, 12.973, 15.856, 98.15, 108.39, 100.91	170
$(\text{NH}_4)_6\text{Bi}(\text{cit})(\text{Hcit})(\text{H}_2\text{O})_5$	$P2_1/c$	8.998, 9.492, 27.021, 99.42	170
$(\text{NH}_4)_6(\text{Bi}_6\text{O}_4)(\text{cit})_4(\text{H}_2\text{O})_5$ initially assigned $(\text{NH}_4)_6(\text{Bi}_6\text{O}_4\text{OH})(\text{cit})_3(\text{H}_2\text{O})_7\text{Hcit}$	$R-3$	17.807, 17.807, 31.596	171, 172

with a tridentate tetra-anionic citrate ligand, which adopts a well-defined dimeric arrangement imposed by chelate coordination of the pendant carboxylate moiety to a neighboring bismuth center **51**. The macrostructures (space groups) are distinguished by the different packing modes of these dimers, governed by water molecules and/or extra citrate ligands (a more detailed structural comparison/assessment is available in Ref. (4)).

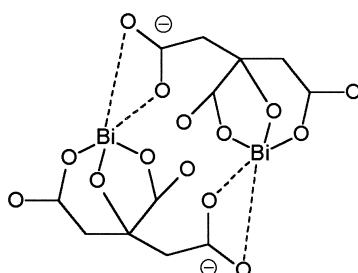
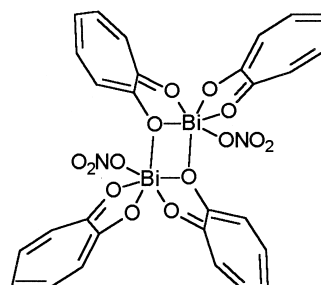
Tridentate (alkoxide/carboxylate/carboxylate) chelation by citrate precludes chelation by the third carboxylate because of the required tetrahedral geometry of the central carbon center of the ligand, so that the five- and six-membered chelate heterocycles are favored over two seven-membered heterocycles imposed by coordination of three carboxylate oxygen atoms. More importantly, the alkoxide has a substantially higher basicity than the carboxylate. In the carboxylate chemistry of bismuth, the citrate salts are uniquely water soluble at high pH with avoidance of hydrolysis, which typically gives BiO for other salts. The tridentate chelate involving the alkoxide dominates this behavior relative to other polycarboxylates and relative to bismuth citrate $[\text{Bi}(\text{HCit})]$ at neutral or low pH, which is deprotonated at high pH.

B. KETOALKOXIDES

Bismuth complexes involving ketoalkoxide ligands are rare and are represented by comprehensively characterized examples of an ethyl-maltolate $\text{Bi}(\text{emal})_3$ (173), a tris(acetylacetonate) (174), an acetylacetonate $\text{Bi}(\mu\text{-O}^i\text{Pr})(\text{O}^i\text{Pr})(\eta^2\text{-acac})$ (175), and series of tropolonate deriva-

tives, which have been extensively derivatized (see Chart 2) in conjunction with assessment of their anti-*Helicobacter pylori* activity (10). Tris(acetylacetonate)bismuth was prepared by ligand exchange from triphenylbismuth, and further alkoxide ligand exchange gave the monoacetylacetonate complex. The maltolate (173) and tropolonate (176–179) complexes are obtained from reactions of the conjugate acid of the ligand with bismuth chloride and bismuth nitrate, respectively. The structures are predictable in terms of the chelate nature of the ligands, the monomeric solid state structure of the maltolate, and the alkoxide bridged dimer arrangement of the acetylacetonate complexes (see Section II,A), with interdimer interactions between the terminal alkoxide and bismuth to give a one-dimensional polymer. The bismuth–acac oxygen bond distances are distinctly different [2.27(3) and 2.43(4) Å] and may represent the bismuth–alkoxide and bismuth–ketone bonding modes, respectively. Consistently, the endocyclic C–C bond is shorter than the ketone carbon C–C bond [1.34(6) vs 1.50(6) Å].

A variety of derivatives of bis-[Bi(tr)₂X, X = Cl or NO₃], tris-(Bitr₃), and tetra-([Bi(tr)₄X][Na]) tropolonate complexes of bismuth (178, 179) have been prepared and spectroscopically characterized (176, 177, 180). Solid-state structures for examples of bis-(tropolonate) derivatives confirm the chelate interaction (171) and in the case of the nitrate derivative, reveal intermolecular alkoxide–bismuth [Bi–O 2.688 and 2.666 Å] dimer contacts **52**, which are slightly longer than the chelate bonds [Bi–O 2.130–2.323 Å].

**51****52**

C. AMINO-, IMINO-, AND AZATHIOLATES

(See Table XII and Chart 5.) The stability of the thiolate–bismuth bond has allowed for the assessment of interactions between bismuth

TABLE XII

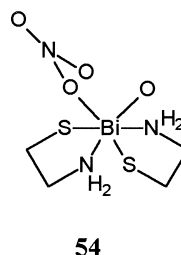
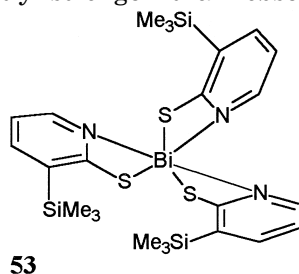
ANALYTICAL DATA FOR BISMUTH AMINO-, IMINO-, AND AZATHIOLATE COMPLEXES

Empirical formula	X-ray structure #	Yield (%)	mp	EA	sol	cond	IR	Raman	UV	NMR	MS	pot	Ref.
Bi(abt) ₃	—	—	x	x	x	x	x	—	—	—	x	x	184, 185
Bi(Habt) ₃ Cl ₃	—	—	—	x	x	x	x	—	x	—	—	—	185
Bi(SCH ₂ CH ₂ NR ₂) ₃ (R = H, Me)	x	38, 22	x	x	—	—	x	x	—	x	x	—	189
Bi(2-SC ₅ H ₃ N-3-SiMe ₃) ₃	53	55	—	x	x	—	x	—	—	—	—	—	186
Bi(mmq) ₃	x	—	—	—	—	—	—	—	—	—	—	—	187
Bi(Hdz) ₃	x	—	x	x	—	—	—	—	—	—	—	—	188
Bi(SCH ₂ CH ₂ NR ₂) ₂ Cl (R = H, Me)	x	17, 31	x	x	—	—	x	x	—	x	x	—	189
Bi(SCH ₂ CH ₂ NH ₂) ₂ (NO ₃)(H ₂ O)	54	35	x	—	x	—	x	x	—	x	—	—	189, 190
Bi(pmq) ₂ Cl	55	78	—	—	—	—	—	—	—	—	—	—	191
Bi(tscR ₁ R ₂) ₂ (NO ₃)	x	76	x	x	—	x	x	—	x	x	x	—	192
Bi(tscR ₁ R ₂)(HtscR ₁ R ₂)Cl ₂ (R ₁ = C ₄ H ₉ S, R ₂ = NC ₆ H ₁₂)	56	55	x	x	—	x	x	—	x	x	x	—	192
Bi(tscR ₁ R ₂) ₂ (NO ₃)	x	71	x	x	—	x	x	—	x	x	x	—	192
Bi(tscR ₁ R ₂)Cl ₂ (R ₁ = C ₆ H ₄ N, R ₂ = NC ₆ H ₁₂)	57	91	x	x	—	x	x	—	x	x	x	—	192
Bi(SCH ₂ CH ₂ NMe ₂)Cl ₂	58	—	—	—	—	—	—	—	—	—	—	—	189
Bi(SCH ₂ CH ₂ NMe ₂ H)Cl ₃	59	97	x	x	—	—	x	x	—	x	x	—	189
Bi(dapts)N ₃	60	—	—	x	—	—	x	—	—	—	—	—	193

and relatively weak donors using bifunctional ligands possessing a thiolate “anchor.” 2-Aminobenzenethiol (Habt) was the first ligand to be examined (181–183) and the trithiolate Bi(abt)₃ (184), as well as the corresponding conjugate acid Bi(Habt)₃Cl₃ (185), have been identified. Although IR data do not suggest interaction of the amino group with bismuth in these complexes, related tris(thiolate) derivatives have been shown to adopt predictable chelate structures in the solid state as illustrated for Bi(2-SC₅H₃N-3-SiMe₃)₃ (**53**) (186), which has a distorted pentagonal pyramidal geometry for bismuth with the sulfur centers in a *cis* configuration. The Bi–S bonds are substantially shorter than the Bi–N bonds [Bi–S 2.544(6)–2.647(7); Bi–N 2.69(2)–2.83(2) Å]. The five membered chelate -BiSCNN- and -BiSCCN- rings of the tris(merecaptoquinoline) Bi(mmq), (187) [Bi–S 2.571(2)–2.623(3); Bi–N 2.689(4)–2.796(4) Å], the tris(dithizone) Bi(Hdz)₃ (188) [Bi–S 2.607(3)–2.613(3) Å; Bi–N 2.678(8)–2.746(10) Å], and the tris(aminothiolate) Bi(SCH₂CH₂NH₂)₃ (189) achieve similar geometrical environments for bismuth and also involve weak interactions with nitrogen.

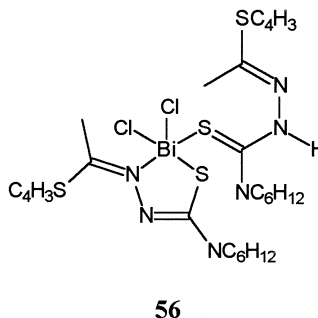
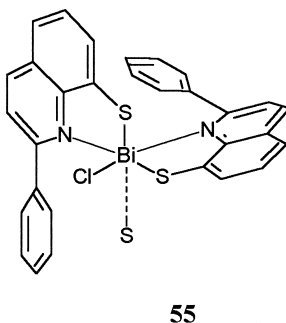
Thiolation is restricted by more effective nitrogen donors or steric limitations. The bis(aminothiolate) complexes are obtained from bismuth nitrate or chloride and the hydrogen chloride adduct of the thiol and essentially independent of stoichiometry. The nitrogen–bismuth interactions in these complexes [e.g., Bi(SCH₂CH₂NH₂)₂(NO₃)(H₂O) **54**,

Bi-S 2.549(2) and 2.589(2) Å; Bi-N 2.462(5) and 2.455(6) Å] (190) are significantly stronger than observed for the tris(*N*-thiolates) pre-

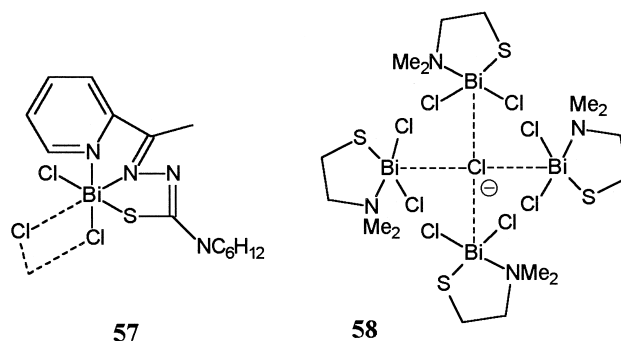


viously. The relatively long Bi-N distances in Bi(pm_q)₂Cl **55** [Bi-S 2.532(3) and 2.591(3) Å; Bi-Cl 2.579(3) Å; Bi-N 2.628(9) and 2.880(7) Å] (191) are likely due to the steric bulk of the ligand, and a long sulfur contact [Bi---S 3.304(3) Å] effects hexacoordination and a meridional arrangement of sulfur ligands.

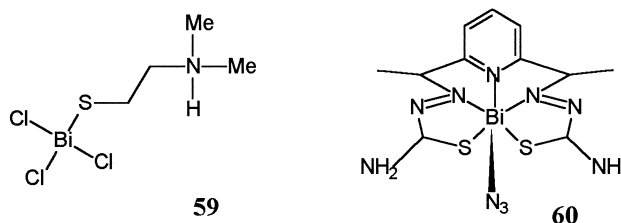
Monothiolates of bismuth are rare and seem to require the influence of auxiliary donors. Bi(tscR₁R₂)(HtscR₁R₂)Cl₂ (R₁ = C₄H₃S, R₂ = NC₆H₁₂) contains an *S,N*-chelate thiolate [Bi-S_{thiolate} 2.527(3); Bi-N 2.518(8); Bi-Cl 2.605(4) and 2.630(4) Å] and a neutral thione (tautomer) ligand [Bi-S_{thione} 2.992(3) Å] (**56**) (192). The dimeric structure of



Bi(tscR₁R₂)Cl₂ (R₁ = C₅H₄N, R₂ = NC₆H₁₂) involves bridging chlorine atoms, but hexacoordination of bismuth includes a tridentate interaction of the tsc ligand **57** [Bi-S 2.583(3); Bi-N_{aza} 2.355(8); Bi-N_{imine} 2.501(8); Bi-Cl 2.585 (3); Bi-Cl 2.791(3) Å] (192). The aminothiolate was isolated as a hydrogen chloride adduct [Bi(SCH₂CH₂NMe₂)Cl₂]₄ · HCl and adopts a cluster arrangement with the unique chloride anion in a tetragonal site, giving a pentacoordinate environment for each bismuth center **58** (189). The chelate interaction of this amine is la



bile and is protonated in aqueous chloride solution to give the aminethiol–bismuth chloride adduct **59**, involving the ammoniumthiolate tautomer of the aminethiol (189, 194). The bis(thiosemicarbazone) daps behaves as a dithiolate ligand in Bi(daps)N_3 , imposing a six-coordinate distorted pentagonal pyramidal environment for bismuth **60** (193). All basal sites are occupied by the S, N, N', N'', S' -pen-



tadentate ligand [Bi-S 2.685(7) and 2.717(8); Bi-N_{aza} 2.46(2) and 2.58(2); $\text{Bi-N}_{\text{imide}}$ 2.44(2) Å] with an azide nitrogen in the apical site [Bi-N 2.25(2) Å].

The most effective synthetic control of the thiolation of bismuth has been achieved using reactions of bismuth chloride with aminethiolate salts (potassium) prepared *in situ*. Although the reactions are not quantitative, the molecular stoichiometry can be reliably selected and a systematic series of mono-, bis-, and tris-thiolates have been isolated and comprehensively characterized. (189).

D. HYDROXY-, ALKOXIDE, ETHER, AND KETOTHIOLATES

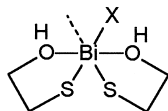
Mercaptoethanol reacts rapidly with most bismuth salts with the typical mineral acid metathesis to give bis(thiolate) $\text{Bi(SCH}_2\text{CH}_2\text{OH)}_2\text{X}$ derivatives as the prominent and most easily isolated

TABLE XIII

ANALYTICAL DATA FOR BISMUTH HYDROXY-, ALKOXIDE, AND KETOTHIOLATE COMPLEXES

Empirical formula	X-ray structure #	Yield (%)	mp	EA	sol	cond	IR	Ram	UV	NMR	MS	Ref.
Bi(SCH ₂ CH ₂ OH) ₂ (NO ₃)(H ₂ O) _{0.5}	61	41–76	x	x	x	x	x	x	x	x	x	195, 197
Bi(SCH ₂ CH ₂ OH) ₂ Cl	61	73–78	x	x	x	—	x	x	—	x	x	197
Bi(SCH ₂ CH ₂ OH) ₂ Br	—	19–22	x	x	x	—	x	x	—	x	x	197
Bi(SCH ₂ CH ₂ OH) ₂ (ClO ₄)	61	—	—	x	—	—	x	—	x	—	—	198
Bi(SCH ₂ CH ₂ O)(SCH ₂ CH ₂ OH)	x	29–47	x	x	x	x	x	x	—	x	—	195, 197
Bi(SCH ₂ CH ₂ OH) ₂ (CH ₃ COO)	61	92	x	—	x	—	x	x	—	x	x	197
Bi(SCH ₂ CH ₂ OH) ₃	—	33–70	x	x	x	x	—	—	x	x	—	16, 195
Bi(dbt) ₃	—	69–90	x	x	x	—	—	—	—	x	—	196
[Bi(PhCH(S)CH ₂ C(O)Ph) ₂] (CH ₂ Cl) ₂	62	85–90	—	x	—	—	x	—	—	x	—	199
Bi(PhCH(S)CH ₂ C(O)C ₆ H ₄ X) ₃ (X = Me, Cl)	—	85–90	—	x	—	—	x	—	—	x	—	199

products (Table XIII), although the tris(hydroxythiolate) has been isolated (195), and the aryl derivative Bi(dbt)₃ has been spectroscopically characterized (196). As observed with aminothiols, restricted thiolation is likely due to a decrease in Lewis acidity of the bismuth center effected by the pendant chelation of two hydroxy moieties. The resulting bicyclic framework **61** is structurally flexible in the solid state,

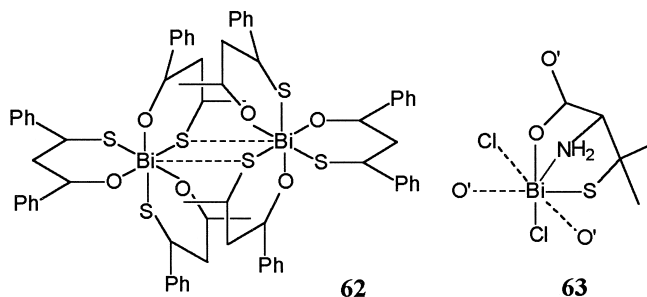
**61**X = NO₃, Cl, ClO₄, CH₃COO

with the chelates adopting *cis*-coplanar and twisted (nonplanar) arrangements depending on the substituent X (X = Cl, NO₃, CH₃COO, ClO₄), but the Bi–S and Bi–O bond distances are not substantially affected. The chloride is polymeric with bismuth in a seven-coordinate environment [Bi–S 2.595(3) and 2.558(4); Bi–O 2.86(1) and 2.80(1) Å] by virtue of two μ_2 -chlorine bridges [Bi–Cl 2.589(3) and 3.488(4) Å], and a sulfur contact [Bi---S 3.124(4) Å] to a third molecule (197). In the absence of water, the nitrate salt engages bismuth in a six-coordinate environment including the bidentate nitrate [Bi–S 2.639(5), 2.655(5); Bi–O 2.63(1), 3.01(2), and 3.17(2) Å] (197). In contrast, the

acetate ligand is monodentate [Bi–O 2.35(2), 2.54(2), and 2.72(2); Bi–S 2.608(7) and 2.577(7) Å] (197).

The alkoxy–hydroxy complex $\text{Bi}(\text{SCH}_2\text{CH}_2\text{O})(\text{SCH}_2\text{CH}_2\text{OH})$ is a rare example of an alkoxythiolate chelate complex and is obtained by either the reaction of bismuth acetate with mercaptoethanol (197) or the deprotonation of the nitrate salt of **61** in basic solution (195). The bicyclic framework is similar [Bi–S 2.527(3) and 2.564(3) Å], but with significantly different Bi–O distances clearly distinguishing the alkoxide [Bi–O 2.195(9) vs 2.577(9) Å]. A polymeric lattice is effected by intermolecular contact between bismuth and an alkoxide oxygen of a neighboring molecule [Bi–O 2.982(8) Å]. The complex is readily reprotonated in acetic acid (197) or by reaction with excess mercaptoethanol to give the tris(thiolate) $\text{Bi}(\text{SCH}_2\text{CH}_2\text{OH})_3$ (195).

The only example of a ketothiolate adopts a dimeric structure $[\text{Bi}(\text{PhCH}\{\text{S}\}\text{CH}_2\text{C}\{\text{O}\}\text{Ph})_3][\text{CH}_2\text{Cl}_2]$ in which one of the three S,O chelate ligands effects a secondary interaction with a neighboring bismuth [Bi---S 3.494(5) and 3.551(5) Å] to impose heptacoordination **62**



(phenyl substituents omitted from drawing for clarity) (199). Interestingly, the bridging sulfur center is more tightly bound [avg. of two unique bismuth centers Bi–S 2.581(4) Å] than the nonbridging sites [Bi–S 2.627(5)–2.731(3); Bi–O 2.536(9)–2.650(9) Å].

E. THIOLATOCARBOXYLATES

Reactions of thioglycolic acids (H_2tga , $\text{H}_2\text{2mpa}$, $\text{H}_2\text{3mpa}$, H_2tsal) with basic bismuth salts or with the addition of base to ensure deprotonation of the carboxylic acid group give complexes of the type $\text{Bi}(\text{A})(\text{HA})$, (Table XIV and Chart 5) in an analogous fashion to thiolates and carboxylates. Infrared spectra of the complexes suggest polymeric structures, with bridging mercaptocarboxylate ligands and

TABLE XIV

ANALYTICAL DATA FOR BISMUTH THIOLATOCARBOXYLATE COMPLEXES

Empirical formula	X-ray structure #	Yield (%)	mp	EA	IR	NMR	MW	Ref.
Bi(tga)(Htga)	—	80	x	x	x	x	x	200
Bi(2mpa)(H2mpa)	—	80	x	x	x	x	x	200
Bi(3mpa)(H3mpa)	—	65	x	x	x	x	x	200
Bi(tsal)(Htsal)	—	77	x	x	x	x	x	200
{Bi ₈ (tsal) ₁₂ (dmf) ₆ }(dmf) ₆	x	28	—	—	—	—	—	201
Bi(pen)Cl	63	96	—	x	—	x	—	202

four-coordinate bismuth atoms (200). A structurally complicated octanuclear arrangement is observed with the tris(thiosalicylate) ligand in $[\{\text{Bi}_8(\text{tsal})_{12}(\text{dmf})_6\}(\text{dmf})_6]$ (201). The cluster has C_3 symmetry with two unique bonding situations for bismuth. One is chelated in an *S,O* (thiolate, carboxylate) manner by three tsal ligands with sulfur atoms in a *fac* arrangement [Bi–S 2.596(8) Å] and all three oxygen atoms bridge to other bismuth centers [Bi–O 2.74(2) Å]. The second bismuth center is chelated by one ligand in an *S,O* manner [Bi–S 2.567(5) Å; Bi–O 2.46(2) Å] and two ligands in an asymmetrical *O,O'* manner [Bi–O 2.20(2)–2.79(1) Å].

A structurally simple complex Bi(pen)Cl **63** is observed with the aminothioloatocarboxylate ligand, which engages bismuth as a tridentate *O,S,N* ligand [Bi–O 2.414(5) Å; Bi–S 2.527(2) Å; Bi–N 2.345(6); Bi–Cl 2.680(2) Å] forming both a -BiSCCN- and a -BiOCCN- ring (202). Long contacts from a chlorine atom [Bi---Cl 3.182 Å] and two carbonyl oxygen atoms of neighboring molecules [Bi---O 2.779(5) and 2.698(5) Å] create a polymeric structure and a seven-coordinate environment for bismuth, which may be important as a model for amino acid complexation by bismuth and heavy metals in general.

F. AMINOCARBOXYLATES

The strong chelating ability of (multi)amino(multi)carboxylate ligands renders complexes of bismuth substantially more hydrolytically stable than those of bifunctional aminocarboxylate ligands (e.g., glycine). Several compounds have been successfully examined as ligands for bismuth, in that complexes are readily isolable as molecular systems with weak intermolecular interactions. The extent and diversity of these complexes is enhanced by substituent derivatization with, for example, cyclohexyl (e.g., cydtpa) and alkoxyethyl (e.g., oedta) groups.

TABLE XV
ANALYTICAL DATA FOR BISMUTH AMINOCARBOXYLATE COMPLEXES

Empirical formula	X-ray	Yield (%)	ea	ir	uv	nmr	ms	tga	pot	Ref.
Bi(qui) ₃ (H ₂ O) ₂	—	80	x	x	—	—	—	—	—	65
Bi(pdc)(Hpdc)(dmsO)	x	—	—	x	—	—	—	—	—	208
Bi(onda)(H ₂ O) ₂	x	—	—	—	—	—	—	—	—	209
[NH ₄][Bi(Honda) ₂ (H ₂ O) ₃]	x	—	—	—	—	—	—	—	—	210
[C(NH ₂) ₃] ₂ [Bi(onda)(Honda)(H ₂ O) ₃]	x	—	—	—	—	—	—	—	—	210
Bi(nta)(H ₂ O) ₂	x	—	x	—	—	—	—	—	—	203
[NH ₄] ₃ [Bi(nta) ₂]	x	—	—	—	—	—	—	—	—	211
[NH ₄] ₄ [Bi(nta) ₂ (NCS)] · 2H ₂ O	x	—	—	—	—	—	—	—	—	205
Bi(Hoedta)(H ₂ O)	—	—	x	x	x	—	—	x	x	206, 212
NaBi(oedta)(H ₂ O) ₄	—	—	x	—	x	—	—	x	x	212
Bi(Hedta)(H ₂ O) ₂	x	—	x	x	—	—	—	—	—	213, 214
Bi(Hedta)	x	—	—	—	—	—	—	—	—	207
Bi(Hedta)(tu) ₂	x	—	—	—	—	—	—	—	—	215
[C(NH ₂) ₃][Bi(edta)(H ₂ O)]	x	—	x	—	—	—	—	—	—	216
[Ca(H ₂ O) ₇][Bi(edta)] ₂ · 2H ₂ O	x	—	—	—	—	—	—	—	—	217
[Co(H ₂ O) ₆][Bi(edta)] ₂ · 3H ₂ O	x	—	—	—	—	—	—	—	—	218
[Ni(H ₂ O) ₆][Bi(edta)] ₂ · 3H ₂ O	x	—	—	—	—	—	—	—	—	218
NaBi(edta)(H ₂ O) ₃	x	—	x	—	—	—	—	x	—	219
[NH ₄][Bi(edta)(H ₂ O)]	x	—	—	—	—	—	—	—	—	207
Bi(Heydta)(H ₂ O) ₅	x	—	x	x	—	—	—	—	—	220
Bi(H ₂ dtpa)(H ₂ O) ₂ (221)	x	47	x	x	—	x	x	—	—	206
Bi(Na ₃ dtpa)(H ₂ O) ₄	—	—	x	x	—	—	—	—	—	206
[C(NH ₂) ₃] ₂ [Bi(dtpa)(H ₂ O) ₄]	x	—	x	—	—	—	—	—	—	203
KBi(Hdtpa)(H ₂ O) ₅	x	—	—	—	—	—	—	—	—	222
[C(NH ₂) ₃] ₂ [Bi(cydtpa)]	x	82	x	—	—	x	—	—	—	221
Bi(H ₄ ttha)(H ₂ O) ₃	x	—	x	x	—	—	—	—	—	220
[C(NH ₂) ₃] ₂ [Bi(Httha)(H ₂ O) ₄]	x	—	x	—	—	—	—	—	—	223

The water solubility of the complexes generally increases with the number of carboxylate groups on the ligand, thereby facilitating crystal growth, and many derivatives have been crystallographically characterized as indicated in Table XV.

Preparative procedures usually involve mixtures of Bi₂O₃, Bi(OH)₃, or (BiO)₂CO₃ with the appropriate ligand set to reflux in water. The neutral hydrated [e.g., Bi(Hedta)(H₂O)₂ (203), Bi(nta)(H₂O)₂ (203), Bi(nta)(H₂O)₃ (204)] (205, 206) and nonhydrated [e.g., Bi(Hedta)] (207) complexes are reportedly synthesized by analogous reactions involving bismuth subcarbonate and bismuth hydroxide, respectively. Addition of a strong base, such as guanidinium carbonate or an alkali hydroxide, to the reaction mixture effects deprotonation of carboxylic acid moieties, thereby increasing the formal charge on the aminocarboxylate ligand above 3. The large covalent radius of bismuth (1.52 Å) allows for maximum chelation by the aminocarboxylate ligand, currently observed up to decadenticity. For complexes with ligands

of relatively low denticity, additional coordination sites are typically occupied by oxygen atoms of water molecules or exocyclic carboxylate groups of neighboring molecules, creating dimers or polymeric arrays.

Dimeric structures are observed for the tetradentate complexes $\text{Bi}(\text{pdc})(\text{Hpdc})(\text{dmsO})$ [Bi—O 2.209(8)–2.507(6); Bi—N 2.418(9) and 2.481(9) Å; Bi---O 2.578(4) Å] (208), $\text{Bi}(\text{onda})(\text{H}_2\text{O})_2$ [Bi—N 2.49(2); Bi—O_{carboxylate} 2.33(1) and 2.34(1); Bi—O_{alkoxide} 2.14(1) Å], $\text{dimer}[\text{Bi}(\text{---O}) 2.46(1) \text{ Å}]$ (209), and $\text{Bi}(\text{nta})(\text{H}_2\text{O})_2$ [Bi—N 2.500(8); Bi—O_{carboxylate} 2.258(6)–2.253(7) Å; Bi---O 2.665(6) and 2.435(6) Å] (203), where high coordination numbers are achieved by auxiliary ligands as with the ionic complexes involving tetradentate ligands. $[\text{NH}_4][\text{Bi}(\text{Honda})_2(\text{H}_2\text{O})_3]$ (210), $[\text{C}(\text{NH}_2)_3]_2[\text{Bi}(\text{onda})(\text{Honda})(\text{H}_2\text{O})_3]$ (210), $[\text{NH}_4]_3[\text{Bi}(\text{nta})_2]$ [Bi—N 2.58(1) and 2.60(2); Bi—O 2.44(1) and Bi—O 2.40(1) Å] (211), and $[\text{NH}_4]_4[\text{Bi}(\text{nta})_2(\text{NCS})(\text{H}_2\text{O})]$ [Bi—O 2.363(4)–2.551(5); Bi—N 2.605(4) Å] (205).

Hexadenticity is observed in all crystallographically characterized bismuth complexes involving conjugate bases of H_4edta , which have been most extensively characterized (214, 217, 218, 224, 224–226). Examples include both hydrated (214, 224, 225, 227, 228) and nonhydrated (229, 224, 227) $\text{Bi}(\text{Hedta})$, as well as the Na (206, 219, 228) K (227), NH_4 (207, 227), Mg (230), Ca (217, 230), Sr, Ba, Ni, Zn, Cd (230), Co (218, 230), Cu (226), and Mo (218) salts of the $[\text{Bi}(\text{edta})]^-$ anion, and the potassium fluoride adduct $\text{K}_2[\text{Bi}(\text{edta})\text{F}] \cdot 3\text{H}_2\text{O}$ (227). $\text{Bi}(\text{Hedta})(\text{H}_2\text{O})_2$ (213) [Bi—N 2.396(10) and 2.577(9); Bi—O 2.295(7)–2.700(10) Å; Bi---O 2.678(7)–2.697(8) Å] is dimeric (214), whereas the dehydrated analogue $\text{Bi}(\text{Hedta})$ (207) [Bi—N 2.465(5); Bi—O 2.399(3)–2.472(4) Å; Bi---O 2.617(5) Å] adopts a one-dimensional polymeric structure. The thiourea ligands in $\text{Bi}(\text{Hendta})(\text{tu})_2$ [Bi—S 3.035(4) Å; Bi—N 2.510(7); Bi—O 2.378(7) and 2.521(9) Å] prevent intermolecular coordinations and result in a monomeric structure (215). A number of ionic complexes are well established, including $[\text{C}(\text{NH}_2)_3][\text{Bi}(\text{edta})(\text{H}_2\text{O})]$ [Bi—N 2.56(1) and 2.59(2); Bi—O 2.34(1)–2.46(1) Å; Bi---O 2.70(1) Å] (216), $[\text{Ca}(\text{H}_2\text{O})_7][\text{Bi}(\text{edta})]_2 \cdot 2\text{H}_2\text{O}$ [Bi—N 2.460(6) and 2.543(6); Bi—O 2.360(6)–2.463(7) Å; Bi---O 2.778(6) and 3.038(7) Å] (217), $[\text{Co}(\text{H}_2\text{O})_6][\text{Bi}(\text{edta})]_2 \cdot 3\text{H}_2\text{O}$ (218), $[\text{Ni}(\text{H}_2\text{O})_6][\text{Bi}(\text{edta})]_2 \cdot 3\text{H}_2\text{O}$ (218), $[\text{NaBi}(\text{edta})(\text{H}_2\text{O})_3]$ [Bi—N 2.495(5) and 2.508(5); Bi—O 2.315(4)–2.521(4); Bi---O 2.636(4) and 2.850(7) Å] (219), and $[\text{NH}_4][\text{Bi}(\text{edta})(\text{H}_2\text{O})]$ [Bi—N 2.479(9) and 2.490(10); Bi—O 2.290(9)–2.494(8); Bi---O 2.792(9) and 2.805(8) Å] (207). $\text{Bi}(\text{Hcydta})(\text{H}_2\text{O})_5$ is analogous to the parent edta complex [Bi—N 2.491(11)–2.513(10); Bi—O 2.286(9)–2.497(11) Å; Bi---O 2.612(9)–2.916(10) Å] (220).

Higher denticities include the heptadentate complex $\text{Bi}(\text{H}_2\text{dtpa})(\text{H}_2\text{O})_2$ (221) [Bi–N 2.449(4)–2.723(4) Å; Bi–O 2.290(3)–2.699(3) Å; Bi---O 2.620(3) Å] (206), the octadentate complexes $[\text{C}(\text{NH}_2)_3]_2[\text{Bi}(\text{dtpa})(\text{H}_2\text{O})_4]$ [Bi–N 2.536(7)–2.639(6); Bi–O 2.368(5)–2.599(5) Å; Bi---O 2.686(6) Å] (203), $\text{KBi}(\text{Hdtpa})(\text{H}_2\text{O})_5$ (222), and $[\text{C}(\text{NH}_2)_3]_2[\text{Bi}(\text{cydtpa})]$ [Bi–N 2.458(5)–2.592(5); Bi–O 2.371(4)–2.610(4) Å] (221), and the decadentate complex $\text{Bi}(\text{H}_3\text{ttha})(\text{H}_2\text{O})_3$ [Bi–N 2.472(8)–2.813(8); Bi–O 2.320(7)–3.055(8) Å] (220), which represents the highest denticity currently observed for bismuth. This distorted bicapped square antiprismatic environment has the external nitrogen atoms (N^1 and N^4) in capping positions. Interestingly, the pentanionic ligand in the bis(guanidinium) salt $[\text{C}(\text{NH}_2)_3]_2[\text{Bi}(\text{Httha})(\text{H}_2\text{O})_4]$ is only non-adentate [Bi–N 2.619(7)–2.688(7); Bi–O 2.327(6)–2.560(6) Å] (223).

G. HYDROXYAMINES AND AMINOALKOXIDES

Many of the multidentate features observed for aminocarboxylate complexes of bismuth are evident in a small, diverse group of complexes involving hydroxyamine and aminoalkoxides ligands (Table XVI). Most of the examples in this section may be considered unique and represent unusual structural arrangements.

The complexes can be classified into two general types. Those involving neutral hydroxy and amine donor sites include complexes of Bi^{3+} with the multidentate, formally neutral ligands cyclenOH and

TABLE XVI

ANALYTICAL DATA FOR BISMUTH HYDROXYAMINE COMPLEXES

Empirical formula	X-ray	Yield (%)	mp	ea	ir	nmr	ms	tga	Ref.
$\text{Bi}(\text{cyclenOH})(\text{ClO}_4)_3(\text{H}_2\text{O})$	x	—	—	x	—	—	—	—	231
$\text{Bi}_3(\text{H}_5\text{taci})_2(\text{NO}_3)_3(\text{CH}_3\text{OH})_{0.5}$	—	97	—	x	x	x	x	—	232
$\text{Bi}_3(\text{H}_5\text{taci})_2\text{Cl}_3(\text{H}_2\text{O})_4$	x	65	—	x	x	x	x	—	232
$\text{Bi}(\text{bta})_3$	x	>90	x	x	—	x	—	—	233
BiCl_3cfh	x	—	—	x	x	—	—	—	234
$\text{Bi}(\text{Hdapt})\text{Cl}_2(\text{dmso})(\text{H}_2\text{O})$	x	~80	—	x	x	—	—	—	235
$\text{Bi}(\text{dapt})\text{Cl}(\text{dmso})$	x	~80	—	x	x	—	—	—	235
$\text{Bi}(\text{Hdapt})\text{X}_2(\text{dmso})$ X = Br, I, NCS	—	—	—	x	x	—	—	—	235
$\text{Bi}(\text{dapt})\text{N}_3(\text{dmso})$	—	—	—	x	x	—	—	—	235
$\text{Bi}(\text{dapt})(\text{OH})(\text{dmso})(\text{H}_2\text{O})$	x	—	—	x	x	—	—	—	193
$\text{Bi}(\text{saltren})$	x	88	—	x	—	—	—	—	236
$\text{Bi}(\text{O}_2\text{CCH}_3)_2(\text{bdmap})(\text{H}_2\text{O})_{0.5}$	x	52	—	x	—	x	—	x	237
$\text{Bi}(\text{Hdpmd})(\text{O}_2\text{CCF}_3)_2(\text{thf})$	x	46	x	x	x	x	—	x	238

taci. $\text{Bi}(\text{cyclenOH})(\text{ClO}_4)_3(\text{H}_2\text{O})$ was isolated from the reaction of Bi_2O_3 in 70% HClO_4 (231) and contains eight-coordinate bismuth interacting with all oxygen and nitrogen atoms of the ligand [Bi–N 2.51–2.544; Bi–O 2.533–2.588 Å]. The hydroxy groups lie on one side of the macrocycle, which is in a “boat”-type conformation, so that the ligand “cradles” the bismuth atom. A weakly bound perchlorate anion coordinates the bismuth center on the opposite side from the macrocyclic ligand [Bi–O 3.34(1) Å]. Bismuth nitrate reacts with taci to give a compound with the empirical formula $\text{Bi}_3(\text{H}_3\text{taci})_2(\text{NO}_3)_3(\text{CH}_3\text{OH})_{0.5}$. The chloride analogue $\text{Bi}_3(\text{H}_3\text{taci})_2\text{Cl}_3(\text{H}_2\text{O})_4$ was obtained from the nitrate by ion exchange (232) and the solid-state structure involves three crystallographically equivalent bismuth atoms sandwiched between two taci ligands in a distorted D_{3h} cluster. The eight-coordinate environment of bismuth is composed of four oxygen atoms [Bi–O 2.28(2)–2.40(1) Å], two nitrogen atoms [Bi–N 2.43(2)–2.71(1) Å], and two weakly bound μ_2 -chlorine atoms [Bi–Cl 3.000(3)–3.002(3) Å], which bridge two Bi atoms of separate adjacent cations.

Complexes involving alkoxide and amine donor sites are slightly more numerous. The trialkoxide chelate complex $\text{Bi}(\text{saltren})$ is formed in the reaction of the sodium saltren (generated *in situ*) with 1 equiv of BiCl_3 in methanol (236). The four amine centers supplement the oxygen donors so that the single ligand accounts for a heptadentate environment for bismuth [Bi–N 2.512(8)–2.82(1); Bi–O 2.197(8)–2.300(8) Å]. $\text{Bi}(\text{bta})_3$ represents the only homoleptic trisalkoxide in this classification and is formed in an unusual redox metathesis reaction between bismuth chloride and Hbta in the presence of triethylamine (233). The tridentate nature of the ligand imposes a D_3 symmetry propeller arrangement and a nine-coordinate environment composed of three alkoxides, three imines, and three ketone donors.

The conjugate bases of the unusual bis(theonylhydrazone) H_2dapt forms complexes in which the anionic ligand can be considered either an amide or an alkoxide. Structural studies on a series of complexes reveal a consistent planar interaction of pentadentate ligand with bismuth in which the ligand occupies the equatorial sites of a pentagonal pyramid or pentagonal bipyramid (235). The apical sites are occupied by chlorine atoms or oxygen atoms of dmsO. The hydroxide complex $\text{Bi}(\text{dapt})(\text{OH})(\text{dmsO})(\text{H}_2\text{O})$ is obtained from the reaction of BiCl_3 with a stoichiometric amount of H_2dapt in acetone, followed by the reaction with excess imidazole in dmsO and water (193).

Alkoxide bridged dimers are observed for $\text{Bi}(\text{O}_2\text{CCH}_3)_2(\text{bdmap})(\text{H}_2\text{O})_{0.5}$ (237) and $\text{Bi}_2(\text{Hdpmd})_2(\text{O}_2\text{CCF}_3)_4(\text{thf})_2$ (238). The stability of the compounds is accredited to the coordinative saturation of bismuth

imposed by the dimeric structure and the crystal lattice packing forces. The ligand engages bismuth in a tridentate fashion via the two pyridyl nitrogen centers and an alkoxide, which bridges the bismuth centers [Bi–N 2.43(2) and 2.44(2); Bi–O 2.20(1) Å]. The eight-coordinate environment of bismuth additionally consists of a thf molecule [Bi–O 2.53(2) Å], two oxygen atoms from a chelating trifluoroacetate ligand [Bi–O 2.50(2) and 2.88(2) Å], and a single oxygen atom from a monodentate trifluoroacetate group [Bi–O 2.48(2) Å]. NMR studies suggest that the complex retains its dinuclear structure in solution.

IX. Conclusions

A diverse coordination chemistry is emerging for bismuth(III) made possible by a spacious and flexible coordination environment, allowing for coordination numbers in excess of 9. Although the available data are still limited, distinct trends are evident, and the polymeric solid-state features that may be assumed on the basis of high coordination numbers can be mediated by appropriate selection of organic-based ligands. The unusual structural arrangements observed for many types of complex may prove to be representative as the number of examples of such systems increases.

ACKNOWLEDGMENTS

We thank the Natural Sciences and Engineering Research Council of Canada and the Killam Foundation for funding (NB), Sciex Canada and the Walter G. Sumner Foundation for scholarships (GGB), Dr. L. Agocs for initial contributions to the literature collection, and T. D. Lawen and A. M. House for assistance with literature management.

REFERENCES

1. Baxter, G. F. *Pharm. J.* **1989**, 243, 805–810.
2. Baxter, G. F. *Chem. Br.* **1992**, 445–448.
3. Sun, H.; Li, H.; Sadler, P. J. *Chem. Ber. / Recueil.* **1997**, 130, 669–681; Sadler, P. J.; Li, H.; Sun, H. *Coord. Chem. Rev.* **1999**, 185–186, 689–709; Guo, Z.; Sadler, P. J. *Angew. Chem., Int. Ed. Engl.* **1999**, 38, 1512–1531.
4. Briand, G. G.; Burford, N. *Chem. Rev.* **1999**, 99, 2601–2657.
5. Subramanian, M. A. *Ceram. Trans.* **1990**, 13(Supercond. Ceram. Supercond.), 59–76. (*Chem. Abs.* **1991**, 114, 33648t).

6. Gopalakrishnan, J. *Chem. High Temp. Supercond.* **1991**, 156–185 (*Chem. Abs.* **1992**, 117, 182316x).
7. Norman, N. C.; Pickett, N. L. *Coord. Chem. Rev.* **1995**, 145, 27–54.
8. McAuliffe, C. A.; Mackie, A. G. *Chem. Org. Arsenic, Antimony Bismuth Compd.* **1994**, 1994, 527–562 (*Chem. Abs.* **1994**, 121, 179654h).
9. Reglinski, J. "Chemistry of Arsenic, Antimony, and Bismuth;" Norman, N. C., Ed.; Blackie Academic & Professional: London, 1998; pp. 403–440.
10. Dittes, U.; Vogel, E.; Keppler, B. K. *Coord. Chem. Rev.* **1997**, 163, 345–364.
11. Freedman, L. D.; Doak, G. O. *Chem. Rev.* **1982**, 82, 15–57.
12. Doak, G. O.; Freedman, L. D. *J. Organomet. Chem.* **1995**, 485, 1–9.
13. Doak, G. O.; Freedman, L. D. *J. Organomet. Chem.* **1994**, 477, 31–44.
14. Doak, G. O.; Freedman, L. D. *J. Organomet. Chem.* **1995**, 496, 1–17.
15. Mehrotra, R. C.; Rai, A. K. *Ind. J. Chem.* **1966**, 4, 537.
16. Wieber, M.; Baudis, U. Z. *Anorg. Allg. Chem.* **1976**, 423, 47–52.
17. Veith, M.; Yu, E.-C.; Huch, V. *Chem. Eur. J.* **1995**, 1, 26–32.
18. Haaland, A.; Verne, H. P.; Volden, H. V.; Papiernik, R.; Hubert-Pfalzgraf, L. G. *Acta Chem. Scand.* **1993**, 47, 1043–1045.
19. Massiani, M.-C.; Papiernik, R.; Hubert-Pfalzgraf, L. G.; Daran, J.-C. *J. Chem. Soc., Chem. Commun.* **1990**, 301–302.
20. Massiani, M.-C.; Papiernik, R.; Hubert-Pfalzgraf, L. G. *Polyhedron.* **1991**, 10, 437–445.
21. Matchett, M. A.; Chiang, M. Y.; Buhro, W. E. *Inorg. Chem.* **1990**, 29, 358–360.
22. Evans, W. J.; Hain, J. H., Jr.; Ziller, J. W. *J. Chem. Soc., Chem. Commun.* **1989**, 1628–1629.
23. Canich, J. M.; Gard, G. L.; Shreeve, J. M. *Inorg. Chem.* **1984**, 23, 441–444.
24. Jones, C. M.; Burkart, M. D.; Whitmire, K. H. *Angew. Chem., Int. Ed. Engl.* **1992**, 31, 451–452.
25. Jones, C. M.; Burkart, M. D.; Whitmore, K. H. *J. Chem. Soc., Chem. Commun.* **1992**, 1638–1639.
26. Jolas, J. L.; Hoppe, S.; Whitmire, K. H. *Inorg. Chem.* **1997**, 36, 3335–3340.
27. James, S. C.; Norman, N. C.; Orpen, A. G.; Quayle, M. J.; Weckenmann, U. *J. Chem. Soc., Dalton Trans.* **1996**, 4159–4161.
28. Hodge, P.; James S. C.; Norman, N. C.; Orpen, A. G. *J. Chem. Soc., Dalton Trans.* **1998**, 4049–4054.
29. Cloutt, B. A.; Sagatys, D. S.; Smith, G.; Bott, R. C. *Aust. J. Chem.* **1997**, 50, 947–950.
30. Smith, G.; Reddy, A. N.; Byriel, K. A.; Kennard, C. H. L. *Aust. J. Chem.* **1994**, 47, 1413–1418.
31. Jones, C. M.; Burkart, M. D.; Bachman, R. E.; Serra, D. L.; Hwu, S.-J.; Whitmore, K. H. *Inorg. Chem.* **1993**, 32, 5136–5144.
32. Lippert, A.; Reid, E. E. *J. Am. Chem. Soc.* **1938**, 60, 2370–2371.
33. Janzen, A. F.; Vaidya, O. C. *J. Inorg. Nucl. Chem.* **1981**, 43, 1469–1471.
34. Boudjouk, P.; Remington, M. P., Jr.; Grier, D. G.; Jarabek, B. R.; McCarthy, G. J. *Inorg. Chem.* **1998**, 37, 3538–3541.
35. Peach, M. E. *J. Inorg. Nucl. Chem.* **1979**, 41, 1390–1392.
36. Farrugia, L. J.; Lawlor, F. J.; Norman, N. C. *Polyhedron* **1995**, 14, 311–314.
37. Clegg, W.; Elsegood, M. R. J.; Farrugia, L. J.; Lawlor, F. J.; Norman, N. C.; Scott, A. J. *J. Chem. Soc., Dalton Trans.* **1995**, 2129–2135.
38. Bochmann, M.; Song, X.; Hursthouse, M. B.; Karaulov, A. *J. Chem. Soc., Dalton Trans.* **1995**, 1649–1652.

39. Atwood, D. A.; Cowley, A. H.; Hernandez, R. D.; Jones, R. A.; Rand, L. L.; Bott, S. G.; Atwood, J. L. *Inorg. Chem.* **1993**, *32*, 2972–2974.
40. Hergett, S. C.; Peach, M. E. *J. Fluor. Chem.* **1988**, *38*, 367–374.
41. Peach, M. E. *Can. J. Chem.* **1968**, *46*, 2699–2706.
42. Farrugia, L. J.; Lawlor, F. J.; Norman, N. C. *J. Chem. Soc., Dalton Trans.* **1995**, 1163–1171.
43. Ikram, M.; Powell, D. B. *Spectrochim. Acta* **1972**, *28A*, 59–64.
44. Agocs, L.; Burford, N.; Cameron, T. S.; Curtis, J. M.; Richardson, J. F.; Robertson, K. N.; Yhard, G. B. *J. Am. Chem. Soc.* **1996**, *118*, 3225–3232.
45. Powell, P. *J. Chem. Soc. (A)* **1968**, 2587–2588.
46. Engler, R. Z. *Anorg. Allg. Chem.* **1974**, *406*, 74–79.
47. Engler, R. Z. *Anorg. Allg. Chem.* **1974**, *407*, 35–39.
48. Hunter, G. *J. Chem. Soc., Dalton Trans.* **1972**, 1496–1498.
49. Hunter, G.; Weakley, T. J. R. *J. Chem. Soc., Dalton Trans.* **1983**, 1067–1070.
50. Donaldson, J. D.; Knifton, J. F.; Ross, S. D. *Spectrochim. Acta* **1964**, *20*, 847–851.
51. Antsyshkina, A. S.; Porai-Koshits, M. A.; Ostriкова, V. N. *Koord. Khim.* **1983**, *9*, 1118–1120 (*Chem Abs.* **1983**, *99*, 131610r).
52. Troyanov, S. I.; Pisarevskii, A. P. *Russ. J. Coord. Chem. (Transl. of Koord. Khim)* **1991**, *17*, 489–492.
53. Donaldson, J. D.; Knifton, J. F.; Ross, S. D. *Spectrochim. Acta* **1965**, *21*, 275–277.
54. Rigby, W. *Acta Chem. Scand.* **1998**, *1*, 1–2.
55. Bensch, W.; Blazsó, E.; Dubler, E.; Oswald, H. R. *Acta Cryst.* **1987**, *C43*, 1699–1704.
56. Pisarevskii, A. P.; Martynenko, L. I.; Dzyubenko, N. G. *Russ. J. Inorg. Chem. (Transl. of Zh. Neorg. Khim.)* **1990**, *35*, 843–846.
57. Troyanov, S. I.; Pisarevsky, A. P. *J. Chem. Soc., Chem. Commun.* **1993**, 335–336.
58. Rae, A. D.; Gainsford, G. J.; Kemmitt, T. *Acta Cryst.* **1998**, *B54*, 438–442.
59. Aurivillius, B. *Acta Chem. Scand.* **1955**, *9*, 1213–1218.
60. Radheshwar, P. V.; Dev, R.; Cady, G. H. *J. Inorg. Nucl. Chem.* **1972**, *34*, 3913–3915.
61. Garner, C. D.; Hughes, B. *Inorg. Chem.* **1975**, *14*, 1722–1724.
62. Reiss, G. J.; Frank, W.; Schneider, J. *Main Group Metal Chemistry.* **1995**, *18*, 287–294.
63. Breeze, S. R.; Chen, L.; Wang, S. *J. Chem. Soc., Dalton Trans.* **1994**, 2545–2557.
64. Stålhandske, C.-I. *Acta Chem. Scand.* **1969**, *23*, 1525–1533.
65. Coin, C.; Zevaco, T.; Dunach, E.; Postel, M. *Bull. Soc. Chim. Fr.* **1996**, *133*, 913–918.
66. Burnett, T. R.; Dean, P. A. W.; Vittal, J. J. *Can. J. Chem.* **1994**, *72*, 1127–1136.
67. Singh, P.; Singh, S.; Gupta, V. D.; Nöth, H. Z. *Naturforsch.* **1998**, *53b*, 1475–1482.
68. Bharadwaj, P. K.; Musker, W. K. *Inorg. Chem.* **1987**, *26*, 1453–1455.
69. Manoussakis, G. E.; Karayannidis, P. *Inorg. Nucl. Chem. Lett.* **1970**, *6*, 71–73.
70. Raston, C. L.; White, A. H. *J. Chem. Soc., Dalton Trans.* **1976**, 791–794.
71. Howard, J. A.; Russell, D. R.; Scutcher, W. *Acta Cryst.* **1975**, *A31*, S141.
72. Venkatachalam, V.; Ramalingam, K.; Casellato, U.; Graziani, R. *Polyhedron* **1997**, *16*, 1211–1221.
73. Battaglia, L. P.; Corradi, A. B. *J. Chem. Soc. Dalton Trans.* **1986**, 1513–1517.
74. Manoussakis, G. E.; Tsipis, C. A.; Hadjikostas, C. C. *Can. J. Chem.* **1975**, *53*, 1530–1535.
75. Raston, C. L.; Rowbottom, G. L.; White, A. H. *J. Chem. Soc. Dalton Trans.* **1981**, 1352–1359.

76. Tsipis, C. A.; Manoussakis, G. E. *Inorg. Chim. Acta.* **1976**, *18*, 35–45.
77. Manoussakis, G. E.; Lalia-Kantouri, M.; Huff, R. B. *J. Inorg. Nucl. Chem.* **1975**, *37*, 2330–2333.
78. Mandal, S.; Mandal, G. C.; Shukla, R.; Bharadwaj, P. K. *Ind. J. Chem.* **1992**, *31A*, 128–130.
79. Bharadwaj, P. K.; Lee, A. M.; Skelton, B. W.; Srinivasan, B. R.; White, A. H. *Aust. J. Chem.* **1994**, *47*, 405–410.
80. Shukla, R.; Bharadwaj, P. K. *Polyhedron* **1993**, *12*, 1079–1081.
81. Cras, J. A.; van de Leemput, P. J. H. A. M.; Willemse, J.; Bosman, W. P. *Rec. Trav. Chim.* **1977**, *96*, 78–80.
82. Raston, C. L.; Rowbottom, G. L.; White, A. H. *J. Chem. Soc., Dalton Trans.* **1981**, 1372–1378.
83. Raston, C. L.; Rowbottom, G. L.; White, A. H. *J. Chem. Soc., Dalton Trans.* **1981**, 1369–1371.
84. Hounslow, A. M.; Lincoln, S. F.; Tiekink, E. R. T. *J. Chem. Soc., Dalton Trans.* **1989**, 233–236.
85. Snow, M. R.; Tiekink, E. R. T. *Aust. J. Chem.* **1987**, *40*, 743–750.
86. Winter, G. *Aust. J. Chem.* **1976**, *29*, 559–563.
87. Tiekink, E. R. T. *Main Group Metal Chem.* **1994**, *17*, 727–736.
88. Hoskins, B. F.; Tiekink, E. R. T.; Winter, G. *Inorg. Chim. Acta* **1985**, *99*, 177–182.
89. Hoskins, B. F.; Tiekink, E. R. T.; Winter, G. *Inorg. Chim. Acta* **1984**, *81*, L33–L34.
90. Tiekink, E. R. T. *J. Cryst. Spec. Res.* **1992**, *22*, 231–236.
91. Gable, R. W.; Hoskins, B. F.; Steen, R. J.; Tiekink, E. R. T.; Winter, G. *Inorg. Chim. Acta* **1983**, *74*, 15–20.
92. Raston, C. L.; White, A. H.; Winter, G. *Aust. J. Chem.* **1978**, *31*, 2207–2212.
93. Kheiri, M.-N.; Tsipis, C. A.; Manoussakis, G. E. *Inorg. Chim. Acta* **1977**, *25*, 223–227.
94. Hoskins, B. F.; Tiekink, E. R. T.; Winter, G. *Inorg. Chim. Acta* **1985**, *105*, 171–176.
95. Raston, C. L.; Rowbottom, G. L.; White, A. H. *J. Chem. Soc., Dalton Trans.* **1981**, 1366–1368.
96. Pilipenko, A. T.; Mel'nikova, N. V.; Bankovskii, Yu. A. *Ukrainskii Khimicheskii Zhurnal* **1980**, *46*, 1311–1315.
97. Manoussakis, G. E.; Tsipis, C. A.; Christophides, A. G. *Inorg. Chem.* **1973**, *12*, 3015–3017.
98. Frank, W.; Reiss, G. J.; Schneider, J. *Angew. Chem., Int. Ed. Engl.* **1995**, *34*, 2416–2417.
99. Carmalt, C. J.; Clegg, W.; Elsegood, M. R. J.; Errington, R. J.; Havelock, J.; Lightfoot, P.; Norman, N. C.; Scott, A. J. *Inorg. Chem.* **1996**, *35*, 3709–3712.
100. Breunig, H. J.; Denker, M.; Schulz, R. E.; Lork, E. Z. *Anorg Allg. Chem.* **1998**, *624*, 81–84.
101. Rogers, R. D.; Bond, A. H.; Aguinaga, S. *J. Am. Chem. Soc.* **1992**, *114*, 2960–2967.
102. Rogers, R. D.; Bond, A. H.; Aguinaga, S.; Reyes, A. *J. Am. Chem. Soc.* **1992**, *114*, 2967–2977.
103. Alcock, N. W.; Ravindran, M.; Willey, G. R. *J. Chem. Soc., Chem. Commun.* **1989**, 1063–1065.
104. Drew, M. G. B.; Nickolson, D. G.; Sylte, I.; Vasudevan, A. *Inorg. Chim. Acta* **1990**, *171*, 11–15.
105. Schäfer, M.; Frenzen, G.; Neumüller, B.; Dehnicke, K. *Angew. Chem., Int. Ed. Engl.* **1992**, *31*, 334–335.

106. Garbe, R.; Vollmer, B.; Neumüller, B.; Pebler, J.; Dehnicke, K. *Z. Anorg. Allg. Chem.* **1993**, 619, 271–276.
107. Kelley, C. J.; McCusker, P. A. *J. Am. Chem. Soc.* **1943**, 65, 1307–1309.
108. Alcock, N. W.; Ravindran, M.; Willey, G. R. *Acta Cryst.* **1993**, B49, 507–514.
109. Willey, G. R.; Lakin, M. T.; Alcock, N. W. *J. Chem. Soc., Dalton Trans.* **1992**, 591–596.
110. Willey, G. R.; Lakin, M. T.; Alcock, N. W. *J. Chem. Soc., Dalton Trans.* **1992**, 1339–1341.
111. Blake, A. J.; Fenske, D.; Li, W.-S.; Lippolis, V.; Schroder, M. *J. Chem. Soc., Dalton Trans.* **1998**, 3961–3968.
112. Genge, A. R. J.; Levason, W.; Reid, G. *J. Chem. Soc., Chem. Commun.* **1998**, 2159–2160.
113. Clegg, W.; Norman, N. C.; Pickett, N. L. *Polyhedron*. **1993**, 12, 1251–1252.
114. Carmalt, C. J.; Farrugia, L. J.; Norman, N. C. *Z. Anorg. Allg. Chem.* **1995**, 621, 47–56.
115. Jameson, G. B.; Blazsó, E.; Oswald, H. R. *Acta Cryst.* **1984**, C40, 350–354.
116. Battaglia, L. P.; Corradi, A. B.; Pelizzi, G.; Tani, M. E. V. *J. Chem. Soc., Dalton Trans.* **1977**, 1141–1144.
117. Battaglia, L. P.; Corradi, A. B.; Pelizzi, G.; Tani, M. E. V. *Cryst. Struct. Comm.* **1975**, 4, 399–402.
118. Battaglia, L. P.; Corradi, A. B. *J. Chem. Soc., Dalton Trans.* **1981**, 23–26.
119. Battaglia, L. P.; Corradi, A. B. *J. Chem. Soc., Dalton Trans.* **1983**, 2425–2428.
120. Battaglia, L. P.; Corradi, A. B.; Pelosi, G. *J. Cryst. Spec. Res.* **1992**, 22, 275–279.
121. Praeckel, U.; Huber, F.; Preut, H. *Z. Anorg. Allg. Chem.* **1982**, 494, 67–77.
122. Battaglia, L. P.; Corradi, A. B. *J. Chem. Soc., Dalton Trans.* **1984**, 2401–2407.
123. Drew, M. G. B.; Kisenyi, J. M.; Willey, G. R.; Wandiga, S. O. *J. Chem. Soc., Dalton Trans.* **1984**, 1717–1721.
124. Drew, M. G. B.; Kisenyi, J. M.; Willey, G. R. *J. Chem. Soc., Dalton Trans.* **1984**, 1723–1726.
125. Reglinski, J.; Spicer, M. D.; Garner, M.; Kennedy, A. R. *J. Am. Chem. Soc.* **1999**, 121, 2317–2318.
126. Ando, F.; Hayashi, T.; Ohashi, K.; Koketsu, J. *J. Inorg. Nucl. Chem.* **1975**, 37, 2011–2013.
127. Clegg, W.; Compton, N. A.; Errington, R. J.; Fisher, G. A.; Green, M. E.; Hockless, D. C. R.; Norman, N. C. *Inorg. Chem.* **1991**, 30, 4680–4682.
128. Clegg, W.; Compton, N. A.; Errington, R. J.; Norman, N. C.; Wishar, N. *Polyhedron* **1989**, 8, 1579–1580.
129. Scherer, O. J.; Hornig, P.; Schmidt, M. *J. Organomet. Chem.* **1966**, 6, 259–264.
130. Gynane, M. J. S.; Hudson, A.; Lappert, M. F.; Power, P. P. *J. Chem. Soc., Dalton Trans.* **1980**, 2428–2433.
131. Burford, N.; Macdonald, C. L. B.; Robertson, K. N.; Cameron, T. S. *Inorg. Chem.* **1996**, 35, 4013–4016.
132. Wirringa, U.; Roesky, H. W.; Noltemeyer, M.; Schmidt, H.-G. *Inorg. Chem.* **1994**, 33, 4607–4608. See also [Bi₂(N^tBu)₄]₂Li₂, Edwards, A. J.; Beswick, M. A.; Galsworthy, J. R.; Paver, M. A.; Raithby, P. R.; Rennie, M.-A.; Russell, C. A.; Verhorevoort, K. L.; Wright, D. S. *Inorg. Chim. Acta* **1996**, 248, 9–14.
133. Veith, M.; Bertsch, B. *Z. Anorg. Allg. Chem.* **1988**, 557, 7–22.
134. Veith, M.; Bertsch, B.; Huch, V. *Z. Anorg. Allg. Chem.* **1988**, 559, 73–88.
135. Raston, C. L.; Rowbottom, G. L.; White, A. H. *J. Chem. Soc., Dalton Trans.* **1981**, 1379–1382.

136. Raston, C. L.; Rowbottom, G. L.; White, A. H. *J. Chem. Soc., Dalton Trans.* **1981**, 1389–1391.
137. Roper, W. R.; Wilkins, C. J. *Inorg. Chem.* **1964**, *3*, 500–502.
138. Bowmaker, G. A.; Hannaway, F. M. M.; Junk, P. C.; Lee, A. M.; Skelton, B. W.; White, A. H. *Aust. J. Chem.* **1988**, *51*, 325–330.
139. Bowmaker, G. A.; Harrowfield, J. M.; Lee, A. M.; Skelton, B. W.; White, A. H. *Aust. J. Chem.* **1998**, *51*, 311–315.
140. Bowmaker, G. A.; Hannaway, F. M. M.; Junk, P. C.; Lee, A. M.; Skelton, B. W.; White, A. H. *Aust. J. Chem.* **1998**, *51*, 331–336.
141. Barbour, L. J.; Belfield, S. J.; Junk, P. C.; Smith, M. K. *Aust. J. Chem.* **1998**, *51*, 337–342.
142. Raston, C. L.; Rowbottom, G. L.; White, A. H. *J. Chem. Soc., Dalton Trans.* **1981**, 1383–1388.
143. Bertazzi, N.; Alonzo, G.; Battaglia, L. P.; Corradi, A. B.; Pelosi, G. *J. Chem. Soc., Dalton Trans.* **1990**, 2403–2405.
144. Alonzo, G.; Consiglio, M.; Bertazzi, N.; Preti, C. *Inorg. Chim. Acta* **1985**, *105*, 51–57.
145. Bowmaker, G. A.; Junk, P. C.; Lee, A. M.; Skelton, B. W.; White, A. H. *Aust. J. Chem.* **1998**, *51*, 317–324.
146. Bertazzi, N.; Alonzo, G.; Consiglio, M. *Inorg. Chim. Acta* **1989**, *159*, 141–142.
147. Willey, G. R.; Daly, L. T.; Meehan, P. R.; Drew, M. G. B. *J. Chem. Soc., Dalton Trans.* **1996**, 4045–4053.
148. Willey, G. R.; Daly, L. T.; Rudd, M. D. *Polyhedron* **1995**, *14*, 315–318.
149. Luckay, R.; Cukrowski, I.; Mashishi, J.; Reibenspies, J. H.; Bond, A. H.; Rogers, R. D.; Hancock, R. D. *J. Chem. Soc., Dalton Trans.* **1997**, 901–908.
150. Ostendorp, G.; Homborg, H. Z. *Anorg. Allg. Chem.* **1996**, *622*, 873–880.
151. Hancock, R. D.; Cukrowski, I.; Antunes, I.; Cukrowska, E.; Mashishi, J.; Brown, K. *Polyhedron* **1995**, *14*, 1699–1707.
152. Hancock, R. D.; Cukrowski, I.; Baloyi, J.; Mashishi, J. *J. Chem. Soc., Dalton Trans.* **1993**, 2895–2899.
153. Bowmaker, G. A.; Junk, P. C.; Lee, A. M.; Skelton, B. W.; White, A. H. *Aust. J. Chem.* **1998**, *51*, 293–309.
154. Clegg, W.; Errington, R. J.; Flynn, R. J.; Green, M. E.; Hockless, D. C. R.; Norman, N. C.; Gibson, V. C.; Tavakkoli, K. *J. Chem. Soc., Dalton Trans.* **1992**, 1753–1754.
155. Clegg, W.; Elsegood, M. R. J.; Graham, V.; Norman, N. C.; Pickett, N. L.; Tavakkoli, K. *J. Chem. Soc., Dalton Trans.* **1994**, 1743–1751.
156. Clegg, W.; Errington, R. J.; Fisher, G. A.; Green, M. E.; Hockless, D. C. R.; Norman, N. C. *Chem. Ber.* **1991**, *124*, 2457–2459.
157. Clegg, W.; Elsegood, M. R. J.; Norman, N. C.; Pickett, N. L. *J. Chem. Soc., Dalton Trans.* **1994**, 1753–1757.
158. Willey, G. R.; Daly, L. T.; Drew, M. G. B. *J. Chem. Soc., Dalton Trans.* **1996**, 1063–1067.
159. Sutton, G. J. *Aust. J. Chem.* **1958**, *11*, 415–419.
160. Herrmann, W. A.; Herdtweck, E.; Scherer, W.; Kiprof, P.; Pajdla, L. *Chem. Ber.* **1993**, *126*, 51–56.
161. Sagatys, D. S.; O'Reilly, E. J.; Patel, S.; Bott, R. C.; Lynch, D. E.; Smith, G. S.; Kennard, H. L. *Aust. J. Chem.* **1992**, *45*, 1027–1034.
162. Kiprof, P.; Scherer, W.; Pajdla, L.; Herdtweck, E.; Herrmann, W. A. *Chem. Ber.* **1992**, *125*, 43–46. (*Chem. Abs.* **1992**, *116*, 98078t).

163. Asato, E.; Hol, C. M.; Hulsbergen, F. B.; Klooster, N. T. M.; Reedijk, J. *Inorg. Chim. Acta* **1993**, *214*, 159–167.
164. Barrie, P. J.; Djuran, M. J.; Mazid, M. A.; McPartlin, M.; Sadler, P. J. *J. Chem. Soc., Dalton Trans.* **1996**, 2417–2422.
165. *Merck Index* **1989**, *11*, 197.
166. *Merck Index* **1996**, 421.
167. Herrmann, W. A.; Herdtweck, E.; Pajdla, L. *Inorg. Chem.* **1991**, *30*, 2579–2581.
168. Asato, E.; Katsura, K.; Mikuriya, M.; Fujii, T.; Reedijk, J. *Inorg. Chem.* **1993**, *32*, 5322–5329.
169. Herrmann, W. A.; Herdtweck, E.; Pajdla, L. *Z. Krist.* **1992**, *198*, 257–264.
170. Asato, E.; Driessen, W. L.; de Graaff, R. A. G.; Hulsbergen, F. B.; Reedijk, J. *Inorg. Chem.* **1991**, *30*, 4210–4218.
171. Asato, E.; Katsura, K.; Mikuriya, M.; Turpeinen, U.; Mutikainen, I.; Reedijk, J. *Inorg. Chem.* **1995**, *34*, 2447–2454.
172. Asato, E.; Katsura, K.; Mikuriya, M.; Fujii, T.; Reedijk, J. *Chem. Lett.* **1992**, 1967–1970.
173. Burgess, J.; Fawcett, J.; Parsons, S. A.; Russell, D. R. *Acta Cryst.* **1994**, *C50*, 1911–1913.
174. Fukin, G. K.; Pisarevskii, A. P.; Yanovskii, A. I.; Struchkov, Yu. T. *Russ. J. Inorg. Chem. (Transl. of Zh. Neorg. Khim.)* **1993**, *38*, 1118–1123.
175. Parola, S.; Papiernik, R.; Hubert-Pfalzgraf, L. G.; Jagner, S.; Håkansson, M. *J. Chem. Soc., Dalton Trans.* **1997**, 4631–4635.
176. Muetterties, E. L.; Roesky, H.; Wright, C. M. *J. Am. Chem. Soc.* **1966**, *88*, 4856–4861.
177. Diemer, R.; Keppler, B. K.; Dittes, U.; Nuber, B.; Seifried, V.; Opferkuch, W. *Chem. Ber.* **1995**, *128*, 335–342.
178. Muetterties, E. L.; Wright, C. M. *J. Am. Chem. Soc.* **1965**, *87*, 21–24.
179. Muetterties, E. L.; Wright, C. M. *J. Am. Chem. Soc.* **1964**, *86*, 5132–5137.
180. Hulett, L. G.; Thornton, D. A. *J. Inorg. Nucl. Chem.* **1973**, *35*, 2661–2668.
181. Steiger, N. U.S. Pat. No. 2,490,717, 1949 (*Chem. Abs.* **1950**, *44*, 3526i).
182. Olszewski, E. J.; Albinak, M. J. *J. Inorg. Nucl. Chem.* **1965**, *27*, 1431–1433.
183. Charles, R. G.; Freiser, H. *J. Am. Chem. Soc.* **1952**, *74*, 1385–1387.
184. Alonzo, G. *Inorg. Chim. Acta* **1983**, *73*, 141–144.
185. Casassas, E.; Visa, T. *Polyhedron* **1986**, *5*, 1513–1518.
186. Block, E.; Ofori-Okai, G.; Kang, H.; Wu, J.; Zubieta, J. *Inorg. Chem.* **1991**, *30*, 4784–4788.
187. Silina, E.; Bankovsky, Yu.; Belsky, V.; Stass, A.; Asaks, J. *Latv. Khim. Zh.* **1996**, 57–62.
188. Niven, M. L.; Irving, H. M. N. H.; Nassimbeni, L. R. *Acta Cryst.* **1982**, *B38*, 2140–2145.
189. Briand, G. G.; Burford, N.; Cameron, T. S.; Kwiatkowski, W. *J. Am. Chem. Soc.* **1998**, *120*, 11374–11379.
190. Herrmann, W. A.; Kiprof, P.; Scherer, W.; Pajdla, L. *Chem. Ber.* **1992**, *125*, 2657–2660.
191. Berzinya, I. R.; Matyakhina, O. G.; Bel'skii, V. K.; Ashaks, Y. V.; Bankovskii, Y. A. *Latv. PSR Zinat. Akad. Vestis, Khim. Ser.* **1985**, 161–165.
192. Diemer, R.; Dittes, U.; Nuber, B.; Seifried, V.; Opferkuch, W.; Keppler, B. K. *Metal Based-Drugs* **1995**, *2*, 271–292.
193. Battaglia, L. P.; Corradi, A. B.; Pelizzi, C.; Pelosi, G.; Tarasconi, P. *J. Chem. Soc., Dalton Trans.* **1990**, 3857–3860.

194. Briand, G. G.; Burford, N.; Cameron, T. S. *J. Chem. Soc., Chem. Commun.* **1997**, 2365–2366.
195. Asato, E.; Kamamuta, K.; Akamine, Y.; Fukami, T.; Nukada, R.; Mikuriya, M.; Deguchi, S.; Yokota, Y. *Bull. Chem. Soc. Jpn.* **1997**, *70*, 639–648.
196. Wada, M.; Natsume, S.; Suzuki, S.; Uo, A.; Nakamura, M.; Hayase, S.; Erabi, T. *J. Organomet. Chem.* **1997**, *548*, 223–227.
197. Agocs, L.; Briand, G. G.; Burford, N.; Cameron, T. S.; Kwiatkowski, W.; Robertson, K. N. *Inorg. Chem.* **1997**, *36*, 2855–2860.
198. Jackson, G. E.; Hancock, R. D. *Polyhedron* **1984**, *3*, 71–73.
199. Mishra, A. K.; Gupta, V. D.; Linti, G.; Nöth, H. *Polyhedron* **1992**, *11*, 1219–1223.
200. Praeckel, U.; Huber, F. Z. *Naturforsch.* **1981**, *36b*, 70–73.
201. Asato, E.; Katsura, K.; Arakaki, M.; Mikuriya, M.; Kotera, T. *Chem. Lett.* **1994**, 2123–2126.
202. Herrmann, W. A.; Herdtweck, E.; Pajdla, L. *Chem. Ber.* **1993**, *126*, 895–898.
203. Summers, S. P.; Abboud, K. A.; Farrah, S. R.; Palenik, G. J. *Inorg. Chem.* **1994**, *33*, 88–92.
204. Rajablee, F. J. M. *Spectrochim. Acta.* **1974**, *30A*, 891–906.
205. Suyarov, K. D.; Shkol'nikova, L. M.; Davidovich, R. L.; Fundamenskii, V. S. *Russ. J. Coord. Chem. (Transl. of Koord. Khim)* **1991**, *17*, 242–248.
206. Iyer, R. K.; Shankar, J. *Ind. J. Chem.* **1972**, *10*, 97–99.
207. Shkol'nikova, L. M.; Suyarov, K. D.; Davidovich, R. L.; Fundamenskii, V. S.; Dyatlova, N. M. *Russ. J. Coord. Chem. (Transl. of Koord. Khim)*. **1991**, *17*, 126–132.
208. Zevaco, T.; Postel, M.; Benali-Cherif, N. *Main Group Metal Chemistry*. **1992**, *15*, 217–224.
209. Davidovich, R. L.; Shkol'nikova, L. M.; Huang, U.-Q.; Hu, S.-Z. *Russ. J. Coord. Chem. (Transl. of Koord. Khim)* **1996**, *22*, 858–862.
210. Khuan, Y.-T.; Khu, C.-D.; Shkol'nikova, L. M.; Davidovich, R. L. *Koord. Khim.* **1995**, *21*, 891.
211. Suyarov, K.D.; Shkol'nikova, L. M.; Porai-Koshits, M. A.; Fundamenskii, V. S.; Davidovich, R. L. *Dokl. Chem. (Trans. of Dokl. Akad. Nauk. SSSR)* **1990**, *311*, 93–95.
212. Bhat, T. R.; Iyer, R. K.; Shankar, J. Z. *Anorg. Allg. Chem.* **1996**, *343*, 329–336.
213. Shkol'nikova, L. M.; Porai-Koshits, M. A.; Davidovich, R. L.; Hu, C.-D.; Ksi, D.-K. *Russ. J. Coord. Chem. (Transl. of Koord. Khim)* **1994**, *20*, 559–562.
214. Summers, S. P.; Abboud, K. A.; Farrah, S. R.; Palenik, G. J. *Inorg. Chem.* **1994**, *33*, 88–92.
215. Shkol'nikova, L. M.; Porai-Koshits, M. A.; Davidovich, R. L.; Sadikov, G. G. *Koord. Khim.* **1993**, *19*, 633–636 (*Chem. Abs.* **1994**, *120*, 19819s).
216. Shchelokov, R. N.; Mikhailov, Yu. N.; Mistryukov, V. E.; Sergeev, A. V. *Dokl. Chem. (Trans. of Dokl. Akad. Nauk. SSSR)* **1987**, *293*, 162–164.
217. Shkol'nikova, L. M.; Porai-Koshits, M. A.; Poznyak, A. L. *Russ. J. Coord. Chem. (Transl. of Koord. Khim)* **1993**, *19*, 634–640.
218. Porai-Koshits, M. A.; Antsyshkina, A. S.; Shkol'nikova, L. M.; Sadikov, G. G.; Davidovich, R. L. *Russ. J. Coord. Chem. (Transl. of Koord. Khim)* **1995**, *21*, 295–302.
219. Jaud, J.; Marrot, B.; Brouca-Cabarrecq, C.; Mosset, A. *J. Chem. Cryst.* **1997**, *27*, 109–117.
220. Wullens, H.; Devillers, M.; Tinant, B.; Declercq, J.-P. *J. Chem. Soc., Dalton Trans.* **1996**, 2023–2029.

221. Brechbiel, M. W.; Gansow, O. A.; Pippin, C. G.; Rogers, R. D.; Planalp, R. P. *Inorg. Chem.* **1996**, *35*, 6343–6348.
222. Ilyukhin, A. B.; Shkol'nikova, L. M.; Davidovich, R. L.; Samosonova, I. N. *Russ. J. Coord. Chem. (Transl. of Koord. Khim)* **1991**, *17*, 484–489.
223. Wullens, H.; Devillers, M.; Tinant, B.; Declercq, J.P. *Acta Cryst.* **1998**, *C54*, 770–773.
224. Davidovich, R. L.; Logvinova, V. B.; Medkov, M. A.; Loginov, A. A.; Teplukhina, L. V.; Dyatlova, N. M. *Koord. Khim.* **1988**, *14*, 1511–1516 (*Chem. Abs.* **1989**, *110*, 87438k).
225. Bhat, T. R.; Iyer, R. K. *Z. Anorg. Allg. Chem.* **1965**, *335*, 331–336.
226. Sobanska, S.; Wingacourt, J.-P.; Conflant, P.; Drache, M.; Bulimestru, I.; Gulea, A. *Eur. J. Solid State Inorg. Chem.* **1996**, *33*, 701–712 (*Chem. Abs.* **1996**, *125*, No. 24, 315175q).
227. Zemnukhova, L. A.; Davidovich, R. L.; Rykovanov, V. N.; Dyatlova, N. M. *Izv. Akad. Nauk. SSSR, Ser. Khim.* **1989**, *1989*, 1915–1918 (*Chem. Abs.* **1989**, *111*, 246533b).
228. Iyer, R. K.; Shankar, J. *Indian J. Chem.* **1972**, *10*, 97–99.
229. Brintzinger, H.; Munkelt, S. *Z. Anorg. Chem.* **1948**, *256*, 65.
230. Loginov, A. A.; Medkov, M. A.; Karasev, V. E.; Davidovich, R. L. *Ukr. Khim. Zh. (Russ. Ed.)* **1989**, *55*, 1134–1138 (*Chem. Abs.* **1990**, *113*, 143957e).
231. Luckay, R.; Reibenspies, J. H.; Hancock, R. D. *J. Chem. Soc., Chem. Commun.* **1995**, 2365–2366.
232. Hegetschweiler, K.; Ghisletta, M.; Gramlick, V. *Inorg. Chem.* **1993**, *32*, 2699–2704.
233. Stewart, C. A.; Calabrese, J. C.; Arduengo, A. J. *J. Am. Chem. Soc.* **1985**, *107*, 3397–3398.
234. Kyriakidis, C. E.; Christidis, P. C.; Rentzeperis, P. J.; Tossidis, I. A.; Bolos, C. A. *Z. Krist.* **1990**, *193*, 101–110.
235. Battaglia, L. P.; Corradi, A. B.; Pelosi, G.; Tarasconi, P. *J. Chem. Soc., Dalton Trans.* **1989**, 671–675.
236. Bharadwaj, P. K.; Lee, A. M.; Mandal, S.; Skelton, B. W.; White, A. H. *Aust. J. Chem.* **1994**, *47*, 1799–1803.
237. Breeze, S. R.; Wang, S.; Thompson, L. K. *Inorg. Chim. Acta* **1996**, *250*, 163–171.
238. Breeze, S. R.; Wang, S.; Greedman, J. E.; Raju, N. P. *Inorg. Chem.* **1996**, *35*, 6944–6951.

PHANES BRIDGED BY GROUP 14 HEAVY ELEMENTS

HIDEKI SAKURAI

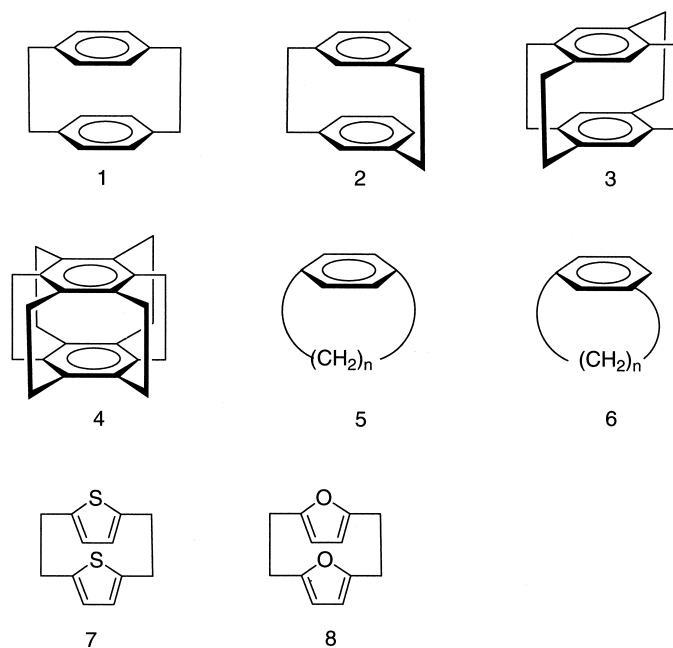
Department of Industrial Chemistry, Faculty of Science and Technology,
Science University of Tokyo, Noda, Chiba 278-8510, Japan

- I. Introduction
- II. An Introductory Case Study on 3,4,7,8-Tetrasilacycloocta-1,5-diyne
- III. [2.2]Cyclophanes
 - A. Octamethyltetrasila[2.2]paracyclophane, Metacyclophane, and Orthocyclophane
 - B. Octamethyltetragerma[2.2]paracyclophane
 - C. Tetrastanna[2.2]paracyclophane
 - D. Comparison of Structures of [2.2]Paracyclophanes Bridged by Group 14 Elements
 - E. Through-Space and Through-Bond interactions in [2.2]paracyclophanes Bridged by Group 14 Elements
- IV. Tetrasila[2.2](2,5)heterophanes
 - A. Octamethyl-1,2,8,9-tetrasila[2.2](2,5)furanophane and Thiophenophane
 - B. Tetrasila[2.2](2,5)pyrrolophane
 - C. NMR Studies and Molecular Structure
 - D. Reactions of Octamethyl-1,2,8,9-tetrasila[2.2](2,5)furanophane
- V. Hexasila[2.2.2](1,3,5)cyclophane
 - A. Preparation and Properties of 1,2,9,10,17,18-Hexasila[2.2.2](1,3,5)cyclophane
 - B. Molecular Structure of 1,2,9,10,17,18-Hexasila[2.2.2](1,3,5)cyclophane
- VI. [2ⁿ]Paracyclophanes Bridged by Si, Ge, and Sn
- VII. [n]Cyclophanes Bridged by Si
 - A. Heptasila[7]paracyclophane
 - B. Pentasila[5](2,5)thiophenophane and Hexasila[6](2,5)thiophenophane
- VIII. Conclusion
- References

I. Introduction

The chemistry of cyclophanes may be traced back to the work of Pellegrin on [2.2]metacyclophane in 1899 (1). Although the first

[2.2]paracyclophane was isolated by Brown and Farthing from the polymerization residue of *p*-xylene in 1949 (2), the chemistry of cyclophanes has been developed greatly by the direct synthesis of a series of paracyclophanes by Cram *et al.* (3). The name paracyclophane (1) originates from the work of Cram.



Subsequently, over more than four decades, numerous studies have been devoted to exploring this fascinating class of compound (4). In addition to metacyclophane (2), analogues with more than two bridges between rings such as 3 (5) are a part of the family. The limit is superphane (4) (6). Compounds with a single benzenoid skeleton as a part of a large cycle such as 5 and 6 are also synthesized (7). In a strict sense, the name of cyclophane should be limited to analogues with benzene ring(s), since phane comes from phenyl, but similar compounds with other aromatic ring(s) are also included to the family. In these cases, "cyclo" is replaced by the ring name to denote, for example, thiophenophane (7) and furanophane (8) (8). Phanes have been suggested as a general name for all such bridged aromatic com-

pounds (8). The phane family expanded its scope further to include non-benzenoid aromatic compounds.

Thus in the past decades, almost all types of phanes have been prepared and structures and reactions have been investigated in detail. One remaining interest in the chemistry is to replace the C–C bridge(s) of phanes with bonds of other elements, in particular of Group 14 heavy elements such as Si, Ge, and Sn.

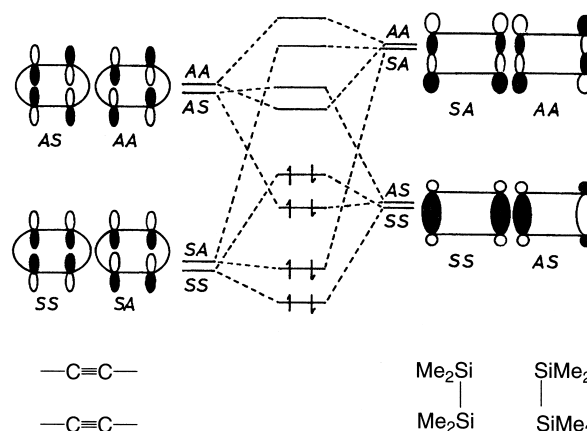
What is the interest associated with pursuing the chemistry of such compounds? First, the synthetic challenges to the compounds is obvious, because weaker M–M bonds ($M = \text{Si, Ge, Sn}$) than the C–C bond require special precautions for synthesis. In addition to this, physical properties due to the extensive mixing of σ – π orbitals are interesting. Higher σ -orbital energies of these element bonds such as Si–Si, Ge–Ge, and Sn–Sn should enable these bonds to mix with π -orbitals of aromatic rings to result in through-bond conjugation. Bond lengths that are longer than those of C–C bonds also create additional strains to phanes. In this chapter, the author tries to summarize the present status of the chemistry of phanes bridged by Group 14 heavy elements.

II. An Introductory Case Study on 3,4,7,8-Tetrasilacycloocta-1,5-diyne

Before going into a detailed account of the chemistry of phanes, the author will touch on 3,4,7,8-tetrasilacycloocta-1,5-diyne briefly, since the compound illustrates the importance of σ – π mixing. The ionization potential of the Si–Si bond is estimated by photoelectron spectroscopy to be 8.69 eV (9). Thus, the HOMO level of the Si–Si is comparable to most HOMOs of π systems. Consequently, the Si–Si bond can conjugate efficiently with carbon–carbon double and triple bonds, benzene rings, and other π systems. Most Si–Si bonds are stable enough to construct sophisticated structures by themselves and with organic molecules (10).

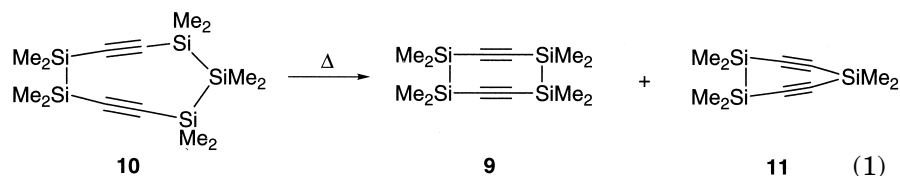
The first UV spectral evidence of the σ – π mixing between the Si–Si σ and the benzene π bonds was reported by three independent groups in 1964 (11). Since then, extensive σ – π mixing has been shown to occur between the Si–Si bond and various π systems in spectra and reactions (12).

In 1983, prior to the studies on phanes, the author tried to construct a new ring system, 3,4,7,8-tetrasilacycloocta-1,5-diyne, composed of two Si–Si σ and two $\text{C}\equiv\text{C}$ π bonds (13). As shown in the

FIG. 1. Qualitative MO diagram of **9**.

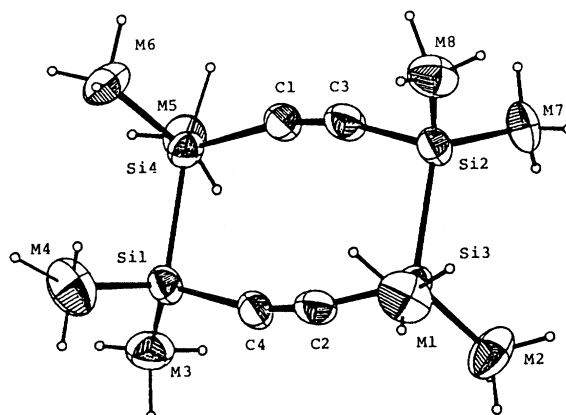
qualitative MO diagram (Fig. 1), two Si-Si σ orbitals can overlap with one of the two π orbitals of each $\text{C}\equiv\text{C}$ bond to make up new molecular orbitals with through-bond conjugation. This is a unique situation for the system since neither spatial nor through-bond interaction between two $\text{C}\equiv\text{C}$ bonds was observed for the corresponding cycloocta-1,5-diyne, the smallest known cyclic diyne (**14**).

3,3,4,4,7,7,8,8-Octamethyl-3,4,7,8-tetrasilacycloocta-1,5-diyne (**9**), prepared first by the ring contraction reaction of **10** together with a seven-membered compound (**11**), exhibited a large bathochromic shift in UV spectra at 250 nm ($\epsilon = 13,400$) compared with an open chain analogue, $\text{Me}_3\text{Si}-\text{C}\equiv\text{C}-\text{SiMe}_2\text{SiMe}_2-\text{C}\equiv\text{C}-\text{SiMe}_3$ ($\lambda_{\text{max}} = 230$ nm).



This is a good indication of strong mixing between Si-Si σ orbitals and $\text{C}\equiv\text{C}$ π orbitals with through-bond conjugation as expected. The molecular structure itself was not very much distorted, as evidenced by the X-ray crystallographic analysis shown in Fig. 2.

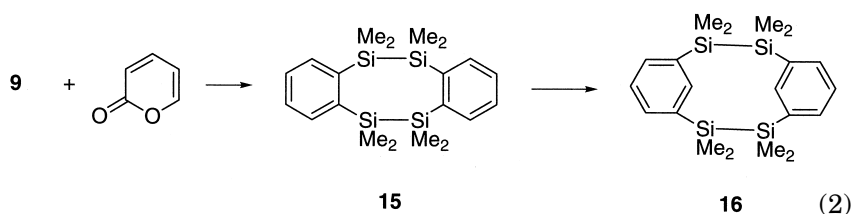
The through-bond conjugation with strong σ - π mixing for tetrasilacycloocta-1,5-diyne is further demonstrated by photoelectron spectroscopic (**15**) and *ab initio* (3-21G basis set) studies (**16**).

FIG. 2. ORTEP drawing of **9**.

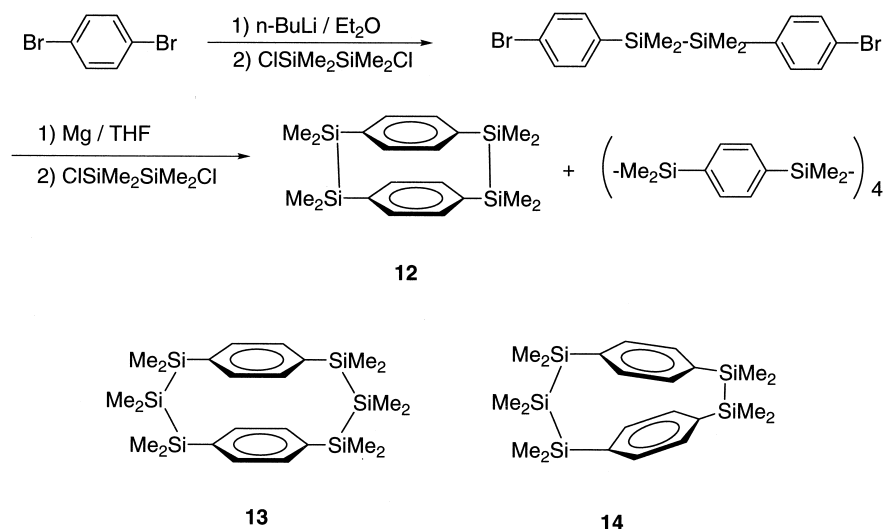
III. [2.2]Cyclophanes

A. OCTAMETHYLTETRASILA[2.2]PARACYCLOPHANE,
METACYCLOPHANE, AND ORTHOCYCLOPHANE

In view of the interesting physical properties of **9** described earlier, similar or even more interesting properties were expected for a [2.2]paracyclophane bridged by two Si_2Me_4 units. The target compound, 1,1,2,2,9,9,10,10-octamethyl-1,2,9,10-tetrasilal[2.2]paracyclophane (**12**), was prepared according to Scheme 1 in low yield (1.6%) (**17**). Related compounds **13** and **14** were also prepared. The reaction of **9** with α -pyrone gave **15**, and acid-catalyzed isomerization of **15** afforded **16** (**18**). The yield of **12** was very low, but in spite of several attempts, such as ring contraction reactions of **13** and **14** by photochemical silylene extrusion, **12** was obtained only by the direct process shown in Scheme 1.



Compound **12** is readily sublimed as colorless crystals. The crystal belongs to the space group $P2_1/n$, the molecular structure being

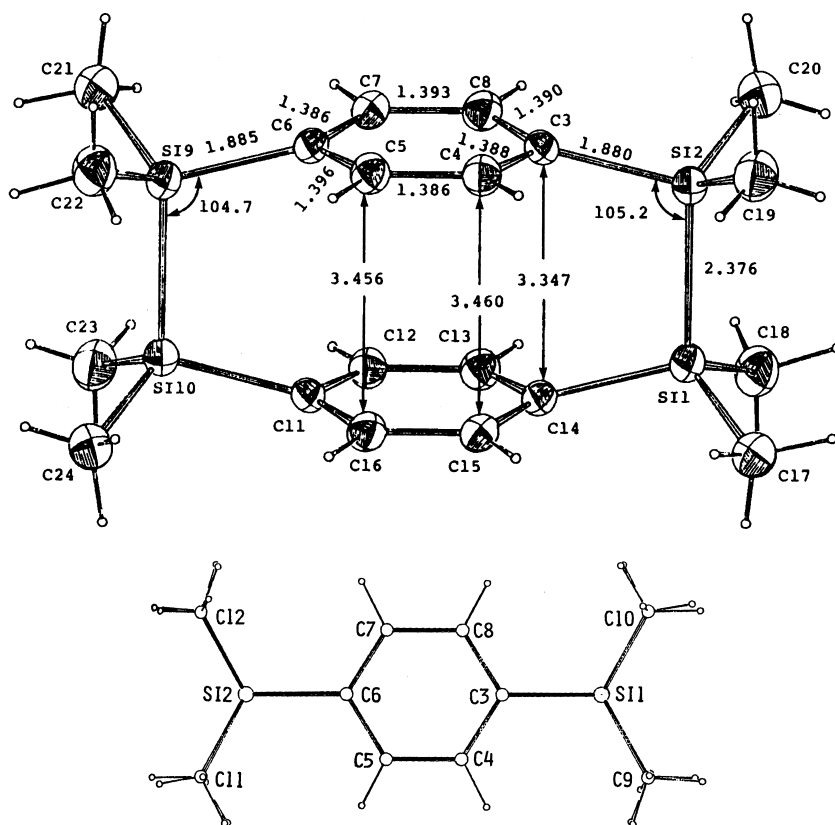


SCHEME 1

shown in Fig. 3. The compound **12** is highly symmetric with a center of symmetry. The Si–Si bond lengths of **12** (3.376 Å) deviate only slightly from the normal values (3.34 Å). The 3 and 6 (and 11 and 14) carbon atoms of the aromatic rings are displaced slightly out of the plane of the other four atoms inward. The degree of the displacement is 4.3, which is far smaller than that of the [2.2]paracyclophane (12.6°), indicating a smaller degree of distortion of the benzene rings of **12** than those of [2.2]paracyclophane (**19**). However, the silicon atoms of the bridges are displaced appreciably from the aromatic ring toward the cyclophane cavity. The degree of this displacement is 15.0°, larger than that of [2.2]paracyclophane (11.2°). The distances between aromatic rings, 3.347 Å for C3–C14 and 3.456–3.460 Å for C4–C15 and C5–C16, are close to that observed in graphite (3.40 Å) and longer than the mean intramolecular aromatic ring separation of [2.2]paracyclophanes around 3.00 Å. Two benzene rings and methyl groups eclipse completely.

Figure 4 compares the structures of tetrasila[2.2]paracyclophane **12**, [2.2]paracyclophane **1**, and [3.3]paracyclophane. Reflecting the longer Si–Si bond (2.376 Å) than the C–C bond (1.562 Å), distortion of the benzene ring in **12** (4.3°) is much less than that of **1** (12.6°), being close to the value for [3.3]paracyclophane (6.4°).

Because of the symmetric structure, ¹H NMR spectra of **12** show only two signals assignable to methyl and phenyl protons at δ 0.50

FIG. 3. Molecular structure of **12**.

and 6.75 ppm, respectively. The latter signal is shifted to the high field by 0.45 ppm from unsubstituted benzene. This is similar to **1** (δ 6.47 ppm) (**10**), but the degree of shift is smaller.

These structural data demonstrate that **12** is a rather less distorted molecule than [2.2]paracyclophane. However, a dramatic effect of the strong $\sigma(\text{Si-Si})-\pi$ interaction was observed in UV spectra as shown in Fig. 5. In the UV spectrum of phenylpentamethyldisilane, an intramolecular $\sigma(\text{Si-Si})-\pi$ charge-transfer band appears around 231 nm (**11a**, **12**). Octamethyltetrasil[2.2]ortho- (**15**) and metacyclophane (**16**) show similar absorptions, but the band splits into two bands at 223 nm ($\epsilon = 19,100$) and 263 nm ($\epsilon = 22,500$) in **12**. This type of red shift in the UV spectra occurs only in **12** among other polysilapara-cyclophanes such as **13** and **14**.

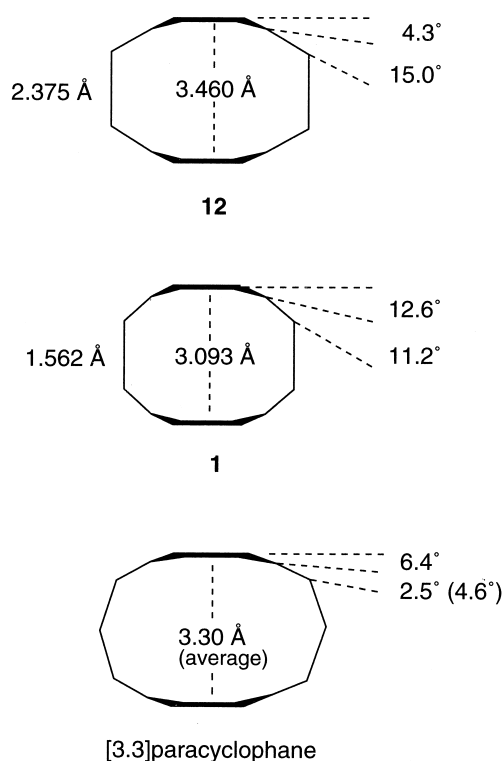
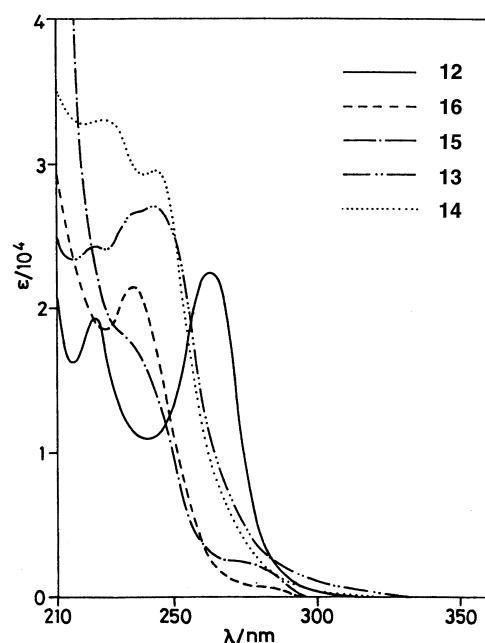


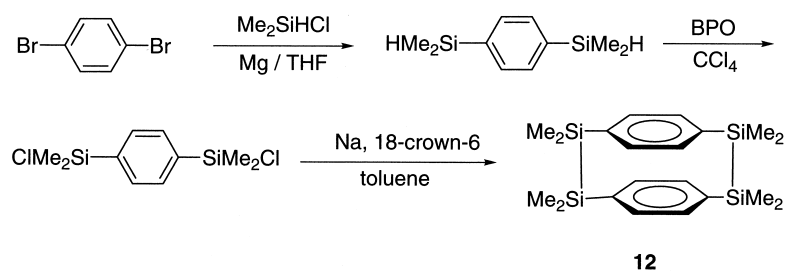
FIG. 4. Comparison of structures of paracyclophanes.

The photoelectron spectrum of **12** was observed and the measured ionization energies were compared with the orbital energies calculated for the parent tetrasil[2.2]paracyclophane (**21**). The He I photoelectron spectra of **1** was recorded to have a broad first band at 8.1 eV that was well separated from other bands (**22**). The first bands of **12** are remarkably different from those of **1**. A shoulder at 7.8 eV and a broad band centered at 8.3 eV was observed. A comparison between the band sequence of **12** and **1** based on both empirical and quantum chemical studies shows a smaller through-space and a larger through-bond interaction for **12**. The through-bond interaction between the b_{3u} (σ) orbital and the corresponding π orbital yielded a different orbital sequence in **12** as compared to **1** (Fig. 6).

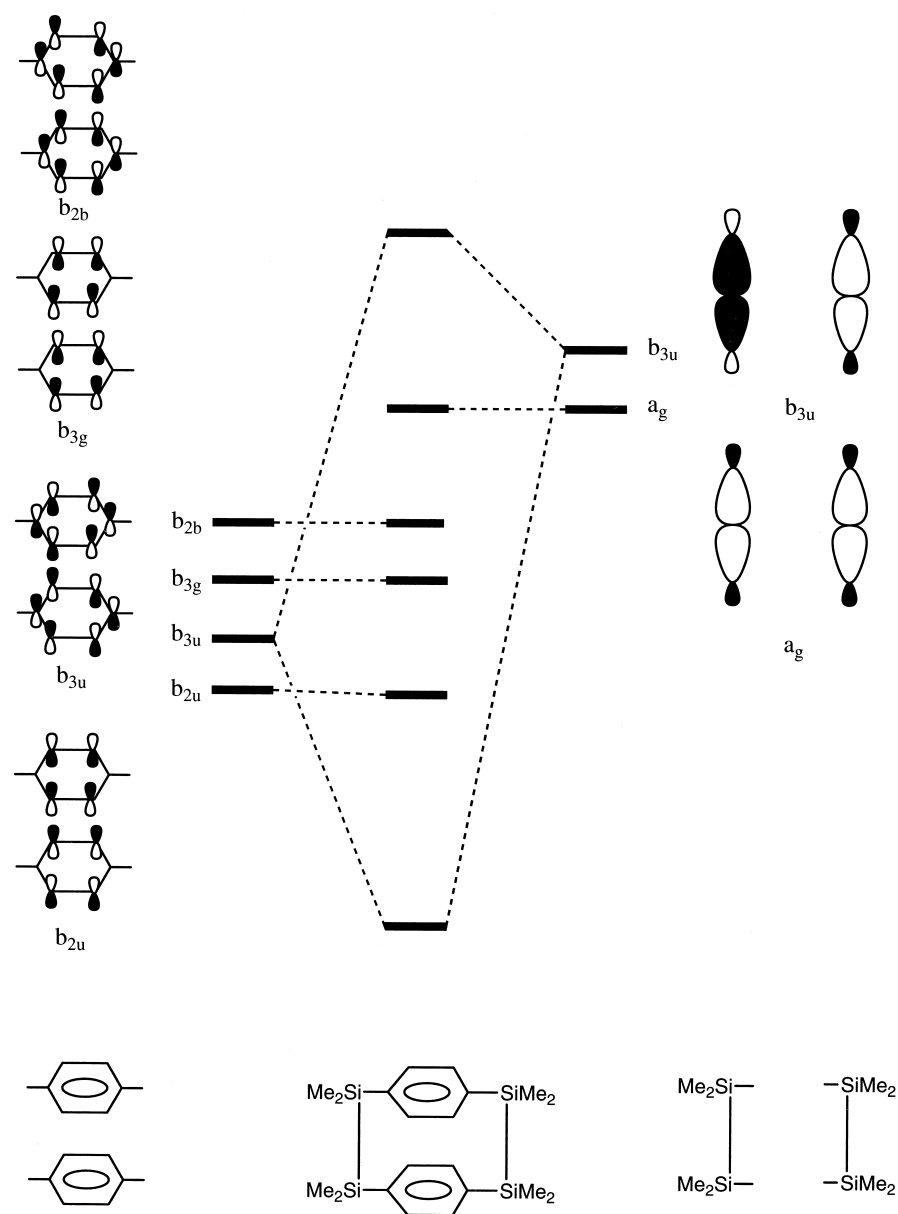
Yatabe has developed a slightly modified process for preparing **12** (**23**). Thus, the reductive coupling reaction of 1,4-bis(chlorodimethylsilyl)benzene with sodium in toluene in the presence of 18-crown-6 pro-

FIG. 5. UV spectra of **12** and related compounds.

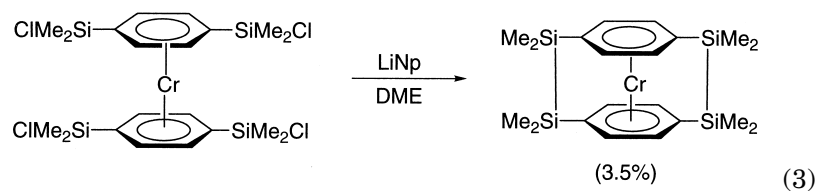
vided the cyclophane **12** (Scheme 2). After removal of the solvent and the resulting salt, silica gel chromatography with hexane followed by recrystallization from ethanol gave **12** in 2.2% yield as colorless crystals. The presence of 18-crown-6 is essential; otherwise the reaction resulted in the formation of intractable polymers. In fact, Ishikawa *et al.* (24) reported the polycondensation reaction of various 1,4-bis(chlorodialkylsilyl)benzenes with sodium in toluene in the absence of the crown ether. They did not succeed in the isolation of the corre-



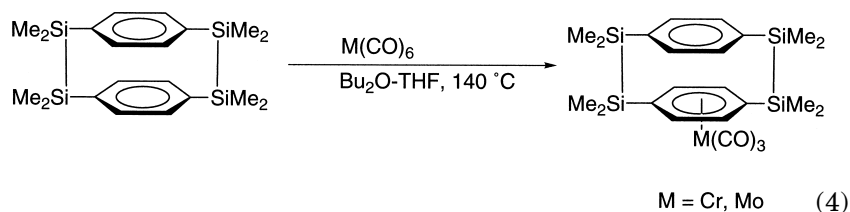
SCHEME 2

FIG. 6. Molecular orbital sequence for **12**.

sponding [2.2]paracyclophanes. The Wurtz-type coupling reaction is highly affected by the reactivity of the silyl anion. The crown ether would be expected to increase the reactivity of the silyl anions by forming a crown ether–sodium ion complex in the hydrocarbon solvent, resulting in an increase in the intramolecular reaction, although the net yields are still very low. In relation to this work, Elschenbroich reported that dechlorinative coupling of bis[bis(chlorodimethylsilyl)- η^6 -benzene]chromium with lithium naphthalenide in dimethoxyethane (DME) led to the formation of (1,2,9,10-tetrasilal- η^6 -[2.2]paracyclophane)chromium as red crystals in 3.5% yield (25).

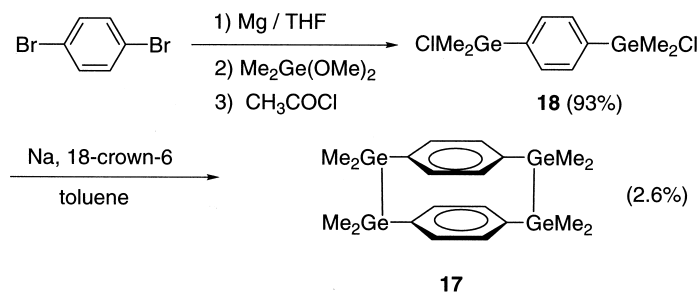


The reaction of **12** with $\text{Cr}(\text{CO})_6$ and $\text{Mo}(\text{CO})_6$ gave the corresponding monocoordinated complexes in 54 and 47% yields, respectively (26).



B. OCTAMETHYLTETRAGERMA[2.2]PARACYCLOPHANE

Although the one-pot process shown in Scheme 2 did not increase the yield of **12** dramatically, the process can be applied to the synthesis of a higher analogue of **12**, octamethyltetragerma[2.2]paracyclophane (**17**) (27). The precursor, 1,4-bis(chlorodimethylgermyl)benzene (**18**), was prepared according to Scheme 3. 1,2,9,10-Tetragerma[2.2]paracyclophane was synthesized in 2.6% yield as colorless crystals by reductive condensation of the chlorogermane **18** with molten sodium metal in refluxing toluene in the presence of 18-crown-6. After removal of the solvent and the resulting salt, silica gel chromatography



SCHEME 3

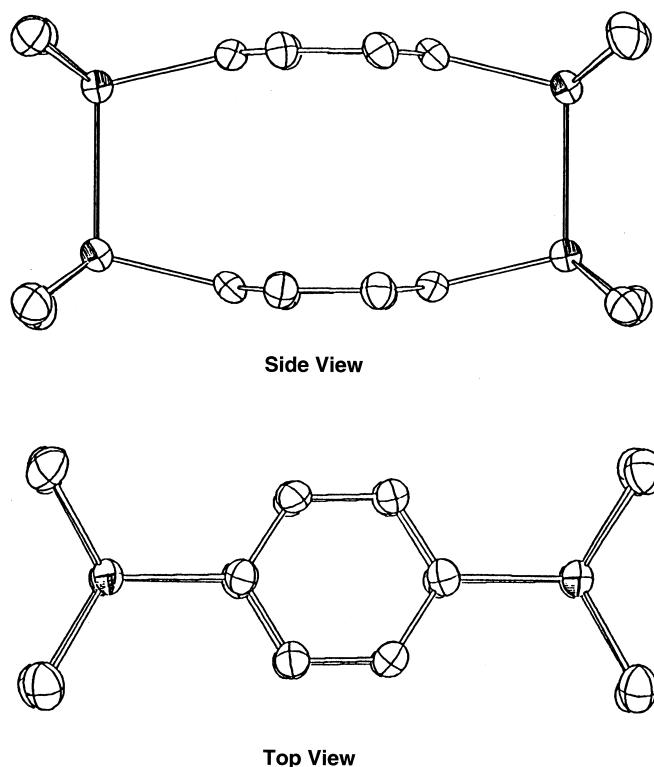
with a 1:1 hexane/benzene mixed solvent as an eluent followed by recrystallization from benzene gave **17** as colorless crystals.

The [2.2]paracyclophane structure of **17** was confirmed by the following spectroscopic data. The mass spectrum showed the M⁺ cluster ion in the range of m/z 554–572, in agreement with the calculated formula of C₂₀H₃₂Ge₄. The ¹H and ¹³C NMR spectra are fully consistent with the highly symmetrical structure: ¹H NMR (CDCl₃, δ) 0.55 (s, 24 H, Me), 6.74 (s, 8 H, ArH); ¹³C NMR (CDCl₃, δ) –4.78 (Me), 133.07 (ortho C), 140.12 (ipso C). In the proton NMR spectra, the aromatic protons of **7**, **6**, and [2.2]paracyclophane **17** appear at 6.74, 6.79, and 6.48 ppm, respectively. Because of the shielding effect of each facially arrayed benzene ring, these aromatic protons appreciably shift up-field (Δδ = 0.59–0.63 ppm) relative to 1,4-bis(pentamethyldigermanyl)benzene (7.35 ppm), 1,4-bis(pentamethyldisilanyl)benzene (7.38 ppm), and 1,4-diethylbenzene (7.11 ppm).

The cyclophane **17** is quite stable and does not change upon heating to 300°C. Furthermore, the Ge–Ge bonds are inert to trimethylamine *N*-oxide or sulfur in refluxing benzene, contrary to the case of **12**. The compound **12** can be oxidized easily to disiloxane-bridged paracyclophane by oxidation with trimethylamine *N*-oxide.

The molecular structure of 1,2,9,10-tetragerma[2.2]paracyclophane **17** was determined by the X-ray diffraction study. The single crystals of **17** for X-ray crystallography were obtained from a toluene solution. Similar to **12**, the crystal belongs to the space group *P*2₁/*n*, and the data collection was carried out at 13°C. The ORTEP drawing of **17** is shown in Fig. 7.

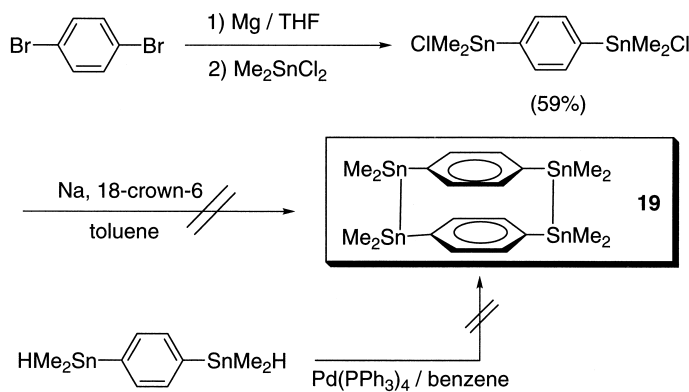
The molecule is highly symmetric with a center of symmetry. The length of the bridging Ge–Ge bonds (2.438(1) Å) is close to that of normal Ge–Ge bonds. The Ge–C_{ar} bond lengths (1.941(10)–1.946(10) Å, av. 1.944 Å) are also normal. The bridged aromatic carbons bend

FIG. 7. Molecular structure of **17**.

inward from the planes of the other aromatic four carbons by 3.1° (C1) and 5.9° (C4) (av. 4.5°). In addition, the germanium atoms at the bridges deviate from benzene rings by 10.4 (Ge1) and 8.8 deg (Ge2) (av. 9.6 deg). As a result, the two benzene rings are distorted slightly into a boat form. The two aromatic rings completely eclipse each other with interplanar space distances of 3.382 Å (C1–C4') and 3.496 Å (av. C2–C5' and C3–C6'). Interestingly, the value is very close to those observed for **12** and is close to that observed in graphite (3.40 Å), as indicated in the case of **12**.

C. TETRASTANNA[2.2]PARACYCLOPHANE

For comparison, it seemed extremely interesting to prepare octamethyltetrastanna[2.2]paracyclophane (**19**). However, the attempted reductive coupling of 1,4-bis(chlorodimethylstannyl)benzene did not



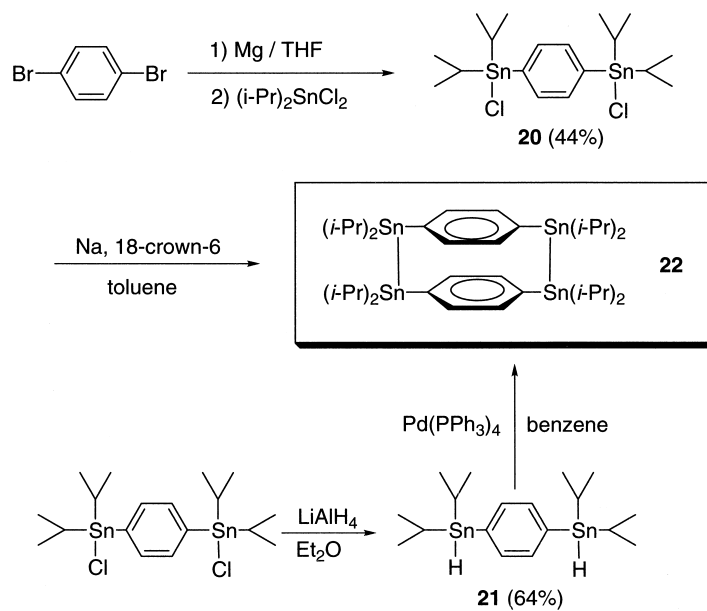
SCHEME 4

afford the desired product **19** (**28**). Fine grains of tin metal were liberated during the reflux of toluene. Next, the synthesis of **19** was attempted by dehydrogenative coupling reaction of 1,4-bis(dimethylstannyl)benzene with tetrakis(triphenylphosphine)palladium. However, the reaction afforded only hexastanna[2.2.2]paracyclophane. The methyl group on tin seemed to be too small to protect against oxidative cleavage of the Sn–Sn bond (Scheme 4).

Then dehalogenative coupling of chlorostannane **20** and dehydrogenative condensation of hydrostannane **21**, both of which contain isopropyl groups as protecting groups, were examined. Dechlorination coupling of **20** gave octa(isopropyl)tetrastanna[2.2]paracyclophane **22** in 0.3% yield as colorless crystals together with dodeca(isopropyl)hexastanna[2.2.2]paracyclophane **23**. Alternatively, dehydrogenative condensation of hydrostannane **21** in benzene with a palladium catalyst at 40°C afforded the cyclophane **22** in 1.1% yield. Both processes gave **22** only in very low yield, but the first paracyclophane bridged by Sn–Sn bonds has been thus obtained (Scheme 5). The cyclophane **22** is stable toward atmospheric oxygen and moisture, although it decomposes upon heating to 200°C.

The molecular structure of 1,2,9,10-tetrastanna[2.2]paracyclophane **22** was determined by the X-ray diffraction method. The crystal belongs to the space group $P2_1/a$, and the data collection was carried out at 13°C. The ORTEP drawing of **22** is shown in Fig. 8.

The molecule is also highly symmetric with a center of symmetry. The two methyl groups of the two isopropyl groups on the tin atoms protect efficiently the Sn–Sn bonds. One of the methyl groups is located above the tin atom as viewed along the Sn–Sn bond. The other



SCHEME 5

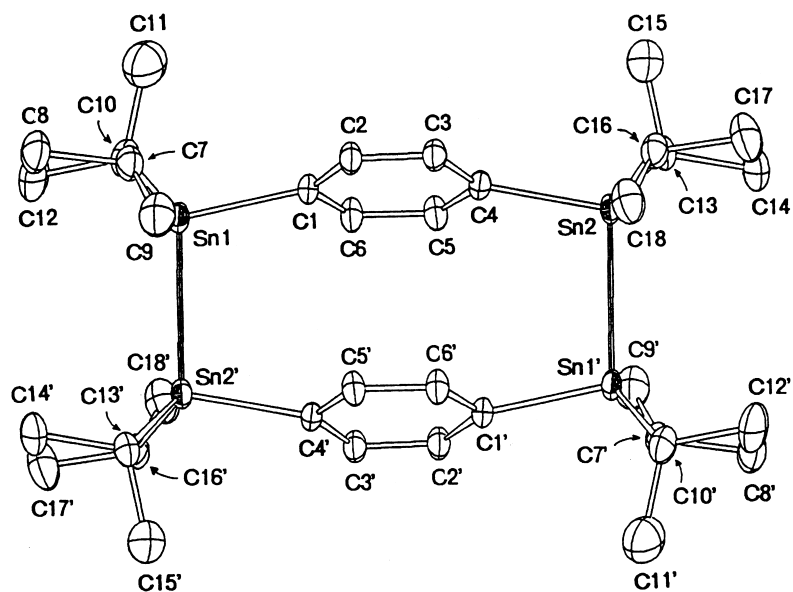


FIG. 8. Molecular structure of **22**.

is located around the Sn–Sn bond. The lengths of the bridging Sn–Sn bonds (2.808(1) Å) are close to those of the normal Sn–Sn bonds (e.g., 2.780 Å in Ph_6Sn_2) (29). The Sn–C bond lengths (2.160(5)–2.164(5), av. 2.162 Å) are also normal. The benzene rings are nearly planar. Thus, the bridged aromatic carbons (C1, C4) are displaced only slightly inward out of the plane of the other four aromatic carbons (C2–C3–C5–C6) by 1.9° (C1) and 2.5° (C4) (av. 2.2°). In contrast, the C–Sn bonds at the bridges are appreciably inclined from the benzene ring by 8.3° (C1–Sn1) and 9.5° (C2–Sn2) (av. 8.9°).

Of great interest is the conformation between the aromatic rings and the bridging Sn–Sn bonds. The benzene rings are connected by the bridging Sn–Sn bonds not perpendicularly but in a stepped conformation; surprisingly, the dihedral angle is 67.4°! The two benzene rings are completely parallel with an interplanar space distance of 3.48 Å; again it is very close to that found for graphite (3.4 Å).

The side view of the molecular structure is illustrated in Fig. 9. Interestingly, C1', C5, C6, and C4' atoms are arranged in a plane. The conformation between the two separated rings is apparently similar to that of the layered structure of graphite. The steric congestion among the neighboring alkyl groups is very small because of the relatively long the Sn–Sn and Sn–C bonds. The shortest distance be-

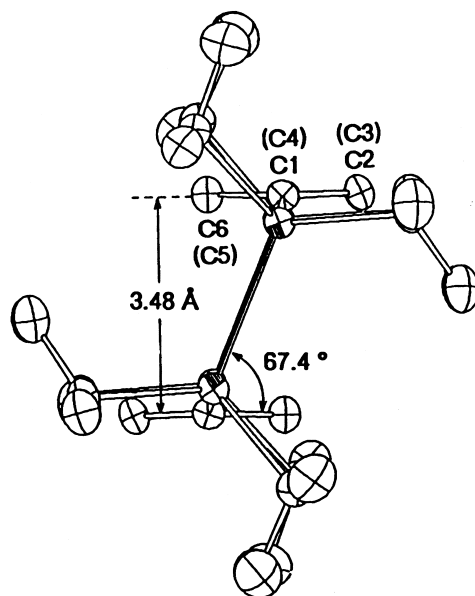


FIG. 9. ORTEP drawing of **22** viewed down the vector C2–C3.

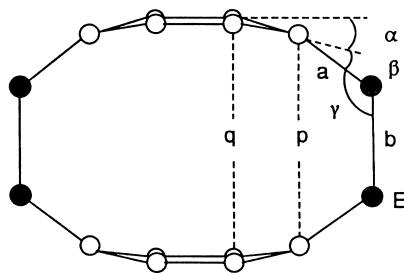
tween the hydrogen atoms is 2.54 Å between H2 (aromatic) and H9 (methyl), indicating that the steric repulsion is also very small. Furthermore, the crystal packing is normal and probably does not influence the conformation between the benzene rings. Therefore, it is reasonable that the stepped conformation in **22** results from the factor similar to that on graphite structure.

D. COMPARISON OF STRUCTURES OF [2.2]PARACYCLOPHANES BRIDGED BY GROUP 14 ELEMENTS

An interesting systematic comparison of the geometries by X-ray diffraction in a series of [2.2]paracyclophanes, **1**, **12**, **17**, and **22**, is given in Table I and Fig. 10. In all the [2.2]paracyclophanes, the bridging bonds (*b*) are somewhat elongated from the normal bond lengths, and the benzene rings are distorted into boat conformations. The strain angles α of the aromatic rings appreciably decrease in the order 12.6 (C) > 4.3 (Si) > 4.5 (Ge) > 2.2 (Sn). The rings of the cyclophane **1** bridged by carbon atoms are considerably deformed into boat

TABLE I
BOND LENGTHS AND ANGLES IN [2.2]PARACYCLOPHANES
BRIDGED BY GROUP 14 E-E BONDS

	C	Si	Ge	Sn
<i>a</i> (Å)	1.511	1.883	1.944	2.163
<i>b</i> (Å)	1.593	2.376	2.438	2.808
<i>p</i> (Å)	2.778	3.347	3.382	3.454
<i>q</i> (Å)	3.093	3.458	3.496	3.482
α (deg)	12.6	4.3	4.5	2.2
β (deg)	11.2	10.6	9.6	8.9
γ (deg)	113.7	105.0	104.1	101.0



E = C, Si, Ge, Sn

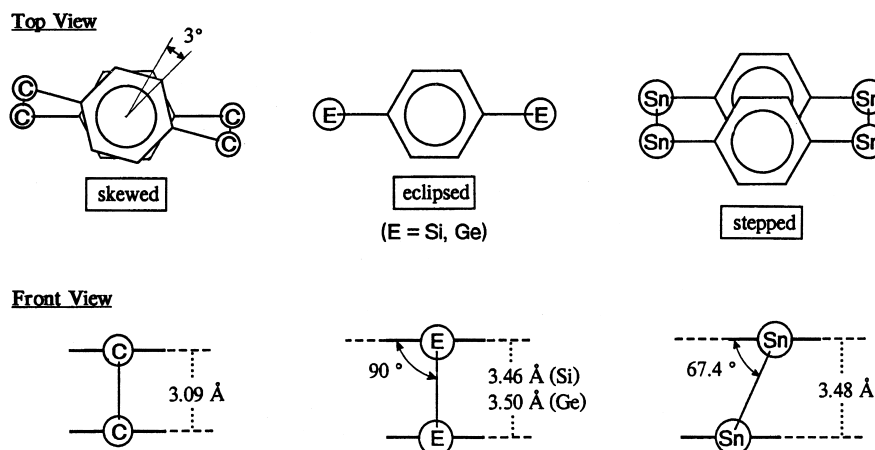


FIG. 10. Conformations of two benzenes in [2.2]paracyclophanes bridged by Group 14 E-E bonds.

shapes, whereas those of the cyclophane **22** bridged by tin atoms are quite flat.

On the other hand, the bending angles β of the bridging atoms slightly decrease in the order 11.2 (C), 10.6 (Si), 9.6 (Ge), and 8.9 (Sn). As a result, the β angles of **12**, **17**, and **22** are larger than the corresponding α angles. In the cyclophane **1**, however, the situation is opposite. The distortions in cyclophanes **12**, **17**, and **22** are accumulated in the E-C (E = Si, Ge, and Sn) bonds to a larger extent than the benzene rings. In contrast, the distortion of **1** is concentrated on the benzene rings. This can evidently be ascribed to the marked differences in the bond lengths at the bridge.

Of particular interest are both the conformations between the separated aromatic rings and the interplanar space distances (q). In the cyclophane **1**, a slight twist (3°) of the aromatic rings occurs in opposite directions due to the transannular repulsion resulting from the quite shorter distance (3.09 Å) than the van der Waals contact distance (3.4–3.6 Å) (30). On the other hand, the two benzene rings of the cyclophanes **12** and **17** eclipse each other completely with the distances (3.46 Å for **12**; 3.50 Å for **17**) just equal to the van der Waals contact distance. In sharp contrast, the benzene rings of the cyclophane **22** are connected by the bridging Sn–Sn bonds not perpendicularly, as in **12** and **17**, but in a stepped conformation, the dihedral angle being 67.4° . The rings of **22** are parallel with an interplanar space distance 3.48 Å, which is almost the same as those of **12** (3.46 Å) and **17** (3.50 Å).

[2.2]Paracyclophanes bridged by Group 14 heavy elements try to keep interplanar distances constant to the value for graphite, regardless of any increase in the bridging bond lengths: 2.38 Å for Si–Si, 2.44 Å for Ge–Ge, and 2.81 Å for Sn–Sn! Such a motive is impossible for the carbon analogue.

E. THROUGH-SPACE AND THROUGH-BOND INTERACTIONS IN [2.2]PARACYCLOPHANES BRIDGED BY GROUP 14 ELEMENTS

A systematic comparison of through-space and through-bond interactions in a series of [2.2]paracyclophanes bridged by Group 14 E–E σ -bond (E = C, Si, Ge, and Sn) is now possible. The UV spectra of [2.2]paracyclophanes **1**, **12**, **17**, and **22**, bridged by E–E bonds (E = C, Si, Ge, and Sn), are shown in Fig. 11 (23).

The cyclophane **12** bridged by two silicon atoms exhibits two absorption bands with maxima at 223 nm ($\epsilon = 18,400$) and 263 nm ($\epsilon = 22,400$). Similar to **12**, two absorption bands with maxima at 223 nm ($\epsilon = 25,000$) and 254 nm ($\epsilon = 23,500$) were observed for the cyclophane **17** bridged by two germanium atoms. On the other hand, the cyclophane **22** bridged by two tin atoms shows an absorption band

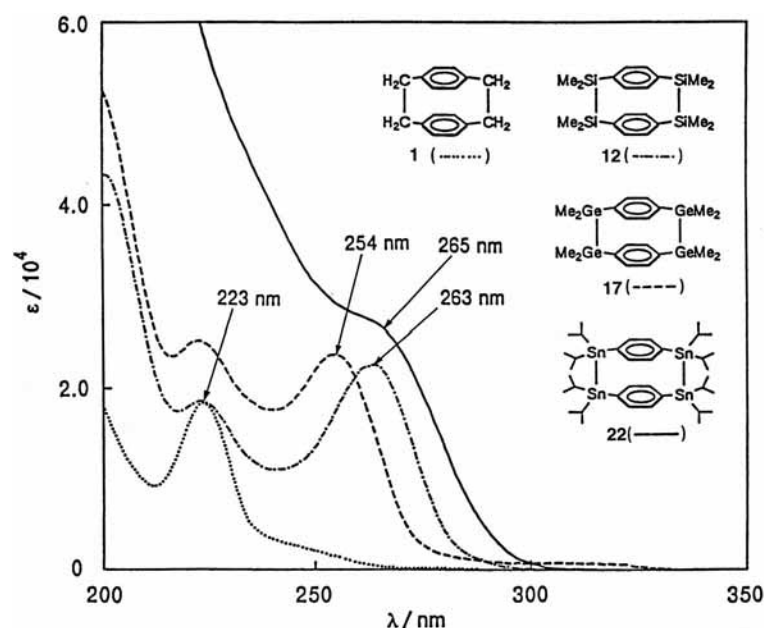


FIG. 11. UV spectra of [2.2]paracyclophanes, **1**, **12**, **17**, and **22**.

with maximum at 265 nm ($\epsilon = 26,500$, sh). In the latter case, the absorption bands observed for **12** and **17** are superimposed on the absorption band attributed to the electronic transition between σ and σ^* orbitals of the Sn–Sn bonds in the 220–240 nm region. Actually, an absorption band with maximum at 215 nm ($\epsilon = 38,500$), tailing into the 280 nm region, was observed for hexaisopropyldistannane. In sharp contrast, an absorption band with maximum at 223 nm ($\epsilon = 18,200$) and a shoulder at 245 nm ($\epsilon = 2,800$) was observed for the cyclophane **1** bridged by the C–C bonds. The compound **1** exhibits no appreciable absorption band in the long wavelength region as found for **12**, **17**, and **22**.

These observations are best explained by accounting for the difference of the HOMO levels resulting from through-space and through-bond interactions (Fig. 12). In [2,2]paracyclophane systems, the two facing benzene π -systems interact strongly because of the through-space overlap. As a consequence, the bonding combinations are stabilized (b_{3u} and b_{2u}), whereas the antibonding combinations are destabilized (b_{2g} and b_{3g}). From the four linear combinations of the benzene π MOs, the b_{3u} linear combination depends very strongly on the nature of the bridge due to through-bond interaction (31).

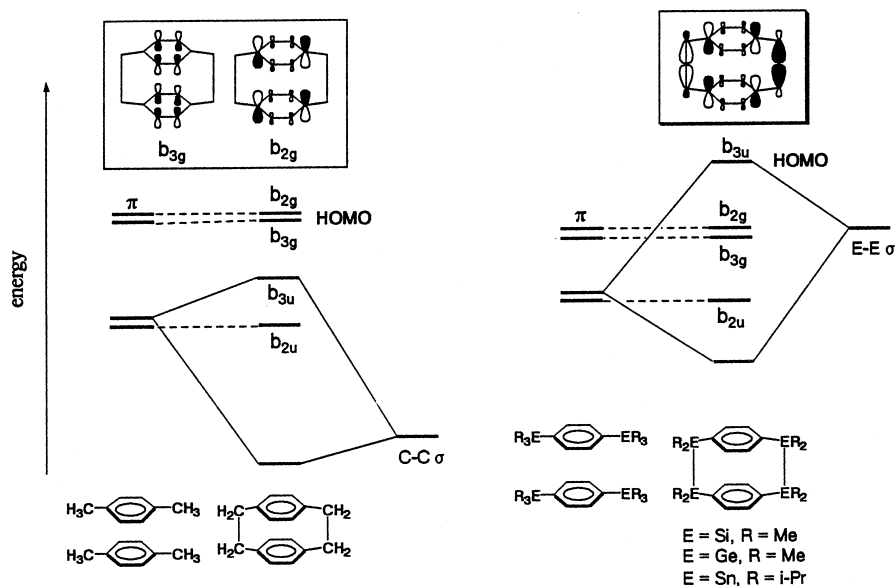


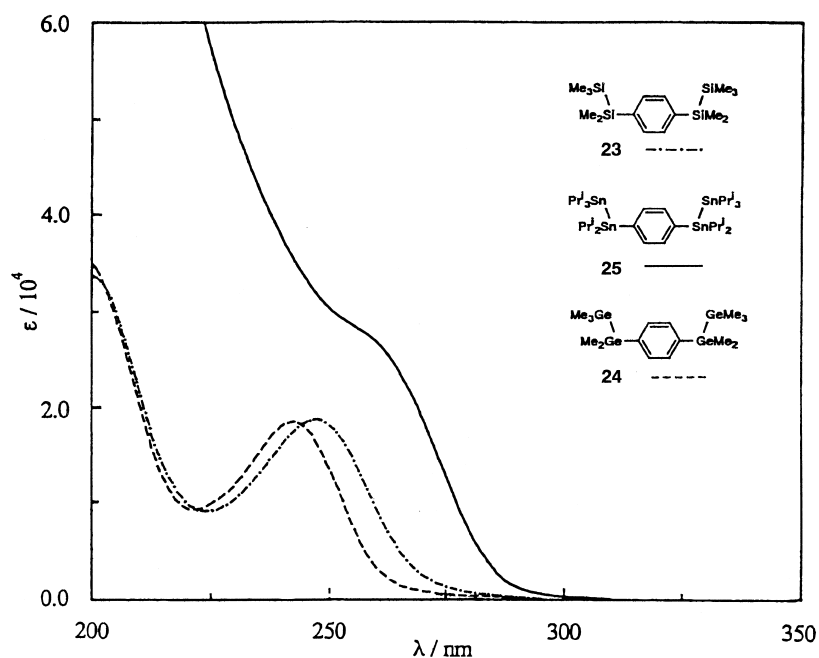
FIG. 12. MO energy diagram of [2,2]paracyclophanes bridged by Group 14 E–E bonds.

In the cyclophane **1**, although the overlap between the π -system ($2p$) and the bridging σ -bonds ($2s2p$) is most effective, these orbital energy levels match worst, the first ionization potentials being 9.25 eV for benzene and 12.1 eV for ethane. As a result, the HOMOs are the almost pure π MOs with the b_2g and b_3g combinations. Both the PE spectrum and theoretical calculation demonstrate the degeneracy of the two HOMO levels. The absorption bands are attributed to the π - π^* transitions associated with the HOMOs.

On the other hand, in the systems with high-lying σ -orbitals, the through-bond interaction effect can be predominant. In the cyclophane **12** bridged by Si_2Me_4 units, the energy level of the σ -bridge is greatly raised compared to the C_2H_4 bridge of the parent system **1**. The first ionization potential of $\text{Me}_3\text{Si-SiMe}_3$ is 8.69 eV. Consequently, the HOMO of **12** is the MO by σ - π mixing with the b_3g combination resulting from the through-bond interaction. Such an orbital interaction causes considerable destabilization of the HOMO level. The first absorption band in the long wave length region of **12** is attributed to the $(\sigma-\pi)-\pi^*$ transitions associated with the HOMO. The second band is probably attributed to the π - π^* transition between the pure π MOs, judging from the fact that the absorption band appears at the same region as that observed for **12**. Like **12**, in the cyclophanes **17** and **22** bridged by the Ge-Ge and Sn-Sn bonds, respectively, the HOMOs are formed with the b_3g linear combination and the HOMO levels are similarly destabilized relative to those of MOs with the b_2g and b_3g symmetries. The absorption bands in the long wavelength region for **17** and **22** are the result of the effective through-bond interaction.

Among the cyclophanes **12**, **17**, and **22**, the absorption band of **22** appears at the longest position. However, the bathochromic shifts in these cyclophanes should be compared with the corresponding acyclic compounds: 1,4-bis(pentamethyldisilanyl)benzene **23**, 1,4-bis(pentamethyldigermanyl)benzene **24**, and 1,4-bis(pentaisopropyldistannanyl)benzene **25** (Fig. 13).

The degree of bathochromic shift decreases in the following order: $(\Delta\nu/\text{cm}^{-1})$ 2500 (**12-23**) > 2000 (**17-24**) > 1100 (**22-25**). This is a consequence of the decreasing effect of the orbital interaction due to both the higher lying orbital energy level of the bridging E-E σ -bond ($\text{Me}_3\text{Si-SiMe}_3$: 8.69; $\text{Me}_3\text{Ge-GeMe}_3$ 8.57; $\text{Me}_3\text{Sn-SnMe}_3$: 8.20 eV) and the less effective overlap of the benzene π -system ($2p$) with the bridging σ -orbitals (Si: $3s3p$; Ge: $4s4p$; Sn: $5s5p$) as the bridging units are replaced by the heavier atoms.

FIG. 13. UV spectra of acyclic compounds **23**, **24**, and **25**.

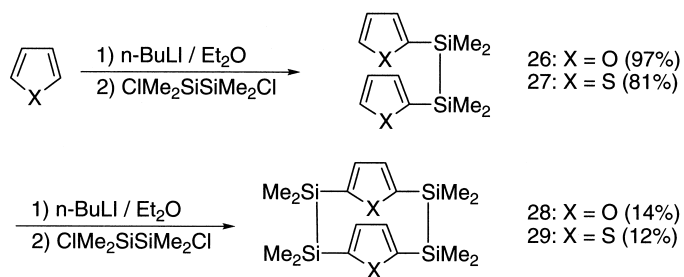
IV. Tetrasil[2.2](2,5)heterophanes

Effects of σ - π interaction are maximized if the interacting orbitals match energetically. Since the HOMOs of heteroaromatic systems such as furan (8.89 eV), thiophene (8.80 eV), and pyrrole (8.20 eV) are higher than that of benzene (9.25 eV), better energy matching with σ (Si-Si; 8.69 eV) orbitals is expected. Therefore, tetrasil[2.2](2,5)heterophanes should be interesting synthetic targets.

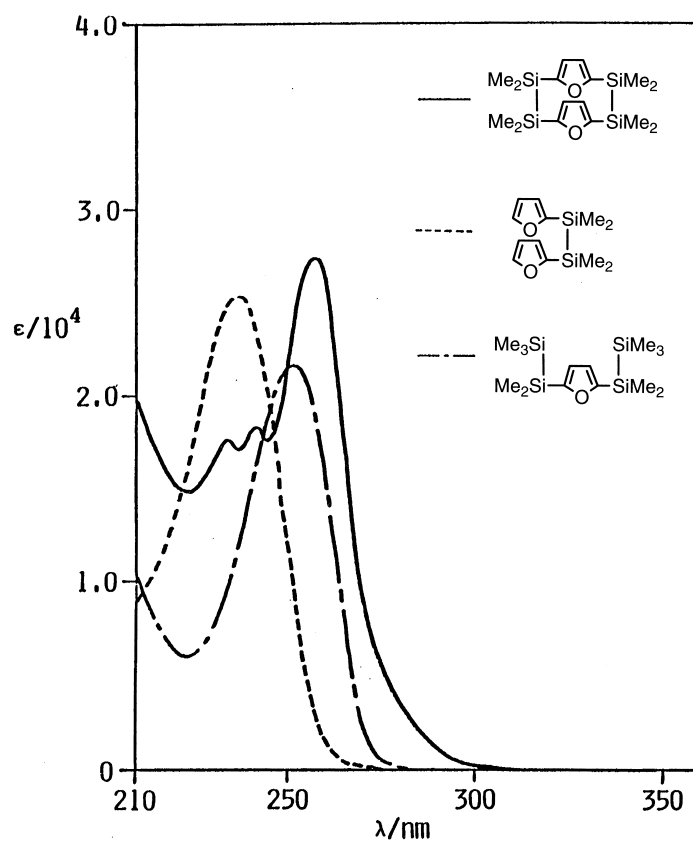
A. OCTAMETHYL-1,2,8,9-TETRASIL[2.2](2,5)FURANOPHANE AND THIOPHENOPHANE

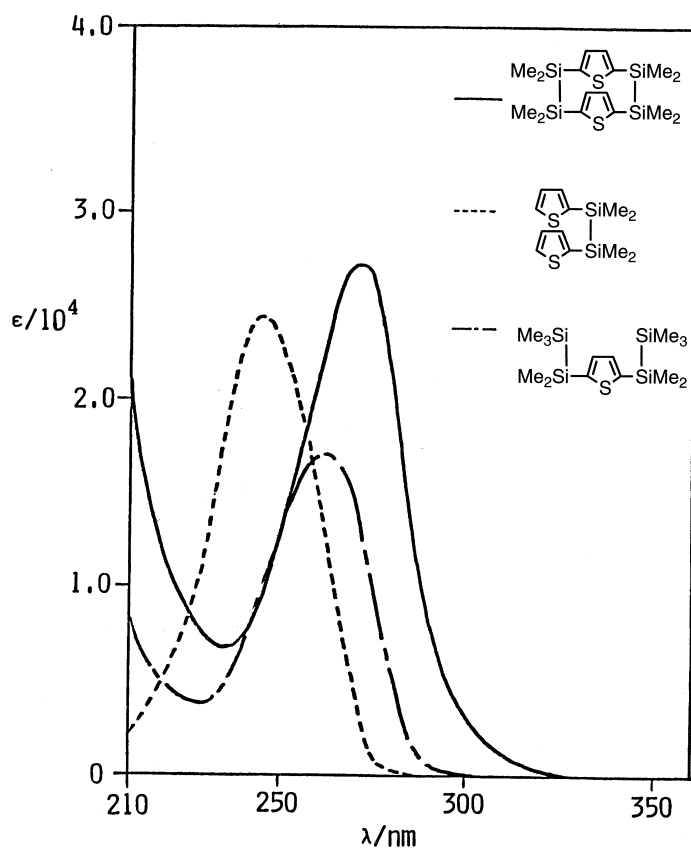
Lithiation of furan and thiophene, followed by the reaction with 1,2-dichlorotetramethyldisilane, gave linear compounds **26** and **27** (Scheme 6). The second lithiation and reaction with 1,2-dichlorotetramethyldisilane under the conditions of high dilution afforded the desired furanophane (**28**) and thiophenophane (**29**) (32).

Figures 14 and Fig. 15 show UV spectra of furanophane (**28**) and



SCHEME 6

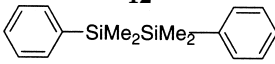
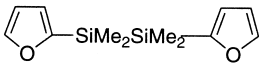
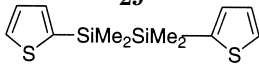
FIG. 14. UV spectra of **28** and related compounds.

FIG. 15. UV spectra of **29** and related compounds.

thiophenophane (**29**), respectively. UV spectra of the corresponding derivatives are also included in both figures.

As clearly shown, the absorption maxima of **28** and **29** are red-shifted considerably as compared with the corresponding acyclic compounds. The C–C bridged parent thiophenophane (**7**) also shows a redshift in UV spectra. Thus, **7** gave two absorption maxima at 245 nm ($\epsilon = 7700$) and 275 nm ($\epsilon = 5720$), quite different from that of 2,5-dimethylthiophene ($\lambda_{\text{max}} = 238$ nm; $\epsilon = 7250$). This is attributed to the transannular π – π interaction between two thiophene rings (33). However, furanophane (**8**) did not show such a redshift and indicated no such π – π interaction between two furan rings. At room temperature by NMR studies, it is reported that two furan rings in **8** rotate freely,

TABLE II
IONIZATION ENERGIES AS DETERMINED BY PHOTOELECTRON SPECTRA

Compound	Band (eV)			
 12	7.8	8.4	9.3	9.9
	8.2		9.0	— 9.8
 28	7.4	8.1	8.9	9.4
	8.1	8.5	9.3	10.0
 29	7.4	8.0	8.7	
	8.0	8.6	9.0	9.3

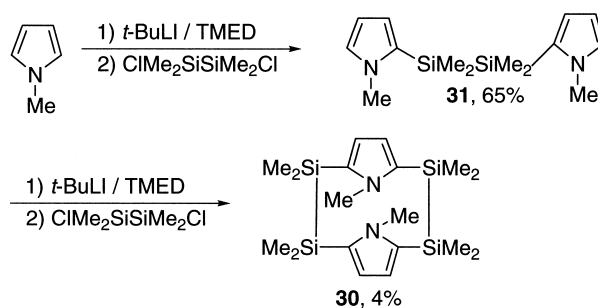
whereas in **7**, rotation of two thiophene rings is frozen to force a transannular interaction (34).

NMR studies on **28** and **29** indicate that both the thiophene and furan rings rotate freely at room temperature (*vide infra*) and therefore, anomalies in the UV spectra of **28** and **29** should be attributed to the through-bond interaction between the Si–Si σ bonds and aromatic π bonds. This was further confirmed by photoelectron spectral studies. As shown in Table II, the lift of HOMO for **12** relative to the model compound was 0.4 eV, but those for **28** and **29** were 0.7 and 0.6 eV, respectively. Apparently, more effective through-bond interaction occurs for **28** and **29** (21).

B. TETRASILA[2.2](2,5)PYRROLOPHANE

N,N,1,1,2,2,8,8,9,9-Decamethyl-1,2,8,9-tetrasilal[2.2](2,5)pyrrolophane (**30**) is prepared by a procedure similar to that applied to **28** and **29** through 1,2-bis(*N*-methylpyrrolyl)disilane **31** with slight modification of the reagents. The lithiation was performed with *t*-BuLi/TMED. Under dilute conditions pyrrolophane **30** was obtained in 4% yield from **31** as air-stable colorless crystals besides a polymeric residue (35) (Scheme 7).

The UV spectrum of **30** (Fig. 16) exhibits a large bathochromic shift ($\lambda_{\max} = 270$ nm) compared to other related compounds such as 2-pentamethyldisilanyl-*N*-methylpyrrole ($\lambda_{\max} = 248$ nm). A similar bathochromic shift is observed in charge-transfer complexes of pyrrolo-

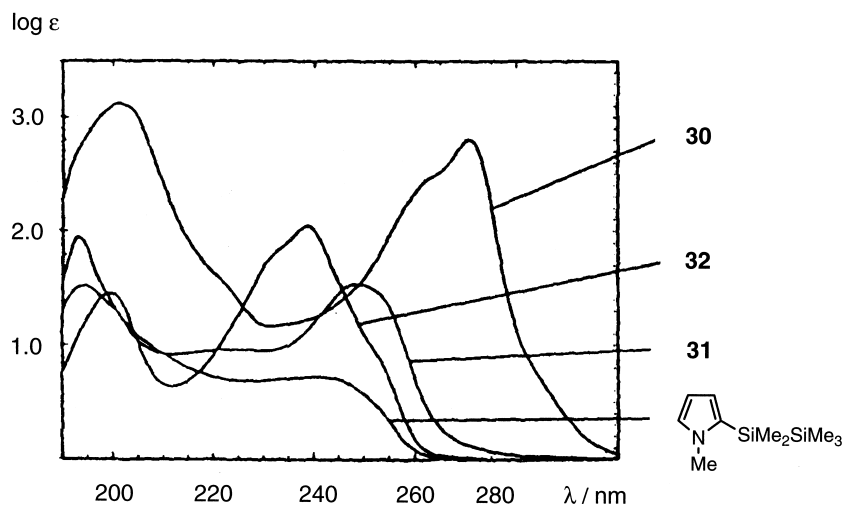


SCHEME 7

phane **30** and related compounds with TCNE (Fig. 17). Thus, the maximum absorption of the CT complex of **30** and TCNE occurs at 718 nm compared with, e.g., 630 nm for the complex of **30** and TCNE. The spectroscopic behavior of **30** reveals the strong interaction between the Si-Si σ bonds and the π systems of the pyrrole rings. Such an interaction has been shown to result in a destabilization of HOMO and thus a bathochromic shift in electronic spectra.

C. NMR STUDIES AND MOLECULAR STRUCTURE

Similar to [2.2]metacyclophane (**2**), relative conformations of two aromatic rings in [2.2](2,5)heterophanes have been studied in detail

FIG. 16. UV spectra of **30** and related compounds.

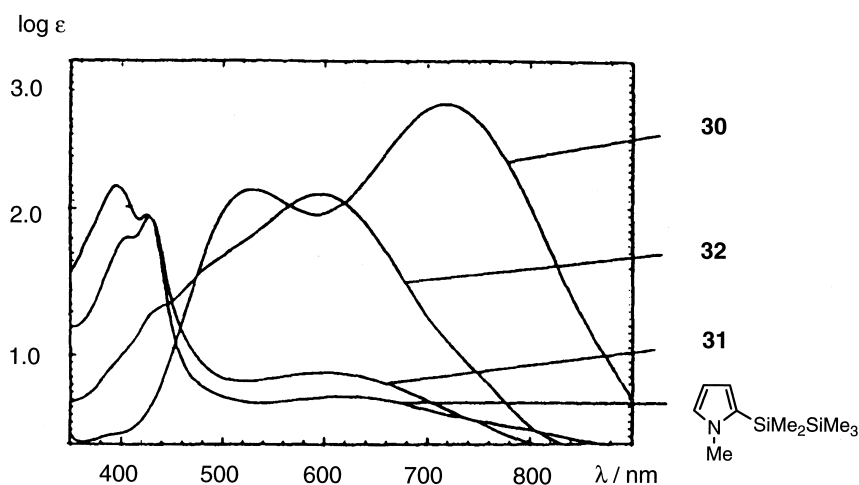
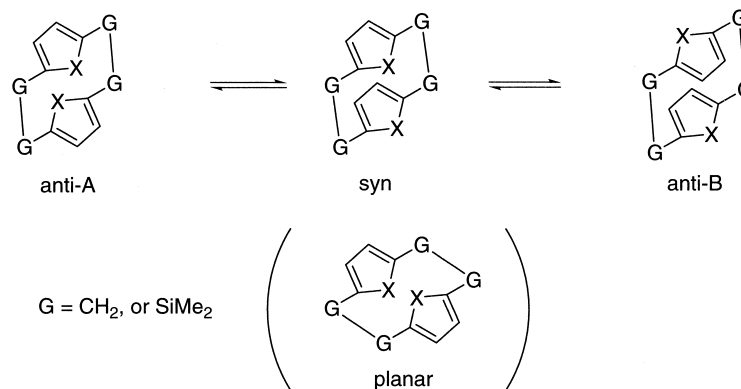


FIG. 17. CT spectra of **30** and related compounds with tetracyanoethylene.

by NMR. Scheme 8 shows equilibration of conformational isomers in heterophanes. The most stable conformation of heterophanes are believed to be *anti-A* or *anti-B*. In fact, *anti* conformations are observed in crystals (36). In solution, furanophane **8** undergoes rapid equilibration between *anti-A* and *anti-B* at room temperature. Dynamic NMR studies indicate that the energy barrier between two conformations is $\Delta G = 16.8$ kcal/mol for [2.2](2,5)furanophane **8**. However, no change was observed for proton signals of [2.2](2,5)thiophenophane **7** even at 200°C, indicating a very high rotational barrier for **7**. Namely, at



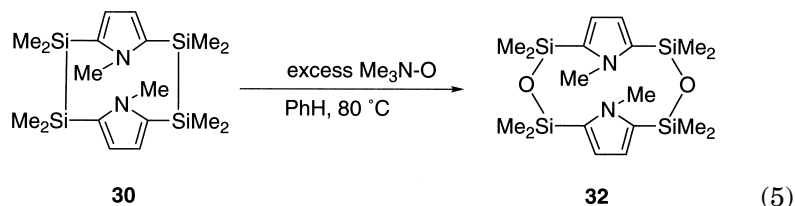
SCHEME 8

room temperature, flipping of rings occurs in furanophane but not in thiophenophane.

Tetrasil[2.2](2,5)thiophenophane **29** shows a singlet for SiMe signals at room temperature. Thus, contrary to the parent thiophenophane **7**, thiophene rings of **29** undergo free rotation at room temperature. However, at low temperature, the methyl signal starts to split into two signals. The coalescent temperature is 15.0°C and inversion barrier is determined to be 14.9 kcal/mol. The greater length of the Si–Si bond is reflected in the smaller barrier to rotation. Contrary, the methyl signal of furanophane **28** retains singlet even at –78°C, indicating a very low barrier for rotation.

¹H NMR of pyrrolophane **30** shows two singlets for SiMe groups that do not coalesce in the temperature range of –80 to +110°C, in contrast to furanophane **28**, which shows rapid *anti/syn* isomerization down to –78°C, and thiophenophane **29**, with a coalescence temperature of 15°C. The rigidity of **30** is obviously due to the steric bulk of the *N*-methyl groups.

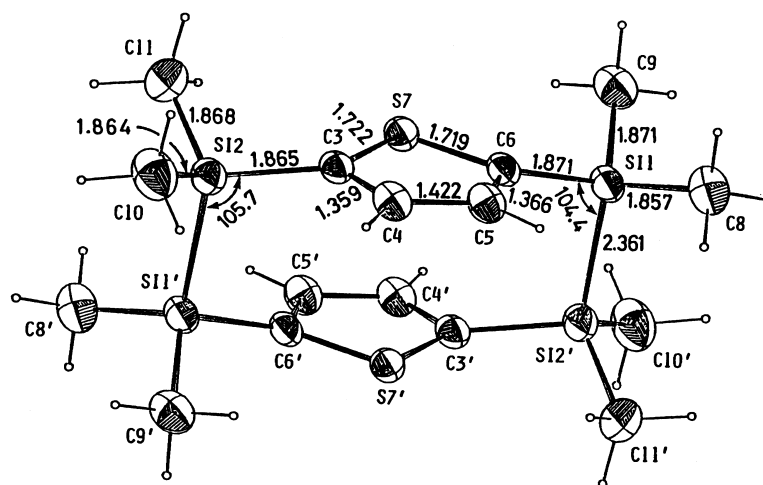
The great steric demand of the methyl group on N was further demonstrated by NMR characteristics of Si–O–Si bridged pyrrolophane **32** prepared by oxidation of **30** with excess Me₃N–O in refluxing benzene (74% yield). Even with the considerably longer Si–O–Si bridges, no *anti/syn* isomerization occurs for **32** between –80 and +110°C.



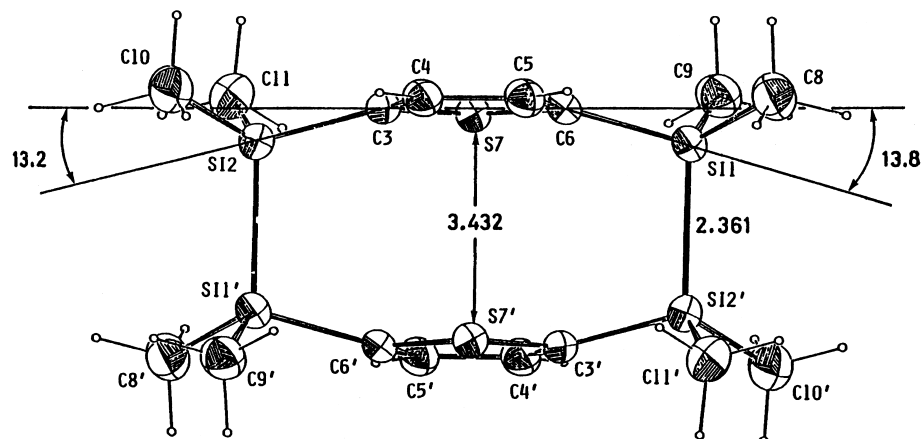
Insertion of oxygen into the Si–Si bond of **30** also blocks σ – π conjugation effectively. The fact can be seen by the shift toward short wavelength for both absorption of **31** in UV ($\lambda_{\text{max}} = 239$ nm) (Fig. 16) and the CT complex with TCNE ($\lambda_{\text{max}} 593$ nm) as compared to pyrrolophane **30** (Fig. 17).

The crystals of thiophenophane **29** belong to the $P2_1/n$ group and are monoclinic, with two molecules in a unit cell similar to that for **12**. An ORTEP drawing is shown in Fig. 18 with pertinent distances and angles. Figure 19 shows a side view of **29**.

In crystals, two thiophene rings take an *anti* conformation. The Si–Si bond length is 2.361 Å, which is slightly longer than the normal

FIG. 18. Molecular structure of **29**.

value (2.34 Å) but shorter than that observed for **12** (2.376 Å). This indicates smaller distortion for **29** than for **12**. The sulfur atoms are not on the plane composed of four carbons but deviate outward by 1.9°. This results from avoiding interactions between the lone-pair and π electrons, and the phenomenon is also observed for the carbon analogue **7** (37). Two thiophene rings are staggered with respect to each other in the direction where each sulfur atom directs the center of the five-membered ring.

FIG. 19. Side view of **29**.

Suitable single crystals of **30** for X-ray analysis were also obtained by slow crystallization from toluene at 10°C. Results for the molecular structure of pyrrolophane **30** are shown in Fig. 20. Pyrrolophane **30** crystallizes in *anti* configuration, with the *N*-methyl groups placed directly above the plane of the opposite pyrrole ring. The Si–Si bond (2.386 Å) is the same length as that found in paracyclophane **12** (2.376 Å) and is inclined against the plane of the pyrrole rings by about 64°.

The same characteristic is observed in the corresponding tetrasila[2.2](2,5)furanophane **28**. In contrast, in the case of thiophenophane **29**, the Si–Si bond is nearly perpendicular to the aromatic rings. Table III summarizes important characteristics of these compounds. All tetrasila[2.2](2,5)heterophanes show only a small deviation of the heteroatoms from ideal planar arrangement in the rings. Also the Si–ring bonds are bend inwards with the biggest deviation occurring in the thiophenophane, which also has the biggest interplanar distance between the heterocycles (3.21 Å). In the case of furanophane **28** the bridge torsion angle of 47° is relatively close to a staggered arrangement (60°) of substituents around the Si–Si bond. In pyrrolophane **30**,

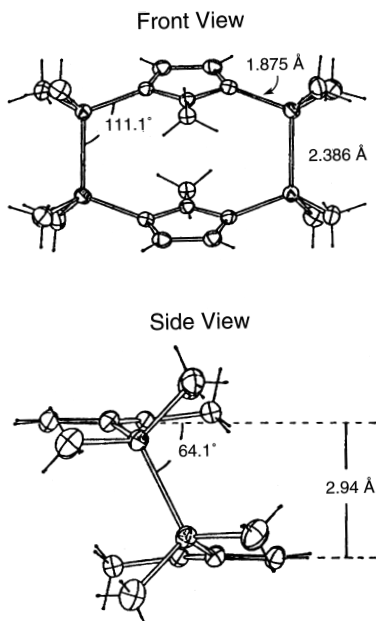
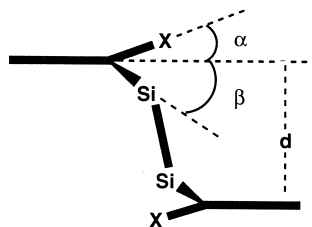


FIG. 20. Molecular structure of **30**.

TABLE III
STRUCTURAL DATA FOR TETRASILA[2.2](2,5)HETEROPHANES

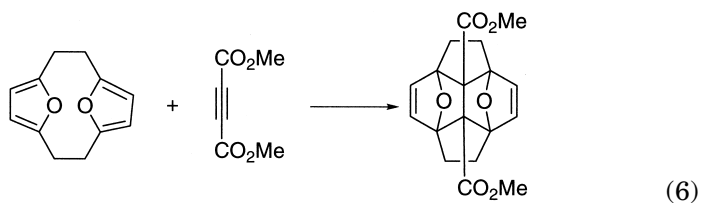
X =	O (28)	S (29)	NMe (30)
Envelope-shaped ring (α) ($^\circ$)	1.3	1.9	1.1
Bending of bridge atom (β) ($^\circ$)	7.0	13.4	13.0
Distance between rings (d) (\AA)	2.63	3.21	2.94
Si–Si bond length (\AA)	2.347	2.361	2.363
Bridge torsion ($^\circ$)	47.0	30.6	25.1



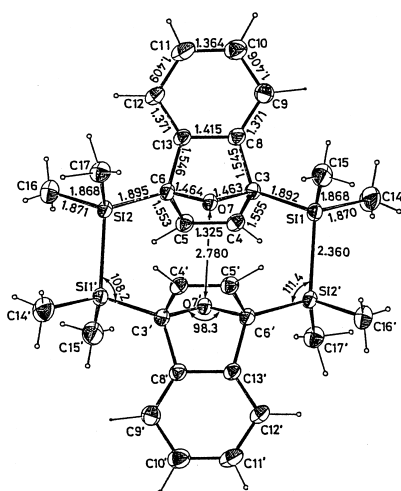
however, the bridge is considerably twisted towards eclipsed conformation (torsion angle 25°) possibly reflecting the greater steric demand of the methyl group.

D. REACTIONS OF OCTAMETHYL-1,2,8,9-TETRASILA[2.2](2,5)FURANOPHANE

[2.2](2,5)Furanophane **8** is reactive and undergoes interesting reactions with dienophiles. The reaction of **8** with dimethyl acetylenedicarboxylic acid gave a polycyclic compound, as shown in the following equation. The compound was derived by intramolecular Diels–Alder reaction of the initially formed 1:1 adducts (38).



Tetrasilabridged furanophane **28** did not react with dimethyl acetylenedicarboxylic or with 4-phenyl-1,2,4-triazoline-3,5-dione. Low distortion of the furan rings in **28** together with steric hindrance of

FIG. 21. ORTEP drawing of **33**.

methyl groups prevented the reaction. However, the reaction of **28** with benzyne did afford **33** in good yield.

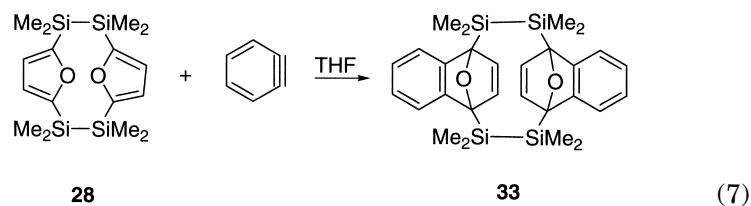
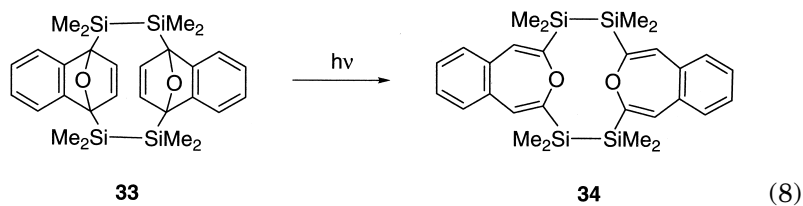
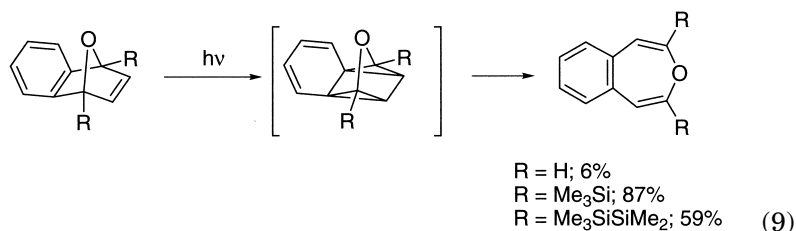


Figure 21 shows an ORTEP drawing of **33**. Photochemical reaction of **33** gave a new Si-Si bridged benzoxepinophane **34**. The latter is a new type of phane. In general, photochemical conversion of 1,4-epoxy-1,4-dihydronaphthalene to benzoxepin occurs only in very low yield, but 1,4-bis(trimethylsilyl)- and 1,4-bis(pentamethyldisilanyl)-1,4-epoxy-1,4-dihydronaphthalene gave the corresponding benzoxepin in 87 and 59% yield. Apparently steric hindrance of silyl groups protects the unstable oxepin structure.





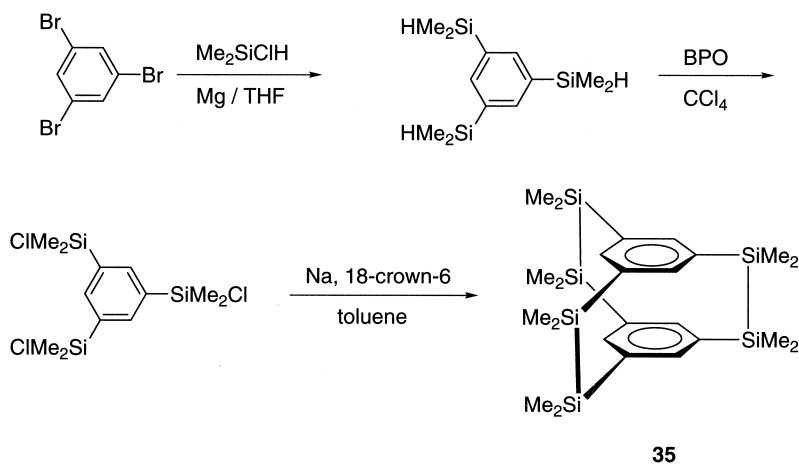
V. Hexasila[2.2.2](1,3,5)cyclophane

A. PREPARATION AND PROPERTIES OF 1,2,9,10,17,18-HEXASILA [2.2.2](1,3,5)CYCLOPHANE

The degree of through-bond interaction in [2.2]paracyclophane **12** bridged by two Si–Si bonds is the greatest among the series of the cyclophanes bridged by Group 14 elements. Therefore, the properties of [2.2.2](1,3,5)cyclophane **35** bridged by three Si_2Me_4 units are of special interest because of the extremely rigid structure and the expectedly strong σ – π conjugation.

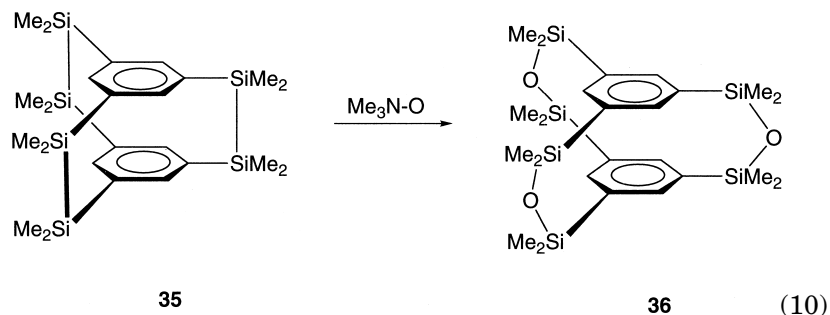
The cyclophane **35** was obtained by a reductive coupling reaction of 1,3,5-tris(chlorodimethylsilyl)benzene with molten sodium metal in refluxing toluene in the presence of 18-crown-6. The GCMS spectrum of the reaction mixture showed the presence of a very small amount of the cyclophane **35** with its parent ion ($M^+ = 498$). After careful isolation, pure samples of **35** were obtained as white solids. This provides the most direct route to **35**, but the yield is very low (0.22%) (39) (Scheme 9).

The structure of [2.2.2](1,3,5)cyclophane **35** was first confirmed by the mass spectrum, which showed the M^+ cluster ion in the range of m/z 498–502 in agreement with the calculated formula of $C_{24}H_{42}Si_6$. The 1H and ^{13}C NMR spectra are fully consistent with the highly symmetrical structure. In the proton NMR spectrum, the aromatic protons of **35** appear at 6.69 ppm and are shifted appreciably upfield ($\Delta\delta = 0.79$ ppm) compared to 1,3,5-tris(pentamethyldisilanyl)benzene (7.48 ppm). The magnitude of the $\Delta\delta$ value is somewhat larger than that between [2.2]paracyclophane **12** (6.79 ppm) and the acyclic compound (7.38 ppm); the fact points to the shortening of the inter-ring distance. The ^{29}Si NMR ($CDCl_3$) spectrum of **35** revealed a single resonance at -15.08 ppm, which shifts somewhat downfield compared with that observed for **12** (-18.36 ppm).



SCHEME 9

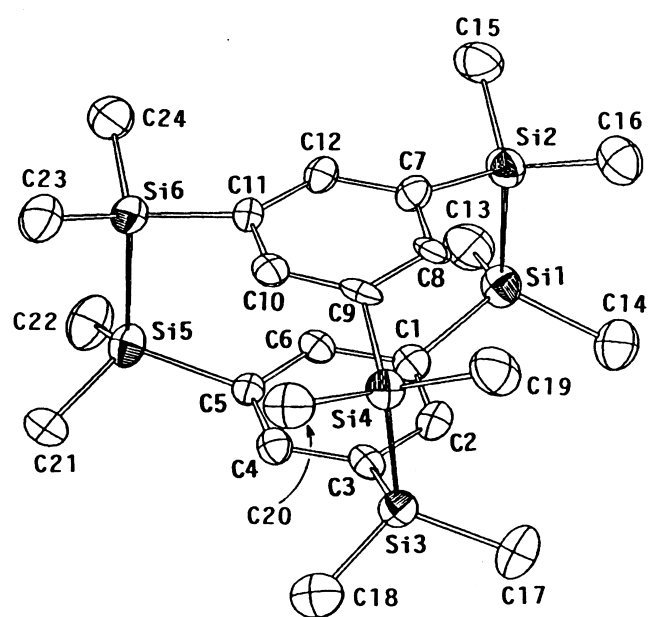
The cyclophane **35** is stable and remains unchanged upon heating to 300°C. The compound **35** is, however, readily oxidized at the Si–Si units by trimethylamine oxide in refluxing benzene, giving the cyclophane **36** containing three Si–O–Si bonds.



B. MOLECULAR STRUCTURE OF 1,2,9,10,17,18-HEXASILA [2.2.2](1,3,5)CYCLOPHANE

The crystals of 1,2,9,10,17,18-hexasila[2.2.2](1,3,5)cyclophane belong to the space group $P2_1/n$. The ORTEP drawing is shown in Fig. 22. The molecule has no crystallographic symmetry. The three Si–Si bonds, Si1–Si2: 2.378(6), Si3–Si4: 2.373(6), and Si5–Si6: 2.384(5) Å (av. 2.378 Å), are different in length and somewhat longer than the normal Si–Si bond (2.34 Å), whereas those in **12**, which has a center of symmetry, are identical (2.376 Å). The benzene rings of the cyclophane **35** are almost flat.

a



b

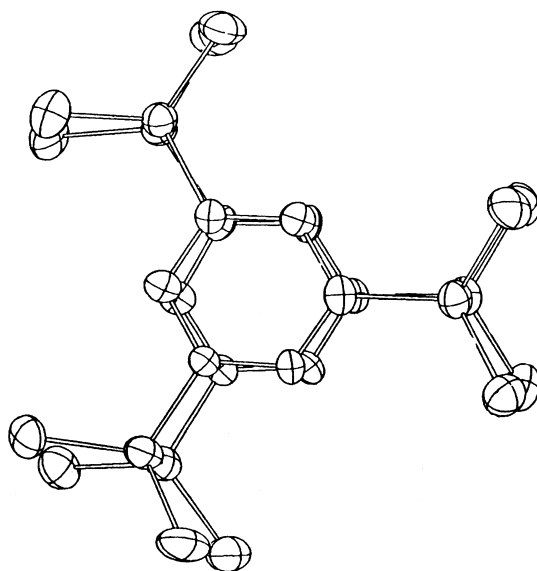


FIG. 22. ORTEP drawing of **35**.

The aromatic carbons (C1, C3, C5, C7, C9, C11) attached to the silicon atoms lie only slightly (0.003–0.029 Å) outside the mean planes of the aromatic rings. However, the Si–C(ring) bonds deviate considerably from the planes of the benzene rings (Si1–C1/C1–C2–C6: 11.0°, Si2–C7/C71–C8–C12: 14.8°, Si3–C3/C2–C3–C4: 13.5°, Si4–C9/C8–C9–C10: 16.6°, Si5–C5/C4–C5–C6: 12.6°, Si6–C12/C10–C11–C12: 16.2° av. 14.1°). The deviation angles are greater than that of **12** (10.6°). The two aromatic rings are so arranged to take the eclipsed position. The average distance between the two aromatic rings of **35** is 3.32 Å, somewhat shorter than that in **12** (3.35 and 3.46 Å). Because the Si–Si bond is 1.5 times longer than the C–C bond, the strain in the cyclophane must be much smaller than that of the carbon analogue.

The UV spectra of hexasila[2.2.2](1,3,5)cyclophane **35** and tetrasila[2.2]-paracyclophane **12** are shown in Fig. 23. The cyclophane **35** exhibits two absorption bands with maxima at 224 nm ($\epsilon = 35,200$, sh) and 264 nm ($\epsilon = 20,900$) and a shouldered absorption band at 240 nm ($\epsilon = 25,000$) similar to those for **12** (223 nm ($\epsilon = 18,400$) and 263 nm ($\epsilon = 22,400$)). Furthermore, the absorption band with maximum at 264 nm for **35** is largely redshifted compared to that for 1,3,5-tris(pentamethyldisilanyl)benzene ($\lambda_{\text{max}} = 233$ nm, $\epsilon = 30,500$). The through-bond interaction between the three Si–Si σ -bonds and the benzene π -systems should be the origin of the bathochromic shift.

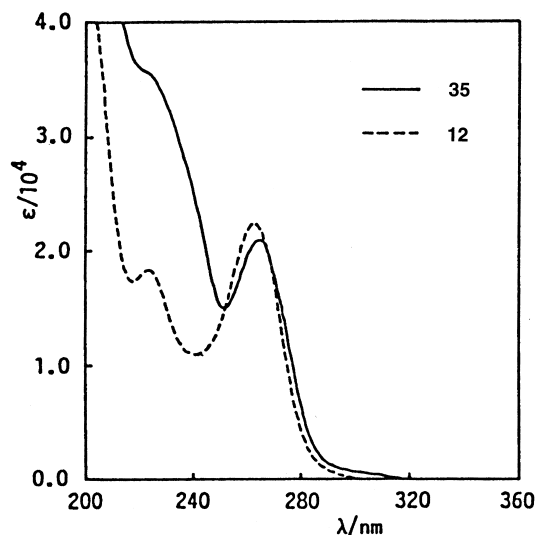
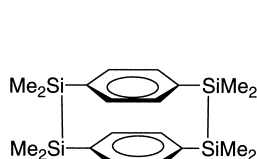
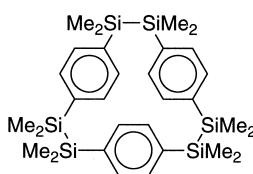
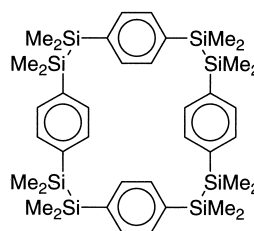
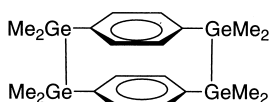
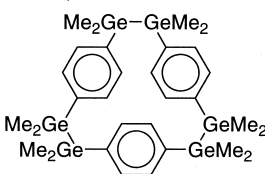
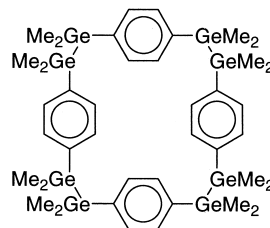
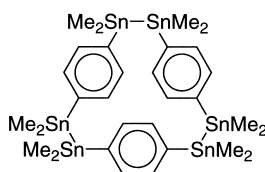
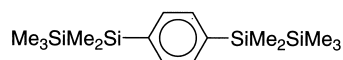
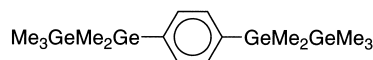


FIG. 23. UV spectra of **12** and **35**.

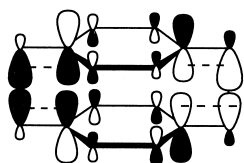
VI. $[2^n]$ Paracyclophanes Bridged by Si, Ge, and Sn

The direct coupling reactions of $\text{ClMe}_2\text{M}-\text{C}_6\text{H}_4-\text{MMe}_2\text{Cl}$ with sodium naphthalenide in toluene at -78°C afforded $[2.2]$ paracyclophanes ($\text{M} = \text{Si}$, **12**, 2.5%; $\text{M} = \text{Ge}$, **17**, 1.7%) as described earlier. Careful examination of the products has revealed that several macrocyclic $[2^n]$ paracyclophanes such as **37** and **38** ($\text{M} = \text{Si}$) and **39** and **40** ($\text{M} = \text{Ge}$) exist as well in low yield. The corresponding reaction for $\text{M} = \text{Sn}$ gave no $[2.2]$ paracyclophane **19** with the $\text{Me}_2\text{SnSnMe}_2$ bridge, but produced dodecamethyl hexastanna $[2^3]$ paracyclophane **41** in 12% yield.

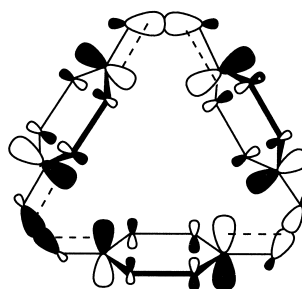
**12****37****38****17****39****40****41****42****43**

The possible through-bond interactions in these compounds are schematically indicated in Scheme 10.

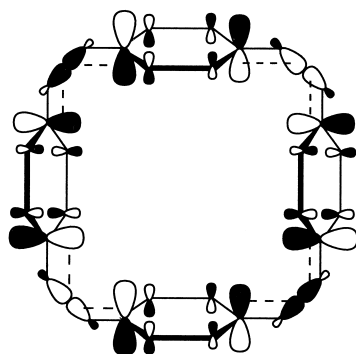
Through-bond conjugation is possible for [2.2]paracyclophane and [2.2.2.2]paracyclophane because of the Hückel overlap between the interacting orbitals, but is not possible for [2.2.2]paracyclophane because of the Möbius conjugation. Thus, it is interesting to examine the point by UV spectra. Figures 24 and 25 show UV spectra of silicon and germanium series of paracyclophanes. In both cases, [2.2]paracyclophanes **12** and **17** exhibit absorption at the longest wavelength in the series. [2.2.2]Paracyclophanes, **37** and **39**, exhibit absorptions at almost the same position as acyclic reference compounds, **42** and **43**, although absorption intensities increase about three times more.



[2.2]paracyclophane

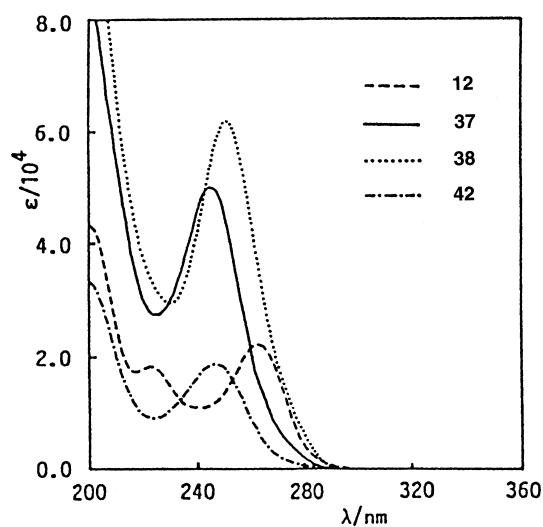


[2.2.2]paracyclophane

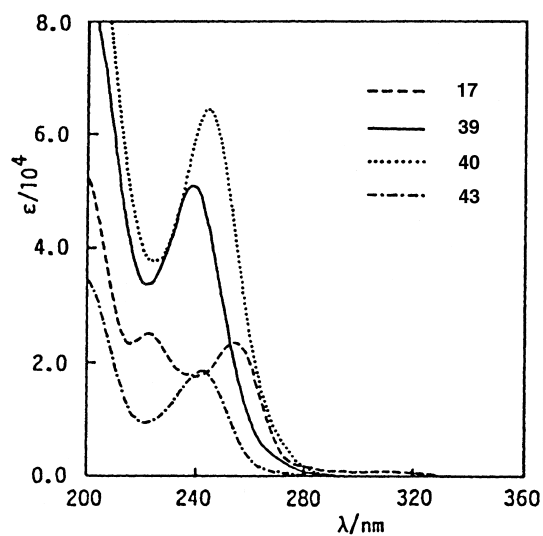


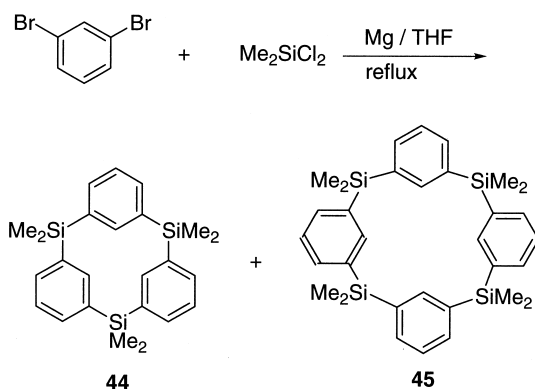
[2.2.2.2]paracyclophane

SCHEME 10

FIG. 24. UV spectra of [2ⁿ]paracyclophane bridged by Si.

This indicates that effective through-bond conjugation does not exist in [2.2.2]paracyclophanes. In contrast, [2.2.2.2]paracyclophanes, **38** and **40**, show slightly redshifted absorptions, indicating the existence of through conjugation, although the degree of conjugation is smaller

FIG. 25. UV spectra of [2ⁿ]paracyclophane bridged by Ge.

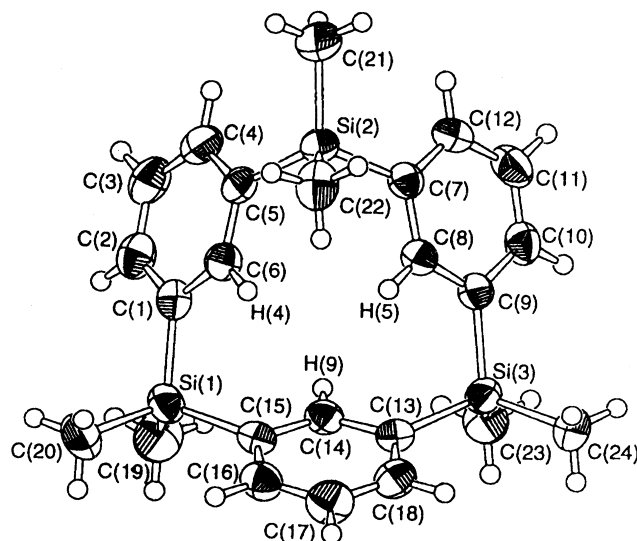


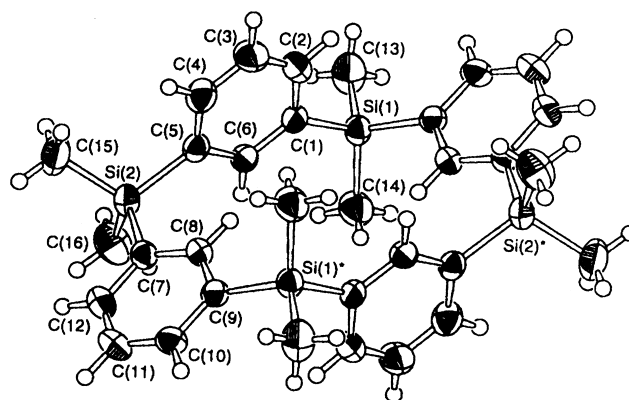
SCHEME 11

than in **12** and **17**. Hexastanna[2.2.2]paracyclophane **41** shows similar absorption to **37**.

Yoshida *et al.* have reported the preparation of trisila[1.1.1]metacyclophane (trisilacalix[3]arene, **44**) and tetrasila[1.1.1.1]metacyclophane (tetrasilacalix[4]arene, **45**) (40) (Scheme 11) and indicate conformational analyses by using semiempirical MO calculations.

A one-pot reaction gave the two different organosilicon macrocyclic compounds concomitantly. The structures of these metacyclophanes,

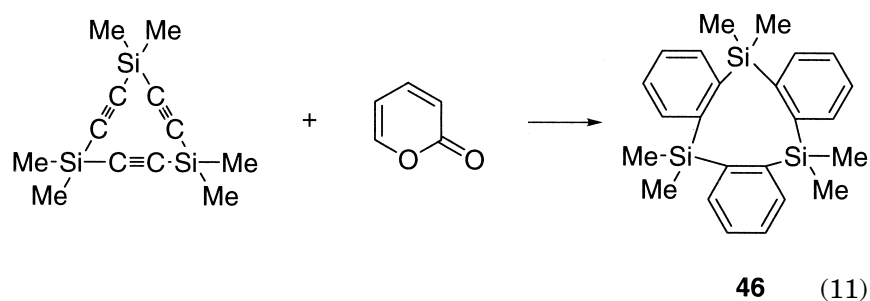
FIG. 26. Molecular structure of **44**.

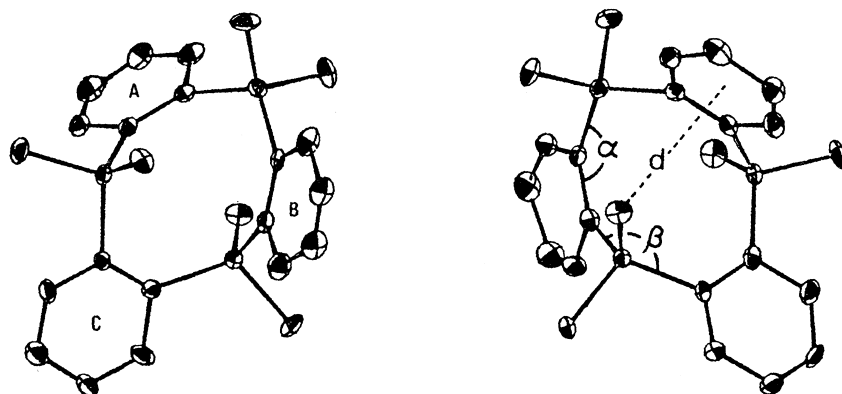
FIG. 27. Molecular structure of **45**.

44 and **45**, were determined by X-ray crystallography. As shown in Figs. 26 and 27, **44** and **45** adopted a saddle structure and a 1,2-alternate structure, respectively. The conformations of these silacalixarenes were also analyzed by semiempirical PM3 calculations, which indicate that the conformations of the silacalixarenes in the crystal do not represent an energy minimum. A completely C_3 symmetric cone structure of **44** and a 1,3-alternate structure of **45**, respectively, were estimated as the most stable conformations.

They have also examined the formation of the π -complex between the silacalixarenes and silver cation by FAB mass spectrometry. Similar π -complex formation with silver cation was observed for hexasila[2,2,2]paracyclophanes **37** (41).

Trisila[1.1.1]orthocyclophane (**46**) was prepared by the reaction of 3,3,6,6,9,9-hexamethyl-3,6,9-trisilacyclonona-1,4,7-triyn and α -pyrone. The structure of **46** determined by X-ray crystallographic analysis (Fig. 28) indicates a twisted saddle conformation (10).



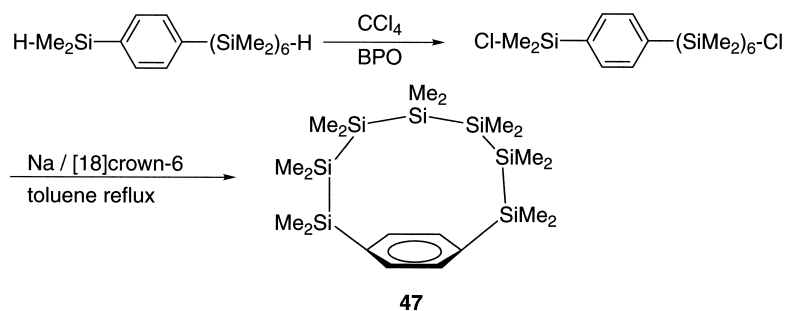
FIG. 28. Molecular structure of **46**.

VII. [n]Cyclophanes Bridged by Si

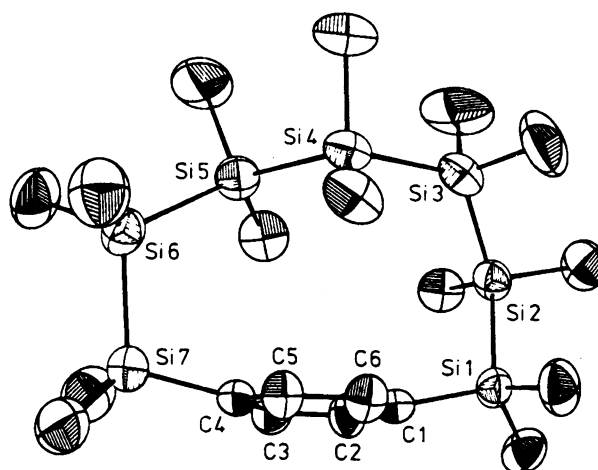
A. HEPTASILA[7]PARACYCLOPHANE

The smallest [n]paracyclophane so far isolated is the [6]paracyclophane, first prepared by Jones *et al.* in 1974. Bickelhaupt prepared and succeeded in spectroscopic characterization of [5]paracyclophane, which is stable at low temperature in solution, but not isolable. As the first example of [n] paracyclophanes bridged by heteroatom chains, Ando *et al.* reported preparation and the crystal structure of heptasila[7]paracyclophane (**47**) (42) (Scheme 12).

Reductive coupling of 1-chloro-6-[4-(chlorodimethylsilyl)phenyl]-1,1,2,2,3,3,4,4,5,5,6,6-dodecamethylhexasilane with sodium in refluxing toluene in the presence of [18]crown-6 afforded heptasila[7]paracyclophane **47** in 1.2% yield. Compound **47**, obtained as colorless crys-



SCHEME 12

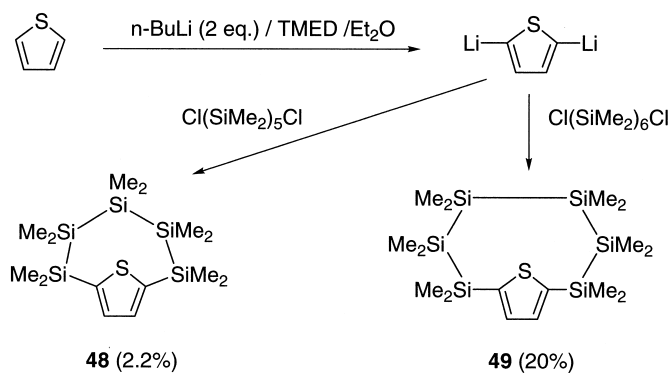
FIG. 29. Molecular structure of **47**.

tals (UV (hexane) = 248 nm ($\log \epsilon = 4.63$)), is stable toward atmospheric oxygen and moisture and does not decompose even when heated to its melting point of 88–88.5°C. Similar to the previous cases, the presence of [1.8]*crown*-6 is also essential; otherwise, only polymeric materials were obtained. In addition to NMR studies, the X-ray structural determination established the molecular structure of **47** as shown in Fig. 29. The molecule had no crystallographic symmetry.

Although the Si–Si bond lengths are normal and range between 2.336(5) and 2.371(4) Å, an alternation in the bond angles around the polysilane chain is observed. Similar to other cyclophanes, the benzene ring of **47** deformed from planarity. The strain angles α of the aromatic rings are 6.6 and 4.5°, while the bending angles β of the bridging atoms are 6.5 and 9.0°. These values are comparable with those observed in **12** and are smaller than those of the [7]paracyclophane derivative **43** and the [8]paracyclophane derivative **44**. Thus, the deformation in the benzene ring is smaller in **47** than in the analogous compounds. However, it should be noted that an appreciable increase in the deformation in the polysilane chain was observed.

C. PENTASILA[5](2,5)THIPHENOPHENE AND HEXASILA[6](2,5)THIPHENOPHANE

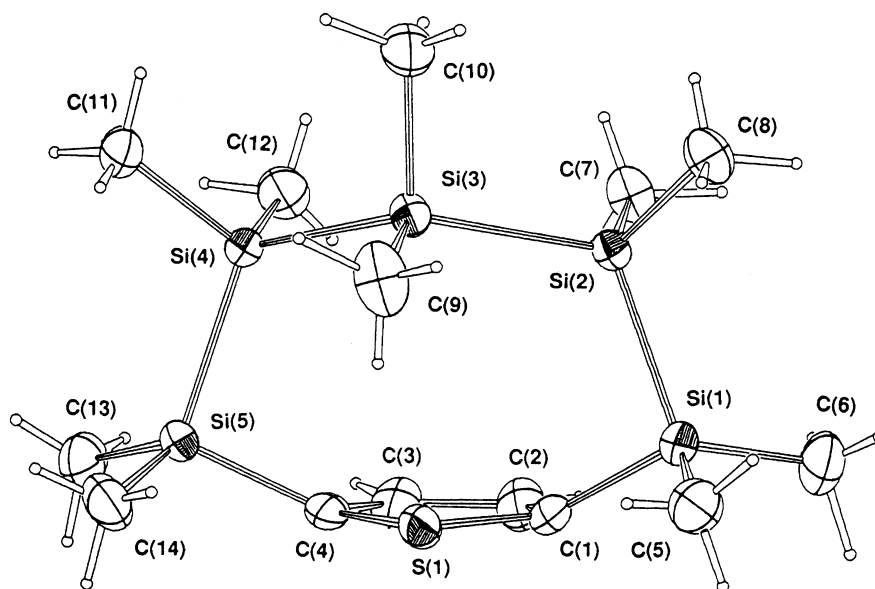
Decamethylpentasila[5](2,5)thiophenophane (**48**) and dodecamethylhexasila[6](2,5)thiophenophane (**49**) were prepared as shown in

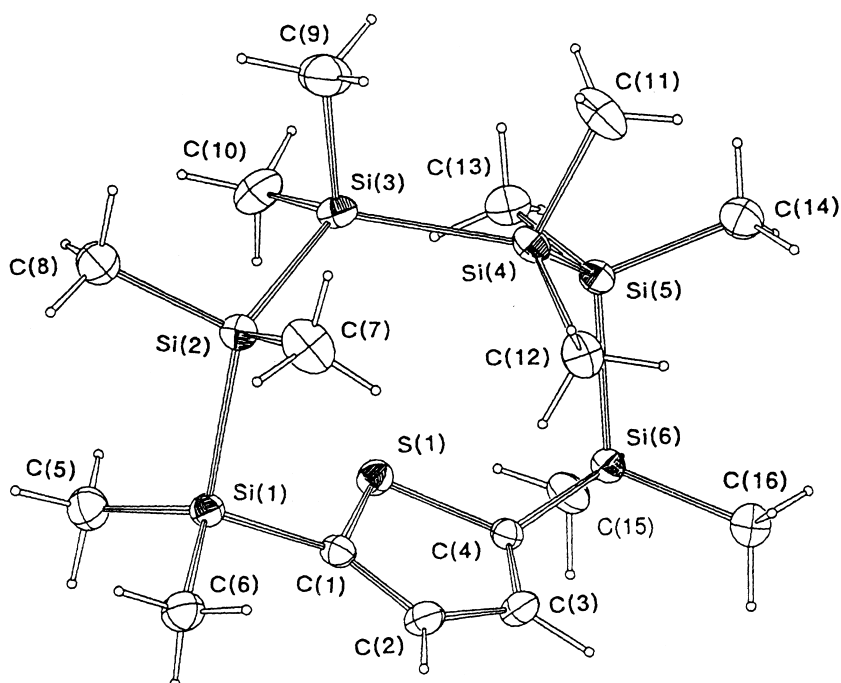


SCHEME 13

Scheme 13 (45). Major by-products are unidentified polymeric materials. Both compounds are stable to air and water.

Molecular structures of **48** and **49** are shown in Figs. 30 and 31. The strain angles α of the thiophene rings of **48** and **49** are 1.1° and 2.1° , while the bending angles β of the bridging atoms are 9.9° and 13.7° , respectively. Thiophene rings are almost planar in

FIG. 30. Molecular structure of **48**.

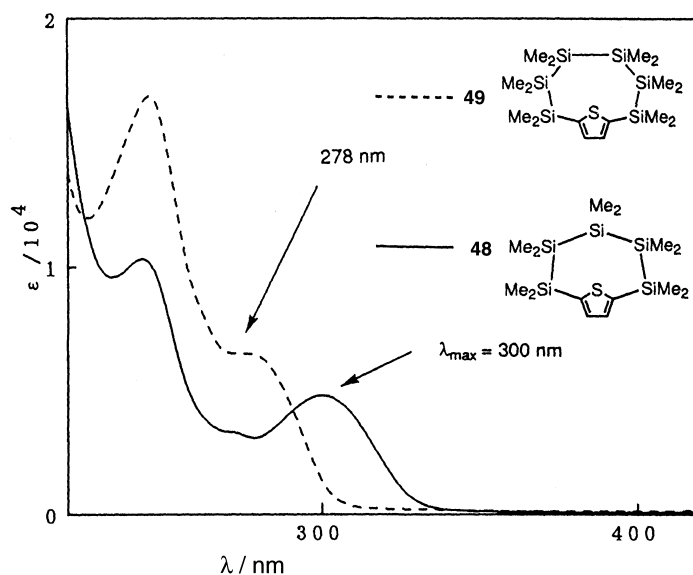
FIG. 31. Molecular structure of **49**.

both compounds, but the pentasilane chain in **49** is much more distorted.

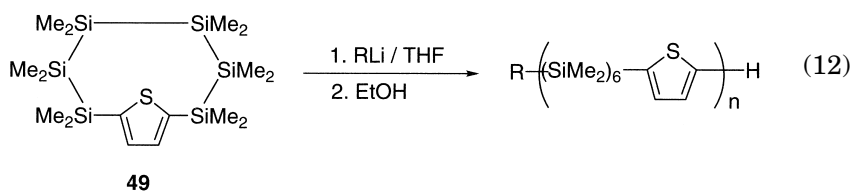
Figure 33 shows UV spectra of **48** and **49**. Since the reference compounds, 1,5-dithienyl-1,1,2,2,3,3,4,4,5,5-decamethylpentasilane and 1,6-dithienyl-1,1,2,2,3,3,4,4,5,5,6,6-dodecamethylpentasilane, have absorption maxima at 258 and 265 nm, respectively, considerable bathochromic shifts are observed for **48** and **49**.

Ring opening polymerization of hexasila[6](2,5)thiophenophane **49** was examined (46). Anionic ring opening polymerization of **49** with

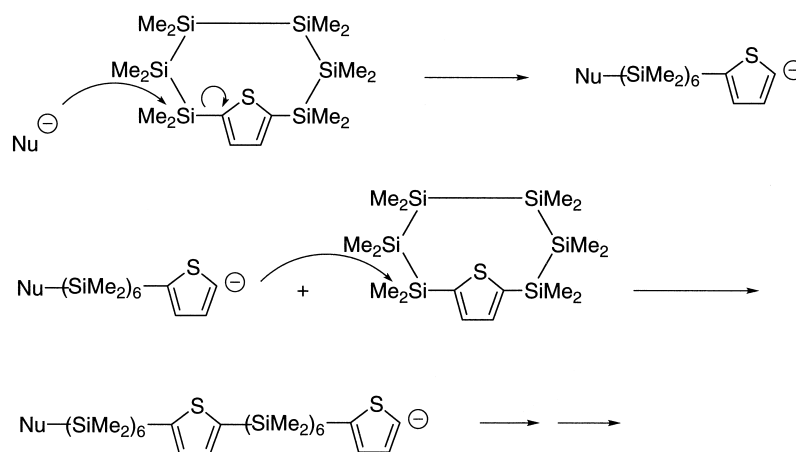
FIG. 32. Comparison of structures of **48** and **49**.



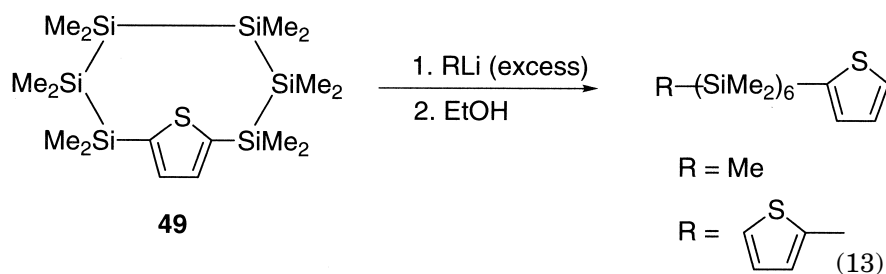
BuLi, Ph₂MeSiNa + cryptand[2.2.1], Ph₂MeSiK + cryptand[2.2.2], and 2-lithiothiophene gave poly[2,5](dodecamethyl-1,6-hexasilanylene)thienylene (**50**) in 15–76% yield. The molecular weight (M_{wt}) was 5500–9500 and $M_{\text{wt}}/M_{\text{n}}$ was 1.5–1.8.



Interestingly, ^1H NMR of **50** shows three sharp signals at 0.05, 0.10, and 0.38 ppm in addition to the signal assigned to the thiophene ring at 7.20 ppm. The ^{29}Si NMR also shows three sharp signals at -43.1 , -39.0 , and -20 ppm. These facts indicate that the polymer **50** has a perfectly regulated alternate structure. The reaction of **49** with excess RLi (R = Me and 2-thienyl), followed by quenching with ethanol, gave R-(SiMe₂)₆-substituted thiophen, exclusively.



SCHEME 14



Based on this observation, the mechanism of polymerization was proposed as indicated in Scheme 14.

It has been reported that anionic polymerization of tetraphenylgermole-*spiro*-cyclogermatetrasilane proceeds by a similar mechanism involving 2-germolyll anions as propagating species (47). In contrast, ring opening polymerization of similar silole derivatives, tetraphenylsilole-*spiro*-pentasilane, occurs in a different way involving pentacoordinate silicon species (48).

VIII. Conclusion

To date, almost all types of phanes bridged by silicon have been prepared, whereas those bridged by germanium and tin are fewer. Much remains to be explored. At present, a particular drawback of

the field is the low yield of products; new methods are needed therefore for further development. However, structures and reactions of these compounds are quite interesting and polymerization of the phanes to polymers of σ - π systems is expected to be important as a contribution to materials science of the future. The author wishes to thank all his co-workers whose names are listed in relevant references.

REFERENCES

1. Pellegrin, M. *Rec. Trav. Chim.* **1988**, *18*, 457.
2. Brown, C. J.; Farththing, A. C. *Nature (London)* **1949**, *164*, 915.
3. Cram, D. J.; Steinberg, H. *J. Am. Chem. Soc.* **1951**, *73*, 5691.
4. For reviews see: (a) Boekelheide, V. *Acc. Chem. Res.* **1980**, *13*, 65; (b) Hopf, H. *Naturwiss.* **1983**, *70*, 349. (c) The Cyclophanes. Vols. I and II; Keehn, P. M.; Rosenfeld, S. M., Eds.; Academic Press: New York, 1983; (d) "Cyclophanes;" Vögtle, F., Ed.; Springer-Verlag: Berlin, 1983.
5. Nakazaki, M.; Yamamoto, K.; Yasuhiro, M. *J. Org. Chem.* **1978**, *43*, 1041.
6. (a) Sekine, Y.; Brown, M.; Boekelheide, V. *J. Am. Chem. Soc.* **1979**, *101*, 3126. (b) Sekine, Y.; Boekelheide, V. *J. Am. Chem. Soc.* **1981**, *103*, 1777.
7. Griffin, R. W., Jr. *Chem. Rev.* **1963**, *63*, 45.
8. Vögtle, F. *Tetrahedron Lett.* **1969**, 3193.
9. Pitt, C. G.; Bock, H. *J. Chem. Soc. Chem. Commun.* **1972**, 28.
10. Sakurai, H. *Pure Appl. Chem.* **1987**, *59*, 1637.
11. (a) Sakurai, H.; Kumada, M. *Bull. Chem. Soc. Jpn.* **1964**, *37*, 1894. (b) Hague, D. N.; Prince, R. H. *Chem. Ind. (London)* **1964**, 1492, (c) Gilman, H.; Atwell, W. H.; Schebke, G. L. *J. Organomet. Chem.* **1964**, *2*, 369.
12. Sakurai, H. *J. Organomet. Chem.* **1982**, *200*, 261.
13. Sakurai, H.; Nakadaira, Y.; Hosomi, A.; Eriyama, Y.; Kabuto, C. *J. Am. Chem. Soc.* **1983**, *105*, 3359.
14. Koster-Jensen, E.; Wirz, J. *Angew. Chem. Int. Ed. Engl.* **1973**, *12*, 671.
15. Gleiter, R.; Schäfer, W.; Sakurai, H. *J. Am. Chem. Soc.* **1985**, *107*, 3046.
16. Morokuma, K. In "Organosilicon and Bioorganosilicon Chemistry;" Sakurai, H., Ed.; Ellis Horwood: Chichester UK, 1984.
17. Sakurai, H.; Hoshi, S.; Kamiya, A.; Hosomi, A.; Kabuto, C. *Chem. Lett.* **1986**, 1781.
18. Sakurai, H.; Nakadaira, Y.; Hosomi, A.; Eriyama, Y. *Chem. Lett.* **1982**, 1971.
19. Singler, R. E.; Cram, D. J. *J. Am. Chem. Soc.* **1971**, *93*, 4443.
20. Wilson, D. J.; Boekelheide, V.; Griffin, Jr. R. W. *J. Am. Chem. Soc.* **1960**, *82*, 6302.
21. Gleiter, R.; Schäfer, W.; Krennirch, G.; Sakurai, H. *J. Am. Chem. Soc.* **1988**, *110*, 4117.
22. Koenig, T.; Wielessek, R. A.; Snell, W.; Balle, T. *J. Am. Chem. Soc.* **1975**, *97*, 3225 and references therein.
23. Yatabe, T. Ph.D. Thesis, **1992**, Tohoku University.
24. Ishikawa, M.; Ni, H.; Watanabe, H.; Saheki, Y.; Nate, K. *Organometallics* **1987**, *6*, 1673.
25. Elschenbroich, C.; Hurley, J.; Massa, W.; Baum, G. *Angew. Chem. Int. Ed. Engl.* **1988**, *27*, 684

26. Hoshi, S. Unpublished results.
27. Sekiguchi, A.; Yatabe, T.; Kabuto, C.; Sakurai, H. *J. Organomet. Chem.* **1990**, *390*, C27.
28. Sakurai, H.; Yatabe, T.; Sekiguchi, A. To be published.
29. (a) Preut, Von H.; Haupt, H.-J.; Huber, F. Z. *Anorg. Allg. Chem.* **1973**, *81*, 396.
(b) Piana, H.; Kirchgassner, U.; Schubert, U. *Chem. Ber.* **1991**, *124*, 743.
30. Bondi, A. *J. Phys. Chem.* **1964**, *68*, 443.
31. Gleiter, R. *Tetrahedron Lett.* **1969**, 4453.
32. Sakurai, H.; Hoshi, S.; Kabuto, C. To be published.
33. Winberg, H. E.; Fawcett, F. S.; Mochel, W. E.; Theobald, C. W. *J. Am. Chem. Soc.* **1960**, *82*, 1428.
34. Fletcher, J. R.; Sutherland, I. O. *Chem. Commun.* **1969**, 1504.
35. Kobs, U.; Sekiguchi, A.; Kabuto, C.; Sakurai, H. 38th Symposium on Organometallic Chemistry, Kyoto, 1991; abstracts, p. 196.
36. Pahor, N. B.; Calligaris, M.; Randaccio, L. *J. Chem. Soc., Perkin II* **1978**, 42.
37. Theodore, F. J.; Seyferth, D. *Inorg. Chem.* **1968**, *7*, 1245.
38. Cram, D. J.; Montgomery, C. S.; Knox, G. R. *J. Am. Chem. Soc.* **1966**, *88*, 515.
39. Sekiguchi, A.; Yatabe, T.; Kabuto, C.; Sakurai, H. *Angew. Chem., Int. Ed. Engl.* **1989**, *28*, 757.
40. Yoshida, M.; Goto, M.; Nakanishi, F. *Organometallics* **1999**, *18*, 1465.
41. Yatabe, T. Unpublished results.
42. Ando, W.; Tsumuraya, T.; Kabe, Y. *Angew. Chem., Int. Ed. Engl.* **1990**, *29*, 778.
43. Allinger, N. L.; Walter, T. J.; Newton, M. G. *J. Am. Chem. Soc.* **1974**, *96*, 4588.
44. Newton, M. G.; Walter, T. J.; Allinger, N. L. *J. Am. Chem. Soc.* **1973**, *95*, 5652.
45. Sakurai, H.; Furuya, M.; Sakamoto, K. *Chem. Lett.*, submitted for publication.
46. Furuya, M. Unpublished results.
47. Sanji, T.; Furuya, M.; Sakurai, H. *Chem. Lett.* **1999**, 547.
48. Sanji, T.; Sakai, T.; Kabuto, C.; Sakurai, H. *J. Am. Chem. Soc.* **1998**, *120*, 4552.

SUBJECT INDEX

A

- Acid solution, beryllium, 116–125
- Acyclic molecular ionic PON compounds, crystal structure, 196–197
- Alkali metal complexes
 - with carbenes, 3–5
 - with lithium phosphinomethanides, 72–82
 - with mesityl- and supermesitylphosphides, 56–57
- Alkaline-earth amides, synthesis and characterization, 183–185
- Alkaline-earth metals, carbene complexes, 5–9
- Alkaline metal salts, beryllium ion complexes, 144–145
- Alkaline solution, beryllium, 125
- Alkoxide chemistry, Group 2 metals, 177–179
- Aluminum
 - Li, in arsandiide and phosphandiide derivatives, 274–276
 - P–O–N system, characterization, 224–225
- Aluminum arsandiides
 - NMR spectroscopy, 270
 - preparation, 267–270
 - X-ray structures, 270–272
- Aluminum phosphandiides
 - NMR spectroscopy, 270
 - preparation, 267–270
 - X-ray structures, 270–272
- Aluminum trihydride, carbene complex, 11–13
- Amino acids, interaction with beryllium ion, 153–154
- Aminocarboxylate ligands, with beryllium ion, 153–154
- Aminophosphine, complexes of lithium phosphides, 48
- Aminopolycarboxylate ligands, with beryllium ion, 154
- Antimony, Li/Sb-mixed clusters of arsandiides and phosphandiides, 276–277
- Arsandiides
 - Al, Ga, and In
 - NMR spectroscopy, 270
 - preparation, 267–270
 - X-ray structures, 270–272
 - Li/Al-mixed derivatives, 274–276
 - Li/Sn-mixed derivatives, 276–277
 - mixed-metalated
 - dynamic processes in solution, 277–278
 - X-ray structure, 278–280
- Arsanes, primary
 - dilithium derivatives, synthesis and complexation, 242–243
 - dimeric $\text{Na}_4\text{As}_{12}$ cluster
 - NMR and cryoscopy, 255–257
 - X-ray structure, 252–253
 - disodium derivatives, 244–246
 - fluoride-complexed clusters
 - NMR and cryoscopy, 253–255
 - X-ray structure, 246–251
 - Li_2O -complexed clusters
 - NMR and cryoscopy, 253–255
 - X-ray structure, 246–251
 - lithium-deficient mixed-valent clusters, synthesis, 243–244
 - mixed-valent clusters
 - NMR and cryoscopy, 255
 - X-ray structure, 251–252
 - Na_2 -complexed clusters, NMR and cryoscopy, 253–255
 - Na_2O -complexed clusters, X-ray structure, 246–251
 - reactivity

- Li₂O-filled clusters *vs.* mixed-valent clusters, 257
 - Na₄-dication cluster, 257–258
 - tetrasodium-dication cluster, 244–246
 - NMR and cryoscopy, 255–257
 - X-ray structure, 252–253
 - Arsenide complexes, 67–70
 - Arsenidene, carbene complex, 20–21
 - Arsinediide complexes, 67–70
 - Arsinomethanides, nonexistence, 87–89
 - Aurin tricarboxylate, complex with beryllium, 152–153
- B**
- Barium aryloxides, characterization, 180–181
 - Barium bis-tetramethylheptanedionate, synthesis and characterization, 187
 - Benzyllithium complex, phosphine-substituted, preparation, 92
 - Beryllium
 - health and safety aspects, 163–164
 - hydrolysis
 - enthalpy and entropy, 128–129
 - precipitation equilibria, 129–131
 - soluble hydrolysis products
 - acid solutions, 116–125
 - alkaline solutions, 125
 - structures, 125–128
 - properties, 115
 - Beryllium ion
 - aliphatic hydroxycarboxylate ligands, 146–149
 - aminocarboxylate ligands, 153–154
 - aminopolycarboxylate ligands, 154
 - aromatic hydroxycarboxylate ligands, 149–153
 - dihydroxy ligands, 155–156
 - existence, 115–116
 - interaction with inorganic ligands
 - fluorides, 131–135
 - inorganic anions, 135–136
 - interaction with organic ligands
 - biscarboxylate ligands, 138–145
 - monocarboxylate ligands, 136–138
 - organic ligands, 161–163
 - phosphonate ligands, 157–160
 - 2,2'-Bipyridyl adducts, Bi amines, 320–322
 - Bis(amino)silabismetidine heterocycle, geometry, 319–320
 - Bis(carbene) complex, isolation, 7–8
 - Biscarboxylate ligands, interaction with beryllium ion, 138–145
 - 1,4-Bis(chlorodimethylsilyl)benzene, reductive coupling with sodium, 366–369
 - Bismuth acetate complexes, preparation, 301–302
 - Bismuth alkoxide carboxylate complexes, preparation, 328–331
 - Bismuth alkoxide complexes
 - chelate complexes, 294–295
 - coordination, 291–292
 - fluorinated compounds, 292–293
 - geometries, 293–294
 - halide substitution, 294
 - preparation, 290–291
 - Bismuth alkoxidthiolate complexes, preparation, 337–340
 - Bismuth amide complexes, preparation, 318–320
 - Bismuth amine complexes
 - 2,2'-bipyridyl adducts, 320–322
 - dithiocarbamate complex, 322–323
 - formation constants, 320
 - nitrate complexes, 324–325
 - 1,10-phenanthroline adducts, 323–324
 - Bismuth aminoalkoxide complexes, preparation, 346–349
 - Bismuth aminocarboxylate complexes, preparation, 341–346
 - Bismuth aminothioliolate complexes, preparation, 333–337
 - Bismuth arsine complexes, preparation, 328
 - Bismuth azathioliolate complexes, preparation, 333–337
 - Bismuth carboxylate complexes, preparation, 300–302
 - Bismuth dicyanoethylene-1,2-dithiolate complexes, 299–300
 - Bismuth diselenocarbamate complexes, preparation, 309
 - Bismuth diselenocarboxylate complexes, preparation, 309
 - Bismuth dithiocarbamate complexes, preparation, 303–309, 322–323

- Bismuth dithiocarboxylate complexes,
 preparation, 303–309
 Bismuth dithioxanthate complexes, prepa-
 ration, 303–309
 Bismuth ether complexes, preparation,
 309–313
 Bismuth formate complexes, preparation,
 300–301
 Bismuth hydroxyamine complexes, prepa-
 ration, 346–349
 Bismuth hydroxycarboxylate complexes,
 preparation, 328–331
 Bismuth hydroxythiolate complexes,
 preparation, 337–340
 Bismuth iminothiolate complexes, prepa-
 ration, 333–337
 Bismuth ketoalkoxide complexes, prepa-
 ration, 331–333
 Bismuth ketone complexes, preparation,
 315–317
 Bismuth ketothiolate complexes, prepara-
 tion, 337–340
 Bismuth nitrate complexes
 crown ether complex, 311–312
 nitrate anion substitution, 311
 Bismuth phosphine complexes, prepara-
 tion, 325–328
 Bismuth selenolate complexes, prepara-
 tion, 300
 Bismuth thiocarboxylate complexes, prep-
 aration, 302–303
 Bismuth thioether complexes, prepara-
 tion, 313–314
 Bismuth thiolate complexes
 chlorobismuthdithiolates, 298–299
 from dithiols, 298
 MS studies, 295, 297
 overthiolation, 297–298
 preparation, 295
 Bismuth thiolatocarboxylate complexes,
 preparation, 340–341
 Bismuth thione complexes, preparation,
 315–317
 Bromium, Bi complex, 306
 2-Bromo-2,3-dihydro-1*H*-1,3,2-
 diazaborole, reaction with carbenes,
 15
n-Butyl lithium, reaction with 2,6-
 (Me₂PCH₂)₂C₆H₃Br, 90–92
- C**
- Calcium, Ca/Sn-mixed clusters of arsandi-
 ides and phosphandiides, 276–277
 Carbanions, center in phosphinometha-
 nide ligands, 77–78
 Carbenes
 alkali metal complexes, 3–5
 alkaline earth metal complexes, 5–9
 arsenidene complex, 20–21
 germanium halide complexes, 17–19
 germanium tin complexes, 19–20
 Group 13 trialkyl complexes, 13–16
 Group 13 triaryl complexes, 13–16
 Group 13 trihalide complexes, 9–11
 Group 13 trihydride complexes, 11–13
 halogen complexes, 25–28
 Hg complexes, 5–9
 hydrogen complexes, 3–5
 lead amide complexes, 19–20
 organosilicon complexes, 16–17
 organotin halide complexes, 17–19
 phosphinidene complex, 20–21
 phosphorane complex, 22
 selenium complexes, 22–25
 silicon halide complexes, 16–17
 sulfur complexes, 22–25
 tellurium complexes, 22–25
 tin halide complexes, 17–19
 Zn complexes, 5–9
 Carbon-donor ligands, phosphine-func-
 tionalized, synthesis, 89–93
 Charge-delocalized ligands
 arsinomethanides, 87–89
 charge stabilization, 70–71
 dianionic phosphinomethanides, 84–85
 heavier alkali metal phosphinometha-
 nides, 82–84
 heterometallic phosphinomethanides,
 85–87
 iminophosphides–phosphinoamides,
 87–89
 lithium phosphinomethanides, 72–82
 phosphinomethanides, 72
 polyanionic phosphinomethanides,
 84–85
 Charge-localized ligands
 arsenides, 67–70
 arsinediides, 67–70

- heterometallic alkali metal (di)organo-phosphides, 64–67
 - heterometallic alkali metal phosphine-diides, 64–67
 - homometallic alkali metal phosphine-diides, 61–64
 - homometallic alkali metal polyphosphides, 61–64
 - homometallic heavier alkali metal (di)-organophosphides, 51–61
 - homometallic lithium (di)organophosphides, 38–51
 - phosphides, 35–37
 - phosphinediides, 35–37
 - Chemical vapor deposition, Group 2 element precursors
 - alkaline-earth amides, 183–185
 - barium aryloxides, 180–181
 - barium bis-tetramethylheptanedionate, 187
 - categories, 174–175
 - components, 173–174
 - definition, 173
 - β -ketoiminate ligand, 189–190
 - metallocene compounds, 182–183
 - organomagnesium reagent preparation, 181–182
 - semiconductors, 175–177
 - superconductors, 175–177
 - tetraglyme with β -diketones, 187–189
 - 2,2,6,6-tetramethylheptanedionate, 185
 - Chlorobismuthdithiolates, characterization, 298–299
 - Chlorophosphine, metalation, 50–51
 - Chlorophosphole, reduction, 97–98
 - Complexones, with beryllium ion, 154
 - Conformation, tri- and tetrametaphosphimate ions, 200–201
 - Cristobalite-type PON, phosphorus oxynitride, 212
 - Crown ethers
 - complex with bismuth nitrate, 311–312
 - halide, Bi complexes, 312–313
 - Crown thioethers, Bi complexes, 313–314
 - Cryoscopy, phosphoranes and arsanes, complexed clusters, 253–255
 - Crystallization, silylarylphosphide, 46
 - $\text{Cs}_3\text{M}^{\text{II}}_2\text{P}_6\text{O}_{17}\text{N}$, crystal structure, 221–222
 - CVD, *see* Chemical vapor deposition
 - Cyclic PON compounds
 - phosphimatometallates, 206–208
 - polymetaphosphimates, 197–200
 - tetrametaphosphimate
 - crystal structures, 204–206
 - ion conformations, 200–201
 - trimetaphosphimate
 - crystal structures, 201–204
 - ion conformations, 200–201
 - trimetaphosphimatometallate crystal structures, 208–209
 - Cyclopentadienide ligand, in organometallic chemistry, 182
 - [n]Cyclophanes, Si-bridged, heptasila[7]-paracyclophane, 400–401
 - Cyclopropenylidene, complexes of Ge, Sn and Pb amides, 19–20
- D**
- Decamethylpentasila[5](2,5)thiophenophane, preparation, 401–402
 - Dianionic phosphinomethanides, synthesis, 84–85
 - 2,6-Di-*tert*-butyl 4-methylphenol, reaction with strontium metal, 179–180
 - Dicarboxylates, interaction with beryllium ion, 139
 - Dicopper phosphandiides
 - preparation, 258–259
 - X-ray structure, 259
 - Diethyl magnesium, reaction with carbenes, 5–6
 - Diethyl zinc, reaction with carbenes, 5–6
 - Differential pulse polarography, for Bi polyamine complex formation constants, 320
 - Dihydroxy ligands, with beryllium ion, 155–156
 - Diisopropylaniline, lithiated, reaction with bismuth chloride, 318–319
 - 1,3-Diisopropyl-4,5-dimethylimidazol-2-ylidene, reaction with indium trihalides, 10–11
 - β -Diketonates
 - isolation and characterization, 185–187
 - with tetraglyme, 187–189
 - Dilithiation, primary phosphanes and arsanes, 242–243

- Diphosphine diamide ligand, complex
with lithium, 95
- Diphosphino-phosphide complexes, with
lithium, 50
- Diphospholide complex, structure, 98
- Disodium, derivatives of phosphanes and
arsanes, 244–246
- Dithiols, in bismuth thiolate synthesis,
298
- Dodecamethylhexasila[6](2,5)thiopheno-
phane, preparation, 401–402
- E**
- Electrical resistance, in superconductors,
176
- Electronic materials, CVD, Group 2 ele-
ment precursors
barium bis-tetramethylheptanedionate,
187
categories, 174–175
CVD components, 173–174
CVD definition, 173
 β -ketoiminate ligand, 189–190
photonic devices, 184
semiconductors, 175–177
superconductors, 175–177
tetraglyme with β -diketones, 187–189
2,2,6,6-tetramethylheptanedionate,
185
- Electronics, pnictides, 237–240
- Enthalpy, beryllium hydrolysis, 128–129
- Entropy, beryllium hydrolysis, 128–129
- Equilibrium constants, notation,
112–114
- F**
- Fluorides
complexed clusters of primary phos-
phanes and arsanes
NMR and cryoscopic measurement,
253–255
X-ray structure, 246–251
interaction with beryllium ion,
131–135
- Fluorosilyl groups, substituted lithium
phosphides, 47–48
- G**
- Gallium arsandiides
NMR spectroscopy, 270
preparation, 267–270
X-ray structures, 270–272
- Gallium phosphandiides
NMR spectroscopy, 270
preparation, 267–270
X-ray structures, 270–272
- Gallium trihydride, carbene complex,
11–13
- Germanium amides, cyclopropenylidene
complexes, 19–20
- Germanium-bridged [2ⁿ]paracyclophanes,
395–399
- Germanium halides, carbene complexes,
17–19
- Group 1, carbene complexes, 3–9
- Group 2
alkoxide chemistry, 177–179
carbene complexes, 3–9
- Group 2 element precursors, CVD
alkaline-earth amides, 183–185
barium aryloxides, 180–181
barium bis-tetramethylheptanedionate,
187
categories, 174–175
components, 173–174
definition, 173
 β -ketoiminate ligand, 189–190
metallocene compounds, 182–183
organomagnesium reagent preparation,
181–182
semiconductors, 175–177
superconductors, 175–177
tetraglyme with β -diketones, 187–189
2,2,6,6-tetramethylheptanedionate, 185
- Group 12, carbene complexes, 3–9
- Group 13, carbene complexes
trialkyls, 13–16
triaryls, 13–16
trihalides, 9–11
trihydrides, 11–13
- Group 14 elements, bridged [2.2]para-
cyclophanes
structure comparison, 375–377
through-bond interactions, 377–379
through-space interactions, 377–379

- Group 15
 arsenidene carbene complex, 20–21
 phosphinidene carbene complex, 20–21
 phosphorane carbene complex, 22
- H**
- Halide crown ether, Bi complexes,
 312–313
 Halides, substitution on bismuth alkox-
 ides, 294
 Halogens, carbene complexes, 25–28
 Health, beryllium compounds, 163–164
 Heavier alkali metal phosphinometha-
 nides, complexes, 82–84
 Heptasila[7]paracyclophane, preparation,
 400–401
 Heterometallic alkali metal (di)organo-
 phosphides, 64–67
 Heterometallic alkali metal phosphinedi-
 ides, metathesis reactions, 64–67
 Heterometallic phosphinomethanides,
 synthesis, 85–87
 Heterometallic phospholide complex, syn-
 thesis, 99
 Hexachlorocyclotriphosphazene, hydroly-
 sis, 198–199
 Hexadenticity, bismuth complexes, 344
 Hexasila[2.2.2](1,3,5)cyclophane
 molecular structure, 392–394
 preparation, 391–392
 properties, 391–392
 UV spectrum, 394
 1,2,9,10,17,18-Hexasila[2.2.2](1,3,5)
 cyclophane
 molecular structure, 392–394
 preparation, 391–392
 properties, 391–392
 UV spectrum, 394
 Hexasila[6](2,5)thiophenophane
 molecular structure, 402–403
 NMR studies, 404–405
 preparation, 401–402
 UV spectrum, 403
 Homometallic alkali metal phosphinedi-
 ide complexes, 61–64
 Homometallic alkali metal polyphosphide
 complexes, 61–64
 Homometallic heavier alkali metal (di)or-
 ganophosphides, synthesis, 51–61
- Homometallic lithium (di)organophos-
 phides, synthesis, 38–51
 Hydrogen, carbene complexes, 3–5
 Hydrolysis
 beryllium
 enthalpy and entropy, 128–129
 precipitation equilibria, 129–131
 soluble hydrolysis products
 acid solutions, 116–125
 alkaline solutions, 125
 structures, 125–128
 hexachlorocyclotriphosphazene,
 198–199
 octachlorocyclotetraphosphazene,
 198–199
 Hydroxycarboxylate ligands, with beryl-
 lium ion
 aliphatic ligands, 146–149
 aromatic ligands, 149–153
- I**
- Imidazole-2-thione, carbene complex,
 22–23
 Iminophosphides–phosphinoamide com-
 plexes, 87–89
 Indium arsandiides
 NMR spectroscopy, 270
 preparation, 267–270
 X-ray structures, 270–272
 Indium(III) halides, carbene complexes,
 9–11
 Indium phosphandiides
 NMR spectroscopy, 270
 preparation, 267–270
 X-ray structures, 270–272
 Infrared spectroscopy, tri- and tetrameta-
 phosphimates, 199–200
 Inorganic anions, interaction with beryl-
 lium ion, 135–136
 Inorganic ligands, interaction with beryl-
 lium ion
 fluorides, 131–135
 inorganic anions, 135–136
 Iodine, Bi complex, 306
- K**
- β -Ketoiminate ligand, synthesis,
 189–190

L

- Lead amides, cyclopropenylidene complexes, 19–20
- Lithium
- in arsendiides and phosphandiides
 - Li/Al derivatives, 274–276
 - Li/Sb derivatives, 276–277
 - Li/Sn derivatives, 276–277
 - complex with diphosphine diamide ligand, 95
 - deficient phosphanes and arsanes, synthesis, 243–244
 - diphosphino–phosphide complexes, 50
 - reaction with tetraphosphafulvalene, 99
 - treatment of trichlorosilanes, 99–100
- Lithium diphenylphosphide, characterization, 39–41
- Lithium diphosphinomethanides, structures, 76–77
- Lithium monophosphinomethanide complexes, 74
- Lithium oxide, complexed clusters of primary phosphanes and arsanes
- comparison to mixed-valent clusters, 257
 - NMR and cryoscopy, 253–255
 - X-ray structures, 246–251
- Lithium phosphides
- aminophosphine-functionalized complexes, 48
 - fluorosilyl-substituted complexes, 47–48
 - isolation, 41–44
 - Si-substituted complexes, 46
- Lithium phosphinomethanides, alkali metal complex, 72–82

M

- Magnesium phosphandiides
- synthesis
 - solvated derivative, 261
 - solvent-free derivative, 261
 - X-ray structures, 261–262
- Magnetically levitated trains, superconductors, 176–177
- Magnetic resonance imaging, superconductors, 176–177
- Main group metal, pnictides, electronics and structure, 237–240
- Malonato complex, beryllium ion, 139, 144
- Mass spectrometry
- bismuth thiolates, 295, 297
 - octamethyltetragerma[2.2]paracyclophane, 370
- Measurement methods, notation, 114
- Meissner effect, in superconductors, 176
- 2,6-(Me₂PCH₂)₂C₆H₃Br, reaction with *n*-butyl lithium, 90–92
- Mercury, carbene complexes, 5–9
- Mesitylphosphides, alkali metal complexes, 56–57
- Metacyclophane, preparation, 363–369
- Metalation, chlorophosphine, 50–51
- Metal halides, metathesis reactions with alkali metal complexes, 64–67
- Metallocenes, oligomeric nature, 182–183
- Metals, as CVD precursors, 174–175
- Metathesis reactions, alkali metal complexes and metal halides, 64–67
- M^I₂M^{III}P₃O₈N, preparation, 222–223
- M^I₂M^{II}₂P₃O₉N, preparation, 219–220
- M^I₃M^{III}P₃O₉N, preparation, 219–220
- Moganite-type PON, phosphorus oxynitride, 215–216
- Molecular PON compounds, crystal structures, 195
- Molecular structure
- 1,2,9,10,17,18-hexasila[2.2.2](1,3,5) cyclophane, 392–394
 - hexasila[6](2,5)thiophenophane, 402–403
 - octamethyltetragerma[2.2]paracyclophane, 370–371
 - pentasila[5](2,5)thiophenophane, 402–403
 - tetrasila[2.2](2,5)heterophanes, 384–389
 - 1,2,9,10-tetrastanna[2.2] paracyclophane, 372–375
 - tin(II) metalated phosphandiides, 265–267
- Monocarboxylate ligands, interaction with beryllium ion, 136–138

Mono-dithiocarbamatedihalo complex,
with Bi, 307
Monomeric barium bis-alkoxide, first ex-
ample, 178–179
MS, *see* Mass spectrometry

N

$\text{Na}_3\text{AlP}_3\text{O}_9\text{N}$, preparation, 219–220
 $\text{Na}_4\text{As}_{12}$, dimeric cluster, phosphoranes
and arsanes, 252–253, 255–257
 $\text{Na}_2\text{Mg}_2\text{P}_3\text{O}_9\text{N}$, preparation, 219–220
Nitrate anions, substitution on bismuth
nitrate, 311
Nitrate complexes, Bi, 324–325
Nitridooxophosphate PON
Al–P–O–N system, 224–225
 $\text{Cs}_3\text{M}^{\text{II}}_2\text{P}_6\text{O}_{17}\text{N}$, 221–222
general considerations, 209–210
 $\text{M}^{\text{I}}_2\text{M}^{\text{II}}\text{P}_3\text{O}_8\text{N}$, 222–223
 $\text{M}^{\text{I}}_2\text{M}^{\text{II}}_2\text{P}_3\text{O}_9\text{N}$, 219–220
 $\text{M}^{\text{I}}_3\text{M}^{\text{III}}\text{P}_3\text{O}_9\text{N}$, 219–220
PON sodalite structure, 217–219
Nitrogen-donor ligands, phosphine-func-
tionalized, synthesis, 94–95
Nonmetals, as CVD precursors, 174–175
Nuclear magnetic resonance
Al, Ga, and In arsandiides and phos-
phandiides, 270
hexasila[6](2,5)thiophenophane,
404–405
octamethyltetragerma[2.2]paracyclo-
phane, 370
octamethyl-1,2,8,9-tetrasilasil[2.2](2,5)
furanophane, 382–383
octamethyl-1,2,8,9-tetrasilasil[2.2](2,5)
thiophenophane, 382–383
pentasila[5](2,5)thiophenophane,
404–405
phosphoranes and arsanes
complexed clusters, 253–255
dimeric $\text{Na}_4\text{As}_{12}$ cluster, 255–257
mixed-valent clusters, 255
superconductors, 176–177
tetrasilasil[2.2](2,5)heterophanes,
384–389
tin(II) metalated phosphandiides,
265

Nucleophilicity, phosphinomethanide
carbanion center, 77–78

O

Octachlorocyclotetraphosphazene, hydro-
lysis, 198–199
Octamethyltetragerma[2.2]paracyclo-
phane
MS, 370
NMR, 370
synthesis, 369–370
X-ray diffraction study, 370–371
3,3,4,4,7,7,8,8-Octamethyl-3,4,7,8-
tetrasilacycloocta-1,5-diyne, 362
Octamethyl-1,2,8,9-tetrasilasil[2.2](2,5)
furanophane
NMR studies, 382–383
reactions, 389–390
UV spectrum, 380, 382
1,1,2,2,9,9,10,10-Octamethyl-1,2,9,10-
tetrasilasil[2.2]paracyclophane
photoelectron spectrum, 366
preparation, 363–364, 366–369
 $\sigma(\text{Si-Si})-\pi$ interaction, 365
structure, 364–365
Octamethyl-1,2,8,9-tetrasilasil[2.2](2,5)
thiophenophane
NMR studies, 382–383
UV spectrum, 380, 382
Octamethyltetrastanna[2.2]paracyclo-
phane, preparation, 371–372
Organic ligands
abbreviations, 287–289
interaction with beryllium ion,
161–163
biscarboxylate ligands, 138–145
monocarboxylate ligands, 136–138
Organomagnesium reagents, preparation,
181–182
Organometallic chemistry, with cyclop-
tadieneide ligands, 182
Organosilicon compounds
carbene complexes, 16–17
as lithium phosphide substituent,
44–46
Organotin halides, carbene complexes,
17–19
Orthocyclophane, preparation, 363–369
Oxalato complex, beryllium ion, 139, 144

Oxygen-donor ligand, phosphine-functionalized, synthesis, 96–97
 Oxynitride P_4N_6O , composition, 216–217

P

- [2.2]Paracyclophanes
 Group 14-bridged
 structure comparison, 375–377
 through-bond interactions, 377–379
 through-space interactions, 377–379
 structure, 364–365
 [2ⁿ]Paracyclophanes, Si, Ge, and Sn-bridged compounds, 395–399
 [3.3]Paracyclophanes, structure, 364–365
 Pentamethyl cyclopentadienide pyrazine barium compound, 183
 Pentasila[5](2,5)thiophenophane
 molecular structure, 402–403
 NMR studies, 404–405
 preparation, 401–402
 UV spectrum, 403
 1,10-Phenanthroline adducts, Bi, 323–324
 Phosphandiides
 Al, Ga, and In
 NMR spectroscopy, 270
 preparation, 267–270
 X-ray structures, 270–272
 Li/Al-mixed derivatives, 274–276
 Li/Sn-mixed derivatives, 276–277
 mixed-metalated
 dynamic processes in solution, 277–278
 X-ray structure, 278–280
 Phosphanes, primary
 dilithium derivatives, synthesis and complexation, 242–243
 dimeric Na_4As_{12} cluster
 NMR and cryoscopy, 255–257
 X-ray structure, 252–253
 disodium derivatives, 244–246
 fluoride-complexed clusters
 NMR and cryoscopy, 253–255
 X-ray structure, 246–251
 Li_2O -complexed clusters
 NMR and cryoscopy, 253–255
 X-ray structure, 246–251
 lithium-deficient mixed-valent clusters, synthesis, 243–244
 mixed-valent clusters
 NMR and cryoscopy, 255
 X-ray structure, 251–252
 Na_2O -complexed clusters
 NMR and cryoscopy, 253–255
 X-ray structure, 246–251
 reactivity
 Li_2O -filled clusters *vs.* mixed-valent clusters, 257
 Na_4 -dication cluster, 257–258
 tetrasodium-dication cluster, 244–246
 NMR and cryoscopy, 255–257
 X-ray structure, 252–253
 Phosphides
 heterometallic alkali metal (di)organo-phosphides, 64–67
 homometallic alkali metal phosphinidides, 61–64
 homometallic heavier alkali metal (di)-organophosphides, 51–61
 homometallic lithium (di)organophosphides, 38–51
 preparation, 35–37
 Phosphimatometallates, as cyclic PON compounds, 206–208
 Phosphine, substituted benzyllithium complex, 92
 Phosphinidides
 heterometallic alkali metal phosphinidides, 64–67
 homometallic alkali metal polyphosphides, 61–64
 preparation, 35–37
 Phosphine-functionalized C-donor ligands, preparation, 89–93
 Phosphine-functionalized N-donor ligands, preparation, 94–95
 Phosphine-functionalized O-donor ligands, preparation, 96–97
 Phosphine-functionalized S-donor ligands, preparation, 96–97
 Phosphine-functionalized thiolate complex, preparation, 97
 Phosphinidene, carbene complex, 20–21
 Phosphinoamides–iminophosphides, development, 71
 Phosphinomethanides
 arsinomethanides, 87–89
 development, 71
 dianionic phosphinomethanides, 84–85

- heavier alkali metal phosphinomethanides, 82–84
 - heterometallic phosphinomethanides, 85–87
 - lithium phosphinomethanides, 72–82
 - polyanionic phosphinomethanides, 84–85
 - preparation, 72
 - Phosphole tetramer, reaction with Na and K, 98–99
 - Phosphonate ligands, with beryllium ion, 157–160
 - Phosphorane, carbene complex, 22
 - Phosphorus oxynitride PON
 - cristobalite-type PON, 212
 - general considerations, 209–210
 - moganite-type PON, 215–216
 - preparation, 211–212
 - quartz-type PON, 212–214
 - Photoelectron spectrum, 1,1,2,2,9,9,10,10-octamethyl-1,2,9,10-tetrasil[2.2]
 - paracyclophane, 366
 - Photonic devices, from alkaline-earth amides, 184
 - pnictides
 - main group metal, electronics and structure, 237–240
 - structure–reactivity relationships, 240–241
 - Polyamine complex, with Bi, 320
 - Polyanionic phosphinomethanides, preparation, 84–85
 - Polymetaphosphimates, as PON compounds, 197–200
 - PON compounds
 - acyclic molecular ionic, 196–197
 - Al–P–O–N system, characterization, 224–225
 - cristobalite-type, 212
 - cyclic, *see* Cyclic PON compounds
 - moganite-type, 215–216
 - molecular, 195
 - Na–P–O–N system, composition, 223–224
 - nitridooxophosphate, 209–210
 - phosphorus oxynitride, 212
 - quartz-type, 212–214
 - sodalites, structure, 217–219
 - solid-state, *see* Solid-state PON compounds
 - Potassium phosphide, complex with alkali metals, 51–55
 - Potassium reactions
 - with phosphole tetramer, 98–99
 - with tetraphosphafulvalene, 99
 - Precipitation, equilibria for beryllium hydrolysis, 129–131
 - Pyridone, complex with beryllium ion, 161–163
 - Pyrimidinedione, complex with beryllium ion, 161–163
 - Pyrone, complex with beryllium ion, 161–163
- Q**
- Quartz-type PON, phosphorus oxynitride, 212–214
- R**
- Raman spectroscopy, tri- and tetrametaphosphimates, 199–200
 - Reductive coupling, for 1,1,2,2,9,9,10,10-octamethyl-1,2,9,10-tetrasil[2.2]
 - paracyclophane preparation, 366–369
- S**
- Safety, beryllium compounds, 163–164
 - Salicylic acid, ligands with beryllium ion, 149–153
 - Selenium, carbene complexes, 22–25
 - Semiconductors, definition, 175–177
 - σ – π mixing, 3,4,7,8-tetrasilacycloocta-1,5-diyne, 361–362
 - σ (Si–Si)– π interaction, 1,1,2,2,9,9,10,10-octamethyl-1,2,9,10-tetrasil[2.2]
 - paracyclophane, 365
 - Silicon
 - bridged [n]cyclophanes
 - heptasila[7]paracyclophane, 400–401
 - hexasila[6](2,5)thiophenophane, 401–405
 - pentasila[5](2,5)thiophenophane, 401–405
 - bridged [2ⁿ]paracyclophanes, 395–399

- Silicon halides, carbene complexes, 16–17
- Silylarylphosphide, crystallization, 46
- Sodium
 Na–P–O–N system, composition, 223–224
 reaction with phosphole tetramer, 98–99
- Sodium oxide, complexed clusters of primary phosphanes and arsanes
 NMR and cryoscopy, 253–255
 X-ray structure, 246–251
- Sodium phosphide, synthesis and characterization, 51–55
- Solid-state PON compounds
 Na–P–O–N system, 223–224
 nitridooxophosphate
 Al–P–O–N system, 224–225
 $\text{Cs}_3\text{M}^{\text{II}}_2\text{P}_6\text{O}_{17}\text{N}$, 221–222
 general considerations, 209–210
 $\text{M}^{\text{I}}_2\text{M}^{\text{II}}\text{P}_3\text{O}_8\text{N}$, 222–223
 $\text{M}^{\text{I}}_2\text{M}^{\text{II}}_2\text{P}_3\text{O}_9\text{N}$, 219–220
 $\text{M}^{\text{I}}_3\text{M}^{\text{III}}\text{P}_3\text{O}_9\text{N}$, 219–220
 PON sodalite structure, 217–219
 oxynitride $\text{P}_4\text{N}_6\text{O}$, 216–217
 phosphorus oxynitride
 cristobalite-type PON, 212
 general considerations, 209–210
 moganite-type PON, 215–216
 preparation, 211–212
 quartz-type PON, 212–214
- Solutions
 arsandiide and phosphandiide dynamic processes, 277–278
 beryllium
 acid solution, 116–125
 alkaline solution, 125
- Strontium metal, reaction with 2,6-di-*tert*-butyl 4-methylphenol, 179–180
- Structure–reactivity relationships, pnictides, 240–241
- Substituent effects, in malonato complexes, 144
- Succinato complex, beryllium ion, 139, 144
- Sulfur, carbene complexes, 22–25
- Sulfur-donor ligand, phosphine-functionalized, synthesis, 96–97
- Superconductors, definition, 175–177
- Supermesitylphosphides, alkali metal complexes, 56–57
- ### T
- Tellurium, carbene complexes, 22–25
- Tertiary phosphine-functionalized ligands
 C-donor ligands, 89–93
 N-donor ligands, 94–95
 O-donor ligands, 96–97
 S-donor ligands, 96–97
- Tetraglyme, with β -diketones, 187–189
- Tetrametaphosphimate ions, conformation, 200–201
- Tetrametaphosphimates
 characterization, 199
 crystal structures, 204–206
 formation and decomposition, 200
 IR and Raman studies, 199–200
- 2,2,6,6-Tetramethylheptanedionate, for CVD precursor preparation, 185
- Tetraphosphafulvalene, reaction with Li or K, 99
- 3,4,7,8-Tetrasilacycloocta-1,5-diyne, σ – π mixing, 361–362
- Tetrasila[2.2](2,5)heterophanes
 molecular structure, 384–389
 NMR studies, 384–389
 octamethyl-1,2,8,9-tetrasila[2.2](2,5) furanophane, 380–383, 389–390
 octamethyl-1,2,8,9-tetrasila[2.2](2,5) thiophenophane, 380–383
 tetrasila[2.2](2,5)pyrrolophane, 383–384
- Tetrasila[2.2](2,5)pyrrolophane
 preparation, 383
 UV spectrum, 383–384
- Tetrasodium dication cluster, phosphanes and arsanes, 244–246, 252–253, 257–258
- 1,2,9,10-Tetrastanna[2.2]paracyclophane, molecular structure, 372–375
- Thiolate complex, phosphine-functionalized, synthesis, 97

Tin

- bridged [2ⁿ]paracyclophanes, 395–399
- mixed clusters of arsanides and phosphandiides, 276–277
- Tin amides, cyclopropenylidene complexes, 19–20
- Tin halide, carbene complexes, 17–19
- Tin(II) metalated phosphandiides
 - molecular structures, 265–267
 - NMR characterization, 265
 - preparation, 263–264
- Trains, magnetically levitated, superconductors, 176–177
- Trialkyl compounds, carbene complexes, 13–16
- Triaryl compounds, carbene complexes, 13–16
- Trichlorosilanes, treatment with Li complex, 99–100
- Trihalides, Group 13, carbene complexes, 9–11
- Trimetaphosphimates
 - characterization, 199
 - crystal structures, 201–204
 - formation and decomposition, 200
 - ion conformation, 200–201
 - IR and Raman studies, 199–200
- Trimetaphosphimatometallates, crystal structures, 208–209
- Triorganoboron complexes, with carbenes, 14
- Tris(dithiocarbamate) complex, with Bi, 303

U

- Ultraviolet spectroscopy
 - 1,2,9,10,17,18-hexasila[2.2.2](1,3,5) cyclophane, 394
 - hexasila[6](2,5)thiophenophane, 403
 - octamethyl-1,2,8,9-tetrasila[2.2](2,5) furanophane, 380, 382
 - octamethyl-1,2,8,9-tetrasila[2.2](2,5) thiophenophane, 380, 382
 - pentasila[5](2,5)thiophenophane, 403
 - tetrasila[2.2](2,5)pyrrolophane, 383–384

X

- X-ray structure
 - acyclic molecular ionic PON compounds, 196–197
- Al, Ga, and In arsanides and phosphandiides, 270–272
- amorphous metallophosphate oxynitrides, characterization, 224–225
- Cs₃M^{II}₂P₆O₁₇N, 221–222
- dicopper phosphandiides, 259
- Group 14-bridged [2.2]paracyclophanes, 375–377
- 1,2,9,10,17,18-hexasila[2.2.2](1,3,5) cyclophane, 392–394
- homometallic lithium (di)organophosphides, 38–51
- magnesium phosphandiides, 261–262
- mixed-metalated arsanides and phosphandiides, 278–280
- molecular PON compounds, 195
- octamethyltetragerma[2.2]paracyclophane, 370–371
- pentamethyl cyclopentadienide pyrazine barium compound, 183
- phosphoranes and arsanes
 - complexed clusters, 246–251, 253–255
 - dimeric Na₄As₁₂ cluster, 252–253
 - mixed-valent clusters, 251–252
 - tetrasodium-dication cluster, 252–253
- Si, Ge, and Sn-bridged [2ⁿ]paracyclophanes, 399
- tetrametaphosphimates, 204–206
- tetrasila[2.2](2,5)heterophanes, 386–389
- 1,2,9,10-tetrastanna[2.2] paracyclophane, 372–375
- trimetaphosphimates, 201–204
- trimetaphosphimatometallates, 208–209

Z

- Zinc, carbene complexes, 5–9
- Zintl ions, characterization, 100

CONTENTS OF PREVIOUS VOLUMES

VOLUME 39

Synthetic Approach to the Structure and
Function of Copper Proteins
Nobumasa Kitajima

Transition Metal and Organic Redox-
Active Macrocycles Designed to
Electrochemically Recognize Charged
and Neutral Guest Species
Paul D. Beer

Structure of Complexes in Solution
Derived from X-Ray Diffraction
Measurements
Georg Johansson

High-Valent Complexes of Ruthenium
and Osmium
*Chi-Ming Che and Vivian
Wing-Wah Yam*

Heteronuclear Gold Cluster Compounds
*D. Michael P. Mingos and
Michael J. Watson*

Molecular Aspects on the Dissolution and
Nucleation of Ionic Crystals in
Water
Hitoshi Ohtaki

INDEX

VOLUME 40

Bioinorganic Chemistry of Pterin-
Containing Molybdenum and
Tungsten Enzymes
*John H. Enemark and
Charles G. Young*

Structure and Function of Nitrogenase
*Douglas C. Rees, Michael K. Chan, and
Jongsun Kim*

Blue Copper Oxidases
A. Messerschmidt

Quadruply Bridged Dinuclear Complexes
of Platinum, Palladium, and Nickel
Keisuke Umakoshi and Yoichi Sasaki

Octacyano and Oxo- and
Nitridotetracyano Complexes of
Second and Third Series Early
Transition Metals
*Johann G. Leipoldt,
Stephen S. Basson, and Andreas Roodt*

Macrocyclic Complexes as Models for
Nonporphine Metalloproteins
Vickie McKee

Complexes of Sterically Hindered
Thiolate Ligands
J. R. Dilworth and J. Hu

INDEX

VOLUME 41

The Coordination Chemistry of
Technetium
John Baldas

Chemistry of Pentafluorosulfanyl
Compounds
*R. D. Verma, Robert L. Kirchmeier,
and Jean'ne M. Shreeve*

The Hunting of the Gallium Hydrides
*Anthony J. Downs and
Colin R. Pulham*

The Structures of the Group 15
Element(III) Halides and
Halogenoanions
*George A. Fisher and
Nicholas C. Norman*

Intervalence Charge Transfer and
Electron Exchange Studies of
Dinuclear Ruthenium Complexes
Robert J. Crutchley

Recent Synthetic, Structural,
Spectroscopic, and Theoretical

- Studies on Molecular Phosphorus
Oxides and Oxide Sulfides
J. Clade, F. Frick, and M. Jansen
- Structure and Reactivity of Transferrins
E. N. Baker
- INDEX
- VOLUME 42
- Substitution Reactions of Solvated Metal
Ions
*Stephen F. Lincoln and
André E. Merbach*
- Lewis Acid–Base Behavior in Aqueous
Solution: Some Implications for
Metal Ions in Biology
*Robert D. Hancock and
Arthur E. Martell*
- The Synthesis and Structure of
Organosilanols
Paul D. Lickiss
- Studies of the Soluble Methane
Monooxygenase Protein System:
Structure, Component Interactions,
and Hydroxylation Mechanism
*Katherine E. Liu and
Stephen J. Lippard*
- Alkyl, Hydride, and Hydroxide
Derivatives in the *s*- and *p*-Block
Elements Supported by
Poly(pyrazolyl)borato Ligation:
Models for Carbonic Anhydrase,
Receptors for Anions, and the Study
of Controlled Crystallographic
Disorder
Gerard Parkin
- INDEX
- VOLUME 43
- Advances in Thallium Aqueous Solution
Chemistry
Julius Glaser
- Catalytic Structure–Function
Relationships in Heme Peroxidases
Ann M. English and George Tsaprailis
- Electron-, Energy-, and Atom-Transfer
Reactions between Metal Complexes
and DNA
H. Holden Thorp
- Magnetism of Heterobimetallics: Toward
Molecular-Based Magnets
Olivier Kahn
- The Magnetochemistry of Homo- and
Hetero-Tetranuclear First-Row
d-Block Complexes
Keith S. Murray
- Diiron–Oxygen Proteins
*K. Kristoffer Andersson
and Astrid Gräslund*
- Carbon Dioxide Fixation Catalyzed by
Metal Complexes
Koji Tanaka
- INDEX
- VOLUME 44
- Organometallic Complexes of Fullerenes
*Adam H. H. Stephens
and Malcolm L. H. Green*
- Group 6 Metal Chalcogenide Cluster
Complexes and Their Relationships
to Solid-State Cluster Compounds
Taro Saito
- Macrocyclic Chemistry of Nickel
Myunghyun Paik Suh
- Arsenic and Marine Organisms
*Kevin A. Francesconi
and John S. Edmonds*
- The Biochemical Action of Arsonic Acids
Especially as Phosphate Analogues
Henry B. F. Dixon
- Intrinsic Properties of Zinc(II) Ion
Pertinent to Zinc Enzymes
Eiichi Kimura and Tohru Koike
- Activation of Dioxygen by Cobalt Group
Metal Complexes
*Claudio Bianchini
and Robert W. Zoellner*

Recent Developments in Chromium
Chemistry
Donald A. House

INDEX

VOLUME 45

Syntheses, Structures, and Reactions of
Binary and Tertiary Thiomolybdate
Complexes Containing the (O)Mo(S_x)
and (S)Mo(S_x) Functional Groups
($x = 1, 2, 4$)
Dimitri Coucouvanis

The Transition Metal Ion Chemistry of
Linked Macrocyclic Ligands
Leonard F. Lindoy

Structure and Properties of Copper–Zinc
Superoxide Dismutases
*Ivano Bertini, Stefano Mangani, and
Maria Silvia Viezzoli*

DNA and RNA Cleavage by Metal
Complexes
*Genevieve Pratviel, Jean Bernadou,
and Bernard Meunier*

Structure–Function Correlations in High
Potential Iron Problems
J. A. Cowan and Siu Man Lui

The Methylamine Dehydrogenase
Electron Transfer Chain
*C. Dennison, G. W. Canters,
S. de Vries, E. Vijgenboom,
and R. J. van Spanning*

INDEX

VOLUME 46

The Octahedral M₆Y₆ and M₆Y₁₂ Clusters
of Group 4 and 5 Transition Metals
Nicholas Prokopuk and D. F. Shriver

Recent Advances in Noble–Gas
Chemistry
John H. Holloway and Eric G. Hope

Coming to Grips with Reactive
Intermediates
*Anthony J. Downs and
Timothy M. Greene*

Toward the Construction of Functional
Solid-State Supramolecular Metal
Complexes Containing Copper(I) and
Silver(I)
*Megumu Munakata, Liang Ping Wu,
and Takayoshi Kuroda-Sowa*

Manganese Redox Enzymes and Model
Systems: Properties, Structures, and
Reactivity
*Neil A. Law, M. Tyler Caudle, and
Vincent L. Pecoraro*

Calcium-Binding Proteins
*Bryan E. Finn and
Torbjörn Drakenberg*

Leghemoglobin: Properties and Reactions
*Michael J. Davies, Christel Mathieu,
and Alain Puppo*

INDEX

VOLUME 47

Biological and Synthetic [Fe₃S₄] Clusters
*Michael K. Johnson,
Randall E. Duderstadt, and
Evert C. Duin*

The Structures of Rieske and Rieske-
Type Proteins
Thomas A. Link

Structure, Function, and Biosynthesis of
the Metallosulfur Clusters in
Nitrogenases
Barry E. Smith

The Search for a “Prismane”
Fe–S Protein
*Alexander F. Arendsen and
Peter F. Lindley*

NMR Spectra of Iron–Sulfur Proteins
*Ivano Bertini, Claudio Luchinat, and
Antonio Rosato*

Nickel–Iron–Sulfur Active Sites:
Hydrogenase and CO Dehydrogenase
*Juan C. Fontecilla-Camps and
Stephen W. Ragsdale*

FeS Centers Involved in Photosynthetic
Light Reactions

- Barbara Schoepp, Myriam Brugna,
Evelyne Lebrun, and
Wolfgang Nitschke*
- Simple and Complex Iron–Sulfur
Proteins in Sulfate Reducing
Bacteria
*Isabel Moura, Alice S. Pereira,
Pedro Tavares, and
José J. G. Moura*
- Application of EPR Spectroscopy to the
Structural and Functional Study of
Iron–Sulfur Proteins
*Bruno Guigliarelli and
Patrick Bertrand*
- INDEX
- VOLUME 48
- Cumulative Index for Volumes 1–47
- VOLUME 49
- Inorganic and Bioinorganic Reaction
Mechanisms: Application of High-
Pressure Techniques
- Rudi van Eldik, Carlos Dücker-Benfer,
and Florian Thaler*
- Substitution Studies of Second- and
Third-Row Transition Metal Oxo
Complexes
*Andreas Roodt, Amira Abou-Hamdan,
Hendrik P. Engelbrecht, and
Andre E. Merbach*
- Protonation, Oligomerization, and
Condensation Reactions of
Vanadate(V), Molybdate(VI), and
Tungstate(VI)
J. J. Cruywagen
- Medicinal Inorganic Chemistry
Zijian Guo and Peter J. Sadler
- The Cobalt(III)-Promoted Synthesis of
Small Peptides
*Rebecca J. Browne,
David A. Buckingham,
Charles R. Clark, and Paul A. Sutton*
- Structures and Reactivities of Platinum-
Blues and the Related Amidate-
Bridged Platinum^{III} Compounds
Kazuko Matsumoto and Ken Sakai
- INDEX